Agronomy Research

Established in 2003 by the Faculty of Agronomy, Estonian Agricultural University

Aims and Scope:

Agronomy Research is a peer-reviewed international Journal intended for publication of broad-spectrum original articles, reviews and short communications on actual problems of modern biosystems engineering incl. crop and animal science, genetics, economics, farm- and production engineering, environmental aspects, agro-ecology, renewable energy and bioenergy etc. in the temperate regions of the world.

Copyright:

Copyright 2009 by Estonian University of Life Sciences, Latvia University of Life Sciences and Technologies, Aleksandras Stulginskis University, Lithuanian Research Centre for Agriculture and Forestry. No part of this publication may be reproduced or transmitted in any form, or by any means, electronic or mechanical, incl. photocopying, electronic recording, or otherwise without the prior written permission from the Estonian University of Life Sciences, Latvia University of Life Sciences and Technologies, Aleksandras Stulginskis University, Lithuanian Research Centre for Agriculture and Forestry.

***Agronomy Research* online:**

Agronomy Research is available online at: http://agronomy.emu.ee/

Acknowledgement to Referees:

The Editors of *Agronomy Research* would like to thank the many scientists who gave so generously of their time and expertise to referee papers submitted to the Journal.

Abstracted and indexed:

SCOPUS, EBSCO, CABI Full Paper and Thompson Scientific database: (Zoological Records, Biological Abstracts and Biosis Previews, AGRIS, ISPI, CAB Abstracts, AGRICOLA (NAL; USA), VINITI, INIST-PASCAL.)

Subscription information:

Institute of Technology, EULS
St. Kreutzwaldi 56, 51014 Tartu, ESTONIA
E-mail: timo.kikas@emu.ee

Journal Policies:

Estonian University of Life Sciences, Estonian Research Institute of Agriculture, Latvia University of Life Sciences and Technologies, Aleksandras Stulginskis University, Lithuanian Institute of Agriculture and Lithuanian Institute of Horticulture and Editors of *Agronomy Research* assume no responsibility for views, statements and opinions expressed by contributors. Any reference to a pesticide, fertiliser, cultivar or other commercial or proprietary product does not constitute a recommendation or an endorsement of its use by the author(s), their institution or any person connected with preparation, publication or distribution of this Journal.

ISSN 1406-894X

CONTENTS

Agronomy Research **16**(3), 621–633, 2018
https://doi.org/10.15159/AR.18.143

Comparison of consumption of tractor at three different driving wheels on grass surface

R. Abrahám[1,*], R. Majdan[1] and R. Drlička[2]

[1]Slovak University of Agriculture in Nitra, Faculty of Engineering, Department of Transport and Handling, Tr.A. Hlinku 2, SK949 76 Nitra, Slovak Republic
[2]Slovak University of Agriculture in Nitra, Faculty of Engineering, Department of Quality and Engineering Technologies, Tr.A. Hlinku 2, SK949 76 Nitra, Slovak Republic
[*]Correspondence: rudolf.abraham@uniag.sk

Abstract. The paper deals with possibility of reduction of tractor fuel consumption when working on grass surface, and compares use of two versions of spike devices embedded to the original tyre body. The device was designed at Department Transport and Handling (Slovak University of Agriculture in Nitra). Older as well as newer system proposed in 2017 comprises spikes and it is assembled to common tractor tyre tread pattern with auxiliary grooves cut in. Same device can be set to two positions, allowing to work as 8-spikes and 16-spikes system. The spikes are tilted in grooves when moving on paved road. The spikes are ejected out to reduce wheels slip when operated in field. Remaining eight spikes are tilted in case of 8-spikes system. Measurements were realised on grass surface. Tractor Mini 070 type was loaded with heavier tractor MT8-065 type in tests with 3 different driving wheels, balancing the actual weight in all cases. Drawbar pull and fuel consumption were measured in tests, allowing to compute specific drawbar consumption and fuel consumption per hour for three different loads. The results pointed out a fact the tyre slip loss and energy consumption of tractor movement increase at the soil humidity 19.45%. It follows from results achieved that use of both 8- and 16-spikes wheel device versions reduced fuel consumption when cultivating higher humidity soil, preferable for tillage. Eight spikes system with semi-tilted remaining spikes is the most efficient method.

Key words: tyres, spikes devices, consumption of fuel, agriculture, drawbar pull.

INTRODUCTION

The testing of tractors used in agriculture is continuously increasing because these machines directly influence the results of agricultural production. Agricultural tractors are losing a lot of energy by the slip of driving wheels. The wheels properties can be theoretically researched using the numerical computation methods (Nadikto et al., 2015; Adamcuk et al., 2016) or under laboratory conditions using the special testing device (Kučera et al., 2016) or under real tractor operation conditions (Semetko et al., 2002). To reduce the tyre slip, tractors are loaded with a heavy weight, which increases the drawbar pull but excessively increases soil compaction and tyre wear on a hard surface (Semetko at al., 2004).

Nowadays, diesel oil and petroleum products belong to the most used fuels. Unfortunately, fossil fuels are non-renewable and exhaustible sources of energy

(Müllerová et al., 2012). The increase of tractor drawbar pull influences the fuel consumption and emissions of exhaust gases.

Tractor fuel consumption is influenced considerably by used transmission system and drive type of tractor in transportation and field operation. Fuel consumption is achieved using new concepts of combustion control in engines. Fuel consumption at high engine slip contributes to environment impacts much more than it is at low slip. Significant savings of fuel used by tractor combustion engines can be achieved by tractor wheel slip reduction using crawler adapters (Molari et al., 2012).

The results of a theoretical analysis reveal that, for a four-wheel-drive tractor to achieve the optimum tractive performance under a given operating condition, the thrust (or driving torque) distribution between the front and rear axles should be such that the slips of the front and rear tyres are equal. Field test data confirm the theoretical findings that, when the theoretical speed ratio is equal to 1, the efficiency of slip and tractive efficiency reach their respective peaks, the fuel consumption per unit drawbar power reaches a minimum, and the overall tractive performance is at an optimum (Wong et al., 1998).

Subsoil tillage is a remedy for adverse soil compaction (Malý & Kučera 2014 and Malý et al., 2015) that results in improved conditions for crop growth.

Not least the drawbar properties improvement of the driving wheels influences the soil compression since lower slip and higher operation speed means lower soil compression (Rataj et al., 2009, Hrubý et al., 2013 and Jobbágy et al., 2016).

MATERIALS AND METHODS

Measurement system and conditions

The drawbar pull measurement of the tractor Mini 070 type (Fig. 2) equipped with different wheels was performed by means of a tensometric force sensor marked as EMS 150, as shown in Fig. 1. The force sensor is connected between the loading tractor MT8-065 and the tractor Mini 070 type through a chain. A portable recording unit HMG 3010 (Hydac GmbH, Germany) was used to record electrical signals from the force sensor. A description of measurement devices and sensor are presented in the works published by Tulík et al. (2013) and Tkáč et al. (2017).

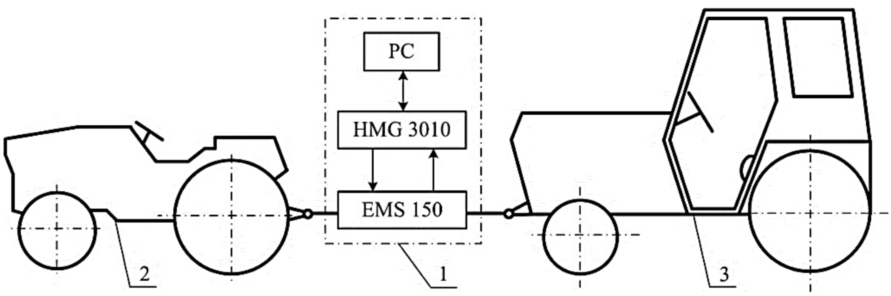

Figure 1. System for measurement of tractor drawbar pulls.
1 – measurement system; 2 – tractor Mini 070 type equipped with different wheel types; 3 – loading tractor type MT8-065; HMG 3010 – digital portable recording device; EMS 150 – force sensor; PC – personal computer.

Technical parameters and specification of tractor Mini 070 type equipped with different wheels types and the loading tractor MT8-065 type used to brake the first one are listed in Table 1.

Table 1. Specifications of the tractors

Tractor type	Tractor part	Parameter	Value
MT8-065	All tractor	Construction weight	970 kg
	Engine	Type and manufacturer	Petrol four-stroke water-cooled (Škoda)
		Number of cylinders	4
		Displacement	1,200 cm^3
		Max. performance	20 kW
Mini 070	All tractor	Construction weight	310 kg
	Engine	Type and manufacturer	Petrol four-stroke air-cooled (Briggs & Stratton)
		Number of cylinders	1
		Displacement	400 cm^3
		Max. performance	8 kW

Drawbar pull measurements procedure is as follows:

– attachment of tractor MT8-065 type (no gear engaged) to the tractor via drawbar pull sensor for the first measurement,
– removal of four spark from engine head of the loading tractor MT8 – 065 type to achieve constant drawbar pull with 1st and 4th gear engaged and stopped engine for the second and third measurements,
– system start in sufficient distance before the sector start,
– start of the stopwatch when the tractor front part passing the staring rods, start the drawbar pull measurement Hydac 3010 and count the drive wheel rotates,
– stop of the stopwatch and tractor when tractor front part passes finish rods,
– repetition of measurements using the tractor Mini 070 type at first and second gear with loading tractor at no, first and fourth gears engaged,
– repetition of measurements with tractor equipped with standard tyres Mitas 6.5/75–14 TS – 02 type (Mitas a. s., Czech Republic), spikes device with all 16 spikes ejected to the angle 90° (16-spikes tyres) and spikes device with 8 spikes ejected to angle 90°and 8 spikes to angle 30° (8-spikes tyres); 8 spikes at angle 90° alternate with 8 spikes at angle 30° around the wheel circumference (Fig. 3).

The measurements of tractor drawbar pull and fuel consumption with three different driving wheels were realised in October 2017 with average volume soil humidity 19.45% and soil volume weight 1.24 g cm^{-3}. The measurement were realised on the grass plane surface at sunny weather in Slovak Agricultural Museum in Nitra. The area for measurement was approximately 0.5 ha. Measuring sector limited by rods had rectangular shape with dimensions 30 x 25 m.

Spikes device

The spike device was designed based on previous research of wheel drawbar pull transfer to surface improvement (Abrahám et al., 2014), where the wheel ploughing sleeves used on two-wheel walking tractors was clearly the best solution.

Fig. 2 shows the spikes device assembled to the tractor tyre body. It consists of eight segments connected together by carrying wire rope 3 and operated by control wire rope 4. Control wire rope 4 provides spikes tipping from tyre body and mutual holding of individual segments in the same position.

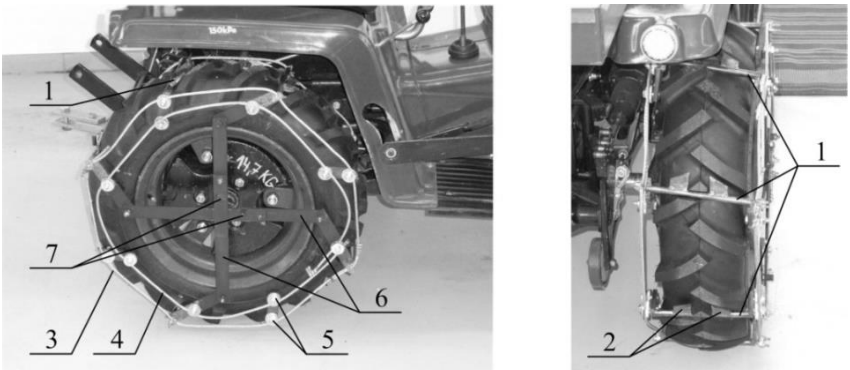

Figure 2. The tractor type Mini 070 equipped with standard tyres and special spikes device: 1 – spike segment; 2 – spikes; 3 – carrying wire rope; 4 – control wire rope; 5 – pivot pins; 6 – lever mechanism; 7 – locking screws.

Spike segments (Fig. 5) are tilting to avoid need for removal when moving on the road and reduce the health risks for operator. The tilting is realised by spikes 2 rotation to tangential position not outreaching the tyre body (tread). Spikes 2 eject automatically due to tractor drive wheel slip, when lever mechanism 6 is locked-off using the locking screws 7. It is necessary to lock tilted position of spikes 2 using lever mechanism 6 and locking screws 7 to prevent spikes recline to transport position when generating drawbar pull back in reverse motion. Locked transport position suitable for movement on paved roads is shown in Fig. 2.

Fig. 3 shows the spikes positioning in the tyre-tread pattern. 8 spikes are ejected to the angle 90° and 8 spikes to 30°. This experiment tests the influence of the spikes position on the drawbar pull of the tractor.

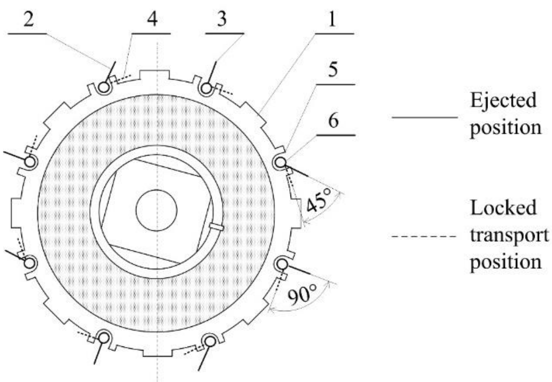

Figure 3. Spikes positioning during drawbar pull measurements: 1 – tractor tyre; 2 – spikes ejected to angle 30°; 3 – spikes ejected to angle 90°; 4 – spikes in locked transport position; 5 – groove in tyre-tread pattern; 6 – spike segment.

Figure 4. Spikes device on tractor wheel tyres TS – 02 type with 8 active spikes.

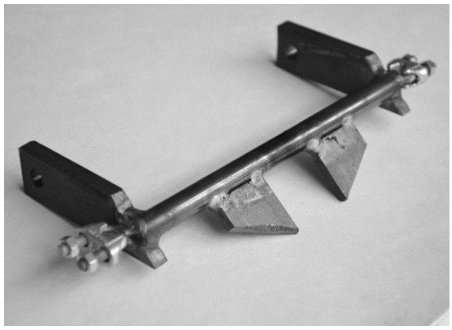

Figure 5. Detail of spike segment.

Measurement and calculation of fuel consumption

Fuel consumption of the small tractor Mini 070 type at stable load is measured by weight method using three-way valve (Fig. 7) and particularly adapted measuring tank (Fig. 6) with volume 1dm^3, fixed to main fuel tank. Three-way valve is set to position reachable to driver. It has three positions: first for fuel flow from main fuel tank to tractor fuel system. Second position allows fuel flow from measuring tank to tractor fuel system. Third position blocks fuel flow from and to any direction above mentioned.

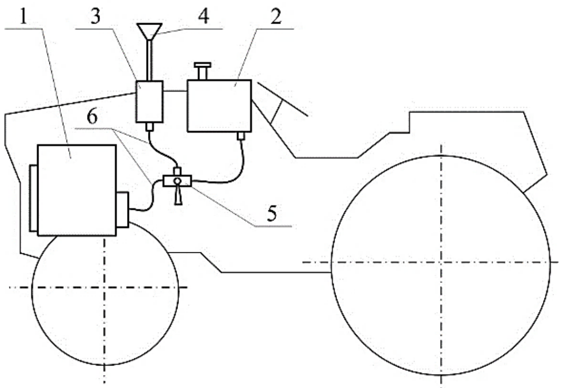

Figure 6. Modified tractor fuel system for fuel consumption measurment: 1 – tractor engine; 2 – main fuel tank; 3 – measuring tank; 4 – funel with gauge line; 5 – three-way valve; 6 – hoses.

Filling hole of measuring tank is funnel with 8 mm pipe internal diameter and gauge line indicating full fuel level to be filled before measurement fuel consumption is determined based on weight of the fuel in doser used for filling.

Filling hole of measuring tank is funnel with 8 mm pipe internal diameter and gauge line indicating full fuel level to be filled before measurement fuel consumption is determined based on weight of the fuel in doser used for filling. Fuel is refilled after each tractor ride to full measuring tank level and remaining fuel in doser is then weighed. Used fuel is the weight difference on digital scale (Fig. 8) of full doser and doser after measuring tank refilling (after tractor ride).

Figure 7. Three-way valve set to flow from the measuring tank.

Figure 8. Doser and digital scale with precision 0.01 g.

Fuel consumption pre hour (M_{ph}) is calculated using this formula:

$$M_{ph} = \frac{m_1 - m_2}{t}, \text{ g h}^{-1} \quad (1)$$

where m_1 – weight of full doser, g; m_2 – weight of doser after filling measuring tank (after tractor ride), g; t – time of ride, h.

Specific drawbar fuel consumption (m_{pe}) as a function of drawbar power at actual load level and speed is calculated using equation:

$$m_{pe} = \frac{M_{ph}}{P_t} = \frac{M_{ph}}{F_t v}, \text{ g kW}^{-1}\text{ h}^{-1} \quad (2)$$

where P_t – drawbar power, kW; F_t – drawbar pull in one ride, kN; v – tractor speed in one ride, m s^{-1}.

The average drawbar power is determined by average drawbar pull and motion speed of tractor. Drawbar characteristics of tractor determine tractor drawbar capacity defined by its drawbar pull F_t at particular motion speed, specifying tractor drawbar power P_t. Tractor drawbar power determines significantly driving wheels slip δ, particularly on unpaved supports. Slip values are therefore accompanying specification of drawbar parameters. Average drawbar power (P_t) can be calculated according to:

$$P_t = F_t v, \text{ W} \quad (3)$$

where F_t – average drawbar pull, N; v – tractor speed, m s^{-1}.

A standard arithmetical average formula and measured values of drawbar pull were used to calculate the average drawbar pull F_t.

Fuel consumption and drawbar pull measurements were realised at the same time. The fuel consumption measurement procedure is as follows:

- staking of the measuring sector of 30 m on grass using two rods at the sector start and finish,
- connection of the tractor fuel tank with the engine using the three-way valve (engine consumes the fuel from the tractor fuel tank and not from the measuring tank),
- passage of the tractor to the sector start,

– refilling measuring tank with fuel up to gauge line (Fig. 9, a),
– connection of measuring tank with engine fuel system using three-way valve, tractor start along with time measurement start using stopwatch,
– tractor stop at the sector finish and block the fuel from measuring tank to the tractor engine using the three-way valve to stop the fuel consumption from the capillary (Fig. 9, b),
– refilling used fuel from the full doser up to gauge line (Fig. 9, c),
– doser weighing (Fig. 8, 9, c),
– calculation of used fuel weight as a weight difference of full doser and doser after measuring tank refilling,
– measurement repetition at no, first and four gear on the loading tractor,
– realization of measurements at full tractor engine power at the full throttle.

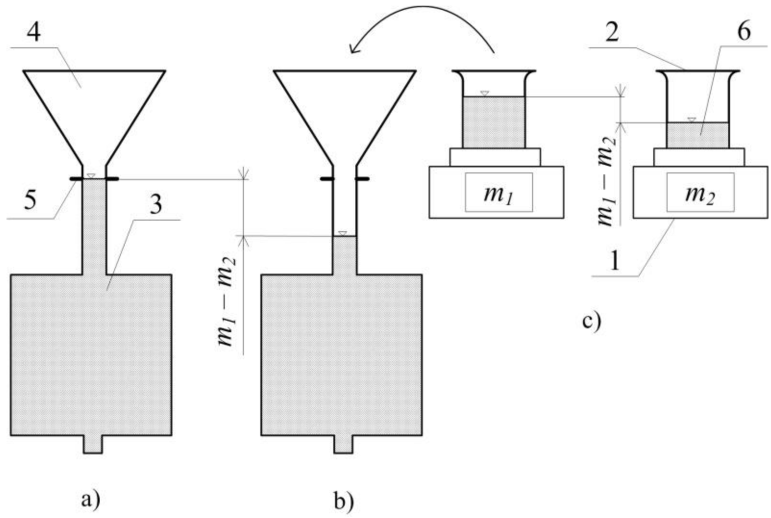

Figure 9. Fuel consumption measurement: 1 – digital scale; 2 – doser; 3 – measuring tank with fuel; 4 – funnel with gauge line; 5 – gauge line; 6 – fuel; a) fuel level corresponds gauge line befor the tractor start; b) fuel level decrease after the tractor ride; c) weighting of consumed fuel.

RESULTS AND DISCUSSION

Tables 2, 3 and 4 show the measured and calculated values describing the fuel consumption of tractor with different driving wheels under three load levels (no, fourth and first gear of loading tractor). The tractor was tested under smallest load at the no gear, medium load at the fourth gear and the highest one at first gear using the loading tractor.

Jenane et al. (1996) achieved minimum specific fuel consumption at values of slip varying between 10% and 30% depending on the soil surface. The author presented that a tractor should be operated at a minimum dynamic traction ratio of 0.4 and at its maximum tractive efficiency to ensure minimum specific fuel consumption. In our case, the spikes device reduces the wheels slip and also the fuel consumption.

Janulevicius & Damanauskas (2015) show that in order to reach the lowest fuel consumption, the following is needed: first, to choose the lowest permissible air pressures in the tyres, and the second to choose the efficient ballast weights. This fact also corresponds with the results of Battiato & Diseren (2013). The spikes device allows reducing the tractor fuel consumption without the need for tyres air pressure change and ballast weight.

Table 2. Measured values of tractor with tyres

Parameter	Unit	Transmission gear of the tractor Mini 070 type					
		1st gear engaged			2nd gear engaged		
Transmission gear of the loading tractor		no gear	4.	1.	no gear	4.	1.
Time of ride t	s	79.28	81.47	118.28	44.33	46.49	79.27
Tractor speed v	m s^{-1}	0.378	0.368	0.254	0.677	0.645	0.378
Weight of full doser m_1	g	163.1	182.2	184.9	150.5	173.8	181.2
Doser weight after filling measuring tank (after ride) m_2	g	142.0	159.2	140.9	133.0	145.4	139.1
Fuel consumption $m_1 - m_2$	g	21.0	23.0	44.1	17.5	28.4	42.1
Fuel consumption per hour M_{ph}	g h^{-1}	955.4	1,017.2	1,340.7	1,417.1	2,195.3	1,913.3
Specific drawbar fuel consumption m_{pe}	g kW^{-1} h^{-1}	2,231.2	1,928.7	2,288.2	1,984.1	2,169.5	1,635.7
Average drawbar pull F_t	N	1,131.6	1,432.3	2,310.1	1,055.4	1,568.1	3,090.9
Average drawbar power P_t	W	428.2	527.4	585.9	714.2	1,011.9	1,169.7

Table 3. Measured values of tractor with 8-spikes tyres

Parameter	Unit	Transmission gear of the tractor Mini 070 type					
		1st gear engaged			2nd gear engaged		
Transmission gear of the loading tractor		no gear	4.	1.	no gear	4.	1.
Time of ride t	s	79.91	82.47	85.87	41.93	37.21	61.87
Tractor speed v	m s^{-1}	0.375	0.364	0.349	0.715	0.806	0.485
Weight of full doser m_1	g	148.0	178.4	174.1	178.9	161.1	169.7
Doser weight after filling measuring tank (after ride) m_2	g	128.8	154.6	144.6	164.9	144.7	145.0
Fuel consumption $m_1 - m_2$	g	19.2	23.8	29.5	14.0	16.4	24.7
Fuel consumption per hour M_{ph}	g h^{-1}	862.7	1,038.1	1,234.7	1,202.9	1,587.6	1,438.4
Specific drawbar fuel consumption m_{pe}	g kW^{-1} h^{-1}	2,348.5	1,698.5	1,325.8	1,348.0	1,309.5	927.3
Average drawbar pull F_t	N	978.5	1,680.1	2,665.6	1,247.1	1,503.8	3,199.1
Average drawbar power P_t	W	367.3	611.2	931.3	892.3	1,212.4	1,551.2

Results achieved (Tables 2, 3 and 4) were divided for evaluation according to gear used on tractor Mini 070 type when testing. Variances were observed in drawbar pull when using common tyres, 8-spikes tyres and 16-spikes tyres. These differences are caused by higher motion speed achieved by tractor with spikes device leading to higher engine speed of tractor MT8-065, resulting in recorded higher drawbar pull and higher mechanical resistance. Similar variances were observed with second gear engaged, with differences even more significant due to higher motion speed.

Table 4. Measured values of tractor with 16-spikes tyres

Parameter	Unit	Transmission gear of the tractor Mini 070 type					
		1st gear engaged			2nd gear engaged		
Transmission gear of the loading tractor		no gear	4.	1.	no gear	4.	1.
Time of ride t	s	75.41	76.59	96.81	42.75	45.3	61.5
Tractor speed v	m s^{-1}	0.398	0.392	0.310	0.702	0.662	0.488
Weight of full doser m_1	g	180.9	151.9	163.1	151.4	178.1	155.0
Doser weight after filling measuring tank (after ride) m_2	g	158.2	131.2	120.4	136.2	157.1	132.7
Fuel consumption $m_1 - m_2$	g	22.7	20.8	42.7	15.2	21.0	22.3
Fuel consumption per hour M_{ph}	g h^{-1}	1,083.7	975.8	1,589.0	1,282.5	1,669.7	1,306.0
Specific drawbar fuel consumption m_{pe}	g kW^{-1} h^{-1}	2,356.5	2,074.1	1,939.0	1,796.0	1,738.2	839.4
Average drawbar pull F_t	N	1,156.0	1,201.1	2,644.4	1,017.6	1,450.4	3,189.4
Average drawbar power P_t	W	459.9	470.5	819.5	714.1	960.6	1,555.8

Figs 12 and 13 are the best representation of the comparison of efficiency of drawbar pull transfer of wheel to surface. An improvement of drawbar pull transfer and reduction of fuel consumption can be observed from the dependency of specific drawbar fuel consumption the on load level in Fig. 12 when 1st gear engaged for both versions of spikes driving wheels with tilting spikes used, starting from medium load at the fourth gear. This improvement can be characterised as a decrease of specific drawbar fuel consumption with load level increase besides the standard tyres. Tyres have the most favourable fuel consumption at medium load. The most favourable fuel consumption dependency was found in case of 8-spikes tyres with partially ejected remaining 8 spikes. It also results from comparison of the both versions of spikes tyres it is more efficient to eject the spikes to the angle less than 90°. Likely due to cable mechanism allowances the spikes ejected to 90° are tilted to more than 100° angle when drawbar pull is generated and the drawbar efficiency is falling.

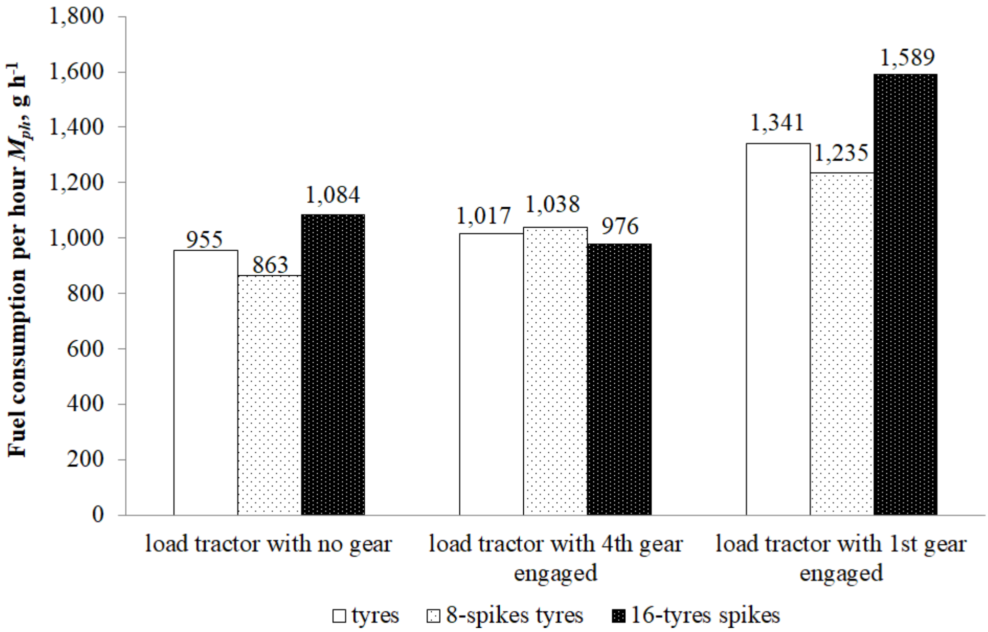

Figure 10. Comparison of fuel consumption per hour, 1st gear engaged.

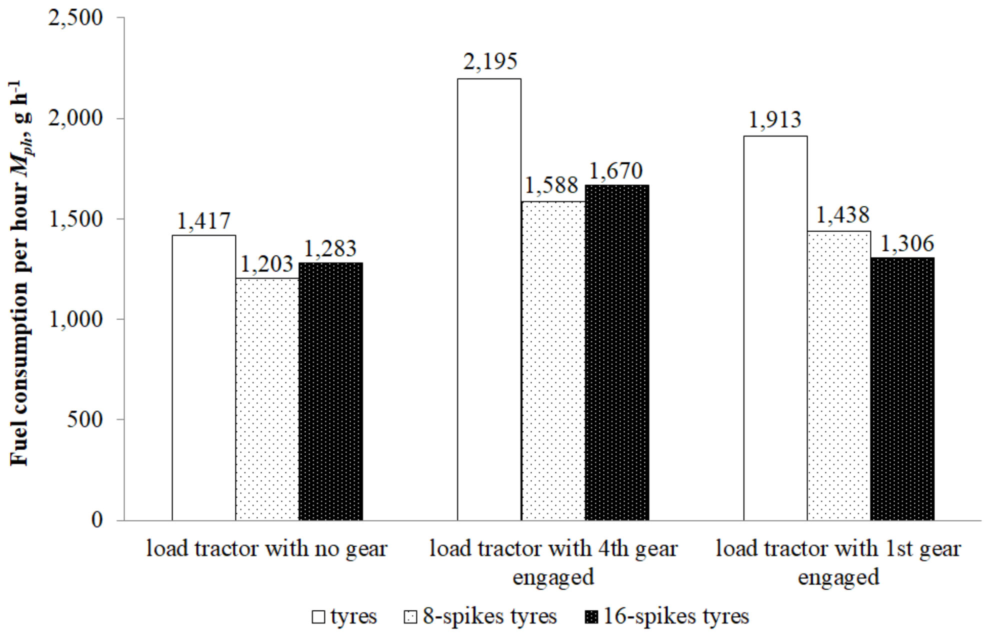

Figure 11. Comparison of fuel consumption per hour, 2nd gear engaged.

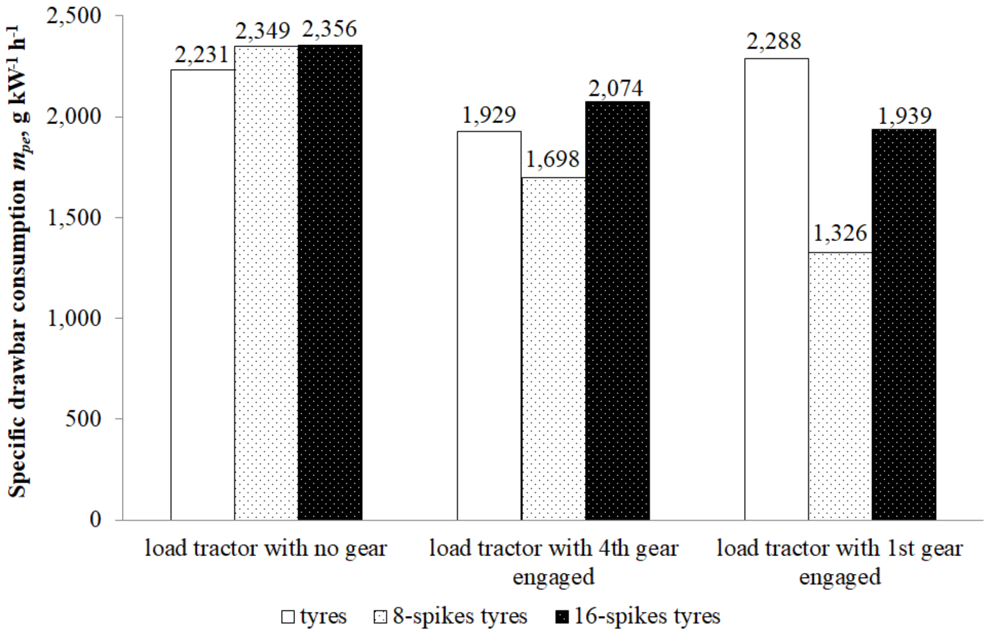

Figure 12. Comparison of specific fuel consumption, 1st gauge engaged.

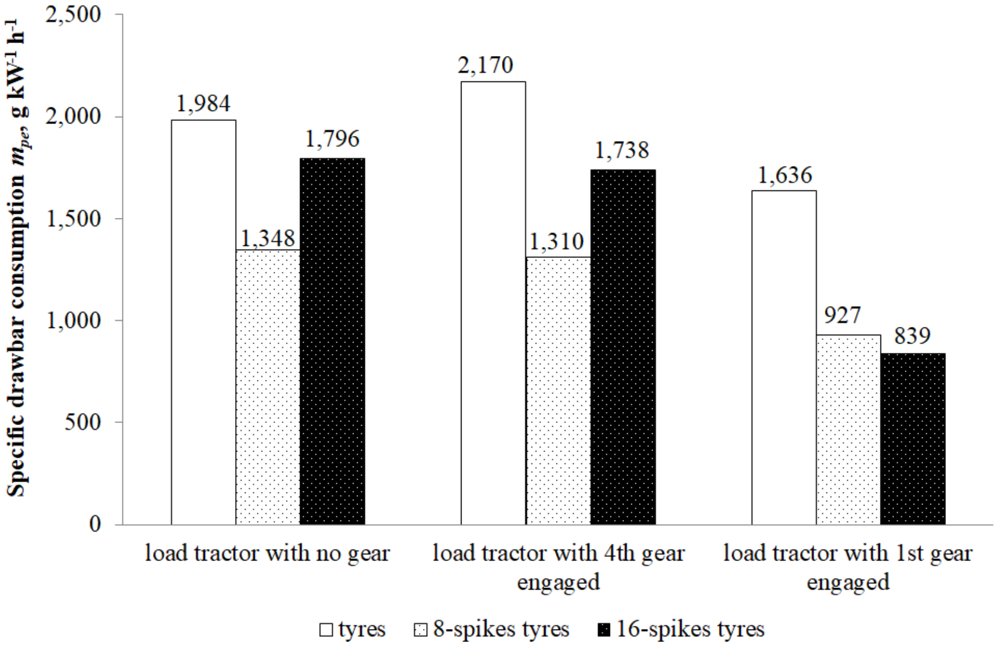

Figure 13. Comparison of specific fuel consumption, 2nd gauge engaged.

The most improvement of the drawbar pull transfer to surface is observed with 1st gear engaged and 8-spikes tyres with partially ejected remaining spikes, based on resulting of dependency of fuel consumption per hour on load level (Fig. 10, 11). This improvement can be characterised as a proportional slip growth up to certain value in case of all three types of driving wheels (Kielbasa & Korenko, 2006). In contrast, with the 2nd gear engaged, 16-spikes tyres and particularly 8-spikes tyres with remaining 8 spikes partially ejected are able to generate higher drawbar power up to medium load as it is evident from Fig. 13. Tyres itself change the dependency from increasing to decreasing at the medium load already and the fuel consumption falls with additional drawbar power due to tyres tread clogging and multiple slip of the driving wheels. It is worth to mention the efficiency improvement of drawbar pull transfer by tyres to surface when 2nd gear engaged (Fig. 11) compared to the 1st (Fig. 10) gear engaged, with the fuel consumption per hour.

CONCLUSIONS

The spikes mechanism was designed to allow comparison of drawbar of different number of spikes engaged in one device. The device was tested intentionally in real soil moisture conditions suitable for soil tillage to let express to the greatest extent differences in drawbar properties of tyres itself and both spikes devices. The next step is to build the spike mechanism into off-road car tyre body and to compare it in long term-test in varied conditions as forest road ride or winter conditions. If needed, the spike device can be easy removed from the tyres in couple minutes similarly as snow chains. The tyres can be used regularly without spikes device after being worn to the tilted spikes diameter, for instance in summer dry conditions. It is first time the devices were compared in this version. The drawbar improvements found will be even more significant in more difficult conditions as dry oil covered by manure, or frozen soil with melted surface layer.

It results from test the spikes device affects the tractor fuel consumption favourably cutting it down and thus improves drawbar pull to elastic surface transfer efficiency at the soil moisture 19.45% compared to common tyres.

ACKNOWLEDGEMENTS. Supported by the Ministry of Education of the Slovak Republic, Project VEGA 1/0155/18 'Applied research of the use of environmentally friendly of energy sources in the agricultural, forestry and transport technology'.

REFERENCES

Abrahám, R., Majdan, R. & Tkáč, Z. 2014. *Research streamlining traction drive wheels of the tractor.* Slovak university of agriculture in Nitra, Nitra, 150 pp. (in Slovak).

Adamchuk, V., Bulgakov, V., Nadykto, V., Ihnatiev, Y. & Olt, J. 2016. Theoretical research into the power and energy performance of agricultural tractors. *Agronomy Research* **14**(5), 1511–1518.

Battiato, A. & Diseren, E. 2013. Influence of Tyre Inflation Pressure and Wheel Load on the Traction Performance of a 65 kW MFWD Tractor on a Cohesive Soil. *Journal of Agricultural Science* **5**(8), 197–215.

Hrubý, D., Bajla, J., Olejár, M., Cviklovič, V. & Tóth, L. 2013. New generation portable vertical penetrometer design. In: *Trends in agricultural engineering 2013*. University of Life Sciences Prague, Prague, pp. 223–227.

Janulevicius, A & Damanauskas, V. 2015. How to select air pressure in the tires of MFWD (mechanical front-wheel drive) tractor to minimize fuel consumption for the case of reasonable wheel slip. *Energy* **90**, 691–700

Jenane, C., Bashford, L.L. & Monroe, G. 1996. Reduction of fuel consumption through improved tractive performance. *Journal of Agricultural Engineering Research* **64**(2), 131–138.

Jobbágy, J., Krištof, K. & Findura, P. 2016. Soil compaction caused by irrigation machinery. *Agronomy Research* **14**(3), 790–800.

Kielbasa, P. & Korenko, M. 2006. Influence of machine working resistance on slippage rate of driving wheels of tractor. *Acta Technologica Agriculturae* **9**(3), 44–47.

Kučera, M., Helexa, M. & Čedík, J. 2016. Link between static radial tire stiffness and the size of its contact surface and contact pressure. *Agronomy Research* **14**(4), 1361–1371.

Malý, V. & Kučera, M. 2014. Determination of mechanical properties of soil under laboratory conditions. *Research in agricultural engineering* **60**(special iss.), 66–69.

Malý, V., Tóth, F., Mareček, J. & Krčálová, E. 2015. Laboratory test of the soil compaction. *Acta Universitatis Agriculturae et Silviculturae Mendelianae Brunensis* **63**(1), 77–85.

Molari, G., Bellentani, L., Guarnieri, A., Walker, M. & Sedoni, E. 2012. Performance of an agricultural tractor fitted with rubber tracks. *Biosystems Engineering* **111**(1), 57–63.

Müllerová, D., Jablonický, J., Hujo, Ľ., Tkáč, Z., Kučera, M. & Kosiba, J. 2012. Measurement of operating parameters and emissions of tractor with diesel oil and biofuel. In: *TEAM.* Josip Juraj Strossmayer University, Osijek-Baranja, pp. 299–302 (in English).

Nadykto, V., Arak, M. & Olt, J. 2015. Theoretical research into the frictional slipping of wheel-type undercarriage taking into account the limitation of their impact on the soil. *Agronomy Research* **13**(1), 48–157.

Rataj, V., Galambošová, J. & Macák, M. 2009. Experiences in GPS application in Slovak Republic (Skúsenosti so zavedením systému CTF na Slovensku). In: *GPS autopilots in agriculture.* Czech University of Life Sciences Prague, Prague, pp. 34–38 (in Slovak).

Semetko, J., Janoško, I. & Pernis, P. 2002. Determination of driving force of tractor and trailer wheels. *Acta technologica agriculturae* **5**(1), 1–4.

Semetko, J., Janoško, I. & Pernis, P. 2004. Determination of power of multidrive vehicles. *Acta technologica agriculturae* **7**(1), 20–23.

STN 72 1010 The statement of soil bulk density. 1989.

Tkáč, Z., Čorňák, Š., Cviklovič, V., Kosiba, J., Glos, J., Jablonický, J. & Bernát, R. 2017. Research of biodegradable fluid impacts on operation of tractor hydraulic system. *Acta technologica agriculturae* **20**(2), 42–45.

Tulík, J., Kosiba, J., Hujo, Ľ., Jablonický, J. & Šinský, V. 2013. The durability of a tractor gear-hydraulic circuit. In: *Trends in agricultural engineering 2013*. Czech University of Life Sciences Prague, Prague, pp. 617–621 (in English).

Wong, J.Y., McLaughlin, N.B., Knezevic, Z. & Burtt, S. 1998. Optimization of the tractive performance of four-wheel-drive tractors. *Proceedings of the Institution of Mechanical Engineers, Part D: Journal of Automobile Engineering* **212**(4), 285–297.

Agronomy Research **16**(3), 634–645, 2018
https://doi.org/10.15159/AR.18.145

Optimising cold compressive recovery of oil from the seeds of Sesame (*Sesamum indicum* L.)

O.L. Akangbe[1,*], R. Adamovský[1] and F. Mošna[2]

[1]Czech University of Life Sciences, Faculty of Engineering, Department of Mechanical Engineering, Kamýcka 129, CZ16521 Praha 6 – Suchdol, Prague, Czech Republic
[2]Czech University of Life Sciences, Faculty of Engineering, Department of Mathematics, Kamýcka 129, CZ16521 Praha 6 – Suchdol, Prague, Czech Republic
[*]Correspondence: akangbe@tf.czu.cz

Abstract. Effects of the time rate of deformation and aspect ratio on mechanical response and performance in single cycle cold compression scheme were investigated for bulk sesame seeds and response forms fitted using forward stepwise multiple regression technique. The degree of deformation was dependent on the time rate of its induction and the equipment's aspect ratio. Energy requirement correlated positively with deformation rate and aspect ratio. Energy expenditure was however more efficient with larger aspect ratios than with smaller ones, given the associated volume energy demands. Strain resistance correlated positively with each of the two influence factors. The time rate of deformation was the most important predictor of oil yield and performance. All the fitted forms had highly significant effects in predicting the responses investigated with 76.7–99.6% of the behaviours of the system explained. The results are valid within the ranges of the influence parameters investigated.

Key words: oilseed, cold pressing, compressive stress, strain, energy.

INTRODUCTION

Abstracting oil from bulk volumes of oilseeds using cold compressive means is particularly dependent on the extent and effectiveness of the deformation of the material matrix that is achievable under the physical, machine and process conditions obtaining during expression. Cold oils are arguably the best quality edible vegetable oils available (Wroniak et al., 2008; Prescha et al., 2014) and the process for obtaining them is well specified to preclude techniques such as physico-chemical or thermo-mechanical treatments capable of altering the natural oil or its quality (Siger et al., 2008; FAO/WHO, 2015). Cold expression is only guaranteed using pure mechanical means (FAO/WHO, 2015). Selecting proper crop, machine and process parameters is the main perceptible route for optimising the yield and performance of the scheme. Existing studies on cold compressive expression detail process limiting parameters to include limit deformation, understood chiefly as attainable via loss of void capacity (Faborode & Favier, 1996; Raji & Favier, 2004). These are all however reported in relation to single cycle compressions and treatment considerations for optimisation were concentrated within physical, chemical and thermo-mechanical domains (Willems et al., 2008; Wiacek et al., 2012;

Lazouk et al., 2015). Multiple cycle compression schemes have been proposed which offer promise of significant improvements in the efficiency of cold compression schemes (Akangbe & Herák, 2018). An alternative approach however is to maximise the yield of single cycle systems through proper understanding of the process. Geometrical parameters have been shown to influence the performances of compression schemes (Owolarafe et al., 2007; Wiacek et al., 2012; Divišová et al., 2014). A generalisable rendition of some of these parameters such as the depth of the product charge to the characteristic dimension of the compression chamber as some aspect ratio (Tumuluru, 2015) is therefore a fitting treatment of the presenting constraints by which the behaviour of the system may be better understood and which will serve to characterise hydraulic compression machines. Deformation in biological materials translates into strain. Productive deformation is that which accomplishes an intended outcome. Many studies appear to present results on observable strain during compressive expression of oil from oilseeds (Faborode & Favier, 1996). However, only very little mention or reference to the rate of induction of such strains may be found in literature (Bargale et al., 2000; Santoso & Inggrid, 2014). One major determinant of the rate of strain is the time rate of induction of deformation, perceivable through the linear approach velocity of the plunger head.

Sesame is an important food crop and an emerging oilseed (Tunde-Akintunde & Akintunde, 2004). In this study, the effects of a geometrical characteristic crop and machine parameter, namely the aspect ratio and the time rate of induction of deformation were investigated and response surfaces modelled using forward stepwise regression technique with a view to optimising the yield and performance of a cold compression scheme.

MATERIALS AND METHODS

Material

The oilseed material used was a batch of whole and cleaned seeds of sesame (*Sesamum indicum* L.) obtained from Czech Republic. The moisture content of the batch of oilseeds used was $6.04 \pm 0.66\%$, in dry basis.

Test procedure, Instrumentation and Design of Experiment

The apparatus used is described in an earlier study (Akangbe & Herák, 2017a). In this study, the internal diameter of the pressing vessel was 60 mm. The base plate was 20 mm thick and oil was discharged laterally through 10 orifices (ϕ 3 mm) equispaced along the circumference of the pressing vessel, and just above the top face of the base plate. For each test, a sample of sesame seeds was fed to a depth in the pressing chamber corresponding to an aspect ratio. The pressing rate was then set and compression induced gradually from zero (0) to a full load corresponding to 26.53 MPa. The load source was a 50 tonne capacity Tempos® model universal test rig – the ZDM50 (TEMPOS, spol. s.r.o., Czech Republic) – operated using the TIRAtest software (TIRA GmbH, Germany). Subsequently, the setup was unloaded and ancillary data acquired. Crop moisture content was determined using oven drying method in accordance with ASAE standards S352.2 for moisture determination in unground grains and seeds. A Gallenkamp type hot air oven (Memmert GmbH, Germany) was used. Temperatures were maintained at 103 ± 2 °C for this purpose. All weight measurements were obtained using the Kern 440–35N (Kern & Sohn GmbH, Stuttgart, Germany) top loading type balance. Pressure applied at the oil point was measured using an auxiliary device with digital output mounted adjacent to the pressing vessel during the test. This is the minimum pressure required to occasion the show and flow of oil. For the determination of the initial bulk density of the seeds, the capacity of the test cylinder used was 0.00035 m^3.

The aspect ratio is the ratio of the depth of product in the compression chamber of the pressing vessel to its diameter and is dimensionless. The time rate of deformation on the test rig was effectuated as the linear velocity of the crosshead (in mm min^{-1}). Three aspect ratios (0.5, 1.0 and 1.5) and three pressing rates (1, 5.5 and 10 mm min^{-1}) were investigated necessitating $3 \times 3 = 9$ treatments. These were implemented in 3 repetitions leading to $3 \times 3 \times 3 = 27$ experimental runs. The study was conducted as a full (3×3) factorial experiment, fitted into a completely randomized design and thus provided more data points for optimising the response surfaces than would normally be required.

Physical, Mechanical Response and Performance Parameters

Physical parameters of the batch of sesame seeds used which are relevant to the measurement of the behaviour of the bulk seeds and the performance of the cold compression scheme adopted were determined using standard methods described in literature (Mohsenin, 1986; Sirisomboon et al., 2007). Bulk density of sesame seeds before oil expression was obtained by dividing the mass of replicate samples by the respective known free–fill volumes they occupy without compaction, as outlined in literature (Arozarena et al., 2012). The true density was established using solvent displacement technique, that is the method of the pycnometer and toluene. True density was determined as a function of the specific gravity of the crop (γ_S), specific gravity of the batch of toluene used (γ_T), mass of the seed sample (m_S) and mass of the displaced volume of toluene (m_{TD}) as shown in Eq. 1 (Mohsenin, 1986):

$$\gamma_s = \left(\gamma_T \times \frac{m_s}{m_{TD}} \right) \tag{1}$$

The material's porosity (or packing factor), P_f (%) was computed based on the bulk density, ρ_b (kg m^{-3}) and the true density, ρ_t (kg m^{-3}) using Eq. 2 (Mohsenin, 1986; Sirisomboon et al., 2007):

$$P_f = \left(1 - \frac{\rho_b}{\rho_t} \right) \times 100 \tag{2}$$

Peak deformation refers to highest value of deformation attainable during a compression test. Induced strain ϵ (–) was measured as the ratio of peak deformation, δ_c (mm) to initial product depth, δ_o (mm) (Eq. 3).

$$\epsilon = \frac{\delta_c}{\delta_o} \tag{3}$$

The initial volume of compressed material, V (mm^3) may be determined using Eq. 4.

$$V = \frac{\pi D^2}{4} \times \delta_O \tag{4}$$

D (mm) is the internal diameter of the pressing vessel. The bulk density of the compressed oilseed material, γ_{CM} (kg m^{-3}) was determined as a function of the mass, m_c of the compressed material and its attained volume, V_c (Eq. 5).

$$\gamma_{CM} = \frac{m_c}{V_c} \tag{5}$$

The volume of the compressed material, V_c (mm^3) was determined using Eq. 6

$$V_c = \frac{\pi D^2}{4} \times \delta_f \tag{6}$$

δ_f (mm) is the depth of the compressed oilseed material in the pressing vessel.

The methods used to compute mechanical parameters and the relevant performance indices are as set forth in literature (Herák et al., 2012). Requisite energy E (J) for achieving observed deformation in the compressed sample was evaluated using Eq. 7:

$$E = \sum_{n=0}^{n=i-1} \left[\left(\frac{F_{n+1} + F_n}{2} \right) \times \left(\delta_{n+1} - \delta_n \right) \right] \tag{7}$$

where, i is the number of subdivisions of the deformation axis, which in this case was logged by the test equipment in incremental steps of 0.01 mm; F_n (N) is the compressive force for a known deformation, δ_n (mm). Volume specific mechanical energy demand was evaluated as a function of the initial volume of the compressed oilseed material (Akangbe & Herák, 2017a).

The deformation modulus, M_n (MPa) of the compressed oilseed was determined as the slope of the stress and strain or deformation curve at the specified force. This is numerically given by Eq. 8:

$$M_n = \left[\frac{4 \times \delta_o}{\pi \times D^2} \left(\frac{F_{n+1} - F_n}{\delta_{n+1} - \delta_n} \right) \right]_{n=0}^{n=i-1} \tag{8}$$

The applied pressure required to occasion the show of oil during each test was observed using the auxiliary digital indicator mounted adjacent to the pressing vessel on the test rig (Akangbe & Herák, 2017b).

For any mass of pressed seeds, m_{ss} (g) and the amount of oil recovered from it during expression, m_O (g) oil yield, OY (kg t^{-1}) may be obtained as (Eq. 9):

$$OY = \frac{m_o}{m_{ss}} \cdot 1{,}000 \tag{9}$$

The percentage yield of oil, POY (%) may be similarly determined (Ajibola et al., 1993) as (Eq. 10):

$$POY = \frac{m_o}{m_{ss}} \cdot 100 \tag{10}$$

Oil expression efficiency is determinable only in reference to the actual quantity of oil present in each batch of pressed seeds. It was therefore necessary to determine the quantity of oil present in the batch of oilseeds used for this study using Soxhlet extraction technique, in accordance with the ISO 659: 2009 reference method for oilseeds. The seeds were milled sufficiently to pass through a size 10 sieve. Samples were defatted in a soxhlet unit using petroleum ether. Standard evaporation techniques were used for solvent recovery as stipulated in the guideline. Three replicate tests were conducted. Oil content, *OC* (%) was then determined using Eq. 11 as the ratio of extracted oil to the mass of the seeds sample (International Organization for Standardization, 2009):

$$OC \frac{m_{OC}}{m_s} \cdot 100 \tag{11}$$

where m_{OC} (g) is the mass of oil extracted and m_S (g) is the mass of the sample. Mechanical oil expression efficiency, η_{OE} (%) was thereafter determined, using Eq. 12, as a ratio of the expressed oil to the total quantity of oil contained in the oilseed (Ajibola et al., 1993):

$$\eta_{OE} = \frac{POY}{OC} \cdot 100 \tag{12}$$

Data analysis

Data obtained in the course of this study were subjected to the analysis of variance using the generalised linear model in Genstat. Numerical computations were done using MS Excel. Treatment effects were compared using Duncan's multiple range test. Curvilinear forms were fitted to the response data on Minitab 17 platform using forward-stepwise multiple regression technique. Detailed description of the curve fitting and validation procedure is reported in literature (Kutner et al., 2005). Surfaces of the form presented below (Eq. 13) were obtained.

$$Y = \beta_0 + \beta_1 D_R + \beta_2 A_R + \beta_3 D_R^2 + \beta_4 A_R^2 + \beta_5 A_R D_R \tag{13}$$

where Y is the response parameter and β_0 is the intercept. β_1, β_2, β_3 β_4 *and* β_5 are slope coefficients. A_R is aspect ratio and D_R is the time rate of deformation. There are ample treatments of the suitability of curvilinear forms to problems of this nature in literature (Granato & Calado, 2014). The equations were fitted with a view to establishing conditions for optimum performance. Optimisation was carried out using the response optimiser in Minitab.

RESULTS AND DISCUSSION

Physical properties of the batch of sesame seeds used for this study showing the initial state of the seeds are presented in Table 1. The seed moisture content was approximately 6%, in dry basis. Bulk and true densities ranged between 626.4 to 696.3 kg m^{-3} and 1,064.9 to 1,099.7 kg m^{-3}, respectively and porosity between 36.2 to 42.5%.

Table 1. Physical properties of the batch of sesame seeds used depicting initial condition of the seeds

Measure	Moisture Content, %, d.b.	Mass, g	Porosity, %	†Bulk density, kg m^{-3}	True density, kg m^{-3}
Mean	6.04	227.9	40.3	651.2	1,091.6
SD*	0.66	5.9	1.6	17.0	13.6

*SD = standard deviation. †n = 20.

Results of the analysis of variance on the test data are presented in Table 2. Both time rate of deformation and equipment aspect ratio had significant effects on mechanical response and the performance parameters investigated. Main effects of the two factors and those of their interactions on deformation, energy and deformation modulus were highly significant. Each of the two factors had a highly significant effect on oil point pressure, but not their interaction. Only the time rate of deformation had significant effect on induced strain, amount of recoverable oil and the performance of the cold expression scheme.

Table 2. Effects of deformation rate and aspect ratio on response variables

Response parameter	Source of Variation		
	Deformation Rate, D_R	Aspect Ratio, A_R	$D_R \times A_R$
Deformation, δ	0.001**	0.001**	0.001**
Strain, ϵ	0.001**	0.094^{ns}	0.202^{ns}
Deformation Energy, E	0.001**	0.001**	0.001**
Volume Energy, e_v	0.001**	0.001**	0.001**
Deformation Modulus, M_n	0.001**	0.001**	0.001**
Bulk Density of Compressed Material, γ_{CM}	0.329^{ns}	0.416^{ns}	0.414^{ns}
Oil Point Pressure, OPP	0.001**	0.001**	0.981^{ns}
Oil Yield, OY	0.001**	0.362^{ns}	0.111^{ns}
Oil Expression Efficiency, η_{OE}	0.001**	0.362^{ns}	0.111^{ns}

ns = not significant at the 5% level; * = significant (at the 5% level); ** = highly significant (at the 1% level).

When treatment means were compared using Duncan's multiple range test, deformation was observed to increase significantly as aspect ratio increased (Table 3) and as the rate of deformation slowed (Table 4). From the force and deformation profiles of the seeds it (Fig. 1), it can be seen that very wide margins are indicated between deformation recorded at lower rates of deformation over those obtained at higher ones; the lower the rate of deformation, the higher the deformation. This was true for all aspect ratios. The incidence of higher deformation at higher aspect ratios is due in part to the larger initial void capacity and volume of the solid material. In their work (Divišová et al., 2014) deformation was positively correlated with the depth of product in the compression chamber. The effectiveness of the compression process appears however to be more dictated by the rate of induction of deformation.

Higher levels of strain were induced as deformation rate was lowered. The slower the rate of induction, the higher was the strain. This effect establishes the time dependence of deformation since strain induction is more effective at the slower rates and agrees with similar observations by Liu et al. (2015). However, in their treatment, reciprocal strain is presented as compression ratio. Deformation and strain improve with time and are functions of the sensitivities of the compressed material under the influence conditions (Savoire et al., 2010). Average strain appeared to be similar for all the aspect ratios investigated (Tables 3 and 4).

Reducing the rate of deformation had the effect of elevating energy requirement for deformation significantly (Table 3), as did also increasing the aspect ratio. Energy expenditure at the lower pressing rates is a function of time as more energy is expended in sustaining incremental compression while working the product mass for much longer periods. Higher aspect ratios however result in better energy efficiency when factored around each bulk volume of material processed. For example, energy expenditure per unit volume of pressed oilseeds reduced significantly from 8.80–0.91 MJ m^{-3} when the aspect ratio was changed from 0.5 to 1.5. The implication therefore is that whereas higher amounts of energy might be required in mills operating with high aspect ratios, the energy efficiency in such systems is better than in mills which may be operated with lower aspect ratios.

Table 3. Main effects of the time rate of deformation on oil expression and compression parameters (*Mean* ± *SD**, *n* = *9*)

Response Parameters	Deformation rate, D_R (mm min^{-1})		
	1.0	5.5	10
Deformation, δ (mm)	35.77 ± 15.90^a	31.35 ± 13.65^b	30.39 ± 12.99^c
Strain, ϵ (-)	0.5932 ± 0.0155^a	0.5218 ± 0.00708^b	0.5066 ± 0.0099^c
Deformation energy, E (J)	407.5 ± 179.0^a	340.8 ± 134.0^b	323.6 ± 122.0^c
Volume energy, e_v (MJ m^{-3})	4.34 ± 3.96^a	3.86 ± 3.65^b	3.66 ± 3.42^c
Deformation modulus, M_n (MPa)	343.6 ± 13.21^b	383.7 ± 38.24^a	370.5 ± 67.63^a
Bulk density of compressed material, γ_{CM}(kg m^{-3})	$1{,}503.0 \pm 986.0^a$	$1{,}141.0 \pm 23.6^a$	$1{,}150.0 \pm 22.5^a$
Oil point pressure, OPP (MPa)	$3{,}247 \pm 0.447^c$	$4{,}077 \pm 0.202^b$	$4{,}626 \pm 0.255^a$
Oil yield, OY (kg t^{-1})	266.5 ± 51.0^a	177.0 ± 6.6^b	144.5 ± 9.23^c
Oil expression efficiency, η_{OE} (%)	59.8 ± 11.5^a	39.7 ± 1.5^b	32.4 ± 2.1^c

Means comparison is row-wise. Similar alphabets indicate homogeneous subsets. Significant effects are valid at the 5% level of significance.

The modulus of deformation represents the compressed material's resistance to strain. At deformation rates of 5.5 and 10 mm min^{-1}, deformation moduli were statistically similar. However, deformation modulus was much less when the rate of deformation was lowered to 1 mm min^{-1}. In essence, the compressed materials were more easily deformed at the lower rates. Increasing aspect ratio does have a significant impact on deformation modulus (Table 4). The mass of material processed given each unit of applied compressive stress increases, as does strain resistance as aspect ratio increases.

Table 4. Main effects of equipment aspect ratio on oil expression and compression parameters (*Mean* ± *SD**, *n* = *9*)

Response Parameters	Aspect ratio, A_R (-)		
	0.5	1.0	1.5
Deformation, δ (mm)	16.04 ± 1.16^c	32.74 ± 2.16^b	48.73 ± 4.36^a
Strain, ϵ (-)	0.5346 ± 0.0385^a	0.5456 ± 0.0361^a	0.5414 ± 0.0484^a
Deformation energy, E (J)	186.6 ± 13.5^c	365.1 ± 30.1^b	520.1 ± 74.7^a
Volume energy, e_v (MJ m^{-3})	8.80 ± 0.64^a	2.15 ± 0.18^b	0.91 ± 0.13^c
Deformation modulus, M_n (MPa)	330.3 ± 15.9^c	357.5 ± 28.7^b	410.0 ± 48.8^a
Bulk density of compressed material, γ_{CM} (kg m^{-3})	$1{,}475.0 \pm 995.9^a$	$1{,}163.0 \pm 23.5^a$	$1{,}156.0 \pm 45.6^a$
Oil point pressure, OPP (MPa)	$4{,}299 \pm 0.690^a$	$3{,}840 \pm 0.618^b$	$3{,}811 \pm 0.603^c$
Oil yield, OY (kg t^{-1})	185.2 ± 51.8^a	203.3 ± 62.7^a	199.5 ± 69.9^a
Oil expression efficiency, η_{OE} (%)	41.6 ± 11.6^a	45.6 ± 14.1^a	44.8 ± 15.7^a

Means comparison is row-wise. Similar alphabets indicate homogeneous subsets. Significant effects are valid at the 5% level of significance.

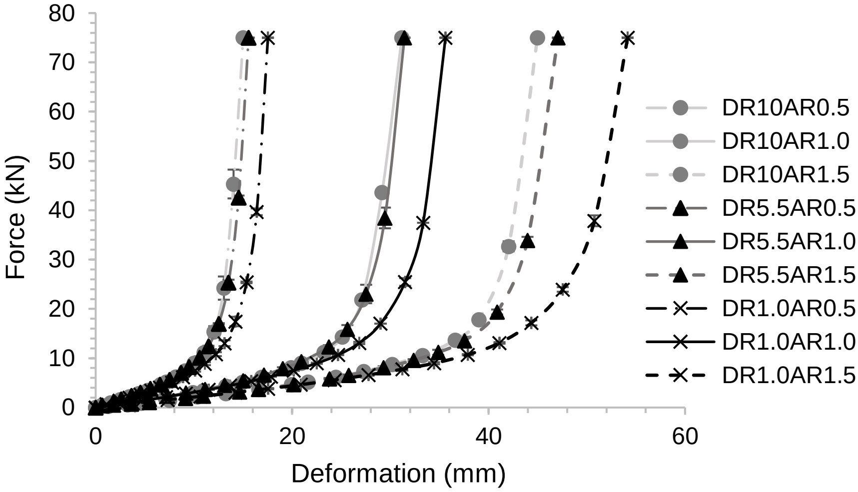

Figure 1. Force and deformation characteristics for aspect ratios of 0.5, 1.0 and 1.5 (AR0.5, AR1.0 and AR1.5, respectively) and at deformation rates of 10, 5.5 and 1.0 mm min^{-1} (or DR10, DR 5.5 and DR 1.0, respectively).

Similar amounts of densification were achieved at all aspect ratios and deformation rates investigated (Tables 3 and 4). The bulk density of the compressed oilseed mass represents a state of loss of void capacity. Whereas the two parameters influenced mechanical response and performance variedly, the bulk density of the compressed seed mass represented an attainable limit, which was similar at the levels of each investigated parameter, the relative contributions of each parameter to the system's response notwithstanding.

At the lower deformation rates, the onset of oil was obtained at lower levels of stress. Oil point pressures increased as deformation rates increased (Table 3). Oil point pressures were, however, lower as aspect ratios increased. In other words, the bigger the aspect ratio, the less was the magnitude of applied stress required to occasion the show and flow of oil (Table 4).

The occasioning of the show and flow of oil at lower pressures observed with bigger aspect ratios did not translate into significant improvements in the yield of oil from the compressed material (Table 4) but higher strains and deformations did which were better as the rate of deformation slowed. The correlation of these parameters with oil yield is in consonance with observations by Liu et al. (2015). The main contributor to improvement in the yield of oil was the time rate of deformation (Table 3). As deformation rate decreased, oil yield increased significantly, and so did the oil expression efficiency. At a deformation rate of 1 mm min^{-1}, an average of 266 kg of oil may be recovered from every tonne of sesame seeds compressed. This represented an oil expression efficiency of 60% and compares favourably with expression at higher pressing rates (Table 3). Existing works (Bargale et al., 2000) confirm the time-dependence of oil yield during compressive expression. As the deformation rate slows, more time is expended in working the product mass. Some attributions of this are with respect to the effectiveness of the process and flow (Adesina & Bankole, 2013; Adekola, 2014).

Table 5. Summary of curvilinear trends fitted to the response indices

Response and performance indicators	β_0	β_1	β_2	β_3	β_4	β_5	S	P > F	R^2	$R^2_{adj.}$
Deformation, δ (mm)	0.450	-0.793	36.765	0.0851		-0.741	0.9427	< 0.001	99.61	99.54
Strain, ϵ (-)	0.6167	-0.0249		0.001385			0.0114	< 0.001	92.55	91.92
Deformation energy, E (J)	-25.1	-7.94	508.8	1.222	-46.9	-14.83	14.8253	< 0.001	99.17	98.97
Volume energy, e_v (MJ m^{-3})	22.063	-0.276	-30.190	0.00712	10.811	0.123	0.1601	< 0.001	99.84	99.80
Deformation modulus, M_n (MPa)	318.5	4.63	9.0	-1.318		12.86	22.4248	< 0.001	80.66	77.14
Oil point pressure, OPP (Pa)	4,230,591	2,29,180	-2,210,485	-6,904	861,402		223,660	< 0.001	90.11	88.31
Oil yield, OY (kg t^{-1})	294.1	-29.0		1.404			30.1934	< 0.001	76.65	74.7
Oil expression efficiency, η_{OE} (%)	65.98	-6.51		0.315			6.7744	< 0.001	76.65	74.70

β_0 is the intercept on the response axis. β_1 – β_5 are slope coefficients to model parameters D_R, A_R, D_R^2, A_R^2, and $D_R A_R$, repectively. S is the standard error of model estimate. P > F is the model probability statistic, significant at p < 0.05. R^2 and R^2_{adj} are the coefficient of determination and adjusted coefficient of determination of the model, respectively.

Table 6. Regions of maximum response on the fitted trends

Response and performance indicators	Regions				95%*CI*		95%*PI*	
	D_R	A_R	*Fit*	*SE Fit*	*LL*	*UL*	*LL*	*UL*
Deformation, δ (mm)	1.0	1.5	53.78	0.471	52.80	54.76	51.59	55.96
Strain, ϵ (-)	1.0		0.5932	0.0038	0.5854	0.6010	0.5685	0.6180
Deformation energy, E (J)	1.0	1.5	603.64	7.680	587.66	619.62	568.92	638.36
Volume energy, e_v (MJ m^{-3})	1.0	1.5	9.46	0.083	9.29	9.64	9.09	9.84
Deformation modulus, M_n (MPa)	9.07	1.5	440.40	9.520	420.66	460.15	389.88	490.93
Oil point pressure, OPP (Pa)	10	0.5	4.94	0.096	4.74	5.14	4.44	5.48
Oil yield, OY (kg t^{-1})	1.0	1.5	266.5	10.1	245.70	287.20	200.8	332.2
Oil expression efficiency, η_{OE} (%)	1.0	1.5	65.97	3.020	59.71	72.24	51.97	79.98

LL – lower limit; *UL* – upper limit; *CI* – confidence interval; *PI* – prediction interval; *Fit* – maximised value of the response parameter; *SE Fit* – standard error of fit.

A summary of equations fit to mechanical response and pressing performance data with respect to the influence of the time rate of deformation and equipment aspect ratio is presented in Table 5. The model fit was Eq. 10. The effects of all the fitted forms in predicting mechanical response and pressing performance were highly significant ($p < 0.001$). Between 76.65%–99.61% of the various responses were explained by the generated trends, given their respective coefficients of determination.

The aspect ratio was the more important contributor to predicting achievable deformation, deformation modulus, deformation energy and volume energy demand than the time rate of deformation. Deformation rate contributed more to predicting strain, oil point pressure, oil yield and oil expression efficiency than the aspect ratio. Regions of maxima for the presented trends and the prediction intervals are presented in Table 6. From the results, maximum yield may be obtained at a deformation rate of 1.0 mm min^{-1} with an aspect ratio of 1.5. This region coincides exactly with those of the occurrences of maximum deformation, strain, deformation energy and volume energy demand but not the maximum resistance of the material to strain (9.08 mm min^{-1} and 1.5) or maximum oil point pressure (10 mm min^{-1} and 0.5). In essence, operating in this region will result in maximum yield and performance of the cold compression scheme.

CONCLUSIONS

In this study, the effects of equipment aspect ratio, time rate of deformation and their interactions on mechanical response and performance in single cycle cold compressive expression of oil from sesame seeds was investigated at 6.04% crop moisture content (in dry basis) and an applied compressive stress of 26.53 MPa. The amount of deformation achieved was dependent on the rate of its induction and the aspect ratio, as well as their interaction. Energy requirement was lower at the higher rates of deformation and smaller aspect ratios. For every unit volume of oilseeds processed, more energy was expended at the lower deformation rates while less energy was expended using bigger aspect ratios. Energy expenditure is therefore more efficient with bigger aspect ratios. The moduli of deformation indicate that resistance to strain is less at lower rates of deformation and smaller aspect ratios compared to the higher settings. Time rate of deformation was the most important predictor of the quantity of oil recovered and the efficiency of the single cycle cold compression scheme. This dependence is explained by the magnitude of induced strain which correlated positively and was dependent mainly on the time rate deformation. The effectiveness of the fitted forms in predicting the respective response parameters was highly significant ($p < 0.001$) with 76.7 to 99.6% of the behaviour of the system explained.

ACKNOWLEDGEMENTS. This study has been supported by Integral Grant Agency of Faculty of Engineering, Czech University of Life Sciences Prague, grant number: 2017: 31130/1312/3111.

REFERENCES

Adekola, K.A. 2014. Optimum processing parameters for coconut oil expression. *Agricultural Engineering International: The CIGR Ejournal*, *XVI*, 240–244.

Adesina, B.S. & Bankole, Y.O. 2013. Effects of particle size, applied pressure and pressing time on the yield of oil expressed from almond Seed. *Nigerian Food Journal* **31**(2), 98–105. https://doi.org/10.1016/S0189-7241(15)30082-5

Ajibola, O.O., Owolarafe, O.K., Fasina, O.O. & Adeeko, K.A. 1993. Expression of oil from sesame seeds. *Canadian Agricultural Engineering* **35**, 83–88.

Akangbe, O.L. & Herák, D. 2017a. Mechanical behaviour of selected bulk oilseeds under compression loading. *Agronomy Research* **15**, 941–951. https://doi.org/10.22616/ERDev2017.16.N206

Akangbe, O.L. & Herák, D. 2017b. Oil point determination of selected bulk oilseeds under compression loading. In V. Osadcuks (Ed.), *Proceedings of the 16th International Scientific Conference on Engineering for Rural Development* (pp. 988–993). Jelgava, Latvia.

Akangbe, O.L. & Herák, D. 2018. Compressive stress, repetitive strain, and optimum expression of oil from bulk volumes of sesame seeds. *Journal of Food Process Engineering*, (October 2017), e12682. https://doi.org/10.1111/jfpe.12682

Arozarena, I., Iguaz, A., Noriega, M.J., Bobo, G. & Virseela, P. 2012. Physical properties of cereal products: measurement techniques and applications. In I. Ariana (Ed.), *Physical properties of foods: novel measurement techniques and applications* (p. 303). New York: CRC Press.

Bargale, P.C., Wulfsohn, D., Irudayaraj, J., Ford, R.J. & Sosulski, F.W. 2000. Prediction of oil expression by uniaxial compression using time-varying oilseed properties. *Journal of Agricultural Engineering Research* **77**(2), 171–181. https://doi.org/10.1006/jaer.2000.0566

Divišová, M., Herák, D., Kabutey, A., Šleger, V., Sigalingging, R. & Svatoňová, T. 2014. Deformation Curve Characteristics of Rapeseeds and Sunflower Seeds Under Compression Loading. *Scientia Agriculturae Bohemica* **45**, 180–186.

Faborode, M.O. & Favier, J.F. 1996. Identification and significance of the oil-point in seed-oil expression. *Journal of Agricultural Engineering Research* **65**, 335–345.

FAO/WHO. 2015. Standard for Named Vegetable Oils Codex Stan 210-1999. *Codex Alimentarius*, 1–13. https://doi.org/10.1017/CBO9781107415324.004

Granato, D. & Calado, V.M. de A. 2014. The use and importance of design of experiments (DOE) in process modelling in food science and technology. In D. Granato & G. Ares (Eds.), *Mathematical and Statistical Methods in Food Science and Technology* (pp. 1–8). UK: John Wiley and Sons, Inc. Retrieved from https://doi.org/10.1146/annurev.energy.28.050302.105521

Herák, D., Kabutey, A., Sedláček, A. & Gurdil, G. 2012. Mechanical behaviour of several layers of selected plant seeds under compression loading. *Research in Agricultural Engineering* **58**(1), 24–29.

International Organization for Standardization. 2009. Oilseeds - determination of oil content (reference method) (ISO 659:2009). Retrieved from https://www.iso.org/standard/23297.html

Kutner, M.H., Nachtsheim, C.J., Neter, J. & Li, W. 2005. *Applied Linear Statistical Models* (5th ed.). Chicago: McGraw-Hill.

Lazouk, M.A., Savoire, R., Kaddour, A., Castello, J., Lanoisellé, J.L., Van Hecke, E. & Thomasset, B. 2015. Oilseeds sorption isoterms, mechanical properties and pressing: Global view of water impact. *Journal of Food Engineering* **153**, 73–80. https://doi.org/10.1016/j.jfoodeng.2014.12.008

Liu, R. kuan, Xu, F. lei, Xiao, Z. hong, Li, C. zhu, Li, H., Zeng, F. tao, & Ye, H. qi. 2015. Effects of compression ratio on variation of stresses and residual oil of cake in pressing process of castor beans and its curve fitting. *Journal of Central South University* **22**(11), 4476–4482. https://doi.org/10.1007/s11771-015-2995-7

Mohsenin, N.N. 1986. *Physical properties of plant and animal materials. Vol. I: Structure, physical characteristics and mechanical properties*. New York: Gordon and Breach Science Publishers.

Owolarafe, O.K., Osunleke, A.S. & Oyebamiji, B.E. 2007. Effect of hydraulic press parameters on crude palm oil yield. *International Agrophysics* **21**, 285–291.
Prescha, A., Grajzer, M., Dedyk, M. & Grajeta, H. 2014. The antioxidant activity and oxidative stability of cold-pressed oils. *Journal of the American Oil Chemists' Society* **91**(8), 1291–1301. https://doi.org/10.1007/s11746-014-2479-1
Raji, A.O. & Favier, J.F. 2004. Model for the deformation in agricultural and food particulate materials under bulk compressive loading using discrete element method . II : Compression of oilseeds. *Journal of Food Engineering* **64**, 373–380. https://doi.org/10.1016/j.jfoodeng.2003.11.005
Santoso, H. & Inggrid, M. 2014. Effects of temperature, pressure , preheating time and pressing time on rubber seed oil extraction using hydraulic press. *Procedia Chemistry* **9**, 248–256. https://doi.org/10.1016/j.proche.2014.05.030
Savoire, R., Carre, P., Chardot, T., Lanoiselle, J.L., Miquel, M., Nesi, N., … & Vorobiev, E. 2010. Micro-pressing of rapeseed (brassica napus L.) and Arabidopsis thaliana seeds for evaluation of the oil extractability. *Oilseeds and Fats, Crops and Lipids (Oleagineux Corps Gras Lipides)*, **17**(2), 115–119. https://doi.org/10.1684/ocl.2010.0300
Siger, A., Nogala-Kalucka, M. & Lampart-Szczapa, E. 2008. The content and antioxidant activity of phenolic compounds in cold-pressed plant oils. *Journal of Food Lipids* **15**(2), 137–149. https://doi.org/10.1111/j.1745-4522.2007.00107.x
Sirisomboon, P., Kitchaiya, P., Pholpho, T. & Mahuttanyavanitch, W. 2007. Physical and mechanical properties of Jatropha curcas L. fruits, nuts and kernels. *Biosystems Engineering* **97**(2), 201–207. https://doi.org/10.1016/j.biosystemseng.2007.02.011
Tumuluru, J.S. 2015. High moisture corn stover pelleting in a flat die pellet mill fitted with a 6 mm die: Physical properties and specific energy consumption. *Energy Science and Engineering* **3**(4), 327–341. https://doi.org/10.1002/ese3.74
Tunde-Akintunde, T.Y. & Akintunde, B.O. 2004. Some physical properties of sesame seed. *Biosystems Engineering* **88**(1), 127–129. https://doi.org/10.1016/j.biosystemseng.2004.01.009
Wiacek, J., Molenda, M., Horabik, J. & Ooi, J.Y. 2012. Influence of grain shape and intergranular friction on material behavior in uniaxial compression: Experimental and DEM modeling. *Powder Technology* **217**, 435–442. https://doi.org/10.1016/j.powtec.2011.10.060
Willems, P., Kuipers, N.J.M. & De Haan, A.B. 2008. Hydraulic pressing of oilseeds: Experimental determination and modeling of yield and pressing rates. *Journal of Food Engineering* **89**(1), 8–16. https://doi.org/10.1016/j.jfoodeng.2008.03.023
Wroniak, M., Krygier, K. & Kaczmarczyk, M. 2008. Comparison of the quality of cold pressed and virgin rapeseed oils with industrially obtained oils. *Polish Journal of Food and Nutrition Sciences* **58**(1), 85–89.

Agronomy Research **16**(3), 646–655, 2018
https://doi.org/10.15159/AR.18.124

Comparison between different types of bedding materials for horses

G. Bambi, G. Rossi and M. Barbari*

University of Firenze, Department of Agricultural, Food and Forestry Systems (GESAAF), Via San Bonaventura 13, IT50145 Firenze, Italy
*Correspondence: matteo.barbari@unifi.it

Abstract. The sports horse lives a large part of the time inside the pen in constant contact with the bedding. Therefore the bedding material can deeply affect the welfare and health of horses kept in pens. The materials have to ensure the realization of a double aim: to create a comfortable and soft surface on which the animal can stand and relax; to give appropriate hygienic and sanitary conditions. Other important factors influence the choice, such as: the material must not be appetizing for the horse; the litter has to maintain a proper level of moisture, so that the hoof is kept healthy, elastic and hydrated. Also the costs for material and litter management have to be taken into account. In the present study, different organic materials are compared: wood chips, hemp, rice, flax and coconut. The trials took place in five box stalls, with square plan of 3 x 3 m. Environmental data were collected during the trials (air temperature and humidity, ammonia concentration, litter moisture). Management data were also collected, regarding the use of bedding materials, working time, costs. In the paper the main results of the comparison between the different litter materials used in horses pens are presented.

Key words: horse husbandry, bedding material, housing, sanitary and hygienic conditions.

INTRODUCTION

In the housing of the sport horse inside stables, the use of litter has always played a fundamental role on the physical wellbeing of the animal. The horse's foot, more if shod, can pose serious problems if the litter used inside the pen is not suitable. Over the years there have been many attempts with different materials such as cereal straw, flax straw, paper, cardboard, sawdust, pine shavings and other types of wood, peat, sand, rice husks, cobs of corn, hemp and coconut.

The continuous increase in the cost of litter in wood chip pellets and the lowering of the average quality (often derived from the shredding of waste products from sawmills and wood industries) has favoured the entry of alternative types of litter into the market.

Many types of natural litter arrived on the market, some ones very popular years ago and others discovered more recently (like the coconut). New producers and importers, who sell different litter materials on the market, exalt their products that often have no practical confirmation in reality.

It is therefore necessary to understand what makes one litter better from another. This research aimed to find an answer to this question, analysing factors that concern the welfare of the horse and the practical and economic aspects of the human activities.

The litter must have the following characteristics for the horse: not to be wet to avoid foot infections; not to be edible; to be free of detrimental substances (chemical and bacteriological); not to be dusty; to ensure physical comfort; to reduce the gaseous emissions.

For the man the litter has to present the following characteristics: to reduce the daily management time; to have a low price; to be easy to dispose of; to be easy to transport and storage; to be easily available.

The horse husbandry usually takes place in box stalls (3 x 3 m or 3.5 x 3.5 m), arranged in two rows with a central lane, where the horse is kept for much of its time stopped, getting out only for training and/or grazing in the paddock. It is therefore essential for the health of a horse that the litter in the box stall, on which the animal spends most of the day, is kept clean and in the best hygienic-sanitary conditions (Fig. 1). To reach this goal there are at least two different ways to manage the litter, which generally depend on the type of litter used:

- with daily aeration of the whole litter and continuous removal of urine and solid dejections;
- with permanence of a bottom layer of the litter (mixed urine) and daily removals of the superficial solid faeces.

Figure 1. Horse lying in the resting phase (left); detail of the horse's foot in contact with the litter (right).

The environmental factors that most influence the physical condition of the horse, and on which the study has focused, are detrimental gases, air humidity and litter moisture.

Air quality is a fundamental environmental condition not only for humans, but also for animals kept inside a barn. A significant accumulation of gases occurs inside the box stall, with some heavy (carbon dioxide, nitrous oxide and hydrogen sulphide) and other light (methane, carbon monoxide and ammonia), detrimental both for man and for animals.

To guarantee good conditions inside a barn the ventilation is really important. The quality of the air is influenced by the ventilation rate. Ventilation system is the most effective airborne particle clearance action (Woods et al., 1993; Curtis et al., 1996). For horse health it is necessary to have enough fresh air distributed to the areas inside the barn where horses are kept (Lundval, 2013). However, when the horses are kept in stall boxes in open paddocks this requirement is less impressive.

Usually in horse sport husbandry, the horses exercise outdoors usually for 1 to 2 h and, consequently, spend the major part of the day (often up to 23 h) indoors. Because of this, stable air quality is of considerable importance. Furthermore the respiratory disorders are common problems, and respiratory allergy is commonly diagnosed as a condition affecting the equine lung (Saastamoinen et al., 2015). When the condition becomes protracted it is referred to as chronic obstructive pulmonary disease (COPD) or heaves (or RAO, recurrent airway obstruction), an animal model of asthma. Some reports suggest that the condition is rare in climates where animals are outside all year around but is common in climates where horses are stabled indoors (Derksen, 1991). Clinical signs in horses with this chronic lung disease include poor athletic performance, chronic couching, purulent nasal discharge, and ultimately difficulties in breathing (Elfman et al., 2011).

People working in and visiting horse stables may also be exposed to the effects of the stable air. Causes of chronic airway disease both in horses and humans usually involve exposure to excessive concentrations of airborne dust, moulds, viruses, bacteria, spores, aeroallergens, and endotoxins which mostly originate from bedding and feed (Tanner, 1998). Furthermore, the inhalation of gaseous irritants such as ammonia may initiate airway obstruction and exacerbate or prolong the clinical signs of COPD in affected horses (Saastamoinen et al., 2015) as well as humans (Elfman et al., 2011).

The ammonia, resulting from the catabolism of nitrogenous substances, has 10 ppm as a limit recommended by the Scientific Committee of the CE Commission (for cattle and pigs, the reference for horses is missing). Ammonia derives from the biological degradation of nitrogenous organic substances: about 85% comes from the demolition of urea and uric acid contained in the urine, the remaining part comes from various compounds present in the faeces (Curtis et al., 1996). The factors that determine the atmospheric concentration of ammonia are mainly temperature, humidity, ventilation, animal load, flooring, debris removal systems and frequency of cleaning and washing (Kwiatkowska-Stenzel et al., 2016).

High concentrations of air humidity, besides favouring the onset of bacteria, parasites and moulds, cause respiratory problems for the horse and the man who must operate inside the stall. Unlike low levels of humidity when combined with high concentrations of dust cause cough and allergies. Optimal relative humidity values are between 50% and 75% and the maximum level of RH has not to exceed 80% in uninsulated stables (Lundval, 2013). An excessive moisture of the litter causes problems related to the hoof, such as the 'worm' (a fungus) and rotting (a bacterium) which, if neglected, become 'cancer' and irreparably compromise the horse. Otherwise a too dry litter tends to dry the nail which will lose elasticity and become more fragile.

Also the role of bedding material in recycling the nutrients of horse manure represents an important issue to take into account during the choice of a proper material. The manure should be efficiently recycled in agriculture avoiding any uncontrollable loss of its nutrients into the environment (Nikama et al., 2014). Keskinen et al. (2017) assessing the nutrient cycling properties of three bedding materials (peat, wood shavings and pelleted straw) in horse manure found that manure with pelleted straw bedding had superior composting characteristics, which favoured an increase of the nutrient concentrations and a decrease of the C:N ratios.

MATERIALS AND METHODS

During the trials the following bedding materials were tested: flax straw, hemp litter, rice husk, coconut litter, wood chips.

Flax straw is a completely vegetable product, very spread in Italy around ten years ago, absolutely free of dust and pests. The tested flax comes from organic farming in Flanders, an area between Belgium and France. A de-dusting system guarantees the absolute absence of any form of powders and substances that create allergies. Usually the flax straw is healthy and convenient, completely vegetable litter. Furthermore, the manure is removed perfectly compostable, thanks to the absolutely neutral pH value.

Hemp litter, obtained from the central and soft part of the hemp stalk, is completely biodegradable. It consists mainly of cellulose and lignin and is highly absorbent. The hemp stalk is also rich in silica, a chemical that in nature is found in sand or flints. It is well accepted by farmers and easy to store and distribute.

Rice husk has a brown/beige colour and a hard consistency, much more resistant than that of wheat. It is lightweight and voluminous and is virtually rot-proof and resistant to insects. It contains silica, has low absorption and is often dusty. It is cheap in areas suitable for rice cultivation and is not easy to dispose of.

Coconut litter is an extremely natural and ecological product, it has a very pleasant appearance (soft, homogeneous, easy to distribute). Due to its high absorption capacity, the litter is always very dry on the surface. It guarantees the total elimination of bad smells. It is characterized by total absence of dust and is not appetizing for the horse. It maintains optimal hygienic conditions and prevents the onset of serious diseases. The use of coconut allows you to reduce the amount of manure to be disposed of, which is still of excellent quality and acceptable for agronomic uses such as fertilizer simple or composted.

Wood chips have been the most used litter in Italy for the housing of horses until recently. Wood chips have a medium-high cost, are easy to store and process and produce an acid material that is not liked by farmers. There are different types of wood chips depending on the type of tree from which they are produced. The two large groups are: fir wood chips and wood chips of other species. In this study two kinds of wood chips were tested, one of only fir and one of beech and another fir.

Fir wood chips (wood chip A), produced exclusively with fir curls, free from toxic substances and impurities. They are de-dusted, dried and ventilated. The chemical-bacteriological analyses attest to the quality and certify the total absence of streptococci, colibacteria, tetanus, fungal moulds, etc. The fir fibre develops considerable hygroscopic values, has good resistance to foot traffic and high thermal insulating effects. It is the litter most used for keeping purebred horses.

Beech and fir wood chips (wood chip AF): contains only selected beech curl with the addition of a large fir leaf dried and de-dusted. Chemical analysis attest the absence of pesticides, fertilizers, aflatoxins, etc. It is a specific horse litter with high hygroscopic power and excellent resistance to wear. It guarantees a valid thermal coefficient and an excellent softness, reducing the moisture and the acute smell of urine.

Table 1 shows the costs of the tested litters, including transport, for the trials.

Table 1. The costs of the tested litter, including transport carried out in the province of Arezzo, site of the study

Litter	Bale size	Bale added/week	Cost/kg (€)
Hemp	7 kg – 80 L	2	0.64 + vat 10%
Flax straw	21 kg – 120 L	1	0.34 + vat 10%
Rice husk	20 kg – 200 L	1	0.18 + vat 10%
Coconut	15 kg – 250 L	1/3	0.80 + vat 4%
Wood chip A	23 kg – 145 L	1	-
Wood chip A/F	23 kg – 145 L	1	-

Instrumentation used and parameters detected

For the trials 5 box stalls (3 x 3 m) arranged in line, with in front a roof (3 m) and walls of 2 cm thick fir wood were used. The base is made in concrete with a central grid and 2% inclination. The roof is a sandwich panel, 2.70 m high at the ridge and 2.20 m in the eaves. The stalls between them are not communicating, not even in the upper part, in order to reduce the exchange of air between adjacent boxes. The horse boxes are all the same and in the same conditions. The air exchange is guaranteed by the upper part of the entrance door to the facility.

The horses examined are of the same body size. They all follow the same diet as type and quantity, with feeding of the food at scheduled times.

Several parameters were monitored during the whole trials. Among them, the parameters taken into account for the present study are the following: relative humidity of the air; moisture of the litter (surface and background layer); amount of ammonia in the air (ppm); quantity of waste; degree of fatigue and perception of smell by the operator; operating times for the daily cleaning of the box.

For the study, the following instrumentation was used: portable data-logger (DO9847 of Delta OHM) with probes for air temperature and humidity and contact temperature; moisture analyser (Rad Radwag Mac50) with heating at 160 °C; ammonia detector (Dräger X-am® 5000). A digital video recording system with five infrared CCTV cameras (Proeye Bullet AHD Multistandard 1.0 Mpixel) was installed with the only purpose to check the state of the horses inside the stalls during the trials.

The data were not collected to provide a statistical analysis most likely due to a limited number of samples and variability in used source materials.

The measured parameters were marked on specific tables. All measurements were taken regularly, in order to cover 2–3 days per week, in the morning before redoing the box stalls and following this method:

- the air temperature and humidity were obtained through measurements taken in five points of the stalls (vertices of a square 2 x 2 m and in the middle) and averaged;
- the measurement of the quantity of ammonia in the air, carried out with the Dräger meter, respectively at the top of a 2 x 2 m square and in the middle;
- the moisture survey was carried out by taking five small points (with the same pattern as in the previous surveys) with a small quantity of litter both from the bottom layer and from the surface layer, mixed separately, and brought to the Radwag analyser for the measurement of moisture.

In this research both of the box stalls management techniques were tested (daily airing of entire litter, layer permanently cross and daily manure removal of surface), for a period of about five weeks; the horses were kept in boxes and sent out to the paddock for 2–3 hours a day in order to simulate the most common horse keeping conditions.

Data on the practical use of the different litters were obtained thanks to the experience of an operator who has been working with horses and cleaning the boxes for years. A table was prepared on which the operator, at the end of the cleaning of the stall box, could express a value in units (U) related to the perception of odours (odours: 1 not detectable, 2 barely perceptible, 3 perceptible, 4 strongly perceptible), express a value in units (U) related to fatigue (fatigue: 1 little, 2 normal, 3 more than normal, 4 a lot), and sign the time employed (in minutes).

Before starting the trials an analysis of the moisture of the different types of litter was conducted (Table 2).

Table 2. Litter moisture in the respective bales (%)

Coconut	Flax Straw	Rice husk	Hemp	W.ch. A	W.ch. A/F
20.0	14.0	9.5	14.1	11.0	13.3

The trials began on 06/04/16 and the box stalls were filled with the quantities of bedding recommended and reported in each pack (Table 3). Subsequently the boxes were cleaned every day in the morning and, until 26/04/16, with the technique of turning the litter completely; from 26/04 regarding the litter of coconut, flax and hemp, leaving a layer at the bottom and removing only the solid superficial faeces (for the litter in wood chips, instead, it continued as usual). The trials of the rice husk, which started later, were carried out with the technique of 'surface removal'.

Table 3. Amounts of litter used for the beginning and for the renewal (number of bales)

Date	Coconut	Flax Straw	Rice husk	Hemp	Wood chips A	Wood chips A/F
06-04	7	4	4	11	3	3
13-04	1/3	1	1	2	1	1
20-04	2/3	1	1	2	1	1
27-04	-	1	1	2	1	1
04-05	1/3	1	1	1	1	1

RESULTS AND DISCUSSION

During the trials a significant amount of data was collected. In this study, the main results regard the analysis of litter moisture and air humidity parameters (Table 4) and ammonia concentration (Table 5). Results related to ergonomic aspects and to the costs of single litters are shown as well. The values concerning the production of manure, the level of smell, the time consumed for the daily work, and the level of fatigue, expressed by the operator during the cleaning and renewal of every single bedding, are summarized in Table 6.

The moisture is related to the depth of the litter, as shown in Table 4. With a relative humidity inside the stable more or less constant (minimum 70.7% and maximum 82.5%) and a total average RH of 77.61%, the lowest values of moisture were reached by beech and fir wood chips (wood chip AF), which presented little differences between moisture at surface and ground levels (26.32 and 29.85% respectively). Also hemp litter showed low values of moisture at surface level (26.00 %), but at the ground level the moisture value increased till 43,01% on average. The highest values were reached by fir wood chips (wood chip A) at surface level (50.21%) and by coconut litter at ground level (55.30%).

Table 4. Litter moisture values (%) at ground and surface level, and air relative humidity (%)

Date	Level	Coconut	Flax Straw	Rice husk	Hemp	W.ch. A	W.ch. A/F
12-04	Ground	51.6	35.8	-	41.8	42.7	29.5
	Surface	40.0	25.6	-	17.8	41.1	20.9
	Air	75.0	76.5	-	76.8	80.6	79.2
14-04	Ground	52.8	33.8	-	43.5	51.7	28.5
	Surface	42.6	27.6	-	18.6	46.8	20.8
	Air	74.8	70.7	-	74.0	71.0	73.8
17-04	Ground	53.6	50.6	-	45.8	54.3	29.7
	Surface	41.3	37.9	-	18.1	50.5	21.0
	Air	73.0	74.0	-	75.0	75.0	74.8
19-04	Ground	58.2	47.6	-	33.9	58.4	32.4
	Surface	44.5	38.7	-	28.8	51.9	31.6
	Air	76.5	75.0	-	77.0	71.8	73.9
23-04	Ground	56.5	43.0	-	45.6	55.1	28.0
	Surface	40.3	37.5	-	29.9	52.2	24.9
	Air	79.0	76.5	-	80.7	82.0	75.0
26-04	Ground	59.1	44.5	-	47.8	56.4	31.0
	Surface	43.2	38.4	-	31.1	52.8	28.2
	Air	77.8	78.4	-	78.7	79.4	76.4
30-04	Surface	56.0	40.1	29.4	31.9	56.2	29.8
	Air	79.0	79.8	80.9	80.6	80.5	76.0
04-05	Surface	53.7	43.7	38.6	33.3	-	34.3
	Air	82.3	80.8	82.1	80.4	-	81.9
06-05	Surface	50.9	48.6	38.5	24.3	-	25.4
	Air	82.5	81.0	80.2	82.0	-	79.8

The highest ammonia concentrations were recorded in flax and hemp litter, and then in the wood chip litter. The coconut litter is the one that recorded the lowest ammonia concentration values. In the first week it presented values of 1 ppm and subsequently higher, with a maximum of 5 ppm. The rice husk litter, even though it does not have great absorbent capacity, recorded very low values in the first week, probably due to the high amount of litter on the first implant (20–30 cm in height). From 26/04/16 the technique of maintaining the ground layer (hemp, flax, coconut and husk) was adopted and, as can be seen in the Table 5, the values lowered.

Generally, the litter ground layer, within one or two months, must be completely renewed. This operation must be carried out with extreme caution: the ammonia detected at the removal of the flax straw after a month of trials was almost 30 ppm.

Concerning the moisture of the litter, in particular concerning the surface layer, which can influence horse's hoof state, the lowest values were recorded in the fir-beech (AF), while the highest in the chip of only fir (A), in the coconut and in the flax. An explanation of this may be that the horse with wood chips (A) recorded an intense walking activity inside the stall box compared to the one with the fir-beech shavings (AF), spreading faeces and urine in all parts of the pen. High moisture values of the litter, i.e. over 50%, must be carefully evaluated, also according to the seasonal period, as they can be a predisposing index to the onset of diseases.

Table 5. Ammonia concentrations (ppm) measured in box stalls with different types of litter

Date	Coconut	Flax Straw	Rice husk	Hemp	Wch. A	Wch. A/F
06-04	Beginning of trials					
09-04	1	8		8	5	8
12-04	1	8		8	7	8
13-04	Added weekly litter					
14-04	3	7		7	3	7
17-04	1	8		5	2	3
19-04	5	6		5	6	5
20-04	Added weekly litter					
23-04	5	7		8	3	3
26-04	4	7		6	6	8
27-04	Added weekly litter					
30-04	3	4	2	6	2	2
04-05	2	6	1.5	6	3	3
04-05	Added weekly litter					
06-05	2	6	2	6	3	3

The hemp litter remained dry and smooth on the surface after just a week, providing an excellent comfort and an excellent filtering function: the urine is filtered by the hemp and ends up at the bottom of the stall box. It is therefore necessary to distribute a certain thickness of litter on the bottom so as to allow the surface to always remain perfectly dry. Daily litter care is also easy.

Flax straw recorded high values of surface moisture and high ammonia concentrations with the drying technique. The wood chips showed good absorption and in particular the fir wood chips (A) presented very high values of surface and background moisture, while the wood chips (AF) were the driest.

Horses never ingested the litter used in the trials, except in rare cases at the beginning of the rice husk and hemp plant.

From the point of view of the work for the man (saving time and fatigue), the technique of total litter aeration has appeared more expensive than the removal of only the surface layer, in particular in the litter of coconut given its height (20–30 cm). The rice husk appeared to be the lightest to be turned over and managed even if, to guarantee low ammonia values, a height of over 20 cm must always be achieved. The rice husk has the advantage of lower costs than other litters and a good availability especially in northern Italy. The coconut used at 20% moisture appears at first glance not convenient considering the high cost and the long preparation during planting and addition due to the necessary shattering of the clods. However, it has low ammonia values in the box and is favourable from the point of view of the work: low labour costs per day thanks to the fact that the care of the litter can be carried out once every two days.

Table 6. Values of manure, smell, time and fatigue expressed by the operator during the cleaning and renewal of every single litter

	Date								
	10-04	12-04	14-04	17-04	19-04	23-04	27-04	30-04	06-05
Manure Kg									
Coconut	5	6	7	4	7	5	5	7	6
Flax	8	8	8	6	6	7	6	6	6
Rice husk								4	5
Hemp	5	3	3	2	2	1	2	4	4
W.ch. A	4		4	1	5	4	4	5	
W.ch. AF	5	7	6	7	6	6	7	6	8
Time min									
Coconut	12	13	12	10	10	14	12	7	7
Flax	5	10	8	10	10	10	10	6	7
Rice husk								8	8
Hemp	5	6	7	8	8	10	8	9	7
W.ch. A	10		12	12	10	12	10	10	
W.ch. AF	10	10	10	10	10	10	10	10	10
Smell U									
Coconut	1	1	1	1	1	1	1	1	2
Flax	4	4	4	4	4	3	3	3	4
Rice husk								3	2
Hemp	3	3	2	2	2	2	2	2	3
W.ch. A	4		3	4	3	3	3	3	
W.ch. AF	3	4	3	2	3	3	3	2	2
Fatigue U									
Coconut	2	2	3	3	3	3	3	1	1
Flax	2	2	2	2	2	2	2	1	1
Rice husk								1	1
Hemp	2	2	2	2	2	2	2	1	1
W.ch. A	1		2	2	2	2	2	3	
W.ch. AF	1	2	2	2	2	2	3	2	2

CONCLUSIONS

The comparison of six different types of litter produced interesting results about the convenience or not to use one or the other litter from an environmental, as well as a commercial perspective.

The coconut litter recorded the lowest values of ammonia concentrations in all the phases of the experiments and, even if it presents high purchase prices, is favourable from the point of view of the work with low labour costs.

Beech and fir wood chips presented very good results in terms of litter moisture, also at ground level, showing to be an excellent product for bedding. Anyway, wood chips have medium-high cost and produce an acid material that is not liked by farmers.

The rice husk, although tested for a short period, showed to have some advantages, such as the acceptable ammonia and moisture values when used with a minimum height of 20 cm, besides the low cost and the good availability especially in northern Italy.

REFERENCES

Curtis, L., Raymond, S. & Clarke, A. 1996. Dust and ammonia in horse stalls with different ventilation rates and bedding. *International Journal of Aerobiology* **12**, 239–247.

Derksen, F.J. 1991. *Chronic Obstructive Pulmonary Disease. In Equine Respiratory Disorders*. Beech, J., Ed.; Lea & Febiger: Malvern, PA, USA, 223–235.

Elfman, L., Wålinder, R., Riihimäki, M. & Pringle, J. 2011. *Air quality in horse stables. In Chemistry, Emission Control, Radioactive Pollution and Indoor Air Quality*. Mazzeo, D., Ed.; Intech: Rijeka, Croatia, 655–680.

Keskinen, R., Saastamoinen, M., Nikama, J., Särkijärvi, S., Myllymäki, M., Salo, T. & Uusi-Kämppä, J. 2017. Recycling nutrients from horse manure: effects of bedding type and its compostability. *Agricultural and Food Science* **26**(2), 68–79.

Kwiatkowska-Stenzel, A., Sowinska, J. & Witkowska, D. 2016. The Effect of Different Bedding Materials Used in Stable on Horses Behavior. *J. Equine Vet. Sci.* **42**, 57–66.

Lundval, J. 2013. *Comparison of stable environment in prior approved and non-prior approved horse stables*. Swedish University of Agricultural Sciences. Student report n. 454, 56 pp.

Nikama, J., Keskinen, R., Närvänen, A., Uusi-Kämppä, J., Särkijärvi, S., Myllymäki, M. & Saastamoinen, M. 2014. The role of bedding material in recycling the nutrients of horse manure. In: *Proceedings Equi-meeting infrastructures horses and equestrian facilities*. Le Lion d´Angers, France, pp. 34–37.

Saastamoinen, M., Särkijärvi, S. & Hyyppä, S. 2015. Reducing respiratory health risks to horses and workers: A comparison of two stall bedding materials. *Animals* **5**, 965–977.

Tanner, M.K., Swinker, A.M., Beard, M.L., Cosma, G.N., Traub-Dargatz, J.L., Martinez, A.B. & Olenhock, S.A. 1998. Effect of phone book paper versus sawdust and straw bedding on the presence of airborne gram-negative bacteria, fungi and endotoxin in the horse stalls. *J. Equine Vet. Sci*. **18**, 457–461.

Woods, P.S., Robinson, N.E., Swanson, M.C., Reed, C.E., Broadstone, R.V. & Derksen, F.J. 1993. Airborne dust and aeroallergen concentration in a horse stable under two different management systems. *J. Equine Vet. Sci.* **25**, 208–213.

Agronomy Research **16**(3), 656–668, 2018
https://doi.org/10.15159/AR.18.113

Agricultural residues in Indonesia and Vietnam and their potential for direct combustion: with a focus on fruit processing and plantation crops

A. Brunerová[1,*], H. Roubík[2], M. Brožek[1] and J. Velebil[3]

[1]Czech University of Life Sciences Prague, Faculty of Engineering, Department of Material Science and Manufacturing Technology, Kamýcká 129, CZ165 00 Prague, Czech Republic
[2]Czech University of Life Sciences Prague, Faculty of Tropical AgriSciences, Department of Sustainable Technologies, Kamýcká 129, CZ165 00 Prague, Czech Republic
[3]Czech University of Life Sciences Prague, Faculty of Engineering, Department of Technological Equipment of Buildings, Kamýcká 129, CZ165 00 Prague, Czech Republic
[*]Correspondence: brunerova@tf.czu.cz

Abstract. Energy consumption in Indonesia and Vietnam has grown rapidly in recent decades. To meet the energy needs of both countries, a higher utilisation of waste biomass sources may represent an adequate solution. Investigated samples represent major crop residues (waste biomass) originating mainly from the agriculture sector of the selected countries. Herbaceous waste biomass from Indonesia is, namely, cassava stems and root peelings (*Manihot esculenta*), coffee leaves (*Coffea arabica*), cacao leaves (*Theobroma cacao*), banana leaves (*Musa acuminata*), bamboo leaves (*Bambusoideae* spp.) and aloe vera leaves (*Aloe vera*). Furthermore, fruit and aquatic waste biomass originating from Vietnam is, specifically, sugarcane bagasse (*Saccharum officinarum*), durian peelings (*Durio zibethinus*), rambutan peelings (*Nephelium lappaceum*), banana peelings (*Musa acuminata*), water milfoil (*Myriophyllum spicatum*) and water hyacinth (*Eichhornia crassipes*). All mentioned types of waste biomass were subjected to proximate and calorimetric analysis: moisture, ash and volatile matter contents (%) and higher and lower heating values (MJ kg^{-1}). Obtained values indicated the highest level of ash content in fruit biomass samples in the case of sugarcane bagasse (0.84%), in herbaceous biomass in the case of cassava stems (3.14%) and in aquatic biomass in the case of water hyacinth (14.16%). The highest levels of lower heating values were achieved by following samples (best samples from each biomass type): cassava stems (17.5 MJ kg^{-1}); banana peelings (17.3 MJ kg^{-1}) and water hyacinth (12.8 MJ kg^{-1}). The overall evaluation of all observed samples indicated that the best suitability for energy utilisation by direct combustion of investigated representatives is fruit waste biomass, followed by herbaceous waste biomass and then aquatic waste biomass.

Key words: renewable energy, waste management, biological residues, waste biomass, calorific value, energy potential.

INTRODUCTION

Energy is generally considered a crucial component for ensuring sustainable livelihood, and the world needs an enormous amount of energy to support future economic developments. A reliable energy supply is essential in all economies for heating, lighting, industrial equipment, transport etc. (IEA, 2014). However, almost one quarter of the world's population, most in developing countries, have basic energy needs that are not being adequately met (Mendu et al., 2012).

Therefore, there are efforts to increase the use of renewable energy resources in the developing world (Ahuja & Tatstani, 2009), especially from waste biomass (Brunerová et al., 2017b). Biomass energy is an important source of energy in most Asian countries (fuelwood, charcoal and other biomass energy such as agricultural residues), which is used by households and small-scale farms (Koopmans & Koppejan, 1998). One option of renewable energy resource utilisation is to extend the use of agricultural residues as potential energy sources because agricultural residual biomass can be used to produce energy (Li & Hu, 2003; Lozano & Lozano, 2018). As papers by Picchi et al. (2013), Obi et al. (2016), Romallosa & Kraft (2017) or Rezania et al. (2016) indicate, not only solid biofuels from wood waste biomass provide satisfactory energy potential, but also different waste biomass types (herbaceous, fruit, mixed) can represent a suitable source of renewable energy that can compete with fossil fuels. The current subsequent utilisation of waste biomass in developing countries occurs at a low level (Brunerová et al., 2017a).

It needs to be stated that knowledge about the current use of crop residues is very limited (Bentsen et al., 2014) as very few countries are collecting data on residue production and use (Bentsen et al., 2018).

Using biomass as an energy source is generally considered an option to mitigate greenhouse effects (Owusu & Asumadu–Sarkodie, 2016; Lozano & Lozano, 2018) and such biomass can be from agricultural residues. Crop residues represent more than half of the world's agricultural phytomass (Lozano & Lozano, 2018). That amount of residue is large and may have a significant energy potential (Nonheber, 2007). But it has to be mentioned that a significant amount of residue is also being used as livestock feed (Nonheber, 2007), and it should not be forgotten that a certain amount of residue is being left onsite to protect soil productivity (Bentsen et al., 2018). According to Scarlat et al. (2010), the amount left on site should usually be between 15% and 60% for most crops; however, the remaining amounts still leave potential for further processing and use.

Very little information is available on how the farmers themselves see their situation regarding the use of agricultural residues in developing countries (Koopmans & Koppejan, 1998; Winkler et al., 2018). However, the farmers' opinions will determine the adoption and increased use of agricultural residues on a farm scale level. Furthermore, as a study by Bilgili et al. (2017) shows, the use of agricultural residues can also be an efficient policy tool for sustainable development. In the issue of waste biomass (herbaceous or fruit) generation of an agricultural crop investigated in the present research, the area of their cultivation in target countries was monitored; detailed values are noted in Table 1.

Energy consumption in Indonesia and Vietnam has grown rapidly in recent decades. To meet the possibilities and needs of both countries, higher utilisation of waste biomass sources may represent an adequate solution. Therefore, this study covers the energy potential from various agricultural residues from major crops in Indonesia and Vietnam.

Table 1. Harvested areas of specific agriculture crop cultivation in 2016

Country	Plantation plant	Cultivated area, ha
Indonesia	Banana tree	139,964.0
	Cassava plants	867,495.0
	Cacao tree	1,701,351.0
	Coffee tree	1,228,512.0
	Sugar cane plants	472,693.0
Vietnam	Banana tree	120,041.0
	Cassava plants	579,898.0
	Coffee tree	597,597.0
	Sugar cane plants	256,322.0

ha – hectares (Source: FAO, 2018).

MATERIALS AND METHODS

All investigated materials were produced as agricultural residues, thus, they were characterised as a waste biomass (renewable source of energy) because of their biological origin and the nature of their origin. As a result, performed experimental methods were defined by technical standards related to the bio-briquette fuel production and its subsequent quality testing, namely, by the technical standards EN 14918 (2010), EN 15234–1 (2011), EN ISO 16559 (2014), EN 18134–2 (2015), EN ISO 17225–1 (2015), ISO 17225–7 (2014), EN ISO 18122 (2015), EN ISO 18123 (2016), whose requirements must be followed and achieved in biofuel commercial production. Each standard is described in the following text related to the biofuels' specific quality indicators, and their full names are noted in the References.

Materials and samples

Investigated waste biomass samples originated from Southeast Asia, namely, from the Socialist Republic of Vietnam and the Republic of Indonesia, as shown in Fig. 1. The specific areas of sample collection in each country are identified by red frames.

Figure 1. The areas of sample collection in the Republic of Indonesia and the Socialist Republic of Vietnam (Adopted from: Wikipedia Commons, CC BY-SA 3.0).

The official administrative division of sample collection target areas in each visited country is noted in detail in Table 2.

Table 2. Administrative division of target areas of sample collection

Country	Province	District	Capital city
Republic of Indonesia	Sumatera Utara	Toba Samosir	Balige
Socialist Republic of Vietnam	Thừa Thiên - Huế	Huế	Huế

Research activities in the Republic of Indonesia were done in the summer of 2016, and the investigated waste biomass samples were collected from July to September. Collection of investigated waste biomass samples in the Socialist Republic of Vietnam were done in January and May 2017. All chosen waste biomass samples were collected in rural areas of districts listed in Table 1, were properly processed directly after their collection and were preserved for subsequent experimental analysis in Prague, Czech Republic (see the subchapter 'Experimental measurements').

Table 3. Characteristic description of investigated waste biomass types

Name of plant species	Biomass type	Country of origin	Plant part
Bambusoideae spp.	Herbaceous	IDN	Leaves
Coffea arabica	Herbaceous	IDN	Leaves
Musa acuminata	Herbaceous	IDN	Leaves
Theobroma cacao	Herbaceous	IDN	Leaves
Aloe vera	Herbaceous	IDN	Leaves
Manihot esculenta[1]	Herbaceous	IDN, VN	Stem
Manihot esculenta[2]	Herbaceous	IDN	Root peel
Saccharum officinarum	Fruit	VN	Stem
Durio zibethinus	Fruit	VN	Peel
Nephelium lappaceum	Fruit	VN	Peel
Musa acuminata	Fruit	VN	Peel
Myriophyllum spicatum	Aquatic	VN	Stem, leaves
Eichhornia crassipes	Aquatic	VN	Stem, leaves

VN – Socialist Republic of Vietnam; IDN – Republic of Indonesia.

Different parts of bodies or fruits of the following plants were investigated: bamboo (*Bambusoideae* spp.), coffee tree (*Coffea arabica*), banana tree (*Musa acuminata*), cacao trees (*Theobroma cacao*), aloe vera (*Aloe vera*), cassava (*Manihot esculenta*), sugarcane (*Saccharum officinarum*), durian tree (*Durio zibethinus*), rambutan tree (*Nephelium lappaceum*), water hyacinth (*Eichhornia crassipes*) and aquatic weed (*Myriophyllum spicatum*). These plants were selected because they represent commonly cultivated agriculture crops in the target areas and their cultivation covers extensive areas, thus, a great amount of unutilised waste biomass originates from this cultivation. The characterisation of collected waste biomass samples is described in Table 3, the main focus of the present research was the production of waste biomass originating from plant cultivations at plantations and from processing plantations of crops or fruits. Moreover, the Socialist Republic of Vietnam has been struggling with water pollution issues for decades; entire populations of invasive aquatic plants are occupying water areas, which results in their removing, thus, production of great amount of aquatic waste biomass. Therefore, the aquatic waste biomass produced when cleaning polluted water areas was investigated, namely, water milfoil *Myriophyllum spicatum* and water hyacinth *Eichhornia crassipes*.

The collection of herbaceous waste biomass samples was performed in close proximity to the plantations, where the redundant and unwanted agriculture residues were mainly stored in the open field. Fruit waste biomass samples were collected near the processing plants or factories where the agriculture crop or fruits were processed. The location of these agriculture residues in practice is shown in Fig. 2.

Figure 2. Investigated agriculture residues left as waste without any subsequent utilisation: a) cassava stems (VN); b) banana tree residues (IDN); c) cacao tree residues (IDN); d) cassava root peels (IDN); e) durian peels (VN); f) sugar cane stems (VN).

Fig. 3 illustrates the reality of water pollution, which resulted in aquatic waste biomass production. Aquatic waste biomass samples were collected in the places they grow-directly from the water surface.

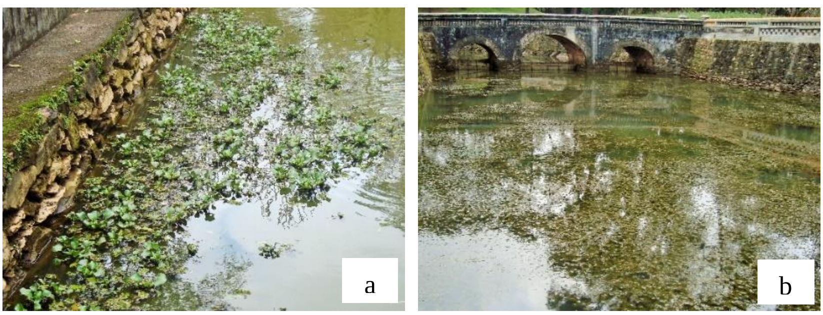

Figure 3. Water pollution results in the production of aquatic waste biomass of: a) water hyacinth (VN); b) aquatic weed (VN).

Experimental measurements

The aim of all experimental tests was to find the suitability of investigated waste biomass samples for direct combustion for energy utilisation. The following methods were chosen in an attempt to determine the samples' safety and efficiency during burning processes, with special emphasis on environmental conservation and competition with fossil fuels.

Initial sample preparation

Collected waste biomass samples were initially crushed and dried in a laboratory drier (at 105°C for 24 hours) in an attempt to stabilise their properties. Processed samples were stored in hermetically sealed laboratory vessels for transportation to the laboratory located in Prague (Czech Republic). The form of waste biomass samples after initial processing is shown in Fig. 4.

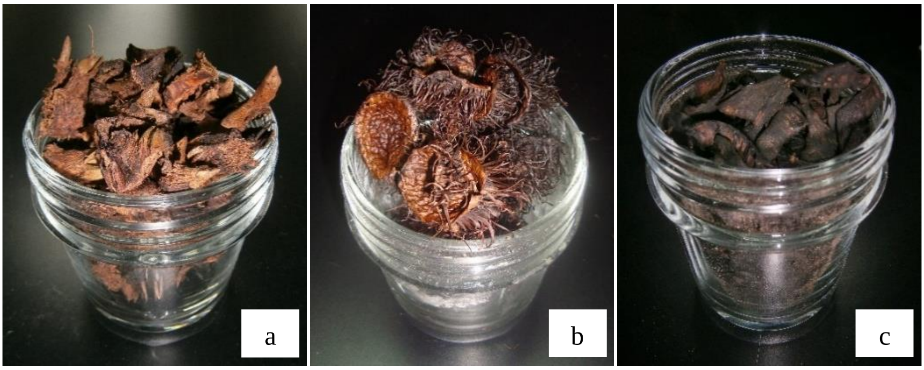

Figure 4. Investigated waste biomass samples prepared for preservation within their transport: a) durian fruit peels; b) rambutan fruit peels; c) banana fruit peels.

Fuel analysis

Proximate analyses and calorimetric measurements were performed in laboratories in Prague, Czech Republic. A set of chosen tests described the basic fuel properties of samples in the statement of their suitability for direct combustion purposes. Primarily, all samples were milled by a cutting mill into a particle size suitable for subsequent testing, i.e. particle size < 0.1 mm. The speed of the equipment was set to 20,000 rpm·min^{-1}. Subsequently, moisture content M_c (%), ash content A_c (%), volatile matter content VM_c (%) and higher heating value HHV (MJ kg^{-1}) of the samples were measured; while lower heating value LHV (MJ kg^{-1}) was estimated. Within each specific test in the case of all tested samples, several measurements were performed; prevalently, two or three suitable measurements and supporting software were used for the statement of final values.

The methodology of measurements of moisture content M_c (%), ash content A_c (%) and volatile matter content VM_c (%) was performed in respect to the ordinance of technical standards EN ISO 18122 (2015), ISO 18134–2 (2017) and EN ISO 18123, (2015). In the first step, a tested sample was dried at 107 °C until constant weight was reached to measure moisture content M_c (%). Subsequently, the dried samples were subjected to the ash content A_c (%) determination. The samples were burned in the presence of oxygen at 550 °C until their weights were constant, which indicated the end of the test. Both of the described tests were performed using a laboratory oven and laboratory thermogravimetric analyser.

The evaluation of energy potential of investigated waste biomass samples, and thus their suitability as an efficient biofuel, was expressed by determining their higher heating value HHV (MJ kg^{-1}). This indicator was determined by an isoperibol calorimeter, and the whole methodology of measurement was conducted according to the technical standard EN ISO 18125 (2017). Before testing itself, milled samples were densified into small pellets of 0.7 g weight. Subsequently, the pellets were burned, and obtained result values were sorted and analysed by the analyser's software. An estimate of lower heating value LHV (MJ kg^{-1}) was calculated from the higher heating value by the same technical standard, assuming hydrogen content at 6% wt. and combined oxygen and nitrogen content at 43% wt. in dry ash free state in all samples. These values were chosen as typical for many types of biomass.

RESULTS AND DISCUSSION

The obtained results of the experimental measurements performed in the present study primarily described the suitability of investigated waste biomass samples for direct combustion for energy generation purposes. Such information was combined with the statistical data of production (harvested areas and production quantity) of several investigated crops, which can indicate the amount of their produced waste biomass. By combining these factors (chemical analysis combined with the theoretical amount of produced waste biomass), the overall monitoring of such waste biomass potential within the energy generation was evaluated.

Materials and samples

Data published by statistical databases of Food and Agriculture Organization of the United Nations (FAO) provided information about agriculture production in specific countries, inter alia, in the Socialist Republic of Vietnam and the Republic of Indonesia (noted also in Table 1). As mentioned in the Introduction, due to the extensive areas of specific crop plantations, the greatest theoretical potential for waste biomass generation can be estimated for the plantation of cacao trees and coffee trees, followed by plantations of cassava plants. Because of the diversity of investigated waste biomass samples, the theoretical production quantity of specific fruits was monitored (expressed in Table 4) in the fruit waste biomass production.

Table 4. Production quantity of specific agriculture crop in 2016

Country	Crop	Production quantity, t
Indonesia	Bananas	7,007,125.0
	Cassava	20,744,674.0
	Cacao (beans)	656,817.0
	Coffee (green beans)	639,305.0
	Sugar cane stem	27,158,830.0
Vietnam	Bananas	1,941,935.0
	Cassava root	11,045,184.0
	Coffee (green beans)	1,460,800.0
	Sugar cane stem	16,313,145.0

t – tonnes (Source: FAO, 2018).

Data noted in Table 4 can also help upgrade the knowledge about the production of fruit waste biomass, which can also be a renewable source for energy generation. The ratio (expressed in percentage of the whole fruit mass) of the used part of fruit and the unused fruit waste biomass of specific exotic fruits was published in the research of Brunerová et al. (2017b). This research proved an extremely high ratio of fruit waste biomass in fruit like cacaos, bananas or coffee fruits. Using data published in the mentioned study (amount of waste biomass from specific fruit types in g and %), the following theoretical production of specific fruit waste biomass (t) was calculated; see Table 5.

Table 5. Estimated potential of specific fruit waste biomass production

Country	Fruit	Mass from one fruit sample, g	Mass proportion of fruit waste biomass*, %	Theoretical production of fruit waste biomass, t
Indonesia	Banana	23.8 ± 6.1	39.4 ± 8.8	2,760,807.3
	Cacao	523.7 ± 176.7	83.8 ± 8.9	550,412.6
	Coffee	0.7 ± 0.1	43.4 ± 9.9	277,458.4
Vietnam	Banana	23.80 ± 6.05	39.4 ± 8.8	765,122.4
	Coffee	0.7 ± 0.1	43.4 ± 9.9	633,987.2

*proportion of fruit waste biomass mass of total fruit sample mass in percentage; ± – standard deviation (Source: Brunerová et al., 2017b).

Experimental measurements

The chemical analysis and related experimental measurements were performed for all investigated waste biomass samples equally. Unfortunately, several samples occurred in a form unsuitable to perform experimental measurements (too heterogeneous), thus, all defined tests in the case of several samples were unable to be performed. Nevertheless, the obtained result values of successfully tested waste biomass samples are expressed in Table 6.

Table 6. Chemical parameters of investigated agriculture waste biomass kinds (in w.b.)

Biomass sample	M_c, %	A_c, %	VM_c, %	HHV, MJ kg^{-1}	LHV, MJ kg^{-1}
Bambusoideae spp.	7.38	12.50	81.79	16.71	15.5
Coffea arabica	9.33	9.42	<u>88.37</u>	17.82	16.5
Musa acuminata	4.56	9.16	<u>88.41</u>	17.18	15.9
Theobroma cacao	8.73	<u>13.50</u>	84.23	16.34	15.1
Aloe vera	4.01	<u>13.53</u>	85.82	16.90	15.7
Manihot esculenta[1] (IDN)	6.31	**3.14**	–	**18.55**	**17.2**
Manihot esculenta[1](VN)	5.93	**2.75**	–	**18.81**	**17.5**
Manihot esculenta[2]	1.52	<u>32.15</u>	**59.15**	12.68	11.8
Saccharum officinarum	7.00	**0.84**	–	17.84	16.5
Durio zibethinus	8.53	5.13	–	16.61	15.3
Nephelium lappaceum	7.55	**3.21**	–	17.03	15.7
Musa acuminata	8.27	12.02	–	**18.56**	**17.3**
Myriophyllum spicatum	5.18	<u>53.31</u>	**42.48**	<u>8.63</u>	<u>7.9</u>
Eichhornia crassipes	7.48	<u>14.16</u>	81.59	<u>13.97</u>	<u>12.8</u>

[1] – stem; [2] – root peel; VN – Socialist Republic of Vietnam; IDN – Republic of Indonesia; M_c – moisture content; A_c – ash content; VM_c – volatile matter content; HHV – higher heating value; LHV – estimated lower heating value; w.b. – wet basis.

Outstanding values, both good and bad, are highlighted in Table 5, bold font indicates good results, while underlined values indicate bad results. The result values of moisture content M_c (%) noted in Table 6 represented the moisture content of the samples processed and prepared for experimental testing. The initial moisture content of investigated samples was not measured because of the limited local conditions during sample collection and transportation. As other research papers indicate, the moisture content of aquatic waste biomass ranges between 85.3%–89.6%, while fruit waste biomass ranges between 63.4%–84.5% (Brunerová et al., 2017b; 2017c).

Waste biomass from aquatic weed (*Myriophyllum spicatum*) resulted in extremely high ash content A_c, which is unwanted. In addition, the ash content of cassava root peels (*Manihot esculenta*) was also very high. In both cases, such results could be caused by admixtures, which is highly arguable in the case of cassava root peels. Those are removed from the root with a certain amount of earth impurities. Focusing on energy potential, the cassava stems (*Manihot esculenta*) from both target countries of origin exhibited a high level of quality indicators, as did the banana peels. Very low values of high heating value were achieved by the aquatic waste biomass (both samples, *Myriophyllum spicatum, Eichhornia crassipes*) and cassava root peel (*Manihot esculenta*). Here, the relation between ash content and high heating value is apparent. The energy potential is lower in the case of samples that exhibited high ash content.

The high energy potential of such agriculture residues (fruit waste biomass) intended for combustion processes was also proved in the research of Brunerová et al. (2017b); namely, it found lower heating values LHV ($MJ \cdot kg^{-1}$) in the dry basis (d.b.) of fruit waste biomass originating from the processing of: banana – 17.79 MJ kg^{-1}, cacao – 16.73 MJ kg^{-1} and coffee – 17.37 MJ kg^{-1}.

Table 7. Calorific value of investigated agriculture waste materials in dry ash free state (d.a.f.)

Biomass sample	HHV, MJ kg^{-1}	LHV, MJ kg^{-1}
Bambusoideae spp.	20.62	19.3
Coffea arabica	21.70	20.4
Musa acuminata	19.82	18.5
Theobroma cacao	20.70	19.4
Aloe vera	20.36	19.1
Manihot esculenta[1] (IDN)	20.49	19.2
Manihot esculenta[1](VN)	20.60	19.3
Manihot esculenta[2]	18.98	17.7
Saccharum officinarum	19.36	18.1
Durio zibethinus	19.24	17.9
Nephelium lappaceum	19.09	17.8
Musa acuminata	23.29	22.0
Myriophyllum spicatum	19.49	18.2
Eichhornia crassipes	17.59	16.3

[1] – stem; [2] – root peel; VN – Socialist Republic of Vietnam; IDN – Republic of Indonesia; HHV – higher heating value; LHV – estimated lower heating value; d.a.f. – dry ash free state.

In respect to the fact that heating value is one of the most important indicators of fuel energy potential, the conversion to a dry ash free state was performed. The result values noted in Table 7 express the exact values of such indicators without the presence of ash, which should be influenced by the contamination of samples, thus, they can sometimes be misleading. The waste biomass samples were collected in the original form to reflect the waste management reality, thus, the contamination of samples was not removed.

Within the overall evaluation of specific biomass types (herbaceous, fruit and aquatic), the average values from all investigated samples were calculated and used to create charts in Figs 5, 6 and 7.

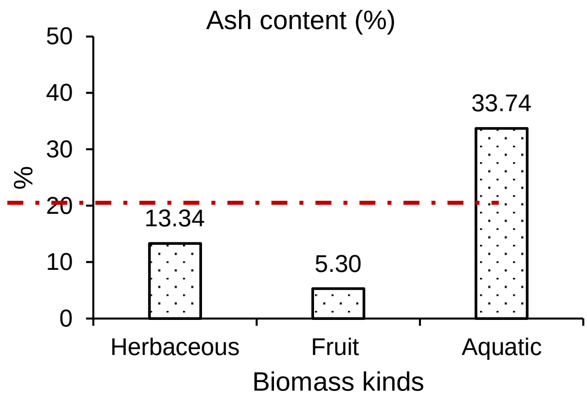

Figure 5. Comparison of ash content of specific investigated biomass types.

Based on the requirements of technical standard ISO 17225–7 (2014), the allowed level of ash content A_c (%) in the case of commercially produced bio–briquette fuel should be lower than 10%. This level is expressed by the dashed line in Fig. 5.

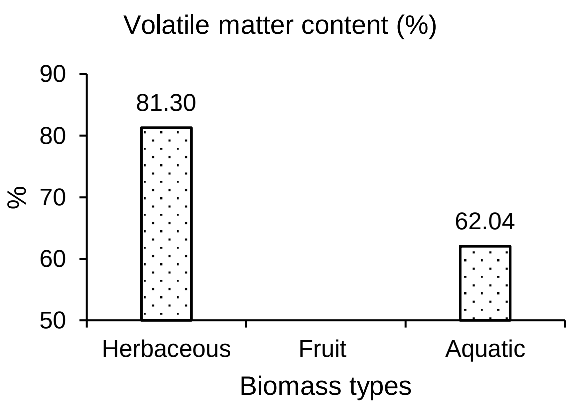

Figure 6. Comparison of volatile matter content of specific investigated biomass types.

The results of aquatic biomass volatile matter content VM_c (%) were not obtained due to the problematic behaviour of samples during testing. The acceptable level of volatile matter content in bio–briquette samples is not strictly stated, but it should be approximately 80%. In the case of wood biomass, the results will always be higher than

80%, but these results do not indicate bad properties of the fuel; they indicate that fuel will burn differently than, for example, coal (EN ISO 18123, 2015).

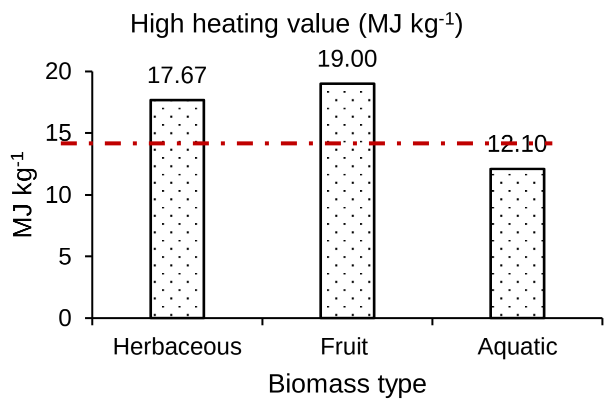

Figure 7. Comparison of higher heating values of specific investigated biomass types.

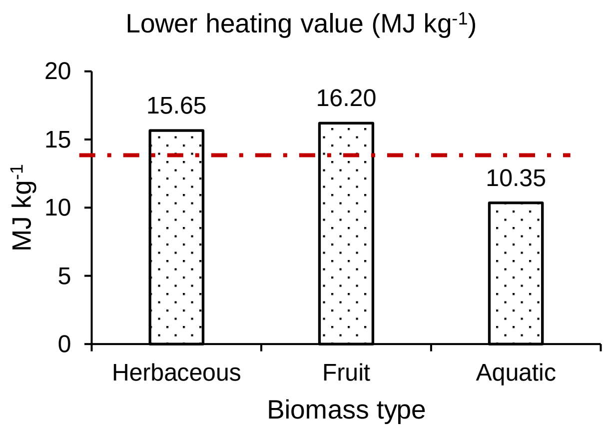

Figure 8. Comparison of lower heating values of specific investigated biomass types.

The required level of lower heating value LHV (MJ kg^{-1}) is expressed in Fig. 8 by the dashed line, thus, LHV > 14.5 MJ kg^{-1} (ISO 17225-7, 2014). This clearly shows which biomass types fulfilled the required levels and which were not suitable for investigation purposes. In both cases, the aquatic biomass samples exhibited unsatisfactory results, thus, proved their inappropriateness for energy utilisation by direct combustion.

CONCLUSIONS

As considerable quantities of agricultural residues remain unused in the developing world, there is potential to use energy from those waste sources. However, the current utilisation of waste biomass in developing countries occurs at a low level. Experimental analysis of fuel parameters of investigated waste biomass samples proved suitability of herbaceous and fruit waste biomass for energy utilisation by direct combustion, while values of aquatic waste biomass showed very low fuel quality indicators. These results could, in practice, cause low energy efficiency of biofuel or could be detrimental to the environment. In the future, having a database system on residue generation and utilisation at a national level could be beneficial; however, there is a need to be cautious and not to lose sight of the implications of social aspects, such as using agricultural residues as domestic fuel. In addition, future studies should focus on the possible effects of an increased use of residues at the farm level, for example, on soil conservation and degradation, income generation, effects on the environment and local communities.

ACKNOWLEDGEMENTS. The research was supported by Internal Grant Agency of the Faculty of Engineering, Czech University of Life Sciences Prague, 2018 grant: 'Energetické využití zemědělských residuí (odpadní biomasy) pomocí procesu densifikace (produkce bio–briket) v domácích i komerčních podmínkách'. and by the Internal Grant Agency of the Czech University of Life Sciences Prague, grant number 20173005 (31140/1313/3108).

REFERENCES

Ahuja, A. & Tatsutani, M. 2009. Sustainable energy for developing countries. *S.A.P.I.E.N.S.* **2**(1), 1–16.

Bentsen, N.S., Felby, C. & Thorsen, B.J. 2014. Agricultural residue production and potentials for energy and materials services. *Progress in Energy and Combustion Science* **40**(0), 59–73.

Bentsen, N.S., Nilsson, D. & Larsen, S. 2018. Agricultural residues for energy - A case study on the influence of resource availability, economy and policy on the use of straw for energy in Denmark and Sweden. *Biomass and Bioenergy* **108**, 278–288.

Bilgili, F., Kocak, E., Bulut, U. & Kuskaya, S. 2017. Can biomass energy be an efficient policy tool for sustainable development? *Renewable and Sustainable Energy Reviews* **71**, 830–845.

Brunerová, A., Malaťák, J., Müller, M., Valášek, P. & Roubík, H. 2017a. Tropical waste biomass potential for solid biofuels production. *Agronomy Research* **15**(2), 359–368.

Brunerová, A., Roubík, H., Brožek, M., Herák, D., Šleger, V. & Mazancová, J. 2017b. Potential of Tropical Fruit Waste Biomass for Production of Bio-Briquette Fuel: Using Indonesia as an Example. *Energies* **10**(12), 2119. doi:10.3390/en10122119

Brunerová, A., Roubík, H. & Herák, D. 2017c. Suitability of aquatic biomass from Lake Toba for energy generation by combustion process. 2017. In: *1st Nommensen International Conference on Technology and Engineering*. Medan, Indonesia, pp. 1–8.EN 14918 (2010): Solid biofuels – Determination of calorific value; ISO: Geneva, Switzerland, 2017.

EN 15234–1 (2011): Solid biofuels – Fuel quality assurance – Part 1: General requirements; ISO: Geneva, Switzerland, 2017.

EN 18134–2 (2015): Solid biofuels – Determination of moisture content – Oven dry method – Part 2: Total moisture – Simplified method; ISO: Geneva, Switzerland, 2017.

EN ISO 16559 (2014): Solid biofuels – Terminology, definitions and descriptions; ISO: Geneva, Switzerland, 2017.

EN ISO 17225–1 (2015): Solid biofuels – Fuel specifications and classes – Part 1: General requirements; ISO: Geneva, Switzerland, 2017.

EN ISO 18122 (2015): Solid biofuels – Determination of ash content; ISO: Geneva, Switzerland, 2017.

EN ISO 18123 (2015): Solid biofuels – Determination of the content of volatile matter; ISO: Geneva, Switzerland, 2017.

International Energy Agency, 2014. World Energy Outlook Special Report. Retrieved August 17, 2015, from http://www.iea.org/publications/freepublications/publication/WEO2014_AfricaEnergyOutlook.pdf

ISO 17225–7 (2014): Solid biofuels – Fuel specifications and classes – Part 7: Graded non-woody briquettes, ISO: Geneva, Switzerland, 2017.

ISO 1928 (2010): Solid mineral fuels – Determination of gross calorific value by the bomb calorimetric method, and calculation of net calorific value; ISO: Geneva, Switzerland, 2017.

Koopmans, A. & Koppejan, J. 1998. Agricultural and forest residues – generation, utilization and availability. In: Paper presented at the regional consultation on modern applications of biomass energy, 6–10 January 1997, Kuala Lumpur, Malaysia. Available at: http://www.fao.org/docrep/006/AD576E/ad576e00.pdf

Li, J.F. & Hu, R.Q. 2003. Sustainable Biomass Production for Energy in China. *Biomass and Bioenergy* **25**, 483–499.

Lozano, F.J. & Lozano, R. 2018. Assessing the potential sustainability benefits of agricultural residues: Biomass conversion to syngas for energy generation or to chemicals production. *Journal of Cleaner Production* **172**(20), 1462–4169.

Mendu, V., Shearin, T., Campbell, J.E., Stork, J., Jae, J., Crocker, M., Huber, G. & DeBolt, S. 2012. Global bioenergy potential from high-lignin agricultural residue. *Proceedings of the National Academy of Sciences* **109**(10), 4014–4019.

Nonhebel, S. 2007. Energy from agricultural residues and consequences for land requirements for food production. *Agricultural Systems* **94**, 586–592.

Obi, O.F. & Okongwu, K.C.H. 2016. Characterization of fuel briquettes made from a blend of rice husk and palm oil mill sludge. *Biomass Conversion and Biorefinery* **6**, 449–456.

Owusu, P.A. & Asumadu-Sarkodie, S. 2016. A review of renewable energy sources, sustainability issues and climate change mitigation. *Cogent Engineering* **3**(1), 1167990.

Picchi, G., Silvestri, S. & Cristoforetti, A. 2013. Vineyard residues as a fuel for domestic boilers in Trento Province (Italy): Comparison to wood chips and means of polluting emissions control. *FUEL* **113**, pp. 43–49.

Rezania, S., Din, M.F., Kamaruddin, S.F., Taib, S.M., Singh, L., Yong, E.L., Dahalan, F.A. 2016. Evaluation of water hyacinth (Eichhornia crassipes) as a potential raw material source for briquette production. *Energy* **111**, 768–773.

Romallosa, A.R.D. & Kraft, E. 2017. Feasibility of Biomass Briquette Production from Municipal Waste Streams by Integrating the Informal Sector in the Philippines. *Resources* **6**(1), doi:10.3390/resources6010012

Scarlat, N., Martinov, M. & Dallemand, J.F. 2010. Assessment of the availability of agricultural crop residues in the European Union: potential and limitations for bioenergy use. *Waste Management* **30**(10), 1889–1897.

Winkler, B., Lewandowski, I., Voss, A. & Lemke, S. 2018. Transition towards Renewable Energy Production? Potential in Smallholder Agricultural Systems in West Bengal, India. *Sustainability* **10**(3), doi:10.3390/su10030801.

Agronomy Research **16**(3), 669–678, 2018
https://doi.org/10.15159/AR.18.127

Air flow conditions in workspace of mulcher

J. Čedík[1,*], J. Chyba[2], M. Pexa[1], S. Petrásek[2], J. Jedelský[3] and M. Malý[3]

[1]Czech University of Life Sciences, Faculty of Engineering, Department for Quality and Dependability of Machines, Kamýcká 129, CZ16521 Prague 6, Czech Republic
[2]Czech University of Life Sciences, Faculty of Engineering, Department of Agricultural Machines, Kamýcká 129, CZ16521 Prague 6, Czech Republic
[3]Brno University of Technology, Faculty of Mechanical Engineering Department of Thermodynamics and Environmental Engineering, Technická 2896/2, CZ616 69 Brno, Czech Republic
[*]Correspondence: cedikj@tf.czu.cz

Abstract. Currently, there has been a great effort on increasing the efficiency of agricultural machinery. The energy demands of mulching with the vertical axis of rotation depends on the amount of processed material per unit of time, its properties and efficiency of material processing. Another important factor that is affecting the overall energy demands is the energy losses, which can be even higher than energy, required for the processing of material. The efficiency of the material processing and the energy losses are influenced to a large extent by the air flow inside the mulcher workspace, which is created by the movement of working tools. The air flow ensures the repeated contact of the processed material with the working tools, affects the energy losses and the quality of work. The contribution deals with the air flow conditions inside the workspace of mulcher with the vertical axis of rotation. The velocity of the air flow was measured my means of LDA (Laser Doppler Anemometry) method in three planes above the surface (180, 100 and 20 mm) and in two directions (peripheral and radial). The laboratory model of one mulcher rotor from mulcher MZ 6000 made by BEDNAR Ltd. company was used for the measurement. From the results it is evident that the maximum values of peripheral velocity of the air flow reach approx. 50% of the velocity of the tools. In the radial plane an air vortex is created between 20 and 100 mm planes above the surface around the tip of the blade.

Key words: mulcher, airflow velocity, cutting tool, mower.

INTRODUCTION

In present time there is a great pressure on manufacturers of agriculture machinery in terms of decreasing the energy demands and increasing the work efficiency. Mulching is energy demanding operation which has many utilizations. Mulchers can be used for treatment of permanent grasslands, fallow lands or crop residues on arable land. During mulching the plants are crushed and left on the soil surface. The principle of mulching is to enable easy and quick decomposition of plants or plant residues (Mayer & Vlášková, 2007; Syrový et al., 2013)

Mulchers with vertical or horizontal axis of rotation are in principle rotational mowers. Other authors found that common rotational mowers have the energy demands between 3.5–16 kW m^{-1} (kW per meter of working width of the machine) (McRandal & McNulty, 1978; Tuck et al., 1991; Srivastava et al., 2006; Syrový et al., 2008; ASABE D497.7, 2011). Mulchers with horizontal or vertical axis of rotation have typically higher energy demands than common rotational mowers since the mulchers are used to crush and disperse the plants on the surface. In previous studies, it was found that the energy demands of the mulcher with vertical axis of rotation highly depend on the amount of processed material (mass performance) and may have value up to 22.6 kW m^{-1} (Čedík et al., 2015; Kumhála et al., 2016; Čedík et al., 2017c).

The mulchers have higher energy losses than common rotational mowers, which mainly causes the higher energy demands. In the workspace of the mulcher with the vertical axis of rotation the so-called ventilation effect is created as a result of movement of cutting tools. The ventilation effect is vital for proper function of mulcher with vertical axis of rotation. Total energy losses may be greater than the energy used for cutting plant material (O'Dogherty & Gale, 1991; Čedík et al., 2016b; Kumhála et al., 2016).

The other authors (Persson, 1987; O'Dogherty & Gale, 1991) identified the following energy losses of the mower machine:

- Acceleration of the material to the output speed
- Friction forces between the material and the cover of the mower mechanism
- Friction forces between the blade and the stubble/soil
- Air movement in the cut area
- Mechanical friction forces of the drive mechanism.

The energy demands and quality of work of mulcher highly depends on the air movement inside the workspace of mulcher (ventilation effect) (Chon et al., 1999a; 1999 b). The energy demands are influenced by aerodynamic resistance of the working tools, which depends on relative speed and direction of the air flow and working tools inside the workspace. From the viewpoint of work quality, the air movement inside the workspace is essential for repeated contact of the cut plant matter with blades of cutting tools and ensures the uniform dispersion of chopped plant matter on the surface. (Čedík et al., 2016a; 2016b).

Direction and speed of the air flow are influenced by the cutting speed, the shape of working tools and the shape of workspace cover (Hagen et al., 2002; Zu et al., 2011; Hosseini & Shamsi, 2012; Kakahy et al., 2014; Čedík et al., 2017a; Čedík et al., 2017b). Hagen et al. (2002) reported that the shape of workspace cover has equal significance as the shape of cutting tool as regards to air flow.

The rotational mower has the cutting speed commonly in the range of 71–84 m s^{-1} (O'Dogherty, 1982; Jun et al., 2006). According to Srivastava et al. (2006), the cutting speed of rotational mower should be in the range of 50–75 m s^{-1} in dependence on the sharpness of the cutting tool.

Other authors (Chon & Amano, 2003; Chon & Amano, 2004; Chon & Amano, 2005) measured the air flow velocity inside the workspace of municipal mowers in tangential and axial direction. They found that in the tangential direction the air flow velocity increases with the distance from rotor centre. Near the side cover the tangential velocity slightly decreases due to wall friction. In axial direction the air flow velocity peaks at the tip of the blade near the circumference of the rotor.

This paper aims to experimentally determine the velocity of air flow inside the workspace of the mulcher with the vertical axis of rotation at different rotation speeds.

MATERIALS AND METHODS

The measurement took place at the Department of Agricultural Machines at Czech University of Life Sciences Prague. In order to determine the velocity of the airflow inside the workspace of the mulcher, a laboratory model of a single mulcher rotor was used. The working mechanism of three-rotor mulcher MZ 6000 produced by the BEDNAR FMT, Ltd. company was used as a base for the laboratory model. The Mulcher MZ 6000 has a working width of 6 m and rotor speed of 1,000 rpm. The diameter of the rotor of the laboratory model is 2 m and an 22 kW asynchronous electromotor MEZ was used to drive the model. The speed of the electromotor was controlled by a frequency converter. The laboratory model of the mulcher rotor is shown in Fig. 1.

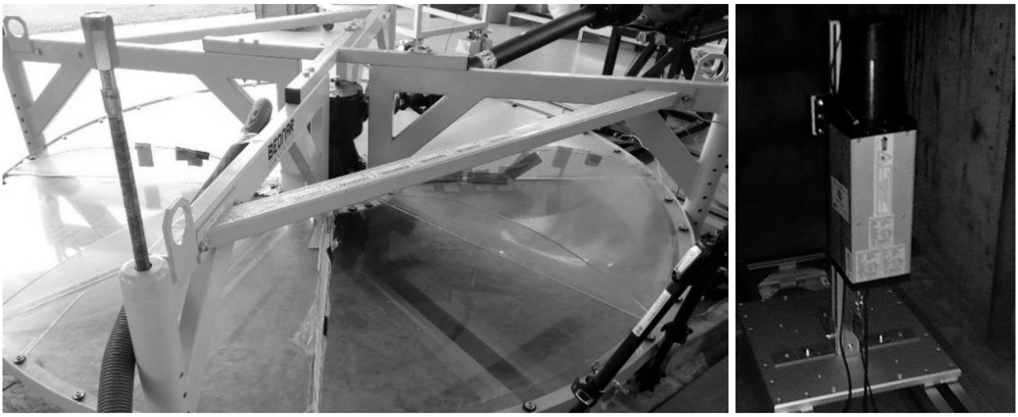

Figure 1. Laboratory model of one mulcher rotor (left) and the FlowExplorer Mini LDA measuring device in the assembly pit (right).

The working tools with the rake angle of 0° and the trailing edge angle of 35° was used for the measurement. The angles on the working tool are schematically illustrated in Fig. 2. The cutting tool and influence of its shape on energy demands during operation are described in (Čedík et al., 2017c), the influence of cutting tool shape on air resistance is described in (Čedík et al., 2016b).

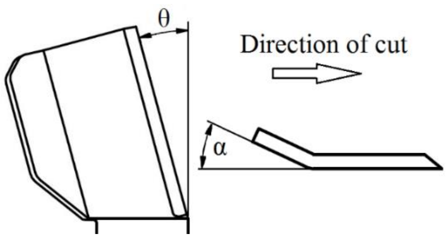

Figure 2. Schematically illustrated angles on the cutting tool (θ – rake angle; α – trailing edge angle).

During the measurement the velocity of the air flow inside the workspace of mulcher, the rotation speed of the rotor and ambient conditions, such as air pressure and temperature were measured.

The velocity of air flow inside the workspace was measured by means of LDA (Laser Doppler Anemometry) method. The FlowExplorer Mini LDA (Fig. 1) made by Dantec Dynamics A/S was used for the measurement (calibration coefficient uncertainty lower than 0.1%). The LDA was configured in the backscatter mode. A built-in, diode-pumped solid-state laser generated beams with 660 and 785 nm wavelength. The beams were split into two pairs of parallel beams with the power of 30 mW each. One beam in each pair was shifted by 80 MHz. A converging transmitting/receiving lens with 300 mm focal length was used to form an ellipsoidal measurement volume with the size of app. $0.1 \times 0.1 \times 1$ mm. Dantec BSA P80 signal processor was used to process the measured signal. BSA flow software v5.20 was used to control the data acquisition and the following setting was used: Photomultiplier sensitivity 1,050 V, signal gain 20 dB. The measurement was limited to 20,000 samples acquired or a 10-second acquisition duration at each measured point. The LDA device measures the velocity of particles traversing the measured volume, but not the air molecules, so seeding the flow field must be performed, for that purpose the oil fog generator was used.

The measuring LDA device was placed under the laboratory model in the assembly pit. Two directions of the air flow were measured, peripheral and radial. The measurement was performed in three heights above the surface, 20 mm (under the working tool), 100 mm (approx. at the level of the working tool) and 180 mm (above the working tool). Because of the limitations of the measurement device the air flow velocity was measured between 440 mm and 980 mm from the centre of the rotor. The step between individual measurement points in the radial direction was 20 mm.

The measurement was performed at rotation speeds of 400, 500 and 600 rpm, which corresponds to cutting speeds of approx. 41.9, 52.4 and 62.8 ms^{-1}. Higher rotation speeds were problematic in terms of data validation. The speed of the rotor of the model of mulcher was measured by means of optical sensor with one pulse per revolution since the measurement was carried out in stable rotation speeds. The data from the optical sensor was stored at the hard drive of measuring computer via a module for impulse sensors Papouch Quido 10/1.

RESULTS AND DISCUSSION

Peripheral air flow velocity

In Fig. 3 the peripheral air flow velocity in the height of 20 mm above the surface in dependence on the distance from the centre of the rotor is shown. It can be seen that under the working tools the peripheral velocity increases almost linearly with the distance from the centre. At all measured rotation speeds the maximum values of peripheral air flow velocity are reached at the 980 mm from the centre of the rotor at the tip of the blade. This result is in good agreement with results of Chon & Amano (2003) who also found the maximum values of tangential air flow velocity near the circumference of the rotor. Compared with the velocity of the tip of the working tool (cutting speed) (41.89 ms^{-1}), at 400 rpm, the maximum value of the peripheral air flow velocity reaches approx. 49.75%. At 500 rpm the maximum value of the peripheral air flow velocity reaches approx. 49.96% of the velocity of the working tool (52.36 ms^{-1}) and at 600 rpm the maximum value of the peripheral air flow velocity reaches approx. 49.96% of the velocity of the working tool (62.83 ms^{-1}). Compared with peripheral air flow velocity at 400 rpm the maximum peripheral air flow velocity at 500 rpm is by approx. 25.5% higher, at 600 rpm the maximum peripheral air flow velocity is by approx. 45.7% higher in comparison with air flow velocity at 400 rpm.

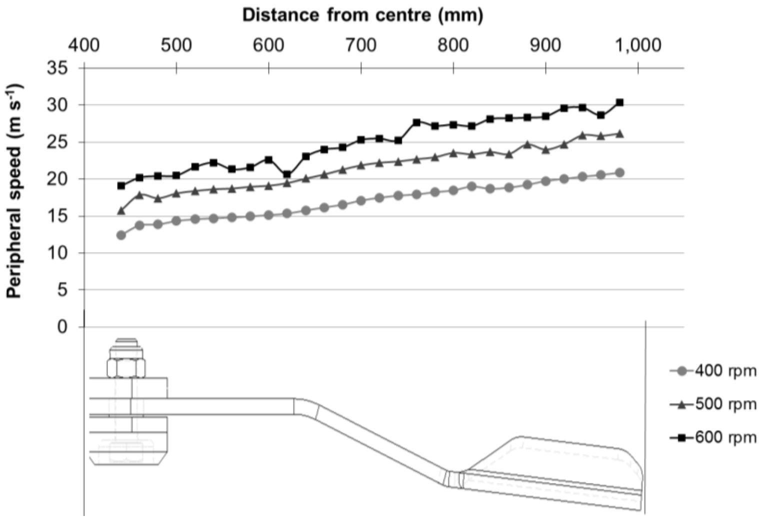

Figure 3. The peripheral air flow velocity profile at the height of 20 mm above the surface at different rotation speeds.

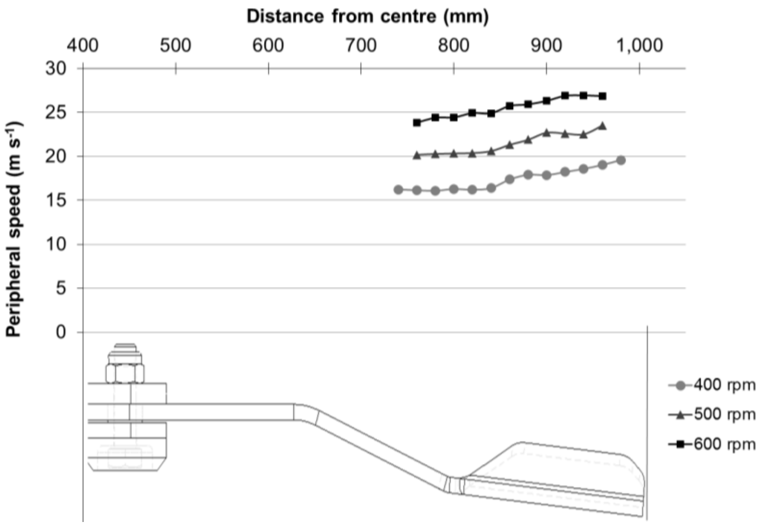

Figure 4. The peripheral air flow velocity profile at the height of 100 mm above the surface at different rotation speeds.

In Fig. 4 the peripheral air flow velocity in the height of 100 mm above the surface in dependence on the distance from the centre of the rotor is shown. At this height it was not possible to measure all determined points because the LDA device was capturing reflections from the cutting tool and data were not valid. The data were valid only between approx. 740–960 mm from the centre of the rotor. From the figure it is evident that the peripheral velocity of the air flow increases almost linearly with distance from the centre of the rotor but it reaches slightly lower values compared with the height of 20 mm. The maximum measured values of the peripheral air flow velocity are reached in the range of 940–980 mm from the rotor centre.

In Fig. 5 the peripheral air flow velocity profile at the height of 180 mm above the surface in dependence on the distance from the centre of the rotor can be seen. From the figure it is evident that up to approx. 740 mm from the rotor centre the peripheral velocity of the air flow increases almost linearly. Between 740–980 mm from the rotor centre the air flow velocity is almost constant at 400 rpm. At 500 and 600 rpm the rapid increase of peripheral velocity between 740–780 mm from the rotor centre can be seen. Between 780–980 mm from the rotor centre the velocity of the air flow remains nearly constant at 500 and 600 rpm. This phenomenon is probably caused by the shape of the trailing edge of the working tool and its angle. It can be assumed that with increasing rotation speed this phenomenon will have a stronger effect. Near the rotor periphery the slight decrease of air flow velocity can be seen, this decrease is caused by the wall friction between the air and side cover of the workspace. Similar phenomena was reported also by Chon & Amano (2004) and Chon & Amano (2005). The maximum values of air flow velocity at height of 180 mm is reached between approx. 780–920 mm from the rotor centre. Compared with the cutting speed of the tip of the blade the maximum measured values of peripheral air flow velocity at 400, 500 and 600 rpm reaches 42.2%, 42.9% and 42% respectively. Compared with the air flow velocity in the height of 20 mm and 100 mm the lower values were reached in the height of 180 mm.

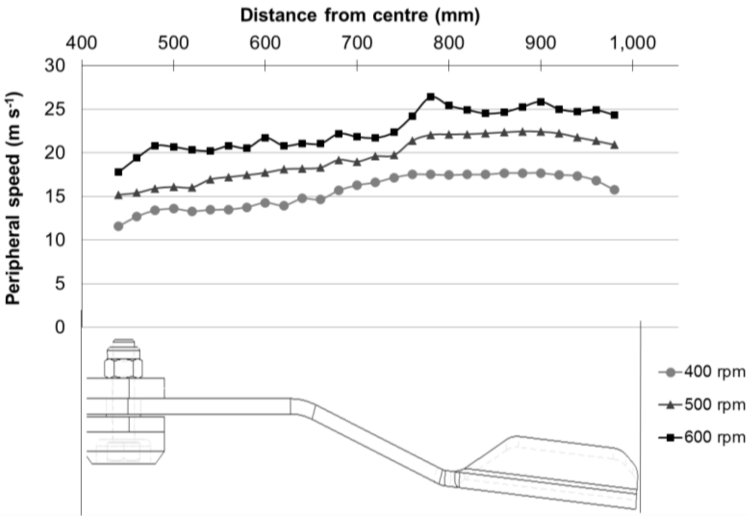

Figure 5. The peripheral air flow velocity profile at the height of 180 mm above the surface at different rotation speeds.

Also, the results can be compared with measured pressure profile inside the workspace, presented in (Čedík et al., 2016a; Čedík et al., 2017a). It was found that inside the workspace the vacuum is created and it is increasing almost linearly from periphery towards to the rotor centre. This result is in good agreement with results obtained from air flow velocity measurement, since it was confirmed that the higher pressure at the rotor periphery is caused by centrifugal forces of rotating air inside the workspace because the peripheral direction of velocity is predominant.

Radial air flow velocity

The radial air flow velocity is important in terms of quality of work, because it ensures repeated contact of the cut material with the blades of the working tools. In Fig. 6 the radial air flow velocity profile at the height of 20 mm above the surface is shown. It can be seen that under the working tools the air flow reaches positive values, it means that the cut material is pushed away from the centre of the rotation towards to the rotor periphery. Further, it can be seen that for all measured rotation speeds the maximum measured values are reached at 980 mm from the rotor centre, this is probably caused by the centrifugal forces of the rotating volume of air inside the workspace. Also, it may be noted that in the height of 20 mm above the surface the significant radial air flow appears only in the range of approx. 800–980 mm from the centre of the rotor, in the range of 440–800 ms^{-1} the radial air flow velocity is lower than 1 ms^{-1}.

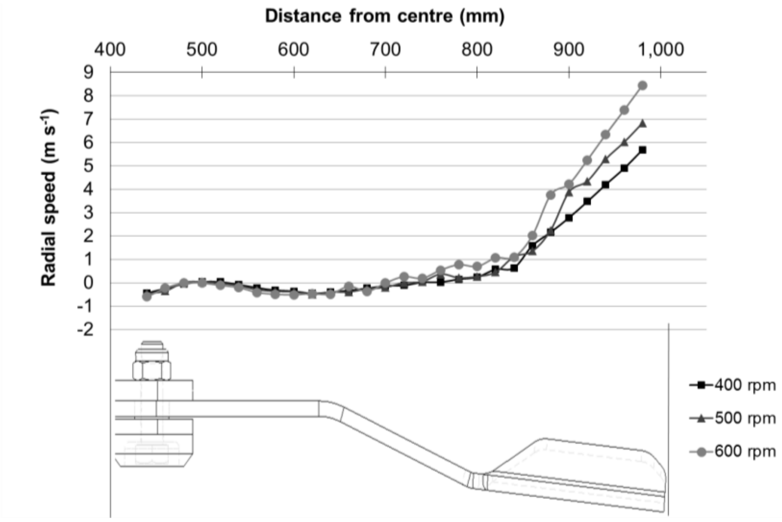

Figure 6. The radial air flow velocity profile at the height of 20 mm above the surface at different rotation speeds.

In Fig. 7 the radial air flow velocity profile at the height of 100 mm above the surface is shown. From the figure it is evident that at 100 mm above the surface the radial air flow velocity reaches negative values which means that the cut plant material is pushed back towards the rotor centre. Also, it can be seen that the higher values of the radial air flow velocity are reached between approx. 800–980 mm from the rotor centre. In the range of approx. 800–900 mm from the rotor centre the rapid increase of radial air flow velocity can be seen, then it remains nearly constant up to 980 mm from the rotor centre. A peak of radial air flow velocity, located at the distance of 680 mm from the rotor centre, is probably caused by the cranked part of the working tool, the value of air flow velocity at this peak was nearly the same for all measured rotation speeds.

A combination of radial air flow velocity at the height of 20 mm and 100 mm creates the air vortex, which ensures the circulation of the material trough the blades of the working tools. This air vortex appears in a range of approx. 800–980 mm from the rotor centre where the blades of the working tools are located, however, the air flow velocity at the height of 20 mm is decreasing more rapidly with decreasing distance from the rotor centre in comparison with the air flow velocity at the height of 100 mm. Results of other authors (Chon & Amano, 2003; Chon & Amano, 2004), who found the peak of axial upward air flow velocity near the rotor periphery, confirms the air vortex around the tip of the blade.

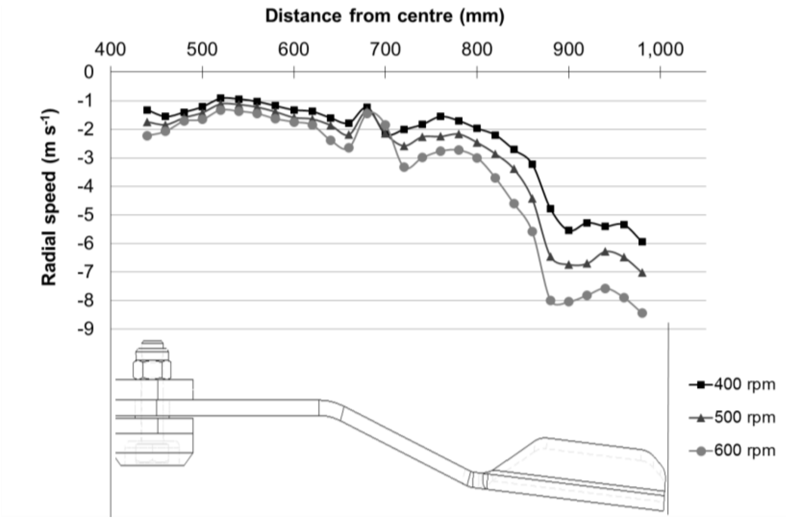

Figure 7. The radial air flow velocity profile at the height of 100 mm above the surface at different rotation speeds.

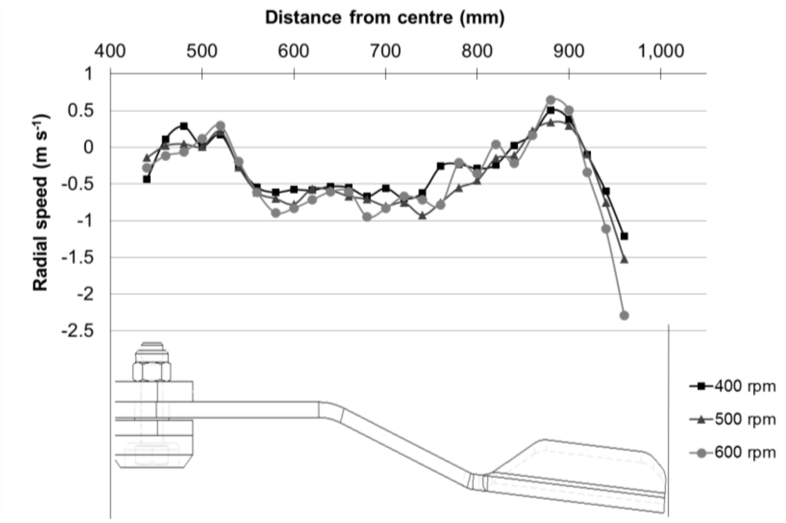

Figure 8. The radial air flow velocity profile at the height of 180 mm above the surface at different rotation speeds.

In Fig. 8 the radial speed in the height of 180 mm above the surface is shown. From the figure it can be seen that the radial air flow velocity in the range between 440–900 mm from the rotor centre is close to zero, changes direction and does not exceed the range from -1 to –0.5 ms^{-1}. For all measured rotation speeds, the peak values are negative and are reached at the distance of 980 mm from the rotor centre.

CONCLUSIONS

From the results of the measurement following conclusions were made:

- The peripheral air flow velocity increases with the distance from the rotor centre.
- The peak values of peripheral air flow velocity reach approx. 50% of the velocity of the tools. Near the side cover of the workspace the peripheral air flow velocity may decrease due to wall friction.
- In the radial plane the air vortex is created. This air vortex appears between the heights of 20 mm and 100 mm above the surface around the tip of the blade.

The contribution is focused on the experimental description of the air flow conditions inside the workspace of mulcher with the vertical axis of rotation. The air flow conditions affect the quality of work and energy demands of the mulcher. From the viewpoint of quality of work the higher radial and axial velocity could improve the work quality. That may be achieved by modification of working tool or workspace cover in order to redirect the radial and upward velocity at the tip of the blades and ensure better recirculation of cut plant material around the blades of the working tools (Čedik et al., 2017a; Čedik et al., 2017b). Also, the shape of workspace cover could be optimized according to course of the radial air flow velocity so that the volume with low values of radial velocity would be minimized.

ACKNOWLEDGEMENTS. The paper was created with the grant support – CULS IGA 2016: 31190/1312/3116 – Effect of cutting tool shape on air flow in working area of mulcher with vertical axis of rotation and CULS IGA 2017:31190/1312/3119 – Analysis of the impact of biofuels on the pressure profile in the combustion chamber of turbocharged diesel engine. The authors also acknowledge the financial support from the project Reg. No. FSI-S-17-4444 funded by the Brno University of Technology. The authors also acknowledge BEDNAR FMT, Ltd. for providing blade section of mulcher and help with the design of mulcher model.

REFERENCES

ASABE D497.7. Agricultural Machinery Management Data. 2011.

Čedík, J., Chyba, J., Pexa, M. & Petrásek, S. 2017a. Influence of shape of cutting tool on pressure conditions in workspace of mulcher with vertical axis of rotation. *Agronomy Research* **15**(4), 1530–1539.

Čedik, J., Chyba, J., Pexa, M. & Petrásek, S. 2017b. Effect of top cover shape on energy demands and workspace pressure of mulcher. *MM Science Journal* **2017**(5), 2050–2054.

Čedík, J., Pexa, M. & Pražan, R. 2017c. Effect of rake angle and cutting speed on energy demands of mulcher with vertical axis of rotation. *Agronomy Research* **15**(4), 1540–1549.

Čedík, J., Pexa, M., Chyba, J. & Pražan, R. 2016a. Pressure conditions inside the workspace of mulcher with vertical axis of rotation. In: *Proceeding of 6th International Conference on Trends in Agricultural Engineering 2016 – Part I*. TAE, Prague, pp. 129–134.

Čedík, J., Pexa, M., Chyba, J., Vondrášek, Z. & Pražan, R. 2016b. Influence of blade shape on mulcher blade air resistance. *Agronomy Research* **14**(2), 337–344.

Čedík, J., Pexa, M., Pražan, R., Kubín, K. & Vondřička, J. 2015. Mulcher energy intensity measurement in dependence on performance. *Agronomy Research* **13**(1), 46–52.

Hagen, P.A., Chon, W. & Amano, R.S. 2002. Experimental Study of Aerodynamics Around Rotating Blades in a Lawnmower Deck. *American Society of Mechanical Engineers, Fluids Engineering Division (Publication) FED* **257**, 67–76.

Hosseini, S.S. & Shamsi, M. 2012. Performance optimization of a rotary mower using Taguchi method. *Agronomy Research* **10**(S1), 49–54.

Chon, W., Jensen, M., Amano, R.S., Caceres, D., Sunjic, A. & Tetzlaff, P. 1999a. Investigation of flows around a rotating blade in a lawn mower deck. In: *Proceedings of the 1999 3rd ASME/JSME Joint Fluids Engineering Conference*, FEDSM'99, San Francisco, California, USA, 18-23 July 1999 (CD-ROM), 1.

Chon, W., Tetzlaff, P., Amano, R.S., Triscari, A., Torresin, J. & Johnson, K. 1999b. Experimental study of aerodynamics around co-rotating blades in a lawn mower deck. *American Society of Mechanical Engineers, Fluids Engineering Division (Publication) FED* ***250***, 57–64.

Chon, W. & Amano, R.S. 2003. Experimental and Computational Investigation of Triple-rotating Blades in a Mower Deck. *JSME International Journal Series B: Fluids and Thermal Engineering* **46**(2), 229–243.

Chon, W. & Amano, R.S. 2004. Experimental and computational studies on flow behavior around counter rotating blades in a double-spindle deck. *KSME International Journal* **18**(8), 1401–1417.

Chon, W. & Amano, R.S. 2005. Investigation of Flow Behavior around Corotating Blades in a Double-Spindle Lawn Mower Deck. *International Journal of Rotating Machinery* **1**, 77–89.

Jun, H.J., Choi, Y. & Lee, C.K. 2006. Development of a side-discharge mid-mower attached to a tractor. In: *Proc. 3rd international symposium on Machinery Mechatronics for agricultural and Biosystems Engineering*, ISMAB, Seoul, pp. 484–490.

Kakahy, A.N.N., Ahmad, D., Akhir, M.D., Sulaiman, S. & Ishak, A. 2014. Effects of knife shapes and cutting speeds of a mower on the power consumption for pulverizing sweet potato vine. *Key Engineering Materials* **594**, 1126–1130.

Kumhála, F., Chyba, J., Pexa, M. & Čedík, J. 2016. Measurement of mulcher power input in relation to yield. *Agronomy Research* **14**(4), 1380–1385.

Mayer, V. & Vlášková, M. 2007. Set-aside land cultivation by mulching. *Agritech Science* **1**(2), 1–5, http://www.agritech.cz/clanky/2007-2-1.pdf, Accessed 18.12.2017. (in Czech)

McRandal, D.M. & McNulty, P.B. 1978. Impact cutting behaviour of forage crops II. Field tests. *Journal of Agricultural Engineering Research* **23**(3), 329–338.

O'Dogherty, M.J. 1982. A review of research on forage chopping. *Journal of Agricultural Engineering Research* **27**(4), 267–289.

O'Dogherty, M.J. & Gale, G.E. 1991. Laboratory Studies of the Effect of Blade Parameters and Stem Configuration on the Dynamics of Cutting Grass. *Journal of Agricultural Engineering Research* **49**(2), 99–111.

Persson, S. 1987. *Mechanics of cutting plant material*. American Society of Agricultural Engineers, St. Joseph, 288 pp.

Srivastava, A.K., Goering, C.E. & Rohrbach, R.P. 2006. *Engineering principles of agricultural machines*. American Society of Agricultural Engineers, St Joseph, 588 pp.

Syrový, O., Bauer, F., Gerndtová, I., Holubová, V., Hůla, J., Kovaříček, P., Krouhlík, M., Kumhála, F., Kvíz, Z., Mašek, J., Pastorek, Z., Podpěra, V., Rybka, A., Sedlák, P., Skalický, J. & Šmerda, T. 2008. *Energy savings in crop production technologies*. Research Institute of Agricultural Engineering, p.r.i., Prague, 101 pp. (in Czech).

Syrový, O., Světlík, M., Pražan, R., Pastorek, Z., Kubín, K. & Gerndtová, I. 2013. *Mobile energy devices and the approximate values of unit fuel and energy consumption.* Research Institute of Agricultural Engineering, p.r.i., Prague, 56 pp. (in Czech).

Tuck, C.R., O'Dogherty, M.J., Baker, D.E. & Gale, G.E. 1991. Field Experiments to Study the Performance of Toothed Disk Mowing Mechanisms. *Journal of Agricultural Engineering Research* **50**, 93–106.

Zu, L., Zhang, L. & Wang, H.K. 2011. Optimization Design of the Lawn Mowing Vehicle's Blade Based on Aerodynamics. *Advanced Materials Research* **199–200**, 173–181.

Agronomy Research **16**(3), 679–687, 2018
https://doi.org/10.15159/AR.18.086

Alarm guard systems for the prevention of damage produced by ungulates in a chestnut grove of Middle Italy

L. Conti*, S. Bartolozzi, S. Iacobelli, V. Racanelli and F. Sorbetti Guerri

University of Florence, Department of Agricultural, Food and Forestry Systems – Via San Bonaventura 13, IT50145 Firenze, Italy
*Correspondence: leonardo.conti@unifi.it

Abstract. Wildlife populations, in particular ungulates and carnivores, have had a significant increase in most Italian regions over the last decades and for this reason ecosystems and agricultural and forest productions are threatened by damage produced by wildlife. In order to evaluate effective methodologies and technologies to mitigate the impact of this phenomenon, innovative protection systems, such as electronic acoustic alarm guard sensors, were tested. These devices are able to randomly produce a significant number of sounds and light projections. At the same time, camera traps were used, as a support instrument to show the presence or absence of wild fauna. Video analysis has provided information on the effectiveness of security systems, on the most suitable methods of installation and management of devices and their ecological impact. Experimental trials were carried out in a chestnut grove located in an Apennine area of the Middle Italy during the harvesting period (autumn). The results obtained have shown that these technologies seem to be particularly suitable for crops that concentrate production in a short time (e.g. vine and chestnut) and in areas not excessively large. Widespread use of devices could mitigate the conflict between public bodies involved in the management of wildlife and farmers.

Key words: alarm guard systems, camera trapping, forest productions, wildlife populations.

INTRODUCTION

In the last fifty years, the Italian territory has undergone significant changes in the structure of the rural territory due to the radical changes in the socio-economic characteristics of the country.

Many wild animal species were strongly affected by the transformations of the agricultural and forest ecosystems. In particular, the reappearance and the spatial and numerical spread of the large mammal populations (herbivores and carnivores) was observed. Repopulation actions, not accompanied by the adoption of suitable management techniques, together with the abandonment of marginal agricultural areas and the spread of forest ecosystems, have encouraged the increase of some wild species (especially ungulates). This phenomenon has led to significant problems of cohabitation between wild fauna and human activities. In Tuscany, from 2000 to 2009 the increase of ungulates around 51% was estimated (Ponzetta et al., 2010).

The abundant presence of wild fauna has led to a series of problems such as damage that animals cause to agricultural and forest productions, in addition to those determined by carnivores (e.g. wolf) to livestock activities. In the last years, the requirement to identify suitable technologies to prevent damage has represented a primary need of the agricultural and forest sector, in order to mitigate the conflicts between wildlife and agricultural activities. In Tuscany, negative impacts on agricultural and forest crops were produced by wild boar, roe deer and deer. The kinds of damage were mainly due to the direct consumption of the product, in addition to behavioral aspects such as the search for food (browsing, rooting, fraying, etc.). The consequences of these actions were a decrease of productions and, in some cases, the modification of the evolution of the forest structure (e.g. affects the natural regeneration). Many solutions were proposed, but most of these lack information experimentally verified on the methods of realization and management of the equipment.

Among the prevention methods adopted, it is useful to remember the use of dissuasive feeding based on the stimulation of smell and taste (Avery & Mason, 1997), of shelter protections for the defense of plants, in addition to the traditional and electrified fences (Berzi et al., 2010; Capaccioli et al., 2017). In the past other acoustic alarm guard systems (e.g. compressed air or propane guns, detonators loaded with blanks, etc.), and bio-acoustic and ultrasonic emitters were widely used, especially tested on birds (Bishop et al., 2003; Arnet et al., 2013). The effectiveness of these protection systems was limited for the animals' habit towards repeated sounds and lights, which were always the same. Furthermore, not all alarm systems are worrying for the animals, also in relation to the different degree of anthropization of the environment.

The aim of the research was to verify the efficacy of last-generation remote alarm guard systems, able to randomly emit a significant number of different sounds and noises, in addition to light projections. This research was carried out to test the capacity of these devices in order to remove wildlife populations and safeguard the production of a chestnut grove in an Apennine area in the Province of Florence (Middle Italy). Camera traps were a support equipment to record the movement of animals within the protected area (Kays et al., 2009; Rovero et al, 2013). These non-invasive devices, effective in any environmental and meteorological conditions, of simple setting and installation, have recently found different applications in faunal field as for the study of habitat use patterns and behavioral patterns of wildlife fauna (Silveira et al., 2003; Bowkett et al. 2007; Rovero & Marshall, 2009; Manzo et al., 2012; Meek & Pittet, 2012).

MATERIALS AND METHODS

Electronic devices

For the purpose of the research, remote automatic devices of alarm guard and detection were tested.

The protective device was the Alarm Guard (patent N° R 2011 000010) manufactured by Ziboni srl Company. The Alarm Guard (AG) is internally composed of loudspeaker, SD card slot (1Gb), on which the audio files (in mp3 format) are archived and modified, a keyboard for setting with display and a rechargeable load acid battery of 12V – 7.2 Ah. Both the loudspeaker and the SD card slot card are equipped with their electronic circuit. The power autonomy of battery depends on the number of events recorded by the AG but if the system works well, this battery type allows a long operation time (minimum 30 days). Externally, the loudspeaker output, the passive infrared sensor (PIR), the flashing light (or LEDs) and a socket to connect the alarm guard sensor battery to any supplementary solar panels are located (Fig. 1, a, b). The hardware components are protected by a special polypropylene box, which isolates the electrical circuits and makes the device waterproof.

Figure 1. Alarm guard sensor (AG): a) device fixed on wooded pole at 1 m above ground in the study area; b) internal view of device with electrical and electronic components.

Two metal brackets for fixing the instrument on any support are placed behind the device.

The AG are automatic devices activated by timer and by the passage of animals in front of the passive infrared sensor (PIR) which, by detecting the animal body heat , triggers the emission of sounds in a random way. Sounds for animals potentially accustomed to anthropic disturbance were selected (e.g. noises of human activities), not easily recognizable by the wild fauna. The devices were also provided with high brightness LEDs (blue and white lights), which are activated before the sound emission. The detection distance of the AG is variable from 8 to 15 m, according to the setting of the sensitivity of the PIR (normal or high). This detection distance can be increased by adding wireless sensors (WS), which remotely activate the AG through a specific emission radio module. The wireless sensors can be positioned up to a maximum distance of 100 m from the main device, depending on the morphology of the territory.

The camera traps Scout Guard SG-550 model were used as device of detection. Camera traps combine a video-photographic recording device with a passive infrared sensor, working automatically in the same way of the AG. Cameras take a picture whenever they sense movement in the surrounding environment. These instruments can be set in order to define their sensitivity, the working time, the video length and the intervals between them. Pictures or videos are stored in a SD card. Another technical component of the camera is the IR-flash for night video with a detection distance of about 10–12 m.

Study Area

The study area was located in the municipality of San Godenzo (FI). The municipal territory falls partly within the National Park of ‘Foreste Casentinesi, Monte Falterona e Campigna’ and partly outside the borders of the Park. The study area was about 3 ha and was exclusively suited for chestnut growing. It was located at an altitude of 700 m, characterized by average slopes around 30%. The surrounding wooded areas were represented by the intercropping of oaks (in particular, *Quercus cerris*), black hornbeam (*Ostrya carpinifolia*) and chestnut (*Castanea sativa*).

The economic and historical-cultural value of chestnut growing in Tuscany until the end of the nineteenth century by the presence of over 150,000 ha was witnessed (Maltoni et al., 2009). The demographic abandonment of the mountain territories in the '70s and' 80s has led to a reduction of the chestnut areas up to about 32,000 ha. Many areas are in a state of neglect due to the recent attacks of the cinipid insect (*Dryocosmus kuriphilus*), which has strongly reduced the production. This criticality was particularly felt in the Central Apennines in order to safeguard fruit productions of recognized importance at Community level (Council Regulation EEC No 2081/92).

The study area (Fig. 2) consists of 2 areas: area A, with central watershed and a flat summit area, and area B, connected to the previous one through an obliged passage.

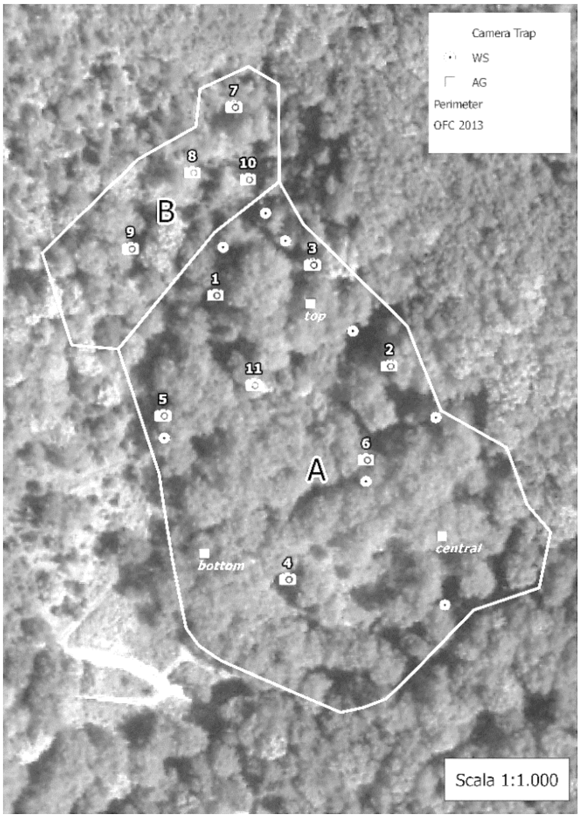

Figure 2. Study area and placement of electronic devices.

Area B is an area with few chestnut trees but with a pool of water used by animals as a watering area. For the research, the area A was considered as a protected area, while the area B as a free zone, without any protection systems.

Study design and methodology

The sampling design of trial was carried out in 4 phases for about 5 months.

The preliminary phase (1), from 23/09/2016 to 7/10/2016, has allowed to identify the access points to the study area, basing on the recognition of wildlife trails, footprints, dung piles, etc. According to them, the placement of 11 camera trap sites was selected: 7 devices were placed in area A, 4 in the top zone (No 1, 2, 3, 11) and 3 in the bottom zone (No 4, 5, 6); 4 camera traps were placed in area B (No 7, 8, 9, 10). In this phase, it was decided not to use food baits, since the fruits on the ground already represented the element of attraction.

In the phase 2 (from 8/10/2016 to 30/10/2016), 3 AG were placed inside the area A (one in the top, one in the bottom and one the central zone) when the fruits were ripe. In order to enhance the action of AG and obtain the maximum protection of the area, 8 WS were used. During the processing/working of the protection systems, camera trapping was also active with 8 devices. The sampling design of the research was flexible in terms of spatial arrangement of devices, even if the camera's detection parameters and sensitivity values of the PIR sensors were respected, in order to ensure a total coverage of the area (Tobler et al., 2008).

AG with following settings were scheduled: triggering of devices by PIR during the night time interval (5.00 pm–8.00 am), AG with maximum volume, triggering interval time after each event (1 s), high sensitivity of PIR sensor. The higher degree indicates that the devices are more easily to be triggered by motion, recording more videos. Camera traps were programmed for video length of 30 s, to allow the recognition and behavior of the target species, trigger interval time (1 s), date and time stamp on. During the trial the cameras and AG were checked every 7 days to download videos, PIR events and check the batteries.

The phase 3 (from 31/10/2016 to 30/12/2016), concerned the shutdown of the protection systems after the chestnut harvesting and the continuation of the camera-trapping, to assess the time of return of the animals in the protected area.

In the phase 4 (from 31/12/2016 to 15/02/2017), the second period of operation of the AG was scheduled.

RESULTS AND DISCUSSION

The data recorded by each camera trap, considered as a sampling unit, were elaborated in order to understand the effective functioning of the AG, in respect of the wild fauna.

The 11 camera traps were operational for 170 days, recording 188 videos for 1,870 camera days; the average video for camera trap was 17.09 No video/camera (Table 1).

Table 1. Camera traps data

	Placements	Days	Camera days	Videos	Video for camera trap (No video/camera)		
					Mean rate	Min.	Max.
Cameras	11	170	1,870	188	17.09	2	35

Estimating the frequency for each camera station, it was observed that devices No 7, 10 and 2 had higher values than the others which are between 2 and 17 trap events per camera (Fig. 3). The highest number of animals photographed per three unit areas may suggest to monitor carefully these zones placed along intensively used wildlife trails and very close to dense forest.

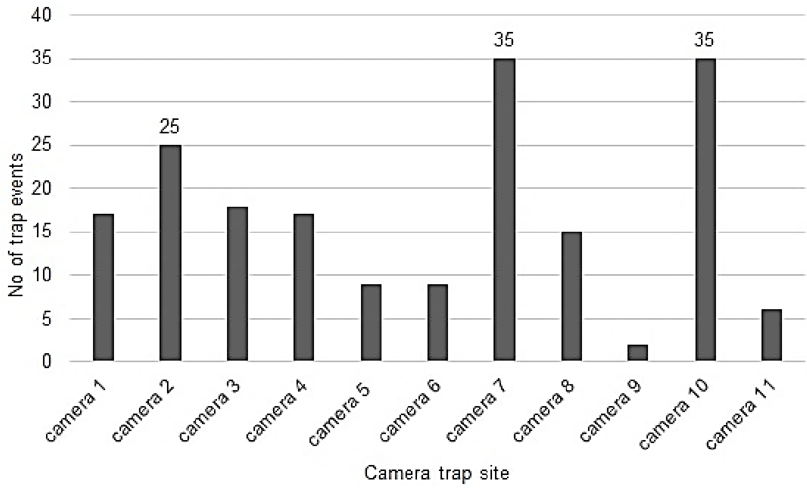

Figure 3. Frequency of detection for each **c**amera trap site.

The AG were operating in two separate periods for 71 days. In the phases 2 and 4 with AG working, the total number of videos recorded was 53: 31 events in protected area A (58%), 22 events in area B (42%). The highest values for zone A could be in contrast with the predicted forecasts, but the most conspicuous food supply of the protected area (A) could have represented an element of attraction for the animals. Behavioral analyses have been shown that attempts to enter were followed by immediate waivers for the activation of AG. The number of AG events recorded in these phases, were respectively 84 (40 AG events in the top zone, 44 AG events in the bottom and central zone), and 361 (154 AG events in the top zone, 207 AG events in the bottom and central zone), highlighting an intense wildlife activity (Table 2).

Table 2. Videos and AG events recorded for each phase

	Phase 1	Phase 2	Phase 3	Phase 4
No video – area B	5	4	57	18
No video – area A	24	2	54	29
No AG events – area A	-	84	-	361

A greater attendance of the animals in the two areas was evident when the AG were not activated (phase 1 and 3).

Another aim of the research was to assess the permanence of the animals inside the study area, multiplying the video length (30s) by the number of animals recorded. Therefore, the movie length of each event was counted and the simultaneous presence of a group of animals was evaluated in terms of grazing time (Forconi et al., 2009; Sorbetti et al., 2011). Processing camera-trapping data, it was calculated a grazing time of 3 min 30 s during the phase 2 and of 1 h 42 m 30 s during the phase 4. Most of the events (54.7%) were made by camera traps No 2 and 10, located in the top zone of the chestnut grove, while 23% of movies were made by camera traps No 4, 5, and 6, located in the central part of the study area (Fig. 4).

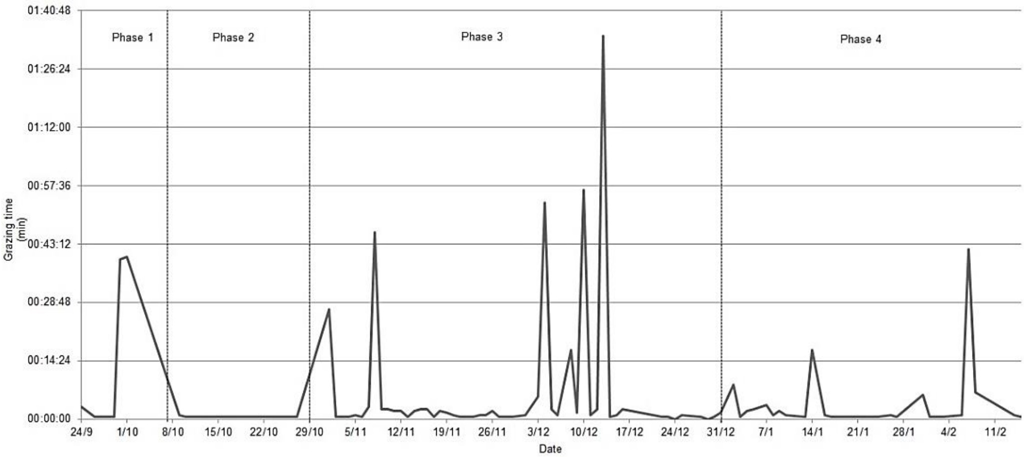

Figure 4. Wild fauna grazing time during the trial.

In phase 3, it was possible to calculate a wild fauna grazing time of 11 h 51 min 30 s: 39.8% of movies from cameras No 7 and 10 (area B) were taken, 33.9% and 14% of videos were respectively made in the top and in the central zone of area A.

Analyzing videos, it was possible to observe that the most numerous detections were made for Roe deer (*Capreolus capreolus*), Deer (*Cervus elaphus*) and Wild boar (*Sus scrofa*) during the phase 3 without disturbance. The presence of Roe deer (*Capreolus capreolus*) was more frequent, but the feeding activity of the animals inside the area was reduced if compared to the events connected to the simple passage in front of devices. Few attendance instead for other species during the working of devices were recorded.

CONCLUSIONS

The acoustic alarm guard method was particularly suitable for crops that concentrate their production in a short time, such as vine and chestnut. For surfaces that are not too large (max 2 ha) these devices were suitable. A behavior of removal in relation to the type of selected sound event was shown by the monitored animal species. Furthermore, it should be observed that this system is an ecological method of prevention, unlike traditional fences, which can represent barriers for some species and obstacles for agricultural, forest, hunting, hiking activities, etc.

The camera traps have represented a non-invasive investigation device for monitoring the ungulates reactions to the AG activation, without interfering with the animal behavior. An attitude of curiosity or indifference towards the camera traps was expressed by the wild fauna; not perceiving them as a potential source of danger. The video analysis was also useful to provide suggestions to improve the effectiveness of the AG equipment, in terms of selection of sounds and light emissions.

The effectiveness of AG cannot be separated from their correct application. Non-specialized employees can also manage these electronic devices, but it is useful to provide some essential precautions both during placement in the field and during the period of working.

At the end of trial, a positive opinion on the equipment tested was expressed by the farmer. In fact, the production of chestnuts of the year 2016 (8,000 kg) was higher if compared to that of previous years (5,000 kg in 2015).

The authors hope to disseminate the use of these devices, both through an awareness-raising project on prevention methods and through a system of supplies funded by public institutes responsible of wildlife management. The authors also suggest a continuous development of the equipment (hardware, software, etc.), to be done between companies and research institutions. Improving the performance of devices will be possible to think about the design of a remote sensor network for the protection of agricultural productions on large scale.

REFERENCES

Arnett,E.B., Hein,C.D., Schirmacher,M.R., Huso,M.M.P. & Szewczak, J.M. 2013. Evaluating the Effectiveness of an Ultrasonic Acoustic Deterrent for Reducing Bat Fatalities at Wind Turbines. *PLoS ONE* **10**, https://doi.org/10.1371/annotation/a81f59cb-0f82-4c84-a743-895acb4b2794.

Avery, M.L. & Mason, J.R. 1997. Feeding responses of red-winged blackbirds to multisensory repellents. *Crop Protection* **6**, 159–164.

Berzi, D., Conti, L., Innocenti, S., Morgenni, F. & Sorbetti Guerri, F. 2010. Electric fences: analysis of the efficacy in preventing damage produced by wolf in Tuscany. In: *International Wolf Conference 'Wolves, people and territories – Wolf managementi in Europe: conservation, monitoring, damage prevention, and conflict mitigation'*, Turin, Italy, pp. 5–5 (in Italian).

Bishop, J., McKay, H., Parrott, D. & Allan, J. 2003. *Review of International Research Literature Regarding the Effectiveness of Auditory Bird Scaring Techniques and Potential Alternatives.* York, UK: Central Science Laboratory. MS. 53 pp.

Bowkett, A.E., Rovero, F. & Marshall, A.R. 2007. The use of camera trap data to model habitat use by antelope species in the Udzungwa Mountain forests, Tanzania. *African Journal of Ecology* **46**, 479–487.

Capaccioli, A., Racanelli, V. & Sorbetti Guerri, F. 2017. *Defense strategies against damage caused by wildlife. Realization and management of electric fences.* Canterano (Rome): Aracne Editrice – Gioacchino Onorati Editore S.r.l. – Unipersonale, ISBN: 978-88-548-9945-2 (in Italian).

Council Regulation (EEC) No 2081/92 on the protection of geographical indications and designations of origin for agricultural products and foodstuffs. Official Journal of the European Communities, Brussels.

Forconi, P., Di Martino, V. & Forlini, P. 2009. *Mammals, how to study them with camera traps.* Tipografia Editrice Temi s.a.s., 145 pp. (in Italian).

Kaysy, R., Kranstauber, B., Jansen, P.A., Carbone, C., Rowcliffe, M., Fountain, T. & Tilak, S. 2009. Camera traps as sensor networks for monitoring animal communities. In: *34th IEEE Conference on Local Computer Networks,* pp. 1–8.

Maltoni, A., Mariotti, B., Jacobs, D.F. & Tani, A. 2012. Pruning methods to restore Castanea sativa stands attacked by Dryocosmus kuriphilus. *New Forests*, pp. 1–17, ISSN: 0169-4286 DOI.

Manzo, E., Bartolommei, P., Rowcliffe, J.M. & Cozzolino, R. 2012. Estimation of population density of European pine marten in central Italy using camera trapping. *Acta Theriologica* **57**, 165–172.

Meek, P.D. & Pittet, A. 2012. User-based design specifications for the ultimate camera trap for wildlife research. *Wildlife Research* **39**, 649–660.

Ponzetta, M.P., Sorbetti Guerri, F., Banti, P. & Nuti, S. 2009. Road accidents caused by wildlife in the Tuscany Region - Analysis of the phenomenon in the period 2001–2008. Ed. Regional Council of Tuscany Press Center, Florence, Italy (in Italian).

Rovero, F. & Marshall, A.R. 2009. Camera trapping photographic rate as an index of density in forest ungulates. *Journal of Applied Ecology* **46**, 1011–1017.

Rovero, F., Zimmermann, F., Berzi, D. & Meeke, P. 2013. 'Which camera trap type and how many do I need?' A review of camera features and study designs for a range of wildlife research applications. *Hystrix* **24**(2), 148–156.

Silveira, L., Jacomo, A.T.A. & Diniz-Filho, J.A.F. 2003. Camera trap, line transect census and track surveys: a comparative evaluation. *Biological Conservation* **114**, 351–355.

Sorbetti Guerri, F., Conti, L., Camiciottoli, S., Innocenti, S. 6Pini, L. 2011. Automatic systems for the wildlife monitoring and prevention of damage to agricultural and forest production. *Proceedings of AIIA National Conference Management and control of agricultural and forest systems,* Belgirate, Italia, pp. 1–6 (in Italian).

Tobler, M.W., Carrillo-Percastegui, S.E., Leite Pitman, R., Mares, R. & Powell, G. 2008. An evaluation of camera traps for inventorying large- and medium-sized terrestrial rainforest mammals. *Animal Conservation*, **11**, 169–178.

Agronomy Research **16**(3), 688–695, 2018
https://doi.org/10.15159/AR.18.100

Anaerobic co-fermentation of molasses and oil with straw pellets

V. Dubrovskis*, I. Plume and I. Straume

Latvia University of Life Sciences and Technologies, Faculty of Engineering, Institute of Energetics, Cakstes blvd. 5, LV3001 Jelgava, Latvia
*Correspondence: vilisd@inbox.lv

Abstract. The average grain and straw production in Latvia is increasing in last decade. Straw is not always managed properly and its utilisation in biogas plants can be considered as an alternative. Straw is not the best feedstock for methane production, because it has high C/N ratio. Co-fermentation with other biomass with higher N content can improve the methane production. Purpose of investigation is to evaluate the wheat straw pellets biomass suitability for production of the methane and effect of its co-fermentation with molasses, fried sunflower oil and catalyst Metaferm. The anaerobic digestion process for biogas production was investigated in 0.75 L digesters, operated in batch mode at temperature 38 ± 1.0 °C. The average biogas yield per unit of dry organic matter added from digestion of wheat straw pellets was 0.540 L g^{-1}_{DOM} and methane yield was 0.285 L g^{-1}_{DOM}. Average biogas yield from co-fermentation of wheat straw pellets and molasses was 0.777 L g^{-1}_{DOM} and methane yield was 0.408 L g^{-1}_{DOM}. Average biogas yield from fermentation of wheat straw pellets with 1ml Metaferm was 0.692 L g^{-1}_{DOM} and methane yield was 0.349 L g^{-1}_{DOM}. Average biogas yield from co-fermentation of wheat straw pellets and sunflowers oil was 1.041 L g^{-1}_{DOM} and methane yield was 0.639 L g^{-1}_{DOM}. All investigated biomasses can be used for methane production.

Key words: anaerobic digestion, biogas, methane, molasses, sunflower oil, wheat straw pellets.

INTRODUCTION

Agricultural production generates a lot of waste and residue, which would be a substantial biomass resource for biogas production. 59 biogas plants are running in Latvia, and different raw materials are utilised for methane production. One of the biomass most widely used by dairy farmers owing biogas plants is the maize silage, due to high biogas and methane volumes obtainable per unit of area (Dubrovskis & Adamovics, 2012). However, some farmers' organizations have recently been influenced by the Ministry of Agriculture in agreeing in repealing an excise tax relief on diesel sold for farmers for corn production. This government decision was based on the need to use the arable land for food production. The production of corn silage is an expensive technology and in situation, when excise tax relief is not more available for corn production, energy corn growing for biogas production turns unprofitable. Therefore, it is essential for biogas producers to find inexpensive raw biomasses capable to substitute corn in feedstock for biogas plants. A more cost effective raw material could be the straw, especially the cereals straw. Straw in Latvia is not used properly and part of straw is wasted in harvesting process or in biodegradation process during storage. Also, emissions of greenhouse gases (CO_2, N_2O, and others) ongoing from straw biomass left on the ground surface or during storage in heaps or bales should be considered. Especially high dry mass losses are observed from straw biomass if uncovered straw biomass is exposed to weather conditions. Low natural density of straw or straw bales increase the transport expenses so limiting, to a certain extent, the straw usage for biogas production.

There can be different ways in straw usage for the biogas production. Usually, straw is used in livestock barns and poultry houses as the litter, so forming the mixture with manure utilisable as cheap raw material in biogas plants. According to the literature, many researchers have obtained biogas from different straw materials (Table 1).

There are only a few studies in Latvia about the potential of biogas from different straw and grasslands. From the crushed and pre-soaked barley straw, a relatively good (0.296 L g^{-1}_{DOM}) methane yield was obtained, mainly due to the positive effect of pre–treatment (Dubrovskis & Adamovics, 2012). Also good (0.280 L g^{-1}_{DOM}) average specific methane yield was obtained from chopped barley (Dubrovskis et al., 2012).

Table 1. Biogas (methane) production from different straw biomass

Raw material	Methane, $m^3\ kg^{-1}_{DOM}$	Methane content, %	Biogas, $m^3\ kg^{-1}_{DOM}$	Literature source
Wheat straw		58.0	0.342	Angelidaki et al., 2009
Flax straw		59.0	0.359	Angelidaki et al., 2009
Rice straw	0.161	57.4		Leyrica et al., 1984
Wheat straw 30 mm		50.0	0.306	Baader et al., 1978
Wheat straw 2 mm		51.0	0.343	Baader et al., 1978
Wheat straw	0.189	51.0	0.370	Becker et al., 2007
Straw		52.0	0.388	Cenian et al., 2012

In other countries straw is also used for biogas production. The relatively low yield of biogas (methane) from roughly chopped wheat straw substrate was 188.4

L·kg^{-1}_{DOM} (78.4 L kg^{-1}_{DOM}). If the same wheat straw was pre-treated with NaOH, then better biogas (methane) yield of 353.2 L kg^{-1}_{DOM} (165.90 L kg_{DOM}^{-1}) was observed. Hydrothermal treatment of the same straw resulted into specific biogas (methane) production yield 205.7 L kg^{-1}_{DOM} (94.1 L kg^{-1}_{DOM}). Compared to untreated wheat straw, methane yield increases by 111.6% from straw treated with NaOH and by 20% from hydrothermally pre-treated straw (Chandr et al., 2012).

In Germany, FNR shows, that a specific biogas yield of 370 L kg^{-1}_{DOM} is obtainable from wheat straw with methane content 51% in biogas (Becker et al., 2007).

In Denmark, at University of Arhus extensive studies were carried out on the use of the straw briquettes for biogas production. Laboratory studies show, that 250 m^3 of methane was obtained per ton of straw briquettes (Moller & Hansen, 2014). Studies show, that methane yield from the briquettes was higher by 19% compared to that from the roughly chopped straw.

Straw was also studied in Sweden for the production of biogas. Studies at the Biogas Research Centre in Wadsworth show that the use of straw in combination with manure is effective (Duong, 2014).

In Denmark, the co-fermentation of straw briquettes with bovine and porcine manure is foreseen as the main raw material for biogas production. According to the program, at least 50% of all manure is expected to utilise for biogas in 2020. The great advantage of briquetting technology is the reduced straw transport costs, especially in transporting over long distances. Due to increased briquettes density the transport costs decreases drastically, as the truckload capacity increases from 12 to 33 tonnes with the straw briquettes compared to capacity with the straw bales (www.kineticbiofuel.com).

Use of the straw pellets for biogas production is investigated in Denmark also. It is supposed that 10% of the pellets by the weight are acceptable percentage for its co–fermentation with the manure. Company Xergi was built a biogas plant using the manure and the straw pellets for production of 8 million m^3 biogas per year (Walsh, 2015).

Purpose of investigation is evaluation the biogas and methane output from the wheat straw pellets co-fermentation with molasses and sunflower oil, and effect of added catalyst Metaferm.

MATERIALS AND METHODS

Biomass never fully degrades in practice therefore the studies are needed to assess the potential of methane for each particular biomass. Several methods can be used for this purpose. In our research, we used the methodology approved by the German scientists (Kaltschmitt, 2010).

The research was provided on wheat straw pellets in diameter of 6.0 mm (Fig. 1), marketed commercially and used as bedding material for animal premises usually.

According to observations, when the straw pellets are added in the water, the pellets do not form a floating layer (Fig. 2). The straw pellets have ability to absorb the large volume of liquids and tend to disintegrate in the substrate.

Figure 1. Straw pellets.

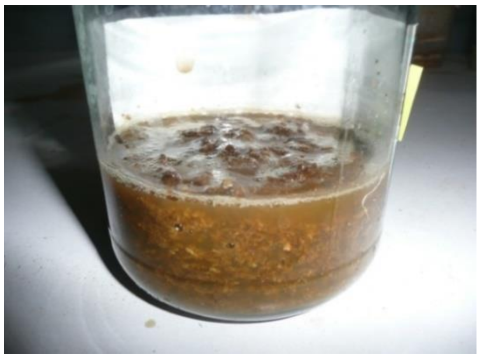

Figure 2. Straw pellets in water (not floating).

Average sample of straw pellets was taken and chemical composition was determined in the LUA laboratory according to standardized methodology ISO 6496:1999. Total dry organic matter, dry matter, ashes content, and content of basic elements was determined for average sample of each group of the raw materials. Each group of raw materials and inoculums was weighed carefully. Each bioreactor (R1-R16) in volume of 0.75 L was filled with the same inoculum (almost finished cows manure digestate taken from a continuously operating bioreactor in volume of 120 L). Bioreactors R1 and R16 with inoculum only were used as control to obtain the values, e.g. volume of biogas and methane produced from pure inoculums needed for correction of biogas and methane volumes obtained from bioreactors R2–R15 with added biomass (straw pellets, molasses, sunflower oil, catalyst Metaferm).

Wheat straw pellets 20 g were added in each reactor R2–R15. Molasses 4.6 g (or 23% of pellets weight) was added in bioreactors R5–R8. Metaferm 1 mL (or 5% of pellets weight) was added in bioreactors R9–R11 and sunflower fried oil 3.8 g (or 19% of pellets weight) was added in bioreactors R12–R15. Molasses is the by-product from sugar beets processing at sugar factories, and were purchased from Belorussia as a feedstock for biogas plant. Actual sample of molasses was obtained at local biogas plant and quality of molasses was impaired.

Fried sunflower oil is the by-product obtained after cooking (frying) process of vegetables (was poured out of the pan).

Metaferm (made in Latvia) is the bio-stimulator for promoting of bacteria activity in anaerobic fermentation process. Catalyst Metaferm contains vitamins, micronutrients and biologically active substances however the precise composition of Metaferm is unknown, due to producer proprietary rights on this product.

Accuracy of raw material sample and additives weight measurement was ± 0.001 g, and accuracy of inoculums weight measurement was ± 0.2 g respectively. Each bioreactor was filled in with planned mixture and sealed carefully. Every bioreactor was connected with gas storage bag fitted with check valve in the input and manually operated tap in the output for gases measurement. All the bioreactors were placed in the thermostat operating at pre-set working temperature 38 ± 0.5 °C. The volume and composition of the produced biogas was measured once a day. The bioreactors were also shaken regularly to reduce the floating layer. Anaerobic fermentation was provided in a single filling (batch) mode and lasted until the biogas production ceases.

After the fermentation process was finished, every digestate from bioreactors was weighed and dry matter, ashes and dry organic matter (DOM) content was measured. The dry matter content was determined in the special unit, model Shimazu, at a temperature of 105°C, and the organic matter content was determined in the oven, model Nabertherm, by burning of the samples at 550 °C according to the special program.

The gas composition (methane, carbon dioxide, oxygen and hydrogen sulphide) was measured with the gas analyser, model GA 2000. Biogas and methane yield from the added biomass (straw pellets, molasses, sunflower oil, catalyst Metaferm) in inoculums was calculated as the biogas (methane) volume from each reactor (R2 to R15) minus the average biogas (methane) volume obtained from the control bioreactors (R1, R16).

The accuracy of the measurements was ± 0.02 for pH, ± 0.025 L for gas volume and ± 0.1 °C for temperature. Methane CH_4, carbon dioxide CO_2 and oxygen O_2 content in biogas was measured periodically with the accuracy ± 2.0%.

Oxygen measurements were provided for control of tightness of gas collection system only. The unit Kern FKB 16KO2 with accuracy ± 0.2 g was used for measurement of total weight of substrates, and the unit Shimazu with accuracy ± 0.001 g was used for weighting of biomass samples to obtain total solids and dry organic matter content. Substrates pH value was measured with pH meter, model PP-50.

Biogas and methane yield from the added biomass (straw pellets, molasses, sunflower oil, catalyst Metaferm) in inoculums was calculated as the biogas (methane) volume from each reactor (R2 to R15) minus the average biogas (methane) volume obtained from the control bioreactors (R1, R16).

RESULTS AND DISCUSSION

Investigation of biogas and methane output from wheat straw pellets and from its co-fermentation with molasses, sunflower oil and catalyst Metaferm was provided according to experimental plan. Results of raw material analysis are shown in Table 2.

Table 2. Results of analysis of raw materials

Bioreactor	Raw material	Weight g	pH	TS %	TS g	ASH %	DOM %	DOM g
R1, R16	IN	500	7.53	2.21	11.050	25.25	74.75	8.260
R2–R4	SP	20		89.37	17.874	9.99	90.01	16.088
R2–R4	IN+SP	520	7.35	5.56	28.924	15.82	84.18	24.348
R5–R8	MO	4.597		89.98	4.136	23.25	76.75	3.174
R5–R8	IN+SP+MO	524.6	7.36	6.31	33.06	16.75	83.25	27.522
R9–R11	IN+SP+MF	521		5.55	28.932	15.82	84.18	24.356
R12–R15	SO	3.829		99.95	3.829	0.30	99.70	3.815
R12–R15	IN+SP+SO	523.8	7.34	6.25	32.753	14.01	85.99	28.163

Abbreviations: TS – total solids; ASH – ashes; DOM – dry organic matter; IN – inoculums; SP – straw pellets; MO – molasses; MF – Metaferm; SO – sunflower oil.

As can be seen from the table, the straw pellets have a high dry matter and organic matter content, and are suitable for biogas production. Straw pellets absorbs moisture and disintegrates in substrate quickly without forming a floating layer, and behave different compared to non-chopped straw forming the floating layer in substrates usually.

The outputs (yields) of biogas and methane from the wheat straw pellets without and with additives are shown in Table 3.

Table 3. Biogas and methane yields from experimental bioreactors

Reactor	Raw material	Biogas, L	Biogas, L g^{-1}_{DOM}	Methane aver. %	Methane, L	Methane, L g^{-1}_{DOM}
R1	IN500	0.00			0.00	
R16	IN500	0.00			0.00	
R2	IN500+SP20	8.60	0.534	52.06	4.472	0.278
R3	IN500+SP20	8.60	0.538	52.97	4.585	0.285
R4	IN500+SP20	8.80	0.550	53.09	4.698	0.292
	Aver. R2–R4	**8.667**	**0.54**	**52.78**	**4.585**	**0.285**
	± st.dev.	**± 0.12**	**± 0.01**	**± 0.56**	**± 0.11**	**± 0.01**
R5	IN500+SP20+MO5	15.90	0.825	52.29	8.314	0.432
R6	IN500+SP20+MO5	16.60	0.862	50.65	8.408	0.437
R7	IN500+SP20+MO5	15.30	0.794	55.93	8.252	0.428
R8	IN500+SP20+MO5	12.10	0.628	53.22	6.44	0.334
	Aver. R5–R8	**14.975**	**0.777**	**53.02**	**7.854**	**0.408**
	± st.dev.	**± 1.19**	**± 0.01**	**± 2.21**	**± 0.94**	**± 0.05**

Table 3 (continued)

R9	IN500+SP20+ MF1	10.00	0.621	51.46	5.146	0.320
R10	IN500+SP20+ MF1	11.50	0.715	48.81	5.613	0.349
R11	IN500+SP20+ MF1	11.90	0.740	50.93	6.061	0.377
	Aver. R9–R11	**11.133**	**10.692**	**50.40**	**5.607**	**0.349**
	± st.dev.	**± 1.00**	**± 0.06**	**± 1.40**	**± 0.46**	**± 0.03**
R12	IN500+SP20+SO4	20.90	1.050	70.22	14.677	0.737
R13	IN500+SP20+SO4	22.20	1.115	57.46	12.757	0.641
R14	IN500+SP20+SO4	20.90	1.050	58.57	12.241	0.615
R15	IN500+SP20+SO4	18.90	0.950	59.22	11.192	0.562
	Aver. R12–R15	**20.725**	**1.041**	**61.38**	**12.717**	**0.639**
	± st.dev.	**±1.36**	**± 0.07**	**± 5.95**	**± 1.46**	**± 0.07**

Oxygen content in biogas was very low, that confirms that tightness of gas collection system was not impaired. Biogas or methane values in Table 3 and in Fig. 3 are presented with subtracted average biogas or methane volumes obtained from the control bioreactors (R1, R16). Specific biogas and methane yield from every bioreactor with wheat straw pellets or wheat straw pellets with additives is shown in Fig. 3.

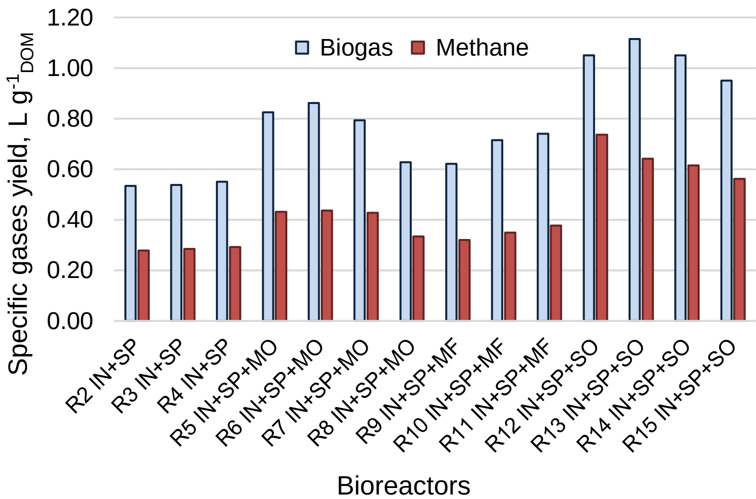

Figure 3. Specific biogas and methane yield from bioreactors with wheat straw pellets or its co-fermentation with molasses, sunflower oil and catalyst Metaferm.

Pre-grinding of wheat straw before pelletizing also may increase methane yield significantly. This could be explained by the fact that the raw materials were well distributed within substrate and microbial access to the raw material was improved. Average specific methane yield and methane percentage in biogas from every group of similar bioreactors is shown in Fig. 4.

As can be seen from the Table 3 and Fig. 4, the co-fermentation results of wheat straw pellets with sunflower oil or with molasses, results increase of average methane production by 124.1% or 43.1% respectively. The addition of catalyst Metaferm 1 mL (5% of pellets weight) in straw pellets substrate increases methane yield by 22.3%. Content of methane in biogas from wheat pellets decreases by 2.3% after addition of the catalyst Metaferm. Methane content increases by 0.3% or 8.7% after addition of the molasses or sunflower oil respectively. Increase of methane content in biogas with sunflower oil can be explained with high content of the fatty acids in additive. Metaferm containing vitamins and micronutrients have the positive effect on anaerobic fermentation of wheat straw pellets.

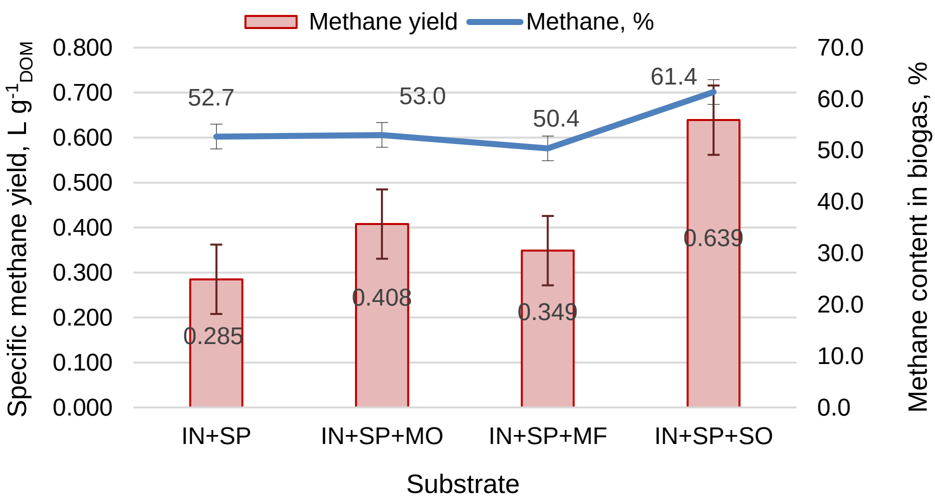

Figure 4. Average specific methane yield and average methane content in biogas from different straw pellets co-fermentation substrates.

Further investigations are needed to explore the biogas and methane potential from different local straw type, straw pellets and briquettes, and from its co-fermentation with different nutrients, micronutrients and biologically active substances.

CONCLUSIONS

Wheat straw pellets sinking in the liquid without forming a floating layer can be regarded as an advantage compared to anaerobic fermentation of roughly chopped straw.

The average specific biogas or methane yield from wheat straw pellets without additives was 0.540 L $g^{-1}{}_{DOM}$ or 0.285 L $g^{-1}{}_{DOM}$ respectively.

The average methane content in biogas from wheat straw pellets in biogas was 52.7%. The results of the study show that wheat straw pellets are a good raw material for methane production.

Co-fermentation of wheat straw pellets with fried sunflower oil (23% of straw pellets weight) produces the specific methane yield 0.639 L $g^{-1}{}_{DOM}$ that was higher by 124% compared to wheat straw pellets without additives.

Specific methane yield obtained from co-fermentation of straw pellets with addition of molasses (19% of pellets weight) was 0.408 L $g^{-1}{}_{DOM}$ that was higher by 43.1% compared to wheat straw pellets without additives.

Addition of 1 mL (5% of pellets weight) catalyst Metaferm in straw pellets substrate increase the specific methane yield by 22.3% compared to wheat straw pellets without additive. Catalyst Metaferm can be recommended as an effective additive to improve the fermentation process and to increase the methane yield from wheat straw pellets.

ACKNOWLEDGEMENTS. This work has been supported by the Latvian National Research Programme LATENERGI.

REFERENCES

Angelidaki, I., Alves, M., Bolzonella, D., Borzacconi, L., Campos, J., Guwy, A., Kalyuzhnyi, S., Jenicek, P. & van Lier, J. 2009. Defining the biomethane potential: proposed protocol for batch assays. *Water Science & Technology* **59(**5), 927–934.

Baader, B., Done, E. & Brenndorfer, M. 1978. Biogas in theory and practice. *KTBL-Schrift* **229**, 133 pp. (in German).

Becker, C. KTBL. 2007. *Faustzahlen biogas*, FNR, ISBN 978-3-930371-46-5. 181 pp. (in German).

Cenian, A., Gołaszewski, J. & Noch, T. 2012. *Eco-Energetic – Biogas*. Proceedings of Baltic Biogas Forum, Gdansk, 188 pp.

Chandr, R., Takeuch, H., Hasegawa, T. & Kumar, R. 2012. Improving biodegradability and biogas production of wheat straw substrates using sodium hydroxide and hydrothermal pretreatments. *Energy* **43**, 273–282.

Dubrovskis, V. & Adamovics, A. 2012. *Bioenergetikas horizonti* (Horizons of bioenergetics), Jelgava, 352 pp. (in Latvian).

Dubrovskis, V., Plume, I., Kazulis, V., Celms, A., Kotelenecs, V. & Zabarovskis, E. 2012. Biogas production potential from agricultural biomass and organic residues in Latvia, in: *11th International Scientific Conference Engineering for Rural Development*, Jelgava, pp. 566–571.

Duong, S. 2014. Systematic Assessment of Straw as Potential Biogas Substrate in Co-digestion with Manure, *Master's thesis*, Linkoping University, 77 pp.

Kaltschmitt, M. 2010. *Methodenhandbuch*, Leipzig, 93 pp. (in German).

Kinetics biofuel. 2015. Brochure, Denmark, Baelum, 8 pp. *http://www.kineticbiofuel.com/brochure-uk.* Accessed 26.01.2018.

Leyerica, J., Valles, S., Flors, A. 1984. Kinetics of rice straw methane fermentation. *Appl. Microbiol. Biotechnol.* **19**, 70–74.

Moller, H. & Hansen, M. 2014. Briquettes of straw and dry grass double biogas production. *FiB* no. **47**, 5 pp.

Walsh, L. 2015. Straw pellets triple biogas yields. *ENDS Report | ENDS Europe*. *https://www.endswasteandbioenergy.com/article/1328673/straw-pellets-triple-biogas-yield*s. Accessed 26.01.2018.

Agronomy Research **16**(3), 696–707, 2018
https://doi.org/10.15159/AR.18.123

On the degradation of metformin and carbamazepine residues in sewage sludge compost

E. Haiba[1], L. Nei[1,*], K. Herodes[2], M. Ivask[1] and M. Lillenberg[3]

[1]Tallinn University of Technology, Tartu College, Puiestee 78, EE51008 Tartu, Estonia
[2]University of Tartu, Institute of Chemistry, Ravila 14A, EE51010 Tartu, Estonia
[3]Estonian University of Life Sciences, Kreutzwaldi 58A, EE51014 Tartu, Estonia
[*]Correspondence: lembit.nei@ttu.ee

Abstract. Recent decades have shown intensive studies devoted to the fate of pharmaceuticals in the environment. These studies have involved the development of analytical tools, determination of pharmaceuticals in different compartments, composting technologies, and plant uptake of pharmaceuticals. The presence of organic pollutants in sewage sludge, including pharmaceuticals, is a problem of major concern. The re-use of sewage sludge should be encouraged since it represents a long-term solution provided that the quality of the sludge re-used is compatible with public health and environmental protection requirements. Composting is a widely recognized way of making the soil application of sewage sludge safer.
In this study, the impact of sewage sludge composting on the degradation of metformin (MET), by far the most often prescribed antidiabetic drug worldwide, and carbamazepine (CBZ), a poorly biodegradable but widely used as an anticonvulsant drug to cure depression and seizures, were analysed. The anaerobically digested and dewatered sewage sludge samples were collected from municipal wastewater treatment plant. Composting experiments were performed under fixed conditions during 30 days. The results of the experiment showed that during a 1-month composting period more than 90% of MET residues degraded, but no degradation of CBZ took place during the composting period. The half-life of MET was 3 days for the compost mixture with the ratios of 1:3 and 1:2 (v:v). The results of this study show that composting maylead to the efficient degradation of MET, whereas for the elimination of CBZ from sewage sludge different means should be used.

Key words: sewage sludge compost, sawdust, fertilizers, metformin, carbamazepine.

INTRODUCTION

The world's pharmaceutical industry has become one of the fastest growing and profitable business sectors. It generates enormous volumes of waste, either directly or indirectly. Hundreds of different active pharmaceutical ingredients (APIs) are discarded in the environment (Agamuthu & Fauziah, 2011). There is clear evidence of impacts of APIs on the building up of bacterial antibiotic resistance (Helwig et al., 2013). As pharmaceuticals are designed to be resistant to biodegradation and current technology at the majority of wastewater treatment plants is unable to remove most APIs, ecosystems are thus exposed to these pollutants (Vallini & Townend, 2010).

Sewage sludge, a residue from the treatment of domestic and industrial wastewater, may be itself regarded as hazardous waste which may cause several undesired consequences due to biological and chemical contaminants, but under certain conditions it can also be used as a fertilizer (Haiba et al., 2016). Taking into account the latter, its safety with respect to pharmaceutical residues (in addition to other potential factors, e.g. pathogens, heavy metals, etc.) must be assessed before use (Kipper et al., 2011). Land application of sewage sludge can be a source of the contamination of food plants by pharmaceutical products (Lillenberg et al., 2010). Plant uptake of pharmaceutical residues, present (even in very small quantities) in soils fertilized with sewage sludge compost, is an obvious reality (Kipper et al., 2011). Although sewage compost is rich in minerals, enabling long-lasting supply for the fast growth of plants (Järvis et al., 2016), antimicrobials consumed even in very small amounts with everyday food can initiate strains of resistant bacteria in human and animal organisms (Kipper et al., 2017). Due to the fact that the use of composted sewage sludge as soil fertilizer is a common practice, knowledge on how the stabilization process affects the reduction of contaminants in this matter is considered crucial (Poluszyńska et al., 2017).

It has been shown that the concentrations of pharmaceuticals decrease after sewage sludge digestion and composting, but they are still present in detectable amounts (Haiba et al., 2016). Amendments of sawdust clearly speed up the degradation of sulfonamides and fluoroquinolones, whereas the mixtures with peat and straw perform lower abilities to decompose the residues of these pharmaceutical (Haiba et al., 2016). In addition to this, sawdust is able to regulate the moisture content and increase the porosity of composting material (Li & Li, 2015). Sawdust has beneficial effects on composting of municipal solid waste. Yousefi et al. (2013) have shown that all compost treatments reached thermophilic temperature rapidly, but the temperature of composting without sawdust showed fluctuations with a rapid drop in the thermophilic temperature and further increase thereafter. On the basis of observed trends in temperature, the composting piles with sawdust required shorter composting periods than those without any sawdust (Yousefi et al., 2013). From an agricultural point of view, sludge co-composted with particularly fine-textured sawdust is the most proper compost material to be applied to soils (Ammari et al., 2012).

The study conducted by Zhong et al. (2018) compared the development of various physicochemical properties and the composition of microbial communities involved in the composting process in the solid fraction of dairy manure (SFDM) with a sawdust-regulated SFDM. The succession of bacteria in both groups proceeded in a similar pattern, suggesting that the effects of the sawdust on bacterial dynamics were minor. Based on this the authors concluded that this confirms the feasibility of composting using only the SFDM. However, this study does not handle the problems associated with different organic pollutants present in dairy manure.

A PhD study was conducted to examine the degradation of some widely used drugs, as fluoroquinolones, sulfonamides, diclofenac (DFC), triclosan (TCS), metformin (MET) and carbamazepine (CBZ) during composting processes, using several bulking agents and different ratios of sewage sludge and sawdust in the mixture (Haiba, 2017). The results reflecting the degradation of sulfonamides and fluoroquinolones, DFC and TCS have been published recently (Haiba et al., 2016 and 2017). Higher proportions of sawdust clearly speeded up the degradation of both DFC and TCS. The current paper is to reflect the results obtained in studying the degradation of MET and CBZ during sewage sludge co-composting with different portions of sawdust, and to compare the outcomes of this work with the results obtained for DFC and TCS, formerly reported in *Agronomy Research* (Haiba et al., 2017) According to the information available from the scientific publications the biodegradation rate of MET is high, whereas the biodegradation of CBZ does not take place (Mrozik & Stefańska, 2014; Blair et al., 2015; Butkovskyi et al., 2016). DFC readily biodegrades in agricultural soils, whereas the degradation of TCS only partly follows this pathway (Xu et al., 2009).

MET is the first-line medication for the treatment of type 2 diabetes (Maruthur et al., 2016). This disease affects more than 200 million people worldwide (Reitman & Schadt, 2007; Trautwein & Kümmerer, 2011). The results published in 2015 by Niemuth & Klaper demonstrated that MET acts as an endocrine disruptor at environmentally relevant concentrations (Haiba, 2017). Unlike many pharmaceutical drugs, MET is not metabolized by humans but passes unchanged through the body. With no natural degradation processes, MET can be easily reintroduced to humans as they enter the food chain (Trautwein et al., 2014). Detection of MET in seawater and tap water proved the absence of an efficient degradation process in ocean environments or drinking water preparation which suggests a high persistence and the potential for ubiquitous distribution (Trautwein et al., 2014; Haiba, 2017). During sewage treatment a significant reduction of MET concentrations is observed which seems to be mainly due to microbial degradation. Despite the high removal efficiency of sewage treatment plants (STPs), MET is still released in significant amounts into the aquatic environment (Scheurer et al., 2009). MET is a mobile compound with low affinity to soils (Mrozik & Stefańska, 2014). This indicates that this drug may be a potential threat to ground and surface water (Benotti & Brownawell, 2007; Haiba, 2017).

CBZ, an antiepileptic drug, is one of the most frequently detected pharmaceuticals in soil and aquatic environments (Zhang et al., 2008; Oosterhuis et al., 2013). CBZ is used for the treatment of seizure disorders, for relief of neuralgia, and for a wide variety of mental disorders. Approximately 72% of orally administered CBZ is absorbed, while 28% is unchanged and subsequently discharged through the feces (RxList4; Zhang et al., 2008; Haiba, 2017). Nieto et al. (2010) determined concentrations between 11 and 42 mg kg^{-1} (dry weight – dw) for CBZ in samples from two STPs. However Miao et al. (2005) detected CBZ at concentration 69.6 μg kg^{-1} (dw) in untreated biosolids and at concentration 258.1 μg kg^{-1} (dw) in treated biosolids. Chefetz et al., 2008 indicated that CBZ exhibits the persistence characteristic of organic contaminants, potentially leading to long-term environmental risks (Haiba, 2017). It is known that CBZ is toxic for some algae, bacteria, invertebrates and fish (Camacho-Munoz et al., 2010). There are no conclusive results confirming the effects (or their lack) of prolonged exposure of organisms to low concentrations of CBZ (Rezka et al., 2015; Haiba, 2017).

CBZ is highly persistent and frequently found in sewage, surface waters and managed aquifer recharge systems (Leclercq et al., 2009; Nieto et al., 2010), and once it is discharged into the environment it causes toxicity (Joss et al., 2006; Verlicchi et al., 2012). Removal of CBZ and its metabolites from municipal sewage treatment plant is very low (~8%). CBZ is persistent in soils (Li et al., 2013; Grossberger et al., 2014; Paltiel et al., 2016) and has been shown to be taken up and accumulate in a variety of crops (Winker et al., 2010; Shenker et al., 2011; Holling et al., 2012; Goldstein et al., 2014; Malchi et al., 2014, Haiba, 2017). CBZ is recalcitrant both in biodegradation and photolysis experiments. This compound is retained by the soil where it is accumulated due to its low degradation rate. Slow degradation rate coupled with plant uptake phenomenon indicates that CBZ present in biosolids amended soils is a significant concern and potential risk (Durán-Álvarez et al., 2015). Researchers have quantified acute toxicity of CBZ < 100 mg L^{-1} (Malarvizhi et al., 2012; Haiba, 2017).

MATERIALS AND METHODS

The procedures described in the current section are identical to those presented in Haiba et al., 2017 with the exception that the drugs used were different: instead of examining the concentration changes of DFC and TCS, the degradation of CBZ and MET was studied during sewage sludge composting. The composting parameters were in excellent agreement with those presented in Haiba et al., 2017, showing the efficiency of the composting process.

Chemicals and materials

CBZ (99.9%) and MET hydroxide (99.8%) were obtained from Sigma-Aldrich. LC-MS eluent components were: methanol (≥ 99.9%; LC-MS Ultra CHROMASOLV; Fluka), water purified in-house using Millipore Milli-Q Advantage A10 system, 1,1,1,3,3,3-hexafluoroisopropanol (HFIP, Sigma-Aldrich), NH_4OH (25%; eluent additive for LC-MS; Fluka) and formic acid (≥ 98%; puriss p.a., Sigma-Aldrich). The samples were prepared using vortex mixer VWR International, shaker Elpan 358S, centrifuge Eppendorf 5430R and ultrasonic bath Bandelin Sonorex were used. Sample extracts were filtered through Sartorius Minisart RC4 (regenerated cellulose, pore size 0.2 μm, membrane diameter 4 mm) syringe filters using disposable 2 mL syringes (Brand).

Sample preparation

The anaerobically digested and subsequently dewatered by centrifugation sewage sludge samples were obtained from a municipal wastewater treatment plant. Prior to the treatment by aerobic composting under laboratory conditions the sewage sludge was mixed with sawdust at two different ratios (1:2 and 1:3 sludge: sawdust, v:v). The initial concentration of both CBZ and MET was 2 mg kg^{-1} in relation to dry weight (dw). Reference piles without additions of pharmaceuticals and with the same ratios of sludge and sawdust were prepared. Samples were thawed at room temperature and mixed by vigorous shaking. For extraction about 5 g of sample was precisely weighted into 50 mL polypropylene centrifuge tube. The following extraction procedure was used:

1. 15 mL of extraction solvent (1% v/v formic acid in ethanol) was added to a sample tube.
2. Vortex mixed for 30 s.
3. The sample tube was tightly capped and placed horizontally on a shaker (200 rpm) for 10 min.
4. The tube was turned into vertical position and shaken manually to ensure that the solid content is in contact with extraction solvent.
5. Extraction was continued by sonicating during 10 min.
6. Samples were centrifuged at 7,830 rpm during 5 min.
7. The extracts were removed from the tube using pipette.

Steps 1-7 were repeated five times with each sample. Extracts were combined in 100 mL polypropylene bottles, mixed and weighted. From each extract 15 mL was taken into 15 mL polypropylene centrifuge tube for further treatment. Prior to LC-MS analysis, sample extracts were diluted: to 100 µl extract 1,400 µl of MilliQ water were added in 1.5 mL Eppendorf tube. Automatic pipette was used for dosing, but all the solutions were weighted. The solutions were vortex-mixed and filtered through syringe filter. First five drops of filtrate were discarded and the remaining (ca 1 mL) was collected into auto-sampler vial (2 mL glass vial).

Calibration samples

Calibration and quality control samples were prepared by diluting stock solutions of analytes. Stock solutions were prepared by dissolving appropriate amount of analytes in ethanol. Working standards were prepared in 1.5 mL Eppendorf tubes by diluting 600 µl of stock solution with 400 µl MilliQ water. Similarly to preparation of sample solutions, all solutions were prepared by weight, vortex-mixed and filtered through syringe filters. Concentrations of the solutions used for calibration were chosen according to the linear range for each analyte.

LC-MS/MS analysis

Sample extracts were analyzed (as described in Haiba et al., 2017) using LC-MS/MS system consisting of ultra-high performance liquid chromatograph UHPLC Agilent 1290 Infinity and mass spectrometer Agilent 6495 Triple Quad. The liquid chromatograph consisted of the following modules: binary high-pressure gradient pump with built-in degasser, autosampler with sample compartment cooling and column thermostat. Waters XBridge C18 (150 mm × 3 mm, 3.5 µm) analytical column and Waters Guard Cartridge (20 mm × 4.6 mm) (Waters) precolumn were used for sample analysis.

For analyte detection triple quadrupole mass spectrometer equipped with heated electrospray interface (HESI) Agilent JetStream was used. Chromatographic separation was carried out using gradient elution. As the weak component of eluent (A), 5 mM HFIP buffer solution (pH adjusted to 9 using NH_4OH) was used. The strong component of the eluent (B) was methanol. The gradient program started from 10% B and content of B was increased to 100% during 33 minutes. For the following 3 minutes isocratic (100% B) elution was used, followed by 3 min gradient to 10% B. For equilibration the column was eluted with 10% B for 4 minutes. Eluent flow rate was 0.3 mL min^{-1}, column temperature maintained at 30 °C and injection volume 10 µl. Multiple reaction monitoring (MRM) mode was used for analyte detection. MRM transitions used are presented in Table 1.

Table 1. MRM transitions, collision energies (CE) and ionization polarities used for analysis

Analyte	Precursor ion, *m/z*	Product ion, *m/z*	CE	Polarity mode
Carbamazepine	237	194	20	positive
	237	179*	40	positive
Metformin	130	71	25	positive
	130	60	10	positive

* – quantitative transition.

The following ion source and MS parameters were used for analysis: drying gas temperature 250 °C and flow rate 14 L min^{-1}, nebulizing gas pressure 20 psi (138 kPa), heating gas temperature 350 °C and flow rate 11 L min^{-1}, capillary voltage 3,000 V. As drying, nebulizing, heating and collision gas nitrogen was used. The instrument was controlled using Agilent MassHunter Workstation ver B.07.00 software. For quantitative analysis Agilent MassHunter Workstation Quantitative analysis ver B.07.01 software was used.

RESULTS AND DISCUSSION

Before spiking the (initial) concentrations of MET in the mixtures of sewage sludge and sawdust were very low: 1 to 2 μg kg^{-1} (dw) (Table 2). As it can be seen from Table 2, none of the compost mixtures was free of CBZ. Its concentrations were from 41 to 62 μg kg^{-1} (dw). This data for CBZ is in reasonable agreement with the results published by Miao et al. in 2005 (Haiba, 2017). Similar concentrations with CBZ were found in compost mixture before spiking for DFC (64 to 86 μg kg^{-1} dw) (Haiba et al., 2017).

Table 2. Concentrations of metformin and carbamazepine in sewage sludge–sawdust mixtures (mg kg^{-1}, dw)

Compound	Mixture ratio (v:v)	Before spiking	1 day	1 week	1 month
Metformin	1:2	0.002 ± 0.000	2.14 ± 0.25	0.44 ± 0.02	0.18 ± 0.01
	1:3	0.001 ± 0.000	1.95 ± 0.15	0.30 ± 0.02	0.14 ± 0.02
Carbamazepine	1:2	0.062 ± 0.002	3.11 ± 0.38	2.59 ± 0.05	3.20 ± 0.10
	1:3	0.046 ± 0.003	2.69 ± 0.26	2.31 ± 0.08	2.32 ± 0.08

lower detection limit for MET – 0.009 ng mL^{-1}; for CBZ – 0.004 ng mL^{-1} in injected solution.

After preparing compost mixtures unexpectedly high concentrations of CBZ were detected. This phenomenon can be explained with the rapid loss of organic matter during the initial stage of composting and is in agreement with the results obtained by Blair et al. (2015), which showed that the concentrations of CBZ and its metabolites increased on a dry weight basis between untreated and treated biosolids. It has been also established that in wastewater treatment plants CBZ sometimes exhibits negative removal efficiency (Collado et al., 2014, Haiba, 2017).

The results measured after 1 week showed that MET had decreased by 79% in compost mixtures with sludge-sawdust ratios 1:2 (v:v). In the case of compost samples with the ratios of 1:3 (v:v) the relevant concentration drop was only 85%.

The results given in Tables 2 and 3 showed that no degradation of CBZ took place, whereas over 90% of MET degraded during a 1-month composting (Haiba, 2017). Butkovskyi et al. (2016) have shown that under specific conditions the partial degradation of CBZ takes place. CBZ is not mineralized in soil but is transformed to a range of transformation products, especially to the recalcitrant acridone-*N*-carbaldehyde (Li et al., 2013). The degradation products of CBZ are more toxic than CBZ (Donner et al., 2013). The formation of these products might also take place during sewage sludge composting (Butkovskyi et al., 2016; Haiba, 2017).

Table 3. Extent of degradation (%) for metformin and carbamazepine during one week and month composting

Sample No	Mixture ratio (v:v)	Metformin		Carbamazepine	
		1 week	1 month	1 week	1 month
1	1:2	79	91	16	-11
2	1:3	85	93	14	13

CBZ readily adsorbs on sludge particles (Blair et al., 2015; Nielsen & Bandosz, 2016; Haiba, 2017). The work carried out by Koba et al. (2016) showed that CBZ and its metabolites are persistent under the studied conditions in soils. According to Li et al. (2013) the values of $t_{1/2}$ for CBZ in soils were between 46 and 173 days (in the studied mixtures $t_{1/2}$ was 178 to 222 days.

CBZ was an exception in the study: this compound was persistent under all studied conditions. According to Collado et al. 2014 in some cases CBZ exhibits even negative removal efficiency with no seasonal variation (Golovko et al., 2014). The results showed this same phenomen in this study (see Table 4). This leads to the conclusion that composting is not an appropriate mean for degrading this compound.

Table 4. The degradation rate constant and half-lives of carbamazepine and metformin

Compound	Mixture ratio (v:v)	Current study			Data from literature		
		k(d^{-1})	$t_{1/2}$ (d)	%	k(d^{-1})	$t_{1/2}$ (d)	%
CBZ	1:2	0.00	222	-11		46…173[a]	
	1:3	0.00	178	13			
MET	1:2	0.22	3	91	0.12–0.26[a]	1–5[a]	99–100[a]
	1:3	0.27	3	93	0.22–0.27[b]	2–3[b]	

[a] – agricultural soil, [b] – compost mixture; CBZ – Li et al. (2013); MET– Mrozik & Stefańska, 2014.

For comparison, the degradation of TCS takes place only partly during one-month composting period, indicating that longer periods are needed for the more complete removal of pharmaceutical residues from sewage sludge based compost (Haiba et al., 2017). TCS gives the following k and $t_{1/2}$ values in the case of agricultural soils (Xu et al., 2009; Haiba, 2017): k = 0.05–0.04 d^{-1}; $t_{1/2}$ = 13–20 d. In sterile soil k = 0.02 d^{-1} and $t_{1/2}$ = 35 d; 45% of TCS degrades during 30 days. In the case of compost mixtures k = 0.03–0.05 d^{-1} and $t_{1/2}$ = 13–26 d. The level of degradation was 55–81%. TCS readily adsorbs on soil particles and due to this its mobility in soils is low (Xu et al., 2009; Haiba, 2017). Bioavailability of TCS greatly decreases in biosolids-amended soils. Biosolids decrease plant uptake primarily by increasing soil organic carbon content and subsequently sorption (Fu et al., 2016; Haiba, 2017).

Results of this study and results presented in Haiba et al. (2017) showed clearly that the degradation of both MET (93%) and DCF (98%) almost fully takes place already during one-month composting period in the case of compost samples with the ratios of 1:3 (v:v). According to Mrozik & Stefańska (2014) MET appears to be a highly mobile compound with a low affinity to soils (K_d = 1.4–0.5 mL g_{ss}^{-1} for MET in different soils). MET is polar and very soluble in water; thus it interacts more strongly with water than with the soil surface. Although the half-lives of MET were 1–5 days in different soils (Table 4), due to its weak sorption MET may be a potential threat to ground and surface water (Benotti & Brownawell, 2007; Haiba, 2017). The degradation of MET takes place rapidly and fully both in soils (from Mrozik & Stefańska, 2014: $k = 0.12–0.26\ d^{-1}$; $t_{1/2} = 1–5$ d) and compost mixtures ($k = 0.22–0.27\ d^{-1}$; $t_{1/2} = 2–3$ d). According to Markiewicz et al. (2017) in most cases MET follows a dead-end pathway with formation of guanylurea. The formed guanylurea does not degrade any further and also does not show toxic properties. In the case of different soils there is a 99–100% degradation of MET during a 30-day period (Mrozik & Stefańska, 2014), whereas in the studied compost mixture degradation was lower at 92–93% (Table 4).

Similarly, DCF is not persistent and is readily biodegradable in soil; its degradation follows the first-order exponential decay model and half-life ($t_{1/2}$) is ranging from 0.4 to less than 5 days (Xu et al., 2009; Al-Rajab et al., 2010; Dalkmann et al., 2012; Carter et al., 2014; Grossberger et al., 2014; Haiba, 2017). The bioconcentration factors found for DCF were high in the case of long-term irrigation with sewage (Christou et al., 2017). In agricultural soils (Xu et al., 2009) $k = 0.23–0.16\ d^{-1}$and $t_{1/2} = 3–4$ d. In the case of sterile soil $k = 0.01\ d^{-1}$ and $t_{1/2} = 70$ d (Xu et al., 2009), and for compost mixtures $k = 0.09–0.1\ d^{-1}$ and $t_{1/2} = 7–8$ d (Haiba, 2017). According to this data in sterile soil only 26% of DCF degrades during a 30-day period, whereas in compost mixtures the level of degradation was 92–98%. This leads to the conclusion that the biodegradation of DCF prevails over its chemical degradation.

Data obtained as a result of degradation experiments were fitted to the exponential decay model: $C = C_0e^{-kt}$ to obtain the degradation rate constant k. Half-lives ($t_{1/2}$) were calculated by the equation: $t_{1/2} = 0.693/k$ (Xu et al., 2009; Haiba, 2017).

As a rule, the degradation rate of pharmaceuticals depends on the media consistency. In agricultural soils biodegradation of pharmaceuticals is faster than in freshly made compost mixtures probably due to the fact that the formation of microbial communities in the latter presumably takes time. Strong adsorption of pharmaceuticals to soil or sludge particles inhibits the degradation of pharmaceuticals. At the same time, this also slaps down the plant uptake of these pharmaceuticals, which is important in the view of food safety (Haiba, 2017).

CONCLUSIONS

This study was carried out to demonstrate the degradation of CBZ and MET in composting processes using different ratios of sewage sludge and bulking agent (sawdust). In the case of MET, compost samples with the sludge-sawdust ratios of 1:3 and 1:2 (v:v) yielded similar degradation of more than 90% during a 1-month composting period. No degradation of CBZ takes place during composting experiments.

The current study (involving MET and CBZ) and the results (for DFC and TCS) published in Haiba et al. (2017) leads to the conclusion that composting might ensure the efficient degradation of DCF, MET and TCS, whereas for the elimination of CBZ from sewage sludge different means should be used. The persistence of pharmaceuticals increases in the following line: MET→DFC→TCS→CBZ.

ACKNOWLEDGEMENTS. The authors would like to thank Environmental Investment Centre of Estonia for funding this work.

REFERENCES

Agamuthu, P. & Fauziah, S.H. 2011. Pharmaceuticals in the environment, a prescription for disaster? *Waste Management & Research* **29**, 349–350.

Al-Rajab, A.J., Sabourin, L., Lapen, D.R. & Topp, E. 2010. The non-steroidal anti-inflammatory drug diclofenac is readily biodegradable in agricultural soils. *Science of the Total Environment* **409**, 78–82.

Ammari, T.G., Al-Omari, Q. & Abbassi, B.E. 2012. Composting sewage sludge amended with different sawdust proportions and textures and organic waste of food industry – assessment of quality. *Environmental Technology* **33**, 1641–1649.

Benotti, M.J. & Brownawell, B.J. 2007. Distributions of Pharmaceuticals in an Urban Estuary during both Dryand Wet-Weather Conditions. *Environmental Science & Technology* **41**, 5795–5802.

Blair, B., Nikolaus, A., Hedman, C., Klaper, R. & Grundl, T. 2015. Evaluating the degradation, sorption, and negative mass balances of pharmaceuticals and personal care products during wastewater treatment. *Chemosphere* **134**, 395–401.

Butkovskyi, A., Ni, G., Hernandez Leal, L., Rijnaarts, H.H.M. & Zeeman, G. 2016. Mitigation of micropollutants for black water application in agriculture via composting of anaerobic sludge. *Journal of Hazardous Materials* **303**, 41–47.

Camacho-Munoz, D., Martin, J., Santos, J.L., Aparicio, I. & Alonso, E. 2010. Occurrence, temporal evolution and risk assessment of pharmaceutically active compounds in Doñana Park (Spain), *Journal of Hazardous Materials* **183**, 602–608.

Carter, L.J., Harris, E., Williams, M., Ryan, J.J., Kookana, R.S., Boxall, A.B.A. 2014. Fate and uptake of pharmaceuticals in soil-plant systems. *Journal of Agricultural and Food Chemistry* **62**, 816–825.

Chefetz, B., Mualem, T. & Ben-Ari, J. 2008. Sorption and mobility of pharmaceutical compounds in soil irrigated with reclaimed wastewater. *Chemosphere* **73**, 1335–1343.

Christou, A., Karaolia, P., Hapeshi, E., Michael, C. & Fatta-Kassinos, D. 2017. Long-term wastewater irrigation of vegetables in real agricultural systems: Concentration of pharmaceuticals in soil, uptake and bioaccumulation in tomato fruits and human health risk assessment. *Water Research* **109**, 24–34.

Collado, N., Rodriguez-Mozaz, S., Gros, M., Rubirola, A., Barcelo, D., Comas, J., Rodriguez-Roda, I. & Buttiglieri, G.2014. Pharmaceuticals occurrence in a WWTP with significant industrial contribution and its input into the river system. *Environmental Pollution* **185**, 202−212.

Dalkmann, P., Broszat, M., Siebe, C., Willaschek, E., Sakinc, T., Huebner, J., Amelung, W., Grohmann, E. & Siemens, J. 2012. Accumulation of pharmaceuticals, *Enterococcus*, and resistance genes in soils irrigated with wastewater for zero to 100 years in Central Mexico. *PLoS ONE* **7**(9), e45397.

Donner, E., Kosjek, T., Qualmann, S., Kusk, K.O., Heath, E., Revitt, D.M., Ledin, A. & Andersen, H.R. 2013. Ecotoxicity of carbamazepine and its UV photolysis transformation products. *Science of the Total Environment* **443**, 870–876.

Durán-Álvareza, J.C., Pradob, B., Gonzálezc, D., Sánchezc, Y. & Jiménez-Cisnerosd, B. 2015. Environmental fate of naproxen, carbamazepine and triclosan in wastewater, surface water and wastewater irrigated soil — results of laboratory scale experiments. *Science of the Total Environment* **538**, 350–362.

Fu, Q., Wu, X., Ye, Q., Ernst, F. & Gan, J. 2016. Biosolids inhibit bioavailability and plant uptake of triclosan and triclocarban. *Water Research* **102**, 117–124.

Goldstein, M., Shenker, M. & Chefetz, B. 2014. Insights into the uptake processes of wastewater-borne pharmaceuticals by vegetables. *Environmental Science & Technology* **48**, 5593−5600.

Golovko, O., Kumar, V., Fedorova, G., Randak, T. & Grabic, R. 2014. Seasonal changes in antibiotics, antidepressants/psychiatric drugs, antihistamines and lipid regulators in a wastewater treatment plant. *Chemosphere* **111**, 418–426.

Grossberger, A., Hadar, Y., Borch, T. & Chefetz, B. 2014. Biodegradability of pharmaceutical compounds in agricultural soils irrigated with treated wastewater. *Environmental Pollution* **185**, 168−177.

Haiba, E. 2017. Optimization of Sewage Sludge Composting: Problems and Solutions, PhD Thesis, Tallinn University of Technology, 162 pp.

Haiba, E., Nei, L., Ivask, M., Peda, J., Järvis, J., Lillenberg, M., Kipper, K. & Herodes, K. 2016. Sewage sludge composting and fate of pharmaceutical residues – recent studies in Estonia. *Agronomy Research* **14**, 1583−1600.

Haiba, E., Nei, L., Kutti, S., Lillenberg, M., Herodes, K., Ivask, M., Kipper, K., Aro, R. & Laaniste, A. 2017. Degradation of diclofenac and triclosan residues in sewage sludge compost. *Agronomy Research* **15**, 395−405.

Helwig, K., Hunter, C. & Maclachlan, J. 2013. Micropollutant point sources in the built environment: Identification and monitoring of priority pharmaceutical substances in hospital effluents. *Journal of Environmental & Analytical Toxicology* **3**, pp. 177.

Holling, C.S., Bailey, J.L., Heuvel, B.V. & Kinney, C.A. 2012. Uptake of human pharmaceuticals and personal care products by cabbage (Brassica campestris) from fortified and biosolids-amended soils. *Journal of Environmental Monitoring* **14**, 3029−3036.

Joss, A., Carballa, M., Kreuzinger, N., Siegrist, H. & Zabczynski, S. 2006. Wastewater treatment. In: Ternes, T.A., Joss, A. (Eds.), Human Pharmaceuticals, Hormones and Fragrances: the Challenge of Micropollutants in UrbanWater Management. IWA Publishing, London, UK, 468 pp.

Järvis, J., Ivask, M., Nei, L., Kuu, A. & Luud, A. 2016. Effect of Green Waste Compost Application on Afforestation Success. *Baltic Forestry* **22**, 90−97.

Kipper, K., Herodes, K., Leito, I. & Nei, L. 2011. Two fluoroalcohols as components of basic buffers for liquid chromatography electrospray ionization mass spectrometric determination of antibiotic residues. *Analyst* **136**, 4587−4594.

Kipper, K., Lillenberg, M., Herodes, K., Nei, L. & Haiba, E. 2017. Simultaneous Determination of Fluoroquinolones and Sulfonamides Originating from Sewage Sludge Compost. *The Scientific World Journal* **2017**, 8 pp.

Koba, O., Golovko, O., Kodesova, R., Klement, A. & Grabic, R. 2016. Transformation of atenolol, metoprolol, and carbamazepine in soils: The identification, quantification, and stability of the transformation products and further implications for the environment. *Environmental Pollution* **218**, 574–585.

Leclercq, M., Mathieu, O., Gomez, E., Casellas, C., Fenet, H. & Hillaire-Buys, D. 2009. Presence and fate of carbamazepine, oxcarbazepine, and seven of their metabolites at wastewater treatment plants. *Archives of Environmental Contamination and Toxicology* **56**, 408−415.

Li, J.Y., Dodgen, L., Ye, Q.F. & Gan, J. 2013. Degradation kinetics and metabolites of carbamazepine in soil. *Environmental Science & Technology* **47**, 3678−3684.

Li, Y. & Li, W. 2015. Nitrogen transformations and losses during composting of sewage sludge with acidified sawdust in a laboratory reactor. *Waste Management & Research* **33**, 139–145.

Lillenberg, M., Kipper, K., Herodes, K. & Nei, L. 2010. Plant Uptake of some Pharmaceuticals from Fertilized Soils. Proceedings of the 2010 International Conference on Environmental Science and Technology (ICEST 2010), pp. 161−165.

Malarvizhi, A., Kavitha, C., Saravanan, M. & Ramesh, M. 2012. Carbamazepine (CBZ) induced enzymatic stress in gill, liver and muscle of a common carp, Cyprinus carpio. *Journal of King Saud University – Science* **24**, 179–186.

Malchi, T., Maor, Y., Tadmor, G., Shenker, M. & Chefetz, B. 2014.Irrigation of root vegetables with treated wastewater: evaluating uptake of pharmaceuticals and the associated human health risks. *Environmental Science & Technology* **48**, 9325−9333.

Markiewicz, M., Jungnickel, C., Stolte, S., Białk-Bielińska, A., Kumirska, J. & Mrozik, W. 2017. Primary degradation of antidiabetic drugs. *Journal of Hazardous Materials* **324**, 428–435.

Maruthur, N.M., Tseng, E., Hutfless, S., Wilson, L.M., Suarez-Cuervo, C., Berger, Z., Chu, Y., Iyoha, E., Segal, J.B. & Bolen, S. 2016. Diabetes Medications as Monotherapy or Metformin-Based Combination Therapy for Type 2 Diabetes: A Systematic Review and Meta-analysis. *Annals of Internal Medicine* **164**, 740–751.

Miao, X-S., Yang, J.-J. & Metcalfe, C.D. 2005. Carbamazepine and its metabolites in wastewater and in biosolids in a municipal wastewater treatment plant. *Environmental Science & Technology* **2005**, 7469–7475.

Mrozik, W. & Stefańska, J. 2014. Adsorption and biodegradation of antidiabetic pharmaceuticals in soils. *Chemosphere* **95**, 281–288.

Nielsen, L. & Bandosz, T.J. 2016. Analysis of the competitive adsorption of pharmaceuticals on waste derived materials. *Chemical Engineering Journal* **287**, 139–147.

Niemuth, N.J. & Klaper, R.D. 2015. Emerging wastewater contaminant metformin causes intersex and reduced fecundity in fish. *Chemosphere* **135**, 38–45.

Nieto, A., Borrill, F., Pocurull, E. & Marce, R.M. 2010. Occurrence of pharmaceuticals and hormoones in sewage sludge. *Environmental Toxicology and Chemistry* **29**, 1484–1489,

Oosterhuis, M., Sacher, F.L. ter Laak, T. 2013. Prediction of concentration levels of metformin and other high consumption pharmaceuticals in wastewater and regional surface water based on sales data. *Science of the Total Environment* **442**, 380–388.

Paltiel, O., Fedorova, G., Tadmor, G., Kleinstern, G., Maor, Y. & Chefetz, B. 2016. Human exposure to wastewater-derived pharmaceuticals in fresh produce: a randomized controlled trial focusing on carbamazepine. *Environmental Science & Technology* **50**, 4476–4482.

Poluszyńska, J., Jarosz-Krzemińska, E. & Helios-Rybicka, E. 2017. Studying the Effects of Two Various Methods of Composting on the Degradation Levels of Polycyclic Aromatic Hydrocarbons (PAHs) in Sewage Sludge. *Water, Air, & Soil Pollution* **228:305**, 10 pp.

Reitman, M.L. & Schadt, E.E. 2007. Pharmacogenetics of metformin response: a step in the path toward personalized medicine. *The Journal of Clinical Investigation* **117**, 1226–1229.

Rezka, P., Balcerzak, W. & Kwaśny, J. 2015. Carbamazepine and other anti-epileptic drugs in the aquatic environment. *Technical Transactions, Environment Engineering* **1-Ś/2015**, 111–118.

RxList4. The Internet Drug Index.http://www.rxlist.com/carbatrol-drug.htm

Scheurer, M., Sacher, F. & Brauch, H.-J. 2009. Occurrence of the antidiabetic drug metformin in sewage and surface waters in Germany. *Journal of Environmental Monitoring* **9**, 1608–1613.

Shenker, M., Harush, D., Ben-Ari, J. & Chefetz, B. 2011. Uptake of carbamazepine by cucumber plants– a case study related to irrigation with reclaimed wastewater. *Chemosphere* **82**, 905−910.

Trautwein, C., Berset, J-D., Wolschke, H. & Kümmerer, K. 2014. Occurrence of the antidiabetic drug Metformin and its ultimate transformation product Guanylurea in several compartments of the aquatic cycle. *Environment International* **70**, 203–212.

Trautwein, C. & Kümmerer, K. 2011. Incomplete aerobic degradation of the antidiabetic drug metformin and identification of the bacterial dead-end transformation product guanylurea. *Chemosphere* **85**, 765–773.

Zhang, Y., Geißen, S-U. & Gal, C. 2008. Review. Carbamazepine and diclofenac: Removal in wastewater treatment plants and occurrence in water bodies. *Chemosphere* **73**, 1151–1161.

Zhong, X.-Z., Ma, S.-C., Wang, S.-P., Wang, T.-T., Sun, Z.-Y., Tang, Y.-Q., Deng, Y. & Kida, K. 2018. A comparative study of composting the solid fraction of dairy manure with or without bulking material: Performance and microbial community Dynamics. *Bioresource Technology* **247**, 443–452.

Vallini, G. & Townend, W.K. 2010. Pharmaceutical waste: as in the Titanic we are only seeing the tip of the iceberg. *Waste Management & Research* **28**, 767–768.

Verlicchi, P., Al Aukidy, M. & Zambello, E. 2012. Occurrence of pharmaceutical compounds in urban wastewater: removal, mass load and environmental risk after a secondary treatment—a review. *Science of the Total Environment* **429**, 123–155.

Winker, M., Clemens, J., Reich, M., Gulyas, H. & Otterpohl, R. 2010. Ryegrass uptake of carbamazepine and ibuprofen applied by urine fertilization. *Science of the Total Environment* **408**, 1902–1908.

Xu, J., Wu, L. & Chang, A.C. 2009. Degradation and adsorption of selected pharmaceuticals and personal care products (PPCPs) in agricultural soils. *Chemosphere* **77**, 1299–1305.

Yousefi, J., Younesi, H. & Ghasempoury, S.M. 2013. Co-composting of Municipal Solid Waste with Sawdust: Improving Compost Quality. *Clean-soil, air, water* **41**, 185–194.

Agronomy Research **16**(3), 708–716, 2018
https://doi.org/10.15159/AR.18.137

Odour reduction of manure through addition of boracic charcoal

G. Hampejs[1,*], A. Jäger[1], S. Steiner[1] and K. Steiner[2]

[1]University of Applied Sciences Upper Austria, Faculty of Engineering, Department of Bio & Environmental Technology, Stelzhamerstr. 23, AT4600 Wels, Austria
[2]HBLA Ursprung, Ursprungstraße 4, AT5161 Salzburg Austria
[*]Correspondence: g.hampejs@fh-wels.at

Abstract: Odours released during the land application of manure results from different gases released from the liquid phase. These gases do create objectionable odours in the vicinity of the land-applied manure. In order to reduce the intensity of odour during manure application, we investigated the effectiveness of combining Borkohle with manure during land application.
Boracic acid is widely used as a flame retardant in cellulose insulation. During demolition of existing buildings, this insulation is sorted into its own residual waste fraction. The cellulose fibres are extracted and pelletized on site. Subsequently, the pellets are charred in a pyrolysis furnace. The resulting Borkohle – charcoal containing boron in various compounds - can be used as a soil enhancer and provides the trace element Boron to the fields. Furthermore, Borkohle provides long-term storage of carbon in the soil. Initial trials of combining boracic charcoal with manure additionally showed that odour emissions seemed to be significantly lower when manure was combined with Borkohle.
This work presents methods to quantify the odour reductions resulting from the addition of Borkohle to manure as well as first results. Parameters like the influence of the amount of charcoal added and exposure time have been investigated.
Charcoal was added at concentrations between 5 and 250 g L^{-1}. While applying typical amounts of charcoal, a reduction of odour concentration of up to 85% was observed. A positive correlation between odour reduction and the amount of charcoal added was observed. Charcoal has a negligible effect when exposure times are less than 30 minutes.

Key words: Olfactometer, charcoal, insulation materials, demolition materials, manure.

INTRODUCTION

Demolishing or renovating a building unavoidably produces a range of waste materials. These can include insulating materials made from cellulose fibres. In order to minimise the risk of a fire, they are mixed with boric acid, which acts as a natural fire retardant (Wieland & Bockisch, 2006). When these cellulose fibres are no longer needed, they are sucked away without producing any dust and pelletized on site to simplify transportation (Bode et al., 1993). In a further step, the pellets are pyrolised in a technical process. This gives rise to boron-laden charcoal, hereinafter referred to as 'Borkohle' (Abbrev. BC). In order to be able to use this charcoal made from waste materials for other purposes, the valuable properties of the product must be investigated and proven and their compliance with relevant limit values demonstrated. The boron-laden organic charcoal – or ‘Borkohle’ – produces in this way can be spread on fields by farmers together with manure as a soil improver and as a source of the trace element boron (Glaser et al., 2015; Schulz et al, 2013). Initial field trials for the spreading of biochar on maize fields indicated that the odour emissions of manure mixed with biochar are lower than the odour emissions of manure applied without additives (Isocell, 2017).

The objective of this project at Upper Austria University of Applied Science / Campus Wels is to investigate the extent of odour reduction due to the charcoal and the underlying modes of action. The first step, which is reported on here, should involve the development of suitable test methods and the investigation of the influences of important constraints, in particular the quantity of charcoal and the reaction time.

MATERIALS AND METHODS

The manner in which the experiments for obtaining representative samples are conducted in the laboratory is explained below. To this end, the three applied trial methods are described in more detail.

Preparation of odour samples

Three different approaches were selected in order to simulate the odour of manure in the laboratory. (1) Direct application on the pasture (2) Desorption using a scrubber (3) Direct method in the bag

(1) In this trial, the manure is applied directly to a piece of pasture measuring 0.24 m x 0.24 m located in a capture hood. In order to simulate a standard spreading quantity of, for example, 30 m^3 manure per ha for maize, 172 mL of manure is added to the pasture located in the hood. Next, an odour sample is taken after a certain reaction time. Before the pasture is treated with manure, the intensity of its inherent odour is determined.

(2) The application of manure is simulated by conveying the manure in a sealed circuit to a packed-bed scrubber, where it is brought into contact with the air also being moved around the circuit, and then returned to the collection tank. This simulates the intense contact experienced during conventional manure spreading through scattering. The odour-laden air is passed through a capture hood, from which the air samples can be taken. First, the storage tank located at the scrubber is filled with manure. Then, the process described above starts. The sample is taken after the scrubber has run for a set time.

(3) With this method of making odour samples, the manure is added to a sample bag made from Nalophan® (approx. 15 litres). The bag is filled with synthetic air. After a dwell time of five minutes, the air is transferred to a sample bag. If the odour concentration is too great for an olfactometric evaluation, the odour sample must be pre-diluted. The dilution is made in a ratio of 1:7.3. The odour sample obtained in this way can be subsequently analysed without any problem with the aid of the olfactometer.

This method of sample creation was developed because the other methods used are very time-consuming and complex by comparison as well as being prone to errors. Less manure is needed than in trials with the scrubber.

Odour measurement with the olfactometer

There are various methods available for assessing odours. In order to assess emissions of the kind produced when spreading manure on agricultural land, the aim must be to determine the odour loads. In turn, the expected level of nuisance can be derived from this. As these loads are to be determined on the basis of quantity and concentration, particular importance is placed on determining the odour concentration.

The odour concentrations were determined by means of dynamic olfactometry with an Olfasense Olfactometer TO8, according to EN13725 – Odour. This involves diluting the air sample with clean, non-odorous air until none of the four to six test subjects are able to notice any more odour. The concentration of the diluted sample is increased in several steps by a factor of 2 or $\sqrt{2}$ until the perception threshold is significantly exceeded in all test subjects. The odour concentration is arithmetically determined from the odour thresholds of all test subjects whose results lie within the required tolerance. This correlates with the concentrations of the substances contained in the samples. (Hauschildt & Mannebeck, 2015)

Another way of presenting the odour concentrations is the unit of 'decibel odour' (dB_{od}). Due to the logarithmic relationship between concentration and intensity, which is analogous to the Fechner law for noise, this logarithmic scale is particularly suitable for comparing odours with each other and against specified limit values (Forrest, 2010).

Preparation of manure

Manure A was used in experiments A, B, C and D. Before the experiments, it was passed through a food mill to remove feed residues and other fibres and solids in order not to cause the pump to malfunction, as had been the case in preliminary tests.

Experimental setup

<u>Experiment A:</u> In this experiment, manure A was applied directly to the pasture. 0.8 g of biochar was added to the 172 mL of manure. This corresponds to a quantity of 5 kg of biochar per m^3 of manure. The biochar was allowed to react with the manure for four hours before spreading. Trials were done with 0.25 m^2 of natural grown pasture per trial which was taken from local meadows including 25 cm of sod. The treated manure was spread by hand, spreading drops of the liquor evenly over the pasture sample.

<u>Experiment B:</u> In experiment B, odour samples were taken using the scrubber. For the experiment without biochar, the storage tank was filled with 10 litres of manure A. The first sample was taken two minutes after starting the scrubber, the second after five minutes. Next, the scrubber was cleaned and the storage tank filled with 10 litres of manure A, which had been mixed five hours previously with 50 g of biochar. The sampling was conducted in the same as the sampling without charcoal. The measurements were outside of the measurement range for all samples, i.e. they were each more than 72,176 GE m^{-3}. Because of this, they could not be analysed and no results are available for experiment B.

<u>Experiment C:</u> In experiment C, the odour samples were also obtained with the aid of the scrubber. The difference from experiment B was that a larger quantity of biochar was used. Thus 150 g and 250 g of charcoal were added to 10 litres of manure respectively. The biochar was allowed to react for five hours. The samples were also taken after two and five minutes after starting the scrubber.

Experiment D: Experiment D involved the use of manure A, which had been pretreated in a food mill. The goal of this experiment was to find out whether the reaction time of biochar has an influence on the odour-reducing effect. To this end, 150 g of charcoal were added to 10 litres of manure. Thus three mixtures of manure and charcoal were made. The different reaction times of the charcoal were 30 min., 1 hr. and 2 hrs. Sampling was conducted after the respective reaction time in the scrubber. Two samples were taken for each mixture, two and five minutes respectively after the start of the scrubber. Samples BK-D01 and BK-D02 were made using the direct approach. The reason for this variation was that the other sampling methods are relatively complicated. This method requires much less manure, and the time taken to make the samples as well as the preparation and follow-up work can be reduced. To this end, 1 litre of manure with 150 g of biochar and 1 litre of manure without biochar were stored in a sample bag with 10 litres of synthetic air for 10 minutes. Next, the air was transferred into a fresh sample bag and analysed using the olfactometer.

Experiment E: Experiment E made use of two different methods for making the samples. Both the scrubber and the direct approach were used. In both cases, manure types B and D were used. In the case of the samples that were made in the experiment with the scrubber, the goal was to find out the extent to which a variation of the reaction time of the biochar in the manure has an impact on the odour concentration. Both manure types (B and D) were sampled. 10 litres of manure were used per sample for this. The amount of biochar used was 50 g per sample. An exception are the samples designated BK-E01 and BK-E02, as these were used to determine the odour concentration of the manure without charcoal. Each of the samples was taken five minutes after starting the scrubber. The reaction time of one and two hours respectively was investigated. For the samples made using the direct approach, the question of the extent to which an increase in the added quantity of biochar has an effect on the odour concentration was investigated. 1 litre of manure types B and D was used for each sample. The samples were taken five minutes after the addition of the synthetic air to the mixing bag. The reaction time of the charcoal was not changed and amounted to 30 minutes for all samples in this experiment setup. Samples were made with a charcoal quantity of 50, 150 and 250 g L^{-1}.

Experiment F: In experiment F, the samples were made with the aid of the direct approach method. All four available types of manure were used. 15 g of charcoal were added to each litre of manure. For each type of manure, two samples were made for which a charcoal reaction time of five and ten minutes respectively was selected.

Experiment G: The samples in experiment G was made according to the direct approach. To this end, 1 litre of manure was mixed with 50 and 150 g of biochar respectively. As this experiment was intended to more closely examine the effect of the reaction time of the charcoal on the odour concentration, only the reaction time was varied. Samples were taken after a reaction time of 5, 15, 30, 45 and 60 minutes.

RESULTS AND DISCUSSION

In the following diagrams, the results are summarised as far as possible in the form of the odour level. This achieves a better comparability of the various results and enables correlations to be identified more quickly. Here, too, a maximum measurement certainty of the odour level of ± 2 dBG is taken into consideration.

Results of the direct approach

The results were divided into two diagrams, as the various experiments involved varying the quantity of the charcoal added (Fig. 1) on the one hand, and varying the reaction time of the charcoal (Fig. 2) on the other. Fig. 1 shows the results of experiments D and E, in which the quantity of added charcoal was varied. It can be seen that the odour level of the manure reduces with the addition of the charcoal. It can also be concluded from this figure that the reduction in the odour level correlates to the increasing addition of charcoal.

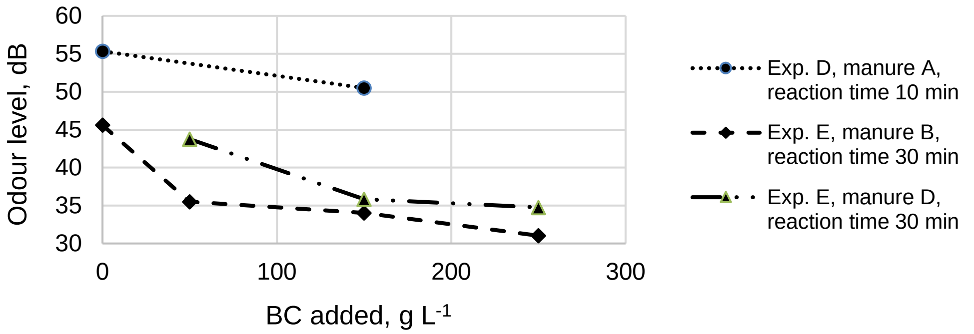

Figure 1. Variation of reaction time at different loads of BC applying experiment D and E showed an important effect at a reaction time of 30 minutes. positive effects were observed for BC loads of 50 gL^{-1}.

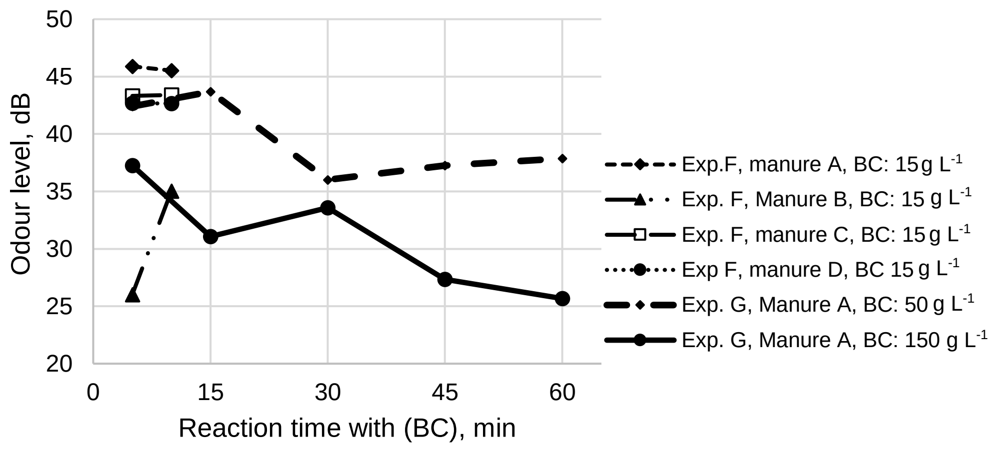

Figure 2. Results for influence of residence time on odor reduction in experiment F and G showed again that effects are poor or unclear at lower loads of BC. For higher loads of BC in experiment G, significant odor reduction could be observed at residence times of 30 to 60 minutes.

Fig. 2 shows the results of experiments F and G, in which the reaction time of the charcoal was varied. On the basis of the available data it is reasonable to conclude that there is hardly any change in the odour level when the reaction time is increased from five to ten minutes. However, if the reaction time is increased to up to one hour, the odour level also falls. It is likely that the combination of an increased quantity of added charcoal and an increased reaction time is responsible for this effect. This becomes clear when the results of experiment G are compared. In each case, manure A was used. The strongest reduction in the odour concentration of up to 12 dB_{OD} was observed with the addition of 150 g L^{-1} of biochar.

Results using the scrubber

The results obtained using the scrubber are presented below. The results were divided into two diagrams according to the varied parameter. On the one hand, the runtime of the scrubber was varied (Fig. 3) and on the other, the reaction time of the charcoal (Fig. 4). Fig. 4 presents the results of experiments C and D. These show that the runtime of the scrubber had a negligible effect on the odour level. The experiment setup proved to be insensitive to the parameter 'runtime of the scrubber'. The main factor here again is the added quantity of charcoal. In some cases (experiment D), no significant reduction in odour could be observed.

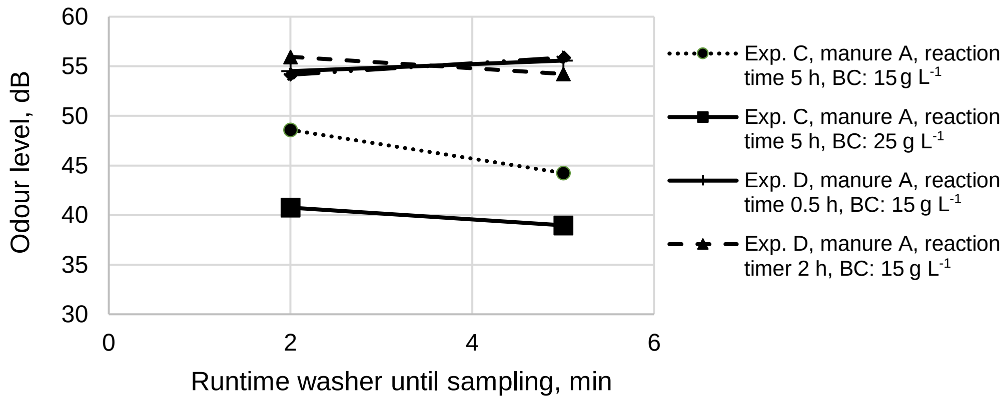

Figure 3. Experiment F and G were used to test if the scrubber experiment is sensitive to washer runtime. The answer is obviously negative. No significant influence of scrubber operation was observed.

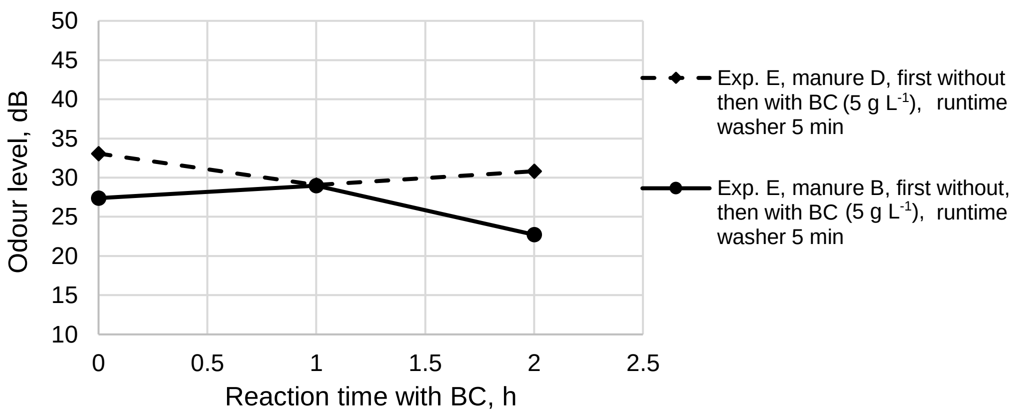

Figure 4. Reduction of odour level at low loads of BC is not clear, even with longer reaction times, applying experiment E.

However, if experiment C is compared with experiment D, the conclusion reached is that the reaction time does indeed have an influence on the odour level. There are concerns here that a reaction time of five hours is set relatively high. The intention in practice is to mix the charcoal with manure only immediately prior to spreading the mixture on the field. In practice, this would give a reaction time of between 30 minutes and one hour. Fig. 4 shows the results of experiment E, in which 2 manures were investigated under the same conditions. The odour level curve is different for the two types of manure used. The results for 2 different manures are an important aspect and require further investigation.

Results of direct spreading

Fig. 5 presents the results of experiment A in graphic form. It is evident that the odour level with added charcoal reduces constantly over time. In contrast, the odour level of the charcoal without additives first rises over time and then falls again towards the end of the observed period, although to a level that is higher than it was at the beginning of the measurement. The odour concentration of the manure treated with charcoal is also consistently at a lower level than the manure without added charcoal. The results of this measurement can be interpreted as an indication of a possible reduction in odour, depending on the manure. At the same time, in comparison to the easier to perform experiments, this complicated method of investigation is not deemed to be any more meaningful than others, but further results showed that the experiment with direct exposure was very sensitive to external influences (failure).

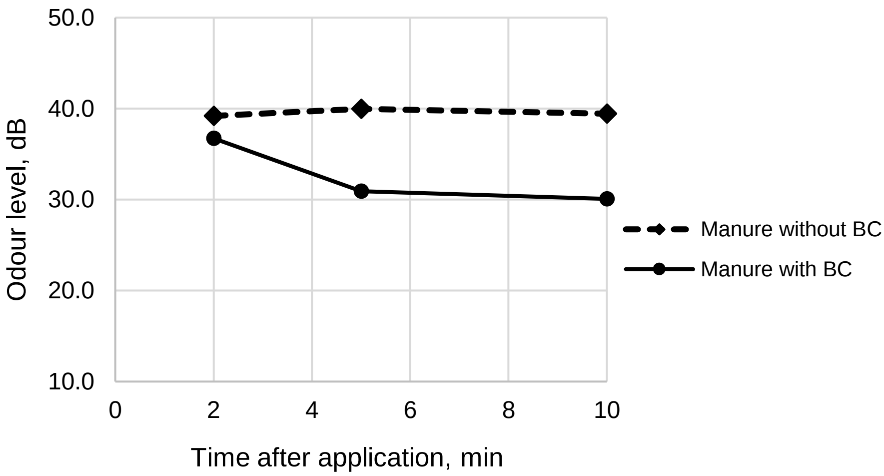

Figure 5. Results of direct spreading on pasture in experiment A showed promising results. With application of BC, odour level was sigificantly lower after a few minutes (> 4).

Relative change in the odour level

Table 1 shows the relative change of the odour level within the various experiments. Note that the change shown is the average change within the respective measurement series. Therefore, the starting value cannot be equated in all cases to the odour level of the untreated manure. It can also come from manure that has been pretreated with charcoal.

Comparing the results increasingly indicates that the reaction time of the charcoal in many instances leads to a reduction in the odour concentration when it lies in the range of about 30 minutes to 4 hours. Furthermore, there is a positive correlation between the reduction in odour and the quantity of charcoal.

Table 1. Relative reduction in the odour level

	Experimental setup	Variable	Odour change
A	direct Application, 4 h react.time, 5 g L^{-1}	amount of BC	- 17.5%
C	scrubber, react.time 5 h, 15 g L^{-1}	amount of BC	- 9.1%
	scrubber, react.time 5 h, 25 g L^{-1}	amount of BC	- 4.2%
D	scrubber, react.time 30 min, 15 g L^{-1}	react.time	+ 2%
	scrubber, react.time 1 h, 15 g L^{-1}	react.time	+ 3.3%
	scrubber, react.time 2 h, 15 g L^{-1}	react.time	- 3.2%
	direct applic., react.time 10 min, 150 g L^{-1}	amount of BC	- 8.7%
E	scrubber, manure D, react.time 1 und 2 h, 5 g L^{-1}	react.time	- 9.7%
	scrubber, manure B, react.time 1 und 2 h, 5 g L^{-1}	react.time	- 5.8%
	direct applic., manure B, react.time 30 min, 50, 150 and 250 g L^{-1}	amount of BC	- 26.5%
	direct applic., manure D, react.time 30 min, 50, 150 and 250 g L^{1}	amount of BC	- 19.3%
F	direct applic., manure A, react.time 5 and 10 min, 15 g L^{-1}	react.time	- 0.9%
	direct applic., manure B, react.time 5 and 10 min, 15 g L^{-1}	react.time	+ 34.6%
	direct applic., manure C, react.time 5 and 10 min, 15 g L^{-1}	react.time	+ 0.2%
	direct applic., manure D, react.time 5 and 10 min, 15 g L^{-1}	react.time	0%
G	direct applic., react.time 5, 15, 30, 45 and 60 min, 50 g L^{-1}	react.time	- 8.7%
	direct applic., react.time 5, 15, 30, 45 and 60 min, 150 g L^{-1}	react.time	- 21.2%

CONCLUSION

It was shown that the testing approaches are suitable for investigating the influence of different parameters on the release of odour when spreading manure. The 'direct approach' method offers the possibility to investigate the reduction in odour in very simple experiments. It was demonstrated that a reduction in the concentration of odour can be achieved by adding biochar to the manure. It was also shown that the measured odour concentration reduced further as the quantity of added charcoal increased. This effect occurred with all methods used. Quantities of charcoal ranging from five to 250 g L^{-1} were added. Important effects of odour reduction could be observed at BC loads of 50 g L^{-1} and higher. Moreover, it was found that, in particular, the differences between shorter reaction times of the charcoal in the manure can be ignored. Over the course of the project, there were increasing signs that where the charcoal has a positive effect, this occurs within the first 30 minutes and continues for several hours. It is therefore possible in practice to use biochar or other organic charcoals immediately before spreading the manure, e.g. when filling suction tankers with it. In conclusion, it can be said that the addition of biochar caused a reduction in odour in all types of manure used, although large differences were observed in the effect it had on various manures.

It can be assumed that odour reduction by 'Borkohle' and other charcoals is mainly related to adsorption of odorous substances and that the effect is reduced with higher residence times. First experiments are widely in accordance to this hypothesis.

In future experiments, an attempt should be made to explain the working mechanisms and to investigate further influencing parameters, such as different manures and manure temperatures. To this end, chemical analyses of the gas phase as well as the solid (charcoal) and liquid phase (manure) will be carried out in addition to odour measurements. This should also explain when – and for which manures – the addition of charcoal can be expected to have positive effects on the emission of odour during spreading. The extent to which the effects found in the laboratory setting can be achieved with standard agricultural equipment, i.e. investigated in field trials, will have to be clarified in a subsequent step. Further investigation of application is under progress. Not all crops need the same amount of boron or do need boron anyway so it will be part of future projects to investigate biochar and combinations of biochar with and without boron to be sure it can be applied due to the needs of different crops.

REFERENCES

Hauschildt, H. & Mannebeck, B. 2015. Measurement, analysis and assessment of environmental odours. *http://www.vivis.de/phocadownload/Download/015_is /2015_IS_131-150_Hauschild.pdf* Accessed 7.1.2018 (in German).

Forrest, W. 2010. Weber-Fechner Law In Plant Pathology and Microbiology Publications. *https://lib.dr.iastate.edu/cgi/viewcontent.cgi?article=1070&context=plantpath_pubs* Accessed 17.2.2018

Glaser, B., Wiedner, K., Seelig, S., Schmidt, H.P. & Gerber, H. 2015. Biochar organic fertilizers from natural resources as substitute for organic fertilizers. In *Agron. Sustain. Dev.* **35**, 667–678.

Hornboden, E., Bode, R. & Donner, P. Edts. 1993. Recycling: materials science aspects, Springer Verlag Heidelberg ISBN-10: 354056408X, pp 118–122. (in German).

Isocell. 2017. Der perfekte Kreislauf. http://www.isocell.com/de/news/77/der-perfekte-kreislauf/ Accessed 26.1.2018 (in German).

Schulz, H., Dunst, G. & Glaser, B. 2014. No Effect Level of Co-Composted Biochar on Plant Growth and Soil Properties in a Greenhouse Experiment. *Agronomy* **4**(1), 34–51. DOI: 10.3390/agronomy4010034.

Wieland, H. & Bockisch, F.J. 2006. Insulating materials produced from renewable raw materials. *Landtechnik* **4**, 218–219 (in German).

Agronomy Research **16**(3), 717–722, 2018
https://doi.org/10.15159/AR.18.105

Development of new elements to automatized greenhouses

J. Hart[1,*] and V. Hartová[2]

[1]Czech University of Life Sciences Prague, Faculty of Engineering, Department of Technological Equipment of Buildings, Kamýcká 129, CZ165 00 Prague, Czech Republic
[2]Czech University of Life Sciences Prague, Faculty of Engineering, Department of Vehicles and Ground Transport, Kamýcká 129, CZ165 00 Prague, Czech Republic
[*]Correspondence: janhart77@gmail.com

Abstract. Development of new elements to automatized of greenhouses is always needed and be it is to improve the current situation because of the increase effectivity in greenhouses or their control. Czech University of Life Sciences Prague was to increase efficiency in greenhouses and therefore, devices designed to improve the automation in greenhouses have been designed and patented. The aim was to propose new improvements for automated greenhouses based on demand. This is primarily about solving the problem of lack of daylight and regularly occurring moss on the roof. This research and development are guided primarily because it is a agriculture branch in the stage of expansion, and it is essential that there is a continuous innovation and research in this field of science. New automatic features or upgrades to existing features in greenhouses, was solved on the basis of the current state of development curent technology. When designet new technologies also help us grants, personal experience with a real installation and cooperation with manufacturers (or with distributors) greenhouses systems. Designs for a light routing system and a system for removing moss from the roof were made.

Key words: greenhouses, light panel, applicator, inhibitor, development, roof

INTRODUCTION

Nowadays, when we place great emphasis on automation in greenhouses, there is a need for constant development. It is also very important to increase the quality and system efficiency of these greenhouses systems. There are many of these simple systems on the market today and many more are being added. Their differences are usually very small, and they frequently vary in terms of cost and reliability. These systems are fully utilized by many companies where the efficiency of the system is not addressed. The design of new low-cost greenhouse systems is therefore highly sought after. It is intended primarily for use in companies where it is necessary to modify the conditions of the greenhouse at a particular moment (Morisse et al., 1997; Hassan et al., 2015; Bradna & Malaťák, 2016; Hart & Hartová, 2016).

Technology focus, which is the constant need for increasing efficiency, is to modify the lighting conditions of greenhouses and protect the roof of greenhouses against unwanted mosses. The most common technology used today to improve the lighting in greenhouses are specific reflectors, whose operation is costly. Removal of the moss also produces recurrent costs. At present, only manual spraying is used. Copper sulfate is most often used to remove mosses. Another is a slaked lime mixed with water. Or, there are combinations of copper sulfate with sodium carbonate or other similar combinations. The aim of our development was therefore to design systems that would eliminate these problems and were not financially unattainable (Gao et al., 2015; Xia et al., 2015).

MATERIALS AND METHODS

Editing of lighting conditions in greenhouses is associated with a number of aspects. Among the most important is the routing sunlight and classical or IR light beams. All of these options are associated with light conditions in the greenhouse. Therefore, a variant has been devised where light can be directed through an automatically light panel (see Fig. 1) or similarly adapted roof (Lee et al., 2015; Liu et al., 2017).

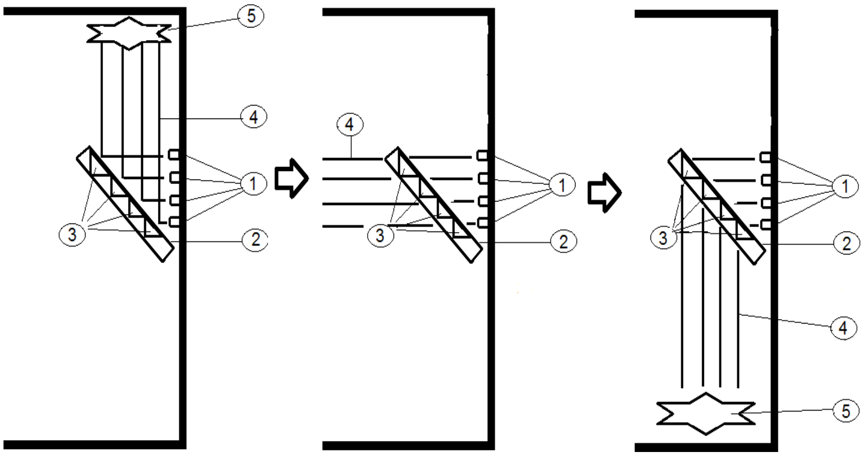

Figure 1. Principle of the automatically light panel: 1 – reflectors or sunlight; 2 – light panel body with rotating mechanism; 3 – light permeable triangles; 4 – light beams; 5 – lighting center. Please refer to the reference if this is not your own drawing.

The light panel consists of permeable triangles (Fig. 2), which together with the light source provide different illumination intensity, the body of the panel with the rotating mechanism and the reflectors. Forward triangles are rotated by the rotating mechanism inside the body of the light panel according to the setting. Light panel can be set a lower light intensity when turning the permeable triangles downwards.

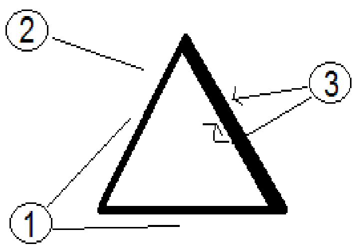

Figure 2. Principle of the light permeable triangle: 1 – light permeable sides; 2 – light permeable triangle; 3 – reflective sides.

Average daily light diffusion light was measured by the measurements. The measurement was carried out on the DT-8809A. It was measured 5 days in October for diffuse lighting. These values were surveyed at the Czech University of Life Sciences

Pargue. Mathematically, the efficiency of light routing into specific points within the greenhouse was derived.

The design of the system for adjusting the lighting conditions of the greenhouse is an easy matter compared to the moss elimination system (Fig. 3). It was necessary to carefully evaluate which substances are suitable for elimination and then select the ‘economical (or cost-effective)’ option.

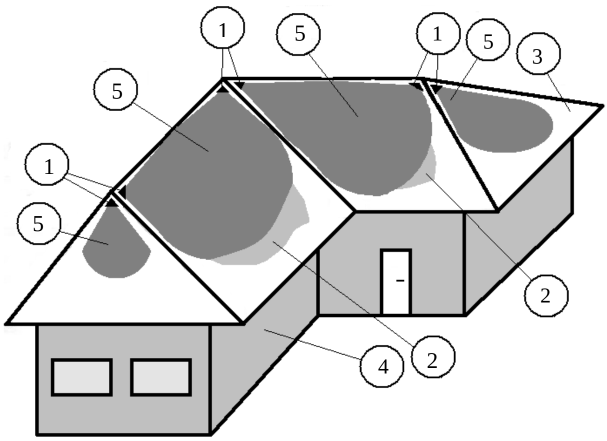

Figure 3. Applicator of inhibitors for protection of roofing: 1 – Sprayers; 2 – Plants of the order Porellales; 3 – Roof; 4 – Greenhouse; 5 – A copper sulphate mixture.

The applicator of inhibitors for protection of roofing consists of a tank containing an integrated refill tank for special inhibitors and mixed chambers, and then from sprayers connected by piping to the mixed chamber. The mixing chamber is then connected to the classical water supply system (Fig. 4).

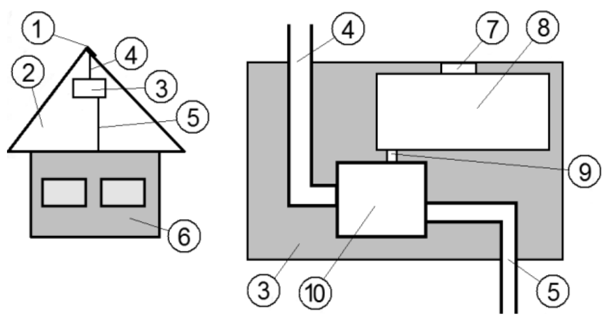

Figure 4. Distribution system: 1 – Sprayers; 2 – Roof; 3 – Tank; 4 – Mixed piping; 5 – Water supply system; 6 – Greenhouse; 7 – refilling opening; 8 – Integrated refilling tank; 9 – Dispenser; 10 – Mixing chamber.

One of the most effective and affordable formulations is copper sulfate (CuSO4), which has to be diluted with water. When the applicator starts running, water is introduced into the mixing chamber and a dispenser is opened, which dispenses special inhibitors from the filling tank to the mixing chamber. The mixture that is formed in the mixing chamber is then distributed via a pipe to the sprayers which was fed through the distribution node. From the distribution node, the mixture is led through the distribution system to the nozzle heads which apply the mixture to the roofing.

The applicator of inhibitors periodically and removes roof coverings of Porellales plants. Repetition is based on the location of the greenhouse and the outdoor climate in the area. In humid environments, there are two applications per year. Cleaning is important because there is sufficient light access to greenhouses. A special mixture (most commonly cuprous sulphate) can be added to the refilling tank by means of a lockable opening. When using this technology, it is important to have the gutter lead in the pit. The economic appreciation was based on several basic price calculations, see Table 1.

Table 1. Price review of the system for the application of inhibitors and periodic cleaning by the company

Service/system price	Price per piece	Price per year
Removal of moss by spraying	300 €	600 €
System price (applicator)	3,200 €	x
The price of chemicals in the applicator	x	80 €

RESULTS AND DISCUSSION

It can be seen from the graph in Fig. 5 that the direction of light leads to improvement of the growing process due to the improvement of the lighting conditions. The plant is able to provide the maximum level of photosynthesis at 35,000 lux. Diffuse light provides about 25,000 luxes. Thanks to light routing, it is possible to stretch the lighting time of a plant to increase its productivity.

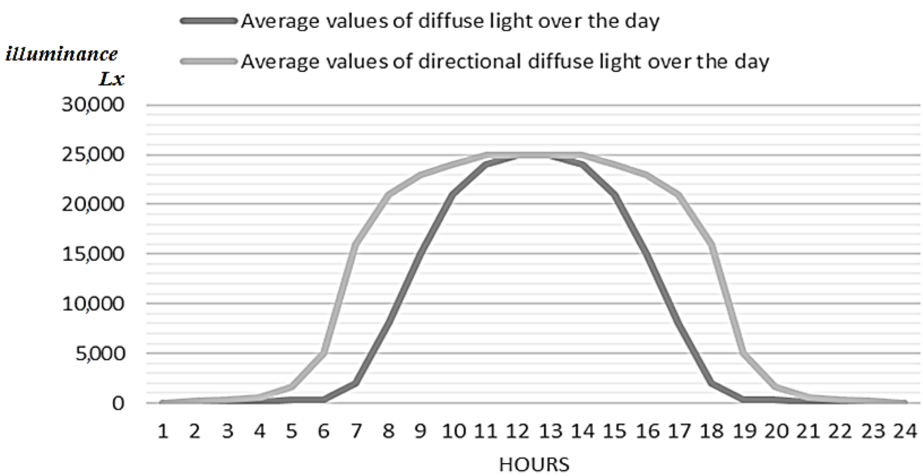

Figure 5. Differential light comparison.

An evaluation of the financial return for the installation of the system was made to compare the costs of the applicator with regular maintenance work of a specialized company. It was found that the applicator would pay back after the sixth year of installation (Fig. 6).

The resulting system is more expensive than spraying, but in the long run, the cost is returned, since there is no need for an intermediary to apply the active substance to the roof. Based on the fixed costs of installing the applicator of inhibitors for the protection of roofing and the periodic maintenance costs performed by an expert firm, a conversion of the return on investment was created.

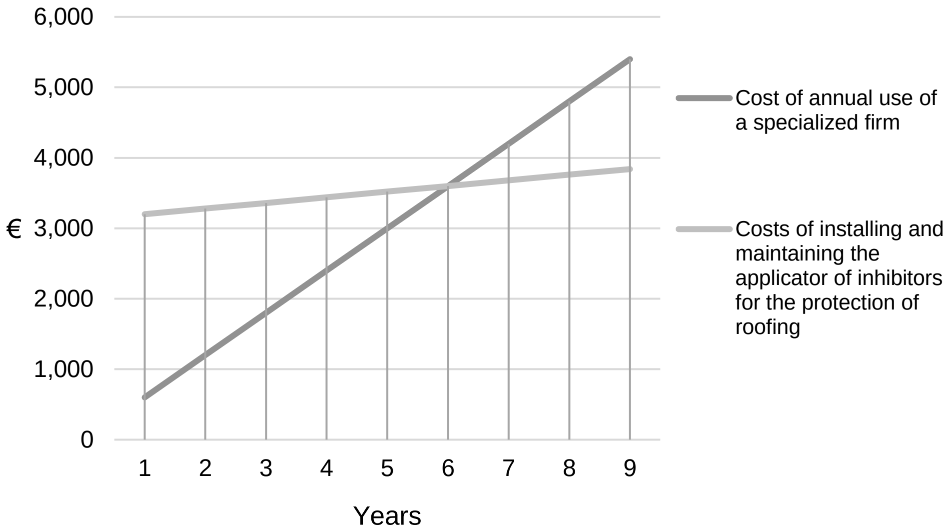

Figure 6. Financial returns using the application of inhibitors for protection of roofing.

Until all the invented systems are real tested, it is possible only to ask whether they will work according to assumptions. The present state of development of systems for greenhouses is at a point of expansion.

The development of light routers follows the research published in the article 'A Solar Automatic Tracking System that Generates Power for Lighting Greenhouses' (Zhang et al., 2015), but the research plan has been viewed from a different point of view. In the same way as in the articles 'Research on Automatic Control System of Greenhouse' (Wen, 2016), 'Design of an intelligent greenhouse automation system based on C language' (Wen, 2016) and 'An Automatic Monitoring and Control System Inside Greenhouse' (Liu at al., 2017), the research was viewed from a fully automatic viewpoint not only for light routing but also for moss removal. Contrary to the above examples, this research was aimed at going in a new direction and making available a financially viable variant of substantial improvements.

CONCLUSIONS

Testing and improving the existing technologies is very important. Due to the continuous development in the field of automated technology research in greenhouses, techniques is always important to continue to develop new and better systems, modules, switchboards and all components. The overall solution of designed system is advantageous for several reasons. Systems should be affordable and should improve the quality of automation in greenhouses.

The resulting design has its selected hardware construction. Thanks to the created system it was demonstrated as well that it enables financial returns on implementation. As long as the future manufacturer has not commenced full cooperation with the other variants of automatization, the system's greenhouse automatization use will remain limited, even when meeting the condition of being a technology which fully conforms to automatic demands.

Light conditions affect plant growth and this is especially true of diffuse light. By bringing daylight to the entire greenhouse and effectively targeting plants, their yields will also increase. This is the basis for a new direction of research to improve lighting and its sustainability.

ACKNOWLEDGEMENTS. It is a project supported by the CULS IGA TF 'The University Internal Grant Agency' (Analisys of the influence of biofuels on operating parameters of combustion engines).

REFERENCES

Bradna, J. & Malaťák, J. 2016. Flue gases thermal emission concentration during waste biomass combustion in small combustion device with manual fuel supply. *Research in Agricultural Engineering* **62**(1), 1–7.

Gao, J., Zhao, L. & Sun, Y. 2015. The Design of Automatic Circulating Temperature Control System of SCM-based Greenhouse. In: *Proceedings of The 2015 International Conference on Applied Science and Engineering Innovation*, vol. **12**, pp. 2019–2026.

Hart, J. & Hartová, V. 2016. Development of new testers to improve quality for data transmissions in intrusion and hold-up alarm systems. In: *15th International Scientific Conference on Engineering for Rural Development*, LUA, Jelgava, pp. 523–528.

Hassan, N., Abdullah, S.I., Noor, A.S. & Alam, M. 2015. An Automatic Monitoring and Control System Inside Greenhouse. In: *2015 3rd International Conference on Green Energy and Technology (ICGET*), art. num. 7315084.

Morisse, J.P., Huonnic, D., Cotte, J.P. & Martrenchar, A. 1997. Relation between mixing solid foods and wellfare into the feed of calves. Study on three groups of 21 calves, *POINT VETERINAIRE*, Volume: **28**, Issue: 184, pp. 71–73.

Lee, Y.J., Park, K.W. & Kim, E.K. 2015, Automatic Dehumidifier Control System for Greenhouse Using Smart Phone. In: *Advanced Multimedia and Ubiquitous Engineering: Future Information Technology*, vol. **352**, pp. 257–264

Liu, Y., Qi, G.Y., Li, Z.Y., Wu, Q.N. & Meng, Y.P. 2017. Research on Automatic Control System of Greenhouse. In: *Advances In Materials, Machinery, Electronics* I, vol. 1820, art. num. 070011.

Wen, J.X. 2016. Design of intelligent greenhouse automatic control system based on C language. In: *Proceedings of the 2016 2nd workshop on advanced research and technology in industry applications*, vol. **81**, pp 1635–1641.

Xia, C.L., Chon, T.S., Ren, Z.M. & Lee, J.M. 2015. Automatic identification and counting of small size pests in greenhouse conditions with low computational cost. *Ecological informatics* **29**, 139–146.

Zhang, Q.X., Yu, H.Y., Zhang, Q.Y., Zhang, Z.Y., Shao, C.H. & Yang, D. 2015. A Solar Automatic Tracking System that Generates Power for Lighting Greenhouses. *Energies* **8**, 7367–7380.

Agronomy Research **16**(3), 723–727, 2018
https://doi.org/10.15159/AR.18.076

Determination of moisture ratio in parts of the hop cone during the drying process in belt dryer

P. Heřmánek*, A. Rybka and I. Honzík

Czech University of Life Sciences Prague, Faculty of Engineering, Department of Agricultural Machines, Kamýcká 129, CZ165 00 Praha 6 - Suchdol, Czech Republic
*Correspondence: hermanek@tf.czu.cz

Abstract. The paper deals with monitoring the moisture content of hop cones and their parts (strigs and bracts) in PCHB 750 hop belt dryer. When drying hop cones, the critical point is the sufficient drying of the strig. These are therefore dried to a moisture content of 6 to 8%. This exact moisture provides a sufficient guarantee ensuring that the strig is dried up. On the other hand, bracts are dried up to such a level which makes pressing the hops impossible. Therefore, after drying, the bracts are remoistened. This is called hops conditioning. After conditioning the moisture content of hops is optimal, ranging between 8 and 11%. There is no doubt that drying or any further moistening does not benefit the hop cone.

During the experiment, the moisture content was determined regarding the whole hop cones as well as the bracts and strigs separately, the samples of which had been taken from the hops prior to entering the dryer, from different parts of belts in the dryer and subsequently before and after the conditioning. The moisture content was determined by means of Mettler HE53 moisture analyzer. After the bracts and strigs had been dried, we calculated their weight ratio which was approx. 90% of bracts and 10% of strigs. Based on this ratio the weighted average was calculated which corresponds to the moisture content of the whole hop cone.

The measured values indicate that the average moisture content of hops below 10% was already at the beginning of the third belt of the dryer. The hops had been unnecessarily overdried along the whole third belt. Another output refers to the moisture ratio of hop cones, bracts and strigs in different parts of the dryer. The obtained values will serve as a basis for the follow-up design of a device for monitoring the dryer parameters and its visualisation.

Key words: hop, hop cone, bract, strig, drying, belt dryer, moisture.

INTRODUCTION

The composition of hops is continuously changing not only during the ripening period and harvest, but more importantly during their drying, storing and processing into various hop products. Moisture is an essential qualitative parameter of hops and other crops (Vitázek & Jurík, 2015; Aboltis & Palabinskis, 2016; Aboltis & Palabinskis, 2017). The optimal moisture content of dried hops is within the range between 8–11%. If the moisture content of dried hops is less than 7%, the hops tend to shatter, i.e. are likely to fall into bracts and strigs, which is undesirable regarding the lupulin losses during any further processing. When the water content is higher than 13%, the hops are at risk of becoming mouldy as well as of deterioration resulting from a change in the colour, or even in an extreme case at risk of self-ignition. Where it is found that there is an excessive water content, those hops are brought back to the grower to be re-dried. Growers are well aware of the risks regarding poor drying of hops, because the number of real cases when the hops had to be re-dried is extremely low (Doe & Menary, 1979; Krofta et al., 2017).

The aim of the article was monitoring the moisture content of hop cones and their parts in hop dryer.

MATERIALS AND METHODS

The monitoring in all the dryers in operation was not focused on the moisture content of hops but of the productive environment inside each dryer. Fig. 1 depicts a scheme of the particular PCHB 750 belt dryer together with data on the speed for each belt.

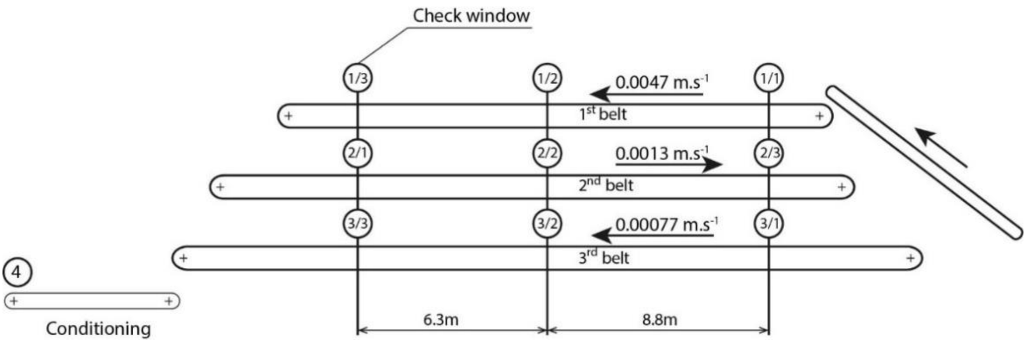

Figure 1. Scheme of the dryer belts indicating the speed of each belt and all sampling points.

Fixed Comet T3419 (Fig. 2) sensors of temperature and relative humidity are installed onto the belt dryers (Fig. 1), nearby the check window (Fig. 3). 8 sensors in the set are always connected to one Comet MS6D multi-channel data logger (Fig. 4). The data from the multi-channel data loggers are stored on the hard drive of the computer (Rybka et al., 2017).

Figure 2. A sensor with transmitter.

The data obtained from these fixed sensors, however, do not indicate an overview of the current hop moisture or even of the individual parts of hops – cone, bract and strig. Therefore, we decided to measure the moisture content of the cone and its parts in the individual sections (the check windows, Figs 1 and 3) of the belt dryer. The actual hop moisture is measured by individual growers by means of various kinds of very out-dated measuring instruments which are not very accurate.

In the laboratory, it is possible to determine the hop moisture content by means of drying a defined amount of ground hops in the laboratory dryer where forced-air ventilation is used, or by the moisture analyser.

Figure 3. A sensor with transmitter and display installed nearby the dryer check window.

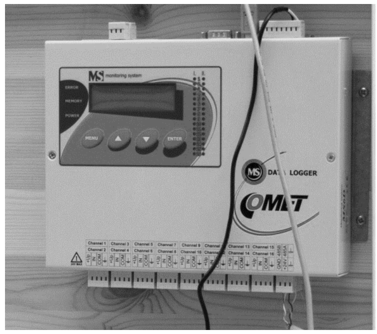

Figure 4. Comet MS6D multi-channel data logger.

When measuring in the laboratory dryer, 5 to 10 grams of ground hops are weighed into an aluminium or glass sample container. The bowl containing the weighed sample is inserted (without the lid) into the dryer that was warmed up to a temperature of 105 °C. This sample is dried for 1 hour. At the end of this period, the bowl with dried hops is closed with a lid and inserted into the desiccator to cool off. After cooling to room temperature, the bowl is weighed. In case we dry fresh green hops, similar procedure is followed, only the cones are cut into smaller pieces in advance and the drying period is longer. In the case of green hops, the drying period of 1.5 h is sufficient.

Another method is determination of the hop moisture content on the moisture analyser, where the sample moisture is continuously shown on the device integral display. The sample amount is approximately 3 grams in this case and the hops need to be evenly spread over the whole surface of the weighing bowl. The end of drying is indicated by the moment when the weight loss of the sample during the defined time interval is lower than its pre-defined value.

Figure 5. HE43 moisture analyser by Mettler-Toledo.

For the purposes of our measurement of the hop moisture content we used the HE43 moisture analyser produced by Mettler-Toledo (Fig. 5). According to the methodology of ‘Assessment of Qualitative Parameters of Hops During Drying and Ageing’ (Green & Osborne, 1993; Krofta et al., 2017), the limit values for the moisture content of hops are:

< 8% overdried hops,
9–11% optimal values,
11–12% acceptable increased moisture,
> 12% high moisture content, hops need to be re-dried.

The laboratory analyses monitored the moisture content of all samples of the hop cone and its parts – bracts and strigs (Fig. 6). The samples (three samples from each check window) taken for the purposes of laboratory measurement were taken at each check window.

Figure 6. Hop cone cross section.

RESULTS AND DISCUSSION

For the Saaz hop variety, the samples had been taken in the PCHB 750 hop belt dryer, the owner of which being Agrospol Velká Bystřice Co., Ltd., from all the check windows and both at the beginning and at the end of conditioning. The hop cone moisture and, separately, the moisture of bracts and strigs was determined on the HE43 moisture analyser provided by the Mettler-Toledo company. These results are presented in Table 1 and the graph in Fig. 7 and are similar Münsterer, (2006).

Table 1. Average measured values to establish the drying curve (Fig. 1)

Check window		1/1	1/2	1/3	2/1	2/2	2/3	3/1	3/2	3/3	4
Measurement time by belt speed, min		0	25	55	70	132	216	235	365	450	555
Cones	Weight, g	8.99	7.05	4.75	3.97	5.54	2.90	2.58	1.85	1.66	1.88
	Moisture, %	75.80	70.60	66.76	60.99	51.70	30.49	11.60	5.58	5.78	7.65
Bracts	Weight, g	7.22	5.57	4.00	3.10	4.26	2.33	2.04	1.60	1.46	1.78
	Moisture, %	75.81	69.34	62.00	58.80	48.50	25.10	9.30	4.69	3.79	7.80
Strigs	Weight, g	1.39	1.15	0.75	0.67	1.03	0.55	0.46	0.23	0.17	0.18
	Moisture, %	80.71	76.13	72.64	71.20	65.20	46.50	39.90	15.44	5.52	5.39

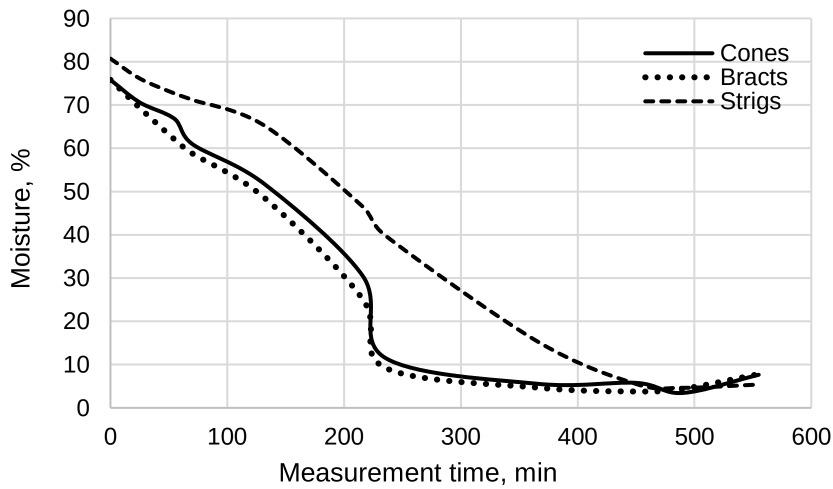

Figure 7. Dependence of the moisture content of cones, bracts and strigs on the measurement time (drying curve).

Fig. 7 shows the drying curve that enables to trace the relationship between the moisture content of bracts and strigs. The figure depicts the reason why hop cones are overdried during regular drying to be moistened again when conditioned at the end of the process. The graph clearly shows that the moisture content of strigs declines slowly compared to the one of bracts. The moment we measure the cone moisture content of e.g. 10%, the strigs may have 40 to 45%. If these hops were pressed, strigs would become a source of high moisture that makes the hops deteriorate. Finally, from the measurements we determined the ratio by mass of bracts to strigs being approximately 8:2 to 9:1.

CONCLUSION

Any deficiencies in the form of dissimilar moisture contents of the separate hop cone parts should be removed by monitoring the moisture content throughout the entire process of drying in the belt dryer and subsequent storage of the hops in conditioning chambers, where the moisture content of bracts and strigs evens out spontaneously. Afterwards, the hops can be pressed without risk. This innovative technology is, however, the subject for future research.

ACKNOWLEDGEMENTS. This paper was created with the contribution of the Czech Ministry of Agriculture as a part of NAZV No: QJ1510004 research project. In the project solution, besides CULS Prague, are involved: Hop Research Institute Co., Ltd., Žatec; Chmelařství, cooperative Žatec; Rakochmel Co., Ltd., Kolešovice and Agrospol Velká Bystřice Co., Ltd.

REFERENCES

Aboltins, A. & Palabinskis, J. 2016. Fruit Drying Process Investigation in Infrared Film Dryer. *Agronomy Research* **14**(1), 5–13.

Aboltins, A. & Palabinskis, J. 2017. Studies of vegetable drying process in infrared film dryer. *Agronomy Research* **15**(S2), 1259–1266.

Doe, P.E. & Menary, R.C. 1979. Optimization of the Hop Drying Process with Respect to Alpha Acid Content. *J. Agric. Engng Res.* **24**, 233–248.

Green, C.P. & Osborne, P. 1993. Effects of solvent quality on the analysis of hops. *J. Institute of Brewing* **99**, 223–225.

Krofta, K., Pokorný, J., Ježek, J., Klapal, I., Mravcová, L., Vondráčková, P., Rybka, A., Heřmánek, P., Honzík, I., Podsedník, J., Melč, J., Šrámek, K., Kolman, Z. & Nádvorník, J. 2017. Evaluation of hops qualitative parameters during drying and aging 2017. Petr Svoboda, Žatec, 17 pp. ISBN 978-80-86836-6-4 (in Czech).

Münsterer, J. 2006. *Optimale Trocknung und Konditionierung von Hopfen*. Bayerische Landesanstalt für Landwirtschaft, Arbeitsgruppe Hopfenbau, Produktionstechnik, Wolnzach 26 pp. (in Germany).

Rybka, A., Heřmánek, P. & Honzík, I. 2017. Theoretical Analysis of the Technological Process of Hop Drying. *Agronomy Research* **15**(3), 859–865.

Vitázek, I. & Jurík, I. 2015. Grain drying and storage technology. Nitra: SPU, 136 pp. ISBN 978-80-5521419-1 (in Slovak).

Agronomy Research **16**(3), 728–736, 2018
https://doi.org/10.15159/AR.18.080

Humus content in a podzolized chernozem after a long-term application of fertilizers in a field crop rotation

H. Hospodarenko[1], I. Prokopchuk[1,*], S. Prokopchuk[1] and A. Trus[2]

[1]Uman National University of Horticulture, Faculty of Agronomy, Department of Agricultural Chemistry and Soil Science, Instytutska street 1, UA20305 Uman, Ukraine
[2]Uman National University of Horticulture, Faculty of Engineering and Technology, Department of Applied Engineering and Labor Protection, 1 Instytutska street, UA20305 Uman, Ukraine
[*]Correspondence: pivotbi@ukr.net

Abstract. The article presents the results of the research into influence of a long-term (50 years) application of different fertilizer rates and fertilizer systems in the field crop rotation on the humus composition and optical parameters of humic acids of a heavy- loamy podzolized chernozem of the Right Bank Forest-Steppe of Ukraine.
It was found that application of fertilizers significantly affects the dominance of humic acids over fulvic acids in the composition of soil, which indicates humate type of soil. Chroma index of humic acids is within 3.56–3.75 depending on a fertilizer. Indicators of the optical properties of humic acids of a podzolized chernozem have a high degree of humification.

Key words: humus, humic acids, fulvic acids, optical density, fertility, podzolized chernozem, fertilizers, field crop rotation.

INTRODUCTION

Humus content in soil is the main indicator of potential soil fertility, therefore conservation, maintenance and restoration of humus are the main tasks of agriculture. The direction of transformation processes of organic matter in the soil in general characterizes the degree of quantitative changes of humus. The study of such changes caused by a long-term influence of fertilizers is especially important for the soils low in organic matter (Mazur, 2002). Podzolized chernozems refer to this type of soils and are prevailing in the Right Bank Forest-Steppe of Ukraine.

Humus level in soil covers a set of morphological features and chemical properties of humus that allows to detect specific forms and types of humus. In this case humus forms are characterized and distinguished according to morphological characteristics, and type of humus is defined as a result of detection of humic substances. The content, reserves and quality of humus belong to the most important indicators, since almost all agronomically valuable soil properties depend from their level (Nosko, 1990).

In contemporary arable farming the issue of soil fertility and efficient soil management remains one of the most urgent. Over recent years the amount of applied mineral fertilizers has decreased by 8–10 times, organic fertilizers – by 4–5 times.

Annual losses of humus under existing structure of cultivated areas in the Forest-Steppe make up 0.6–0.7 t ha^{-1} (Shedey, 2005; Tsvey, 2010). Therefore, this situation requires a comprehensive approach to improving soil fertility, and especially to the efficient use of fertilizers.

The aim of the research was to define the changes in the indexes of humus content of a podzolized chernozem under the influence of a long-term application of various fertilizer rates and fertilizer systems in a field crop rotation in order to improve their monitoring and to specify the rules and recommendations for a safe application of fertilizers.

MATERIALS AND METHODS

This research was carried out on the experimental field of Uman National University of Horticulture in the stationary experiment of the Department of Agrochemistry and Soil Science. The experiment was launched in 1964, and it is based on a 10-field crop rotation extended – in time and space (spring barley + meadow clover, meadow clover, winter wheat, sugar beet, corn, peas, winter wheat, silage corn, winter wheat, sugar beet).

The following fertilizer systems were used in the crop rotation: organic (manure 9 tons, 13.5 tons, 18 tons), mineral ($N_{45}P_{45}K_{45}$; $N_{90}P_{90}K_{90}$; $N_{135}P_{135}K_{135}$) and organic-mineral (manure 4.5 tons + $N_{22}P_{34}K_{18}$; manure 9 t + $N_{45}P_{68}K_{36}$; manure 13.5 t + $N_{67}P_{102}K_{54}$). Fertilizer rates are specified per 1 ha of crop rotation area.

Before the experiment the soil was under a long-term cultivation under field crops, hence it was a degraded, 'plowed-out' soil. Soils samples taken before the experiment (1964) had the following parameters: content of physical clay – 66.5%, base saturation – 95%, humus content – 3.31%; content of easily hydrolysable organic nitrogen (according to the Tiurin – Kononova method); mobile compounds of phosphorus and potassium (according to Chirikov method) – 122 and 135 mg kg^{-1}; pH_{KCl} – 6.2 respectively.

In the soil samples the carbon content was determined by the method of I.V. Tiurin in the modification of the *Central Research Institute* of *Agrochemical* Maintenance of Agriculture (Orlov, 1992), its factional and group composition – by the method of I.V. Tiurin in the modification of V.V. Ponomareva & T.A. Plotnikova (1980). Optical density of sodium humate solutions was determined by photocolorimeter with a set of light filters at the wavelengths of 430, 465 and 665 nμ. Concentration of the 1st and 2nd fractions of humic acids (HA-1 + HA-2) was calculated by the Bouguer-Lambert-Beer general formula. Chroma index of humic acids was determined according to the ratio of optical density of sodium humate solutions at a wavelength 465 nμ to a corresponding value at the wave length 665 nμ. To characterize soil humus we include humification index according to the recommendation of D.S. Orlov in the system of indexes of humus content in soil.

To evaluate the accuracy of experimental data we used confidence interval derived via mathematical statistics program of application software Statistica 6.0

RESULTS AND DISCUSSION

The research results showed that a long-term systematic use of soil in agricultural production led to to the reduction in humus content compared to the figures at the time when the experiment was launched (Table 1).

Table 1. The content of humus in a podzolized chernozem after a long-term (50 years) application of fertilizers in field crop rotation, %

Variant of experiment	Layer of soil, cm				
	0–20	20–40	40–60	60–80	80–100
Before the experiment	3.31 ± 0.13	3.00 ± 0.21	2.74 ± 0.12	1.98 ± 0.15	1.58 ± 0.09
Without fertilizers (control)	2.73 ± 0.22	2.43 ± 0.22	2.19 ± 0.19	1.90 ± 0.14	1.56 ± 0.06
$N_{45}P_{45}K_{45}$	2.76 ± 0.15	2.65 ± 0.22	2.39 ± 0.14	1.93 ± 0.16	1.56 ± 0.07
$N_{90}P_{90}K_{90}$	2.80 ± 0.15	2.61 ± 0.20	2.38 ± 0.12	1.94 ± 0.16	1.54 ± 0.09
$N_{135}P_{135}K_{135}$	2.84 ± 0.16	2.69 ± 0.20	2.36 ± 0.17	1.93 ± 0.10	1.58 ± 0.05
Manure 9 t	2.88 ± 0.10	2.73 ± 0.16	2.40 ± 0.13	1.94 ± 0.13	1.58 ± 0.07
Manure 13,5 t	3.03 ± 0.17	2.80 ± 0.11	2.39 ± 0.12	1.95 ± 0.16	1.59 ± 0.07
Manure 18 t	3.24 ± 0.11	2.95 ± 0.15	2.51 ± 0.14	1.98 ± 0.09	1.55 ± 0.11
Manure 4.5 t + $N_{23}P_{34}K_{18}$	3.16 ± 0.15	2.91 ± 0.13	2.63 ± 0.17	1.98 ± 0.08	1.55 ± 0.09
Manure 9 t + $N_{45}P_{68}K_{36}$	3.34 ± 0.17	3.03 ± 0.12	2.79 ± 0.15	1.98 ± 0.06	1.58 ± 0.05
Manure 13.5 t + $N_{68}P_{101}K_{54}$	3.39 ± 0.17	3.14 ± 0.13	2.89 ± 0.18	1.99 ± 0.08	1.56 ± 0.07

At the same time fertilization systems, that had been studied, influenced the content of humus in different ways. Thus, under mineral system in the layer of 0–20 cm of soil the humus content reduced by 0.47–0.55 abs.% compared with its content at the time when the experiment was launched, however, when we compare it with control, we observe inessential increase (by 0.03–0.11 abs.%), that is, within experimental error. Other scientists observed a similar impact of mineral fertilizers on the humus content in the soil (Brock et al., 2013; Kõlli & Tamm, 2013; Kõlli et al., 2015).

Application of semi decomposed manure contributed to the conservation of the humus content in the soil at the level of 2.88–3.24%. In this case the content of humus depended on the rate of its application and was higher with increasing application rates. That is, in the variant of experiment with a high rate of manure (18 tons ha^{-1}) humus content equaled the index value at the time when the experiment began (3.31%). It proves that organic fertilizers are a source of energetic material for soil microorganisms that contribute to enhancing the process of humus formation. Combined application of organic and mineral fertilizers was the most significant among the variants that were studied in the experiment and contributed to the formation and accumulation of humus in the soil.

In the 0–20 cm layer of soil under the first level of organic-mineral fertilizer system the humus content made up 3.16%, which is by 0.43% more than in the control variant. The concept of qualitative composition of humus is wider and includes both the ratio between the amount of carbon in the different fractions within two groups (humic and fulvic acids), and the amount of carbon of insoluble residue. All above mentioned compounds form the humus of the soil. While studying humus level of the soil it is very important to investigate fraction-group composition of humus (Table 2).

Table 2. Fractional-group composition of humus (layer 0–20 cm) of podzolized chernozem after a long-term (50 years) fertilizers application in field crop rotation

Variant of experiment	C_{total}, %	Humic acids (HA)				Fulvic acids (FA)					$C_{ha}+C_{fa}$	Humin	$C_{ha} : C_{fa}$
		HA–1	HA–2	HA–3	Amount	FA–1a	FA–1	FA–2	FA–3	Amount			
		in % from C_{total}											
Without fertilizers (control)	1.58	6.4	18.1	9.9	34.4	2.4	4.7	6.6	3.5	17.2	51.6	48.4	2.00
$N_{45}P_{45}K_{45}$	1.60	5.7	19.6	9.7	35.0	1.9	4.4	6.9	3.7	16.9	51.9	48.1	2.07
$N_{90}P_{90}K_{90}$	1.62	5.5	20.7	10.4	36.6	2.0	4.5	7.0	3.3	16.8	53.4	46.6	2.18
$N_{135}P_{135}K_{135}$	1.65	6.0	21.6	10.8	38.4	1.9	4.3	7.4	3.1	16.7	55.1	44.9	2.30
Manure 9 t	1.67	5.4	21.9	9.6	36.9	2.6	3.9	6.9	3.3	16.7	53.6	46.4	2.21
Manure 13.5 t	1.76	5.8	22.8	10.9	39.5	2.4	3.5	7.0	3.1	16.0	55.5	44.5	2.47
Manure 18 t	1.88	5.8	23.9	11.6	41.3	1.7	3.2	6.8	3.2	14.9	56.2	43.8	2.77
Manure 4.5 t + $N_{23}P_{34}K_{18}$	1.83	5.9	22.9	10.3	39.1	1.9	3.9	6.3	3.4	15.5	54.6	45.4	2.52
Manure 9 t + $N_{45}P_{68}K_{36}$	1.94	6.1	24.7	11.4	42.2	1.5	3.5	6.1	3.0	14.1	56.3	43.7	2.99
Manure 13.5 t + $N_{68}P_{101}K_{54}$	1.97	6.6	25.4	11.6	43.6	1.5	3.2	6.1	3.0	13.8	57.4	42.6	3.16

Research showed that fractional-group composition of humus changed depending on the particularities of fertilizer application judging by the change in fractions of humic (HA) and fulvic acids (FA) in the humus content, they differed significantly after a long-term application of various fertilizer rates and systems in field crop rotation.

The result of the research into the group composition of humus of podzolized chernozem showed that fertilizers had a significant impact on the content of humic and fulvic acid groups in humus. So, the application of $N_{45}P_{68}K_{36}$ with 9 t ha^{-1} of manure led to the increase in humic acids in the soil layer of 0–20 cm to 42.2%, which is by 2% higher compared to the variant with the application of 18 tons of manure per 1 ha of crop rotation area and the variant $N_{90}P_{90}K_{90}$ – by 15% respectively.

The amount of humic acids in all variants of the experiment of field crop rotation in the layer 0–20 cm varied within 34.4–43.6% of the total carbon content in the soil (C_{total}). This indicates a high degree of humification of organic substances (Borisova et al., 2005). The content of humic acids in the soil in a field crop rotation under mineral, organic and organic-mineral fertilizer systems compared to unfertilized plots was higher by 2–12%, 7–20% and by 14–27% respectively.

The fraction of fulvic acids, depending on the variant of the experiment was within 13.8–17.2% of the total carbon content in the soil. Under mineral fertilizer system fulvic acid amount decreased by 2–3%, under organic – by 2–13%, and under organic-mineral – by 10–20 % compared with unfertilized plots. It indicates that organic fertilizers, either alone or in combination with mineral fertilizers are an important factor in increasing the overall content of humus in the soil, as well as humic acid groups (Graefe & Beylich, 2006; Kõlli, Graefe & Tamm, 2015; Andreetta et al., 2016; Bödeker et al., 2016; Paterson et al., 2016; Baskaran et al., 2017).

Depending on the variant of the experiment the fractional composition of humic acids in the soil layer of 0–20 cm shows that fraction of humic acids bound with calcium (HA–2) prevails and makes up 18.1–25.4% of the amount of C_{total}. Fraction of free humic acids and bound with mobile sesquioxide (HA–1) makes up the smallest part – 5.4–6.6% in the content of organic carbohydrate. Fraction of humic acids bound with clay minerals and stable sesquioxide (HA–3) falls in between in the composition of fulvic acids and made up 9.6–11.6%.

In the composition of fulvic acids prevails the fraction bound with HA–2 (FA–2) and makes up 6.1–7.4% of the total content of organic carbon. Whereas corresponding parts of fractions of free fulvic acids and bound with mobile sesquioxides (FA–1a), bound with HA–1 (FA–1) and bound with HA–3 (FA–3) make up 1.5–2.6%; 3.2–4.7 and 3.0–3.7 % respectively.

The part of insoluble residue (humin) decreased compared with unfertilized plots depending on fertilizer rates by 1–7% under mineral, by 4–9% – under organic and by 6–12% – under organic-mineral fertilizer systems.

A long-term use of fertilizers in a field crop rotation greatly influenced the increase of humic acids in the humus content over fulvic acids, and led to the expansion of ratio C_{ha}: C_{fa}. Therefore, the ratio of carbon of humic and fulvic acids in the 0–20 cm layer of soil in field crop rotation was within 2.07 to 3.16 depending on the particular fertilizing. Accordingly, there was a humate type of humus in all variants of the experiment. Comparing the ratio of C_{ha}: C_{fa} in the soil under various fertilizer systems in a field crop rotation, we can conclude that the application of organic fertilizers and their combinations with mineral fertilizers contributes more to the accumulation of humic acid groups than– fulvic acids and changes the type of humus into humate direction.

Besides fractional-group composition of humus, the study of changes in the optical properties of humic acids under different soil fertilizing is also an important indicator of soil formation. The research carried out by (Kononova, 1972) proved that the data on the optical density of humic acids bound with calcium (HA–2) is essential to determine the patterns of change in the extinction coefficient (E). These acids are the most optically dense as compared with other fractions of humic acids in podzolized soils.

A study of the optical density of the HA–2 in the 0–20 cm layer of podzolized chernozem showed (Table 3) that the extinction coefficient at the wavelength of 430 nμ was 22.14–24.83, at 465 nμ – 16.72–19.35 and at 665 nμ – 4.70–5.86, depending on the rates and systems of fertilizer application. In the experiment with unfertilized plots the optical density coefficient was 21.67, 16.45 and 3.66 respectively, which indicates the saturation of the HA–2 with aliphatic chains and the relatively young nature of their molecules.

Under application of mineral fertilizers in field crop rotation degree of condensation of HA–2 increased compared to unfertilized plots at the wavelength of 430 nμ by 7–11%, at 465 nμ – by 8–12% and at 665 nμ – by 28–31% respectively, indicating mineralization of HA–2 due to the decrease of aliphatic hydrocarbon chains in their structure.

Application of organic fertilizers in the field crop rotation provided accelerated mineralization of aliphatic hydrocarbon chains of HA–2, which is proved by the increase in degree of condensation of HA–2 by 8–13%, 11–16% and 30–38% respectively. Under organic-mineral fertilizer system there was an increase in the depth of humification.

Table 3. Coefficients of the optical density of humic acids HA – 2 fraction (layer 0–20 cm) of podzolized chernozem after a long – term (50 years) usage of fertilizers in field crop rotation

Variant of experiment	Wavelength, nμ			E_{465}/E_{665}	$E_4^{0,001}$
	E_{430}	E_{465}	E_{665}		
Without fertilizers (control)	21.67 ± 0.79	16.45 ± 1.62	3.66 ± 0.21	4.49	0.122
$N_{45}P_{45}K_{45}$	23.14 ± 1.09	17.72 ± 1.68	4.70 ± 0.24	3.56	0.124
$N_{90}P_{90}K_{90}$	23.49 ± 1.82	18.12 ± 1.19	4.74 ± 0.24	3.61	0.128
$N_{135}P_{135}K_{135}$	24.03 ± 1.69	18.39 ± 1.33	4.78 ± 0.17	3.64	0.133
Manure 9 t	23.37 ± 1.14	18.28 ± 1.18	4.77 ± 0.25	3.62	0.128
Manure 13,5 t	23.81 ± 1.27	18.71 ± 1.61	4.83 ± 0.22	3.67	0.132
Manure 18 t	24.45 ± 1.72	19.02 ± 1.43	5.06 ± 0.27	3.56	0.137
Manure 4.5 t + $N_{23}P_{34}K_{18}$	23.73 ± 1.20	18.42 ± 0.68	4.78 ± 0.22	3.64	0.129
Manure 9 t + $N_{45}P_{68}K_{36}$	24.52 ± 2.27	19.17 ± 0.98	4.84 ± 0.25	3.75	0.135
Manure 13.5 t + $N_{68}P_{101}K_{54}$	25.83 ± 2.73	20.35 ± 1.29	5.26 ± 0.25	3.68	0.138

This ensured the maximum value of the optical density of HA–2. The highest level of optical density was at wavelengths 430, 465 and 665 nμ and made up 25.83, 20.35 and 5.26 respectively in the variant, when 13.5 tons of manure was applied per 1 ha of the area under crop rotation.

To compare the characteristics of the optical properties of humic acids it is common to use the ratio of the extinction coefficients at the wavelengths of 465 nμ and 665 nμ (chroma index). Chroma index is not dependent on the carbon concentration in the solution, so it is characteristic value for humic acids of different soils.

The lower the ratio is, the greater participation of concentrated aromatic nucleus and, consequently, less – of aliphatic side chains was in the construction of molecules of humic substances (Boguta et al., 2016). Calculations showed that chroma index was higher in the variant with unfertilized plots and made up 4.49, which means a better structuring of humic acids. In variants of the experiment with the application of fertilizers in the field crop rotation chroma index was within 3.56–3.75, which is typical for a podzolized chernozem and indicates a high optical density due to predominance of black humic acids bound with calcium in its composition. (DiDonato et al., 2016; Kimura et al., 2017; Jin et al. 2018).

Coefficients of the Bouguer-Lambert-Beer equation are widely used (E-value at a wavelength of 465 nμ, solution concentration of 0.001% and a cuvet length of 1 cm – $E_4^{0.001}$) to characterize humic acids. Orlov et al. (1996) gives a mean value $E_4^{0.001}$ of humic acids for chernozems within 0.113–0.131, in the variants under investigation the value of this parameter in the layer of 0–20 cm made up 0.112–0.138, which allows us to refer this soil to a podzolized chernozem.

According to the recommendation of Orlov the humification indicator, that takes into account the amount of humic acids as well as their quantity, was included into the system of parameters defining humus level in soils.

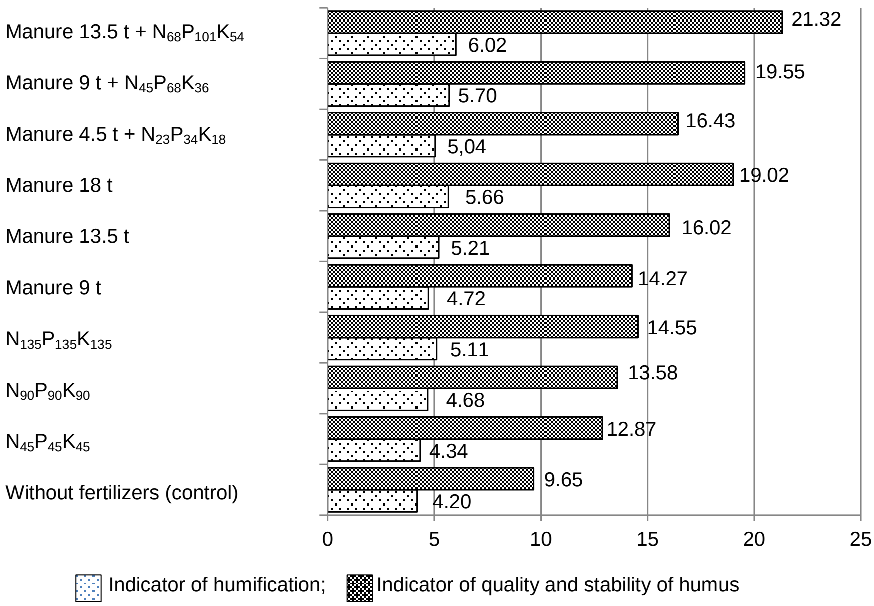

Figure 1. Indicators of the optical properties of humic acids of HA – 2 fraction of podzolized chernozem after a long-term (50 years) usage of fertilizers in field crop rotation.

According to this indicator the soil of studied variants under mineral, organic and organic-mineral fertilizer systems had a high degree of humification (4.34–6.02), that indicates that it is a podzolized chernozem (see Fig. 1). A slight decrease in the index of humification was observed in the soil plots without a long-term fertilizing and made up 4.20, which was by 10% less than in the experimental variant $N_{90}P_{90}K_{90}$ and by 26% in the variant with Manure 18 tons and Manure 9 tons + $N_{45}P_{68}K_{36}$.

One of the important criteria of the optical properties of humic acids is the indicator of the quality and stability of humus proposed by Fernández-Romero et al. (2016) and Melnik & Kowalczuk (2018).

The highest index of quality and stability of humus was 21.32 in the variant when 13.5tons of manure and $N_{68}P_{101}K_{54}$ were applied. The value of this index showed the signs of improving the humus content in soil.

CONCLUSIONS

1. Fractional-group composition of humus of a podzolized chernozem after a long-term (50 years) application of different rates of fertilizers and fertilizer systems in crop rotation is characterized by the predominance of humic acids over fulvic acids and this leads to an expansion of the ratio C_{ha}: C_{fa}, which indicates humate type of soil. The fraction of humic acids bound with calcium (HA–2) makes up 18.1–25.4% of C_{total} and prevails in the fraction of humic acids. The fraction of fulvic acids bound with HA–2 (FA–2) makes up 6.1–7.4% of $C_{total\ and}$ prevails in the fraction of fulvis acids.

2. These data indicate that podzolized chernozem after a long-term systematic application of fertilizers had a high optical density of humic acids which is characteristic for the soils of a chernozem type. Chroma index is characteristic for a podzolized

chernozem (3.56–3.75), and indicates a high optical density due to the predominance of black humic acids bound with calcium in its composition.

3. In terms of the optical properties of humic acids podzolized chernozem had a high degree of humification, which provides high and stable indicators of humus content in soil.

REFERENCES

Andreetta, A., Cecchinia, G., Bonifacio, E., Comolli, R., Vingiani, S. & Carnicellia, S. 2016. Tree or soil? Factors influencing humus form differentiation in Italian forests. *Geoderma* **264**, 195–204.

Baskaran, P., Hyvönen, R.S., Berglund, L., Clemmensen, K., Göran, I., Björn, Å., Lindahl, D. & Manzoni, S. 2017. Modelling the influence of ectomycorrhizal decomposition on plant nutrition and soil carbon sequestration in boreal forest ecosystems. *New Phytologist* **213**(3), 1452–1465.

Bödeker, I.T., Lindahl B.D., Olson, Å. & Clemmensen, K.E. 2016. Mycorrhizal and saprotrophic fungal guilds compete for the same organic substrates but affect decomposition differently. *Functional Ecology* **30**(12), 1967–1978.

Boguta, P., D'Orazio, V., ZofiaSokołowska, Z. & Senesi, N. 2016. Effects of selected chemical and physicochemical properties of humic acids from peat soils on their interaction mechanisms with copper ions at various pHs. *Journal of Geochemical Exploration* **168**, 119–126.

Borisova, T.S., Chimitdorzhieva, G.D. & Tsybekov, Yu.B. 2005. Change of humus state of deflated chestnut soil under the influence of fertilizers under cultivation of forage crops. *Agrochemistry* **3**, 22–29.

Brock, C., Franko, U., Oberholzer, H., Kuka, K., Leithold, G., Kolbe, H. & Reinhold, J. 2013. Humus balancing in Central Europe–concepts, state of the art, and further challenges. *Jornal of Plant Nutrition and Soil Science* **176**, 3–11.

DiDonato, N., Chen, N., Waggoner, D. & Hatcher, P. 2016. Potential origin and formation for molecular components of humic acids in soils. *Geochimica et Cosmochimica Acta* **178**, 210–222.

Fernández-Romero, M.L., Clark, J.M., Collins, C.D., Parras-Alcántara, L. & Lozano-García, B. 2016. Evaluation of optical techniques for characterising soil organic matter quality in agricultural soils. *Soil and Tillage Research* **155**, 450–460.

Graefe, U. & Beylich, A. 2006. Humus forms as tool for upscaling soil biodiversity data to landscape level? *Mitteilungen der Deutschen Bodenkundlichen Gesellschaft* **108**, 6–7.

Jin, J., Sun, K., Yang, Y., Wang, Z., Han, L., Wang, X., Wu, F. & Xing, B. 2018. Comparison between Soil-and Biochar-Derived Humic Acids: Composition, Conformation, and Phenanthrene Sorption. *Environmental Science Technology* **52**(4), 1880–1888.

Kimura, A., Baptista, M. & Scotti, M.R. 2017. Soil humic acid and aggregation as restoration indicators of a seasonally flooded riparian forest under buffer zone system. *Ecological Engineering* **98**, 146–156.

Kõlli, R. & Tamm, I. 2013. Humus cover and its fabric depending on pedo-ecological conditions and landuse: an Estonian approach to classification of humus forms. *Estonian Journal of Ecology* **62**(1), 6–23.

Kõlli, R., Graefe, U. & Tamm, I. 2015. Abundance and species richness of microannelids in humus cover of Estonian forest soils. *Journal of Agricultural Science* **1**, XXVI, 24–29.

Kononova, M.M. 1972. Modern challenges in the field of soil organic matter. *Soil science* **7**, 27–36.

Mazur, G.A. 2002. Potential of soil fertility and productivity of crops. *Collection of scientific papaers of the Institute of Agriculture UAAS* **3**, 3–7.
Mielnik, L. & Kowalczuk, P. 2018. Optical characteristic of humic acids from lake sediments by excitation-emission matrix fluorescence with PARAFAC model. *Journal of Soils and Sediments* **1**, 1–12.
Nosko, B.S. 1990. Handbook of agrochemical and agroecological state of soil in Ukraine. Kyiv,: Urozhay, 328 pp.
Orlov, D.S. 1992. *Soil Chemistry*. Education book. MGU, Moskow, 400 pp.
Orlov, D.S., Biryukova, O.N. & Sukhanova, I.N. 1996. *Soil organic matter of the Russian Federation*. Nauka, Moscow, 256 pp.
Paterson, E., Sim, A., Davidson, J. & Daniell, T.J. 2016. Arbuscular mycorrhizal hyphae promote priming of native soil organic matter mineralization. *Plant and Soil* **408**(1–2), 243–254.
Ponomareva, V.V. & Plotnikova, T.A. 1980. *Humus and soil formation* (methods and results of the study. Nauka, Leningrad, 222 pp.
Shedei, L.O. 2005. Effect of fertilizers on the level of humus and nitrogen of podzolized chernozem and productivity of crop rotation under traditional and resource-saving agriculture: Thesis for obtaining scientific degree of PhD (Agricultural Sciences) speciality. 06.01.04 agrochemistry. Kharkiv, pp. 22.
Tsvei, Ya.P. 2010. Formation of fractional composition of chernozem humus under a long-term fertilization in crop rotation. *Agrochemistry and Soil Science: special issue Soil protection - public support* **3**, 294–295.

Agronomy Research **16**(3), 737–748, 2018
https://doi.org/10.15159/AR.18.144

Evaluation of the fuel commercial additives effect on exhaust gas emissions, fuel consumption and performance in diesel and petrol engine

I. Janoško* and P. Kuchar

Slovak University of Agriculture in Nitra, Technical Faculty, Department of Transport and Handling, Tr.A. Hlinku 2, SK949 76 Nitra, Slovak Republic
*Correspondence: ivan.janosko@uniag.sk

Abstract. The paper deals with the impact assessment of the additives used in diesel and petrol fuel to improve the power and emission parameters of the vehicle and its consumption. The usage of additives in engine fuels have an increasing tendency. The manufacturers claim that additives have positive impact on engine operating parameters, cleaning the fuel supply system and decreasing fuel consumption by improving the engine combustion process. Based on the above statements, measurements were performed to determine change in the engine parameters utilising additives. Measurements were performed under laboratory conditions on the MAHA MSR 500 test bench (dynamometer) to simulate free driving cycle selected by authors, which were carried out at constant engine speeds and constant load. Focus have been given on tracking of the vehicle's external speed characteristic and measurement of selected parameters: CO, HC, O_2, fuel consumption (petrol engine) and smoke, fuel consumption (diesel engine). Resulting values of the driving cycles measured before and after additives application have been then compared. The result of experiment confirmed that tested fuel additives improved performance and torque depending on engine mileage and fuel type. Tested diesel engine with the higher mileage (approx. 388 k km) showed significant increase in power (cca 3.57%) and torque while in newer petrol engine (approx. 73 k km) improvement has not been measured. Emissions were improved in both engines. Difference has been also measured in fuel economy as in petrol engine consumption insignificant increased while in the diesel engine it decreased. This paper brings new complex view on energetical and emission changes in internal combustion engines.

Key words: fuel additive, emission, fuel consumption, engine speed characteristic.

INTRODUCTION

The increase of road transport (especially the individual transport) is a worldwide problem in the major part of cities. The fast growth of the world population and industrial development is linked with an increasing consumption of fossil fuels. Fossil fuels, besides their benefits in terms of tradition and mastered processing technology, have many disadvantages (Jindra et al., 2016). The increasing traffic intensity brings many negative impacts. The most significant negative impacts of transport include the noise, vibration and production of harmful exhaust emissions as CO, CO_2, NOx, HC and particulate matters. The exhaust gases emitted from the engine often get into the human respiratory tract and may cause headaches, irritation of the mucous membranes in eyes and throat and cause cancer (Küüt et al., 2015). The oxides of nitrogen and sulfur which are emitted by internal combustion engines can result in acid rains (Fayyazbakhsh & Pirouzfar, 2017). Globally, the road transport sector is one of the main sources of carbon dioxide emissions and pollution. Therefore, the reduction of emissions from this sector is one of the key objectives in order to meet the Kyoto Protocol and create a sustainable transport system (Beleov et al., 2017).

The combustion of hydrocarbon fuels results in emissions of various kinds. The gaseous pollutants from diesel engines mainly contain carbon monoxide (CO), nitrogen oxides (NOx), sulphur oxides (SOx), hydrocarbons (HC) and small particles (Colbeck et al., 2011; Ma et al., 2011). Nitrogen oxides are usually generated during combustion at high temperature and its concentration increases with the engine combustion efficiency (Yanowitz et al., 2000; et al., 2012). Exhaust gases, thus products of combustion are one of the most serious shortcomings of internal combustion engine (Janoško 1994; Lenďák et al., 2014). To decrease negative impact of the emissions on the environment and mankind it is necessary to establish a regular inspection of the exhaust gases of diesel engines. When air is used as the oxidant, it is always the most significant component of the nitrogen N_2 content in the combustion process. The oxygen O_2 occurs in the exhaust gas, when the entire content does not apply to the fuel oxidation, because there was excess of the fresh air or it has not been used for other reasons (closing in fuel beam, etc.). Oxidation of NOx, which consists mainly of NO_x and a smaller amount of nitric oxide NO_2 is generated in the combustion chamber at high temperatures (Králik et al., 2016). The relationship between the quality of the mixture with the amount and composition of exhaust gases and technical condition of the engine has a great diagnostic meaning (Ogunmola et al., 2013; Jukl et al., 2014).

In order to meet the increasingly strengthened exhaust emissions regulations, much effort has been put into improving existing fuels or innovating novel fuels as well as developing new engine generations (Khalife et al., 2017).

The fuel adulteration method is widely accepted by many researchers, to achieve specific fuel properties to improve performance and achieve good emission control of diesel engine without any modification of the existing engine. There can be used various types of additives, based on different chemical principles such as alcohol, organometallic, nitrate etc. Each of these types has different effects on the parameters of combustion engines (Song et al., 2006; Gidney et al., 2010).

The basic requirements of all catalysts as fuel additives to conventional fuels are: The additive should decrease the exhaust emissions as well as increase the oxidation intensity in the engine. It is necessary to maintain the typical operational properties of engines. If catalytic additives are mixed with fuel, their chemical stability in the mixture must be retained under all conditions. Catalytic additives should not decrease the working effectiveness of the particulate filters and catalytic additives should not increase the emissions of environmentally harmful substances (Polonec & Janosko 2014; Shaafi et al., 2015).

The fuel type associated with a change in the combustion process results in the formation of particle shape and shows that the particle size and number distribution emitted is closely related to the physical and chemical properties of the fuel, suggesting that an increase in the proportion of oxygen in the air–fuel mixture due to the addition of an oxygenate, can lead to a significant change in size distribution and number of emitted particles with one or another fuel blend. Some experiments using combustion engines with oxygenated fuels have reported an emission reduction of total hydrocarbons, CO, and smoke, which means a reduction of PM (Gürü et al., 2002; Barrios et al., 2014).

Several additive manufactures such as: Castrol TDA, STP, Liqui Moly, Sheron, Ekolube, Valvoline, VIF and Tectane claim that their products improve technical state of fuel injection system by cleaning and improve cold engine starts, increase octane number. Some manufacturers guarantee decreases of fuel consumption in range of 2–7% and improvement in emissions. For testing, we chose an additive from company Lang Chemie whose name is VIF because it is one of the most commonly used in Central Europe.

MATERIALS AND METHODS

The aim of the contribution was to evaluate the effect of selected Super diesel and Super benzin additive from VIF manufacturer on the power and emission parameters along with the fuel consumption for the diesel and petrol engine with different mileage. The tested vehicles are Škoda Octavia (Fig. 1) category M1 with the 1.9 TDI diesel engine with a rotary injection pump and Renault Clio (Fig. 2) category M1 with 1.2 L petrol engine. The vehicle's main parameters are displayed in Table 1.

Figure 1. Tested vehicles Škoda Octavia 1.9 TDI (388 k km).

Figure 1. Tested vehicles Renault Clio 1.2 (73 k km).

Table 1. Main parameter of tested vehicle

Vehicle	Škoda Octavia	Renault Clio
Year of manufacture	2002	2008
Engine type	ASV	D7FG7
Cylinders capacity	1,896.0 cm^3	1,149.0 cm^3
Emission regulations	EURO 3	EURO 4
Post-treatment emission systems	NKAT, EGR	NKAT
Highest engine power/speed	81 kW / 4,150 min^{-1}	43 kW / 5,250 min^{-1}
Maximum vehicle design speed	191 km h^{-1}	158 km h^{-1}
Operating weight	1,275 kg	1,010 kg
Number of driven axles	1 / front	1 / front
Tires	195 / 65/ R15 – Barum Polaris 3	175 / 65 / R14
Number of driven kilometres	388,546	73,523

Characteristics of working mediums

Škoda Octavia car used fuel from brand Slovnaft. It was a basic range of fuel without the additive with the trade name Tempo plus winter diesel. Pumped diesel fuel met the requirements of standard EN 590 and also satisfies the conditions of the World Association of Automobile Manufacturers.

Renault Clio used Shell FuelSave Natural gasoline with 95 octane number and winter specification. The gasoline must meet the norm STN EN 228 and law number 725/2004 Z.z. In the both tank contained approximately 25 litres which was half the capacity of the tank.

Figure 3. Used additives by VIF.

VIF additives (Fig. 3) has been chosen as it is well known and often used in real world. It is sold in a plastic bottle with volume of 125 mL. In Škoda with diesel engine, Super diesel additive was used. It is a product constructed on the basis of 2-ethylhexyl nitrate ($C_8H_{17}NO_3$), the manufacturer indicates improvement in the cetane number by 5 units, better combustion, reduced engine noise and lower fuel consumption by 5%.

In Renault, Super benzin additive was used which is constructed on the polyether basis. The additive should improve fuel consumption by 5 to 7%, keeps the engine and the fuel system clean, improves the lubrication properties of the fuel and protects the injection from wear.

The additives serve to improve 40 to 60 litres of fuel. In the tests, the entire volume of the additive was used, ensuring a dosing ratio of up to 1: 200 respectively 0.125 L additive: 25 L fuel.

Characteristics of the instruments

Due to inaccurate measuring of fuel consumption by a vehicle on-board computer, it was necessary to use a different, more accurate system. We used an AIC-5004 Fuel Flowmaster (Fig. 4) external fuel meter from AIC SYSTEMS AG (accurancy ± 1%, the uncertainties K = 2) which joined the car's fuel system in its engine compartment. Due to the fact that the device is connected to a performance dynamometer, it does not need a display unit, but the data is displayed along with the other measured variables on the roller dynamometer. This makes it possible to read the exact values of a specific amount of fuel in specific engine operating modes.

Figure 4. External fuel meter AIC-5004 Fuel Flowmaster by AIC SYSTEMS AG.

Performance dynamometer by the German manufacturer MAHA (Fig. 5) with the designation MSR 500 (accurancy ± 2%, the uncertainties K = 2) with the possibility of measuring 4-wheel drive have been used to measure the performance of the vehicles. Air temperature in laboratory was 21–24 °C, relative humidity 26.8–27.5% and air pressure 994.2–995.6 hPa. From this and other parameters MAHA calculated the corrected performance according reg. EWG 80/1269.

Figure 5. Performance roller dynamometer MAHA MSR 500.

Exhaust gas analyser, model MGT 5 / MDO2 – LON (Fig. 6) by brand MAHA have been used to detect quantity of emissions in the exhaust gas. It is a dual instrument to record the production of both petrol and diesel emissions. Accurancy and measurement uncertainties of analyser: accuracy CO = ± 0.06%, the uncertainties CO K = 0,012, accuracy HC = ± 12 ppm, uncertainties HC K = 1.2, accuracy smoke = ± 0.6%, uncertainties smoke K = 2.0).

Figure 6. Exhaust gas analyser – MGT 5 / MDO2 – LON by brand MAHA.

During the measurement of the petrol engine emissions were measured carbon monoxide CO (% of vol.) and unburned hydrocarbons HC (ppm) and in diesel engine smoke was measured (m^{-1}).

Similarly, as the fuel flow meter, the device is connected to a performance dynamometer, which allows recording and displaying, in addition to the normal emission tests, the quantity of emissions produced depending on the combustion engine operation mode.

Methology of measurement

Experimental measurements of a vehicle with a gasoline and diesel engine were divided into two levels:

At the first level, the engine speed during the entire operating speed range as well as the maximum power and torque values through the MAHA MSR500 cylindrical test were measured and rated. This is a standardized test of measurement.

At the second level, fuel consumption and exhaust emissions were measured and monitored. Focus has been given on the tracking of selected parameters during the selected free driven cycle proposed by the authors, which were performed at constant engine speeds and constant load. The operating engine speed was set at 3,500 rpm and the brake bench load set to 150 N in constant setting. The CO_2, HC, O_2 and fuel consumption were measured with the gasoline engine. The smoke and fuel consumption were measured with the diesel engine.

The process of measurement lasted 150 seconds, from which a 30 second steady state was subsequently selected. These measurements were repeated 5 times prior and 5 times after adding the additive to the fuel for all parameters of the engines, which together is 20 measurements.

The measurement process itself consisted of several important steps: fixing the car on the roller, connection of the flowmeter, exhaust gas analyser, oil temperature probe and pairing the vehicle via OBD diagnostics with a computer to record all values from the control unit and the devices to the computer. After completion of the initial steps, the engine had to be warmed to the operating temperature to ensure the most accurate and trusted results.

It was necessary to calculate and analyse measured parameters using the basic following relationships:

Calculation of performance

$$P = M_k . \omega = M_k . 2 . \pi . n \text{ (kW)} \tag{1}$$

Calculation of torque

$$M_k = \frac{P}{2.\pi.n} \text{ (Nm)} \tag{2}$$

The quantity of fuel consumed for the selected period of time

$$V' = V_{x1} - V_{x2} \text{ (dm}^3\text{ 30 s}^{-1}\text{)} \tag{3}$$

Hourly fuel consumption

$$V = \frac{V' . \rho_{fuel}}{t} \cdot 3{,}600 \text{ (kg hod}^{-1}\text{)} \tag{4}$$

RESULTS AND DISCUSSION

Based on the external engine speed characteristics obtained from the MAHA performance dynamometer, it was possible to assess and compare the performance parameters of the vehicles. As can be seen in Table 2, after comparing the results, it was concluded that the diesel power increased by 4.4 kW and torque by 5.97 Nm. Increase in power by 0.5 kW and torque by 0.55 Nm for petrol engine was in range of dynamometer measurement inaccuracy. Therefore, we do not consider measured values for petrol engine as significant in terms of performance improvement.

Table 2. Comparison of average performance parameters before and after adding additive to diesel

Vehicle	Parameter	Before using the additive	After using the additive
Renault Clio	Corrected performance [P_{norm}]	47.75 kW	48.25 kW
	Torque [M_{norm}]	93.2 N m^{-1}	93.75 N m^{-1}
Škoda Octavia	Corrected performance [P_{norm}]	83.80 kW	88.2 kW
	Torque [M_{norm}]	240.2 N m^{-1}	246.17 N m^{-1}

For a more complex assessment, not only the highest values are important, but also the overall performance of the speed characteristic. Figs 7 and 8 presents the overlap of the power curves before and after the addition of the additive. Significant difference can be seen mainly in speed characteristic of diesel engine. Speed characeristic after application of additive approximated factory set speed charateristic.

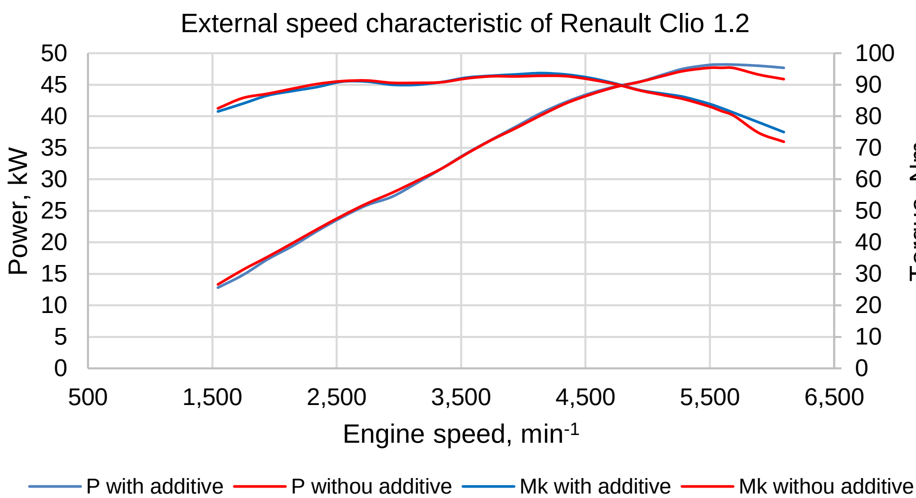

Figure 7. Comparison of average performance and torque curves before and after adding additive to gasoline.

For the Renault Clio 1.2, the manufacturer states a max. power of 45 kW at 5,250 rpm. During the experiments, the power output at these revolutions was measured at 47.2 kW prior additive usage and 47.6 kW after additive usage, which statistically does not represent a fundamental difference. For the Škoda Octavia 1.9 TDI, the manufacturer states max. power 81kw at 4,200 rpm. At these revolutions, the power of 80.87 kW was measured prior additive usage and 83.76 kW after the additive usage which represents a draw of 3.57%.

Another examined parameter was the influence of fuel additive on engine emissions. This was performed as a sequence of 5 consecutive measurements before and 5 measurements after addition within the specified time range.

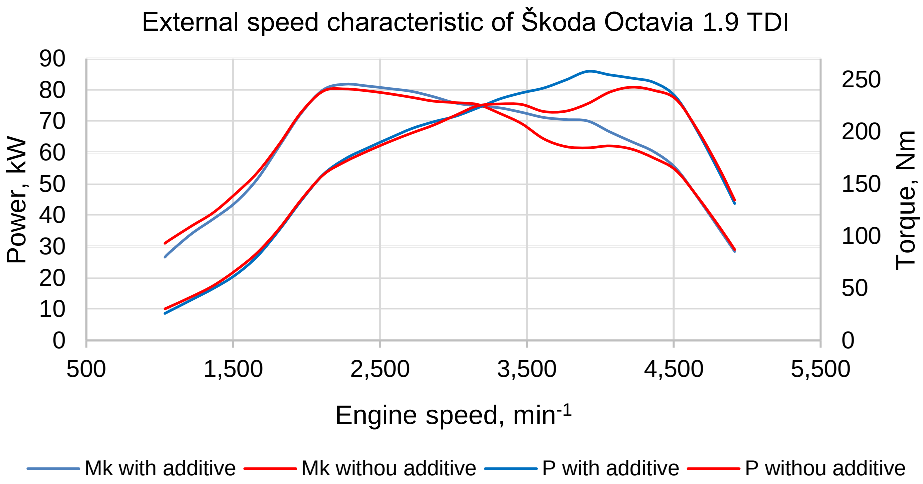

Figure 8. Comparison of average performance and torque curves before and after adding additive to diesel.

Similarly, to the measurement of emissions (Figs 9–12), we measured the fuel consumption by using a flow meter that was connected to the fuel system of the car. The values of these measurements were averaged and statistically analysed. The results are shown in Tables 3 and 4.

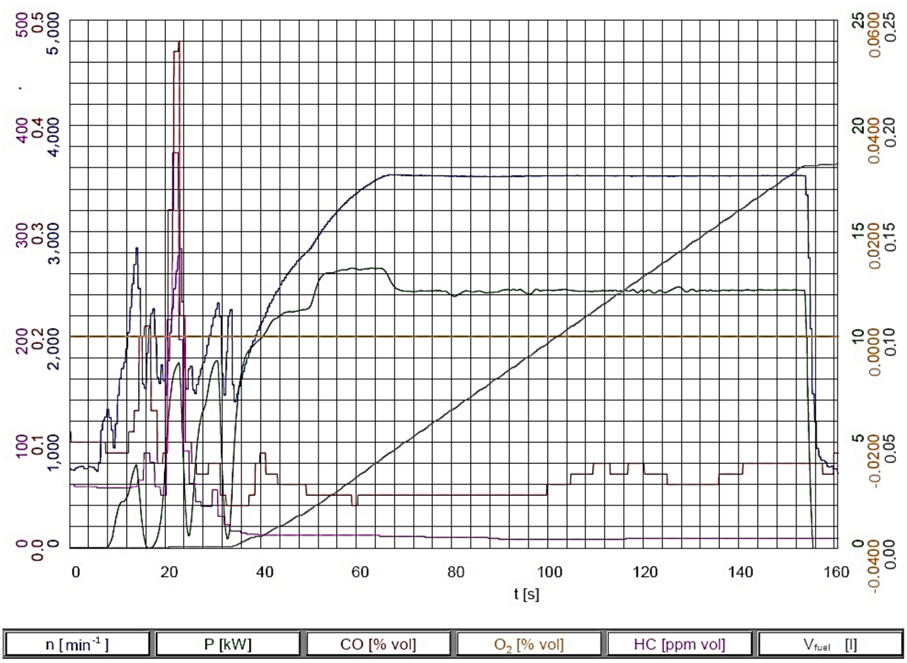

Figure 9. Sample of Renault Clio 1.2 time dependencies of measured parameters: power, speed CO, O_2, HC, fuel consumption before adding additive.

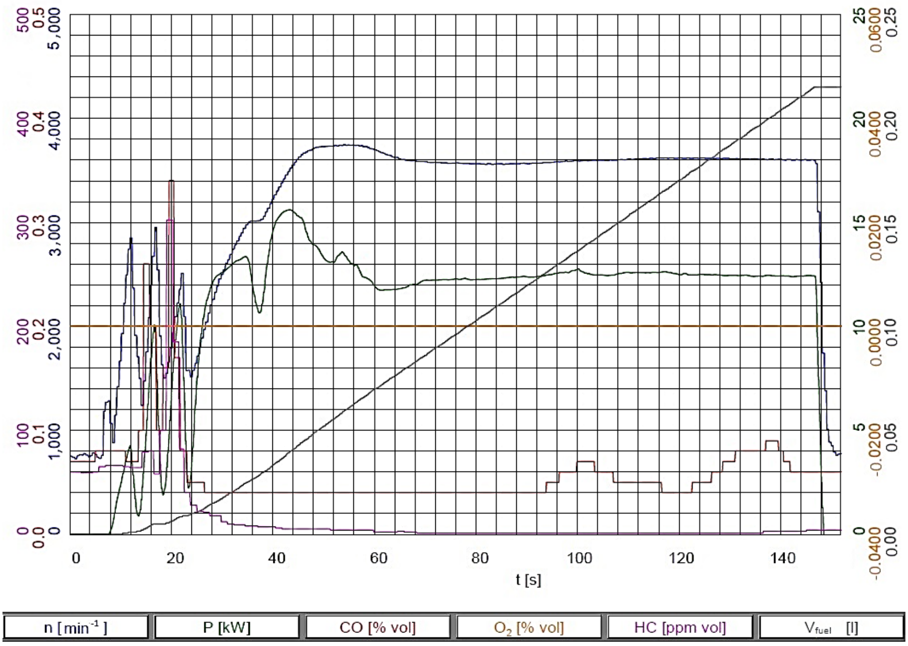

Figure 10. Sample of Renault Clio 1.2 time dependencies of measured parameters: power, speed CO, O_2, HC, fuel consumption after adding additive.

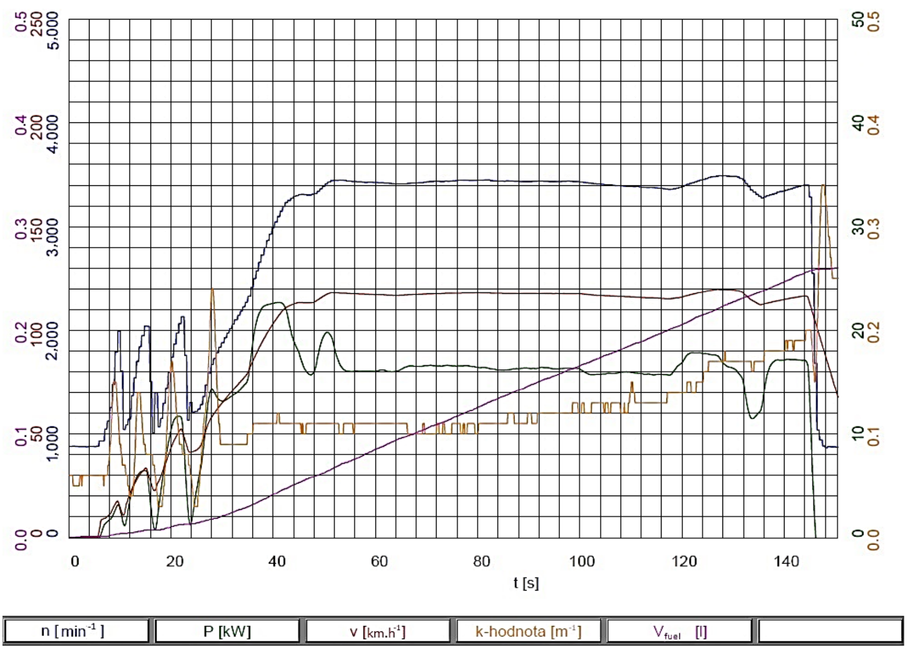

Figure 11. Sample of Škoda Octavia 1.9 TDI time dependencies of measured parameters power, speed, k-value, fuel consumption before adding additive.

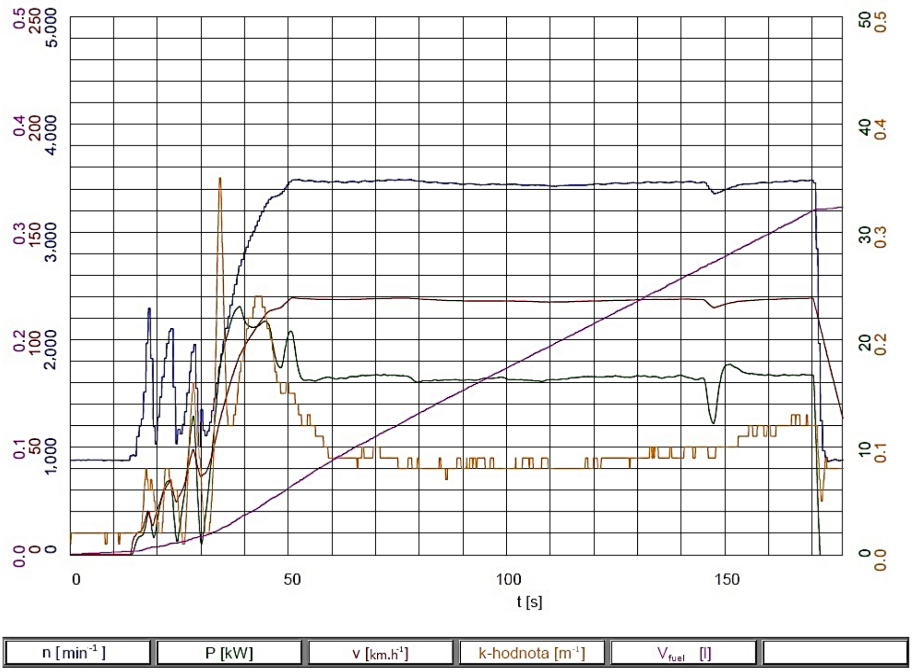

Figure 12. Sample of Škoda Octavia 1.9 TDI time dependencies of measured parameters power, speed, k-value, fuel consumption after adding additive.

Table 3. The results of measuring emissions and fuel consumption on the Renault Clio

Renault Clio	Time of measurement	Value	Different	Standard deviation	Variation coefficient
Carbon monoxide	before addition	0.083	- 0.033	0.025	0.303
CO (% of vol.)	after addition	0.050		0.043	0.865
Unburned	before addition	11.930	- 7.19	4.344	0.364
hydrocarbons HC (ppmo)	after addition	4.740		8.790	1.855
Fuel consumption	before addition	3.940	+ 0.29	0.185	0.047
(kg hod^{-1})	after addition	4.230		0.076	0.018

Table 4. The results of measuring emissions and fuel consumption on the Škoda Octavia

Škoda Octavia	Time of measurement	Value	Different	Standard deviation	Variation coefficient
K-value (m^{-1})	before addition	0.137	- 0.04	0.022	0.163
	after addition	0.097		0,014	0.014
Fuel consumption	before addition	5.432	- 0.184	0.174	0.092
(kg hod^{-1})	after addition	5.248		0.047	0.009

The results of the experimental measurements show partially the positive effect of the selected additive on the fuel consumption and the emissions of the tested passenger cars.

Measurement in Renault Clio showed that CO emission decreased by 39.76%, HC decreased by 60.27%. However, fuel consumption increased by 7.36% therefore claimed statements by VIF producer to decrease fuel consumption in range of 5–7% for petrol engine has not been confirmed by our measurements.

Measured parameters in Škoda Octavia 1.9 TDI showed that smoke (K-value) decreased by 29.20% and fuel consumption decreased too by 3.39% while VIF producer claims decrease by 5%.

CONCLUSIONS

The aim of the paper was to evaluate the impact of the additives on the vehicle's power and emission parameters along with fuel consumption. This complex approach of additives testing brings more precise answers on energetical and emission changes in petrol and diesel engines.

Experimental measurements were performed in a test laboratory on preselected vehicles. For testing purpose, vehicle Skoda Octavia with engine volume of 1,896 cm^3, 81 kW, 388 k km mileage and Renault Clio with engine volume 1,149.0 cm^3, 43 kW, 73 k km mileage were chosen. Both vehicles were equipped with manual transmission and front-wheel drive. The measurements partiality confirmed the additive manufacturer's claims about emissions improvement, fuel consumption and performance parameters. Upon using the diesel additive, a rather significant difference was noticed for torque and engine power. In the case of a petrol engine, the difference was minor in range of dynamometer inaccuracy. We assume that the gasoline additive does not have a significant effect on the engine's performance parameter, but it has a positive cleaning impact on the combustion chamber.

In conclusion it can be stated that tested diesel engine with the higher mileage (approx. 388 k km) showed significant increase in power and torque while in newer petrol engine (approx. 73 k km) improvement has not been measured. Emissions were improved in both engines. Difference has been also measured in fuel economy as in petrol engine consumption increased while in the diesel engine it decreased.

ACKNOWLEDGEMENTS. This work was supported by AgroBioTech Research Centre built in accordance with the project Building 'AgroBioTech' Research Centre ITMS 26220220180.
The contribution was made under the grant project of the Ministry of Education of the Slovak Republic VEGA 1/0464/17 'Monitoring of the impact of ecological fuels derived from agricultural production and impurities in hydrocarbon fuels to technical and environmental performance of internal combustion engines used in agricultural and transport technology'.

REFERENCES

Barrios, C., Martin, C., Domínguez-Sáez, A., Álvarez, P., Pujadas, M. & Casanova, J. 2014. Effects of the addition of oxygenated fuels as additives on combustion characteristics and particle number and size distribution emissions of a TDI diesel engine. *Fuel* **132**(1), 93–100.

Beloev, I., Gabrovska-Evstatieva, K. & Evstatiev, B. 2017. Compensation of CO_2 emissions from petrol stations with photovoltaic parks: Cost-Benefit and risk analysis. *Acta tech. Agric* **4/2017**, 85–90.

Colbeck, I., Nasir, Z. A., Ahmad, S. & Ali, Z. 2011. Exposure to PM10, PM2.5, PM1 and Carbon Monoxide on Roads in Lahore. *Aerosol Air Qual. Res.* **11**(1), 689–695.

Fayyazbakhsh, A. & Pirouzfar, V. 2017. Comprehensive overview on diesel additives to reduce emissions, enhance fuel properties and improve engine performance. *Renewable and Sustainable Energy Reviews* **74**(1), 891–901.

Gidney, J.T., Twigg, M.V. & Kittelson, D.B. 2010. Effect of Organometallic Fuel Additives on Nanoparticle Emissions from a Gasoline Passenger Car. *Environmental Science and Technology* **44**(7), 2562–2569.

Gürü, M., Karakaya, U., ltıparmak, D. & Alıcılar, A. 2002. Improvement of Diesel fuel properties by using additives. *Energy Conversion and Management* **43**(8), 1021–1025.

Janosko, I. 1994. Speed control of diesel engine with microcomputer. *Acta Technologica Agriculturae*

Jukl, M., Polcar, A. & Čupera, J. 2014. Possibilities of monitoring the technical condition of the combustion engine with starter load corrent. *Acta universitatis agriculturae et silviculturae mendelianae brunensis* **62**(1), 961–969.

Jindra, P., Kotek, M., Mařík, J. & Vojtíšek, M. 2016. Effect of different biofuels to particulate matters production. *Agronomy Research* **14**(3), 783–789.

Khalife, E., Tabatabaei, M., Demirbas, A. & Aghbashlo, M. 2017. Impacts of additives on performance and emission characteristics of diesel engines during steady state operation. *Progress in energy and Combustion Science* **59**(1), 32–78.

Králik, M., Jablonický, J., Tkáč, Z., Hujo, Ľ., Uhrinová, D., Kosiba, J., Tulík, J. & Záhorská, R. 2016. Monitoring of selected emissions of internal combustion engine. *Research in agricul. engineering* **62**(1), 66–70.

Küüt, A., Ilves, R., Hönig, V., Vlasov, A. & Olt, J. The impact of bioethanol on two-stroke engine work details and exhaust emission. *Agronomy Research* **13**(5), 1241–1252.

Lenďák, P., Jablonický, J., Uhrinová, D., Kosiba, J. & Polorecký, J. 2014. Possible solutions for checking particulate matter filters (DPF) in motor vehicles. *Advanced Materials Research* **1059**, 119–125.

Ma, C.M., Hong, G.B. & Chang, C.T. 2011. Influence of Traffic Flow Patterns on Air Quality inside the Longest Tunnel in Asia. *Aerosol Air Qual. Res.* **11**(1), 44–50.

Ogunmola, B., Abolarin, S. & Adelaja, A. 2013. On the prediction of pollutant emission (NOx) in internal combustion engine. *Advanced Materials Research* **824**, 505–513.

Polonec, T. & Janoško, I. 2014. Improving performance parameters of combustion engine for racing purposes. *Research in agricultural engineering* **60**(3), 83–91.

Shaafi, T., Sairam, K., Gopinath, A., Kumaresan, G. & Velraj, R. 2015. Effect of dispersion of various nanoadditives on the performance and emission characteristics of a CI engine fuelled with diesel, biodiesel and blends—A review. *Renewable and Sustainable Energy Reviews* **49**(1), 563–573.

Song, C., Zhang, W., Pei, Y., Fan, G. & Xu, G. 2006. Comparative effects of MTBE and ethanol additions into gasoline on exhaust emissions. *Atmospheric Environment* **40**(11), 1957–1970.

Uhrinová, D., Jablonický, J., Hujo, Ľ., Tkáč, Z., Kučera, M. & Kosiba, J. 2012. Measurement of operating parameters and emissions of tractor with diesel oil and biofuel. In Živić, M., Klarić, Š., Milinović, A., (eds): *TEAM*. J.J. Strossmayer University of Osijek, Slavonski Brod, Croatia, pp. 96–98.

Yanowitz, J., McCormick, R.L. & Graboski, M.S. 2000. In-use Emission from Heavy-duty Diesel Vehicles. *Environ. Sci. Technol* **34**(5), 729–740.

Agronomy Research **16**(3), 749–757, 2018
https://doi.org/10.15159/AR.18.134

Evaluation of the RTK receiver's capability of determination the accurate position

J. Kadeřábek[1,*], V. Shapoval[1] and P. Matějka[2]

[1]Czech University of Life Sciences Prague, Faculty of Engineering, Department of Agricultural Machines, Kamýcká 129, CZ16500 Prague, Czech Republic
[2]Czech University of Life Sciences Prague, Faculty of Engineering, Department of Technological Equipment of Buildings, Kamýcká 129, CZ16500 Prague, Czech Republic
[*]Correspondence: jkaderabek@tf.czu.cz

Abstract. The main aim of this experiment was to compare low-cost RTK receiver, that possible can be used for precise agricultural application, another that is currently used for these applications and the third one that suits for static measurement the most and gives the reference point for results comparison. The main idea of this research was to compare the measured positions during static measurement of RTK receivers. Were discovered that the receiver Trimble 750 was not able to work in fix mode (mode when the RTK receivers are capable to measure the most accurately) for the whole time. This fact affects the results from whole measurement and showed that errors were a little higher than producers specifies. The low-cost receiver u-Blox C94-M8P showed satisfying results when in most cases it was capable to solve the problem of ambiguity integer phases. The main parameters in this work that were counted and summarized were: accuracy, precision, RMS error, system status ratio and number of satellites.

Key words: localization, positioning, survey-ing, accuracy, precision, agriculture, RTK, VRS.

INTRODUCTION

Nowadays, one of the most accurate localization methods which is available on market is RTK (Real Time Kinematic). This system uses signal correction by reference stations for more accurate positioning (Feng & Wang, 2007). This method, which has according to its producers the precision around 20 millimetres, already found new uses in many fields of industry. The RTK method which is increasingly common is used for precision farming purposes as an automatic guidance of agricultural machines. RTK system as all satellite navigation systems is affected by different influences that cause errors. These influences are: ephemeris data error, satellite clock error, ionosphere influence, troposphere influence, antennas construction and placement (including multipath error) (Tamura et al., 2002). For minimizing these errors RTK system typically involves two GNSS receivers: the base station and one or more rovers (including technology for transmission of correction data). During operation, the base station and the rover are observing a common set of satellites and simultaneously the base station sends its position and satellite observation to the rover. The rover combines these data with its own satellite observations and determines its position in real time (Berber & Arslan, 2013).

In a certain way the classic principle, which is mentioned above, is simple but still have some disadvantages. The main disadvantage is the requirement of the base station to be located within ten kilometres or in some cases five kilometres close to rover (Mageed, 2013; Carballido et al., 2014). The precision decreases when required maximal distance from the base station increases.

However, the method called Virtual Reference Station (VRS) can solve the problem of the required proximity of base with higher efficiencies and lower costs. The main idea is to generate virtual reference station that simulates reference/base station nearby the user receiver. The wide network covered by multiple reference stations is used to create the virtual station that allows doing precise positioning everywhere in a wide area only by receiving the correction data (Retscher, 2002). The communication network is performed by using common phone data lines.

More affordable low-cost systems emerged on the market in the course of development of RTK receivers. However, it appeared that these low-cost systems exhibit characteristics that negatively affect the accuracy of position determination (Beran et al., 2005). The worse ability of reaching the fix mode is more common for cheaper variants. Probably it is given by the receiver's inability to solve the problem of ambiguity phases.

The main aim of this research was to verify and to compare the properties of modern RTK systems from different price relations. The method for this research was to compare the measured positions during static measurement of RTK receivers. In this research was verified that individual receivers perform different deviations and in most cases do not reach parameters of errors mentioned by producers.

MATERIALS AND METHODS

The main idea of this experiment was to compare low-cost RTK receiver, that possible can be used for precise agricultural application, with another receiver that is currently used for these applications and with the third one which suits the most for static measurement and gives the reference point for results comparison. The reference point was generated from long-term measurement (lasted for 21 hours) from Trimble 5800 receiver.

Three different RTK receivers were chosen for this experiment. All of them used correction data from VRS (Virtual Reference Station) through NTRIP clients (Network Transport of RTCM data over IP) in RTCM 3.1 format and sample rate 1 Hz. Placement of VRS was provided by service 'Trimble VRS Now' in closer area of measurement.

The first device was low-cost receiver u-Blox C94-M8P-C with Novatel GPS-702-GG antenna. The second receiver was Trimble CFX-750 with Trimble AG25 GNSS antenna that is commonly used for precise agricultural applications. And the third receiver was Trimble 5800 set with own built-in antenna and data controller Trimble TSC2 that is more often used for static positioning for example for geodetic targeting positioning.

The notebook model Lenovo E540 was used during measurement for more functions. During all measurements, this notebook was connected on the internet for receiving correction signal for the u-Blox M8P receiver. This correction signal was obtained through the NTRIP client in native application u-center v8.24 and in the same application the logging of NMEA GNGGA messages was conducted. In case of Trimble 750 receiver was used RTKM2 v.01 modem with own NTRIP client for transmission of data corrections. The NMEA messages in the GPGGA protocol format were logged from the serial line to notebooks console in 9,600 baud rate. Trimble 5800 setting communication and logging were provided by Trimble TSC2 with its own modem and NTRIP client through the Bluetooth transmission. Then data exported from controller were obtained by internal software to the computer. All three receivers were receiving and recorded in the period of one second.

The measurements were realized in areal of The Czech University of Life Sciences on the roof of the building of The Faculty of Engineering. The whole experiment took two days with three measurements. Two measurements were realized on the first day and the third measurement was realized the next day. All three measurements were running for one hour period with sampling rate of obtained positions one sample per second (1 Hz). The received signal of all receivers was obtained from sufficient number of satellites, apparent from the Table 1 in values μ_s. Measurements of Horizontal Dilution of Precision (HDOP) were different for each receiver, in average: u-Blox M8P achieved 0.72, Trimble 750 achieved 1.15 and Trimble 5800 achieved 2.24. The antennas were placed in the line on the distance of five meters from each other (further in text: 'PLACE A' and 'PLACE B'). Three antennas were attached to wood construction on the same line on the distance of 0.7 meters. The construction was arranged in a way to be stable and ensure manipulation with antennas without changing the distance from each other. First and third (from day two) measurements were realized on 'PLACE A' and the second on 'PLACE B' (Fig. 1).

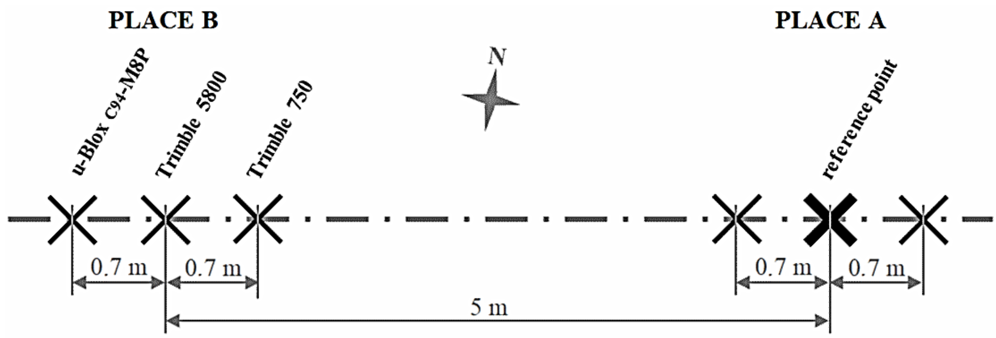

Figure 1. Placement of receiver antennas.

From data processing perspective all measured coordinates were needed to convert to the Cartesian coordinate system END (East-North-Down) for future calculations of horizontally positioning errors. The orientation of this coordinate system allows calculating of the positioning deviations in meters with knowledge of the azimuth and ignored altitude. The logged coordinates by all three receivers was in WGS84 (World Geodetic System 1984) format, i.e. in the spherical coordinate system. The first coordinates were converted to the ECEF (Earth-centred, Earth-Fixed) Cartesian coordinate system and then this obtained cloud of points was rotated to END coordinate system. Then the determination of horizontal distance was calculated for each coordinate from the data set of one measurement (in ENU) toward to the created reference point. The reference point was determined for each antenna placement by deducting of the antennas place offsets on the line (Fig. 1) and deducting of previous calculated azimuth. Were obtained the azimuth from two averaged coordinates in END. Both coordinates were surveyed by receiver Trimble 5800 from 3,600 samples of measurement.

Theory and modelling

For evaluation of the results were chosen these parameters:

1. Accuracy (μ_{err}) – sample mean of deviations from reference point (error offset):

$$\mu_{err} = \frac{1}{n}\sum_{i=1}^{n} d_i \tag{1}$$

where n – data-set of measured samples; d_i – deviation from reference point at the i index of a data-set, m.

2. Precision (σerr) – standard deviation of error (stability of positioning):

$$\sigma_{err} = \sqrt{\frac{\sum_{i=1}^{n}(d_i - \mu_{err})^2}{n-1}} \tag{2}$$

where n – data-set of measured samples; d_i – deviation from reference point at the i index of a data-set; μ_{err} – sample mean of deviations from reference point, m.

3. RMS error (RMSerr) – value specified by the manufacturer (metric emphasizing large errors):

$$\mathrm{RMS}_{err} = \sqrt{\frac{1}{n}\sum_{i=1}^{n} d_i^{\,2}} \tag{3}$$

where n – data-set of measured samples; d_i – deviation from reference point at the i index of a data-set, m.

4. System status ratio (SSR) – ability of the system to solve the problem of ambiguity integer phases:

$$\mathrm{SSR} = \frac{m}{n} * 100 \tag{4}$$

where n – data-set of measured samples; m – data-set of samples with solved ambiguity integer phases, %.

5. Number of satellites (μs) – the average value of the number of received GPS satellites:

$$\mu_s = \frac{1}{n}\sum_{i=1}^{n} s_i \tag{5}$$

where n – data-set of measured samples; s – number of received satellites at the i index of a data-set, -.

RESULTS AND DISCUSSION

All the monitored parameters are summarized in the table (Table 1). For better presentation, ratings were divided into these three categories:

All measurement – represents all values from the range of measurement.

Without fix – represents the values when the receiver was not capable to solve the problem of ambiguity integer phases. It includes states 'RTK float' and 'Only GPS'.

Fixed – represents the values when the receiver was capable to solve the problem of ambiguity integer phases, i.e. in a mode when the RTK receivers are capable to measure the most accurately. This category includes only state 'RTK float'.

Due to the impossibility of logging except the fixed positions by Trimble 5800 receiver (due to logging principle of the receiver), only these positions were evaluated. The results of all three measurements and their average values were always written to the table below.

Table 1. Measured values overview

		Whole measurement		Without fix		Fixed		
	*)	u-Blox M8P	Trimble 750	u-Blox M8P	Trimble 750	u-Blox M8P	Trimble 750	Trimble 5800
μ_{err} [m]	1st	0.013	0.188	0.026	1.096	0.013	0.008	0.009
	2nd	0.012	0.223	0.175	1.293	0.010	0.010	0.013
	3rd	0.016	0.080	0.092	1.318	0.009	0.009	0.012
	mean	**0.014**	**0.164**	**0.098**	**1.236**	**0.011**	**0.009**	**0.011**
σ_{err} [m]	1st	0.004	0.406	0.005	0.080	0.004	0.005	0.005
	2nd	0.027	0.480	0.132	0.103	0.006	0.006	0.006
	3rd	0.019	0.299	0.066	0.199	0.004	0.006	0.007
	mean	**0.014**	**0.156**	**0.122**	**1.282**	**0.010**	**0.009**	**0.012**
	$1\sigma_{err}$	0.014	0.156	0.122	1.282	0.010	0.009	0.012
	$2\sigma_{err}$	0.028	0.311	0.243	2.565	0.020	0.019	0.024
	$3\sigma_{err}$	0.042	0.467	0.365	3.847	0.030	0.028	0.036
RMS_{err} [m]	1st	0.014	0.188	0.027	1.099	0.014	0.009	0.010
	2nd	0.030	0.223	0.219	1.297	0.011	0.011	0.014
	3rd	0.025	0.080	0.113	1.333	0.014	0.011	0.014
	mean	**0.023**	**0.164**	**0.120**	**1.243**	**0.012**	**0.010**	**0.013**
SSR [%]	1st	-	-	-	-	99.31	83.44	81.00
	2nd	-	-	-	-	98.39	83.36	96.58
	3rd	-	-	-	-	96.72	94.61	97.61
	mean	**-**	**-**	**-**	**-**	**98.14**	**87.14**	**91.73**
μ_s [-]	1st	8.015	7.918	7.800	8.000	8.017	7.901	7.568
	2nd	7.743	7.948	8.241	9.302	7.735	7.677	6.916
	3rd	7.976	7.891	8.119	8.000	7.971	7.885	7.224
	mean	**7.911**	**7.919**	**8.053**	**8.434**	**7.907**	**7.821**	**7.236**

*) measurement number.

The means of the errors (μ_{err}, σ_{err} and RMS_{err}) showed that receivers are capable to measure better in a state of 'Fixed' than in a state of 'Without fix'. In case of u-Blox M8P receiver the all of three monitored error parameters were more than eight times higher. In case of Trimble 750 receiver it was even more than one hundred times higher in all three parameters representing the errors. Following two figures of graphs better show the described phenomenon (Figs 2 and 3):

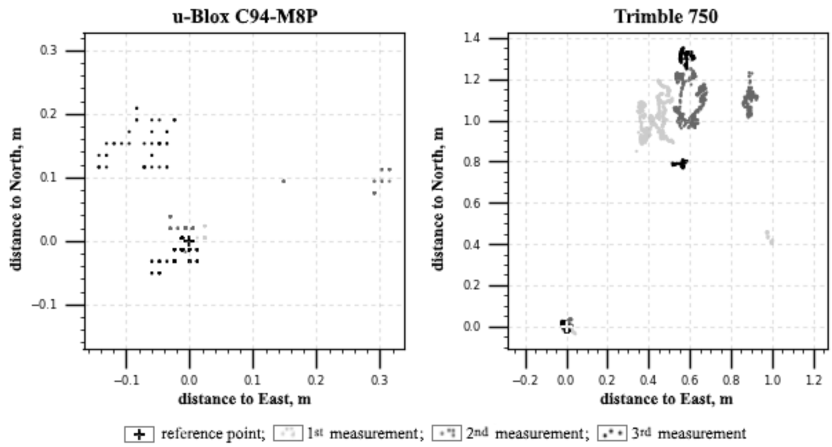

Figure 2. Positioning of the wholle measurement.

If we filtered out the samples when the receivers, were not capable to solve the complete ambiguity of the phase of carrier wave, from all measurement (Fig. 2) we obtained the cloud of points concentrated closer around the reference point (Fig. 3). Then the results of measured errors of all of three receivers had the similar character. The best in this evaluation was Trimble 750 which had the best result of all three error parameters. In all of three errors parameters were in the second place u-Blox M8P and the worst was Trimble 5800. The deviations in this evaluation were small in opposite to errors from whole period of measurement.

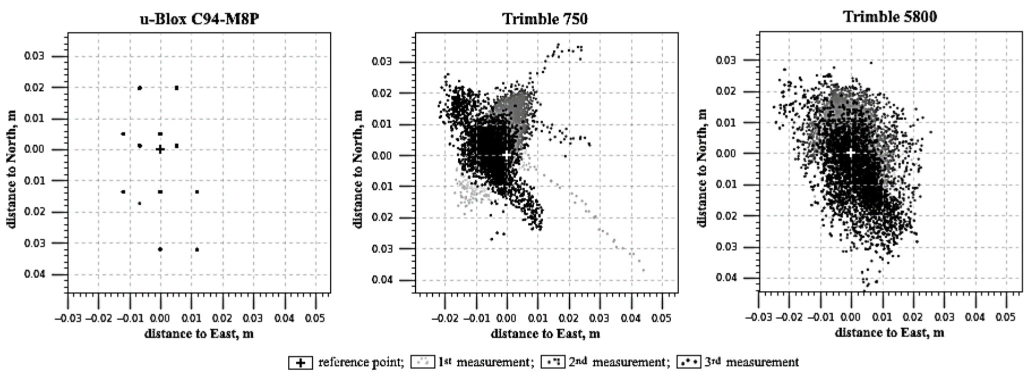

Figure 3. Positioning during fixed ambiguidy.

As we can see u-Blox M8P receiver was not capable to obtain finer resolution. That happened due to less number of decimal places in minutes values of geographic coordinates in NMEA message. Nevertheless, the measured coordinates oscillated mostly in four coordinates around the reference point.

In the range of the whole measurement, the parameters that influenced measured errors can be described by the state of what receivers were listed when they lost the capability to solve the ambiguity of phase. In this work the consequences of loss of ability to solve ambiguity was as follows: u-Blox M8P receiver always entered into state 'Float' (the state when is RTK receiver capable to solve only the decimal part of ambiguity of the carrier phase) and Trimble 750 receiver always entered into state of 'Only GPS' (the state when the RTK receiver is not capable to solve the ambiguity at all). It can be assumed that the complete loss of ambiguity of the Trimble 750 receiver had occurred due to the RTKM2 v.01 modem quality.

Other parameters that also influenced the results were the SSR, i.e. the percentage ratio of samples when the RTK receivers were capable the ambiguity of carrier phase, opposite to other possible states. Both these facts are obvious in graphs below (Figs 4 and 5). However, it is worth pointing out that these graphs have the different scale factor of the vertical axis (the distance deviation).

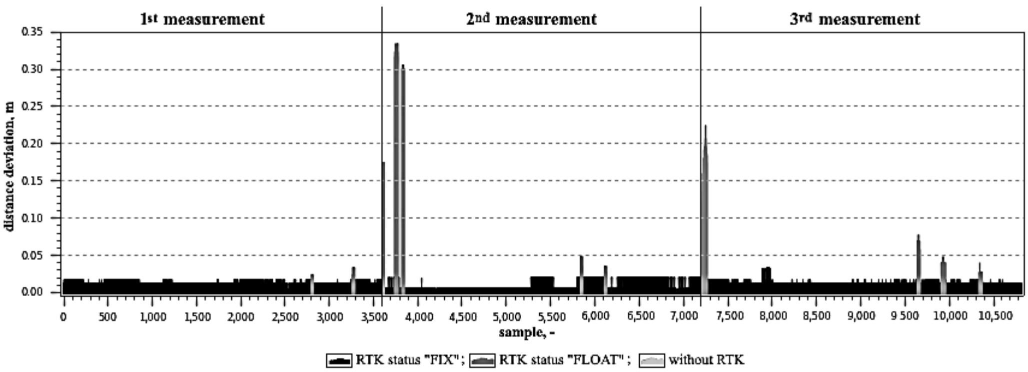

Figure 4. Accuracy deviation and system status of u-Blox M8P.

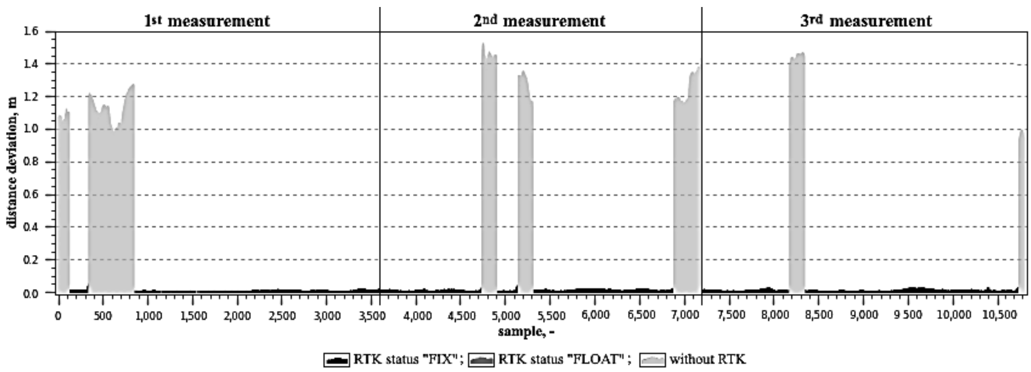

Figure 5. Accuracy deviation and system status of Trimble 750.

Due to results of SSR (87%) the ability of the system Trimble 750 to solve the problem of ambiguity integer phases was the worst during whole measurements. The better result was obtained from Trimble 5800 (92%) and surprisingly the best ability to solve ambiguity phases (98%) was shown by low-cost receiver u-Blox M8P. In this case, we cannot argue that this system provide the best ability to keep the fix mode because this ability can be influenced by different factors. One of them is the base station placement distance. In research of author Feng (2008) it's obvious that the baseline distance to a receiver can affect the system status ratio. In this research was confirmed the dependence of distance when in distance of 21 km the SSR was 99%, at 56 km 87% and at 74 km 77%. It is obvious that with base station placement distance the SSR was decreased.

The accuracy for three receivers was around 0.01 m during fix mode that corresponds with manufactures data's and results from other researches during static measurements (Garrido et al., 2011; Berber et al., 2012). In cases when receivers were measured in float or only GPS mode the errors were in terms of 0.10 m and in some cases more than one meter, that affected and increased errors for whole measurement data. Our next measurement will be based on these knowledge's and focused on finding how the receivers will be able to measure with fix mode and how without fix mode will affect accuracy, precision and RMS error during dynamic measurement.

CONCLUSIONS

The methodology of this research was based on static measurement (antennas had unchanged position during measurement). After evaluation of measurement, we discovered that the receiver Trimble 750 was not able to work in fix mode (the mode when the RTK receivers are capable to measure the most accurately) for the whole time. This fact affects the results from the whole measurement and showed that errors were a little higher than producers specifies. The low-cost receiver u-Blox M8P showed satisfying results when in most cases it was capable to solve the problem of ambiguity integer phases.

This static method can be applied for application where motion monitoring is not required, for example geodetic targeting. Therefore, we can ignore the samples of data with the unsolved ambiguity phase and use only the accurate ones (fix mode). The question is, if accuracy and precision of positioning will be influenced by the long-term monitoring or by the dynamic movement of the antennas. These properties of RTK receivers will be assessed in our next research.

ACKNOWLEDGEMENTS. This study was supported by GA no. 2017/31160/1312/3123 with topic 'Evaluation of Determined Position Accuracy by RTK Receivers'.

REFERENCES

Beran, T., Langley, R.B., Bisnath, S.B. & Serrano, L. 2005. High-Accuracy Point Positioning with Low-Cost GPS Receivers: How Good Can It Get?. In: *Proceedings of the 18th International Technical Meeting of the Satellite Division of The Institute of Navigation (ION GNSS 2005)*, pp. 1524–1534.

Berber, M. & Arslan, N. 2013. Network RTK: A case study in Florida. *Journal of the International Measurement Confederation* **46**(8), 2798–2806.

Berber, M., Ustun, A. & Yetkin, M. 2012. Comparison of accuracy of GPS techniques. *Journal of the International Measurement Confederation* **45**(7), 1742–1746.

Carballido, J., Perez-Ruiz, M., Emmi, L. & Agüera, J. 2014. Comparison of positional accuracy between rtk and rtx gnss based on the autonomous agricultural vehicles under field conditions. *Applied Engineering in Agriculture* **30**(3), 361–366.

Feng, Y.& Wang, J. 2008. GPS RTK Performance Characteristics and Analysis. *Journal of Global Positioning Systems* **7**(1), 1–8.

Feng, Y. & Wang, J. 2007. Exploring GNSS RTK performance benefits with GPS and virtual Galileo measurements. In: *Proceedings of Institute of Navigation National Technical Meetings*, San Diego, CA, USA, pp. 22–24.

Garrido, M.S., Giménez, E., de Lacy, M.C. & Gil, A.J. 2011. Surveying at the limits of local RTK networks: Test results from the perspective of high accuracy users. *International Journal of Applied Earth Observation and Geoinformation* **13**(2), 256–264.

Mageed, K.M.A. 2013. Accuracy evaluation between GPS Virtual Reference Station (VRS) and GPS Real Time Kinematic (RTK) techniques. *World Applied Sciences Journal* **24**(9), 1154–1162.

Retscher, G. 2002. Accuracy Performance of Virtual Reference Station (VRS) Networks. *Journal of Global Positioning Systems* **1**(1), 40–47.

Tamura, Y., Matsui, M., Pagnini, L.C., Ishibashi, R. & Yoshida, A. 2002. Measurement of wind-induced response of buildings using RTK-GPS. *Journal of Wind Engineering and Industrial Aerodynamics* **90**(12–15), 1783–1793.

Agronomy Research **16**(3), 758–768, 2018
https://doi.org/10.15159/AR.18.131

Using the FEM model for design the heat treatment of an agricultural tools

A. Kešner[1,*], R. Chotěborský[1], M. Linda[2] and M. Hromasová[2]

[1]Czech University of Life Sciences Prague, Faculty of Engineering, Department of Material Science and Manufacturing Technology, Kamýcká 129, CZ165 21 Prague, Czech Republic
[2]Czech University of Life Sciences Prague, Faculty of Engineering, Department of Eletrical Engineering and Automation, Kamýcká 129, CZ165 21 Prague, Czech Republic
[*]Correspondence: kesner@tf.czu.cz

Abstract. Agricultural tools need mechanical properties such as abrasive wear, hardness and toughness. These mechanical properties are achieved by choosing a suitable steel and subsequent heat treatment of the steel. Phases of the microstructure affects the final steel properties. The phase composition in the steel is influenced with the designing of the heat treatment. 25CrMo4 steel was investigated for the production of agricultural tools. The heat treatments ware designed for different cooling conditions. The salt bath was used to cooling as a medium with subsequent cooling on the water or in the air. The FEM method was used to designing the heat treatment conditions. The Johnson-Mehl-Avrami-Kolmogorov equation and the Koistinen-Marburger equations were used to prediction the microstructure phases. The microstructures were verified with experimental measurements. The ASTM G65 method was using for abrasion resistance tests. The results show that this procedure can be used to designing parameters of heat treatment of agricultural tools.

Key words: chisel, abrasive wear, microstructure of steel, hardness.

INTRODUCTION

Micro-ploughing (Stawicki et al., 2017), micro-cutting (Ryabov et al., 2016), micro-fatigue (Lin et al., 2008) and micro-cracking (Swain & Biswas, 2017) are abrasive wear mechanisms. Abrasive wear causes damage to the surface of agricultural tools and entrainment of material from the surface (Sidorov et al., 2017; Yazici & Çavdar, 2017). Worn agricultural tools are the cause of lower soil quality such as depth of processing, breadth of processing or soil mixing (Arvidsson & Bölenius, 2006; Manuwa, 2009). Abrasive wear causes a change in shape of the tool causing an increase in force on the tool and the entire machine (Kichler et al., 2011). The microstructure of the steel is important for the intensity of abrasive wear (Sabet et al., 2011; Votava 2014). The articles (Das Bakshi et al., 2013; Gola et al., 2017) state that the most suitable microstructure for abrasive wear is bainite and martensite. Soil resistance affects agricultural tools, so the tool's abrasion resistance is not enough, the toughness, strength and hardness of the tool are also necessary (Votava et al., 2016; Ziemelis & Verdins, 2017).

Experimental tests would be too costly to find a suitable combination of toughness, strength and hardness of steel. The resulting microstructure and hardness can be predicted by mathematical models using finite element method (Serajzadeh, 2004; Teixeira et al., 2009). Heat flux (Babu & Prasanna Kumar, 2009; Prasanna Kumar, 2013), thermal conductivity and specific heat capacity (Telejko, 2004; Telejko & Malinowski, 2004) are important to build FEM models.

The phase transformation of austenite to martensite is non-diffusion process. Non-diffusion process can be described Koistinen-Marburger equations. Transformation of austenite to bainite, ferrite or pearlite is a diffusion process. The diffusion process can be described by Johnson-Mehl-Avrami-Kolmogorov equations (Martin, 2010; Wróbel et al., 2017).

Heat treatment of steels is important for the proportions of the individual phases of the resulting microstructure. Heat treatment in salt baths also called as isothermal hardening is a modern trend in steel processing. Isothermal quenching provides the possibility of setting conditions such as ambient temperature stability, higher cooling temperature required to create bainite, heat transfer from product to salt bath (Beck et al., 2015; Urbanec et al., 2015; Jaason et al., 2016).

The ASTM G65 method is a standardized method for comparing abrasion resistance. ASTM G65 defines the exact parameters of abrasion resistance tests, so results can be comparable to other steel tests (Elalem & Li, 1999; Doering et al., 2011; Hyttel et al., 2013).

The aim of this work is to design a model of microstructure distribution after heat treatment. The microstructure is verified with experimental measurements. Abrasion resistance tests were carried out on tested steels.

MATERIALS AND METHODS

25CrMo4 steel (steel no. 1.7218) has been chosen for this experiment. The chemical composition of the steel is shown in Table 1.

Table 1. Chemical composition of steel 25CrMo4 (wt.%)

Steel	C	Mn	Si	P	S	Cr	Ni	Cu	Al	Mo	Sn	V	Ti
25CrMo4	0.25	0.71	0.23	0.018	0.022	1.03	0.09	0.23	0.023	0.21	0.011	0.004	0.015

Experimental measuring:

Samples were made from a rod of Ø25 mm. The sample was adjusted to the dimensions 25 x 10 x 50 mm (according to the standard ASTM G65). The surfaces of the sample were ground with a diamond wheel. Struers MD Allegro was used with diamond suspension of 9 μm.

All samples were heated in air at 800 °C for 1,200 seconds. Sample cooling was carried out in combinations of the salt bath 50 wt.% $NaNO_2$ + 50 wt.% $NaNO_3$, water and air cooling media – see Table 2.

Table 2. Setting of heat treatment of steel samples

	1. cooling			2. cooling			3. cooling		
Sample [-]	Temp. [°C]	Medium [-]	Time [s]	Temp. [°C]	Medium [-]	Time [s]	Temp. [°C]	Medium [-]	Time [s]
1	400	salt bath	37	400	air	163	20	air	to 20 °C
2	400	salt bath	37	20	water	to 20 °C	-	-	-
3	400	salt bath	20	20	water	to 20 °C	-	-	-
4	400	salt bath	30	20	water	to 20 °C	-	-	-
5	400	salt bath	500	20	water	to 20 °C	-	-	-
6	20	water	to 20 °C	-	-	-	-	-	-

FEM model:

The heat flux was obtained by the procedure described in the work (Kešner et al., 2016). Specific heat capacity and thermal conductivity were obtained by the procedure which was described in (Kešner et al., 2017). Calculation of microstructure and hardness were obtained according to the algorithm shown in Fig. 3.

Steel time transitions are implemented in the model between different cooling media (salt bath 50 wt.% $NaNO_2$ + 50 wt.% $NaNO_3$, water and air). Time transitions are defined in the library software ElmerFem (CSC 2017). Heat flux of steel were used and temperature of cooling media, specific heat capacity and thermal conductivity as boundary conditions.

The model was sketched in 2D with a mapped mesh network with three points created from which the analysis of the resulting data is performed. Created points correspond to the placement of temperature sensors in a laboratory experiment. Point 2 is located 3 mm below the surface in the longitudinal direction, point 1 is located in the center of the longitudinal direction see Fig. 1.

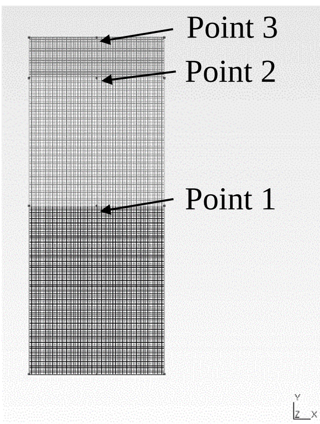

Figure 1. Mesh Network Model with Marked Points.

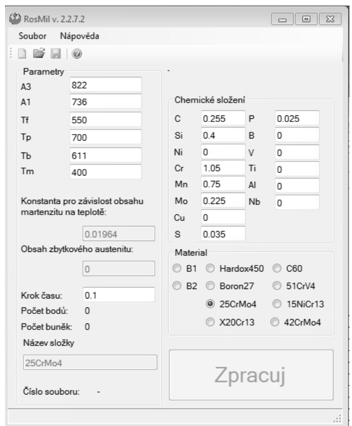

Figure 2. Software for calculating the volume of the phases.

Fig. 3 shows the flowchart of calculating the volume of the final phases and the hardness of the steel after heat treatment. MS Visual basic language (Microsoft 2010) was use for algorithm, which is show in Fig. 3. The software allows you to select the type of steel for analysis – see Fig. 2. The software allows you to select the type of steel for analysis (contains all the properties and constants of the steel to calculate Johnson-

Mehl-Avrami-Kolmogorov and Koistinen-Marburger equations). Johnson-Mehl-Avrami-Kolmogorov and Koistinen-Marburger equations have been taken from the articles (Kirkaldy, 2007; Sinha et al., 2007; Chotěborský & Linda, 2015). The parameters can be changing after selection of the steel.

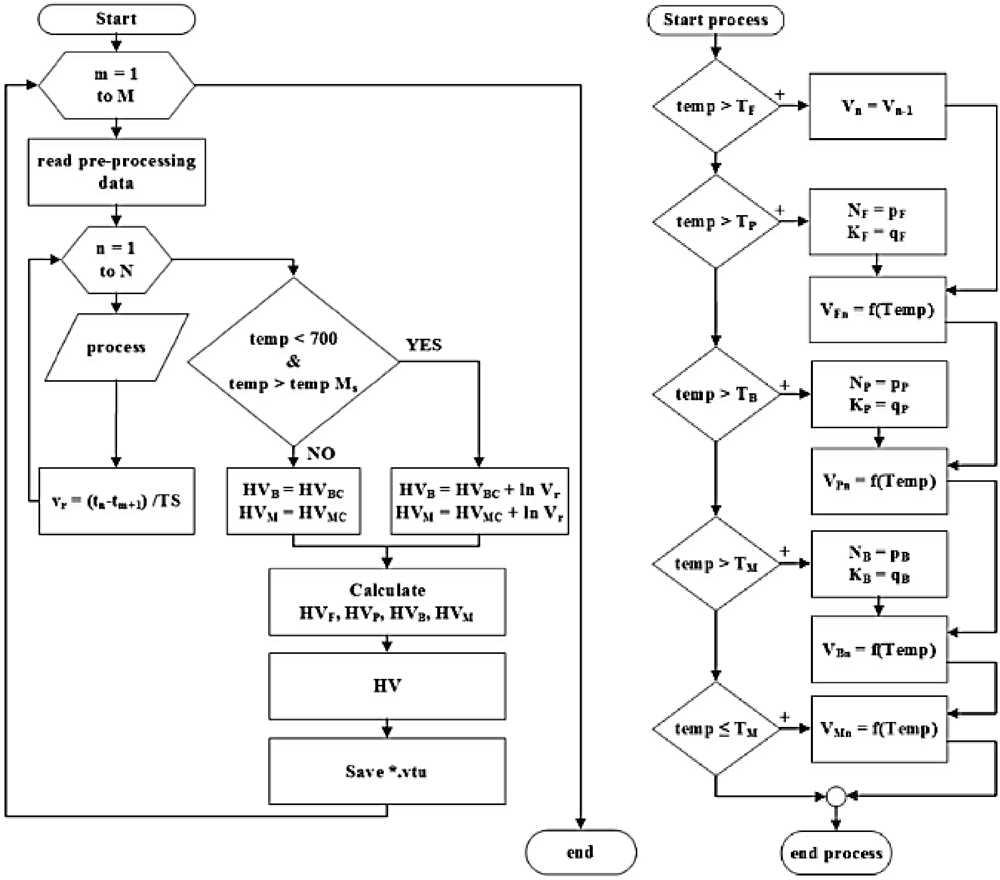

Figure 3. The flowchart of calculating the volume of the final phases and the hardness of the steel after heat treatment.

The calculation procedure use a data of the heat model from the ElmerFem finite element method, where the boundary conditions are present in the Table 2. The **.vtu* files of heat field are loaded to our MS VB.net algorithm, where *m* defines the current calculation step, the loaded input file and *M* defines the total number of input files. The temperature information processing is performed in individual nodes, *n* is the current node of calculation and *N* is the total number of nodes. In the 'process' subroutine, the individual parts of the calculation of volumetric concentrations of the ferrite, perlite, bainite, martensite phases according to the Johnson-Mehl-Avrami-Kolmogorov and Koistinen-Marburger equations were define. A condition for the calculation of the individual phases is always the achievement of the respective temperatures and the phase formation time according to the TTT and CCT diagrams. The cooling rate is included in the calculation. The calculation of hardness starts after the completion of the calculation of the 'process' subroutine and the termination of the calculation loop of all nodes. The hardness is calculated according to the volume of the individual phases and then the total hardness is calculated. The resulting data and temperature are stored in a new **.vtu* file in the same xml format as the original data. Data processing is performed in the program ParaView (Sandia Corporation, 2015).

Fig. 4 shows the temperature gradient of sample 2 at 37 s, at the time of transition to another cooling media.

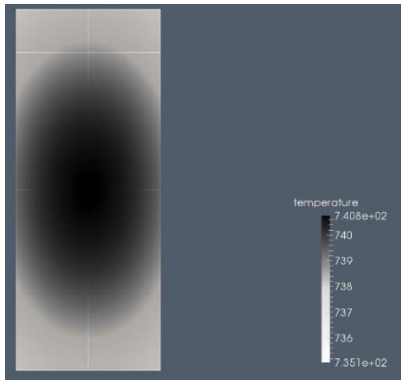

Figure 4. Temperature gradient for sample 2 at the time of 37 s.

Fig. 5 shows cooling of sample 2. The sample was cooled for 37 seconds in a salt bath (400 °C) and then transferred to air (20 °C). The temperature curves are presented for 3 points – Fig. 1. Point 1 is the border point of the model, hence its temperature falls below the set limit of 20 °C.

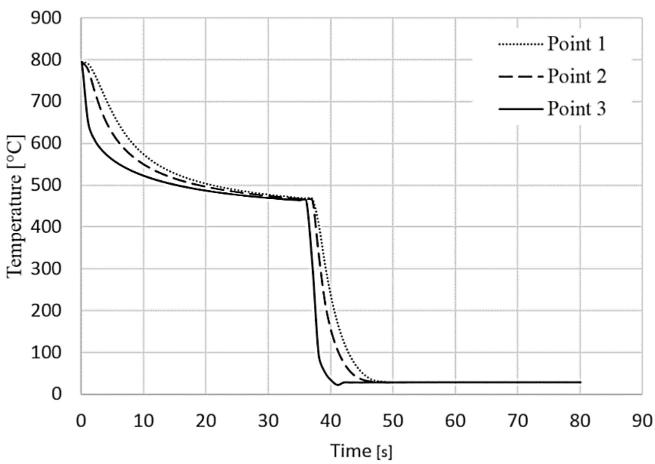

Figure 5. Cooling curves for sample 2.

RESULTS AND DISCUSSION

The microstructure phase volume at points 1, 2, 3 (location on the sample of Fig. 1) is shown in Figs 6–8. The difference was found between the microstructure of the ferrite as determined by the model and the experimentally measured microstructure of the ferrite, especially in models 1, 2 and 5 – shown Fig. 6. The difference of 36% is the largest for sample 1 in point 3. In point 1, the difference dropped to 15%. For sample 2, the greatest difference is 22% at point 2. The 32% difference in point 3 was found in sample 5.

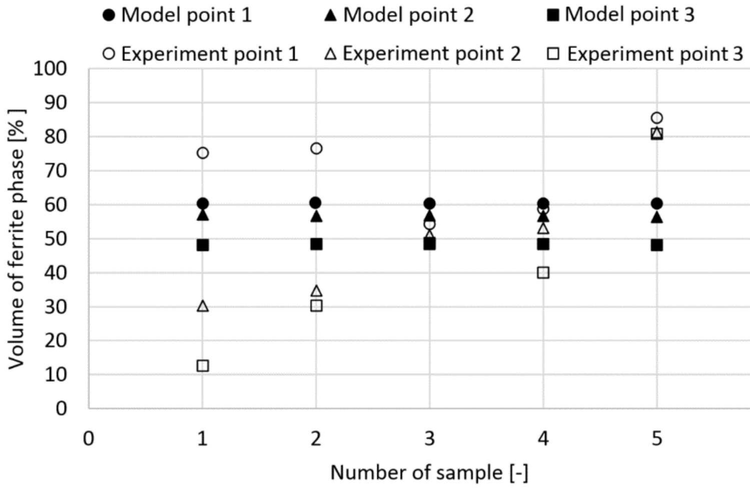

Figure 6. The volume of the ferrite phase in individual samples.

Differences in the bainite microstructure are visible as well as in the ferrite microstructure, ie in samples 1, 2 and 5 – shown Fig. 7. The greatest difference of 35% is measured on the sample is a 1 in the point 3 between the experimentally measured and calculated bainite. Sample 2 at point 3 has a difference of 20% of the microstructure. In point 1, the difference is reduced to 15%. A large difference of 33% was found for sample 5 – at point 3. Samples 3, 4 and 6 had the difference between microstructures measured and calculated by max. 15%.

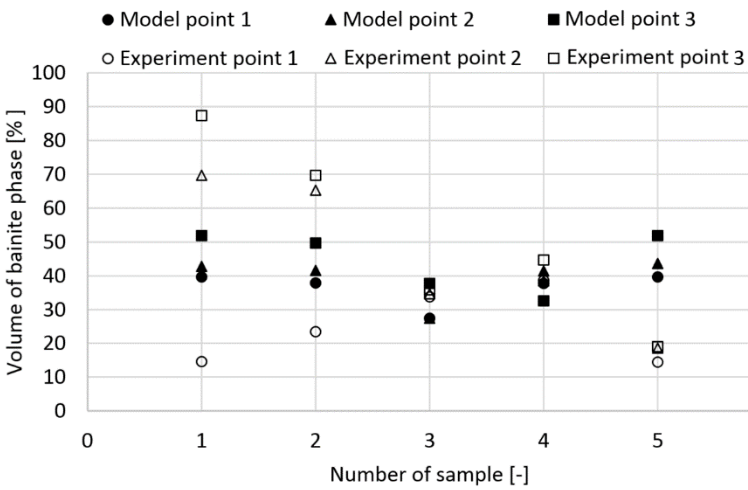

Figure 7. The volume of the bainite phase in individual samples.

The volume of martensite is considerably smaller relative to the microstructure of bainite and ferrite. The occurrence of martensite microstructure was not recorded in samples 1 and 5 – neither in the experimental part nor in the model part. Differences of 2% of the martensite microstructure were found for samples 1 to 5. The difference volume of martensite in sample 6 was 21% in point 3. At point 2, the difference was significantly reduced to 5% and in point 1 it decreased to 12%.

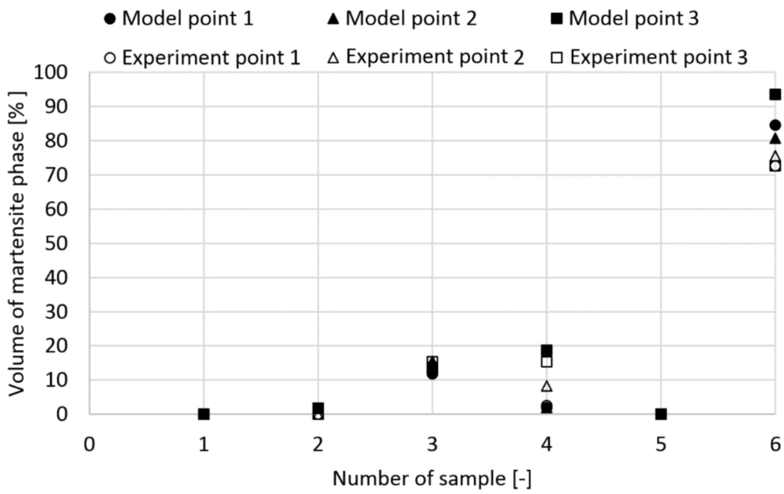

Figure 8. The volume of the martensite phase in individual samples.

Hardness of HV is shown in Fig. 9. Distribution of hardness for the model and the experiment is divided by points 1, 2, 3 (arrangement shown in Fig. 1). The differences are apparent in the samples 1 to 5. Different hardness values are due to the differences between phases between the experiment and the model. The hardness of sample 6 shows the difference in point 3. At point 3, the difference between the microstructure is described above.

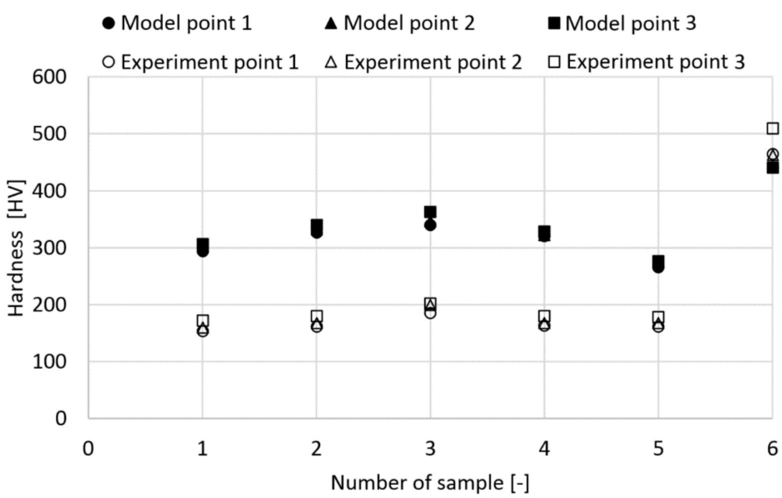

Figure 9. Hardness of HV in individual samples.

The Program Statistica 12 (StatSoft, 2014) was used for statistical evaluation. Dependence was evaluated between loss of weight on the microstructure of bainite, martensite and ferrite. A weight loss of 1 meter was used for the calculation. Equation (1) was compiled to describe the ideal representation of the microstructure for the lowest abrasive wear.

$$\psi = 0.081 + 3.8 \cdot 10^{-6} \cdot V_F^2 + 1.18 \cdot 10^{-6} \cdot V_B^2 + 1.09 \cdot 10^{-6} \cdot V_M^2 \qquad (1)$$

where ψ – weight loss, %; V_F – volume of ferrite phase, %; V_B – volume of bainite phase, %; V_M – volume of martensite phase, %.

The results were evaluated in terms of the lowest weight loss. For the smallest weight loss it is advisable to use a structure that contains a maximum of 10% ferrite and bainite + martensite, each of which is in the range of 40% to 60%.

Specific heat capacity, thermal conductivity and heat flux was measured accurately for the steel 25CrMo4 – samples were prepared from the same rod. For this reason, it can be assumed that the differences found in microstructures between the experimental measurement and the model may be due to the assumed boundaries of the emergence of new phases from the TTT diagram. Border shift occurs when steel is alloyed with some elements such as chrome. The mathematical model then calculates the different beginnings of the boundaries of new phase phases, thus changing the microstructure distribution.

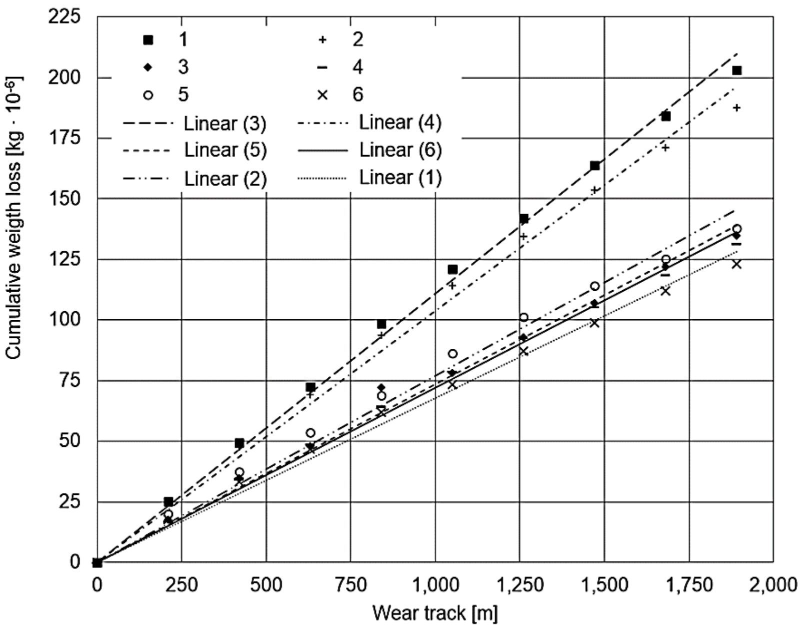

Figure 10. Abrasive wear depending on the cumulative loss of weight over the wear track (distance traveled by the disc).

The cumulative weight loss in relation to the path is shown in Fig. 10. Sample 1 and sample 2 have the least resistance to abrasive wear.

Samples 3 through 6 have significantly better abrasion resistance. The highest resistance to abrasion wear has a sample of 6. Sample 6 has a significantly greater volume of martensite (70%) than samples 1 to 5. At the same time there is a reduction in the volume of ferrite – on the surface of the sample, where the test was conducted with ASTM G65 volume of ferrite is 12%. This value is similar to the statistical model (the proportion of ferrite to 12%). The volume between the structure of bainite and martensite is ideally fifty to fifty – in this case 44% bainite and 44% martensite. A sample experiment shown 72% volume of martensite on the surface for sample 6. For samples 1 to 5, the volume of ferrite is significantly higher – for these samples, abrasion resistance is reduced. This fact corresponds to the statistical model mentioned above.

The suitability of the bainite and martensite structure for abrasion resistance is described in the literature (Hernandez et al., 2016; Narayanaswamy et al., 2016; Trevisiol et al., 2017). This fact confirms the accuracy of the statistical model in terms of the mutual share of bainite, martensite and ferrite for resistance to abrasion wear.

Babu, Prasanna Kumar (2011) in their work, states that the magnitude of the heat flux is affected by the chemical composition of the steel. In this work the chemical composition was taken from the material sheet which was supplied with steel. The chemical composition, that has been inserted into the computational models, may have small deviations, that cause the change in the size of the heat flow. The amount of heat flow is related to the calculation of the phase volume after heat treatment. For this reason, the difference between the mathematical model and the experiment can vary by up to 36% for the phase volume calculation.

CONCLUSIONS

Various heat treatment was chosen for the steel 25CrMo4. The statistical model shows that the most appropriate distribution of the microstructure is up to 10% ferrite, and the martensite content with bainite is 40% to 60% – ideally divided by half. Differences between the experimentally measured and calculated microstructure were found to 35%. This difference may be due to addition of alloying elements in the steel, because the chemical composition of steel was taken from the material sheets supplied together with steel. The hardness for samples 1 through 5 was about 150 HV lower for the model than for the experiment. This fact is due to the accuracy of calculation of the microstructure. The procedure described in this paper could be used to predict the microstructure after heat treatment. Differences between the microstructure measured and the model microstructure can be reduced by refining the chemical composition of the steel.

ACKNOWLEDGEMENTS. Supported by Internal grant 31140/1312/3114 agency of Faculty of Engineering, Czech University of Life Sciences in Prague.

REFERENCES

CSC – IT Center for Science 2014. Elmer finite element software [online]. Available from: *http://www.csc.fi/english/pages/elmer*

Arvidsson, J. & Bölenius, E. 2006. Effects of soil water content during primary tillage – laser measurements of soil surface changes. *Soil and Tillage Research* **90**, 222–229.

Babu, K. & Prasanna Kumar, T.S. 2009. Mathematical Modeling of Surface Heat Flux During Quenching. *Metallurgical and Materials Transactions B* **41**, 214–224.

Babu, K. & Prasanna Kumar, T.S. 2011. Effect of CNT concentration and agitation on surface heat flux during quenching in CNT nanofluids. *International Journal of Heat and Mass Transfer* **54**, 106–117.

Beck, M., Schmidt, C., Ahrenberg, M., Schick, C., Kragl, U. & Kessler, O. 2015. Ionic Liquids as New Quenching Media for Aluminium Alloys and Steels. *HTM Journal of Heat Treatment and Materials* **70**, 73–80.

Das Bakshi, S., Shipway, P.H. & Bhadeshia, H.K.D.H. 2013. Three-body abrasive wear of fine pearlite, nanostructured bainite and martensite. *Wear* **308**, 46–53.

Doering, A., Danks, D., Mahmoud, S. & Scott, J. 2011. Evaluation of ASTM G65 abrasive - Spanning 13 years of sand. *Wear* **271**, 1252–1257.

Elalem, K. & Li, D.Y. 1999. Dynamical simulation of an abrasive wear process. *Journal of Computer-Aided Materials Design* **6**, 185–193.

Gola, A.M., Ghadamgahi, M. & Ooi, S.W. 2017. Microstructure evolution of carbide-free bainitic steels under abrasive wear conditions. *Wear* **376–377**, 975–982.

Hernandez, S., Leiro, A., Ripoll, M.R., Vuorinen, E., Sundin, K.G. & Prakash, B. 2016. High temperature three-body abrasive wear of 0.25C 1.42Si steel with carbide free bainitic (CFB) and martensitic microstructures. *Wear* **360–361**, 21–28.

Hyttel, M.W., Olsson, D.D., Reisel, G. & Bøttiger, J. 2013. Comparison of a newly developed compression-twist abrasive wear test with the ASTM G65 test method. *Wear* **307**, 134–141.

Chotěborský, R. & Linda, M. 2015. FEM based numerical simulation for heat treatment of the agricultural tools. *Agronomy Research* **13**, 629–638.

Jaason, K., Peetsalu, P., Kulu, P., Saarna, M. & Beilmann, J. 2016. Predictive tools for the isothermal hardening of strip steel parts in molten salt. *Proceedings of the Estonian Academy of Sciences* **65**, pp. 152–158.

Kešner, A., Chotěborský, R. & Linda, M. 2016. Determination of the heat flux of steel for the heat treatment model of agricultural tools. *Agronomy Research* **14**, 1004–1014.

Kešner, A., Chotěborský, R. & Linda, M. 2017. Determining the specific heat capacity and thermal conductivity for adjusting boundary conditions of FEM model. *Agronomy Research* **15**, 1033–1040.

Kichler, C.M., Fulton, J.P., Raper, R.L., Mcdonald, T.P. & Zech, W.C. 2011. Effects of transmission gear selection on tractor performance and fuel costs during deep tillage operations. *Soil and Tillage Research* **113**, 105–111.

Kirkaldy, J.S. 2007. Flux-independent theory of nonlinear diffusion for Vegard's law solutions. *Materials Science and Engineering: A*. **444**, 104–111.

Lin, Y.J., Agrawal, A. & Fang, Y. 2008. Wear progressions and tool life enhancement with AlCrN coated inserts in high-speed dry and wet steel lathing. *Wear* **264**, 226–234.

Manuwa, S.I. 2009. Performance evaluation of tillage tines operating under different depths in a sandy clay loam soil. *Soil and Tillage Research* **103**, 399–405.

Martin, D. 2010. Application of Kolmogorov–Johnson–Mehl–Avrami equations to non-isothermal conditions. *Computational Materials Science* **47**, 796–800.

Microsoft. Visual Basic . NET. 2010

Narayanaswamy, B., Hodgson, P., Timokhina, I. & Beladi, H. 2016. The Impact of Retained Austenite Characteristics on the Two-Body Abrasive Wear Behavior of Ultrahigh Strength Bainitic Steels. *Metallurgical and Materials Transactions A* **47**, 4883–4895.

Prasanna Kumar, T.S. 2013. Influence of Steel Grade on Surface Cooling Rates and Heat Flux during Quenching. *Journal of Materials Engineering and Performance* **22**, 1848–1854.

Ryabov, V.V., Motovilina, G.D., Khlusova, E.I., Sidorov, S.A. & Khoroshenkov, V.K. 2016. Study of the Structure of New Wear-Resistant Steels for Agricultural Machinery Components After Operational Tests. *Metallurgist* **60**, 839–844.

Sabet, H., Khierandish, Sh., Mirdamadi, Sh. & Goodarzi, M. 2011. The Microstructure and Abrasive Wear Resistance of Fe–Cr–C Hardfacing Alloys with the Composition of Hypoeutectic, Eutectic, and Hypereutectic at Cr. C. ¼ 6. H. *Tribology Letters* **44**, 237–245.

Sandia Corporation, Kitware Inc, 2015. *ParaView 4.3.1* [online]. 2015. New Mexico PO Box 5800 Albuquerque, NM 87185: Sandia Corporation, Kitware Inc. Available from: www.paraview.org

Serajzadeh, S. 2004. A mathematical model for prediction of austenite phase transformation. *Materials Letters* **58**, 1597–1601.

Sidorov, S.A., Khoroshenkov, V.K., Lobachevskii, Ya.P. & Akhmedova, T.Sh. 2017. Improving Wear Resistance of Agricultural Machine Components by Applying Hard-Alloy Thick-Layer Coatings Using Plasma Surfacing. *Metallurgist* **60**, 1290–1294.

Sinha, V.K., Prasad, R.S., Mandal, A. & Maity, J. 2007. A Mathematical Model to Predict Microstructure of Heat-Treated Steel. *Journal of Materials Engineering and Performance* **16**, 461–469.

Statsoft. 2014. Statistica [online]. 2014. Available from: http://www.statsoft.com/

Stawicki, T., Białobrzeska, B. & Kostencki, P. 2017. Tribological Properties of Plough Shares Made of Pearlitic and Martensitic Steels. *Metals* **7**, 139–158.

Swain, P.T.R. & Biswas, S. 2017. Abrasive Wear Behaviour of Surface Modified Jute Fiber Reinforced Epoxy Composites. *Materials Research* **20**, 661–674.

Teixeira, M.G., Rincon, M.A. & Liu, I.-S. 2009. Numerical analysis of quenching – Heat conduction in metallic materials. *Applied Mathematical Modelling* **33**, 2464–2473.

Telejko, T. & Malinowski, Z. 2004. Application of an inverse solution to the thermal conductivity identification using the finite element method. *Journal of Materials Processing Technology* **146**, 145–155.

Telejko, T. 2004. Analysis of an inverse method of simultaneous determination of thermal conductivity and heat of phase transformation in steels. *Journal of Materials Processing Technology* **155–156**, 1317–1323.

Trevisiol, C., Jourani, A. & Bouvier, S. 2017. Effect of hardness, microstructure, normal load and abrasive size on friction and on wear behaviour of 35NCD16 steel. *Wear* **388–389**, 101–111.

Urbanec, J., Saastamoinen, A., Kivivuori, S. & Louhenkilpi, S. 2015. Fast Salt Bath Heat Treatment for a Bainitic/Martensitic Low-Carbon Low-Alloyed Steel. *Metallurgical and Materials Transactions A*. **46**, 5343–5349.

Votava, J. 2014. Usage of abrasion-resistant materials in agriculture. *Journal of Central European Agriculture* **15**, 119–128.

Votava, J., Kumbár, V. & Polcar, A. 2016. Optimisation of Heat Treatment for Steel Stressed by Abrasive Erosive Degradation. *Acta Universitatis Agriculturae et Silviculturae Mendelianae Brunensis* **64**, pp. 1267–1277.

Wróbel, J., Kulawik, A. & Bokota, A. 2017. The Numerical Analysis of the Hardening Phenomena of the Hot-work Tool Steel. *Procedia Engineering* **177**, 33–40.

Yazici, A. & Çavdar, U. 2017. A Study of Soil Tillage Tools from Boronized Sintered Iron. *Metal Science and Heat Treatment* **58**, 753–757.

Ziemelis, M. & Verdins, G. 2017. Plough parts wear resistance depending on their material composition and processing technology. *Engineering for Rural Development* **16**, 455–460.

Agronomy Research **16**(3), 769–783, 2018
https://doi.org/10.15159/AR.18.146

Effect of alternative sources of input substrates on biogas production and its quality from anaerobic digestion by using wet fermentation

K. Krištof[1,*] and J. Gaduš[2]

[1]Slovak University of Agriculture in Nitra, Faculty of Engineering, Department of Machines and Production Biosystems, Tr.A. Hlinku 2, SK949 76 Nitra, Slovakia
[2]Slovak University of Agriculture in Nitra, Faculty of European Studies and Regional Development, Department of Regional Bioenergy, Tr.A. Hlinku 2, SK949 76 Nitra, Slovakia
[*]Correspondence: koloman.kristof@uniag.sk

Abstract. The aim of the study was to confirm the suitability of alternative input substrates for production of biogas in order to decrese the need of utilization of high quality maize silage. All of the experiments were conducted by employement of wet fermentation process in mesophilic conditions (temperature in fermentor 40 ± 1 °C) in experimental fermentor with volume 5 m^3. The experiments were realised in operating conditions of biogas station designed for utilization of agricultural biowaste. The experiments were divided into two alternatives (I and II cycle) and one controle input substates. In the first alternative (I cycle) was daily dosage formed by 33 kg of *Amaranth* and 250 L of controle manure mixture. In this cycle, more than 3–times greater specific production of biogas was observed with average methan content 63.9% in comparison with controle manure mixture (80 : 20%, liquid manure and manure). In the second alternative (II cycle) was daily dosage formed by 19.5 kg of sugar beer cuts, 3.3 kg of maize silage, 1.9 kg of oil-seed rape moldings, 2.5 kg of glycerine and 250 L of controle manure mixture. In this cycle, more than 5.9–times greater specific production of biogas was observed. The decrease in averare methan content 55.1% however also decrease in average content of hydrogen sulphide (128 ppm) was observed as well. An unquestionable advantage for both tested alternative mixed substrates was increase in biogas production and its quality in comparison with control substrate based on manure. At the basis of these findings can be concluded that both tested alternative input substrate mixtures are suitable as co–fermentation substances with great potential to increase the biogas production and its quality in case of wet fermentation processes.

Key words: biogas, co-fermentation, co-substrates, anaerobic digestion, wet fermentation.

INTRODUCTION

Increased energy security as well as efforts to mitigate climatic changes and impacts on the environment has become the main motivation for transformation of energy production from mainly used fosil fuels into the renewable energy sources. Biomass plays a key role in the considerations how to secure enough amount of energy for next generations while biomass is a source of energy which is available almost everywhere in the world regardless of its form (Piszczalka & Jobbágy, 2011; Gaduš & Giertl, 2016). Furthermore, biosubstrate, which includes suprogenic green waste and bio-waste, represents more than 2/3 of total renewable energy sources which can be successfully transformed into energy supplies. Production of biogas from biomass offers the effective replacement for conventional sources of energy while it represents the source of energy with a great potential. The methan gase produced from biomass provides a lot of interesting ways of its utilization while among its greatest benefits is its storability (storage of energy). Mostly due to its possibility to post-treated and compressed. Therefore the produced energy carrier biogas would decrese our dependency on conventionaly used fosil fuels (Braun, 1982; Crabtree, 1995; Gerardi, 2003; Braun, 2013).

From an environmental point of view, the production of biogas containing methane is more efficient in terms of emissions than fossil fuel energy. Biogas is understood as a source of energy with zero carbon dioxide (CO_2) emissions into the atmosphere. Biogas is considered as CO_2 neutral. The utilization of biomass for energy purposes allows the consumption of air CO_2 during photosynthesis while its release back into the atmosphere is closed in a relatively short time. This fact distinguishes biogas from fossil fuels. Moreover, carbon dioxide produced by the controlled anaerobic digestion process can be again exploited by the plants which allow closing down the carbon cycle in nature (Gunaseelan, 1997; Ward et al., 2008). The emissions resulting from agricultural activities are estimated at between 10 and 12% of the total amount of greenhouse gases which is between 5.1 and 6.1 billion tonnes of carbon dioxide equivalent per year (Piszczalka & Jobbágy, 2011; Gaduš & Giertl, 2016).

The biogas is a mixture of gases that results from a complex of multi-stage process overall described as the biodegradation of organic substances under anaerobic conditions. The main component of the gaseous mixture of biogas is methane. Methan is a colorless, non-degassing gas which with air is forming a flammable mixture in the range 5.3-15% vol., respectively. The overall composition of the biogas is dependent on the input substrate composition and the digestion process. On the average, biogas mixtures contain from 65 to 75% of methane (CH_4), 25 to 35% of carbon dioxide (CO_2), 3 to 4% of water (H_2O) and 0.1 to 0.5% of hydrogen sulphide (H_2S). Among the other traceble elements are hydrogen (H), nitrogen (N), ammonia (NH_3) etc. The calorific value of biogas ranges from 17 to 25 MJ m^{-3} which represents in average of 2/3 of energy produced by natural gas as a source of energy. The energy contained in biogas should be used as efficiently as possible especially in connection with the development of high temperatures (Crabtree, 1995; Møller et al., 2004; Li et al., 2011; Vítěz et al., 2015).

At present, some modern factories, especially those that produce bio–waste, are currently undergoing the possibility of producing biogas directly in the plant within its current processing. The biogas is often produced mainly in production plants that have their own biological waste water treatment where the methane–rich biogas is produced as a byproduct of purification. If it is used further in the factories, for heating for example, it reduces the operating costs and replaces the other sources of energy which are commonly used for that purpose.

In order to achieve a good economically balanced biogas production plant it is necessary to evaluate the advantages of its situation prior to construction. The costs of building and purchasing of technology are considered as financially very demanding. Therefore, prior to construction of the biogas plant, it is necessary to ascertain the amount of available raw material resources, to perform tests and determine the yield of biogas and its quality. The efficiency of the modern biogas plant operation can be increased by a suitable combination of input organic materials (co-fermentation). The term co-fermentation can be understood as the anaerobic treatment of partial substrates (within a fraction) alongside with the main component of the feed mixture (dominant organic materials). Co-fermentation is carried out due to the processing of several types of materials (if available) but also in order to increase of the methane content from the biogas mixture. In addition, by fermentation of suitable co–substrates with the primary types of substrate the total amount of gas produced can also be increased (Álvarez et al., 2010; Zhang et al., 2014).

By co–fermentation it is possible to refer to the anaerobic treatment of several materials. These are different types of biomass mixtures which are added together with the basic (major) substrate into joint fermentation. This process allows achieving higher production of biogas than in the fermentation of these substrates alone. Joint fermentation of materials can also be carried out due to the availability of these materials only in certain quantities whose total weight is sufficient to achieve the required power of the biogas plant. However, not all of organic materials can be fermented together with the production of a sufficient quantity of high–quality biogas. Determination of the suitability for co–fermentation and co–fermentation of individual biomass materials requires tests to be carried out prior to its utilization (Angelidaki & Ahring, 1994; Sosnowski et al., 2003).

As the main advantages of the co–fermentation can be considered the possibility of fermenting several types of biomass that are available directly in the vicinity of the biogas plant it self. In addition, the improvement of the economic efficiency of the biogas plant is therefore also achievable. Moreover, the possibility of increase in the production of biogas or production of biogas with higher methane content (higher energy value) is also considered as an undeniable advantage (Khalid et al., 2010).

The advantage of facilities capable of handling diverse types of organic substances is the rich availability of agricultural and food materials that otherwise would end up as waste. In the fermentation treatment of organic matter, in addition to the production of energy fuel, the carbon cycle is also closed. Therefore, it is considered as a highly rated biomass processing for energy purposes. With a well–established anaerobic decomposition process, co–fermentation can produce high volumes of biogas in comparison to fermentation of the input mono–substrate (Rajeshwari et al., 2000; Clemens et al., 2006; Lin et al., 2013).

The aim of the study was to verify the suitability of alternative substrates usable as input mixtures for anaerobic treatment in the biogas station with the result of production of energy fuel – biogas, under the operating conditions of a real biogas station. Another object was to design suitable alternative substrates with respect to their composition which would provide the required performance parameters while reducing operating costs as well as evaluating the advantages of their anaerobic treatment compared to processing the same volume of input substrate from some conventional fermentation mixtures such as cattle slurry, manure, maize silage, ect.

MATERIALS AND METHODS

Several methods can be used to determine the effect of substrate composition and its suitability for anaerobic fermentation. In addition, measurement of the biogas produced volume and the distribution of individual components volume, particularly methane, were also carried out. The measurements were carried out in order to determine the mixtures composition before the fermentation process itself and during the fermentation process. In these analyses it is possible to observe the process of anaerobic digestion with an increased or reduced content of substances, parameters indicating the state of the fermentation process. Therefore it is possible to describe the substrate distribution options. Since among the important indicators of the fermentation processes are the pH value during the process, the presence of ammonia and unsaturated fatty acids, etc. (Lehtomäki et al., 2007). When determining the suitability of substrates and combinations of substrate in the mixtures, one of the determining factors for the production of sufficient biogas is the presence of organic substances (Rajagopal et al., 2013).

Among one of the laboratories in which the properties and suitability of the substrates composition for anaerobic fermentation can be determined is set up at the workplace of the experimental biogas station VPP SPU in Kolíňany (48°21'47.3"N, 18°12'06.2"E). The laboratory is set up at the Slovak university of agriculture in Nitra, where a 5 m^3 experimental fermentor is installed with an automatic substrate dispenser and a homogenisation input tank. It is adapted and developed for testing substrates for anaerobic fermentation. Gas analyzer (HY-LiTE® 2 system, Merck Millipore, Prague, Czech Republic) and gas chromatograph (WTW PhotoLab S12, Xylem Analytics Germany Sales GmbH & Co. KG, Weilheim, Germany) was used to measure gas composition in experimental biogas plant. The volumes of gas produced were measured by a gas meter (BK-G10, Mahrlo, MAHRLO ltd., Trenčín, Slovakia).

Sampling before fermentor

The samples taken before entering the fermentor suppose to be sufficiently homogeneous. Therefore, before sampling the substrate must be thoroughly mixed to bring the sample as close as possible to the entire composition of the substrate. The sampling temperature and pH should be measured during sampling. Between sampling and sample processing, a long time difference should be avoided due to possible chemical and biological changes in the sample over a longer period of time. After the sample has been transferred to the laboratory, these must be re-homogenized so that it can be further used for testing. Basic measurements of the sample before fermentation are the measurement of COD (chemical oxygen demand), total nitrogen and the presence of sulphates in the sample. The COD content is determined to observed the proportion of organic matter in the sample; the sulfate content predestined the content of hydrogen sulfide in the output biogas.

Chemical test of samples before fermentor (input substrate)

Methodology of determination COD (chemical oxygen demand)

The method is based on the procedure described in the MERCK Sulfate Cell Test Instructions – Cell Test. The chemical oxygen demand value is the amount of oxygen coming from the potassium dichromate that reacts with the oxidizable substances contained in one litre (L) of water under the specified conditions. 1 mol of $K_2Cr_2O_7$ is equivalent to 1.5 mol of O_2. Thus, chemical oxygen demand indicates the amount of oxygen needed to oxidize organic matter with oxidizing agents, a method for expressing the amount of organic matter in the sample.

Methodology of determination slphur content

The method is based on the procedure described in the MERCK Sulfate Cell Test Instructions – Cell Test. The method of determining the sulphate content is based on reactions in which the sulfate ions react with barium ions of mildly soluble barium sulphate. The resulting concentration value is then determined photometrically.

Methodology of determination of nitrogen content

The method is based on the procedure outlined in the MERCK Nitrogen (Total) Cell Test Instructions – Cell Test. The method of determining the concentration of nitrogen is based on reactions in which nitrogen–containing organic and inorganic components are transformed into nitrates by the Koroleff method by the action of oxidizing agents in a thermo-reactor. In sulfuric and phosphoric acid, nitrates are further reacted with 2,6-dimethylphenol (DMP) to form 4-nitro-2,6-dimethylphenol, which is then determined photometrically. If COD is higher than 7,000 mg L it is necessary to dilute the sample with distilled water.

Sampling from fermentor – running process

Samples taken from the fermentor represent a fermentation mixture with the processes of acidogenesis is already started. The sample exhibits sufficient homogeneity as the fermentor is not sufficiently agitated. The sample exhibits a higher temperature as the fermentor is heated with thermophilic processes up to 40 °C. The sampling temperature and pH should be measured during sampling. Between sampling there should be a short time difference due to possible chemical and biological changes in the sample over a longer period of time. After the sample has been transferred to the laboratory, it must be re–homogenized so that it can be further used for testing. Among the basic measurements of the taken sample is determination of the ammonia, iron content, the determination of TS (total solids) as well as the presence of fatty acids.

A high amount of ammonia in the fermentation mixture may inhibit the anaerobic digestion process. The presence of fatty acids is conducted to determine the presence of acetic acid as the main constituent needed for methane formation. For a good fermentation process the pH should be in the slightly alkaline range of 7–8. The proportion of organic matter content is determined in dry matter, subsequently. The dry matter of the fermented mixture is lower than the dry matter of the feed material (Mata–Alvarez et al., 2014).

Chemical and physical tests of samples in process of fermentation (running process)

Determination of total solids (TS)

For measurements, TS is determined from the homogenized taken samples. The basic process for determination of dry matter was conducted by device KERN MLB 50-3 (Merck KGaA, Darmstadt, Germany). Ceramic plates are used to dry the sample in the apparatus, which are combusted in a muffle furnace at a temperature of 550 °C for 20 minutes prior to the drying process, then dried in a desiccator (device with an absorbent material, e.g. silicate gel).

Determination of fatty acids

Samples were analyzed immediately after collection. The samples were thoroughly homogenized. The method was performed by diluting the substrate sample with distilled water 1:50.

Determination of amonia (NH_4)

The method is based on the procedure described in the MERCK Sulfate Cell Test Instructions – Cell Test. Ammonium ions react at pH 12.6 with hypochlorite ions and salicylate ions in the presence of sodium nitrosophoric acid as a catalyst to give intense blue coloration (indophenol). The test was evaluated photometrically.

Determination of iron (Fe)

The method is based on the procedure described in the MERCK Sulfate Cell Test Instructions – Cell Test. Iron ions are the effects of ascorbic acid reduced to divalent iron ions. The thioglycolate–buffered solution is then reacted with the triazine derivative to give a red–colored complex which was photometrically evaluated.

Laboratory equipment

For sampling and homogenisation were used folloeing devices: Disperser for sample homogenization WTW Disper D8 (Xylem Analytics Germany Sales GmbH & Co. KG, Weilheim, Germany) and Test reaction cuvettes for determination of COD content in water. For determination of COD and total nitrogen content in substrate samples and biogas was used Thermoreactor for heating of cuvettes WTW Cr4200 (Xylem Analytics Germany Sales GmbH & Co. KG, Weilheim, Germany) and Photometer WTW PhotoLab S12 (Xylem Analytics Germany Sales GmbH & Co. KG, Weilheim, Germany).

Laboratory equipment includes auxiliary glass banks, measuring cylinders, ceramic bowls, fungi, and pipetting piston dispensers for dosing exact quantities of samples or reagents. For determination of pH values was used device pH meter WTW 3310 (Xylem Analytics Germany Sales GmbH & Co. KG, Weilheim, Germany).

For following analysis of biogas quality and other observed parameters were used distilation device (KjelFlex K-360, Donau Lab, Bratislava, Slovakia), laboratory scales with drying of samples (Kern MLS-D, KERN & SOHN GmbH, Balingen, Germany) and muffle furnace (Witeg FHP-3, Unimed ltd., Praque, Czech Republic).

RESULTS AND DISCUSSION

Experiments with anaerobic fermentation of biomass were conducted in two alternatives. In accordance with the stated objectives of the study there were carried out 2 cycles (Table 1). These cycles were conducted in the operating conditions of the biogas station with duration of 25 to 30 days. During these long–term experiments chemical analyses of the substrate were carried out according to the standard methodology (Donoso–Bravo et al., 2011). Methodology was briefly described in above

Table 1. Overview of realised experiments

Cycle	Time period (days)	Co–substrates	Amout of added co–substrates (kg)
I.	28	amaranth	33
II.	30	sugar beet slices	19.5
		maize silage	3.3
		rape moldings	1.9
		glycerine	2.5

chapters and sampling was conducted regularly (twice a day) along with the analysis of biogas quality.

As a comparative and starting biological material for fermentation the cattle manure was used along with pigs' slurry in a volume ratio of 20:80%. This mixture was mechanically pretreated in the main homogenization tank with a submersible propelled mixer. After coarse homogenization of the manure a daily dose of 250 L of substrate was pumped into an experimental fermentor with a volume of 5 m^3 thus maintaining a residence time of 20 days.

In the first (I) experimental cycle the cosubstrate – amaranth was added to a small homogenization tank in the prescribed quantity into a basic mixture consisting of 20% volume of cattle manure and 80% volume of pigs' slurry. In this tank the substrate was homogenized with a propelled mixer for 30 minutes before dosing. The daily dose was pumped from this tank through a slurry pump into a small fermentor.

In the second (II) experimental cycle a daily dose consit of: 19.5 kg of sugar beet slices, 3.3 kg of maize silage, 1.9 kg of rape moldings and 2.5 kg of glycerine. Used sugar beet slices (biowaste after production of sugar) was dosed in automatic mode via a newly designed and installed solid biomass dosing device after mixing with the rape moldings (biodiesel production waste) and after addition of a small amount of maize silage. Before the filling cycle it was programmed to mix the substrate in the tank with a rocking mixer for 5 minutes. The dosing itself took 4 minutes and the amount corresponding to a 1/4 daily dose was added to the fermentor. Glycerine (liquid waste from production of biodiesel) was added to fermentor by supply pump also in automatic mode directly in about 2/3 of the length of the lying fermentor.

The overall arrangement of the experimental device can be seen in Fig. 1 where the main parts and flow of the substrate, biomass, biogas and water for heating the fermentor are shown.

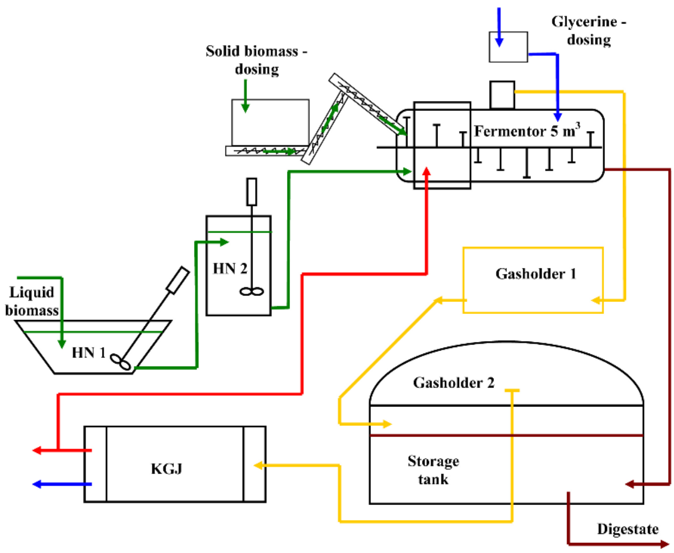

Figure 1. The overall arrangement of the experimental device for co-fermentation (HN1 – great homogenization tank 8 m^3, HN2 – small homogenization tank 1.6 m^3 and KGJ – co–generation unit).

The fermentor is the basic technological equipment for the biogas production. For testing purposes, an experimental (horizontal) 5 m^3 fermentor was used which operates under mesophilic conditions at 40 °C±1 °C. The content of the fermentor was automatically, at regular intervals, driven by the blades of the slow stirrer. Bacteria formed by the raw biogas from the fermentor were accumulated in a small gas jug. From there biogas was pumped through the gas volume meter into a large gas tank located above the final storage tank (Fig. 1).

The main observed parameters were the amount of biogas produced (BP) in terms of its specific production ($m^3\ m^{-3}\ d^{-1}$) per unit of fermentor volume, methane content (CH_4) and other biogas components (CO_2, O_2 and H_2S). The analysis was carried out on a regular basis, twice a week, as well as chemical analysis of the substrate, with total solids (TS) content, organic total solids (OTS), and annealing loss (VSS), ammonium ions (NH^{4+}). For assessing the proper course of the fermentation process the pH and temperature of the substrate in the fermentor were also monitored (Alatriste–Mondragón et al., 2007).

The share of individual components (CH_4, CO_2, O_2 and H_2S) in the raw biogas was detected by the Schmack SSM 6000 gas analyzer (SCHMACK BIOGAS AG, Schwandorf, Germany). The measurement was performed automatically twice a day.

I. cycle of experiments

The experimental measurements were performed for 28 days. The amount of added amaranth to the base substrate was 33 kg. In experiments the same residence time was chosen as the reference biological material (pigs slurry and cattle manure) at least 20 days. The daily dose was maintained as for the base substrate, ie 250 L.

The content of the original biomass in the fermentor was gradually reduced by adding the daily dose of the monitored substrate (250 L). It can be seen from the graph (Fig. 2) that the temperature in the fermentor was on average 38.9 °C and was very stable. Throughout the experiment the methane content was averaged to 63.9%. The content of dry matter in the substrate (5.58%), thanks to the daily addition of 33 kg of amaranth was higher which also ensured a higher average specific production of biogas (0.542 $Nm^3\ m^{-3}\ d^{-1}$) compared to the reference cycle.

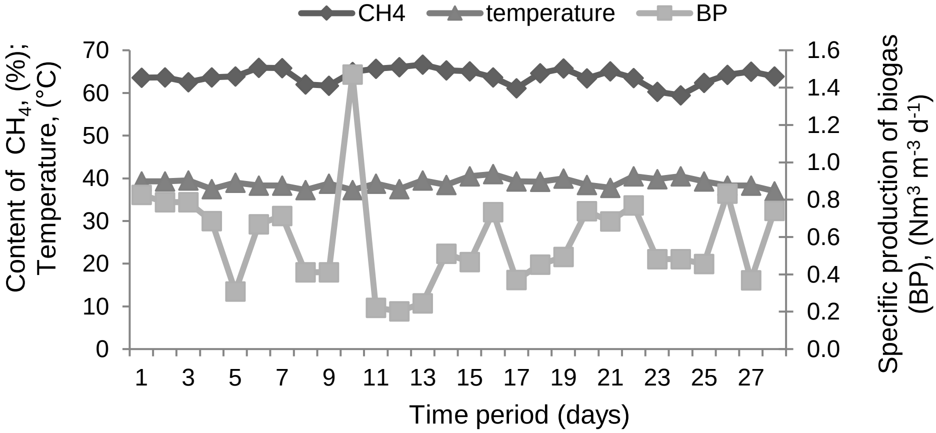

Figure 2. The course of monitored parameters for substrate fermentation – **I. cycle**.

The average values of the monitored parameters are shown in the Table 2 and Table 3. From Table 2 it is possible to extract information that the input substrate (slurry+manure+ amaranth) in fermentor has shown the higher value of organically dispersible organic total solids (OTS = 74.11% TS). In addition, samples from the homogenisation tank (before entering the fermentor) showed an average chemical oxygen demand (COD) of 49,100 mg L^{-1}.

Table 2. Average values of monitored parameters and chemical composition of substrates (slurry+manure+amaranth) – **I. cycle**

Parameter	Unit	Substrate samples	
		MHN	Fermentor
pH	-	5.90	7.33
temperature	°C	20.00	38.9
TS	%	4.90	5.58
VSS	%	-	3.72
OTS	% TS	-	74.11
CHSK	mg L^{-1}	49,100	-
N_{tot}	mg L^{-1}	153	-
NH_4^+	mg L^{-1}	-	1,040
SO_4^{2-}	mg L^{-1}	163	-
Fe	mg L^{-1}	-	8.53

Where TS – dry matter content; VSS – loss on ignition; CHSK – chemical oxygen demand; N_{tot} – total nitrogen; NH_4^+ – amonia ions; SO_4^{2-} – sulphur anions; Fe – iron content.

II. cycle of experiments

The experiment was performed for 30 days. Glycerin was added for up to 10 days. The content of the original biomass (slurry+manure) in the fermentor was gradually reduced by the addition of the daily dose of the monitored substrate. As shown in Fig. 3, an increase in biogas production and slightly methane content (the first 13 days) was recorded immediately. The production of biogas grew gradually and at 14 days (after the start of glycerine dosing) the specific production of biogas was 1.289 $Nm^3\ m^{-3}\ d^{-1}$ which was almost the highest value recorded. Both biogas and methane production were very stable throughout the 30–day trial. Moreover, the temperature in the fermentor was also maintained at a very stable value at average of 39.90 °C. However, very low content of dry matter in the substrate was recorded at average of 3.92%. It can be concluded that the daily dose of the substrate under investigation could be increased to four times to achieve a more efficient use of the fermentor (Raposo et al., 2012; Ariunbaatar et al., 2014; Lee et al., 2014). Moreover, lower dry matter content (5.69%) was recorded during the whole experiment in comparison with the reference substrate and almost the ideal average pH in the fermentor (7.33) was observed as well.

Table 3. Average values of monitored parameters and chemical composition of substrates (slurry + manure + cosubstrates: sugar beet slices, maize silage, rape moldings and glycerine) – **II. cycle**

Parameter	Units	Substrate samples	
		MHN	Fermentor
pH	-	6.25	7.33
temperature	°C	20.00	39.3
TS	%	4.90	2.92
VSS	%	-	2.18
OTS	% TS	-	78.43
CHSK	mg L^{-1}	93,200	-
N_{tot}	mg L^{-1}	1,530	-
NH_4^+	mg L^{-1}	-	298
SO_4^{2-}	mg L^{-1}	263	-
Fe	mg L^{-1}	-	-

Where TS – dry matter content; VSS – loss on ingnition; CHSK – chemical oxygen demand; N_{tot} – total nitrogen; NH_4^+ – amonia ions; SO_4^{2-} – sulphur anions; Fe – iron content.

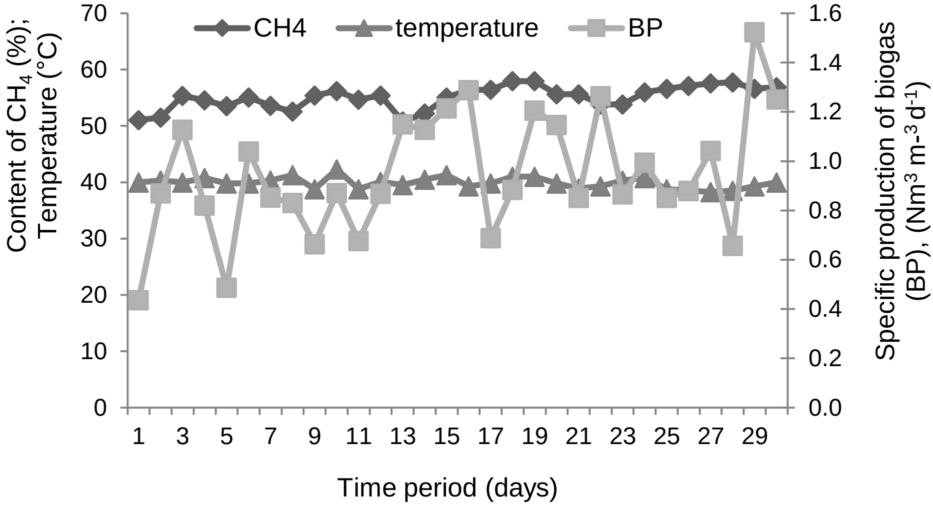

Figure 3. The course of monitored parameters for substrate fermentation – **II. Cycle**.

The average values of the monitored parameters are shown in Table 3 and Table 4. From the values given in Table 3 it can be concluded that the input substrate (slurry + manure + cosubstrates: sugar beet slices, rape moldings, maize silage and glycerine) showed a good value of organic degradable dry matter (OTS = 78.43% TS) in the fermentor. In addition, samples from the homogenisation tank (before entering the fermentor) showed an average chemical oxygen demand (COD) of 93,200 mg L^{-1}.

Table 4. Comparison of the average parameters of biogas production from 2 cycles of experiment with reference biomass (slurry and manure)

Material	CH_4	H_2S	CO_2	Biogas production	Specificproduction of biogas
	obj%	ppm	obj%	$Nm^3\ h^{-1}$	$Nm^3\ m^{-3}\ d^{-1}$
Cosubstrate – 33 kg of amaranth	63.9	998	28.9	0.113	0.542
Cosubstrate – 19.5 kg of sugar beet slices + 3.3 kg of maize silage + 1.9 kg of rape moldings + 2.5 kg of glycerine	55.1	128.3	34.8	0.199	0.955
Slurry:manure (80:20) obj%	60.8	1,343	31.2	0.032	0.160

Where CH_4 – methane; H_2S – hydrogen sulfide; CO_2 – carbon dioxyde; Nm^3 – standardised cubic meter.

Throughout the whole test period, the biogas composition was also monitored by the gas analyzer. The overview of the average values achieved by percentage representation is shown in the Table 4. Moreover, the average content of hydrogen sulphide which is an undesirable component in the biogas reached very acceptable values (on average 128.3 ppm), which is only 9.5% value than in the reference substrate. Therefore, based on the experience of co–generation units and the results obtained by other researchers it can be concluded that no expensive desulphurisation equipment is necessary (Hobson et al., 1974; Yadvika et al., 2004; Nielsen et al., 2007; Cantrell et al., 2008; Karafiát et al., 2012; Menon & Rao, 2012).

Table 4 lists the average parameters describing biogas production compared to the reference substrate parameters (pigs slurry and cattle manure in ration 80 and 20% volume).

In the co–fermentation of the amaranth an increase in biogas production was observed. Moreover, very stable and high methane content in the biogas was achieved. A significant reduction in the production of hydrogen sulphide content, which is an undesirable component due to highly corrosive effects, was also observed. It is important especially for the further processing of biogas in cogeneration units while its removal with the regular biogas cleaning represents the most costly operation (Gelegenis et al., 2007; Parawira et al., 2008; Fodora et al., 2013; Mao et al., 2015; Gaduš & Giertl, 2016).

In comparison with the reference substrate in the I–cycle of experiments (dosing of 33 kg of amaranth) it was observed an increase of specific biogas production in almost 3.39 times higher. Moreover, average methane content of 63.9% was observed as well. This represents very significant results. These results have demonstrated the suitability of using the amaranth as a co–substrate in biogas stations in our study as well as it was concluded by other authors (Gunaseelan, 1997; Seghezzo et al., 1998; Lehtomäki et al., 2007; Khalid et al., 2011).

Based on the results obtained from II. cycle of the experiments it can be concluded that the tested biomass showed very good results at suitable dosages and can therefore be considered as useful for the production of biogas by anaerobic fermentation. Similar conclusions were also indicated in other studies, e.g. Fatih Demirbas et al. (2011), Lee et al. (2014), Mao et al. (2015). The high energy value of both sugar and biodiesel waste, as demonstrated by the results of the experiments, ensures a high biogas production of more than 5.9 times than in case of the reference material. Moerver, there are still reserves of increase in potential increase of the daily dose, which would also provide a multiple times increase in biogas production (Alatriste–Mondragón et al., 2006; Nielsen et al., 2007; Parawira et al., 2008; Wang et al., 2012; Baeyens et al., 2015).

For methane production the most preferable pH is from 7.2 to 7.8 as can be seen from the tables above. In the first substrate measurement cycle the pH was lower than 6 and in the second cycle was less than 7. An unquestionable advantage for both experimental substrates was that the biogas production and specific biogas production were significantly higher than in case of utilization of slurry and manure combination. The differences in the amount of biogas produced are significant despite the lower value of methane from the fermented mixture of sugar beet slices, maize silage, rape moldings and glycerine. However, it should be added that the methane content in biogas of less than 50% may be limiting for its combustion in the cogeneration unit. This criterion is critical in terms of reliable operation while biogas has a lower calorific value (Hansen et al., 1998; Al Seadi et al., 2008; Gelegenis et al., 2007; Demirbas, 2011; Losak et al., 2014; Vítěz et al., 2015; Laštůvka et al., 2016). The methane content in biogas produced by fermentation of amaranth with slurry and manure mixture reached even higher levels of methane till up to 64%.

Based on the above results it is possible to conclude that the tested co–substates like amaranthus, as well as the addition of a mixture of biomass consisting of sugar beet slices, rape moldings, maize silage and glycerin are suitable biomass for the production of biogas by anaerobic fermentation. In addition, experience from biogas station situated in Kolíňany confirms that it is appropriate to look up for and verify the use of other biomass. These findings are more important while it may lead to reduction of utilization of high quality of maize silage for biogas production which is currently used in Slovakia for more than 85% and it is considered as very high demanding from the economic point of view.

CONCLUSIONS

The aim of the study was to verify the suitability of alternative substrates usable as input mixtures for anaerobic treatment in the biogas station with the result of production of energy fuel – biogas, under the operating conditions of a real biogas station. The experiments were divided into two alternatives (I and II cycle) and one controle input substates. In the first alternative (I cycle) was daily dosage formed by 33 kg of Amaranth and 250 L of controle manure mixture. In this cycle, more than 3–times greater specific production of biogas was observed with average methan content 63.9% in comparison with controle manure mixture (80 : 20%, liquid manure and manure). In the second alternative (II cycle) was daily dosage formed by 19.5 kg of sugar beer cuts, 3.3 kg of maize silage, 1.9 kg of oil-seed rape moldings, 2.5 kg of glycerine and 250 L of controle manure mixture. In this cycle, more than 5.9–times greater specific production of biogas was observed. The decrease in averare methan content 55.1% however also decrease in average content of hydrogen sulphide (128 ppm) was observed as well. An unquestionable advantage for both tested alternative mixed substrates was increase in biogas production and its quality in comparison with control substrate based on manure. These findings are more important while it may lead to reduction of utilization of high quality of maize silage for biogas production which is currently used in Slovakia for more than 85% and it is considered as very high demanding from the economic point of view.

ACKNOWLEDGEMENTS. This work was supported by AgroBioTech Research Centre built in accordance with the project Building 'AgroBioTech' Research Centre ITMS 26220220180; and by the Ministry of Education of the Slovak Republic, Project VEGA 1/0155/18.

REFERENCES

Alatriste–Mondragón, F., Samar, P., Cox, H.H.J., Ahring, B.K. & Iranpour, R. 2006. Anaerobic codigestion of municipal, farm, and industrial organic wastes: A survey of recent literature. *Water Environment Research* **78**(6), 607–636.

Al Seadi, T., Rutz, D., Prassl, H., Köttner, M., Finsterwalder, T., Volk, S. & Janssen, R. 2008. *Biogas handbook.* Esbjerg: University of Southern Denmark Esbjerg, Niels Bohrs Vej 9–10, DK-6700 Esbjerg, Denmark, 2008. ISBN 978–87–992962–0–0.

Álvarez, J.A., Otero, L. & Lema, J.M. 2010. A methodology for optimising feed composition for anaerobic co–digestion of agro–industrial wastes. *Bioresource Technology* **101**(4), 1153–1158.

Angelidaki, I. & Ahring, B.K. 1994. Anaerobic thermophilic digestion of manure at different ammonia loads: Effect of temperature. *Water Research* **28**(3), 727–731.

Ariunbaatar, J., Panico, A., Esposito, G., Pirozzi, F. & Lens, P.N.L. 2014. Pretreatment methods to enhance anaerobic digestion of organic solid waste. *Applied Energy* **123**, 143–156.

Baeyens, J., Kang, Q., Appels, L., Dewil, R., Lv, Y. & Tan, T. 2015. Challenges and opportunities in improving the production of bio–ethanol. *Progress in Energy and Combustion Science* **47**, 60–88.

Braun, R. 1982. *Biogas – Methane treatment of organic waste.* Monograph. Wien–New York: Springer Verlag, 1982 (In German).

Braun, R. 2013. *Biogas – Methassification of organic waste materials Basics and application examples.* Wien: Springer, 2013 (in German).

Cantrell, K.B., Ducey, T., Ro, K.S. & Hunt, P.G. 2008. Livestock waste–to–bioenergy generation opportunities. *Bioresource Technology* **99**(17), 7941–7953.

Carlsson, M., Lagerkvist, A. & Morgan–Sagastume, F. 2012. The effects of substrate pre–treatment on anaerobic digestion systems: A review. *Waste Management* **32**(9), 1634–1650.

Clemens, J., Trimborn, M., Weiland, P. & Amon, B. 2006. Mitigation of greenhouse gas emissions by anaerobic digestion of cattle slurry. *Agriculture, Ecosystems and Environment* **112**(2–3), 171–177.

Crabtree, R.H. 1995. Aspects of Methane Chemistry. *Chemical Reviews* **95**(4), 987–1007.

Gerardi, M.H. 2003. *The Microbiology of Anaerobic digesters.* New Jersey: John Wiley & Sons, Inc., Hoboken, 2003. ISBN 0–471–20693–8.

Demirbas, A. 2011. Waste management, waste resource facilities and waste conversion processes. *Energy Conversion and Management* **52**(2), 1280–1287.

Donoso–Bravo, A., Mailier, J., Martin, C., Rodríguez, J., Aceves–Lara, C.A. & Wouwer, A.V. 2011. Model selection, identification and validation in anaerobic digestion: A review. *Water Research* **45**(17), 5347–5364.

Fatih Demirbas, M., Balat, M. & Balat, H. 2011. Biowastes–to–biofuels. *Energy Conversion and Management* **52**(4), 1815–1828.

Fodora, M., Gaduš, J., Mareček, J., Vítěz, T. & Kažimírová, V. 2013. Design of laboratory cyclone separator for biogas purification. *Acta Universitatis Agriculturae et Silviculturae Mendelianae Brunensis* **61**(3), 631–635.

Gaduš, J. & Giertl, T. 2016. Technology for low–temperature thermochemical conversion of biomass. *MM Science Journal* **2016** (DECEMBER), 1545–1548.

Gelegenis, J., Georgakakis, D., Angelidaki, I. & Mavris, V. 2007. Optimization of biogas production by co–digesting whey with diluted poultry manure. *Renewable Energy* **32**(13), 2147–2160.

Gunaseelan, V.N. 1997. Anaerobic digestion of biomass for methane production: A review. *Biomass and Bioenergy* **13**(1–2), 83–114.

Hansen, K.H., Angelidaki, I. & Ahring, B.K. 1998. Anaerobic digestion of swine manure: Inhibition by ammonia. *Water Research* **32**(1), 5–12.

Hobson, P.N., Bousfield, S., Summers, R. & Kirsch, E.J. 1974. Anaerobic digestion of organic matter. *C R C Critical Reviews in Environmental Control* **4**(1–4), 131–191.

Karafiát, Z., Vítěz, T., Somerlíková, K., Gaduš, J., Haitl, M. & Koutný, T. 2012. Employment of maize silage in non–liquid fermentation for biogas production. *Acta Universitatis Agriculturae et Silviculturae Mendelianae Brunensis* **60**(6), 153–160.

Khalid, A., Arshad, M., Anjum, M., Mahmood, T. & Dawson, L. 2011. The anaerobic digestion of solid organic waste. *Waste Management* **31**(8), 1737–1744.

Laštůvka, I., Vítěz, T., Chovanec, J. & Mareček, J. 2016. Zero waste; energy recovery from non–recyclable mixed municipal waste. *Acta Universitatis Agriculturae et Silviculturae Mendelianae Brunensis* **64**(1), 99–107.

Lee, W.S., Chua, A.S.M., Yeoh, H.K. & Ngoh, G.C. 2014. A review of the production and applications of waste–derived volatile fatty acids. *Chemical Engineering Journal* **235**, 83–99.

Lehtomäki, A., Huttunen, S. & Rintala, J.A. 2007. Laboratory investigations on co-digestion of energy crops and crop residues with cow manure for methane production: Effect of crop to manure ratio. *Resources, Conservation and Recycling* **51**(3), 591–609.

Li, Y., Park, S.Y. & Zhu, J. 2011. Solid–state anaerobic digestion for methane production from organic waste. *Renewable and Sustainable Energy Reviews* **15**(1), 821–826.

Lin, C.S.K., Pfaltzgraff, L.A., Herrero-Davila, L., Mubofu, E.B., Abderrahim, S., Clark, J.H., Koutinas, A.A., Kopsahelis, N., Stamatelatou, K., Dickson, F., Thankappan, S., Mohamed, Z., Brocklesby, R. & Luque, R. 2013. Food waste as a valuable resource for the production of chemicals, materials and fuels. Current situation and global perspective. *Energy and Environmental Science* **6**(2), 426–464.

Losak, T., Hlusek, J., Zatloukalova, A., Musilova, L., Vitezova, M., Skarpa, P., Zlamalova, T., Fryc, J., Vitez, T., Marecek, J. & Martensson, A. 2014. Digestate from biogas plants is an attractive alternative to mineral fertilisation of Kohlrabi. *Journal of Sustainable Development of Energy, Water and Environment Systems* **2**(4), 309–318.

Mao, C., Feng, Y., Wang, X. & Ren, G. 2015. Review on research achievements of biogas from anaerobic digestion. *Renewable and Sustainable Energy Reviews* **45**, 540–555.

Mata–Alvarez, J., Dosta, J., Romero-Güiza, M.S., Fonoll, X., Peces, M. & Astals, S. 2014. A critical review on anaerobic co–digestion achievements between 2010 and 2013. *Renewable and Sustainable Energy Reviews* **36**, 412–427.

Menon, V. & Rao, M. 2012. Trends in bioconversion of lignocellulose: Biofuels, platform chemicals & biorefinery concept. *Progress in Energy and Combustion Science* **38**(4), 522–550.

Møller, H.B., Sommer, S.G. & Ahring, B.K. 2004. Methane productivity of manure, straw and solid fractions of manure. *Biomass and Bioenergy* **26**(5), 485–495.

Nielsen, H.B., Uellendahl, H. & Ahring, B.K. 2007. Regulation and optimization of the biogas process: Propionate as a key parameter. *Biomass and Bioenergy* **31**(11–12), 820–830.

Parawira, W., Read, J.S., Mattiasson, B. & Björnsson, L. 2008. Energy production from agricultural residues: High methane yields in pilot–scale two–stage anaerobic digestion. *Biomass and Bioenergy* **32**(1), 44–50.

Piszczalka, J. & Jobbágy, J. 2011. Bioenergy: *Green Energy*. 1st edition. Slovak university of agriculture in Nitra, Nitra, 2011. 143 pp.

Piszczalka, J. & Jobbágy, J. 2012. Bioenergy: *Green energy*. 1st edition. Slovak university of agriculture in Nitra, Nitra, 2012. 149 pp.

Rajagopal, R., Massé, D.I. & Singh, G. 2013. A critical review on inhibition of anaerobic digestion process by excess ammonia. *Bioresource Technology* **143**, 632–641.

Rajeshwari, K.V., Balakrishnan, M., Kansal, A., Lata, K. & Kishore, V.V.N. 2000. State–of–the–art of anaerobic digestion technology for industrial wastewater treatment. *Renewable & sustainable energy reviews* **4**(2), 135–156.

Raposo, F., De La Rubia, M.A., Fernández–Cegrí, V. & Borja, R. 2012. Anaerobic digestion of solid organic substrates in batch mode: An overview relating to methane yields and experimental procedures. *Renewable and Sustainable Energy Reviews* **16**(1), 861–877.

Seghezzo, L., Zeeman, G., Van Lier, J.B., Hamelers, H.V.M. & Lettinga, G. 1998. A review: The anaerobic treatment of sewage in UASB and EGSB reactors. *Bioresource Technology* **65**(3), 175–190.

Sosnowski, P., Wieczorek, A. & Ledakowicz, S. 2003. Anaerobic co–digestion of sewage sludge and organic fraction of municipal solid wastes. *Advances in Environmental Research* **7**(3), 609–616.

Vítěz, T., Koutný, T., Geršl, M., Kudělka, J., Nitayapat, N., Ryant, P., Hejduk, S., Lošák, T., Vítězová, M. & Mareček, J. 2015. Biogas and methane yield from rye grass. *Acta Universitatis Agriculturae et Silviculturae Mendelianae Brunensis* **63**(1), 143–146.

Wang, X., Yang, G., Feng, Y., Ren, G. & Han, X. 2012. Optimizing feeding composition and carbon-nitrogen ratios for improved methane yield during anaerobic co–digestion of dairy, chicken manure and wheat straw. *Bioresource Technology* **120**, 78-83.

Ward, A.J., Hobbs, P.J., Holliman, P.J. & Jones, D.L. 2008. Optimisation of the anaerobic digestion of agricultural resources. *Bioresource Technology* **99**(17), 7928–7940.

Yadvika, Santosh, Sreekrishnan, T.R., Kohli, S. & Rana, V. 2004. Enhancement of biogas production from solid substrates using different techniques - A review. *Bioresource Technology* **95**(1), 1–10.

Zhang, C., Su, H., Baeyens, J. & Tan, T. 2014. Reviewing the anaerobic digestion of food waste for biogas production. *Renewable and Sustainable Energy Reviews* **38**, 383–392.

Agronomy Research **16**(3), 784–793, 2018
https://doi.org/10.15159/AR.18.111

Assessment of soil electrical conductivity using remotely sensed thermal data

K. Křížová[1,2,*], J. Haberle[3], M. Kroulík[1], J. Kumhálová[4] and J. Lukáš[2]

[1]Czech University of Life Sciences Prague, Faculty of Engineering, Department of Agricultural Machines, Kamýcká 129, CZ16500 Prague, Czech Republic
[2]Crop Research Institute, Division of Crop Protection and Plant Health, Drnovská 507/73, CZ 16106 Prague, Czech Republic
[3]Crop Research Institute, Division of Crop Management Systems, Drnovská 507/73, CZ16106 Prague, Czech Republic
[4]Czech University of Life Sciences Prague, Faculty of Engineering, Department of Machinery Utilization, Kamýcká 129, CZ16500 Prague, Czech Republic
[*]Correspondence: krizovak@tf.czu.cz

Abstract. Detection of heterogeneity (crop, soil, etc.) gained a lot of importance in the field of site-specific farming in recent years and became possible to be measured by different sensors. The thermal spectrum of electromagnetic radiation has a great potential today and experiments focused on describing a relation between canopy temperature and various vegetation characteristics are conducted. This paper was aimed to examine the relation between canopy temperature and electrical conductivity as one of staple soil characteristics. The related experiment was undertaken in Sojovice, Czech Republic, within an agricultural plot where winter wheat was grown in 2017 growing season. The examined plot was composed of three sub plots and 35 control points were selected within this area which the data were related to. A canopy was sensed by UAV (eBee carrying thermoMAP (FLIR TAU2) camera). Soil conductivity data were collected by terrestrial sampling using EM38-MK2 Ground Conductivity Meter in 1 m depth and 2 m sampling point distance. This dataset was later interpolated using the kriging method. The correlation analysis results showed a strong negative correlation between conductivity and thermal data (-0.82; $p < 0.001$). When comparing conductivity with NDVI representing the aboveground biomass, there was an opposite trend but also strong result (0.86; $p < 0.001$). Correlation coefficient of thermal data and NDVI comparison was -0.86; ($p < 0.001$). These preliminary results have a potential for further research in terms of soil characteristics studies.

Key words: precision agriculture, winter wheat, heterogeneity, UAV, kriging.

INTRODUCTION

The concept of Precision Agriculture (PA) has developed rapidly in recent decades. As the population grows and the field of specialized technologies are enhanced, the methods of site-specific farming more or less engage the common practice. Many studies are conducted with the aim to describe relations between various soil and vegetation characteristics and different kind of remotely sensed (RS) data. Such knowledge is essential to obtain a complex overview of how the natural processes may be explained by spectral imagery. The major advantage of such approach is especially the fact that the research may be carried out in a non-destructive mode. Related analyses may be thus undertaken repeatedly during one growing season, i.e. it is possible to evaluate crops on particular plot in different growth stages (Richards, 1993; Jones & Vaughan, 2010). It was determined that the spectral characteristics are related to various vegetation characteristics such as biochemical composition, physical structure or plant status (Sahoo et al., 2015). Based on this knowledge there is not only the possibility to evaluate the crop status at the canopy scale, but it is also possible to detect some within-field heterogeneity. This heterogeneity may be caused by variability of elevation or soil texture that in both cases affects at most the water distribution (Kumhálová et al., 2011; Sassenrath & Kulesza, 2017). Detecting of the within-field heterogeneity may be utilized to adjust the agricultural management and delineate so-called production zones. Initially, the concept of PA was based on responses in the visible and near-infrared (NIR) regions of the electromagnetic spectrum. Plenty of vegetation indices (VI) were developed as the ratios of reflectance in different wavelengths. Although many of them are considered to be very effective indicator of soil and vegetation characteristics, the research is focused on thermal infrared region of the spectrum in recent years. The major difference between these two approaches is that optical RS exploits the radiation reflected from the investigated surface, whereas thermal RS methods work with the amount of radiation that is emitted by the particular surface or object (Sabins Jr., 1997). As the temperature is such characteristic that is not visible under standard conditions, the thermal RS converts this information and displays the patterns as the visible image (Ishimwe et al., 2014). According to Khanal et al. (2017) this is especially useful for early detection of stressed vegetation based on the crop temperature on the contrary to optical RS methods, where the stress may be indicated only when visible symptoms appear. This statement is supported also by study of Camoglu et al. (2017), where thermal and hyperspectral data were analyzed to detect four levels of water stress on peppers (*Capsicum annuum L.*). Whereas spectral indices did not indicate the difference between 100% and 75% irrigated vegetation, thermal indices provided significant results. Initially, the obtaining of high resolution thermal imagery was limited by high acquisition costs. However, recently the low-costs platforms were developed. Especially, the utilization of Unmanned Aerial Vehicles (UAV) has lowered the costs and thus the thermal imagery became more accessible for various branches of agricultural research such as nursery and greenhouse monitoring, irrigation management, plant disease detection or yield prediction (Ishimwe et al., 2014). A number of studies focus on fruit trees yield prediction. An algorithm was developed by Stajnko et al. (2004) to estimate apple tree yield prediction using thermal data. Moreover, Bulanon et al. (2008) demonstrated the method how to estimate citrus fruit yield based on the fact that the fruits have approximately 1.6 °C higher temperature than leaves during the night. Nevertheless, the utilization of thermal imagery to predict cereals yield has still some limits in scientific literature. However, there are also studies describing the relation of thermal imagery and soil characteristics. Soil texture was found to be strongly related to a land surface temperature (Mattikalli et al., 1998). It is a factor that besides the others affects the amount of water held in soil profile that on the rebound influences the surface temperature. Soil electrical conductivity (EC) is considered to be a staple soil property. It determines capability of soil to transmit an electrical charge (Logsdon, 2008). According to various studies EC is associated to other soil attributes such as soil texture or soil water content (Corwin & Lesch, 2003; Logsdon, 2008; Malin & Faulin, 2013). Exploration of physical and chemical soil properties within examined area is often expensive and time consuming procedure. Therefore, in terms of PA applications EC became useful and most frequently obtained measurements to determine soil properties. Obtained values of EC are usually processed and thereafter presented as a map. This kind of map thus gives approximate information about soil texture and soil water distribution. It may be utilized not only for appropriate crop selection, but also for evaluation of drainage and irrigation management or spatio-temporal changes in soil properties.

Since thermal RS methods gained attention in recent years and the soil EC is considered to be a staple soil factor, this study aimed to describe the relation between these two variables. Experimental data presented in this paper are aimed to be analysed to determine the level of association of canopy temperature (T_c) and soil EC as the staple soil factor.

MATERIALS AND METHODS

Experimental Site

The experiment was conducted within an agricultural plot near the Sojovice town in Czech Republic. It is located approximately 25 km north-east from Prague [50°13'45"N, 14°45'54"E]. The whole experimental area has nearly 25 ha and it is composed of three smaller plots marked by numbers (Fig. 1). The west side plot [7] has 8.4 ha and there are cambisols as a staple soil type. The northern part of plot [9] has 10.0 ha and the southern one [5] has 5.8 ha. There are regosols as the staple soil type within both of these plots. According to the DEM the elevation ranges between 175–184 m a.s.l. thus there is no significant elevation variability over the area. This agricultural plot has already been monitored in recent years. Certain pattern in crop heterogeneity is observable on different kind of imagery during the growing season (Fig. 2).

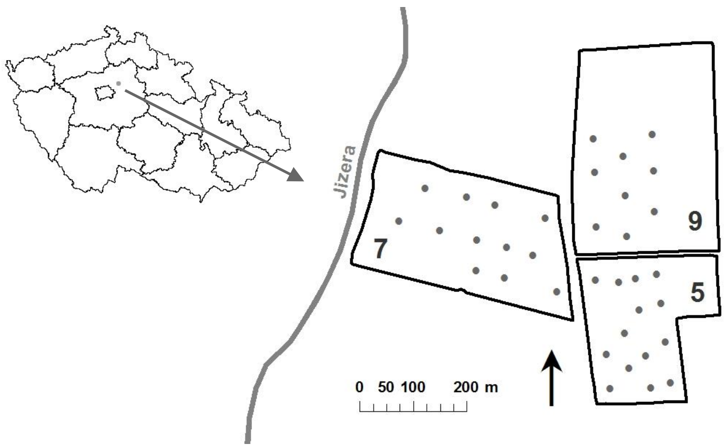

Figure 1. Experimental plot localization and composition (subplots marked by numbers 5, 7, 9) with 35 control points depicted within the field and Jizera river flow on the west side.

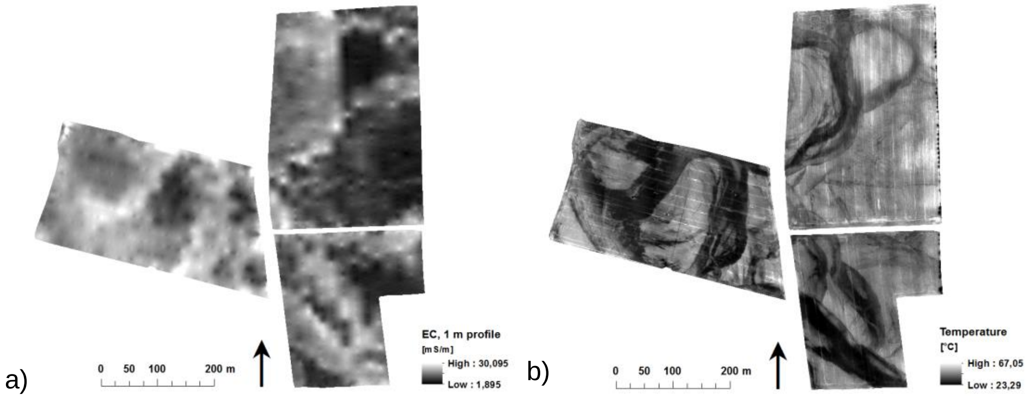

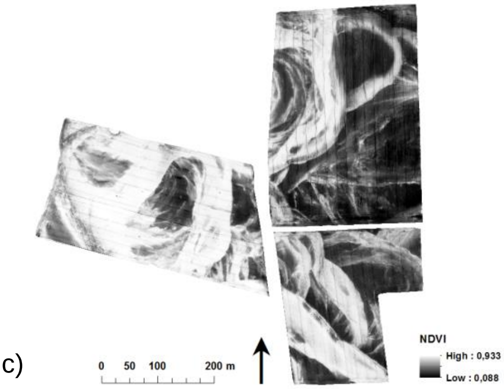

Figure 2. a) Soil electrical conductivity (EC), b) canopy temperature (T_c) and c) Normalized Difference Vegetation Index (NDVI) derived from remotely sensed imagery.

This heterogeneity is very likely influenced by the nearby flow of Jizera river and it is planned to be examined also in upcoming growing season. For a purpose of pedological research in total 35 control points were selected (Fig. 1). This control points selection was based on remotely sensed data from years 2015 and 2016 that were generally poor on precipitation. Therefore, zones of crops stressed by insufficient amount of water appeared in certain pattern during both examined growing season. Thus, points were selected to represent zones with different rate of crop water stress.

Agricultural management of the examined plot works with crop rotation of winter wheat and potato with one-year period. In 2017 growing season there was a winter wheat grown in two varieties. Variety *Patras* was sown on the southern part of the plot [5], while the other two parts were sown with *Epos* variety. Consequently all data analysis and results interpretation are related to winter wheat as one of the staple agricultural crops.

Remotely sensed Data

To obtain spectral data in sufficient spatial resolution the canopy of the experimental plot was sensed using UAV on 19th June 2017. A fully autonomous drone eBee (senseFly, Cheseaux-Lausanne, Switzerland) was utilized to carry two different types of camera. Canopy temperature data were obtained using thermal camera senseFly thermoMap. The images were processed and composed using specialized SW. In order to calculate Normalized Difference Vegetation Index (NDVI) sensing with multispectral camera senseFly multiSPEC 4C was done as well. To acquire absolute reflectance measurements the calibration with calibration target was necessary to be done before flight. This multispectral camera contains four separate sensors that acquire data in four bands – green, red, red-edge and NIR. Based on multispectral imagery NDVI index was calculated using ENVI 5.4 (Exelis Visual Information Solutions, Boulder, Colorado, USA). This index was derived and used in the analysis as the indicator of aboveground biomass. Technical specifications of utilized cameras and their settings for this particular sensing are given by Table 1, whereas Table 2. describes meteorological conditions during the process of data acquisition.

Table 1. Technical parameters of canopy remote sensing at 80 above ground level

	Thermal camera	MS camera
Typ of device	thermoMap	multiSPEC 4C
Sensor	FLIR TAU2, 640 × 512 px	4×1/3" CMOS
Ground resolution at 100 m, cm/px	19	10
Velocity, m s^{-1}	12–13	
Vertical overlap, %	80	
Horizontal overlap, %	80	
SW	eMotion, Pix4D	

Soil Electrical Conductivity Data

In order to gain the soil EC data, a terrestrial sampling was carried out using widely known probe for electromagnetic induction (EMI) (Corwin and Lesch, 2005) measurement EM38 MK2 (Geonics Limited, Ontario, Canada) on 13th September 2017. Weather conditions during the process of measurement are given in Table 2. The probe was pulled by quad by the speed approximately 2.8 m s^{-1}, while the data were acquired in the soil profile 0–1 m. The measurement was performed as the set of points with the distance of 2 m in the direction of quad motion.

Table 2. Meteorological conditions by data collection

	T_c	EC
Date of sensing	19.6.2017	13.9.2017
Time of sensing	2–3 PM	2–4 PM
Aerial temperature, °C	29	16.4
Precipitation, mm	0.0	0.0
Wind velocity, k h^{-1}	8.6	18
Air pressure, hPa	1,020.3	1,005.8

Weather conditions during the process of measurement are given in Table 2. The probe was pulled by quad by the speed approximately 2.8 m s^{-1}, while the data were acquired in the soil profile 0–1 m. The measurement was performed as the set of points with the distance of 2 m in the direction of quad motion. The distance between particular trajectories was approximately 20 m. Data from probe was recorded to the measuring unit together with DGPS signal each second. In order to eliminate recorded errors, some modifications on the original EC values were performed before processing. Data were treated at the extreme values. Data of conductivity were processed using statistical and geostatistical methods. The set of 7,428 points was interpolated in order to get coherent map representing the EC values distribution within the examined area. The maps were created using the kriging interpolation method (see Table 3). Software Microsoft office (Microsoft Corporation, Redmond, USA) and ArcGIS 10.5 (ESRI, Redlands, California, USA) were used.

Table 3. Parameters of Kriging as a method of interpolating the point electrical conductivity (EC) data

Method of estimation	Method of Moments (MoM)
Method of interpolation	Kriging
Variogram model	Spherical
Nugget variance	0.776
Distance parameter (*r*)	43.471
Partial sill	12.349

Data Analysis

Since the data were acquired and processed, it was possible to display numerical values of examined vegetation and soil characteristics in form of raster layer. This kind of visualisation showed certain pattern of data variability within examined agricultural plot. Nevertheless, the analysis needed to be done to describe the relation between T_c and EC more precisely. In addition, analysis of the relation between EC and NDVI, respectively T_c and NDVI was done as well to obtain complex information about the dataset. Since there was set of 35 control points selected within the experimental area, the other data analysis was related to those points. Values from raster layers (T_c, EC and NDVI) were extracted using the *Extract Multi Values to Points* tool in ArcMap 10.5 SW and added to the attribute table of 35 control point vector layer. Thus, the result was the table with in containing exact numerical information about T_c, the soil EC and NDVI at the particular point. Statistical analysis process was done in R Studio SW (RStudio Team, Boston, Massachusetts, USA). Pearson's correlation coefficient was calculated at three levels. At first the relation T_c and EC was evaluated, followed by the calculations for T_c and NDVI and also EC and NDVI.

RESULTS AND DISCUSSION

First, summary statistics of examined variables was done to acquire complex information about the dataset intended to be analysed. Results of the summary are given by Table 4. Mean value of EC was 10.306 mS m^{-1}, whereas median reached only 9.310 mS m^{-1}. These values were in accordance with possitive skewness (0.403) that indicated the data are more distributed on the right side of the mean value, i.e. the field is mostly characterized by lower values of EC, however the mean value is influenced by several parts with higher EC values. Mean canopy temperature was calculated to be 30.4 °C, median 31.6 °C. Negative skewness indicated higher vaules dominating among the dataset. NDVI mean value was 0.66 and slightly negative skewness showed on more values distributed on the left side of the mean.

Table 4. Summary statistics of soil electrical conductivity (EC), canopy temperature (T_c) and Normalized Difference Vegetation Index (NDVI)

	EC	T_c	NDVI
Count	35	35	35
Mean	10.306	30.440	0.660
Median	9.310	31.600	0.679
Sample variance	14.621	5.825	0.040
Standard deviation	3.824	2.413	0.199
Minimum	4.280	26.440	0.323
Maximum	18.048	33.910	0.901
Skewness	0.403	-0.215	-0.179

Relation of soil EC and T_c was evaluated within selected agricultural plot. Additionally, the NDVI was added to the analysis as the aboveground biomass indicator. The analysis was concentrated in 35 control points selected in terms of previous research. Correlation coefficients were calculated for combinations of three examined variables, however, the relation of EC and T_c was the most required one. Fig. 3 gives a complex overview of correlation analysis results. Significantly strong correlation was detected at all levels. Soil EC and T_c were negatively correlated with the correlation coefficient value -0.82. Even stronger negative correlation was observed by T_c and NDVI relation (-0.86), while conversely very strong positive correlation was found by EC and NDVI (0.86). Fig. 4 gives detailed information about the relation of EC and other two examined variables (T_c and NDVI).

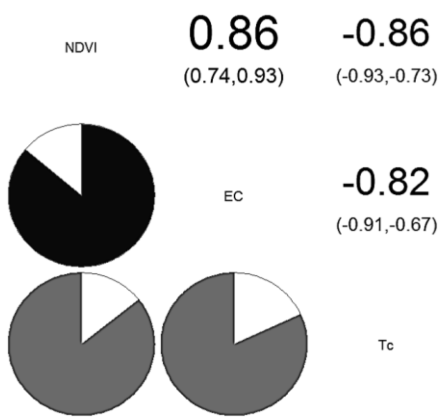

Figure 3. Results of correlation analysis presented as correlogram, where the dark grey colour within a pie chart represents a positive trend of correlation coefficient, while the light grey indicates a negative trend (*p-value < 0.001*). Confidence intervals are given in round brackets.

Based on the results of correlation analysis the relation of soil property and canopy temperature may be described. The negative value of correlation coefficient is the indicator of indirect proportion. In fact, with lower values of EC the canopy temperature tends to increase. It is generally known that plant temperature is associated with the stomatal conductance that further links to the nutrient uptake and therefore it influences actual biomass of the crop (Cai & Cespedes, 2012). This fact is also in accordance with result of analysis of thermal data and NDVI representing aboveground biomass, where the correlation coefficient indicated indirect proportion as well.

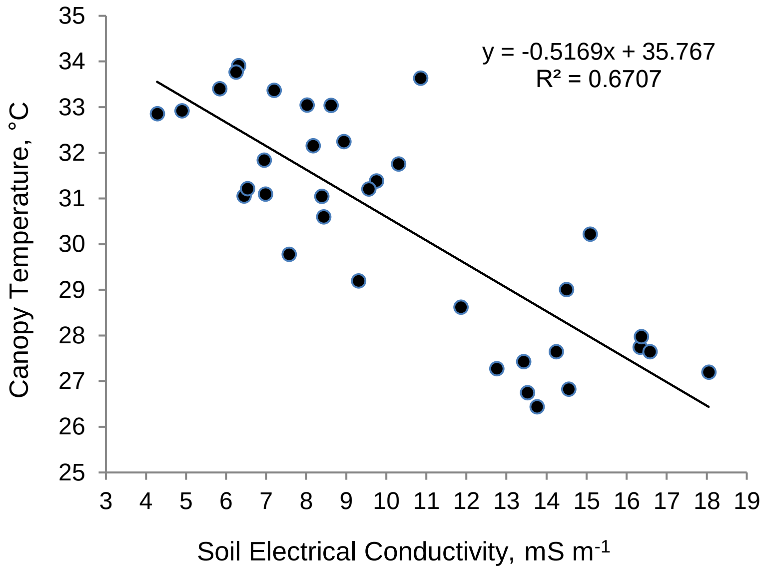

a)

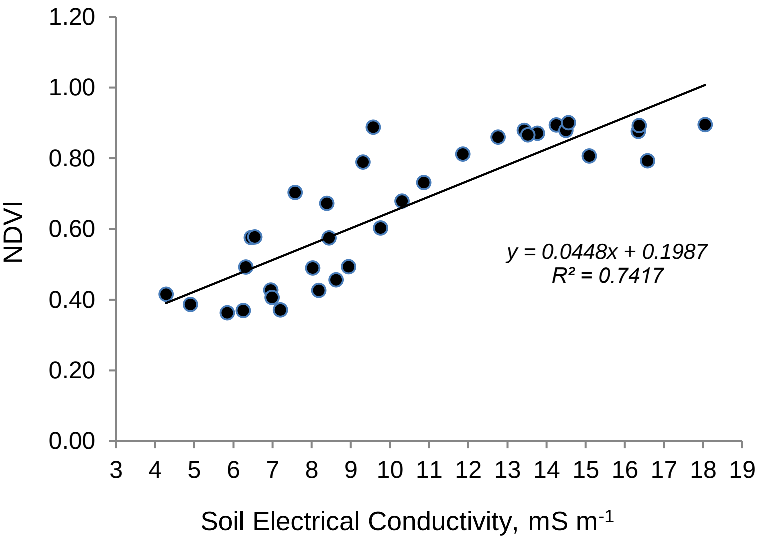

b)

Figure 4. a) Trend of T_c and EC and b) trend of NDVI and EC relation based on the data from 35 control points.

Multispectral imagery can provide quick information about crop biomass within the field by calculating particular VI. In this case, NDVI values ranges from 0.323 to 0.901 and the heterogeneity is apparent also from attached map (Fig. 2, c). When having such information about the crop vegetation status, the cause of such differences should be determined. Various factors may influence the crop growth, e.g. topography (Kumhálová et al., 2011), soil properties variability or presence of pests or effect of plant disease. As was stated above, the elevation variability is not significant within the examined plot. Very likely the heterogeneity is caused by variable soil properties, but the soil sampling is difficult to be conducted during growing season. On the contrary, evaluation of vegetation cover using thermal RS techniques may be carried out regardless of time. T_c and EC correlation analysis showed the value -0.89 and thus the EC may be very likely explained by remotely sensed thermal data. There are studies that describe very tight correlation of EC and other soil properties (Corwin & Lesch, 2003). However, other studies were conducted with different results. Malin & Faulin (2013) evaluated two agricultural plots to determine the relation of EC and clay and water content. Significant results were found only on one of two evaluated plots, where spatial variability of soil texture was higher. Moreover, the study of Valente et al. (2012) found no significant results when evaluating EC and soil texture and moisture, respectively various chemical properties. It is clear that conclusions differ across the scientific literature, so the particular limiting soil factor may not be always identified precisely without soil sampling.

CONCLUSIONS

A number of studies were conducted to describe possible utilization of recently enhanced thermal RS data to predict yield of agricultural plot. However, the potential of thermal data to explain the soil properties that are a major factor influencing the crop growth, i.e. yield as well, is not described yet. In order to determine some basic relation of thermal response and soil characteristics this study was conducted. Soil electrical conductivity was chosen to be analysed as the factor subsuming most of other soil properties. At first, correlation analysis showed that aboveground biomass (presented by NDVI) is strongly influenced by EC (0.86). Based on this piece of information the correlation of canopy temperature and EC was examined and provided significant results, respectively close negative correlation (-0.82) was indicated. Such conclusion may be considered as some preliminary result supporting the thesis on possibility of soil properties to be explained by thermal RS. Further research may be conducted based on this conclusion to explore how are the thermal data capable to explain other soil properties.

ACKNOWLEDGEMENTS. This study was supported by Faculty of Engineering of Czech University of Life Sciences under the internal grant IGA 2017:31160/1312/3118. The section of data acquisition was conducted under financial support from project of Ministry of Industry and Trade TRIO FV10213. The section regarding terrestrial experiments was supported by Ministry of Agriculture of the Czech Republic CRI RO0418.

REFERENCES

Bulanon, D.M., Burks, T.F. & Alchantis, V. 2008. Study on temporal variation in citrus canopy using thermal imaging for citrus fruit detection. *Biosystems Engineering* **101**, 161–171.

Cai, J. & Cespedes, M. 2012. Plant temperature measurement and analysis from infrared images. In: *27th Conference on Image and Vision Computing New Zealand*. IVCNZ, Dunedin, pp. 406–411.

Camoglu, G., Demirel, K. & Levent, G. 2017. Use of infrared thermography and hyperspectral data to detect effects of water stress on pepper. Quantitative InfraRed Thermography Journal, DOI: 10.1080/17686733.2017.1331008.

Corwin, D.I. & Lesch, S.M. 2003. Applicaion of Soil Electrical Conductivity to Precision Agriculture: Theory, Principles, and Guidelines. *Agronomy Journal* **95**, 445–471.

Corwin, D.L. & Lesch, S.M. 2005. Apparent soil electrical conductivity measurements in agriculture. *Computers and Electronics in Agriculture* **46**, 11–43.

Ishimwe, R., Abutaleb, K. & Ahmed, F. 2014. Applications of Thermal Imaging in Agriculture – A Review. *Advances in Remote Sensing* **3**, 128–140.

Jones, H.G. & Vaughan, R.A. 2010. *Remote Sensing of Vegetation: Principles, techniques and applications*. Oxford University Press, Oxford, 353 pp.

Khanal, S., Fulton, J. & Shearer, S. 2017. An overview of current and potential applications of thermal remote sensing in precision agriculture. *Computer and Electronics in Agriculture* **139**, 22–32.

Kumhálová, J., Kumhála, F., Kroulík, M. & Matějková, Š. 2011. The impact of topography on soil properties and yield and the effects of weather conditions. *Precision Agriculture* **12**, 813–830.

Logsdon S.D. 2008. *Soil Science: Step-by-step Field Analysis*. ASA-CSSA-SSSA, Madison, 251 pp.

Malin, J.P. & Faulin, G.CH. 2013. Spatial and Temporal variability of soil electrical conductivity related to soil moisture. *Scientia Agricola* **70**, 1–5.

Mattikalli, N.M., Engman, E.T., Jackson, T.J. & Ahuja, L.R. 1998. Microwave remote sensing of temporal variations of brightness temperature and near-surface soil water content during a watershed-scale field experiment and its application to the estimation of soil physical properties. *Water Resources Research* **34**, 2289–2299.

Richards, J.A. 1993. *Remote Sensing Digital Image Analysis: An Introduction.* Springer-Verlag, Berlin, 340 pp.

RStudio Team 2016. RStudio: Integrated Development for R. RStudio, Inc., Boston, MA URL http://www.rstudio.com/.

Sabbins, Jr. F.F. 1997. *Remote Sensing: Principles and Interpretation, 3rd Edition*. W.H. Freeman, New York, 494 pp.

Sahoo, R.N., Ray, S.S. & Manjunath, K.R. 2015. Hyperspectral remote sensing of agriculture. *Current Science* **108**, 848–859.

Sassenrath, G.F. & Kulesza, S. 2017. Measuring Soil Electrical Conductivity to Delineate Zones of Variability in Production Fields. In: *SEARC Agricultural Research 2017*. Kansas State University, Manhattan, pp. 64–72.

Stajnko, D., Lakota, M. & Hočevar, M. 2004. Estimation of number and diameter of apple fruits in an orchard during the growing season by thermal imaging. *Computer and Electronics in Agriculture* **42**, 31–42.

Valente, D.S.M., DeQueiroz, D.M., Pinto, F.A.C., Santos, N.T. & Santos, F.L. 2012. The relationship between apparent soil electrical conductivity and soil properties. *Revista Ciência Agronômica* **43**, 683–690.

Agronomy Research **16**(3), 794–805, 2018
https://doi.org/10.15159/AR.18.085

Criteria of design for deconstruction applied to dairy cows housing: a case study in Italy

L. Leso, L. Conti, G. Rossi and M. Barbari*

Department of Agricultural, Food and Forestry Systems, University of Firenze, Via San Bonaventura 13, IT50145 Firenze, Italy
*Correspondence: leonardo.conti@unifi.it

Abstract. This work aims at presenting the design process of a new barn for dairy cows. Project embraces several concepts that are rather new to the dairy industry and will deeply affect its environmental, economic and social sustainability. The barn will be built on a green field site located in Cervasca (CN) in the region of Piedmont. Building has been designed applying the emerging principle of "design for deconstruction" extensively. A series of constructive solutions was developed allowing for complete end-of-life disassembly and reuse of building materials. Structural system will consist of locally sourced timber connected by steel joints. Foundations will be realized by means of chestnut wood piles driven into the ground. The employment of an alternative housing system for dairy cows based entirely on cultivated pack will allow limiting the use of cast-in-place concrete, which is largely employed in conventional dairy barns. The cultivated pack needs a large space per cow leading the building to be particularly extended. The large covered area combined with the high snow load of the building site posed several challenges. Accumulation of snow on the roof would increase dramatically the structural load and therefore construction costs. Therefore, the building will consist of several 12m-large modules with 4m free space between them. Given the unusual shape of the barn and the limited use of concrete for flooring, the development of efficient systems for livestock management required the study of dedicated solutions. A first module, already realized to collect useful information for final design, is described.

Key words: design for deconstruction, sustainable building, cattle housing, cultivated pack barns, compost dairy barns.

INTRODUCTION

Housing can play a major role in determining environmental, economic and social sustainability of dairy farming. The construction and materials used for buildings can influence together with technological equipment the microclimatic conditions inside the cowsheds (Kic, 2017). Over the last decades, free stall barns have established as the standard housing system for dairy cattle worldwide. Such solution allowed achieving substantial improvements in labour requirement and cow cleanliness (Bewley et al., 2017). However, recent research highlighted this system may have several shortcomings, especially with respect to animal welfare and waste management (EFSA, 2009). Conventional building design and extensive use of concrete, typical in free stall barns, may also have a negative impact on the sustainability of cattle housing.

Cultivated pack barns (CPB), also known as compost bedded pack barns, are an alternative housing systems for dairy cows, which showed potential to improve animal welfare (Barberg, 2007a; Leso et al., 2013). In CPB, cows are provided with an open bedded pack area for resting and walking rather than individual stalls and concrete alleys. The bedded pack, which is a mixture of bedding material and animal excreta, is cultivated daily to foster the evaporation of water and maintain adequate hygienic conditions for the cows. Such housing system was developed in recent years mainly to improve the welfare of cows.

Scientific research showed that cows housed in compost barns have healthier claws and legs likely due to the reduced concrete surfaces and less injury-causing obstacles in the barn compared with the conventional free stall housing system (Fulwider et al., 2007; Kester et al., 2014). Although some authors expressed concerns about cow cleanliness and udder health, recent findings showed that, if properly managed, this housing would allow maintaining adequate udder health and milk quality (Black et al., 2014). Other advantages of CPB regard cows longevity and improved behaviour (Enders & Barberg, 2007; Leso et al., 2014). Better welfare may result in improved productivity, lower production costs and reduced use of medicines and antibiotics (von Keyserlingk et al. 2009).

Compared with free stalls, employing CPB would also allow producing higher quantities of solid effluents while reducing the amount of liquid wastes. Solid manure can be easily stocked and demonstrated to produce less odour compared with slurry. Recent research also showed this material is a valuable fertilizer, especially due to the very high content of organic matter, which improves soil structure over the long term (de Boer, 2014). Furthermore, employing CPB could reduce the use of (cast-in-place) concrete, especially for paving, in the areas dedicated to the animals.

Construction waste management has become extremely important due to stricter disposal and landfill regulations, and a lesser number of available landfills (Rios et al., 2015). Design for Deconstruction (DfD) is a concept in building science, which has the potential to improve the management of construction waste and thus contributes reducing the environmental impact of a building.

Design for Deconstruction is a concept in building science based on the use of recyclable, renewable, locally available and environmentally friendly raw materials, with low environmental and economic impact according to six main principles for sustainable construction: to minimise resource consumption; to maximise resource reuse; to use renewable and recyclable resources; to protect the natural environment; to create a healthy and non-toxic environment; to pursue quality in creating the built environment (Miyatake, 1996).

These topics are a priority for authors, who over the years have carried out several projects regarding the sustainable development of agricultural buildings (Barbari et al., 2003; Barbari et al., 2012; Conti et al., 2016). The deconstructable anthropization should be considered for reversible changes of the places, in order to increase the temporary business needs of farming without compromising the original conditions of the territory. In fact, buildings that can be destroyed and eliminated at the end of their functional and planning life, using no additional resources and disposed causing no environmental pollution, can be considered deconstructable. The purpose of DfD consists in 'increase resource and economic efficiency and reduce pollution impacts in the adaptation of and eventual removal of buildings, and to recover components and materials for reuse, re-manufacturing and recycling' (Pulasky et al., 2003).

To achieve these objectives, it is necessary to make coherent choices in all phases of the design process. In particular, it is important to consider an integrated design connected to the choice of natural and locally available building materials, of suitable building technologies and to the analysis of economic and environmental costs for the potential decommissioning of the sustainable building. The main criteria of the building systems adopted are based on the disassembly of each element in parts conveniently transportable, storable, and reusable without heavy reconditioning interventions. These criteria seem to find practical applications in the 7th Environment Action Programme, which will address European environment policy until 2020 (EAP, 2016).

To date, concepts of DfD have been poorly implemented in the design of cattle housing. The present work aims at describing and discussing the design process of a new barn for dairy cows. The project embraces several concepts that are rather new to the dairy industry, including CBD and DfD, which can improve its sustainability. The design process started in 2013 and is still on-going. However, main building solutions and general layout of the barn have been identified. A first module, already realized to collect useful information for final design, is also described.

MATERIALS AND METHODS

Case study

The case study presented in this paper resulted from the collaboration between the Department of Agricultural, Food and Forestry Systems (GESAAF) of the University of Firenze and Cascina Bianca, a certified organic dairy farm located in Piedmont, Italy. Cascina Bianca already owns housing facilities for about 70 lactating cows (Fleckvieh breed), delivering about 1,400 kg of milk per day, but the farm aims at expanding the milk production to 7,000 kg day^{-1}. Therefore, one of the main objectives of the project was to build a new barn capable of housing the number of animals required to achieve the target daily milk production. Recent evidence shows that environmental concerns and societal perception of farming are becoming urgently important (Boogaard et al., 2011). Since Cascina Bianca processes and markets directly organic dairy products, developing a project that meets the fast changing needs of consumers was crucial. Hence, the department GESAAF was asked to help identify solutions to improve sustainability of the new housing facility. Besides improving productivity, project was expected to reduce environmental footprint and ensure high levels of animal welfare as well as being economically sound.

Construction site and context

The barn will be built on a green field site located in Cervasca (CN), Piedmont, Italy (44.405583, 7.500528). The area is in the south-western edge of the Po plain, at the foot of the Western Alps. The construction site is mostly flat and approximately rectangular in shape, with the main length lying on the North-South direction. Soil is loam with high presence of gravel. In the area, climate is continental temperate, with cool to cold winters and warm summers. Mean month temperatures range between 1.5 °C in January to 20.5 °C in July (Arpa, 2011). Maximum temperatures can be particularly high (> 30 °C) in summer, potentially causing sever heat stress conditions for dairy cattle (West, 2003). Prevailing wind flow from South-West while average annual precipitation is 1028 mm (Frattiani et al., 2007). Proximity with the Alps makes the area prone to high snowfall during the winter. Italian law sets a minimum design snow load of 240 kg m^{-2} for this particular area (D.M. 14 Gennaio 2008, Italian Government). Besides agriculture, forestry is very well developed in the area, particularly due to the wide availability of chestnut (*Castanea sativa*).

Project constrains

As already noted, project was expected to deliver a high level of sustainability. In particular, the main constrains set by Cascina Bianca were:

– building has to be designed according to the principles of DfD as the entire facility will have to be completely removed (and most materials recycled) when obsolete (expected life time 20 years);

– building has to be pleasant, consumers friendly, provide unobstructed views of the internal spaces and realized mainly with natural and locally sourced materials;

– cows have to be provided with high level of animal welfare, with special focus on limiting risk for painful diseases and fostering natural cattle behaviour;

– production of liquid effluents has to be limited as much as possible while high quality solid effluents are strongly desired.

Prototype building and test

In 2014, Cascina Bianca built a prototype building in order to test the feasibility of the project and measure effects on animal welfare (Fig. 1). The prototype building has been realized employing the same techniques and materials described below and can therefore provide useful indications about the performance of the housing system. The prototype building was 10 m wide and 40 m long with a total covered area of 400 m^2, of which 340 m^2 were bedded.

Figure 1. External view of the prototype building used for test.

RESULTS AND DISCUSSION

One of the first steps in the design process was identifying the housing system for the cows. Several solutions have been investigated and compared. Conventional systems like straw yards (SY) and free stalls (FS) have been quickly discarded due to the need of large volumes of concrete, which would have limited the deconstructability of the building (Salama, 2017). Also, both SY and FS may pose some limitations to animal welfare. Free stall housing showed to increase risk of foot and leg disorders, which represent a major welfare problem for dairy cattle (Kester et al., 2014). On the other hand, SY may result in poor udder health, especially due to high exposure to environmental mastitis-causing bacteria (Fregonesi & Leaver, 2001).

A housing system based on CPB was selected primarily because of the documented benefits regarding animal welfare (Bewley et al., 2017), which was one of the main focus of the project. Besides that, CPB would result in a very simple housing facility, with a unique large open area for the animals. Compared with FS, a CPB requires less steelwork and potentially less concrete. This allows applying extensively the concepts of DfD and has the potential to reduce construction costs. Moreover, employing CPB would limit the amount of liquid effluents produced while increase solid manure.

Normally, CPB consist of two separate areas for resting and for feeding. Resting area is bedded and pack thickness can vary from few cm to more than 1m depending on management (Klaas & Bjerg, 2011). Depending on the country and begging management, the floor beneath the bedded pack can be paved or not. In most cases CPB in Italy have a cast-in-place concrete floor in the resting area (Leso et al., 2013). Barberg et al. (2007b) reported that CPB in Minnesota are commonly bedded upon a clay base. Other research found that most CPB in the Netherlands have a concrete floor, while just one Dutch CPB was provided with a plastic foil under the bedding (Galama et al., 2011). In CPB, 30 to 50% of the total cow excreta are produced in the feeding area (Janni et al., 2007). For this reason, the floor of the feeding area is generally not bedded and made up of concrete (close or slatted) to facilitate frequent removal of manure.

To reduce as much as possible the use of concrete and steelwork, the housing system for the new barn of Cascina Bianca will consist of a unique continuous bedded area on which the cows will rest, walk and eat. Therefore, there will be no distinctions between the resting and the feeding areas. To ensure homogenous distribution of excreta over the bedded area, cows will be fed with movable feed troughs (Fig. 2). The troughs will be filled with fresh feed and moved on a new spot every day. Bedding will be 0.8 to 1.0 m-deep and the floor beneath will be realized with a plastic foil. A layer of sand will be placed above the foil to protect it even though the pack stirring operations, which will be carried out once or twice a day, will occur at a maximum depth of 0.25–0.3 m. Previous experiences in CPB with deep bedding suggest that just the upper part of the bedded pack needs to be removed and substituted periodically (normally once a year) with new material, while the lower layer

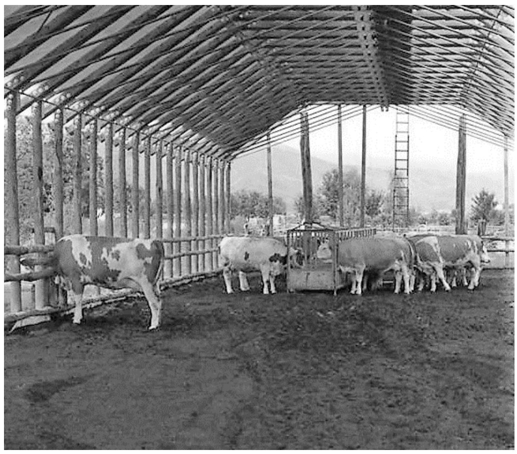

Figure 2. The movable feeding trough system allows spreading the manure over the entire area of the bedded pack, without the need of a concrete alley.

can be left in place (Galama et al., 2011). This management guarantees the plastic foil is not damaged by machines and makes concrete paving beneath bedding unnecessary.

In compost barns throughout the world, several kinds of bedding have been employed, based on climate, local availability and market price. Most common seem to be sawdust and woodchips (Klaas & Bjerg, 2011). However, the price of wood-based materials has increased in recent years mainly due to the use as alternative energy sources. Cascina Bianca will adopt green waste compost sourced from a local composting plant as bedding. Besides being environmentally friendly, this material resulted to be particularly cheap on the local market. Besides reducing costs associated with bedding, employing compost allows shortening the loop of organic wastes within the local economy and can contribute generating a positive perception of the farm. The employment of compost bedding coupled with the movable feeding system will result in the production of a single type of effluent. Such material, being relatively dry and solid, can be easily stocked and managed. Recent research also showed this material is an excellent fertilizer, especially due to the very high content of organic matter, which improves soil structure over the long term (de Boer, 2014). This aspect makes it very well suited to organic farming systems.

Although this kind of CPB housing would allow a high level of animal welfare, as the cows are not exposed to concrete flooring, the cultivated pack needs a large area, leading the building to be particularly extended. First aim of Cascina Bianca is building an housing facility to increase production of milk up to 7,000 kg day^{-1}. Considering a milk yield per animal of 25 kg day^{-1} (which is the actual milk production level at Cascina Bianca), the new barn will need to house 280 lactating cows. Space for 40 dry cows and 40 pregnant heifers will also need to be provided, leading to a total capacity of 360 dairy cattle. Previous research indicates 30m^2 cow^{-1} can be an adequate animal density in CPB systems that are not provided with scraped feeding area (Klaas & Bjerg, 2011). The barn will therefore have a covered area of 10,800 m^2, excluding the milking facility.

Cows will be milked twice a day in a 20+20 herringbone parlour. A dedicated building will accommodate the parlour and other necessary facilities including the milk and equipment rooms, the holding pen and the cows treatment area. Such building will be constructed using the same techniques and materials employed for the superstructure of cattle housing. However, the whole building will be paved with concrete to facilitate cleaning operations. Conventional building solutions (concrete and bricks) will also be used to create the internal and external walls of the milking centre. Effluents generated in this area will be collected in a dedicated tank, and will represent the only liquid waste produced.

Building layout and structure

Structural system consists of locally sourced timber connected by steel joints and supporting truss work in wood. The bearing structure is composed of pillars in solid chestnut wood (diameter 0.15 m, nominal length 6.25 m), the roof has a nominal span of 12 m, and overall height is 8.25 m. The anchor joints with pillars are simply placed flat on a wood beam under the roof truss. Foundations are realized with chestnut wood pillars driven into the underground to a depth of 2.4 m.

The very large covered area combined with the high snow load of the building site (240 kg m^{-2}) posed several challenges. The snow accumulated on the roof increases dramatically the structural load and therefore construction costs. Therefore, it is necessary to adopt a solution that consists to build a simple structure with a moderate clear span of 12 m for a total length of 180 m. This kind of buildings will be replicated throughout 4 modules of building separated between them with a distance of 4 m (Fig. 3).

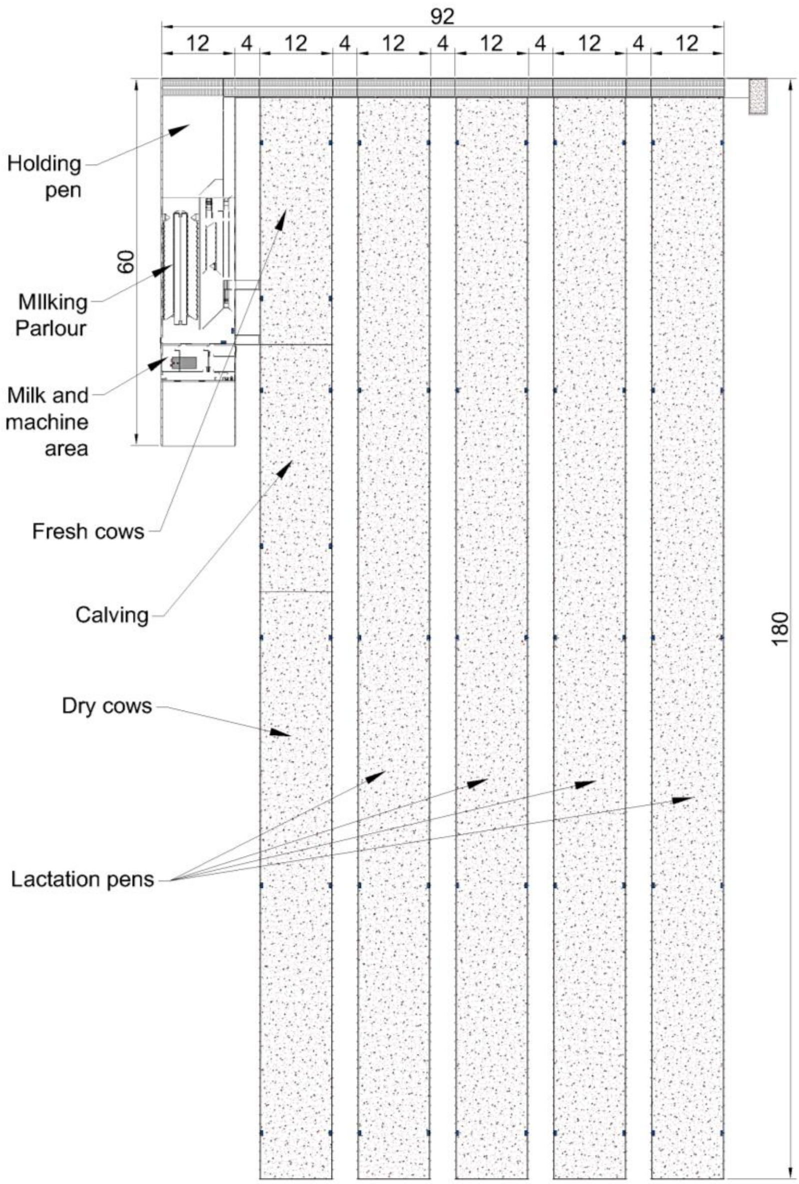

Figure 3. Plan view of the building.

All structures, including the milking centre will be covered with a transparent PVC foil, derived from the greenhouse sector. The transparent covering is recyclable and will help creating bright and pleasant interiors as well as contributing to maintain the bedded pack dry and comfortable for the cows. To avoid excessive heat load, a plastic shading net will be installed over the transparent covering during summer months. Moreover, a row of trees will be planted between each module with the aim of fostering natural shading of the structure as well as creating a more natural-looking environment (Leso et al., 2017). A cross section of one of the building modules is reported in Fig. 4.

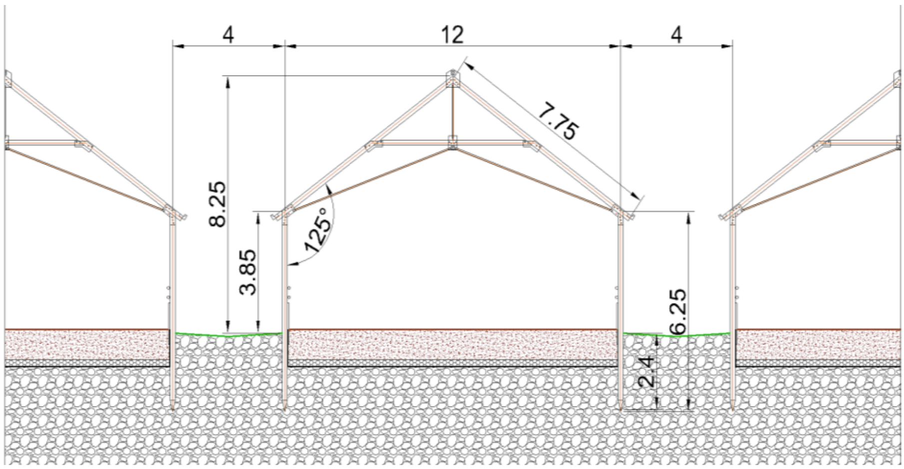

Figure 4. Cross section representing one of the building modules.

Building materials

In the context of building removal, some materials are better suited to recycling, some to reuse. Metals, for example, are well suited to recycling. Steel can be roughly treated (bent, torn apart and otherwise) and still retain a relatively high value. Even if it is intermixed with other materials, metal can be separated (magnetically) for recycling (Falk, 2002). As regards to the selection of building materials for the design of the sustainable cattle housing, the technical features are shown here:

– Chestnut timber: if solid lumber is mistreated and broken up, it is impractical to separate it from other building materials and any value is vastly reduced (Falk, 2002). In order to respect this point only local round chestnut has been used.

– Steel plate joints: simple and standardized structural connections can enhance the assembly and disassembly process. For example, modular connections, such as the new rigid key-type joint or an older modular connection called Saxe clips for structural steel, allow steel members to be easily disassembled and reused. These modular connections require as little as one bolt and no welding for installation, resulting in a simplified construction process and contributing to a shorter construction schedule. Attention to connection details is critical for future reusability of structural elements. Complex and unique connections increase installation time and complicate the deconstruction process. Fewer connections and consolidation of the types and sizes of connectors will reduce the need for multiple tools during deconstruction (Guy & Shell, 2002). Simple and standard connections that facilitate the ease of disassembly and full recovery of reusable materials are necessary to close the loop on material reuse (Pulaski et al., 2003). Metallic joints mainly made of galvanized steel (hot-dip galvanizing or electrogalvanized) are recyclable. Recycling consists of separating steel from zinc, in order to obtain materials with the same initial physical and chemical properties.

– Plastic film: cheap, durable and versatile, plastics bring us multiple benefits. But these materials can also pose problems when plastics end up in the environment, with impacts on nature, the climate and human health. To make recycling easier, plastic manufacturers have implemented a numeric resin identification. DfD must respect this code system in order to simplify reuse and to promote the use of recycle plastic.

Livestock housing and handling solutions

Given the unusual shape of the barn and the limited use of concrete for flooring, the development of efficient systems for livestock feeding and management required the study of dedicated solutions. Housing for cows will be organized in 5 distinct modules (Fig. 3). One of them (the closest to the milking parlour) will accommodate 3 pens for different production stages: 1) dry cows, 2) calving pen, 3) freshly calved and special attention cows. The remaining modules will house all lactating cows, offering flexibility to create up to 4 groups of animals. This allows providing different rations tailored to the nutritional requirement of each group. Also, lactating cows can be separated based on their parity. A sorting gate placed at the exit of the milking parlour will allow separating individual cows that need to be examined, treated or inseminated. A dedicated treatment area, provided with insemination and treatment chutes, will facilitate animal husbandry operations.

Results obtained with the prototype building

The prototype building realized in 2014 allowed Cascina Bianca to assess the feasibility of the project and evaluate construction methods and building materials. After more than four years from construction, the structure and in particular the wooden posts driven into the ground showed no apparent signs of deterioration indicating the building techniques employed can be sustainable over the mid- to long-term.

Furthermore, to assess effects on animal welfare and performance, a trial was organized in cooperation with the University of Turin, Department of Veterinary Science (Bellino, 2014). Twenty two primiparous cows (Fleckvieh breed) were randomly divided in two groups. The first group was housed in a conventional free stall barn while the second was housed in the prototype building with CPB housing system. The 11 cows in the group CPB-TRTM were allocated 30.9 m^2 $animal^{-1}$. All cows were fed the same TMR ration and milked 2 times a day in a 5+5 herringbone parlour. Experiment lasted 8 months (from February 2014 to October 2014), during which the animals were constantly monitored to determine milk production and quality. Animal behaviour was monitored by direct observations carried out by a trained operator. Air temperature and temperature of the bedding in the prototype building were also monitored during the course of the study.

Results of the trial carried out in the prototype building indicated cows housed in CPB were healthier and produced higher quality milk compared with those in the conventional free stalls system (Bellino, 2014). In particular, cows in CPB-TRTM showed lower locomotion score, lower somatic cells count, lower total bacteria count, and higher milk fat content. No differences were detected in milk yield and body conditions score among the two groups. Furthermore, compared with FS-TRTM, cows in CPB-TRTM showed less agonistic behaviours among herd mates and better interactions with humans. During the course of the study, temperature of the bedding was significantly higher than air temperature, indicating that the material was actively composting.

CONCLUSIONS

The concept of DfD has the potential to limit the environmental impact of construction by supporting end-of-life disassembly and reuse of building materials. To date, such concept has been poorly implemented in the design of livestock housing and research in this specific field is still very sparse. The case study described in this paper demonstrates applying DfD extensively to dairy cows housing is feasible. However, novel and dedicated solutions need to be identified during early phases of the design process. Cultivated pack barns seem to be better suited to DfD compared with conventional housing systems, such as FS. Further research is strongly needed to develop viable DfD-oriented building solutions for livestock housing.

ACKNOWLEDGEMENTS. Authors acknowledge Cascina Bianca for their participation and support of this study. We thank Livio Bima, farm manager at Cascina Bianca, for sharing his invaluable experience.

REFERENCES

Arpa Agenzia Regionale per la Protezione Ambientale. 2011. Fifty years of metereological data in Pedmont Region – Daily temperatures and rainfalls (1958–2009). *https://www.arpa.piemonte.it/pubblicazioni-2/pubblicazioni-anno-2011*. Accessed 04/10/2017 (in Italian).

Barbari, M., Conti, L., Monti, M., Pellegrini, P., Rossi, G., Simonini, S. & Sorbetti Guerri, F. 2012. Antropizzazioni decostruibili per il non-consumo del territorio rurale: Progettazione per la decostruibilità. In: *Proceedings of the National Congress of the Italian Society of Agricultural Engineering. L'edilizia rurale tra sviluppo tecnologico e tutela del territorio*. Firenze, Italy (in Italian).

Barbari, M., Monti, M., Pellegrini, P. & Sorbetti Guerri, F. 2003. La costruzione di edifici agricoli in legno massiccio sulla base di progetti tipo. In: *ARSIA Regione Toscana: Costruire in legno - Progetti tipo di fabbricati ed annessi agricoli* (2 ed.). Firenze, Italy (in Italian).

Barberg, A.E., Endres, M.I. & Janni, K.A. 2007b. Compost dairy barns in Minnesota: A descriptive study. *Applied Engineering in Agriculture* **23**, 231–238.

Barberg, A.E., Endres, M.I., Salfer, J.A. & Reneau, J.K. 2007a. Performance and welfare of dairy cows in an alternative housing system in Minnesota. *Journal of Dairy Science* **90**, 1575–1583.

Bellino, C. 2014. Final report of activities carried out within the project "COMPOSTALLA". Grant n. 08000540743, PSR Piemonte 2013. Department of Veterinary Science, Univeristy of Torino, Italy (in Italian).

Bewley, J.M, Robertson, L.M. & Eckelkamp, E.A. 2017. A 100-Year Review: Lactating dairy cattle housing management. *Journal of Dairy Science* **100**(12), 10418–10431.

Black, R.A., Taraba, J.L., Day, G.B., Damasceno, F.A., Newman, M. C., Akers, K. A., Wood, C. L., McQuerry, K.J. & Bewley, J. M. 2014. The relationship between compost bedded pack performance, management, and bacterial counts. *Journal of Dairy Science* **97**, 1–11.

Boogaard, B.K., Oosting, S.J., Bock, B.B. & Wiskerke, J.S.C. 2011. The sociocultural sustainability of livestock farming: an inquiry into social perceptions of dairy farming. *Animal* **5**(9), 1458–1466.

Conti, L., Barbari, M. & Monti, M. 2016. Design of sustainable agricultural buildings.A case study of a wine cellar in Tuscany, Italy. *Buildings* **6**(2), 1–8.

de Boer, H. 2014. *On farm development of bedded pack dairy barns in the Netherlands - Nutrient balances and manure quality of bedding material*. Report 709. Wageningen UR Livestock Research, Lelystad, NL.

EFSA. 2009. Scientific report of EFSA prepared by the Animal Health and Animal Welfare Unit on the effects of farming systems on dairy cow welfare and disease. Annex to the *EFSA Journal* **1143**, 1–284.

Endres, M.I. & Barberg, A.E. 2007. Behavior of Dairy Cows in an Alternative Bedded-Pack Housing System. *Journal of Dairy Science* **90**, 4192–4200.

EU European Commission. 2016. The 7th General Union Environment Action Programme to 2020. Brussel, Belgium. *http://ec.europa.eu/environment/action-programme/*. Accessed 15.9.2017.

Falk, B. 2002. Wood-Framed Building Deconstruction: a source of Lumber Construction? Forest Products Journal **52**(3), 8–15.

Frattiani, S., Cagnazzi, B. & Cremonini, R. 2007. *Il vento in Piemonte*. Regione Piemonte, Turin, Italy (in Italian).

Fregonesi, J.A. & Leaver, J.D. 2001. Behaviour, performance and health indicators of welfare for dairy cows housed in straw yard or cubicle systems. *Livestock Production Science* **68**, 205–216.

Fulwider, W.K., Grandin, T., Garrick, D.J., Engle, T.E., Lamm, W.D., Dalsted, N.L. & Rollin, B.E. 2007. Influence of free-stall base on tarsal joint lesions and hygiene in dairy cows. *Journal of Dairy Science* **90**, 3559–3566.

Galama, P.J., Bokma, S., van Dooren, H.J., Ouweltjes, W., Smits, M. & Driehuis, F. 2011. *Prospects for bedded pack barns for dairy cattle*. Wageningen UR Livestock Research, Lelystad, The Netherlands.

Guy, B. & Shell, S. 2002. Design for Deconstruction. In: *Proceedings of CIB Task Group – 39 Deconstruction*. Karlsruhe, Germany.

Italian Government. 2008. Approval of new technical rules for constructions. Gazz. Uff. 04/02/2008, n. 29. *http://www.camera.it/cartellecomuni/leg15/RapportoAttivitaCommissioni/commissioni/allegati/08/08_all_dm_2008.pdf*. Accessed 20.9.2017 (in Italian).

Janni, K.A., Endres, M.I., Reneau, J.K. & Schoper, W.W. 2007.Compost dairy barn layout and management recommendations. *Applied Engineering in Agriculture* **23**, 97–102.

Kester, E., Holzhauer, M. & Frankena, K. 2014. A descriptive review of the prevalence and risk factors of hock lesions in dairy cows. *The Veterinary Journal* **202**, 222–228.

Kic, P. 2017. Effect of construction shape and materials on indoor microclimatic conditions inside the cowsheds in dairy farms. *Agronomy Research* **15**, 426–434.

Klaas, I.C. & Bjerg, B.S. 2011. Compost barns - An alternative housing system for dairy cows? *CAB Reviews: Perspectives in Agriculture, Veterinary Science, Nutrition and Natural Resources* **6**(45), 1–9.

Leso, L., Morshed, W., Conti, L. & Barbari, M. 2017. Evaluating thermal performance of experimental building solutions designed for livestock housing: the effect of greenery systems. *Agronomy Research* **15**(1), 239–248.

Leso, L., Uberti, M., Morshed, W. & Barbari, M. 2013. A survey of Italian compost dairy barns. *Journal of Agricultural Engineering* **44**(e17), 120–124.

Leso, L., Uberti, M., Morshed, W. & Barbari, M. 2014. Cultivated pack barns improve longevity of dairy cows. In: *18th World Congress of CIGR International Commission of Agricultural and Biosystems Engineering*. Beijing, China, pp. 162–166.

Miyatake, Y. 1996. Technology Development and Sustainable Construction. *Journal of Management in Engineering* **12**(4), 23.

Pulaski, M, Hewitt, C., Horman, M. & Guy, B. 2003. Design for Deconstruction: Material Reuse and Constructability. In: *Proceedings of Green Build Conference*. Pittsburg, PA, USGBC, Washington, D.C, pp. 1–10.

Rios, F.C., Chong, W.K. & Grau, D. 2015. Design for Disassembly and Deconstruction - Challenges and Opportunities. *Procedia Engineering* **118**, 1296–1304.

Salama, W. 2017. Design of concrete buildings for disassembly: An explorative review. *International Journal of Sustainable Built Environment.* In Press, Corrected Proof. https://doi.org/10.1016/j.ijsbe.2017.03.005

Von Keyserlingk, M.A.G., Rushen, J., de Passillé, A.M. & Weary, D.M. 2009. Invited review: The welfare of dairy cattle - Key concepts and the role of science. *Journal of Dairy Science* **92**, 4101–4111.

West, J.W. 2003. Effects of Heat-Stress on Production in Dairy Cattle. *Journal of Dairy Science* **86**, 2131–2144.

Agronomy Research **16**(3), 806–820, 2018
https://doi.org/10.15159/AR.18.125

Performance evaluation of rural areas: the case of Estonian rural municipalities before the administrative reform

H. Luik-Lindsaar*, R. Põldaru, A. Põder and J. Roots

Estonian University of Life Sciences, Institute of Economics and Social Sciences, Kreutzwaldi 1, EE51014 Tartu Estonia
*Correspondence: helis.luik@emu.ee

Abstract. Estonian municipalities have recently passed an administrative reform that has resulted in the reorganisation of municipal management and decreased the number of municipalities. Unfortunately, no thorough scientific research has been done to find out whether the emerging helps to increase the efficiency. The aim of this paper is to estimate the efficiency of Estonian rural municipalities and to identify the factors that influence their efficiency. In this study we use a two stage analysis. In the first stage, we use the DEA Slacks-Based Model's (SBM) output-oriented approach. In the second stage, we use the Fractional Regression Model (FRM) to determine relevant exogenous factors that are associated with efficiency. 170 Estonian rural municipalities have been analysed. According to the DEA results, 28% of municipalities (48) are efficient, the average efficiency of municipalities is 0.762. The analysis implies that there are considerable differences between smaller and larger rural municipalities. FRM results revealed that larger share of subsidies characterize inefficient municipalities. The weaker the municipality, the more state support the municipality must receive. A larger share of people with a higher education increases the efficiency, it is related to higher salaries and therefore higher revenue to the municipality. Elderly residents in the population increases the efficiency, however it isn't sustainable in the long-run because more inputs are needed to offer various public services. The results indicate that the further away a municipality is from the capital, the more inefficient the municipality becomes.

Key words: technical efficiency, rural municipalities, DEA, FRM.

INTRODUCTION

Municipalities manage public money, which is collected and distributed by the government. More than half on local municipalities' revenue comes from income tax (Statistics Estonia, 2016). Therefore, local residents expect high quality services which contribute to the functioning and development of local life.

Municipalities have to provide and ensure services to local residents. As any other organisations, municipalities must follow the theory of the firm: the provision of services must be cost-efficient and at the same time, they have to ensure high quality of services. A limited budget complicates the provision of high quality services and often becomes the decisive factor in calculating the volume of services and outlining the list of required services.

Some municipalities are managing public money better than others, which means that these municipalities are more efficient. We can measure the efficiency in input-output context. The services that municipalities provide are considered as inputs and the population and area describing the output volumes.

Assessing the efficiency of municipalities in respect of the provision of certain services is fully valid since municipalities operating within the same political and economic context and cultural space should provide services in a relatively homogenous way. Benchmarking and identifying the reasons of efficiency at local level provides necessary information to reorganise services in those municipalities that experience problems with the provision of services.

Previous literature shows that efficiency studies differ in terms of methodological approaches, as well as by results. DEA (data envelopment analysis) and SFA (stochastic frontier analysis) are quite extensively used techniques for efficiency analysis (Afonso & Fernandes, 2008; Cuadrado-Ballesteros, et al., 2013; Charles & Zagarra, 2014; Cruz & Marques, 2014; Doumpos & Cohen 2014; Asatryan & De Witte, 2015; Drew et al., 2015; Horta et al., 2016; Storto, 2016; D'Inverno et al., 2018). The performance of municipalities is estimated against a frontier consisting of the observation of the best practices. The municipalities with the best practices, which use resources effectively, serve as references for inefficient municipalities, and can be used as guidance for the future.

It is common to assess the efficiency of the following services which are in the area of responsibility of municipalities: education (Seroa da Motta & Moreira, 2009); environmental protection, and housing and communal services (Rogge & De Jaeger, 2012; Alper et al., 2015), healthcare (Valeira et al., 2010), social security (Iparraquirre & Ma, 2015), leisure and culture (De Witte & Geys, 2011). Some studies have focused on the size (population) and the merger of municipalities with the aim to make conclusions about the occurrence of the scale effect across different services provided in larger municipalities (Slack & Bird, 2013a).

In less populated municipalities, it is difficult to offer services as efficiently as in densely populated municipalities. Sparsely populated municipalities are often situated in the periphery, which are struggling due to urbanisation and outmigration. Owing to the marginalisation process, creation of new jobs is very limited in these municipalities, which leads to both short and long term decrease of the revenue base. The government has provided considerable subsidies for municipalities which have a low revenue base. Since Estonia's population is aging and municipalities are facing a situation where the revenue base is decreasing whilst the number of people who need social assistance is increasing, the state is looking for solutions that would ensure residents significant public services within their own municipalities. The state considers that the merger of municipalities is one of the options, in order to achieve greater efficiency through the scale effect. The merger of municipalities, their efficiency and the optimal size of a municipality have been the focus of increasingly heated public debate in Estonia. Many countries have gone through similar processes of considerable reform of municipal structures and mergers in the recent decades (Bönish et al., 2011). A number of studies have been carried out on the effect that the merger of municipalities has on financial sustainability in the context of providing public services (Nakazawa, 2013; Slack & Bird, 2013b; Allers & Geertsema, 2014).

This research uses a two-stage approach to assess the efficiency of Estonian rural municipalities as many authors have done previously in other countries (Balaguer-Colla et al., 2007; Afonso & Fernandes, 2008; Doumpos & Cohen, 2014; Storto, 2016). In the first stage, the efficiency of municipalities is assessed using the DEA method, followed by identifying efficient and inefficient municipalities. In the second stage, the FRM (fractional regression model) is used to assess the effect that exogenous variables have on efficiency, whereas the DEA model's efficiency score is the dependent variable.

Overview of Estonian municipalities

Estonia is located in the Baltic Sea on the shores of the Gulf of Finland, bordering with Russia in the east and Latvia in the south. With an area of 45,227 km^2 and a population of 1.3 million, it is one of the smallest EU countries. Estonia is territorially divided into 15 counties. It was subdivided into 213 municipalities, including 30 cities and 183 parishes until 1st July of 2017 (Statistics Estonia, 2015).

Due to urbanisation, more populated parishes are mainly situated in North Estonia, around the capital Tallinn. Harju county has 575,000 residents (a remarkable 43% of the total population), with 407,000 of them living in the capital Tallinn. Urbanisation of the population can also be observed elsewhere in Estonia, particularly in suburban parishes. Less populated parishes are situated in West, East and Southeast Estonia.

The single-level municipal system has been in force in Estonia since 1993. Municipalities make decisions and organise all aspects of local life independently (Ministry of Finance, 2016b). The state can only assign obligations to them based upon the law or upon an agreement with the municipality (The parliament of Estonia, 1993). The cornerstone of modern democratic organisation is the principle of subsidiarity, according to which functions must be exercised at a public administration level as close as possible to the citizen. One of the main tasks of the local council is to make the most important decisions that affect local life, and to guide the development of the municipality (The parliament of Estonia, 1993).

Municipalities must provide social assistance and services, housing and communal services, water supply and waste disposal, spatial planning, public transport, maintenance of municipal public roads and city streets, offer primary level healthcare services, organise the upkeep of local preschool childcare institutions, schools, libraries, community centres and other local institutions, and also ensure public order and surveillance. (The parliament of Estonia, 1993)

Municipalities can exercise the functions assigned by the state, using the financial resources at their disposal. Estonian municipality revenues include taxes, sales of goods and services, sales of tangible and intangible property, revenue from property, government subsidies, and other income. Government subsidies refer to central government's grants to local municipalities to guarantee financial resources for carrying out their tasks and for equalizing the disparities in per capita income (Reiljan, 2004, Ministry of Finance, 2016b).

The municipal income analysis shows that in 2013 the largest part of income in municipal budgets comes from personal income tax proceeds (49%), and another part is constituted by government subsidies (34%). A relatively small part is made up by the sales revenue of goods and services (10%) and by land tax (4%). The largest share of expenses are education costs (42%), followed by economic, defence and security costs

(17%), costs related to culture and sport (13%), and environmental protection and communal service costs (10%). (Statistics Estonia, 2016)

The quality of public services can differ between Estonian municipalities. The functions of all municipalities are the same by the law, however, the size of municipalities varies from capital with over 400,000 inhabitants to small island municipalities with less than 100 inhabitants (European Commission, 2013). So municipalities with very different capacities have to provide same kind of broad range of services (Friedrich et al., 2010). Uudelepp et al. (2009) pointed out that problems are caused by the delegation of tasks which are unaffordable to municipalities, and by the insufficient revenue base of municipalities, especially sparsely populated and peripheral ones. Insufficient public services create a multifaceted problem, possibly limiting people's quality of life (lacking social services) and opportunities (lacking educational services). Estonian administrative organisation is often referred to and highlighted as problematic. (Uudelepp et al., 2009)

An analysis of Estonian administrative organisation demonstrates that considering the number of residents and the area of Estonia, there was a lot of municipalities compared to other Nordic countries. In Estonia, the average surface area of a municipality was 212.3 km^2, whereas it is 1,067.6 km^2 in Finland, and 1,512.3 km^2 in Sweden. The average number of residents in Estonian municipalities was 6,165.6, compared to Finland's 17,261.1, and Sweden's 33,577.8 residents (Eurostat, 2015; Eurostat, 2016). Most of local municipalities appeared to be too small to deliver everyone the services they are required to provide by law (European Commission, 2012).

In order to reduce the number of municipalities, the parliament of Estonia passed the Promotion of Local Government Merger Act in 2004, stipulating that the state encourages and supports the merger of municipalities at their own initiative in order to create municipalities with a larger territory and more inhabitants (The parliament of Estonia, 2004). Regardless of the state support, municipalities have not merged extensively. From 2004 to 2016, the number of municipalities decreased only from 241 to 213. In 2016 there was many municipalities (142) fewer than 3,000 inhabitants (Statistics Estonia, 2016). The dissent over the reduction of the number of public servants after the mergers, local communities' fears about marginalization, political and economic future have also contributed to the slow progress of mergers (Olle & Merusk, 2013).

Given that municipalities in Estonia were small and not interested in merging voluntarily, the government decided to enforce an administrative reform to create stronger (administratively more efficient) municipalities that would develop local life as a whole and ensure better accessible and higher quality public services for people. Having a bigger budget would make it possible to hire better qualified staff and public servants, improve the quality and regularity of public transport thanks to a larger territory being involved, contributes to the growth of municipal budgets, thus enabling to draw up and carry out larger projects (Ministry of Finance, 2016a). By the end of 2017, local municipalities in Estonia were either voluntarily and forcedly merged in to 79 municipalities (Ministry of Finance, 2016a).

In theory, one can claim that the merger of municipalities will lead to the anticipated benefits. Nevertheless, research has shown that this is not the case when it comes to forced mergers. Hanes & Wikström (2010) analysed whether voluntary mergers are more efficient compared to forced mergers, as well as the impacts mergers have on the local population and income growth in Sweden. The main finding was that municipalities formed on a voluntary basis had higher population growth, therefore the conclusion could be that local opinions are important to consider when forming a new municipal structure.

There are practically no scientific articles on the administrative technical efficiency of Estonian municipalities, however, the quality of life in Estonian counties has been studied using the DEA-PCA method (Põldaru & Roots, 2014). Reiljan et al. (2013) have studied the impact of merging municipalities and cities to their financial sustainability. Põldnurk (2015) has worked with municipal waste management optimisation in rural areas. The consultancy and training centre Geomedia has studied the capability of municipalities in 2016 (Noorkõiv & Ristmäe), and the Praxis Centre for Policy Studies has assessed the quality of public services (Uudelepp et al., 2009).

Since the efficiency of Estonian municipalities has not been assessed, there is a need to analyse and identify the factors that affect the efficiency of municipalities. On one hand, this is necessary for the better operation of inefficient municipalities in the future by learning from the municipalities with the best practice performances, and on the other hand, policy makers can acquire information that is important to help underdeveloped municipalities.

MATERIALS AND METHODS

Data Envelopment Analysis and fractional regression model

DEA method has many advantages to evaluate the efficiency, therefore it is widely used. There are a lot of different DEA models and model's developments (Cooper et al., 2007). The basic concept is the benchmarking study, where the units to be evaluated (decision making units - DMU) are evaluated against each other. The DEA model returns the efficiency scores (reported as the scalar ρ) for DMU's between in the interval 0 (worst result) to 1 (best result). The DMU is equal to 1 if and only if the DMU is on the efficient frontier without any slacks. The slacks represent input surplus or output scarcity of the DMU. Tone (2001) introduced a slacks-based measure of efficiency (SBM model) which deals with the input excesses and the output shortfalls, the model has some important properties: it is units-invariant and the measure is monotone decreasing in each input and output slack.

We will use the output-oriented approach, which allows assessing how much output could actually be produced with the available inputs, e.g. how many residents could be served using the incurred expenses in municipalities. We will deal with n DMUs ($j = 1,\dots,n$) each using m inputs ($i = 1,\dots\dots,m$) to produce s outputs ($r = 1,\dots,s$). The input and output vectors are $x_o \in R^m$ and $y_o \in R^s$, respectively. For each DMU the input and output matrices are denoted as $X = (x_1,\dots,x_n) \in R^{m\times n}$ and $Y = (y_1,\dots,y_n) \in R^{s\times n}$, respectively. The vector s^+ indicates output shortfall, and it is called slack.

The output-oriented SBM model (1) with the variable returns to scale is formulated as (Tone, 2001; Cooper et al., 2007):

$$\rho_o = \min_{\lambda,s^+} \frac{1}{1 + \frac{1}{s}\sum_{r=1}^{s} s_r^+/y_{ro}} \tag{1}$$

subject to

$x_o \geq X\lambda;\ y_o = Y\lambda - s^+;\ \lambda = 1;\quad s^+ \geq 0\ \frac{1}{s}\sum_{r=1}^{s} s_r^+ / y_{ro}$ is the mean expansion rate of outputs and λ is an intensity vector (Tone, 2001).

We use the fractional regression model (FRM) in the second-stage analysis as suggested by Papke & Wooldridge (1996), and Ramalho et al. (2010). The DEA estimates the technical efficiency scores are in the interval [0, 1]. The advantage of the FRM is that it allows accumulation of non-trivial probability mass at one end of the distribution, which is often the case in the DEA analyses. In addition, the FRM enables to analyse one- and two-part models, which is useful if the probability of observing a DEA score of unity is relatively large or if the sources of technical efficiency may differ from those of inefficiency (Ramalho & Ramalho, 2011).

In our analysis, the DEA score 1.000 was observed in 28% of cases. The first stage of the FRM uses a binary choice model, where the binary indicator has values 0 for inefficient and values one for efficient (TE score = 1.000) municipalities. The second stage of the model is the fractional section that is estimated using only the sub-sample of inefficient municipalities (TE score < 1.000).

Data

The inputs and outputs have differed considerably in previous DEA studies, which is fully justified. The selection of indicators for DEA analysis is crucial because selecting wrong indicators could lead to wrong results. Therefore, the indicators must characterize municipalities and their operation. The inputs must characterize the contribution that municipalities make to serve local residents, whereas the outputs must characterize the value created directly or indirectly by municipalities.

Several studies have used expenses as input – both the total expenditures (Loikkanen & Susiluoto, 2005; Afonso & Fernandes, 2008; Geys & Moesen, 2009) and expenses by offered services (Balaguer-Colla et al., 2007; Storto, 2016). Using expenses by offered services as inputs is common if the aim is to assess the efficiency of a specific offered service (healthcare, education, etc). In such cases, the chosen inputs could be for instance healthcare costs, education costs, environmental protection and communal service costs, public transport and road maintenance costs (Loikkanen & Susiluoto, 2005; Rogge & De Jaeger, 2012). Additonally, in DEA models have used the quantities of specific services: the number of teachers, children's day care centres, comprehensive schools, the length of roads, the number of parks and recreation areas, the amount of waste water, the number of households with central drinking water and sewage (Loikkanen & Susiluoto, 2005; Valeira et al., 2010; Rogge & De Jaeger, 2012).

Studies that focus on assessing the efficiency of a municipality as a whole often use the total cost as a input, and the number of residents and the surface of the municipality as outputs (Cruz & Marques, 2014; Storto, 2016). It is important to note that in this study, expenses made by the municipality are equalized with the amount of services. The outputs describe values indirectly created by the municipality. Four inputs and two outputs have been selected for DEA model (Table 1). Inputs include expenditures to significant public services per annum in euros: education costs (X1), environmental protection and housing and communal service costs (X2), social security costs (X3), leisure, culture and religious costs (X4). Output variables are: number of residents (Y1) and surface area of the municipality (Y2).

Table 1. Summary statistics of inputs and outputs in DEA and variables in FRM to evaluate Estonian rural municipalities

Variables	Name	Avg.	St. Dev.	Min	Max
Inputs in DEA					
X1 – Spending on education (€)	SPEDU	1,301,882	1,296,522	177,556	8,613,914
X2 – Spending on environmental protection (€)	SPENV	71,134	139,230	0,000	999,795
X3 – Spending on social care (€)	SPSC	234,803	246,249	19,551	2,359,321
X4 – Spending on culture, recreational activities and sport (€)	SPCAS	331,603	392,148	19,413	2,630,354
Outputs in DEA					
Y1 – Population (inhabitants) of municipality	POP	2,485	2,347	457	14,373
Y2 – Surface area of the municipality territory (km2)	AREA	232.1	133.5	12.0	871.3
Dependent variable in FRM					
Technical efficiency (score)	PTE	0.762	0.204	0.101	1.000
Independent variables in FRM					
Z1 – Population with higher education (%)	HEDU	0.2	0.0	0.1	0.3
Z2 – Roads (km)	ROAD	204.0	127.2	9.6	828.1
Z3 – Agricultural land (ha)	AGR	5,250	3,621	195	19,512
Z4 – Subsidies (% of total income)	SUB	0.4	0.1	0.1	0.7
Z5 – Distance from capital (km)	DCAP	154.0	70.4	0.0	290.9
Z6 – Quality of land (points)	QOL	41.0	5.3	29.0	53.0
Z7 – Elderly people (%)	ELD	21.0	4.2	9.5	32.1
Z8 – Wage (€)	WAGE	815.6	82.1	634.3	1,244

The technical efficiency score characterizing the efficiency of a municipality is the dependent variable in FRM, and the factors that potentially affect efficiency are independent variables (Z1–Z8). The FRM is used to assess the effect of exogenous variables on Estonian rural municipalities.

As there is not yet data available on the merged municipalities, the present analysis uses the statistical data from the period before the mergers in 2017. The dataset consists of municipalities' annual expenses and other relevant variables from 2013. All the information for the DEA and FRM comes from Statistics Estonia (2016), except for the indicator characterizing the quality of land, which is from the Estonian University of Life Sciences. To obtain outliers before the DEA analysis, we used the DEA super-efficiency model (Cooper et al., 2007) and expert opinions. 27 of the initial 197 rural municipalities have been excluded from the survey. Outliers were the municipalities with a very big or a very small population. Therefore, 170 municipalities are in the analysis.

Based on previous studies (Afonso & Fernandes, 2005; Bönish et al., 2011; Nakazawa, 2013; Doumpos & Cohen, 2014; Drew et al., 2015; Storto, 2016), we can claim that the following factors affect the efficiency of municipalities: the share of residents with higher education (HEDU), the length of roads (ROAD), the size of agricultural land (AGR), the share of subsidies in the municipal budget (SUB), distance from the capital (DCAP), the quality of land (QOL), the share of elderly residents (ELD), wage (WAGE). The effect of size of agricultural land on the efficiency is important because this study focuses on Estonian rural municipalities. In our analysis, the bigger size of agricultural land could refer to the municipality's location in the periphery and therefore it could affect the efficiency negatively. The distance from capital could affect the efficiency negatively. The share of subsidies are presumably bigger in inefficient municipalities. The length of roads describes the municipality on several ways, it refers to the size of municipality, higher costs for road maintenance and also better infrastructure.

RESULTS AND DISCUSSION

Results of DEA

The analysis consisted of 170 Estonian rural municipalities. According to DEA results the number of efficient municipalities is 48 (28%), their pure technical efficiency (PTE) is equal to 1,000. The average technical efficiency of municipalities is 0.762 points. In other words, their average efficiency is 76.2%, which means that municipalities could serve 23.8% more population and area using the same amount of expenses they have used for services. Municipalities with low efficiency (PTE lower than 0.600) are the most problematic, the number of such municipalities is 46 (27.1%), these municipalities should serve at the same level of inputs (expenses) 40% more inhabitants and area.

For a more detailed analysis, municipalities have been divided into five groups based on efficiency score: PTE = 1.000 (Group I); $0.803 \leq \text{PTE} < 1.000$ (Group II); $0.659 \leq \text{PTE} < 0.803$ (Group III); $0.553 \leq \text{PTE} < 0.659$ (Group IV); $\text{PTE} < 0.553$ (Group V). The difference between groups is statistically significant ($P < 0.05$).

Fig. 1 gives an overview of local rural municipalities ($n = 170$) based on efficiency scores (Group I being the most efficient). The figure highlights various efficient municipalities in North and Central Estonia, and inefficient ones in South Estonia. To generalize, it can be said that municipalities situated closer to the capital are relatively more efficient.

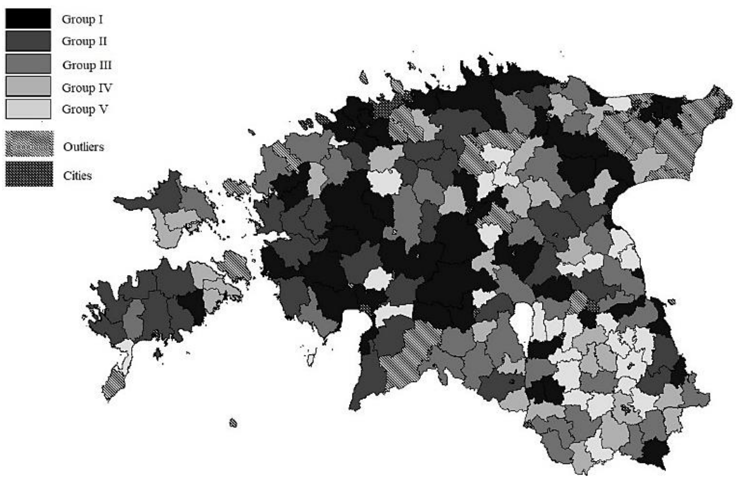

Figure 1. Classification of municipalities based on efficiency scores.

In order to analyse the efficiency of Estonian municipalities from different angles, municipalities have been divided into five groups based on the number of residents (P – population size). Each group contains 34 municipalities. The size groups are: P < 955 (Group 1); 955 ≤ P < 1,318 (Group 2); 1,318 ≤ P < 1,886 (Group 3); 1,886 ≤ P < 3,729 (Group 4); P ≥ 3,729 (Group 5).

Comparing the expenses per resident, it appears that as the number of residents in municipalities grows, the average costs per resident decrease (Table 2). In small municipalities (Groups 1 and 2), average costs per resident are € 1,195–1,219. In large municipalities, expenses per resident are considerably lower. In municipalities with the most residents (Group 5), the average costs per resident were € 1,052. Municipalities with more residents are relatively more efficient, on average their expenses are 14% lower. Efficient municipalities spend less per resident (on average € 1,088), and less efficient municipalities spend considerably more – € 1,121 (Group I compared to Group V). Larger municipalities are hence more efficient since they spend considerably less per resident than small municipalities. Doumpos & Cohen (2014) have reached the same conclusion that smaller municipalities tend to be more inefficient. It appears that expenses are significant factor shaping the efficiency of a municipality.

Table 2. Costs per resident (€) by municipality's size and efficiency

Population of local	Efficiency groups					
municipality	I	II	III	IV	V	Average
Group 1	1,166	1,207	1,301	1,193	1,526	1,219
Group 2	1,085	1,282	1,370	1,171	1,116	1,195
Group 3	0,940	1,020	1,109	1,207	1,083	1,070
Group 4	1,127	1,050	1,059	1,283	1,080	1,101
Group 5	1,078	1,090	0,991	0,979	1,024	1,052
Average	1,088	1,110	1,175	1,168	1,121	1,128

An analysis of the average income by size and efficiency groups shows that average income is 11.8% bigger in large municipalities (Group 5) than in small municipalities (Group 1) (Table 3). As efficiency decreases, so do salaries. Residents of efficient and large municipalities (Group 5, I) have the highest salaries. To keep the workforce, it is important to ensure a competitive salary.

Table 3. Average monthly salaries (€) of local residents by municipality's size and efficiency

Population of local	Efficiency groups					
municipality	I	II	III	IV	V	Average
Group 1	775	810	801	780	831	790
Group 2	748	885	792	832	779	796
Group 3	800	804	800	802	798	801
Group 4	827	803	780	813	821	808
Group 5	917	836	841	861	873	883
Average	834	819	799	813	803	816

The share of subsidies in efficient and less efficient municipalities varies from 37.0% to 43.2% on average (Table 4). In smaller municipalities (Group 1), subsidies make up a larger share, an average of 40.4%, whereas in larger municipalities (Group 5), subsidies constitute 34.7%. The share of subsidies is larger in less efficient municipalities. The weaker the municipality, the more state support the municipality must receive. Doumpos & Cohen (2014) reached a similar conclusion, pointing out that independence from state subsidies improves the efficiency of municipalities.

Table 4. The share of subsidies (%) by municipality's size and efficiency

Population of local municipality	Efficiency groups I	II	III	IV	V	Average
Group 1	42.6	34.0	42.1	40.0	47.9	40.4
Group 2	46.1	39.1	44.4	34.2	44.1	42.3
Group 3	29.9	36.0	41.0	41.4	46.1	39.0
Group 4	36.5	39.7	43.0	44.5	39.8	40.3
Group 5	33.6	36.7	37.4	33.3	35.2	34.7
Average	37.0	37.1	42.0	38.6	43.2	39.3

An analysis of the size and efficiency of municipalities shows that there are significant differences within the groups regarding the following indicators: total cost per resident, average income, and the share of subsidies out of total revenue. In larger municipalities, efficiency is higher mainly thanks to having lower costs per resident. Therefore, we can say that based on the analysis, the dependence of analysed indicators on the size of the municipality and efficiency score is in accordance with economic theory and practice.

Results of fractional regression analysis

The results of the fractional regression analysis are presented in Table 5. The efficiency scores of municipalities obtained in the first stage using the DEA analysis are the dependent variables in the FRM analysis, and 8 factors that may affect the efficiency of a municipal unit serve as independent variables. In the one-part model, 4 factors resulted statistically significant. The share of subsidies (SUB), the share of population with higher education (HEDU), and the share of elderly people (ELD) are the most significant one ($P < 0.05$). The size of agricultural land is also statistically significant ($P < 0.1$).

A positive regression coefficient shows that as the impact factor increases, so does the efficiency of the municipal unit, whereas a negative one denotes an unfavourable association. As the share of people with higher education (HEDU) increases, so does the efficiency of a municipality, which is in compliance with the practice and also demonstrating that more efficient municipalities attract more educated population. As far as the share of people with higher education affects municipalities efficiency positively, it should be kept in mind and bring up in the future. Hopefully, the opportunity to get free higher education will be the case in the future and helps to increase the efficiency at municipal level and also in the state level.

Increase in the number of the elderly people (ELD) has a positive effect on the efficiency of a municipality. Just like other parts of Europe, Estonia is also characterized by aging population. This leads to increased costs (Nakazawa, 2013). The increase of costs combined with the decrease of tax revenue per person should in theory result in the decrease of efficiency in municipalities. The latter should occur in the long run. According to FRM results however, the increase of the share of the elderly increases efficiency. Various leading municipal researchers have reached the same conclusion

(Bönish et al., 2011). We should bear in mind that this correlation exists in the short run, and other tendencies occur in the long run. If the share of elderly people increases the tax revenue will decrease and the amount of social services will increase. The authors of this study agree with Cruz and Marques (2014) that the share of the elderly people and the surface area of the municipality are indicators that the government must consider when distributing resources between municipal budgets, and that state investments must also be made in more sparsely populated areas in order to guarantee the sustainability of these areas.

A negative indicator of the share of subsidies (SUB) is in accordance with economic practices. Based on studies, we can claim that independence from state subsidies improves efficiency in some countries (Bönish et al., 2011; Doumpos & Cohen, 2014; Drew et al., 2015) and reduces it in others (Balaguer-Colla et al., 2007; Cruz & Marques, 2014). The impact of subsidies on efficiency thus primarily depends on the specifics and the policies of the assessed country. The example of Estonian rural municipalities allows us to argue that independence from subsidies increases efficiency.

Increase in the agricultural land (AGR) has a positive effect to the efficiency.

There are some differences in significant variables in the two-part FRM models compared to the one-part FRM model. In the first part of the two-part model, the factors affecting efficiency negatively are: distance from capital (DCAP), wage (WAGE). It means that peripheral municipalities with lower local income levels are less efficient. The share of people with higher education has a positive effect to the efficiency.

In the second part of the two-part model we consider only these municipalities with lower efficiency (PTE < 1). The results of the 2nd part of the two-part model reveal that it bears resemblance to the one-part model. The three exogenous factors that are significant in the one-part model are also significant in the two-part model (AGR, SUB, ELD). In the 2nd part of the model, the importance of the share of higherly educated people did not appear to have significant effect on efficiency, but quality of land appears to be significant factor. Increase in the quality of land (QOL) has a negative effect to the efficiency. The negative effect of quality of land on efficiency could be explained by the fact that municipalities with a better rating on the quality of land are rural municipalities in which the agriculture dominates local economy. Lack of economic diversification has contributed to higher loss of population in recent decades and thus those municipalities have less inhabitants, which is in significant and negative correlation with efficiency.

From DEA results revealed that municipalities with bigger population are more cost-efficient and it might refer to the positive effect of emergization. Policy makers hope that units with a larger surface area and a higher number of inhabitants will be more efficient, referring to the occurrence of the scale effect. The study by Slack and Bird (2013b) showed that scale effect does not occur when it comes to providing services, but it can occur when providing a physical infrastructure to a higher number of users. Nakazawa's (2013) study demonstrated that merging municipalities results in the increase of administrative costs, although one would assume that these decrease as a result of a merger through the reduction of administrative staff at municipalities. Drew et al. (2015) have noted that the number of inhabitants is a factor that does not increase the efficiency of municipalities.

Table 5. Results of cauchit fractional regression models

	One-part model					Two-part model									
						1st part					2nd part				
	Estimate	SE	t-value	P(> |t|)		Estimate	SE	t-value	P(> |t|)		Estimate	SE	t-value	P(> |t|)	
INTERCEPT	2.8846	3.3744	0.8550	0.3930		5.4426	5.4775	0.9940	0.3200		1.4168	2.0423	0.6940	0.4880	
HEDU	8.0947	3.9352	2.0570	0.0400	**	24.7238	8.7152	2.8370	0.0050	***	-2.8721	2.3188	-1.2390	0.2150	
ROAD	0.0008	0.0012	0.6820	0.4950		0.0002	0.0016	0.1030	0.9180		0.0006	0.0005	1.1050	0.2690	
AGR	0.0001	0.0000	1.8020	0.0710	*	0.0000	0.0001	0.3920	0.6950		0.0001	0.0000	4.0910	0.0000	***
SUB	-2.7662	1.3031	-2.1230	0.0340	**	-2.0432	2.8695	-0.7120	0.4760		-2.0668	0.8846	-2.3360	0.0190	**
DCAP	-0.0040	0.0025	-1.5620	0.1180		-0.0115	0.0047	-2.4140	0.0160	**	-0.0008	0.0014	-0.5740	0.5660	
QOL	-0.0437	0.0280	-1.5620	0.1180		-0.0455	0.0561	-0.8110	0.4180		-0.0445	0.0169	-2.6270	0.0090	***
ELD	0.0728	0.0337	2.1600	0.0310	**	0.0428	0.0618	0.6920	0.4890		0.0323	0.0175	1.8480	0.0650	*
WAGE	-0.0019	0.0025	-0.7890	0.4300		-0.0088	0.0048	-1.8180	0.0690	*	0.0012	0.0015	0.8040	0.4220	
	Number of obs. 170					Number of obs. 170					Number of obs. 122				
	R-squared: 0.159					R-squared: 0.149					R-squared: 0.295				

*$P < 0.1$; **$P < 0.05$; ***$P < 0.01$.

CONCLUSIONS

We used the two-stage analysis to evaluate the efficiency of Estonian rural municipalities. In the first stage, we used the DEA and in the second stage the FRM model. The DEA model was an output-oriented SBM with 4 inputs and 2 outputs. In FRM, we evaluated the effect of 8 exogenous variables on efficiency. The dataset consisted of 170 rural municipalities in 2013. According to the DEA model, 48 rural municipalities (28%) are efficient, the average efficiency of municipalities is 0.762, which means that on average 23.8% more outputs should municipalities provide with a given set of inputs.

The analyse showed that there are differences between the size and the efficiency of groups, but on average, smaller units are more likely to be inefficient. To get more information about the effect of exogenous factors on the efficiency of rural municipalities, we used the FRM model. It revealed that the share of subsidies (SUB) affects negatively efficiency, the share of population with higher education (HEDU) increases the efficiency, and also the share of elderly people (ELD) and the size of agricultural land (AGR).

Policy makers must acknowledge that the more elderly residents and the larger their share in the population, the more inputs are needed to offer different public services. In the meanwhile, they must not forget that population aging results in a decrease of tax revenue. Therefore, it is important to review the current arrangement of distributing revenues to municipal budgets. Policy makers must additionally take into consideration the fact that rural municipalities with greater surface areas need more inputs because they have relatively higher fixed costs for maintaining their infrastructure.

Taking the latter into consideration, the authors of this study consider it an important next step to analyse whether the merger of municipalities and the formation of larger units would result in increased efficiency that policy makers hope for and promised people. This is especially the case since the efficiency of rural municipalities has been assessed and the factors affecting their efficiency have been identified.

REFERENCES

Afonso, A. & Fernandes, S. 2005. Assessing and explaining the relative efficiency of local government: Evidence for Portuguese Municipalities. In: *ISEG Economics Working Paper*.

Afonso, A. & Fernandes, S. 2008. Assessing and explaining the relative efficiency of local government. *The Journal of Socio-Economics* **37**, 1946–1979.

Allers, M. & Geertsema, B. 2014. The effects of local government amalgamation on public spending and service levels: Evidence from 15 years of municipal boundary reform Groningen: University of Groningen. In: *SOM Research Reports 14019-EEF*

Alper, D., Sinuany-Stern, Z. & Shinar, D. 2015. Evaluating the efficiency of local municipalities in providing traffic safety using the Data Envelopment Analysis. *Accident Analysis & Prevention* **78**, 39–50.

Asatryan, Z. & De Witte, K. 2015. Direct democracy and local government efficiency. *European Journal of Political Economy* **39**, 58–66.

Balaguer-Colla, M.T., Priorb, D. & Tortosa-Ausina, E. 2007. On the determinants of local government performance: A two-stage nonparametric approach. *European Economic Review* **51**, 425–451.

Bönish, P., Haug, P., Illy, A. & Schreier, L. 2011. Municipality size and efficiency of local public services: Do size matter? In: *IWH Discussion Paper* **18**, 1–39.

Charles, V. & Zagarra, L. 2014. Measuring regional competitiveness through Data Envelopment Analysis: A Peruvian case. *Expert Systems with Applications* **41**, 5371–5381.

Cooper, W., Seiford, L. & Tone, K. 2007. *Data envelopment analysis: a comprehensive text with models, applications, references and DEA Solver Software*. Springer. New York.

Cruz, N. & Marques, R. 2014. Revisiting the determinants of local government performance. *Omega* **44**, 91–103.

Cuadrado-Ballesteros, G.S, Garcia-Sanchez, I.B. & Prado-Lorenzo, J.M. 2013. Effect of modes of public services delivery on the efficiency of local governments: A two-stage approach. *Utility Policy* **26**, 23–35.

De Witte, K. & Geys, B. 2011. Evaluating efficient public good provision: Theory and evidence from a generalized conditional efficiency model for public libraries. *Journal of Urban Economics* **69**, 319–327.

D'Inverno, G., Carosi, L. & Ravagli, L. 2018. Global public spending efficiency in Tuscan municipalities. *Socio-Economic Planning Sciences* **61**, 102–113.

Doumpos, M. & Cohen, S. 2014. Applying data envelopment analysis on accounting data to assess and optimize the efficiency of Greek local governments. *Omega* **46**, 74–85.

Drew, J., Kortt, M. & Dollery, B. 2015. What determines efficiency in local government? A DEA analysis of NSW local government. In: *Economic Papers*, pp. 243–256.

European Commission. 2012. Assessment of the 2012 national reform programme and stability programme for Estonia. In: *Commission staff working document.* Brussels. *http://ec.europa.eu/europe2020/pdf/nd/swd2012_estonia_en.pdf.* Accessed 26.03.16.

European Commission. 2013. Local government & administration in Estonia. *https://ec.europa.eu/europeaid/decentralisation-and-regional-local-government-administration-estonia_en.* Accessed 30.01.16.

Eurostat. 2015. LAU 2 – NUTS 2013, EU-28. *http://ec.europa.eu/eurostat/web/nuts/local-administrative-units*. Accessed 30.01.16.

Eurostat. 2016. Land cover overview. *http://ec.europa.eu/eurostat/web/lucas/data/database.* Accessed 30.01.16.

Friedrich, P., Reiljan, J. & Nam, C.W. 2010. The need of municipal fiscal equalization reform in Estonia. In: *Raudjärv M, Mäeltsemees S, Reiljan J. (Ed.). Eesti majanduspoliitilised väitlused* XVIII. Berlin - Tallinn: Berliner Wissenchafts-Verlag, Mattimar, pp. 52−73.

Geys, B. & Moesen, W. 2009. Measuring local government technical (in)efficiency: an application and comparison of FDH, DEA and econometric approaches. In: *Public Performance and Management Review* **32**, 489–504.

Hanes, N. & Wikström, M. 2010. Amalgamation impacts on local growth: Are voluntary municipal amalgamation more efficient? *Canadian Journal of Regional Science* **33**, 57–70.

Horta, I., Camanho, A. & Dias, T. 2016. Residential building resource consumption: A comparison of Portuguese municipalities' performance. *Cities* **50**, 54–61.

Iparraquirre, J.L. & Ma, R. 2015. Efficiency in the provision of social care for older people. A three-stage Data Envelopment Analysis using self-reported quality of life. *Socio-Economic Planning Science* **49**, 33–46.

Loikkanen, H.A. & Susiluoto, I. 2005. Cost Efficiency of Finnish Municipalities in Basic Service Provision 1994–2002. In: *Urban Public Economics Review* **4**, 39–63.

Ministry of Finance. 2016a. Administrative reform. *http://www.fin.ee/haldusreform.* Accessed 01.03.18.

Ministry of Finance. 2016b. Local Government Finances. *http://www.fin.ee/local-government-finances* Accessed 30.01.17.

Nakazawa, K. 2013. Cost Inefficiency of Municipalities after Amalgamation. *Procedia Economics and Finance* **5**, 581–588.

Noorkõiv, R. & Ristmäe, K. 2016. Kohaliku omavalitsuse üksuste võimekuse indeks. Tartu: Geomedia. *http://geomedia.ee/tehtud-tood/.* Accessed 30.01.16. (in Estonian)

Olle, V. & Merusk, K. 2013. Problems of Estonian Local Government in 2013 and Co-operation as an Instrument of Their Resolution. In: *Juridica International: Law Review of University of Tartu*, pp. 160−168.

Papke, L. & Wooldridge, J. 1996. Econometric methods for fractional response variables with an application to 401 (K) plan participation rates. *Journal of Applied Econometrics* **11**, 619–632.

Põldaru, R. & Roots, J. 2014. A PCA-DEA approach to measure the quality of life in Estonian counties. *Socio-Economic Planning Sciences* **48**, 65–73.

Põldnurk, J. 2015. Optimisation of the economic, environmental and administrative efficiency of the municipal waste management model in rural areas. *Resources, Conservation and Recycling* **97**, 55–65.

Ramalho, E., Ramalho, J. & Henriques, P. 2010. Fractional regression models for second stage DEA efficiency analyses. *Journal of Production Analysis* **34**, 239–255.

Ramalho, E. & Ramalho, J. 2011. Alternative estimating and testing empirical strategies for fractional regression models. *Journal of Economic Surveys* **25**, 19–68.

Reiljan, J., Andresson, K. & Ukrainski, K. 2004. The consequences of attempting to equalize the income of local governments in Estonia. In: *Eesti majanduspoliitilised perspektiivid Euroopa Liidus: XII teadus- ja koolituskonverentsi ettekanded-artiklid: Tartu - Värska, 1.-3. juuli 2004. Berlin, Tallinn: Berliner Wissenschafts-Verlag*, pp. 364−381.

Reiljan, J., Jaansoo, A. & Ülper, A. 2013. The Impact of Amalgamation on the Financial Sustainability of Municipalities in Estonia. *Public Finance and Management* **13**, 167–194.

Rogge, N. & De Jaeger, S. 2012. Evaluating the efficiency of municipalities in collecting and processing municipal solid waste: A shared input DEA-model. *Waste Management* **10**, 1968–1978.

Seroa da Motta, R. & Moreira, A. 2009. Political factors and the efficiency of municipal expenditure in Brazil. *Economia Aplicada* **13**, 353–371.

Slack, E. & Bird, R. 2013a. Does Municipal Amalgamation Strengthen the Financial Viability of Local Government? A Canadian Example. In: *International Centre for Public Policy Working Paper Series* **12**, 1–23.

Slack, E. & Bird, R. 2013b. Merging Municipalities: Is Bigger Better? University of Toronto Institute on Municipal Finance and Governance. In: *IMFG Papers* **14**.

Statistics Estonia. 2015. Minifacts about Estonia. *http://www.stat.ee/90745*. Accessed 30.01.16.

Statistics Estonia. Tallinn. *http://www.stat.ee* Accessed 30.01.16.

Storto, C. 2016. The trade-off between cost efficiency and public service quality: A non-parametric frontier analysis of Italian major municipalities. *Cities* **51**, 52–63.

The parliament of Estonia. 1993. Local Government Organisation Act. Riigi Teataja. *https://www.riigiteataja.ee/en/eli/509012014003/consolide.* Accessed 30.01.16.

The parliament of Estonia. 2004. Promotion of Local Government Merger Act. Riigi Teataja *https://www.riigiteataja.ee/en/eli/513112013014/consolide.* Accessed 30.01.16.

Tone, K. 2001. A slacks-based measure of efficiency in data envelopment analysis. *European Journal of Operational Research* **130**, 498–509.

Uudelepp, A., Uus, M. & Ender, J. 2009. Kuidas arendada kohalikke avalikke teenuseid omavalitsuste ja kodanikeühenduste koostöös? Praxis. *http://www.praxis.ee.* Accessed 30.03.16. (in Estonian)

Valeira, P., Martins, G.A. & Fávero, L.P. 2010. Production efficiency and financing of public health: an analysis of small municipalities in the state of São Paulo – Brazil. *Health Care Management Science* **13**, 112–23.

Agronomy Research **16**(3), 821–837, 2018
https://doi.org/10.15159/AR.18.092

Optimizing the sample size to estimate growth in I-214 poplar plantations at definitive tree density for bioenergetic production

P.A. Marziliano*, D. Russo, V. Altieri, G. Macrì and F. Lombardi

Mediterranean University of Reggio Calabria, Department of AGRARIA, Loc. Feo di Vito, IT89165 Reggio Calabria, Italy
*Correspondence: pasquale.marziliano@unirc.it

Abstract. In Europe, over the last decades, the arboriculture for woody biomass production has significantly expanded, often using poplar plantations. In order to maximize production, the flexibility of the cultivation algorithms becomes necessary. For this reason, it is necessary to apply monitoring tools for the evaluation and estimate of the wood productions, without significantly affect the production costs. In particular, for the estimate of the productions, the choice of the sample size is of particular importance. The aim of this study was to verify a simplified sampling approaches in poplar plantations characterized by constant tree density. The research was conducted in a poplar plantation on the Tuscan hills (Italy). The surveys were carried out each year for 13 years, from 4 to 16 years old. Through different statistical techniques, the change in the social position of each tree over time was evaluated. The results showed that the social position of each tree has been characterized by the first years after the plantation. Consequently, the estimate of the productions can be carried out by analysing the diameter increment of 10% of the trees, included in the diameter classes around the medium-sized tree at the time of the survey. This study provided a valid method for forest managers characterized by a simplified approach useful to estimate the growth and yield of hybrid poplars. This method will permit reliable biomass estimates, but also a reduction of the costs in the sampling activities in the field.

Key words: poplar, woody biomass, basal area, medium rotation forestry, cluster analysis.

INTRODUCTION

In the last decades, forestry activities are supported by structural funds of EU, in order to enhance the afforestation of abandoned agriculture land (Coletta et al., 2016).

Moreover, over the last few years, in Europe the arboriculture for wood production has significantly expanded. The main objectives of these cultivations are linked to the production of woody assortments for the industry, but also for the biomass collection for energetic purposes (Marziliano et al., 2017). Furthermore, the increasing use of renewable energies is a key EU strategy for reducing the greenhouse gases (GHG) emissions, contributing then to strategic policy objectives. The supply of sustainable energy is one of the main challenges that we will face over the coming decades, particularly because of the need to fight the climate change.

Biomass from wood productions can make a substantial contribution to supplying future energy demand in a sustainable way. They have a significant potential to expand in the production of heat and electricity, and could provide significant environmental benefits, by substituting imported fossil fuels with domestic biomass, giving also opportunities for the economic and social development in rural communities (AA.VV., 2001; Grogan & Matthews, 2002; Bergante & Facciotto, 2006; Facciotto et al., 2008; Marziliano et al., 2015).

Tree plantation for energetic production purposes, especially the thermal ones, developed firstly in northern Europe in the ’90, particularly in Sweden (Perttu, 1998). These plantations are characterized by medium-rotation times (typically 10–12 years) and by cultivation algorithms characteristic of the intensive agriculture. In Europe, the most promising tree species usually planted are *Populus* spp. and *Salix* spp. (Armstrong et al., 1999), strongly considered as an optimal source of bio-energy (Hinchee et al., 2009, Fischer et al., 2011). Clones of poplars are characterized by fast growing rates, which are partly induced by a set of physiological intrinsic characteristics (e.g. Ceulemans et al., 1990; Casella & Ceulemans, 2002; Dillen et al., 2010). Considering their fast growth and high yield, poplars are then the most widely used tree species in medium rotation forestry (MRF) and short rotation forestry (SRF). Additionally, intensive breeding programs have selected a wide range of clones with optimal production rates for a wide range of climates. When compared to other tree species, poplars have many characteristics that make them suitable for plantation cultures which enable the production of large quantities of wood in short periods of time. In general, abandoned rural land and marginal and degraded areas are used for plantations, where the rotation turn over ranges from 10 to 20 years, in relation to different management patterns, but also depending to the tree density and the species used. Moreover, the different cultivation systems nowadays available give different opportunities for the use of the biomass produced: from the cellulose for paper industries to the wood burned for energetic purposes (Rosenqvist et al., 2000; Scholz & Ellerbrock, 2002).

In order to maximize the productivity in tree plantations, a flexible approach in the use of the cultivation algorithms is necessary (Macaya-Sanz et al., 2017); they should be modified at any time, also in relation to the geographical and climatic conditions. However, for this purpose, it is necessary to apply appropriate management tools useful to evaluate and estimate the woody productions, without significantly affect the economic costs.

On the other hand, the availability of simplified technical tools for the evaluation and estimation of tree growth and yield is particularly important when the total economic value of a given plantation should be assessed (Pérez-Cruzado et al., 2014). Moreover, at European level, there is a clear demand to find methods useful to optimize the estimates for the plantation productivity, in particular regarding the short-rotation forestry (Arevalo et al., 2007). Moreover, reliable estimates of growth and yield are usually a prerequisite for the establishment of a woody biomass-based industry (Stampfl et al., 2007).

Therefore, these management tools can encourage the cultivation of fast-growing woody tree species within short-rotation forestry. These plantations can provide a significant source of alternative and renewable energy (Isebrands & Karnosky 2001; Hill et al., 2006). Moreover, renewable energy sources play a key role in meeting the CO_2 emission reduction objectives, since they are characterized by a lower net CO_2 emissions when substituted for fossil fuels (Kheshgi et al., 2000). The replacement of fossil fuel with biomass in the generation of energy and heat has recently been an important strategy promoted by the European Union (EU) to mitigate the effects of climate change and to enhance the security of the supply and the diversification of energy sources (IEA, 2003).

In the context of the woody biomass production, the basal area and volume of the plantations (past, present and future) are the most important parameters to be considered and carefully evaluated within a production process (Wang et al., 2013; Perez-Cruzado et al., 2014; Niemczyk et al., 2016).

In order to assess these parameters, various sampling approaches can be suitably exploited. When designing monitoring schemes, scientists should consider their specific objectives in order to define the degree of precision and accuracy required (Lombardi et al., 2015), also through a cost-benefit analysis.

More in detail, for the estimate of the productions (in terms of basal area or volume), the choice of the sample extent is of particular importance: it is essential to reduce as much as possible the sample size, however maintaining the need for statistically reliable estimates.

Starting from these assumptions, the aim of this study was to verify simplified sampling approaches in poplar plantations characterized by constant tree density, in order to optimize the field work in estimating the basal area development. Even if this study refers to a specific context, from a methodological approach, it can however provides a useful contribution to the knowledges on this topic.

In particular, the study assessed the relationships between the number of trees sampled and the accuracy in the estimate of the basal area (BA). The basal area, rather than the volume, was selected as studied parameter since it is directly correlated to the stand volume (Eastuagh, 2014), but also not interested by estimation errors (Hellrigl, 1970).

The questions we tried to answer were the followings: (1) in order to estimate the basal area development of a plantation, what is the minimum size of a reliable sample, in terms of the trees number? (2) Which characteristics should have the trees sampled? (3) Is it possible to sample just one tree, e.g. the average-size tree, then extending the estimate to the whole stand?

However, in order to obtain reliable results, two conditions are necessary: (i) the density of the plantation should be constant; (ii) the trees must always maintain the same social position during the whole plantation cycle. In this paper, the first condition is ensured by the cultivation algorithm adopted, while we tried to verify the second condition as a secondary objective of the current study.

MATERIALS AND METHODS

Study area

The study was carried out on four permanent experimental plots set up within hybrid poplar (*Populus x euroamericana*) plantation located in central Italy, south-west of Greve village in Chianti (Tuscany Region) (43° 34’ N, 11° 22’ E). The plantation was constituted by the I-214 clone, the most widespread in Italy and considered typical and representative of the Italian poplar cultivations (Bergante et al., 2015; Coaloa et al., 2016). The investigated plantation is located on a plateu, at an altitude of about 560 m a.s.l., characterized by fertile loamy soils.

The climate is typically Mediterranean. The annual rainfall is 1,200 mm, with minimum precipitation in summer and a maximum in winter. The average annual temperature is 12.5 °C, the average temperature of the coldest month is 4.2 °C, while the warmest has an average temperature of 21.6 °C. According to the Pavari's phytoclimatic classification (Pavari, 1959), the plantation is located in the warm sub-zones of Castanetum. Geologically, the site is characterized by green and purple Paleozoic schist. According to the FAO soils classification (FAO, 1998), soils are Cambisols. Conventional site preparation was carried out and the planting density was 400 trees per hectar, spaced on a 5 x 5 m grid. No thinning operation was realized, while all the trees were moderately pruned twice, according to conventional schedule (Nervo et al., 2011).

Survey and data analysis

The four experimental plots extend each on 0.18 ha, representing different site-index conditions (Corona et al., 2002). An abundant shrubs layer occurs in two plots (slightly sloping) (*Rubus* spp. and *Dactylis glomerata*), while it is almost absent in the other two plots (flat). Measurements started when the plantation was 4 years old and were repeated every year until the plantation reached 16 years old. Statistics of the main dendrometric variables recorded in each plot are reported in Table 1.

Table 1. Statistics of the main dendrometric variables recorded in the experimental plots. Values refer to the last sampling year (age 16 year old)

Variable	Mean	Minimum	Maximum	S.D.
Stand basal area (m^2 ha^{-1})	22.12	17.31	28.22	4.54
Stand basal area increment (m^2 ha^{-1} $year^{-1}$)	1.04	0.80	1.32	0.21
Average tree basal area (m^2)	0.0572	0.0453	0.0733	0.0118
Average tree basal area increment (cm^2 $year^{-1}$)	0.0030	0.0007	0.0070	0.0001

The diameter at breast height (*DBH*) was measured on each tree. In the first survey, the measured trees were marked with indelible paint, so that the trees were measured at the same height in the overall study period. Moreover, in the first survey, the position of each tree occurring in the surveyed plots was also recorded, identifying each tree with an ID code (i.e. A01, A02… I07, I08).

The following methodological approach was used:

1. Attribution of a social position index to each tree;
2. Evaluation of the variation in the social position index over the years;
3. Splitting of trees into homogeneous groups with respect to their social position index;
4. Test of different sampling methods for the estimation of the basal area, characterized by different number of trees;
5. Statistical comparison between the basal area values obtained through the different sampling methods applied;
6. Statistical comparison between the real basal area per hectare obtained from the surveys carried out annually and the estimated basal area with the chosen sampling extraction method.

In order to assign a social position index to each tree, the diameters measured in the last year of observation (age: 16 years) were ordered according to a decreasing serialization. Consequently, each tree has been assigned to a rank number, according to its position in the rank scale. In detail, the rank number 1 was assigned to the tree with the largest diameter, while the higher rank number referred to the tree with the smaller diameter. This procedure was repeated for all the surveys realized across the years (from the age of 4 to the age of 16 years). Consequently, we obtained for each year a matrix referring to the rank value assigned. Moreover, since the same tree can have a different rank number over the years, also the confidence interval (C.I.) of the rank number was calculated.

Furthermore, the social position of each tree over the years has been evaluated through the variation of the rank number attributed to each tree. We firstly evaluated the correlation between the rank number attributed to each tree at the last survey (age: 16 years) and the number of rank of the previous years. For this purpose, the Spearman's rank correlation coefficient was used. Subsequently, for each tree, we evaluated the size of the confidence interval (C.I.) of the rank numbers. This analysis was carried out (1) evaluating the confidence interval of the rank numbers compared to the rank number assigned in the last survey; (2) through an interval plot showing, for each tree, the lower and upper limits of the interval of confidence of the rank numbers.

In order to identify homogeneous groups of trees with respect to their social position index, a multivariate Cluster Analysis was applied. This analysis allows to identify, starting from each single tree, homogeneous groups of trees characterized by a specific rank number, in each year. As already applied in the clustering methods, we used the average linkage useful to calculate the distance between two sub-groups, considering the mean (Euclidean) distance between any two members referring to opposite groups. When compared to other clustering methods, such as the 'single clustering', the average linkage emphasizes the similarity inside groups rather than the differences among groups (Rand, 1971; Oshumi, 1980; Gordon, 1999). In order to identify the number of clusters, the dendrogram was cut at the step preceding the step determined by the rapid increment in the dispersion within-groups (Fowler & Cohen, 1995). This procedure allows to evaluate the validity of the clusters identified; it is an effective tool for choosing the level of distance at which the dendrogram could be cut (Fowler & Cohen, 1995).

Moreover, in order to quantify the minimum number of trees necessary for a reliable estimate of the basal area, the starting tree used to design the sampling extraction methods was the sample characterized by the average size tree. This choice was made for the following reasons: (i) the average diameter of the mean basal area is easily determinable and commonly adopted in dendrometry; (ii) the basal area estimate per hectare is obtained multiplying the average basal area with the number of trees per hectare. Therefore, starting from the average size tree, we tested five methods for estimating the growth of the woody production in terms of basal area, considering the basal area range as criterion for applying the five different methods, through the selection of the trees with basal area (g), as follow:

Method 1, tree with basal area equal to $\bar{g}$ (average basal area);

Method 2, trees with basal area included in the interval $\bar{g} \pm 0.10 * $ Standard Deviation;

Method 3, trees with basal area included in the interval $\bar{g} \pm 0.15 * $ Standard Deviation;

Method 4, trees with basal area included in the interval $\bar{g} \pm 0.20 * $ Standard Deviation;

Method 5, trees with basal area included in the interval $\bar{g} \pm 0.30 * $ Standard Deviation.

For each plot, Table 2 reports the average basal area values, the standard deviation, and also the minimum and maximum basal area values for each estimation method, regarding the year of the last survey.

Table 2. Average basal area values, standard deviation (SD) and minimum and maximum values for each method of estimate applied

Plot	$\bar{g}$ [cm²]	SD [cm²]	$\bar{g} \pm 0.1$ SD [cm²]	[cm²]	$\bar{g} \pm 0.15$ SD [cm²]	[cm²]	$\bar{g} \pm 0.2$ SD [cm²]	[cm²]	$\bar{g} \pm 0.3$ SD [cm²]	[cm²]
1	569	173	552	586	543	595	534	603	517	621
2	453	70	446	460	443	464	439	467	432	474
3	733	130	720	746	713	752	707	759	694	772
4	533	133	520	546	513	353	506	560	493	573

For each plot, the basal area estimated with the 5 methods was compared with the measured basal area by developing the percentage error (E%):

$$E\% = \frac{BA_{est_i} - BA_{obs_i}}{BA_{est_i}} \cdot 100 \qquad (1)$$

where BA_{est_i} is the basal area estimated with the 5 methods; BA_{obs_i} is the measured basal area in each plot.

The analysis of the variance (ANOVA) was carried out to test the differences in percentage error (*E%*) between the different methods of estimate developed. The significance of the differences was tested with the support of the Tukey’s method.

Finally, both the independent-sample T test and the indipendent-sample Z-Test (Mann-Whitney test) were used to compare the real basal area with the sampling extraction method resulted more efficient. The *T test* is a parametric test known to be more statistically powerful; on the other hand, the *Z-Test* is a non-parametric test and requires no assumptions (Zar, 1996; Montgomery, 2001; Soliani 2008).

RESULTS AND DISCUSSION

Fig. 1 shows the trend of the Spearman's rank correlation coefficient between the rank number attributed to each tree at the last survey (age: 16 years) and the rank number of the previous years (age from 4 to 16). The correlation coefficient tends to decrease when trees are younger, mostly in plots 1, 2 and 4. However, for all the years studied, the correlation is always very strong and significant, ranging from 0.945 to 0.996. These results indicate how the rank number of each tree observed in previous years does not change significantly when compared to the rank number assigned in the last survey.

Fig. 2 reports the interval of confidence in the rank number for each tree. Dots represent the single trees, while the values refer to the interval of confidence. In all the experimental plots, and for each tree, the size of the interval of confidence referring to the rank number is never high. In detail, the plot 3 shows the lowest values (from 0.10 to 2.21), even if also in the other plots it is rather low (from 0.14 to 3.11).

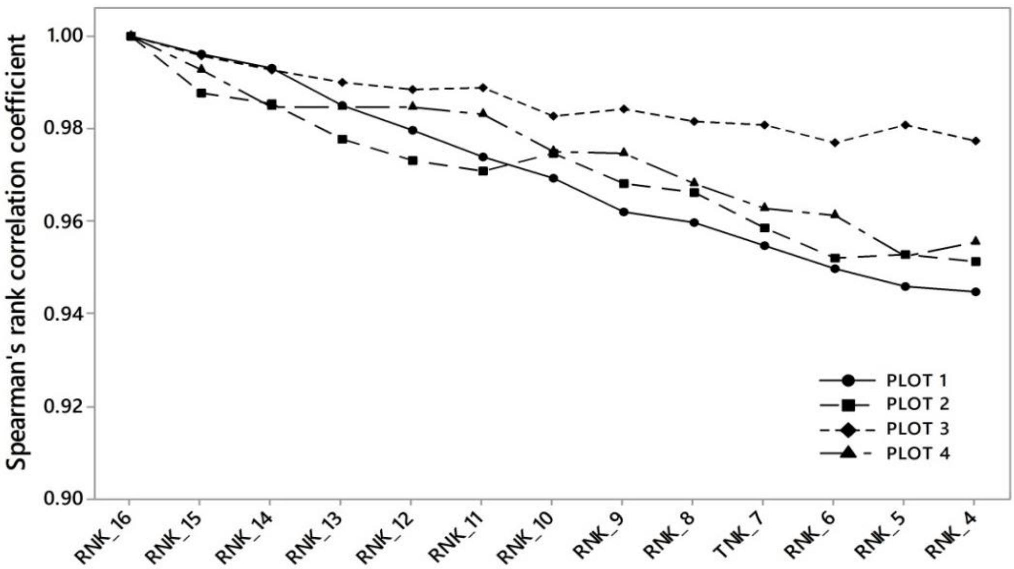

Figure 1. Trend of Spearman's rank correlation coefficient between the rank number attributed to each tree at the last survey and the number of rank of previous years.

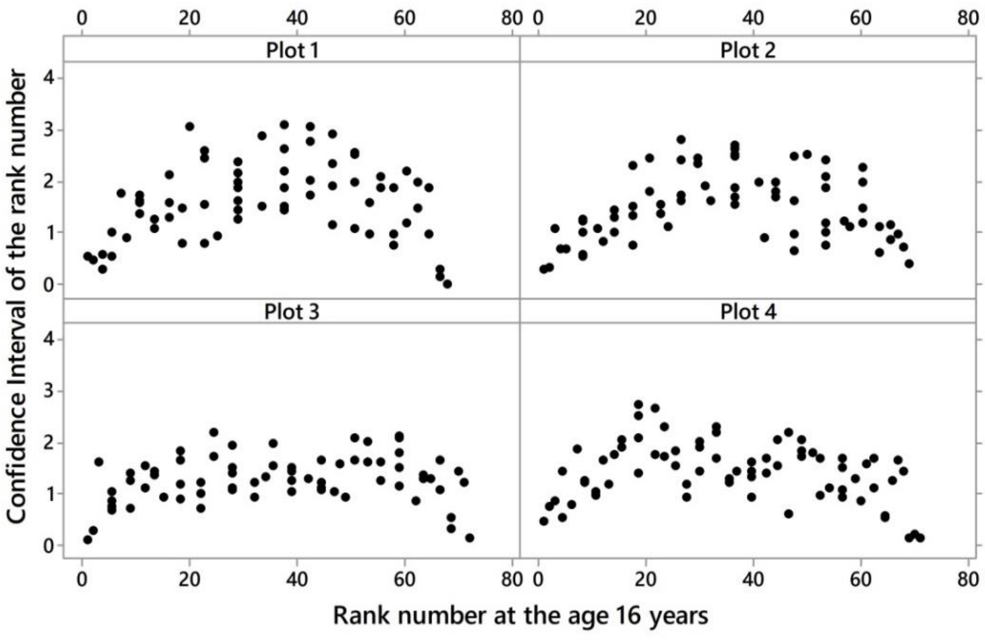

Figure 2. Variation of the rank number across the years, for all the experimental plots. For each tree and in all the experimental plots, the x-axis indicates the rank number of trees at the last survey (age: 16 years), while the y-axis shows the confidence interval (CI) of the rank number in each year of survey (age from 4 to 16 years) for all the sampled trees.

The results obtained confirm what the Spearman's correlation coefficients already showed: even if a small variation in the social position (rank number) for each tree occurred over the years, this variation is not significant.

For each plot, Fig. 3 shows the lower and upper limits of the interval of confidence for each tree. Trees with low rank numbers (larger trees) and those with high rank numbers (smaller trees) are characterized by small and very small confidence intervals. On the contrary, trees referring to intermediate rank numbers, are characterized by slightly larger interval of confidence, especially in plots 1 and 2.

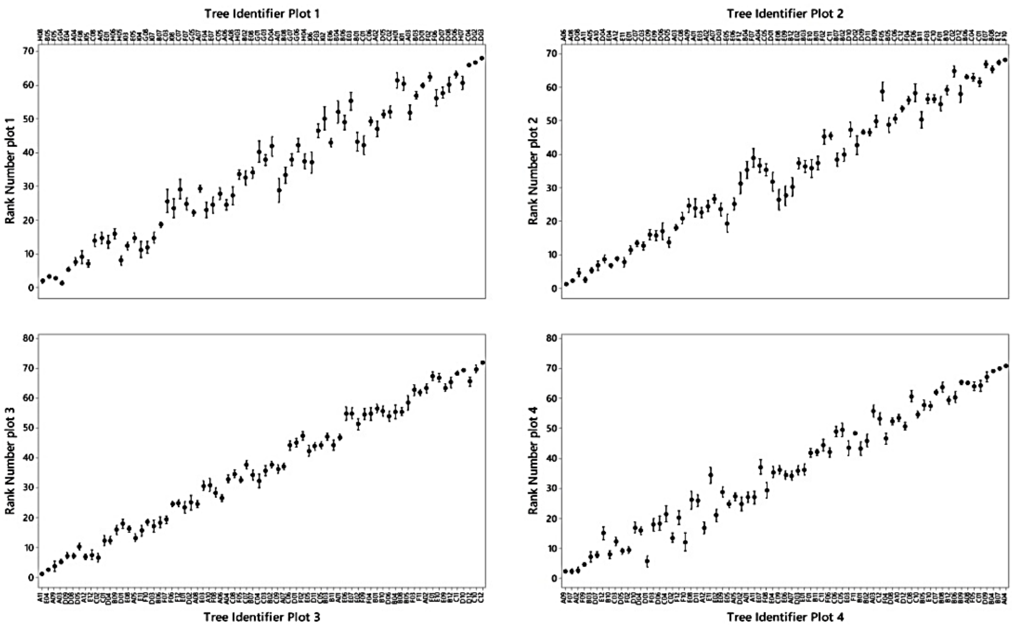

Figure 3. Interval-plot of the rank number over the years in each experimental plot.

The observed low interval of confidence can suggest how, over the years, the individual trees don't significantly modify their social position, maintaining almost the same social position during the whole production cycle. This result implies that if a tree is already characterized by a small (but also medium or large) diameter in the first years after the planting, then it will continue for the whole production cycle to maintain the same social position.

Fig. 4 shows the dendrograms obtained through the cluster analysis. Following the procedure described by Fowler & Cohen (1995) to identify the number of clusters, we observed how the dispersion remains low up to about the 50th step of the agglomeration algorithm, for all the studied plots; after, it rapidly increases. At a distance of 51.01 (Plot 1), 50.58 (Plot 2), 53.88 (Plot 3) and 54.01 (Plot 4), the dendrograms indicate the formation of three well-defined clusters. For each plot, the first group is characterized by trees with large diameters, with a number of trees ranging from 19 to 23. Immediately after, the second group is characterized by trees with small diameters, with a number ranging from 21 to 22 trees. Finally, the third group is characterized by trees with intermediate diameters (27–28 trees). These trees thus identified, are always the same during the entire production cycle.

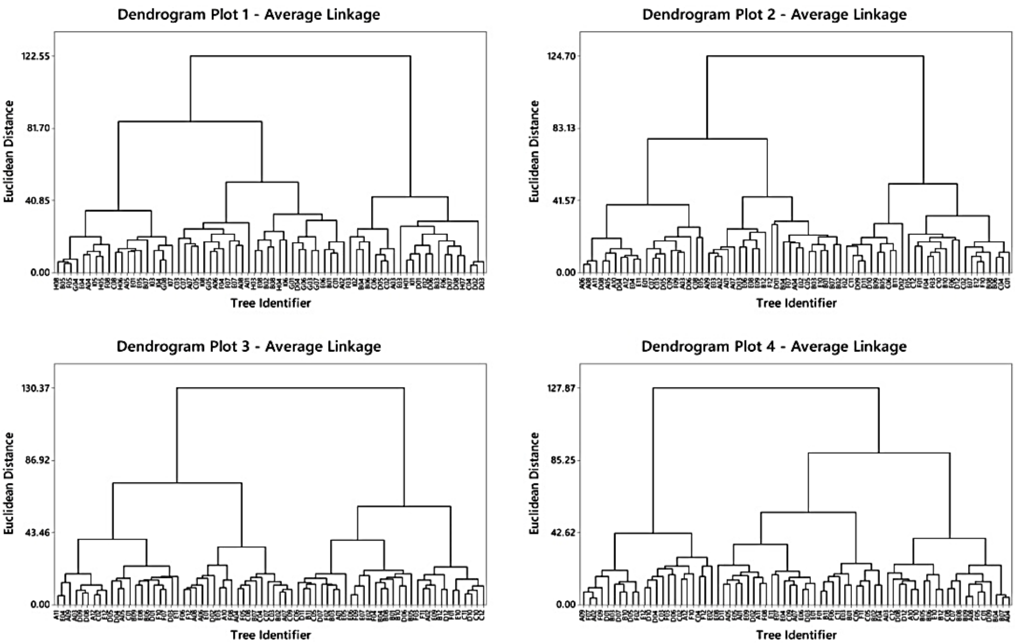

Figure 4. Cluster analysis. For each experimental plot, the x-axis indicates the single sampled trees, while the y-axis refers to the Euclidian distance. Considering the rank number for each plot, at the Euclidian distance of about 50, homogeneous groups of trees are aggregated.

Fig. 5 shows the diameter development observed in Plot 1. For each year, the three groups of trees are always well defined and never intersect each other. The trees, already reported in Fig. 4 (Plot 1), referring to the range H08 – I07 (22 trees) form the larger (diametric) group of trees; those occurring between C03 and A02 (27 trees) refer to a medium-sized group; finally, trees occurring between F03 and D03 (19 trees) form the smaller group of trees. It is interesting to observe that, in each group, trees are always the same: during the whole production cycle, no transition from a group to another are observable. Moreover, when a tree changes its social position, it always happens within the same group. Fig. 5 also reveals, for the groups I and III, that tree diameter increases when the age rises; on the contrary, trees characterized by an average size maintain approximately the same diameter across the years.

The obtained results suggest that, in a plantation with a definitive tree density, the social position of each tree is already defined in the first years of tree growth and did not change in the following years. Therefore, in the first years after the planting, a dimensional hierarchy is established and it is preserved during the following stand growth.

Furthermore, we can underline that the necessary condition to define the sample size useful for the basal area estimate is satisfied: trees always maintain the same social position during the whole plantation cycle.

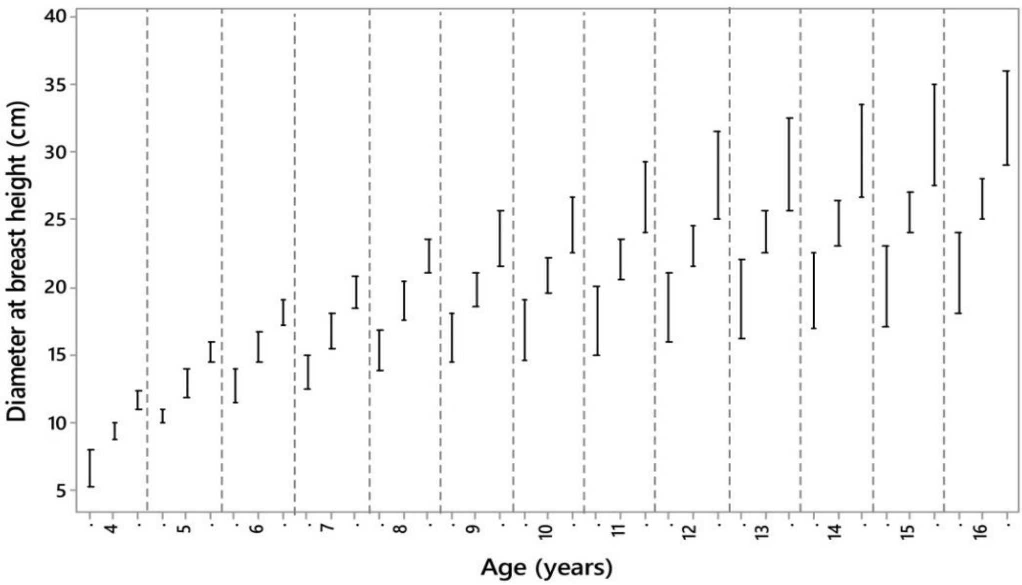

Figure 5. Diameter development observed un experimental plot 1, for each groups of trees.

In Table 3 are reported the values of the annual basal area estimated with the 5 estimation methods tested (for semplication, the values are shown every two years). Table 4 shows the ANOVA results.

They allow to reject the null hypothesis at a level of statistical significance of 95%. The different methods of estimate revealed significant differences in the percentage errors (see Eq. 1), when compared to the real basal area (measured basal area). For each method of estimate applied, Fig. 6 shows the average of the percentage errors and the interval corresponding to the minimum significant difference, according to the Tukey method. The average percentage errors ranges from 2.31% for method 1 (tree with $g = \bar{g}$) to 1.04% for method 5 (trees with $g = \bar{g} \pm 0.3 * SD$). Certainly, the errors observed are higher for the methods of estimate applied on a low number of sample trees. As showed in Fig. 6, two groups of methods can be identified. The first group is characterized by the methods 1 and 2 (respectively tree with $g = \bar{g}$ and trees with $g = \bar{g} \pm 0.1 * SD$), while the second group refers to the methods 3-4-5. Within each group, the methods revealed no significant differences; on the contrary, the differences are significant when comparing the two groups of methods. The methods 1 and 2 (group 1) showed significantly higher percentage errors if compared to the methods of the second group (method 3-4-5).

The results obtained revealed that Method 3 should be the best estimate method, i.e. the method characterized by a number of trees with a basal area (g) = $\overline{g} \pm 0.15 * SD$. This simplified method allows to obtain, measuring a low number of trees, a statistically reliable estimate of the stand growth and productivity. Then, applying this estimate procedure, emerges the advantage to reduce the sampling costs, without affecting the reliability of the estimate. In fact, no statistically significant errors were observed when comparing method 3 with methods in which a higher number of trees should be sampled. More in detail, the number of statistical units of the identified method of estimate varied from a minimum of 7 trees to a maximum of 9 trees, depending on the number of the experimental plots sampled.

Table 3. Estimates of the basal area obtained through the application of the 5 methods of sampling extraction

Plot	Age	Method 1 G m^2 ha^{-1}	Method 2 G m^2 ha^{-1}	Method 3 G m^2 ha^{-1}	Method 4 G m^2 ha^{-1}	Method 5 G m^2 ha^{-1}
1	4	4.49	4.49	4.38	4.37	4.13
1	6	9.36	9.36	9.02	9.05	8.99
1	8	13.32	13.32	12.91	12.92	12.78
1	10	15.55	15.55	15.19	15.18	15.09
1	12	17.51	17.51	17.24	17.21	17.21
1	14	20.37	20.37	20.13	20.14	19.96
1	16	22.15	22.15	21.97	22.09	21.97
2	4	3.18	3.16	3.15	3.15	3.17
2	6	6.64	6.57	6.54	6.53	6.55
2	8	9.67	9.63	9.60	9.58	9.66
2	10	11.37	11.33	11.30	11.28	11.36
2	12	13.28	13.19	13.12	13.11	13.18
2	14	15.53	15.48	15.44	15.45	15.56
2	16	17.28	17.28	17.26	17.30	17.39
3	4	4.92	4.86	4.87	4.93	4.88
3	6	11.27	11.04	11.07	11.12	11.06
3	8	15.87	15.58	15.64	15.79	15.59
3	10	18.76	18.30	18.36	18.59	18.39
3	12	21.33	21.02	21.18	21.56	21.33
3	14	25.36	25.00	25.27	25.79	25.45
3	16	28.14	28.06	28.27	28.51	28.21
4	4	4.05	4.05	4.05	4.06	4.01
4	6	8.44	8.44	8.33	8.38	8.35
4	8	12.14	12.14	11.89	11.90	11.86
4	10	13.98	13.98	13.80	13.92	13.86
4	12	16.23	16.23	15.85	16.02	15.99
4	14	19.30	19.30	18.75	18.94	18.99
4	16	20.87	20.87	20.61	20.81	21.22

Table 4. Values deriving from the ANOVA procedure. The error (%) of each estimate method is compared to the observed values in relation to the 'Methods of estimate' and the 'Age'

Source	Sum of Squares	Df	Mean Square	F	Sig.
Model	770.534	17	45.326	15.619	< 0.0001
AGE	357.359	12	29.780	10.262	< 0.0001
METHODS	70.771	4	17.693	6.097	< 0.0001
Error	705.168	243	2.902		
Total	1475.702	260			

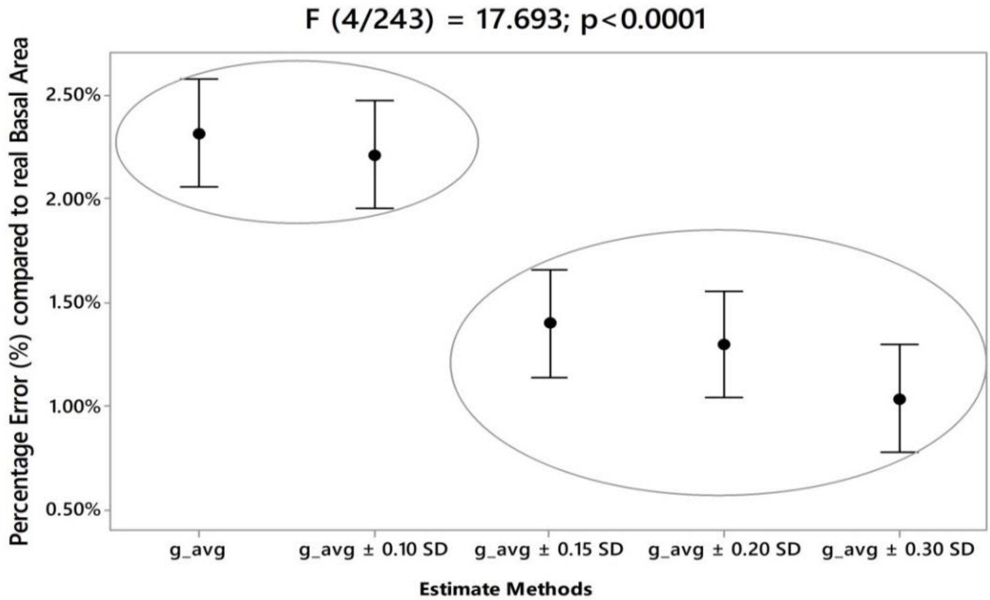

Figure 6. Percentage error (%) (average and interval of confidence) corresponding to the minimum significant difference for each method of estimate compared to the obtained values.

Fig. 7 shows the trends obtained for the real basal area and for the estimated basal area within the proposed methodology. The two lines are almost perfectly overlapped although, for a few years, a very slight underestimation or overestimation was observed; however, these errors can be considered not significant. The differences between the real basal area and basal area estimated with the simplified method and related statistical significance is reported in Table 5. The differences in basal area estimates using the indipendent-sample t test (*T-test*) and the Mann Withney test (*Z-test*) were not significant for all the plots.

We believe that the method applied could be also adopted in other geographical contexts, even if the sample size can be

Table 5. Statistical significance between the real basal area and basal area estimated with the simplified method, assessed by the t test (T) and the Mann-Whitney test (Z)

Plot	T	Prob	Z	Prob.
Plot 1	0.127	0.979	-0.333	0.739
Plot 2	0.053	0.982	-0.333	0.739
Plot 3	0.067	0.992	-0.282	0.778
Plot 4	0.112	0.932	-0.333	0.739

different. Once the sample has been identified, it is sufficient, on these trees, to reconstruct the diameters at breast height of the previous years (for example by taking from each sampled tree a core using the Pressler borer) and thus obtain the planting increment by multiplying the increments of the sampled trees at different ages for the number of trees to which the trees refer.

There are a variety of methods that can help assess a woodland (Dickmann, 2006; Aylott et al., 2008; Perez-Cruzado et al., 2011; Headlee et al., 2012; Marziliano et al., 2012; Tallis et al., 2012), however, in this paper, we have implemented a simplified methodology for estimating basal area development (parameter strongly correlated to the volume and growth of the forest), less expensive and easier to use than others methodologies. Therefore, this methodology can be, also for the accurate estimates it provides, a valid management guideline for choosing the best cultivation options (West, 2015), especially when the energy production deriving from woody biomass is the main objective of the plantation.

This methodology can be useful for medium rotation forestry (MRF) at definitive tree density, where the amount of trees is limited. On the contrary, in short rotation coppice and short rotation forestry (SRC and SRF), where the tree densities are higher, this methodological approach needs more experimentation.

However, the most important limitation of the proposed methodology is its field of application: it is not valid for all those stands that are subject to progressive natural or artificial thinning. In fact, in these stands, from the trees that form the sample size for estimate basal area, it could not be deduced the basal area increment at different ages because it is impossible to reconstruct the number of trees at the previous ages.

However, in all these contexts, the proposed methodology could be applied only for small periods of time (last 3–5 years) provided that in these years neither the vegetative conditions of the individuals trees nor the trees number were modified.

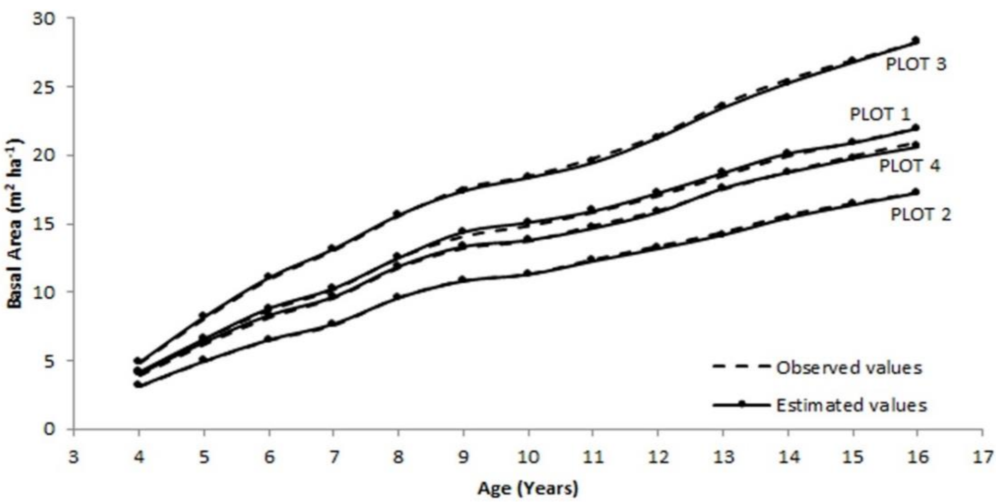

Figure 7. Trends obtained for the measured basal area (dotted lines) and for the basal area estimated (solid lines) with the proposed methodology.

CONCLUSIONS

This study provided a simplified methodological approach for forest managers and policy makers to estimate the basal area of poplar plantations at definitive tree density.

The analysis showed that, in a tree plantation with constant planting density (i.e. not subjected to intercalary thinnings), the estimate of some parameters of productions (in any year of the production cycle), such as basal area, volume and weight, can be carried out by analysing the increment of a few trees with DBH around the tree with average diameter and the multiplication the average basal area of these trees by trees number per hectare will yield an reliable estimate of the basal area per hectare. Our results underline the advantage to sample only few trees, without affecting the reliability of the estimate.

We can therefore finally answer to the questions proposed: (1) and (3) the trees number of reliable sample for basal area estimate is bigger than 1 and varies from a minimum of 7 to a maximum of 9 trees, depending on the variability of the experimental plots, (2) and these trees must have a diameter around the tree of average size.

In conclusion, this method here developed will permit reliable biomass estimates, but also a reduction of the costs in the sampling activities in the field. The availability of simplified technical tools for the evaluation and estimation of tree growth and yield is particularly important when the total economic value of a given tree plantation should be assessed. Finally, we believe that the knowdledge and use of these tools makes a landowner more informed, and better able to make decisions regarding your property.

ACKNOWLEDGEMENTS. We thank the Department of Agraria of Mediterannean University for supporting our research. In addition, we thank the anonymous reviewers for their careful reading of our manuscript and their many insightful comments and suggestions. Following the suggestions, we included several improvements in the manuscript.

REFERENCES

AA.VV. 2011. Cultivation models for wood production in the flatland. Quaderni della ricerca. Regione Lombardia, 127 (in Italian).

Arevalo, C., Volk, T.A., Bevilacqua, E. & Abrahamson, L. 2007. Development and validation of aboveground biomass estimations for four *Salix* clones in central New York. *Biomass and Bioenergy* **31**, 1–12.

Armstrong, A., Johns, C. & Tubby, I. 1999. Effects of spacing and cutting cycle on the yield of poplar grown as an energy crop. *Biomass and Bioenergy* **17**, 305–314.

Aylott, M.J., Casella, E., Tubby, I., Street, N., Smith, P. & Taylor, G. 2008. Yield and spatial supply of bioenergy poplar and willow short-rotation coppice in the UK. *New Phytologist*, **178**, 358–370.

Bergante, S. & Facciotto, G. 2006. Annual, biennal, five-year planting. Productivity and costs in some companies in Northern Italy. *Sherwood* **128**, 25–30.

Bergante, S., Zenone, T. & Facciotto, G. 2015. Short Rotation Forestry for Energy Production in Italy: Environmental Aspects and New Perspectives of Use in Biofuel Industry. In: Sustainable Biofuels. An Ecological Assessment of the Future Energy. ISBN: 978-311027

Casella, E. & Ceulemans, R. 2002. Spatial distribution of leaf morphological and physiological characteristics in relation to local radiation regime within the canopies of 3-year-old *Populus* clones in coppice culture. *Tree Physiology* **22**, 1277–1288.

Ceulemans, R., Stettler, R.F., Hinckley, T.M., Isebrands, J.G. & Heilman, P.E. 1990. Crown architecture of *Populus* clones as determined by branch orientation and branch characteristics. *Tree Physiology* **7**, 157–167.

Coaloa, D., Facciotto, G., Chiarabaglio, P.M., Giorcelli, A. & Nervo, G. 2016. Poplar clones to Larger Environmental Sustainability. *SHERWOOD*, 31–34 (in Italian).

Coletta, V., Menguzzato, G., Pellicone, G., Veltri, A. & Marziliano, P.A. 2016. Effect of thinning on above-ground biomass accumulation in a Douglas-fir plantation in southern Italy. *Journal of Forestry Research* **27**(6), 1313–1320. doi: 10.1007/s11676-016-0247-9.

Corona, P., Marziliano, P.A. & Scotti, R. 2002. Top-down growth modelling: a prototype for poplar plantations in Italy. *Forest Ecology and Management* **161**, 65–73. doi: 10.1016/S0378-1127(01)00481-9.

Dickmann, D.I. 2006. Silviculture and biology of short-rotation woody crops in temperate regions: then and now. *Biomass and Bioenergy* **30**, 696–705.

Dillen, S.Y., Rood, S.B. & Ceulemans, R. 2010. Growth and physiology. In: Genetics and Genomics of *Populus* Plant Genetics and Genomics: Crops and Models (eds Jansson, S, Bhalerao, R, Groover, A), pp. 39–63. Springer, New York, NY.

Eastaugh, C.S. 2014. Relationships between the mean trees by basal area and by volume: reconciling form factors in the classic Bavarian yield and volume tables for Norway spruce. *European Journal of Forest Research* **133**(5), 871–877. https://doi.org/10.1007/s10342-014-0804-8.

Facciotto, G., Di Candilo, M., Bergante, S., Lioia, C. & Diozzi, M. 2008. Poplar clones for biomass production in Italian SRC. In: *Proceedings of 16th European Conference & Exhibition, Biomass for Energy*, Industry and Climate Protection, Valencia, Spain, 2-6 June 2008, pp. 170–173.

FAO. 1998. World reference base for soil resources. The latest WRB classification manual. Food and Agriculture Organization of the United Nations, Rome, Italy, pp. 128.

Fischer, M., Trnka, M., Kučera, J., Fajman, M. & Žalud, Z. 2011. Biomass productivity and water use relation in short rotation poplar coppice (*Populus nigra x P. maximowiczii*) in the conditions of Czech Moravian Highlands. Acta univ. agric. et silvic. *Mendel. Brun. LIX* **6**, 141–152.

Fowler, J. & Cohen, L. 1995. Statistics for Ornithologist. 2nd edition. British Trust for Ornithology, Guide No 22, Distributed by NHBS, UK.

Gordon, A.D. 1999. Classification, 2nd ed. Chapman & Hall, London, 272 pp.

Grogan, P. & Matthews, R. 2002. A modelling analysis of the potential for soil carbon sequestration under short rotation coppice willow bioenergy plantations. *Soil Use and Management* **18**(3), 175–183.

Headlee, W.L., Zalesny, R.S., Donner, D.M. & Hall, R.B. 2012. Using a process-based model (3-pg) to predict and map hybrid poplar biomass productivity in Minnesota and Wisconsin, USA. *BioEnergy Research* **6**, 196–210.

Hellrigl, B. 1970. The sample size in the dendrometric survey. L'Italia Forestale e Montana, **XXV**(6), 312–319 (in Italian).

Hill, J., Nelson, E., Tilman, D., Polasky, S. & Tiffany, D. 2006. Environmental, economic, and energetic costs and benefits of biodiesel and ethanol biofuels. *Proceedings of the National Academy of Sciences USA* **103**, 11206–11210.

Hinchee, M., Rottmann, W., Mullinax, L., Zhang, C., Chang, S., Cunningham, M., Pearson, L. & Nehra, N. 2009. Short-rotation woody crops for bioenergy and biofuels applications. *Vitro Cell.Dev.Biol. Plant* **45**, 619–629. DOI 10.1007/s11627-009-9235-5.

IEA (INTERNATIONAL ENERGY AGENCY) 2003. IEA statistics-renewable in- formation, IEA/OECD, Paris.

Isebrands, J.G. & Karnosky, D.F. 2001. Environmental benefits of poplar culture. In Poplar culture in North America. NRC-CNRC Press, Ottawa, Ontario, Canada, pp. 309–324.
Kheshgi, H.S., Prince, R.C. & Marland, G. 2000. The potential of biomass fuels in the context of global climate change: focus on transportation fuels. *Annual Review of Energy and the Environment* **25**,199–244.
Lombardi, F., Marchetti, M., Corona, P., Merlini, P., Chirici, G., Tognetti, R., Burrascano, S., Alivernini, A. & Puletti N. 2015. Quantifying the effect of sampling plot size on the estimation of structural indicators in old-growth forest stands. *Forest Ecology and Management* **346**, 89–97.
Macaya-Sanz, D., Chen, J.G, Kalluri, U.C., Muchero, W., Tschaplinski, T.J., Gunter, L.E., Simon, S.J., Biswal, A.K., Bryan, A.C., Payyavula, R., Xie, M., Yang, Y., Zhang, J., Mohnen, D., Tuskan, G.A. & Di Fazio, S.P. 2017. Agronomic performance of *Populus deltoides* trees engineered for biofuel production. *Biotechnol Biofuels* 1**0**, 253. DOI 10.1186/s13068-017-0934-6.
Marziliano, P.A., Menguzzato, G., Scuderi, A. & Corona, P. 2012. Simplified methods to inventory the current annual increment of forest standing volume. *iForest* **5**, 276–282.
Marziliano, P.A., Coletta, V., Menguzzato, G., Nicolaci, A., Pellicone, G. & Veltri, A. 2015. Effects of planting density on the distribution of biomass in a douglas-fir plantation in southern Italy. *iForest* **8**, 368-376. [online 2014-09-09] doi: 10.3832/ifor1078-007.
Marziliano, P.A., Menguzzato, G., Scuderi, A., Scalise, C. & Coletta, V. 2017. Biomass conversion and expansion factors in Douglas-fir stands of different planting density: variation according to individual growth and prediction equations. *Forest Systems* **26**, e003. https://doi.org/10.5424/fs/2017261-10239.
Montgomery, D. 2001. *Introduction to statistical quality control* (4th edn). John Wiley & Sons, New York, USA, 795 pp.
Nervo, G., Coaloa, D., Vietto, L., Giorcelli, A. & Allegro, G. 2011. Current situation and prospects for European poplar culture: the role of Italian research. Actas del Tercer Congreso Internacional de Salicáceas en Argentina 16-19 March 2011, pp 117–125.
Niemczyk, M., Wojda, T. & Kaliszewski, A. 2016. Biomass productivity of selected poplar (*Populus* spp.) cultivars in short rotations in northern Poland. *New Zealand Journal of Forestry Science* **46**, 22. DOI 10.1186/s40490-016-0077-8.
Oshumi, N. 1980. Evaluation procedure of agglomerative hierarchical clustering methods by fuzzy relations. In: Diday, E. (Ed.), Data Analysis and Informatics II. *Elsevier Science*, Amsterdam, pp. 509–522.
Pavari, A. 1959. Phytoclimatic classifications and station characteristics. Scritti di ecologia selvicoltura e botanica forestale, pp. 45–116 (in Italian).
Péerez-Cruzado, C., Merino, A., Rodrıguez-Soalleiro, R. 2011. A management tool for estimating bioenergy production and carbon sequestration in *Eucalyptus globulus* and *Eucalyptus nitens* grown as short rotation woody crops in north-west Spain. *Biomass and Bioenergy* **35**, 2839–2851.
Perez-Cruzado, C., Sanchez-Ron, D., Rodriguez-Soalleiro, R., Hernandez, M.J., Sanchez-Martin, M.M., Canellas, I. & Sixto, H. 2014. Biomass production assessment from *Populus* spp. short-rotation irrigated crops in Spain. *GCB Bioenergy* **6**, 312–326, doi: 10.1111/gcbb.12061
Perttu, K.L. 1998. Environmental justification for short rotation forestry in Sweden. *Biomass and Bioenergy* **15**(1), 1–6.
Rand, W.M. 1971. Objective criteria for the evaluation of clustering methods. *Journal of the American Statistical Association* **66**, 846–850.
Rosenqvist, H., Roos, A., Ling, E. & Hector, B. 2000. Willow growers in Sweden. *Biomass and Bioenergy* **18**(2), 137–145.

Scholz, V. & Ellerbrock, R. 2002. The growth productivity and environmental impact of the cultivation of energy crops on sandy soil in Germany. *Biomass and Bioenergy* **23**(2), 81–92.
Soliani, L. 2008. Applied statistics. UNI.NOVA, Parma, Italy, pp. 694 (In Italian).
Stampfl, P.F., Clifton-Brown, J.C. & Jones, M.B. 2007. European-wide GIS-based modelling system for quantifying the feedstock from *Miscanthus* and the potential contribution to renewable energy targets. *Global Change Biology* **13**, 2283–2295.
Tallis, M.J., Casella, E., Henshall, P.A., Aylott, M.J., Randle, T.J., Morison, J.I.L. & Taylor, G. 2012. Development and evaluation of ForestGrowth-SRC a process-based model for short rotation coppice yield and spatial supply reveals poplar uses water more efficiently than willow. *Global Change Biology Bioenergy* **5**, 53–66.
Wang, D., Lebauer, D. & Dietze, M. 2013. Predicting yields of short-rotation hybrid poplar (*Populus* spp.) for the United States through model–data synthesis. *Ecological Applications* **23**(4), 944–958 (USA).
West, P.W. 2015. Tree and Forest Measurement. Third Edition. *Springer International Publishing*, 214. DOI:10.1007/978-3-319-14708-6
Zar, J.H. 1996. Biostatistical analysis (3rd edn). Prentice Hall Inc., Englewood Cliffs, NJ, USA, 718 pp.

Agronomy Research **16**(3), 838–845, 2018
https://doi.org/10.15159/AR.18.110

Influence of soil tillage on oats yield in Central Bohemia Region

J. Mašek* and P. Novák

Czech University of Life Sciences Prague, Faculty of Engineering, Kamýcká 129, CZ165 21 Prague 6 – Suchdol, Czech Republic
*Correspondence: masekj@tf.czu.cz

Abstract. The paper describes results of the field experiment with two technologies of oats crop stand establishment. First technology is conventional technology and second is no-tillage technology. The article describes an experiment which was conducted in years 2013–2017. The experiments were located in Nesperská Lhota at Central Bohemia region. Altitude of selected field is 460 m. The experimental field is covered by a light cambi-soil. The differences between the two technologies stand establishment are discussed. Statistical evaluation was performed on both methods in the parameter number of tillers per m^2 and yield. Crop yield is the basic indicator of agricultural production and usually affected by quality of soil tillage. One of the parameters affecting the yield is tillage (technology, working tools, depth, turning of soil etc.). Tillage depends mainly on the depth of processing and other quality parameters. An examination of the crop yield is necessary in terms of sensitivity, depending on agro-technical conditions. Among those can be included processing plant soil nutrition and plant protection. It's always necessary commemorate, in these experiments can't be excluded some parameters like locality or meteorological parameter influences. Field trial was conceived as multi-year experiment with minimal changes of agro-technical conditions. During the experiment, the positive effect of conventional technology on crop yields was found. This difference was reflected in the number of tillers and in total yield. The measurement shows the beneficial effect of the loosening of soil on the state of the oat crops. The results of experiment show that, the average yield in 5 years observation was 2.11 t ha^{-1} for no-till technology and 4.22 t ha^{-1} for conventional technology of tillage.

Key words: no till technology, conventional technology, yield evaluation.

INTRODUCTION

The basic result of crop production is yield. Yield is affected and limited by many factors. Limiting factors of yield in field crops can be divided into few basic groups: soil conditions, soil fertility, agro-technics factors and meteorological conditions (Karing et al., 1999). Some of these conditions can be affected by agrotechnology. Of course, meteorological factors cannot be influenced (Zute et al., 2010). The main task of soil cultivation is to prepare optimal conditions for crop growth. Contemporary agriculture is characterized by the transition from conventional soil technology to reduced technologies. Berner et al. (2008) describes the necessary change in the cultivation strategy when changing the soil tillage system. Baumhardt & Jones (2002) also emphasizes the need of good management of plant residues.

The problem of no till technology can also be an extension of persistent weeds. Cereals yield loss increased as weeds density increased but the magnitude of the yield loss diminished with increasing cereals plant density (O'Donovan et al., 1999). The main advantage of reduced systems (including no till) is soil protection. Reduced or no-tillage techniques, together with crop residue management and crop rotation are the pillars of CA (conservation agriculture). The term reduced tillage covers a range of tillage practices but it never involves inverting the soil. In this way, soil disturbance is minimized and crop residues are left on the soil. Studies in many European countries have shown that CA can indeed be very effective in combating soil erosion (Van den Putte et al., 2010).

It is also problematic to grow cereals in monocultures without rotation of crops. López-Bellido (1996) found a connection between crop rotation and soil cultivation. The decline in yield over long-term cultivation is also related to the type of tillage. Berzsenyi et al. (2000) also found a decline in crop yields without rotation. The yields of maize and wheat were lower in all cases in a monoculture than in a crop rotation.

Due to lack of studies targeted on spring cereals yield from different soil tillage systems point of view was established this long term field trail. More over this experiment is focused on sustainability of monoculture plant production of spring cereals.

MATERIALS AND METHODS

The field experiment with two variations of tillage and seeding of oat (*Avena Sativa* L.) was based on loamy cambisol at an altitude of 410 m. Growing slope of the land was uniform in all experimental variants. The average slope was 5.4°. The area of experimental plots for individual variants of the experiment was 300 m^2 – width 6 m and length 50 m (3 repeats of each variant), the orientation of the longer side plots the fall line. First variant was no till technology, and the second was traditional variant with ploughing.

First variant: Conventional technology with ploughing in the fall into depth 0.22 m, during winter soil left in rough furrow, in spring time sowing soil preparation with levelling bars and harrows, oats sowing (each year).

Second variant: No till technology with crushing straw from previous year and it was spreading on soil surface like mulch covering for whole winter time, only oat sowing each spring by Ross seeder.

Primary tillage for the foundation of experiment took place in the fall of 2009. Field trial was established in 2009. First four seasons was as a transition between conventional and no till system. First evaluated season for full no till technology was 2013 (due to exclude influence of previously tillage effect). After harvesting of triticale, the straw was crushed and dispersed. The soil was cultivated in the second half of August by disc tiller BDT 3.5 (only variant with conventional tillage). Driving of the machine proceeded in the direction of the contours, hunk pitch against the slope. On half of October the land was processing by mouldboard plough Ross into depth 0.22 m (only variant with conventional tillage). Tillage and sowing in spring is given for each variant of the experiment.

The field experiment was conceived from the beginning as several years. Vantage Vue weather station is located near the experimental plot. In addition, the rainfall was registered and intensity of rainfall and other meteorological variables. The experiment was established for measuring the quantity of water erosion in particular, but additional parameters were monitored, for example elements of the crop yield, soil physical properties etc. Evaluated parameters of biological yield were the height of the stand, tilers' number of evaluated area.

The height of the stand was measured in ten repetitions three times during vegetation in phonological stage BBCH 30, BBCH 50, BBCH 85. The selection was random. Yield of oats plants was determined by manually harvesting in ten repetitions. Each one area was 1 m^2. Biomass of plants was weighed on digital scales Kern. Samples were trashed on laboratory thrasher unit to achieve grains. Data were processed by the programmes MS Excel (Microsoft Corp., USA) and Statistica 12 (Statsoft Inc.,USA).

RESULTS AND DISCUSSION

Table 1 contains meteorological data from all evaluated seasons. The highest rainfall during the vegetation was in 2014. On the contrary, the 2015 and 2017 seasons were relatively dry. During season 2016, rainfall occurred in the form of heavy rains and much of the water drained in the form of a surface runoff.

Table 1. Precipitations and temperatures at different growth stages by BBCH scale recorded in the experimental field for oat in 2013–2017

Year	Growth stages	Temperature, °C	Precipitation, mm
2013	BBCH 20-29	13.4	86.2
	BBCH 30-59	15.3	101.7
	After BBCH 60	20.5	137.9
	Sum	-	320.4
	Mean	16.4	-
2014	BBCH 20-29	12.3	31.9
	BBCH 30-59	16.5	102.8
	After BBCH 60	21.1	143.5
	Sum	-	278.2
	Mean	16.6	-
2015	BBCH 20-29	13.2	31.9
	BBCH 30-59	19.3	82.8
	After BBCH 60	22.4	43.5
	Sum	-	158.2
	Mean	18.3	-
2016	BBCH 20-29	13.4	46.2
	BBCH 30-59	16.3	101.7
	After BBCH 60	19.1	87,8
	Sum	-	230.3
	Mean	15.6	-
2017	BBCH 20-29	14.1	48.7
	BBCH 30-59	16.5	52.8
	After BBCH 60	22.2	84.2
	Sum	-	184.8
	Mean	17.5	-

The physical properties of the soil are shown in Table 2. Porosity and bulk density were monitored parameters. Table shows relatively small differences between variants. Differences over several year experiment were smaller than we expected. Slightly better soil properties were recorded in the variant with a no-till technology. Changes in soil properties are always long term phenomenon, and are also influenced by many other factors (organic matter, etc.).

Table 2. Soil physical properties between years 2013–2017

Year	Depth (m)	Conventional		No till	
		Bulk density, g cm^{-3}	Porosity, %	Bulk density, g cm^{-3}	Porosity, %
2013	0.05–0.1	1.52	37.5	1.47	42.2
	0.1–0.15	1.50	39.4	1.49	41.7
	0.15–0.2	1.54	40.8	1.50	41.9
2014	0.05–0.1	1.49	36.2	1.44	41.9
	0.1–0.15	1.48	40.2	1.47	40.8
	0.15–0.2	1.54	39.2	1.48	43.5
2015	0.05–0.1	1.47	40.0	1.46	41.9
	0.1–0.15	1.49	41.6	1.54	40.0
	0.15–0.2	1.51	37.4	1.47	43.5
2016	0.05–0.1	1.56	42.9	1.48	44.5
	0.1–0.15	1.52	40.3	1.51	41.1
	0.15–0.2	1.53	44.1	1.50	40.8
2017	0.05–0.1	1.47	39.7	1.40	42.7
	0.1–0.15	1.48	38.7	1.41	42.8
	0.15–0.2	1.50	39.6	1.44	44.2

The graph in Fig. 1 shows the number of tillers of oats in each measurement period (BBCH 50). The figure clearly shows greater tillering of oats using conventional technology. This was proven during all years. The number of tillers is an important element of the yield. This parameter suggests a direct effect on yield. Table 3 shows the average value of the number of tillers in each year for each technology. In the years 2013 and 2014, there were statistical differences at the level of alfa = 0.05 below the threshold of statistical significance. In the years 2015–2017, there was a statistically significant difference over the threshold between these two technologies.

Table 3. Average values of tillers number per 1 m^2

Technology	2013	2014	2015	2016	2017
No-till	357	293	248 (***)	186 (***)	197 (***)
Conventional	399	372	368 (***)	407 (***)	398 (***)

*** statistical significance difference.

Value of total yield confirms the positive impact of conventional technology tillage on plant development oats. Tillering of oat plants increased, as well as the other yield components (total yield), as confirmed by the Fig. 2. Conventional technology resulted in higher total yields during all experimental years in comparison with no-till technology. The smallest difference recorded in the 2013 could be caused by the high amount of rainfall during the main growth of oats (BBCH 10-70).A significant decline in yield for no-till technology is reported in following years.

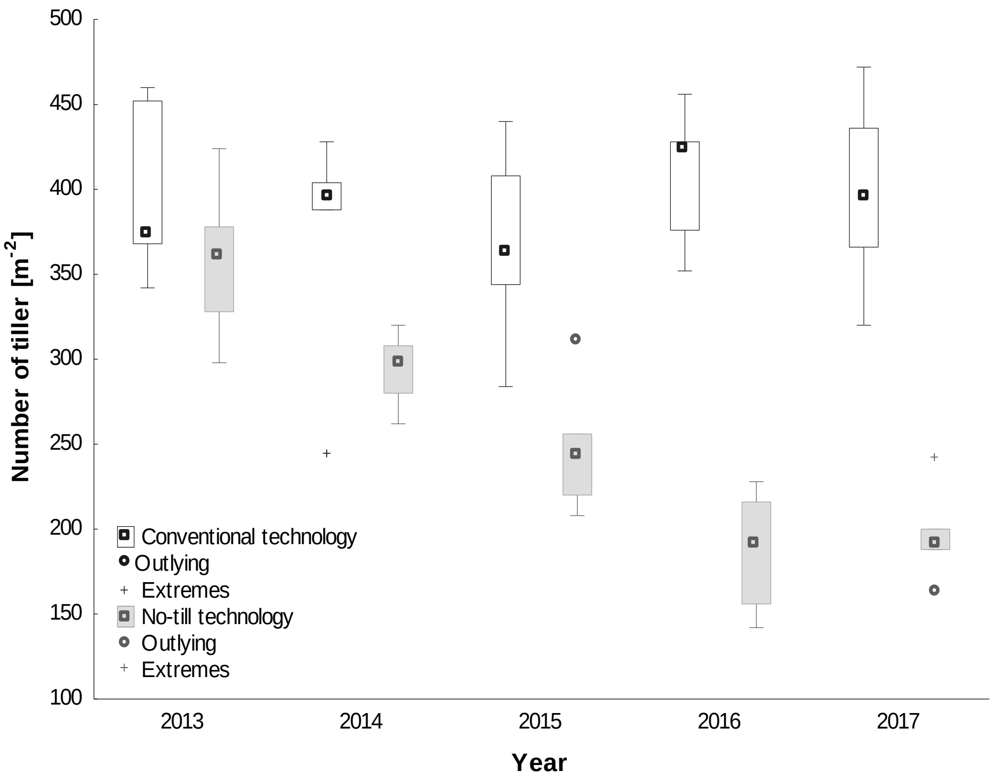

Figure 1. The number of tillers of plants oat in year 2013–2017.

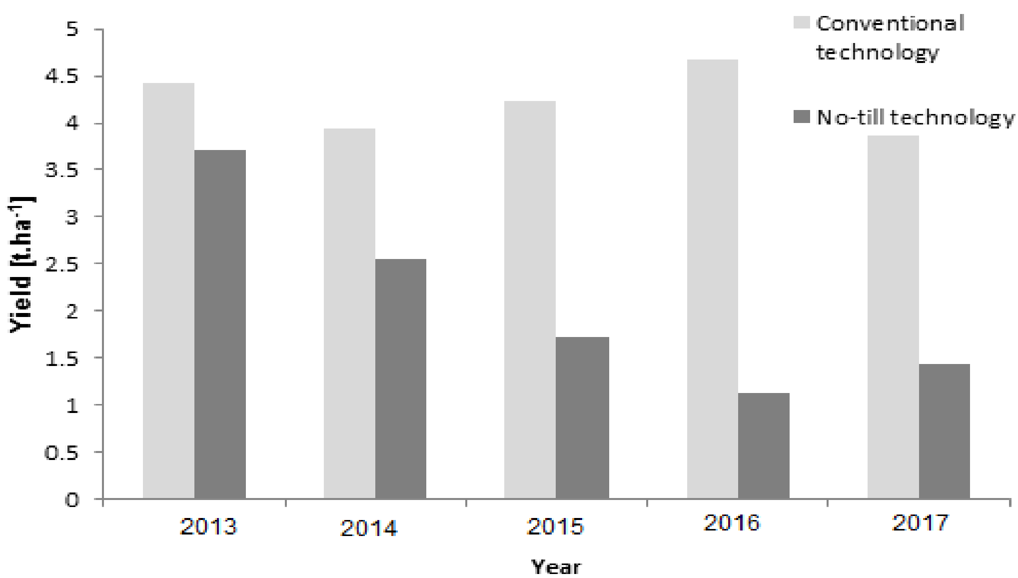

Figure 2. Total yield between 2013–2017.

Fig. 3 shows a comparison of yields for both technologies throughout the given period. It was reported that the conventional technology has more than twice higher yield than no-till technology, suggesting the use of the no-till technology for oats is unsuitable under conditions of central Bohemia region.

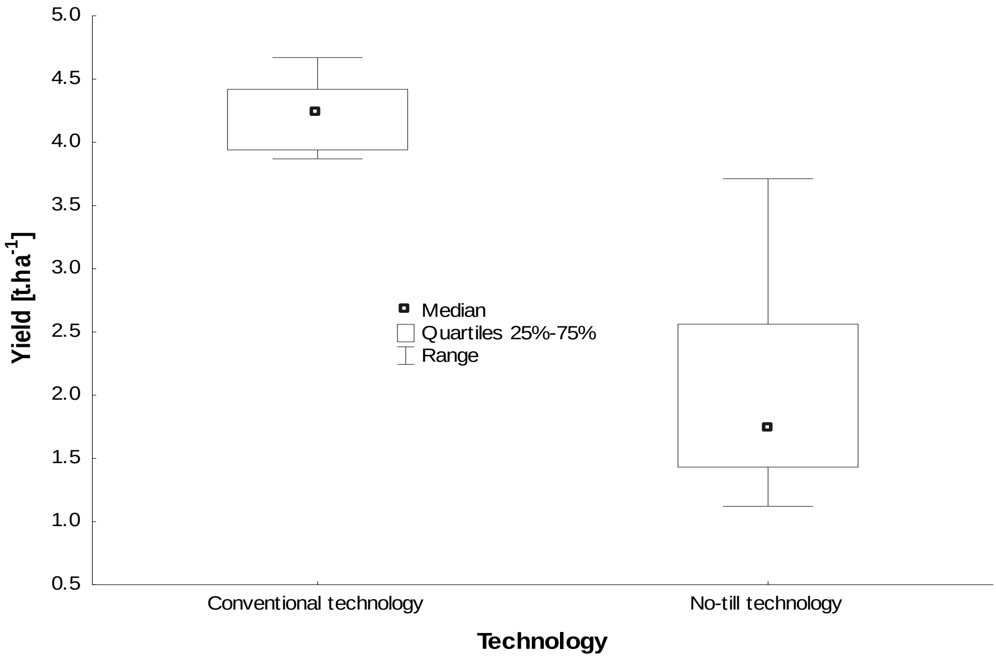

Figure 3. Comparison of each technology in the years 2013–2017.

Tukey test in Table 4 indicates a statistically significant difference between technologies at a significance level alfa = 0.05. Simultaneously shows the average value of each technology.

Table 4. Tukey HSD test- homogeneous group (yield)

Technology	Average yield (t ha^{-1})	1	2
No-till technology	2.11	****	
Conventional technology	4.22		****

The similar results were confirmed by Neumann et al. (2007). They studied effects of crop density and tillage system on grain yield and N uptake from soil and atmosphere of sole and intercropped pea and oat. They also confirmed the beneficial effect of conventional soil cultivation on the yield of oat and the number of tillers. Our results are consistent with results of Riley et al. (2005). They founded that reduced technology (shallow loosening) has a negative impact on total yield compared to conventional technology. Declined yield of oat in no tillage system was confirmed by Seehusen et al. (2017) too. In their work is described reducing the quality of production due to reduced soil tillage for spring cereal production. On the other hand, De Vita et al. (2007) found beneficial effect of no till technology on wheat yields, but only in humid areas. This is confirmed by our research. In the case of higher precipitation during main phonological phases (BBCH 10-60) the difference between technologies was smaller than in the case of lack of rain.

The experiment did not show a decline in yield due to the constant cultivation of one crop using conventional technology. On the other hand, when using no-till technology, decrease of yields was relatively rapid. This is consistent with the study by López-Bellido et al. (1996). It can be stated that for the long-term growing of oats, convection technologies are suitable in these conditions.

CONCLUSIONS

It is evident, that using the conventional technology for oats production has higher yield and more tillers per square meter than using no-tillage technology in this soil conditions. During the research no significant differences were found in the physical properties of the soil. Yield is undoubtedly influenced by other phenomena such as metrological factors and soil properties. The results can't be generalized because the experiment was carried out only in central Bohemia region in one soil type- in this case cambisol. For unambiguous conclusions, it is necessary to test the experiment on multiple sites with different soil conditions.

REFERENCES

Baumhardt, R.L. & Jones, O.R. 2002. Residue management and tillage effects on soil-water storage and grain yield of dryland wheat and sorghum for a clay loam in Texas. *Soil and tillage research* **68**(2), 71–82.

Berner, A., Hildermann, I., Fliessbach, A., Pfiffner, L., Niggli, U. & Mäder, P. 2008. Crop yield and soil fertility response to reduced tillage under organic management. *Soil and Tillage Research* **101**(1–2), 89–96.

Berzsenyi, Z., Győrffy, B. & Lap, D. 2000. Effect of crop rotation and fertilisation on maize and wheat yields and yield stability in a long-term experiment. *European Journal of Agronomy* **13**(2–3), 225–244.

De Vita, P., Di Paolo, E., Fecondo, G., Di Fonzo, N. & Pisante, M. 2007. No-tillage and conventional tillage effects on durum wheat yield, grain quality and soil moisture content in southern Italy. *Soil and Tillage Research* **92**(1–2), 69–78.

Karing, P., Kallis, A. & Tooming, H. 1999. Adaptation principles of agriculture to climate change. *Climate research* **12**(2/3), 175–183.

López-Bellido, L., Fuentes, M., Castillo, J.E., López-Garrido, F.J. & Fernández, E.J. 1996. Long-term tillage, crop rotation, and nitrogen fertilizer effects on wheat yield under rainfed Mediterranean conditions. *Agronomy Journal* **88**(5), 783–791.

Neumann, A., Schmidtke, K. & Rauber, R. 2007. Effects of crop density and tillage system on grain yield and N uptake from soil and atmosphere of sole and intercropped pea and oat. *Field Crops Research* **100**(2–3), 285–293.

O'Donovan, J.T., Newman, J.C., Harker, K.N., Blackshaw, R.E. & McAndrew, D.W. 1999. Effect of barley plant density on wild oat interference, shoot biomass and seed yield under zero tillage. *Canadian Journal of Plant Science* **79**(4), 655–662.

Riley, H.C.F., Bleken, M.A., Abrahamsen, S., Bergjord, A.K. & Bakken, A.K. 2005. Effects of alternative tillage systems on soil quality and yield of spring cereals on silty clay loam and sandy loam soils in the cool, wet climate of central Norway. *Soil and Tillage Research* **80**(1–2), 79–9.

Seehusen, T., Hofgaard, I.S., Tørresen, K.S. & Riley, H. 2017. Residue cover, soil structure, weed infestation and spring cereal yields as affected by tillage and straw management on three soils in Norway. *Acta Agriculturae Scandinavica, Section B—Soil & Plant Science* **67**(2), 93–109.

Van den Putte, A., Govers, G., Diels, J., Gillijns, K. & Demuzere, M. 2010. Assessing the effect of soil tillage on crop growth: A meta-regression analysis on European crop yields under conservation agriculture. *European journal of agronomy* **33**(3), 231–241.

Zute, S., Vicupe, Z. & Gruntina, M. 2010. Factors influencing oat grain yield and quality under growing conditions of West Latvia. *Agronomy Research* **8**, 749–754.

Agronomy Research **16**(3), 846–853, 2018
https://doi.org/10.15159/AR.18.128

Festulolium seed production dependence on fertilizer application system

V. Obraztsov*, D. Shchedrina and S. Kadyrov

Voronezh State Agrarian University named after Emperor Peter the Great, Department of Crop Science, Forage Production and Agricultural Technologies, ul. Mitchurina 1, RU394087 Voronezh, Russia
*Correspondence: ovennn@mail.ru

Abstract. *Festulolium* (× *Festulolium* F. Aschers. et Graebn.) is a new perennial grass *Poaceae* family. The benefits of this culture are good regrow capacity, increased sugars content and higher winter hardiness. It can be used as a green feed when creating cultivated hayfields and pastures. Widespread application of this new culture for forage production is constrained by the shortage of seeds, due to the imperfection of their production technologies. There are still very few of studies on the biology and technology of *Festulolium* cultivation in the forest-steppe of the Central Chernozem Region of Russia (CCR). The experiments involved the VIC-90 *Festulolium* variety with the first crop being the vetch-oat mixture harvested for green fodder. The soil in the experimental plots was leached medium thick medium loamy chernozem. The humus content in the arable horizon was 4.56%, pH was 4.9, degree of base saturation was 74–86%, P_2O_5 content was 129 mg kg^{-1}, K_2O content was 115 mg kg^{-1} (according to Chirikov) and the hydrothermal index was 1.13. The experiment included the following variants: no fertilizer application (control) and application of mineral fertilizers (ammonium nitrate and ammonium nitrate phosphate fertilizer) at different doses. Soil preparation was conventional for seed swards of perennial grasses in the CCR. *Festulolium* was sown in broad drills by coverless sowing to the depth of 0.5–1.0 cm at the seeding rate of 6.0 kg ha^{-1}. Experiments, records, observations and determination of economic and bioenergetic efficiency were carried out according to conventional procedures. It was found that the climatic conditions in the forest steppe of the CCR were favorable for *Festulolium* seed cultivation. Application of mineral nitrogen fertilizers in autumn at a dose of 60 kg ha^{-1} of active ingredient (AI) ensures the formation of high yielding erect seed-producing sward, and can increase harvest energy efficiency an average by 1.45–1.82 times and obtain 591–620 kg ha^{-1} of certified seeds. The greatest profitability of production (179%) and the highest notional farm net income (RUB 43,000 per hectare) are provided by a single application of ammonium nitrate fertilizer at a dose of 60 kg ha^{-1} of active ingredient in autumn (after vegetative mass topping).

Key words: perennial grasses, non-lodged plant stand, overwintering, seasonal fertilizer application, different doses, seed productivity.

INTRODUCTION

One of the main factors for obtaining high yields of *Festulolium* seeds is a rational fertilizer application system. In contrast to cultivation for fodder purposes, when it is necessary to obtain the greatest yield of vegetative mass, fertilizer application system on seed producing plots should correspond to the production of non-lodged or slightly lodged plant stand with even flowering and seed ripening. A lot of researchers (Yansons, 1978; Mikhailichenko, 1987; Rogov, 1989; Meerovsky & Kovalets, 2008; Zolotarev et al., 2008; Perepravo et al., 2012) consider nitrogen to be the main element influencing seed growing potential in seed production of perennial grasses. Phosphate-potassium fertilizers are less important for obtaining high yields of grass seeds, but their lack in soil reduces the efficiency of additional nitrogen fertilizing.

Most Russian and foreign researchers think that the doses and timings of nitrogen fertilizer application are critical factors in seed production of perennial grasses (Griffiths et al., 1971; Mikhailichenko et al., 1999; Zolotarev et al., 2007; Perepravo et al., 2013; Cougnon et al., 2017; Mastalerczuk et al., 2017). According to S.P. Smelov (1966), perennial grasses absorb up to 50–80% of nitrogen from spring tillering to shooting stage. Spring application of nitrogen fertilizers stimulates the formation of reproductive organs, contributes to an increase in the number of seeds in the inflorescences. Nitrogen deficiency decelerates the developmental processes in plants, reduces formation of branching roots and rootlets, as well as chlorophyll content in leaves, CO_2 uptake and water use efficiency, which finely leads to a decrease in dry matter accumulation and seed productivity (Mastalerczuk et al., 2017). Excessive nitrogen nutrition, on the contrary, adversely affects plants development, especially in the seasons of sufficient and excessive depth of precipitation, causes lodging of generative shoots, which leads to a decrease in the potential seed productivity of plants, makes it difficult to harvest seeds mechanically and degrade their quality.

Application of high doses of nitrogen reduces winter hardiness, the content of water-soluble carbohydrates and increases the nitrate content in feeding stuffs. In addition to the above, the efficiency of fertilizers largely depends on the biological properties of the cultivated crop. Therefore, it is of critical importance to determine correctly the doses and timings of the application of mineral fertilizers (Schuppenies, 1988; Mikhailichenko et al., 1999; Perepravo et al., 2003).

In the researches of I. Gutmane (2005; 2012) devoted to the effect of mineral nitrogen fertilizers on *Festulolium* seed productivity and carried out on sod gley soil in climatic conditions of Latvia, it was defined that N_{120} kg ha^{-1} nitrogen dose was the nearest to the optimal quantity of nitrogen fertilizers, that provides seed harvest from 0.6 to 1.0 t ha^{-1}.

Doses of nitrogen fertilizers and timings of their application before *Festulolium* sowing for seeds are not adequately investigated from the perspective of climatic conditions of the Central Chernozem Region. The objective of the presented research is revealing the influence of different types and doses of additional nitrogen fertilizing on the developmental biology of *Festulolium* of different planting period when the crop under study is growing for seed production.

MATERIALS AND METHODS

Experimental part of the study was performed in field trials of the Department of Crop Science, Forage Production and Agricultural Technologies of Voronezh State Agrarian University on the fields of 'Agrotechnology' Training, Research and Technological Center (N51.7140416 E39.21545371) in 2009–2011.

The soil in the experimental plot is leached middle thick middle loamy chernozem. The humus content in the arable horizon was from 4.56 to 5.50%, pH_{salt} was 4.9, and soil base saturation was 74–86%. The content of labile phosphorus (P_2O_5) and exchangeable potassium (K_2O) was 78–129 and 109–118 mg kg^{-1} of soil, the total absorbed bases was from 21.3 to 22.2 mg-eq. per 100 g of soil.

The variation of meteorological conditions during the period of experiments allowed to evaluate objectively the obtained results. In 2009 weather conditions were more favorable for *Festulolium* plantings although precipitation depth was below mean annual rainfall. In 2010 the weather was abnormally hot and dry, the air temperature on the soil surface in flaming summer days reached 60°C, average monthly temperatures of July and August were above 25 °C. In 2011 the conditions of vegetation season were relatively favorable.

The experiments involved the VIK–90 *Festulolium* variety. It was preceded by vetch-oat mixture harvested for green fodder.

The soil preparation to sowing was conventional for seed swards of perennial grasses in the Central Chernozem Region. After harvesting *Festulolium* preceding crop primary tillage was fulfilled to the depth of 8–10 cm, then in two weeks the soil was plowed using jointer shares to the depth of 27–30 cm. In spring, as far as the soil was ready, we performed early tandem disk harrowing, secondary tillage, soil packing before sowing, coverless wide-row (30 cm) sowing to the depth of 0.5–1.0 cm at the seeding rate of 8.0 kg ha^{-1}, and soil packing after sowing. Registration plot area was 20 sq. m., randomized experiments were carried out in fourfold replication.

Experiments, relevant records and observations were carried out according to standard Methodological Instructive Regulations (1986) for perennial grasses seed production.

RESULTS AND DISCUSSION

During the first year of life of *Festulolium* plantings the meteorological conditions of vegetation season, especially during seedling emergence, have a strong effect on the plant growth and development. Weather conditions during the period of research showed to be favorable for *Festulolium* seed sprouting, mean field germination rate reached 75.8%.

More favorable weather conditions for *Festulolium* seedling emergence were in 2009 and 2010: field germination rate average in all variants reached 76.1 –81.8%. In 2011 field germination rate decreased to 69.5% due to dry weather during sowing and seed sprouting stage.

In 2010 for the second part of summer hot and dry weather with air temperature above 25 °C continued during 24 days and thus negatively affected plants safety index during the first year of life. The mean crop failure during vegetation was the highest – 15.2%, whereas in other years it did not exceed 8.3–9.2%.

In the year of sowing *Festulolium* plantings grow slowly and do not form generative shoots. They are formed during the second and the following years, both from overwintered shoots as well as from shoots newly appeared in spring.

The first leaf expansion occurs 4–6 days after seedling emergence, 5–6 days after unfolds the second one. In the phase of 3–4 leaves the first side tillering-branching shoot appears. *Festulolium* plantings of the first year of life vigorously put out side shoots during the whole summer period. The amount of well-developed shoots in the first year of life directly affects overwintering and the amount of yield.

Festulolium is a cross-pollinated plant. Flowering period of a single plant continues from 2 to 4 days, whereas flowering period of the population is extended up to 8–11 days. During the second year of life the period from spring aftergrowing till complete seed ripeness continued 99–107 days.

Nitrogen fertilizers increase the vegetation period of plants, especially spring tillering and shooting stages. In the second year of life the vegetation period of plants as compared to control increased in the variants with additional ammonium nitrate (N) and nitroammophoska (ammonium nitrate phosphate fertilizer) fertilizing by 3–7 days and 3–8 days, respectively (Table 1).

Table 1. The Influence of Fertilizers on the Duration of Stages of *Festulolium* Plantings of the Second Year of Life from the Vegetative Renewal to Shooting, Earing, Flowering and Complete Seed Ripeness (2009–2011 period average)

Fertilizer type	Dosage of fertilizer, kg ha^{-1} of active ingredient (AI)	Duration of stages from spring vegetative renewal to the beginning of the stage			
		Shooting	Earing	Flowering	Complete seed ripeness
	Control (no fertilizers)	32	46	63	99
Ammonium nitrate	N_{45} – in autumn	34	49	66	100
	N_{60} – in autumn	34	51	68	103
	N_{75} – in autumn	35	51	69	104
	N_{90} – in autumn	36	52	71	105
	N_{30} – in autumn + N_{30} – in spring	36	53	71	106
	N_{45} – in autumn + N_{45} – in spring	37	54	72	107
Nitroammophoska 16:16:16	$(NPK)_{45}$ – in autumn	35	50	69	101
	$(NPK)_{60}$ – in autumn	35	51	70	104
	$(NPK)_{75}$ – in autumn	36	52	71	105
	$(NPK)_{90}$ – in autumn	37	53	73	106
	$(NPK)_{30}$ – in autumn + $(NPK)_{30}$ – in spring	37	52	72	107
	$(NPK)_{30}$ – in autumn + $(NPK)_{45}$ – in spring	38	53	74	107

Additional nitrogen fertilization increases the height of plants. In the second year of life in the control variant average height of generative shoots reached 41.8 cm, and when applying additional N_{45} and N_{90} fertilization it increased by 7.3 and 18.0 cm, respectively.

An increase of fertilization doses from 75 to 90 kg ha^{-1} of active ingredient (AI) contributed to the intensification of plant growth at early stages of vegetation leading to high lodging of plants, which negatively affected cross-pollination of flowers, seed formation and ripening, and also worsened the conditions of their harvesting. E.g. in wet weather conditions of 2009 in the variants with N_{45} and N_{60} application the degree of lodging reached 16.8 and 35.2%, and in the variants with N_{75} and N_{90} application it reached 39.0 and 46.8%, respectively.

In 2010 characterized by low amount of precipitation in the second half of vegetation season low degree of grass lodging was observed. It was found that in the lodged plantings the beginning of complete ripeness stage was delayed by 2–4 days as compared to control, and the amount of imperfect (shrunken) weevils in inflorescences increased.

The lowest degree of lodging of *Festulolium* seed crops (14.9%) was observed in the variant with $(NPK)_{45}$. In the variants with N_{90} and $(NPK)_{90}$ application the degree of grass lodging reached on average 33.6 and 34.8%.

It was found that *Festulolium* had high winter hardiness. During all years of study in the variants with mineral fertilizers application the amount of overwintered plants reached 84.9–88.9%.

Favorable conditions for *Festulolium* wintering occurred in the winter of 2010/2011 due to high snowing. In all the variants crop failure was low (4–8%). Better plant safety index (97.8–95.9%) was registered in the variants with higher doses of fertilizers, less plants (92%) survived in the control variant without fertilizers.

Winter weather conditions in 2009/2010 were the most unfavorable. Strong frosts and long-term absence of snow cover led to the considerable crop failure. In the control variant before wintering the density of plantings was 1,030 pcs m^{-2}, after wintering it was only 734 pcs m^{-2}, crop failure reached 28.7%. The application of ammonium nitrate and nitroammophoska increased the amount of overwintered plants to 77.0–81.8%, which is by 5.7–10.5% higher than in the control variant.

Table 2. The Influence of Fertilizers on the Elements of Crop Structure of *Festulolium* of the Second Year of Life (2009–2011 period average)

Fertilizer type	Dosage of fertilizer, kg ha^{-1} of AI	Ear length, cm	Number of generative shoots, pcs m^{-2}	Number of spikelets in a ear	Number of seeds in a ear
	Control (no fertilizers)	16.0	639.3	14.4	48.7
Ammonium nitrate	N_{45} – in autumn	17.1	762.2	15.8	57.8
	N_{60} – in autumn	18.3	853.6	16.7	65.2
	N_{75} – in autumn	18.4	813.1	17.9	66.7
	N_{90} – in autumn	19.7	793.6	18.3	67.1
	N_{30} – in autumn + N_{30} – in spring	17.2	834.0	15.9	63.7
	N_{45} – in autumn + N_{45} – in spring	18.0	815.1	16.6	64.9
Nitroammophoska 16:16:16	$(NPK)_{45}$ – in autumn	18.0	775.1	16.0	61.3
	$(NPK)_{60}$ – in autumn	18.9	868.0	17.2	67.1
	$(NPK)_{75}$ – in autumn	20.0	827.2	18.6	67.1
	$(NPK)_{90}$ – in autumn	21.0	805.8	19.2	66.9
	$(NPK)_{30}$ – in autumn + $(NPK)_{30}$ – in spring	17.8	844.7	17.1	62.8
	$(NPK)_{45}$ – in autumn + $(NPK)_{45}$ – in spring	18.5	822.2	17.6	64.0
LSD_{05} for fertilizer type		0.8	37.2	0.3	1.8
LSD_{05} for fertilizer dose		1.5	24.3	0.5	2.2

The density of generative shoots of *Festulolium* of the second year of life was higher in the variants with fertilization – in the variants with ammonium nitrate and nitroammophoska application it reached 762–853 and 775–868 pcs m^{-2}, respectively; in the control variant this index was by 16–26% lower. However, the increase of doses of both nitrogen and compound fertilizer above 60 kg ha^{-1} of AI did not increase the amount of generative shoots (Table 2).

Mineral fertilizers application increased the size of ears. Their length in the control variant was 16 cm, whereas in the variants with ammonium nitrate and nitroammophoska application it reached 17.1–19.7 cm and 18–21 cm, respectively, i.e. the length of ears were by 11.4–13.2% longer as compared to control variant without fertilizers application. This trend was registered throughout four years of *Festulolium* seed crop life.

Mineral fertilizers application increased the amount of spikelets in a ear by 1.4–4.8 pcs due to more intensive nutrition of generative organs during the period of their growth, flowering and seed formation.

It has been found experimentally that in order to obtain high yielding non-lodged or slightly lodged *Festulolium* grass sward nitrogen fertilizers should be applied in autumn period during sowing or after harvesting of *Festulolium* vegetative mass (i.e. in mid-September) at a dose of 60 kg ha^{-1} of AI.

In our experiments *Festulolium* seed harvest directly depended on the amount of generative shoots per crop area unit and on inflorescence seed content (Table 3).

Table 3. The Influence of Fertilizers on *Festulolium* Seed Harvest in Plantings of Different Year of Life (2009–2011 period average)

Fertilizer type	Dosage of fertilizer, kg ha^{-1} of AI	Year of life		
		Year 2	Year 3	Year 4
	Control (without fertilizers)	410.7	192.0	154.6
Ammonium nitrate	N_{45} – in autumn	489.4	206.4	180.5
	N_{60} – in autumn	591.4	253.3	223.4
	N_{75} – in autumn	540.3	224.5	207.9
	N_{90} – in autumn	514.3	212.6	200.8
	N_{30} – in autumn + N_{30} – in spring	559.7	241.5	208.8
	N_{45} – in autumn + N_{45} – in spring	568.3	246.9	213.8
Nitroammophoska 16:16:16	$(NPK)_{45}$ – in autumn	513.4	247.0	197.9
	$(NPK)_{60}$ – in autumn	620.5	272.5	240.9
	$(NPK)_{75}$ – in autumn	565.8	244.0	227.5
	$(NPK)_{90}$ – in autumn	538.5	230.1	222.6
	$(NPK)_{30}$ – in autumn + $(NPK)_{30}$ – in spring	586.1	260.0	228.0
	$(NPK)_{45}$ – in autumn + $(NPK)_{45}$ – in spring	591.7	271.9	230.8
LSD_{05} for fertilizer type		27.9	14.3	15.7
LSD_{05} for fertilizer dose		24.1	12.1	12.9

Seed harvest in the control variant (without fertilizers) was 410.7 kg ha^{-1}. In the variants with autumn application of nitrogen fertilizers (N_{30}–N_{90}) seed harvest of *Festulolium* plantings of the second year of life increased as compared to control by 16.1–30.6% and totaled from 489.4 to 591.4 kg ha^{-1}. In the variants with nitroammophoska application seed harvest was even higher (by 19.9–35.5% as compared to control) and totaled from 513.4 to 620.5 kg ha^{-1}.

The applied fertilizers practically did not affect sowing qualities of *Festulolium* seeds. Laboratory germination varied from 93 to 95% and the mass of 1,000 seeds was 2.91–2.99 g.

Production cost of 100 kg of *Festulolium* seeds was the lowest (43,000 rubles) and the level of profitability of their production was the highest (179%) in the variants with N_{60} application. It was also rather high (145%) in the variants with $(NPK)_{60}$ application.

CONCLUSIONS

The authors draw following conclusions from the results of research of winter hardiness, growth and seed productivity of *Festulolium* in dependence on fertilizer application system in climatic conditions of the forest-steppe of the Central Chernozem Region conducted in 2009–2011.

1. Agroclimatic conditions of the forest-steppe of the Central Chernozem Region are favorable for seed production of VIK–90 *Festulolium* variety. During all years of study in the variants with mineral fertilizers application the amount of overwintered plants reached 84.9–88.9%. Mineral fertilizers application, including nitrogen ones, improved winter hardiness of *Festulolium* plantings by 3.2–7.2%.

2. In the year of sowing *Festulolium* plantings are characterized by slow growth and development without generative shoots forming. Nitrogen and compound fertilizers increase the duration of vegetation period of plantings in the second year of life by 3–8 days, especially in spring tillering and shooting stages. Generally the period from spring regeneration to complete ripeness in the second year of life amounted 99–107 days, in the third and fourth years of life it continued 95–103 days.

3. Autumn application of ammonium nitrate (N_{60}) or nitroammophoska (NPK_{60}) provides the formation of higher seed harvest of *Festulolium* plantings of the second year of life from 591.4 to 620.5 kg ha^{-1}. In the following years *Festulolium* seed productivity decreases by 2.3–2.7 times. Mineral nitrogen application at a dose of 30 kg ha^{-1} of AI before autumn and spring grass tillering increases seed harvest by 31.4–37.2%.

4. In economic terms it is advisable to apply ammonium nitrate at a dose of 60 kg ha^{-1} of AI once a year in the fall. In this variant the highest notional farm net income of RUB 43,000 per hectare and profitability level of 179% can be obtained.

REFERENCES

Cougnon, M., De Swaef, T. & Lootens, P. 2017. In situ quantification of forage grass root biomass, distribution and diameter classes under two N fertilization rates. *Plant and soil* **411**(1–2), 409–422.

Griffiths, D., Roberts, G. & Spichkin, I. 1971. *Fundamentals of seed forage grasses*. Moscow, Kolos, 182 pp. (in Russian).

Gutmane, I. & Adamovics, A. 2005. Use of *Festulolium* and *Lolium x boucheanum* for forage and seed production. In*: 13th International Occasional Symposium of the European Grassland Federation.* European Grassland Fed., Tartu, pp. 503–506.

Gutmane, I. & Adamovics, A. 2012. *Festulolium* (× *Festulolium* Asch & Graebn.) and hybrid ryegrass (*Lolium* × *boucheanum* Kunth.) seed yield formation at two N fertiliser' rates in Latvian climatic conditions. In*: 24th General Meeting of the European Grassland Federation*. Ministerstwo Rolnictwa Rozwoju Wsi., Lublin, pp. 520–522.

Gutmane, I. & Adamovics, A. 2012. *Festulolium* (× *Festulolium* Asch & Graebn.) and hybrid ryegrass (*Lolium* × *boucheanum* Kunth.) seed production. In*: Conference on Research for Future of Latvia Agriculture – Food, Feed, Fiber and Energy*. Latvia Univ Agr, Fac Agr., Jelgava, pp. 60–64.

Jansons, F. 1978. *Perennial herbs in the north-western zone.* Leningrad, Kolos, 216 pp. (in Russian).

Mastalerczuk, G., Borawska-Jarmulowicz, B. & Kalaji, H. 2017. Gas-exchange parameters and morphological features of *Festulolium* (*Festulolium braunii* K. Richert A. Camus) in response to nitrogen dosage. *Photosynthetica* **55**(1), 20–30.

Meerovsky, A. & Kovalets, G. 2008. *Festulolium* is a new fodder crop. *Belarusian agriculture* **7**(75), 32–33.

Methodological Instructive Regulations on the Conducting of Research in Seed Production of Perennial Grasses. 1989. Moscow, VIK, 135 pp. (in Russian).

Mikhailichenko, B. 1987. *Industrial Seed Production of Perennial Herbs in the Non-Black Soil Region*. Moscow, VIK, 142 pp. (in Russian).

Mikhailichenko, B., Perepravo, N. & Ryabova, V. 1999. *Seed production of perennial grasses. Practical recommendations on mastering the seed production technology of the main species of perennial grasses*. Moscow, Rosselkhozizdat, 143 pp. (in Russian).

Perepravo, N. 2013. *Agroecological seed production of perennial grasses*. Moscow, State Agrarian University of Russia, 54 pp. (in Russian).

Perepravo, N. & Ryabova, V. 2012. *Cultivation and use of a new fodder culture – Festulolium – for fodder and seeds: a methodical manual*. Moscow, Russian State Agrarian University, 26 pp. (in Russian).

Rogov, M. 1989. *Perennial grasses*. Moscow, Agropromizdat, 45 pp. (in Russian).

Schuppenies, R. 1988. Vergleich von Wiesenschweidel und Ausdauerndem Weidelgras bei unterschiedlicher Stickstoffdungung. *Zuchtung und Anbau von Wiesenschweidel* **5**, 111–130.

Smelov, S. 1966. *Theoretical Foundations of Meadow Management*. Moscow, Kolos, 367 pp. (in Russian).

Zolotarev, V. 2008. *Ecological biological and technological fundamentals of tilling Ryegrass*. Astana, 736 pp. (in Russian).

Zolotarev, V. 2007. Scientific principles of production and harvesting of highly productive seed agrophytocenoses of fodder crops. In*: Feed production: Problems and solutions*. VIK, Moscow, pp. 404–417 (in Russian).

Agronomy Research **16**(3), 854–861, 2018
https://doi.org/10.15159/AR.18.140

Irradiation level affects fluctuating asymmetry value of bilateral traits of cucumber in juvenile phase

S. Rakutko[1,*], E. Rakutko[1], A. Avotins[2] and K. Berzina[2]

[1]Institute for Engineering and Environmental Problems in Agricultural Production (IEEP), 3 Filtrovskoje Shosse, RU196625, p.o. Tiarlevo, Saint-Petersburg, Russia
[2]Institute of Industrial Electronics and Electrical Engineering, Riga Technical University, 1 Kalku street, LV-1658 Riga, Latvia
[*]Correspondence: sergej1964@yandex.ru

Abstract. Light is an important factor of the plant's environment. The aim of research was to confirm the hypothesis on the influence of different irradiation levels on the fluctuating asymmetry (FA) value of bilateral traits of plants cultivated in the indoor plant lighting. The object of research was the plants of cucumber (*Cucumis sativus L*) as one of the main glasshouse crops. Young 14-day-old cucumber plants in the first true leaf phase were studied. Different irradiation levels (15.0, 22.5 and 30 W m^{-2}) were maintained by fluorescent lamps. An essential asymmetry of bilateral structures in plants grown under different irradiation levels was observed. It was found that statistically significant lower values of FA, that is greater stability of plant development, correspond to increased plant performance. When the irradiation level was switched from 15 to 30 W m^{-2} (by 100%), the FA index for different bilateral structures varied by different amount: in terms of cotyledons mass it decreased from 0.046 to 0.032 relative units (by 30.2%), in terms of chlorophyll content in cotyledons it increased from 0.038 to 0.073 relative units (by 88.6%). In some bilateral structures the FA index variation was rather small: in terms of the cotyledon area it was zero, in terms of the cotyledon thickness – by 1.8%. It was experimentally prove through the example of cucumber plants that FA index could be used as an indicator of plant developmental stability, characterizing the deviations of the growing environment parameters from the normal state in the indoor cultivating.

Key words: indoor plant lighting, developmental stability.

INTRODUCTION

An important scientific trend, which has been formed at the intersection of biological sciences, is the study how environment affects the individual development (ontogeny) of plants. Investigations in this area should address the issues of quantitative assessment of the relationship between the indices of plant life activity and the environmental factors in ontogeny. The level of irradiation in the range of photosynthetically active radiation (PAR) is an important environmental factor, with which the plants, being organisms with sessile mode of life, is forced to coordinate the processes of their growth and development (Smith, 1982).

In natural conditions, the ambient light changes continuously due to the changing position of the Sun above the horizon throughout the day and the year. Under the indoor plant lighting conditions, the control of irradiation modes provides an opportunity to influence both individual physiological processes in the plant and the plant developmental stability in general (Wheeler, 2008). The latter manifests itself in the interaction of random events in the plant organism and their ability to follow accurately the programme inherent in the genotype, resisting the environmental impacts in the process of development in order to form the optimal phenotype. Accordingly, the inadequate quality of the growing medium leads to developmental instability (Venâncio et al., 2016).

The most striking manifestation of the stable development of a biological object at the macro level is the phenomenon of fluctuating asymmetry (FA), consisting of minor and random deviations of the parameters of bilateral (mirror) morphological structures (Moller & Swaddle, 1997; Graham et al., 2010). Such structures are cotyledons, halves of simple leaves, opposite leaflets of compound leaves, needles of conifers in the whorl, petals of flowers, seed pod walls, and opposite leaves.

The symmetry breaking is identified by comparing the different parameters of bilateral traits (Daloso, 2014). The FA level is minimal only under optimal environmental conditions; it increases under any stress impacts (Zakharov, 1992; Palmer & Strobeck, 2003). In a number of studies it was found that the FA index is closely correlated with the quality of plant growing environment, both natural (Alados et al., 2001; Milligan et al., 2008; Veličković, 2010) and controlled (Kuznetsova et al., 2013). Therefore, it can be used as an indicator of the developmental stability of an organism, characterizing even subtle deviations in the ambient parameters, irradiation in our case, from the background state. Other studies show, however, the absence of environmental influence on FA (Bjorksten et al., 2000; Veličković & Perišić, 2006; Sandner & Matthies, 2017; Zverev et al., 2018).

Assumption that non-optimality of irradiation parameters affecting the plants is a stress factor makes it possible to use the level of FA as a plant status indicator in order to estimate the effectiveness and ecological compatibility of the indoor plant lighting, with due account for the irradiation quality (Rakutko et al., 2017).

For natural plant growing conditions, the interrelation between the level of plant FAs and the stress and quality of environment is described in numerous scientific publications (Tucić & Miljković, 2010; Silva et al., 2016; Venâncio et al., 2016), while for the indoor plant lighting more detailed research is still needed.

The aim of research was to test the hypothesis on the influence of different irradiation levels on the value of FA of bilateral traits of plants cultivated in the indoor plant lighting.

MATERIALS AND METHODS

Cucumber (*Cucumis sativus* L) was chosen for the investigations as one of the main greenhouse crops. To optimise its cultivation conditions for higher yields is a topical task for modern greenhouse complexes. Several periods are identified in the ontogenesis of cucumber, based on a set of morphological and morpho-physiological characters and histological signs. The early periods and age states are of particular interest. These are the latent period, with the age state being a seed, and the pre-generative period with two age states: (1) a sprout with heterotrophic mode of nutrition, starting from the seed planting and ending with the emergence of the folded cotyledons over the substrate surface; (2) a sprout with mesotrophic nutrition ending with the appearance of the 1st true leaf. Then comes the juvenile plant from the 1st to the 2nd true leaf; the immature plant, from the 2nd to the 4th leaf, and the virginile plant, from the 4th to the 9th leaf (Vasilevskaya, 1991).

In the pre-generative period of ontogenesis, the internal structures of a plant organism are formed; therefore, the study of growth and development processes during this period depending on environmental factors at the whole organism level is of both theoretical and practical interest.

The plants were grown on peat, the acidity of which was neutralised with dolomite meal to pH of 6.0. One kg of peat included the following mineral nutrients: K_2O – 330.2 mg, P_2O_5– 42.8 mg, CaO – 151.6 mg, mgO – 102.8 mg, N_2O_5 – 63.1 mg. The seeds of middle-early cucumber hybrid Safaa F1, were sown on February 14, 2017 to a depth of 1 cm under the 5 x 5 cm pattern. Fully sprouted cucumbers appeared on the fourth day – February 17, 2017. From February 21, 2017, the photoperiod of 16 hours was set from 07.00 to 23.00. On the ninth day, February 22, 2017, the unfolding of the first true leaf was registered. The growing was stopped on the 14th day, February 27, 2017, when the second true leaf appeared.

A comparative experiment was carried out in the three zones of the laboratory room, separated by a light-tight curtain. The air temperature of +26 °C and humidity 65–72% were maintained by an automatic control system. The moisture content of the substrate was 70%; the soil temperature was + 25–26 °C. Irradiators of the own design with fluorescent lamps L 58W / 77 Fluora OSRAM and PHILIPS MASTER TL–D Xtra 58W / 840 we used. The radiation spectrum of the light sources was characterised by approximately equal flux share in blue, green, and red bands of PAR. Different levels of irradiation (15.0, 22.5 and 30 Wm^{-2}) during the experiment in the growing zones were ensured by maintaining the required height of the irradiator suspension over the tops of the plants.

The length (L_L, R_L) and the width (L_W, R_W) of the left and right cotyledons, respectively, were used as metric parameters. The length of the secondary leaf veins from the base of the blade to their forking (first trait L_1, R_1), the distance from the forking to the leaf apex (second trait L_2, R_2) and the distance from the leaf apex to the characteristic points on the leaf edge (third trait L_3, R_3) were measured on the left and right half of the leaf, correspondingly. In addition, the chlorophyll meter CCM-200 determined the chlorophyll content index in the cotyledons (L_{cc}, R_{cc}) and on the sides of the leaf (L_{cl}, R_{cl}) in CCI relative units; mass (L_{mc}, R_{mc}), thickness (L_T, R_T) and area (L_S, R_S) of the cotyledons, as well as the mass M_L and area of the leaves S_L were measured. 40 plants from each container were used for measurements.

Linear dimensions were measured on the images obtained by the Power Five Evo camera using the XnView program. The data were processed by mathematical statistics methods ($P < 0.05$) using Excel 2003 and Statistica 6.0 software packages.

RESULTS AND DISCUSSION

Even preliminary analysis of the data obtained showed fairly high frequency of asymmetric signs in cucumber plants grown under different levels of irradiation. The frequency values of a number of traits increased monotonically with higher irradiation level (cotyledon length – from 0.73 to 0.90, chlorophyll content in individual cotyledons – from 0.80 to 0.90, chlorophyll content in the leaf halves – from 0.50 to 0.71).

The values of biometric indicators and the level of FA for individual bilateral traits are shown in Table 1. The meaning of ΔP is how much the value of the parameter P changes with a change in the irradiance level from 15.0 to 30.0 W m^{-2}.

Table 1. The values of biometric indicators and the level of FA for individual bilateral traits

Bilateral traits (indicators)	Parameters *P*	Irradiation, W m^{-2}			ΔP, %
		15.0	22.5	30.0	
1. Cotyledon width (L_W, R_W), mm	$\bar{X} \pm \sigma$	23.93 ± 1.42	24.62 ± 1.69	22.59 ± 2.43	-5.6
	FA	0.028	0.020	0.040	42.3
2. Cotyledon length (L_L, R_L), mm	$\bar{X} \pm \sigma$	41.62 ± 2.60	42.00 ± 3.11	40.04 ± 3.72	-3.8
	FA	0.024	0.027	0.033	35.5
3. Cotyledon area (L_S, R_S), cm^2	$\bar{X} \pm \sigma$	6.88 ± 0.93	7.04 ± 1.00	6.07 ± 1.11	-11.8
	FA	0.071	0.060	0.071	0.0
4. Cotyledon mass (L_{mc}, R_{mc}), g	$\bar{X} \pm \sigma$	0.36 ± 0.04	0.46 ± 0.05	0.39 ± 0.05	8.3
	FA	0.046	0.021	0.032	-30.2
5. Cotyledon thickness (L_T, R_T), mm	$\bar{X} \pm \sigma$	0.81 ± 0.05	0.80 ± 0.05	0.84 ± 0.05	3.7
	FA	0.019	0.017	0.019	1.8
6. Cotyledon CCI (L_{cc}, R_{cc}), rel.u.	$\bar{X} \pm \sigma$	85.28 ± 10.26	103.46 ± 13.53	120.47 ± 15.84	41.3
	FA	0.038	0.046	0.073	88.6
7. Leaf first trait (L_1, R_1), mm	$\bar{X} \pm \sigma$	14.00 ± 2.22	16.23 ± 2.70	18.16 ± 3.13	29.7
	FA	0.055	0.042	0.066	19.2
8. Leaf second trait (L_2, R_2), mm	$\bar{X} \pm \sigma$	26.34 ± 2.82	29.93 ± 4.46	31.95 ± 4.31	21.3
	FA	0.095	0.118	0.097	3.0
9. Leaf third trait (L_3, R_3), mm	$\bar{X} \pm \sigma$	25.36 ± 3.02	30.20 ± 4.92	32.68 ± 5.42	28.9
	FA	0.042	0.047	0.038	-9.3
10. Leaf CCI L_{cl}, R_{cl}), rel.u.	$\bar{X} \pm \sigma$	30.95 ± 2.31	37.65 ± 5.51	39.69 ± 6.65	28.2
	FA	0.069	0.062	0.059	-13.7
11. Leaf mass M_L, g	$\bar{X} \pm \sigma$	0.35 ± 0.05	0.50 ± 0.09	0.65 ± 0.12	85.7
12. Leaf area S_L, cm^2	$\bar{X} \pm \sigma$	12.12 ± 2.43	16.51 ± 4.22	20.30 ± 4.63	67.5

At the same time, other traits demonstrated the biggest values (the width of the cotyledons, their mass, area and thickness, the geometric dimensions of the leaf). Nonparametric methods of statistical analysis were applied. Most of the leaf traits had a normal distribution, except for the third trait in plants in the first experimental room zone.

The analysis revealed fluctuations in the asymmetry of traits around the zero mean that is a diagnostic sign of FA. Anti-symmetry in the analyzed traits was not observed.

Using the Spearman rank correlation coefficient, a statistically significant ($p < 0.05$) correlation was revealed between the asymmetry value of the trait and its average size for a number of traits.

Therefore, to calculate the value of FA, the normalizing formula was applied:

$$FA_i = \frac{1}{N}\sum_{i=1}^{N}\frac{|L_i - R_i|}{(L_i + R_i)} \qquad (1)$$

where L_i – the value of the i-th trait for the bilateral structure on the left; R_i – the value of the i-th trait for the bilateral structure on the right; N – the number of measurements.

Significant correlation of traits between each other was revealed; therefore, FA values for individual traits were used for the analysis, without applying the complex index. Various environmental stress factors can influence different traits of FA in various ways (Roy & Stanton, 1999).

Analysis of Table 1 shows that when the irradiation level was switched from 15 to 30 W m^{-2} (by 100%), the FA index for different bilateral structures varied by different amount: in terms of cotyledons mass it decreased by 30.2%, in terms of chlorophyll content in cotyledons it increased by 88.6%.

However, in some bilateral structures, the FA level did not change: for the cotyledon area, ΔFA = 0%, for the cotyledon thickness ΔFA = 1.8%.

The above Table also presents the average values of the measured biometric indicators with the standard deviation of each indicator. Differences between the largest and smallest values of all indicators are statistically significant ($p < 0.05$).

It is of interest to identify the relationship between the FA level and the plant performance. Fig. 1 shows the dependence of the average cotyledon mass on the irradiation level. Fig. 2 shows the dependence of the FA level in terms of cotyledon mass on the irradiation level.

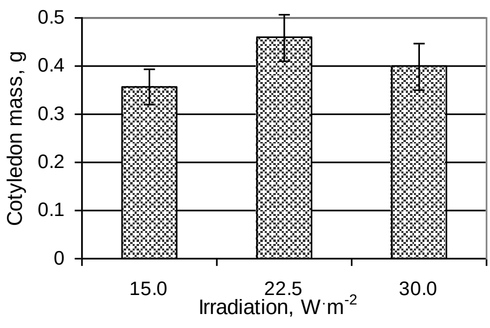

Figure 1. Dependence of the average cotyledon mass on the irradiation level.

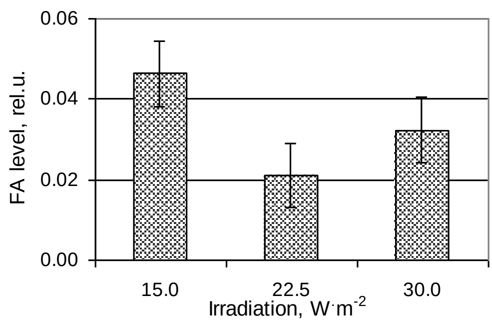

Figure 2. Dependence of the FA level in terms of cotyledon mass on the irradiation level.

It was found that statistically significant lower values of FA, that is greater stability of plant development correspond to increased plant performance in terms of raw mass of cotyledons. Plant signaling systems control their development depending on environmental conditions. Light is the most important environmental factor, the regulatory role of which is to ensure the growth and development of plants. The photosynthesis processes play a significant role in the life support system for plants. These processes are very sensitive to any changes in environmental factors, even slight ones (Darko et al., 2014).

Under heterotrophic nutrition, during the sprout stage, intensification of physiological processes under the influence of environmental factors increases the rate of metabolite efflux from the cotyledons. With the involvement of autotrophic nutrition, the processes of synthesis start along with dissimilation, and therefore the factors of the light environment are of paramount importance. When the structural and functional state of the organism becomes more complex, one of the criteria for becoming self-organised is to change the nature of the links with environmental factors from passive proportional response to differentiated perception (Belousov, 1987). In favour of the latter is the mere fact that there exist optimal values of factors, including illumination.

According to one of the approaches, the optimal parameters are those parameters of the environment under which the minimum duration of ontogeny stages is observed. Thus, for cucumber plants in juvenile and immature age states under all temperatures, the illumination of 10 kLx was found optimal by this criterion. If the accumulation rate of dry mass is taken as the growth index, then the optimal illumination is 25 kLx (Sysoeva, 1991)

In this study, the accumulation of green mass, characterized by a number of biometric indicators, was taken as a measure of the growth process intensity. Plant developmental stability was assessed by the FA index of bilateral structures. Usually this indicator is applied to the right and left halves of one leaf (Kaligarič et al., 2008).

It was assumed that the impact of environmental factors would result in greater asymmetry in the development of more distance-separated bilateral structures, which were nevertheless under the same conditions. So in this study the parameters of cotyledon were measured.

CONCLUSIONS

1. As a result of the study, a significant asymmetry of bilateral structures in juvenile cucmber plants, grown under different irradiation levels, was revealed. Frequency of asymmetry in individual structures reached 90%.

2. The asymmetry of bilateral traits was found non-directional, with the anti-symmetry not in place. This allowed classifying the observed asymmetry as fluctuating.

3. Significant correlation between individual bilateral traits was revealed. This provides an opportunity for a well-grounded choice of one specific trait or their combination to characterize the FA. The size-dependence of some traits was also revealed.

4. It was found that statistically significant lower values of FA, that is greater stability of plant development, correspond to increased plant performance in terms of raw mass of cotyledons. This confirms the original hypothesis that bigger values of FA are observed under conditions, which are less favourable for plants.

5. Using the example of cucumber plants, it was experimentally proved that FA indexes can be used to assess the quality the light environment for plant indoor cultivation.

ACKNOWLEDGEMENTS. Publication is created with support of European Regional Development Fund project ‘New control methods for energy and ecological efficiency increase of greenhouse plant lighting systems (uMOL)’, Grant Agreement Nr. 1.1.1.1/16/A/261.

REFERENCES

Alados, C.L., Navarro, T., Escos, J., Cabezudo, B. & Emlen, J.M. 2001. Translational and fluctuating asymmetry as tools to detect stress in stress–adapted and nonadapted plants. *International Journal of Plant Sciences* **162**(3), 607–616.

Belousov, L.V. 1987. *Biological morphogenesis*. MSU, Moskva, 239 pp. (in Russian).

Bjorksten, T., David, A.P. & Pomainkowski, A. 2000. Fluctuating asymmetry of sexual and non–sexual traits in stalkeyed files: a poor indicator of developmental stress and genetic quality. *Journal of Evolutionary Biology* **13**, 89–97.

Daloso, D.M. 2014. The ecological context of bilateral symmetry of organ and organisms. *Natural Science* **6**(4), 184–190.

Darko, E., Heydarizadeh, P., Schoefs, B. & Sabzalian, MR. 2014 Photosynthesis under artificial light: the shift in primary and secondary metabolism. *Philosophical Transactions of the Royal Society* B 369: 2013024.

Graham, J.H., Raz, S., Hel–Or, H. & Nevo, E. 2010. Fluctuating asymmetry: methods, theory, and applications. *Symmetry* **2**, 466–540.

Kaligarič, M., Tognetti, R., Janžekovič, F. & Raschi, A. 2008. Leaf fluctuating asymmetry of *Myrtus Communis L.*, affected by increases in atmospheric CO2 concentration: evidence from a natural CO2 spring. *Polish Journal of Environmental Studies* **17**(4), 503–508.

Kuznetsova, E.A., Chelpanov, O.M., Belova, E.E., Hotuleva, O.V. & Kolontzov, A.A. 2013. Evaluation of the influence of cadmium ions on the fluctuating asymmetry of the leaves of a cucumber inoculum (*Cucumis Sativus L.*). *Vestnik MGOU* **2**, 1–9 (in Russian).

Milligan, J.R., Krebs, R.A. & Mal, T.K. 2008. Separating developmental and enviromental effects on fluctuating asymmetry in *Lythrum salicaria* and *Penthorum sedoides. International Journal of Plant Sciences* **169**(5), 625–630.

Moller, A.P. & Swaddle, J. 1997. *Asymmetry, Developmental stability, and Evolution.* Oxford University Press, Oxford, 302 pp.

Palmer, A.R. & Strobeck, C. 2003. Fluctuating asymmetry analysis revisited. In Polak, M. (ed.): *Developmental instability (DI): causes and consequences.* Oxford University Press, New York, pp. 279–319.

Rakutko, S.A., Rakutko, E.N., Kaposhko, D.A., Vaskin, A.N. & Tranchuk, A.S. 2017. Influence of light quality on fluctuating asymmetry of bilateral traits of forced parsley leaves. In *Engineering for Rural Development*. *The 16-th International Scientific Conference.* Latvia University of Agriculture, Latvia, pp. 42–47.

Roy, B.A. & Stanton, M.L. 1999. Asymmetry of wild mustard, *Sinapsis arvensis* (*Brassicaceae*), in response to severe physiological stresses. *Journal of Evolutionary Biology* **12**, 440–449.

Sandner, T.M. & Matthies, D. 2017. Fluctuating asymmetry of leaves is a poor indicator of environmental stress and genetic stress by inbreeding in Silene vulgaris. *Ecological Indicators* **79**, 247–253.

Silva, H.V., Alves–Silva, E. & Santos, J.C. 2016. On the relationship between fluctuating asymmetry, sunlight exposure, leaf damage and flower set in Miconia fallax (Melastomataceae). *Tropical Ecology* **57**(3), 419–427.

Smith, H. 1982. Light quality, photoperception, and plant strategy. *Annual Review of Plant Physiology* **33**, 481–504.

Sysoeva, M.I. 1991. *The influence of environmental factors on the growth and development of cucumber plants in the early stages of ontogeny: a multidimensional approach.* Extended abstract of Cand. Sc. (Biology) dissertation. Petrozavodsk, 21 pp. (in Russian).

Tucić, B. & Miljković, D. 2010. Fluctuating asymmetry of floral organ traits in natural populations of *Iris pumila* from contrasting light habitats. *Plant species Biology* **25**, 173–184.
Vasilevskaya, N.V. 1991. *Ontogenetic reactions of Cucumis Sativus L. to the action of the temperature factor*. Extended abstract of Cand. Sc. (Biology) dissertation. MSU, Moskva, 23 pp. (in Russian).
Veličković, M. 2010. Reduced developmental stability in *Tilia cordata* leaves: effects of disturbed environment. *Periodicum Biologorum* **112**(3), 273–281.
Veličković, M. & Perišić, S. 2006. Leaf fluctuating asymmetry of common plantain as an indicator of habitat quality. *Plant Biosystem* **140**(2), 138–145.
Venâncio, H., Alves–Silva, E. & Santos, J.C. 2016. Leaf phenotypic variation and developmental instability in relation to different light regimes. *Acta Botanica Brasilica* **30**(2), 296–303.
Wheeler, R.M. 2008. A historical background of plant lighting: an introduction to the workshop. *HortScience* **43**(7), 1942–1743.
Zakharov, V.M. 1992. Population phenogenetics: analysis of developmental stability in natural populations. *Acta Zoologica Fennica* **191**, 7–30.
Zverev, V, Lama, A.D. & Kozlov, M.V. 2018. Fluctuating asymmetry of birch leaves did not increase with pollution and drought stress in a controlled experiment. *Ecological Indicators* **84**, 283–289.

Agronomy Research **16**(3), 862–871, 2018
https://doi.org/10.15159/AR.18.147

Changes in composition and spatial distribution of knowledge-based economy in rural areas of Latvia

B. Rivza, M. Kruzmetra and L. Sunina

Latvia University of Life Sciences and Technologies Faculty of Economics and Social Development, Institute of Economics and Regional Development, 18 Svetes street, LV-3001 Jelgava, Latvia
Correspondence: swonders@apollo.lv

Abstract. One of the features in the 21st century is growth of knowledge-based economic sector, which is referred as new growth theory. New growth theory reflects the attempt to understand the role of knowledge and technology in driving productivity and economic growth. In this view, key factors are investments in research and development, education and training and new managerial work structures. The aim of research is to estimate the composition and geographic location of knowledge economy and its perspectives in rural areas of Latvia in post-crisis stage. A special focus was placed on the mentioned processes in territorial units of the regions – municipalities, as the life of residents is influenced not only by national policies, but also by on-going processes in the administrative territories of local governments. The Eurostat classification of industries was used for the analysis of changes in composition and spatial distribution of knowledge-based economy. Data were processed by quantitative and qualitative statistical analysis, as well as grouping methods. The analysis of the information allows concluding that: municipalities with high and medium-high business is increasing and the business directions with bioeconomic features are the fastest growing ones in terms of composition. It must be stated that the economic growth in the rural territories was greatly affected by the quality of local governance and the fact that local community residents' readiness for active, innovative and inclusive action is strengthened.

Keywords: knowledge-based economy, Eurostat classification of industries, composition and spatial distribution, local governance, local community.

JEL codes: O30, P31, R12.

INTRODUCTION

Expansion of knowledge-based economy sector is treated as a development model or stage in 21th century. 'The knowledge based economy' is an expression coined to describe trends in advanced economies towards greater dependence on knowledge, information and high skill levels, and the increasing need for ready access to all of these by the business and public sectors (OECD, 2005). The classification of economic sectors developed by EUROSTAT clearly indicates, which processing industries and services are a part of the knowledge economy segment (EUROSTAT, NACE Rev.2, 2008), thus opening up the possibilities for current in-depth analysis of the national economy segment.

Firstly, the theoretical basis of the research is a spatial approach to the analysis of the phenomenon, which includes both its territorial disposition and its socio-economic and environmental objective-subjective characteristics and ongoing changes. In general, these processes are characterized by significant sociologists (Sztompka, 1993; Castells, 2000; Macionis, 2004), as well as leading researchers in rural development in Europe (Ploeg J.D. van der, etc., 2000; Woods M., 2012). The abovementioned researchers indicate that developments in the field of rural development at the beginning of the 21st century include multi-level changes in agricultural and public relations, changes in the agricultural sector itself, as well as the combination of various activities within the agricultural sector.

In the 21th century, the question of rural viability and, hence, the optimization of opportunities provided by rural areas has been raised. Researchers focus on the impact of rural space on economic growth, including the knowledge economy, the use of riches provided by the rural environment for the production of organic food and other needs (Chotovinsky & Altmann, 2017; COTER, Territorial impact, 2017; Ronkkoi & Aarrevaara, 2017; etc.).

Secondly, research is based on theoretical understanding of structural changes in economics and a set of practical evidence. The economy functioning in the territory of the state, region, municipality (local territory) is a system consisting of economic activity sectors and industries. The change in the share of sectors and industries in the system reflects the potential directions for the economic development of the territorial unit and points to the tasks to be solved in the first place (Hartwig, 2010; Campligio, 2014; Lankauskiene, 2015; Sipilova, 2015, etc.). The increase in the productivity of economic activity is set as the main desired benefit of structural change is. (Padilla-Perez & Villareal, 2017; Vu, 2017). Research concludes that quantitative and qualitative growth does not occur at the same time – at the beginning there is a quantitative growth and qualitative changes begin and develop only after a certain period of time (Chen et al., 2011). During analysis of the situation, certain steps must be taken: Economic structure → Economic sectors → Economic sector performance → Economic growth (Lankauskiene & Tvaronaviciene, 2013), a successive implementation of which can provide an assessment for the ongoing processes and conclude, whether the structural upgrading has yielded expected results.

A knowledge-based economy together with its formation and functioning processes and its problems has become a significant research field in the whole world. Therefore, rural communities must participate in the knowledge economy to fully utilize the advances in research and development. All types and sizes of rural business must have access to appropriate technology, state-of-the-art connectivity, as well as new management tools to deliver economic, social and environmental benefits (CORK 2.0. Declaration 2016).

A group of researchers working on the development of rural viability analysis and smart development has carried out quantitative growth of the economy in 2009–2016 (Rivza et al., 2016; Rivza et al., 2017; Rivza & Kruzmetra 2017). An extensive evaluation of the knowledge economy segment was performed, the results of which are summarized in this article.

The aim of research is to estimate the composition and geographic location of knowledge economy and its perspectives in rural areas of Latvia in post-crisis stage. A special focus was placed on the mentioned processes in territorial units of the regions – municipalities, as the life of residents is influenced not only by national policies, but also by on-going processes in the administrative territories of local governments.

Methodology and methods: For the analysis of the knowledge economy, the Eurostat methodology for classifying NACE Rev. 2 industries and the Latvian Bioeconomy Strategy 2030 for the classification of bioeconomy have been used. The Latvian Business Register (LURSOFT) data for the period 2009–2016 and Central Statistical Bureau data for the period 2009–2016 were used as information sources. The data were processed by quantitative (growth) and qualitative (structural changes) statistical analysis methods, as well as cluster analysis – the grouping of Latvian municipalities in terms of the composition and spatial structural changes in the segment of high and medium-high technology processing industry. The development of knowledge economy is assessed based on the changes in the number of businesses involved in high-tech (HT) and medium-high tech (MHT) activities and the changes in the share of specific activities.

RESULTS AND DISCUSSIONS

1. Composition changes in the knowledge economy of HT and MHT manufacturing industry segments

Changes in the economy can take place and be evaluated: among sectors, within the sectors, i.e. among industries of the sector, including changes in sector and industry specialization (Palan, 2010). The research part of the present article provides extensive analysis of the knowledge economy, consisting of HT and MHT manufacturing enterprises. This share of 0.9% of the economy in total has increased slightly to 0.98% over the period under review. The study reveals the content of this process.

As shown in the Fig. 1, the growth is observed in all sector groups, but rapid increase can be seen in five of the seven industry groups – in both high-tech groups (C21, C26) and in three medium-high technology groups (C20, C27 and C28). In absolute numbers, the number of hi-tech enterprises in 110 municipalities has increased 2.43 times, while the medium-high technology – 1.77 times. Since C20 and C21 are considered as traditional bioeconomic sectors (Bioeconomic Strategy..., 2017), the authors carried out an internal analysis of the C20 and C21 enterprises for determining the composition. The obtained data indicate that C21 industry had the largest increase in number of pharmaceutical enterprises, but in the case of C20 – among enterprises, specializing in fertilizer and nitrogen compound production, as well as soap and detergent manufacturing enterprises. These trends justify the nomination of a bioeconomy as a significant direction of rural business in Latvia also in the segment of high and medium technology business segment (Pilvere et al., 2016). The data also confirms that Latvia is involved in implementing the EU policy of bio-economic strategy (European Commission, 2017).

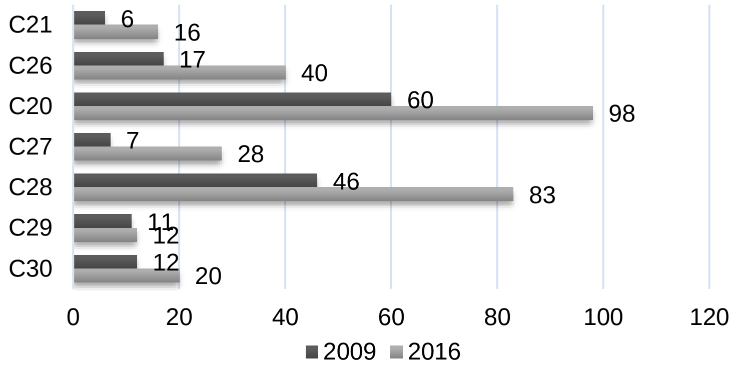

where C21 – manufacture of basic pharmaceutical products and preparations; C26 – manufacture of computer, electronic and optical products; C20 – manufacture of chemicals and chemical products; C27 – manufacture of electrical equipment; C28 – Manufacture of machinery and equipment; C29 – manufacture of motor vehicles, trailers and semi-trailers; C30 – manufacture of other transport equipment.

Figure 1. Increase of knowledge economy enterprises in the rural space of Latvia in 2009–2016 (number of enterprises).
Source: classification of HT and MHT manufacturing industry groups by division of NACE Rev. 2.

Different growth pace in the composition of high and medium-high technology enterprises has also been initiated by changes in the share of enterprises in a particular group. Three directions – C27 Manufacture of electrical equipment, C26 Manufacture of computer, electronic and optical products and C21 Manufacture of basic pharmaceutical products and pharmaceutical preparations have increased their impact (Table 1).

Table 1. Changes in the share of high-tech and medium tech enterprises by their economic activity between 2009 and 2016

	C21	C26	C20	C27	C28	C29	C30	Total
2009	3.8	10.7	37.7	4.4	28.9	6.9	7.5	100.0%
2016	5.4	13.5	33.0	9.4	27.9	4.0	6.7	100.0%
Changes	+1.6	+ 2.8	- 4.7	+ 5.0	- 1.0	- 2.9	- 0.8	

However, this has not changed the situation the dominant sector in high and medium technology group is C20 Manufacture of chemicals and chemical products and C28 Manufacture of machinery etc. As a result, it can be concluded that the group of high and medium-high technology enterprises in the country's rural economy has grown overall and its internal restructuring has taken place in the desired direction.

2. Changes in the spatial location of the knowledge economy in HT and MHT manufacturing industry segment

The analysis of LURSOFT data shows not only the increase in the number of HT and MHT enterprises and the changes in composition within these groups of enterprises, but also the changes in spatial layout. As a result, it is possible to distinguish five municipality groups or clusters, the common feature of which is the existence and absence of a HT and MHT enterprises groups, but different feature – the growth, stagnation or decline of the particular group of enterprises.

In all 110 municipalities of Latvia, the growth of the HT and MHT manufacturing industry group is characterized in 53 municipalities (48.2% of the total number of municipalities – Clusters 2 and 4). In addition, the HT and MHT manufacturing industry group has emerged and continues to function in the post-crisis period in 25 districts (22.7% – Cluster 4). Stagnation has occurred in 14 municipalities (12.7% – Cluster 1), where the HT and MHT manufacturing industry group has been maintained, but expansion has not been achieved. The decline in the significant segment of the national economy has taken place in 11 municipalities (10.0% – Cluster 3). Finally, it should be noted that there are 32 municipalities in Latvia (29.1% – Cluster 5), where the group of such enterprises did not exist at all and has not appeared during post-crisis period. Such processes took place in common rural area of Latvia outside cities of national significance (Fig. 2).

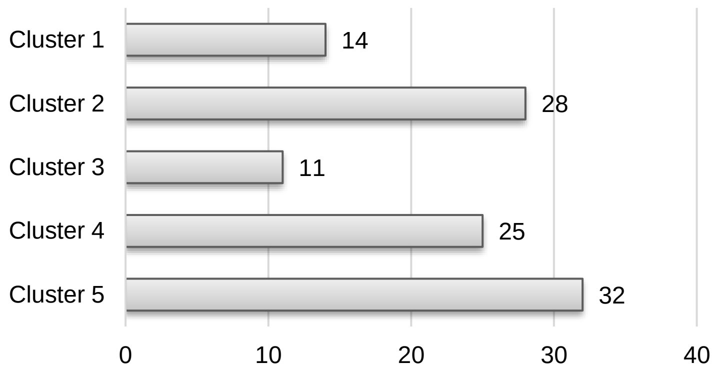

where Cluster 1 – municipalities, where corresponding enterprise group existed in 2009 and continue to work also in 2016, but the number of enterprises over the present period has not changed; Cluster 2 – municipalities, where corresponding enterprise group existed in 2009, but the number of enterprises increased rapidly by 2016; Cluster 3 – municipalities, where corresponding enterprise group existed in 2009, but the number of enterprises decreased or stopped its activity by 2016; Cluster 4 – Municipalities, where corresponding enterprise group did not exist in 2009, but emerged by 2016; Cluster 5 – municipalities, where corresponding enterprise group did not exist in 2009, and has not emerged by 2016.

Figure 2. Spatial view of development processes in enterprises of knowledge economy (year 2016 in comparison to 2009) (number of municipalities).

Territorial differences in the entry of the HT and MHT manufacturing industry into the rural area raise new challenges for further research. It is necessary to answer the questions – what facilitates and what hinders the process? – to what extent they are objective factors (natural environment, geographic location, etc.) and to what extent they are subjective factors (quality of management, citizens' readiness for the new economic model, etc.)? – how to promote knowledge transfer processes from research findings to practical work both in management system and business better?

3. Common and different in the group of HT and MHT enterprises in Zemgale and Kurzeme regions

The analysis of individual regions in previously performed divisions, of course, shows some differences. For comparison, the authors selected HT and MHT group companies of two regions for the analysis of the composition and spatial changes – Kurzeme and Zemgale. Kurzeme and Zemgale regions are spatially encountered, since they are neighboring regions, as well as they both belong to medium-sized regions of Latvia in terms of size and population. Both regions consist of two national cities each and municipalities – eighteen municipalities in Kurzeme, and twenty municipalities in Zemgale. The changes in HT and MHT manufacturing industry composition occurring in these municipalities over the revised period reveal differences.

In the rural area of the Zemgale region, as in all 110 municipalities, the number of HT companies has increased more rapidly than the number of MHT companies (HT – 3.0 times, but MHT – 1.8 times). In the high technology group, two directions stand out – C21 and C26, and two in the medium high technology group – C20 and C28 (Fig. 3).

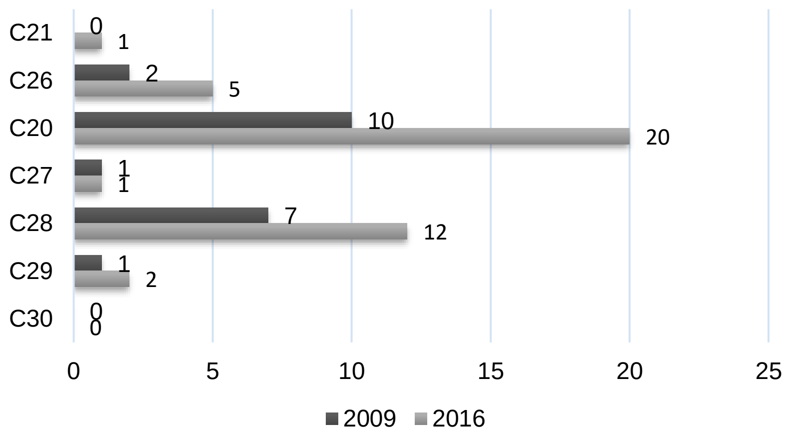

where C21 – manufacture of basic pharmaceutical products and preparations; C26 – manufacture of computer, electronic and optical products; C20 – manufacture of chemicals and chemical products; C27 – manufacture of electrical equipment; C28 – Manufacture of machinery and equipment;, C29 – manufacture of motor vehicles, trailers and semi-trailers; C30 – manufacture of other transport equipment.

Figure 3. Growth of knowledge economy enterprises in the rural area of Zemgale Region in 2009–2016 (number of enterprises).

The analysis of Kurzeme region data shows three differences in comparison with Zemgale region. Firstly, the highest growth was not observed in the HT group (2.5 times), but in the MHT group (3.3 times). This growth rate is almost twice as the average in Latvia. Secondly, the high-technology group consists only of C26 – Manufacture of computer, electronic and optical products, but the group of medium-high technology companies distinguishes three directions – C20, C27 and C28 (Fig. 4). Thirdly, bioeconomic direction is growing more rapidly in Zemgale region, in comparison with Kurzeme region, while in Kurzeme region, compared to Zemgale region, a faster breakthrough is in the production of electrical and mechanical equipment.

where C21 – manufacture of basic pharmaceutical products and preparations; C26 – manufacture of computer, electronic and optical products; C20 – manufacture of chemicals and chemical products; C27 – manufacture of electrical equipment; C28 – Manufacture of machinery and equipment; C29 – manufacture of motor vehicles, trailers and semi-trailers; C30 – manufacture of other transport equipment.

Figure 4. Growth of knowledge economy enterprises in the rural area of Kurzeme Region in 2009–2016 (number of enterprises).

The different growth rates of the composition growth, of course, lead to a change in their share. There are also differences and common features in the process for both regions.

As data show, the largest increase in the share of Zemgale region is for HT companies (C21 and C26), although the majority of HT and MHT companies retain the largest share (even slightly increasing) C20 – Manufacture of chemicals and chemical products, with the decrease of the C28 share (Table 2). In Kurzeme region, HT and MHT companies generally have an increase in the share of only two directions: C26 and C27. C20 dominance remains, but declines by 5.6%. So again, from another aspect of view (the proportion of HT and MHT companies in general), the conclusion can be confirmed that the production of electrical and mechanical equipment is becoming more important in Kurzeme region. At the same time with the growth and restructuring of the HT and MHT processing industry in Zemgale and Kurzeme region, the results of the research showed changes in the spatial arrangement of this processing industry group (Table 3).

Table 2. Changes in the share of high- tech and medium high-tech companies in Zemgale and Kurzeme regions

	C21	C26	C20	C27	C28	C29	C30	Total
Zemgale region								
2009	0.0	9.5	47.6	4.8	33.3	4.8	0.0	100.0%
2016	2.4	12.2	48.8	2.4	29.3	4.9	0.0	100.0%
Changes	**+ 2.4**	**+ 2.7**	**+1.2**	-2.4	-4.0	**+ 0.1**	0.0	
Kurzeme region								
2009	0.0	14.3	50.0	0.0	28.6	7.1	0.0	100.0%
2016	0.0	18.5	44.4	11.1	25.9	0.0	0.0	100.0%
Changes	0.0	**+4.2**	-5.6	**+ 11.1**	-2.7	0.0	0.0	

Table 3. The changes in the spatial distribution of HT and MHT enterprises in Zemgale and Kurzeme regions during 2009–2016

Indicators	Cluster 1	Cluster 2	Cluster 3	Cluster 4	Cluster 5	Total
Changes in the location of enterprises in municipalities of Zemgale region						
2009	7	9	5	0	0	21
2016	7	20	2	12	0	41
The number of municipa-lities	2 municipa-lities	4 municipa-lities	2 municipa-lities	6 municipa-lities	6 municipa-lities	20
Changes in the location of enterprises in municipalities of Kurzeme region						
2009	7	2	5	0	0	14
2016	7	9	3	8	0	27
The number of municipa-lities	3 municipa-lities	2 municipa-lities	2 municipa-lities	7 municipa-lities	4 municipa-lities	18

Source: Calculation by the authors after LURSOFT data,
where Cluster 1 – municipalities, where corresponding enterprise group existed in 2009 and continue to work also in 2016, but the number of enterprises over the present period has not changed; Cluster 2 – municipalities, where corresponding enterprise group existed in 2009, but the number of enterprises increased rapidly by 2016; Cluster 3 – municipalities, where corresponding enterprise group existed in 2009, but the number of enterprises decreased or stopped its activity by 2016; Cluster 4 – Municipalities, where corresponding enterprise group did not exist in 2009, but emerged by 2016; Cluster 5 – municipalities, where corresponding enterprise group did not exist in 2009, and has not emerged by 2016.

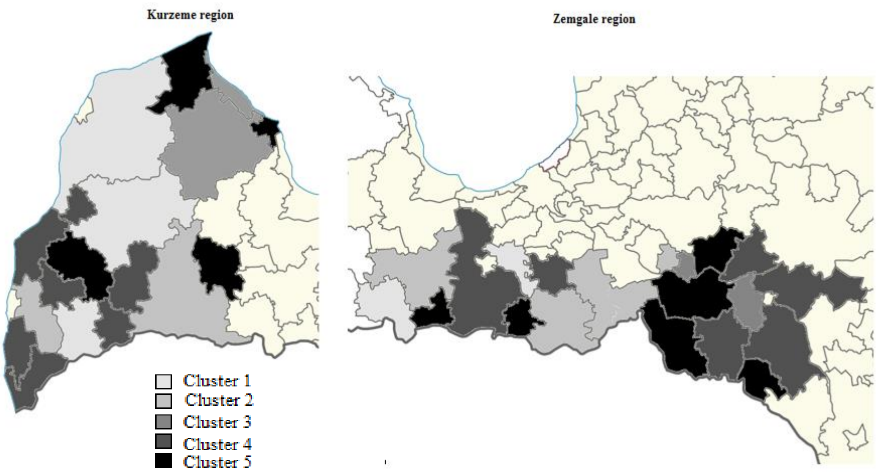

Figure 5. Spatial distribution of HT and MHT manufacturing industry groups in Kurzeme and Zemgale regions.

In terms of spatial analysis, both regions are characterized by two common qualitative features:

- there are municipalities in both regions where the HT and MHT enterprises until 2016 has not entered (Cluster 5);
- both regions have municipalities where in 2009 there were no HT and MHT manufacturing industries, but it has formed by 2016 (Cluster 4).

The difference is in the pace of spatial changes. In Kurzeme region spatial expansion, including new municipalities has occurred more rapidly than in Zemgale region. In Kurzeme region, the number of municipalities where HT and MHT processing enterprises operate over eight-year period has increased from 38.9% to 77.8% of the total number of municipalities, but in Zemgale region – from 40.0% to 70.0%. Within the framework of the research, the spatial expansion of HT and MHT is significant because it confirms that the knowledge-intensive industry does not have the tendency to focus only on selected sites, but it has the opportunity to expand sufficiently widely in rural areas outside large national cities (Fig. 5).

CONCLUSIONS

Changes in the knowledge economy, including high and medium-high technology business, are happening. At the same time, there are also substantial changes in this part of the business. The direction of the bio-economy and the production of innovative equipment in the economy has a tencdency to increase. The high and medium-high technology business is expanding not only in the municipalities where it operated already in 2009, but also expanding spatially, starting its activity in completely new areas. So, the business of high and medium technology is expanding substantially and spatially.

Comparison of data in Zemgale and Kurzeme regions shows that the composition and spatial changes in the processing industry of the knowledge economy result in differences between regions over time. Data analysis for municipalities of Zemgale and Kurzeme region indicates that the process of composition and spatial change in the knowledge economy processing industry takes place within the region as well. There are municipalities where innovation expands in all territory of municipality, there are municipalities where innovations are expanding, but at the same time, there are municipalities where the high and medium-high technology processing industry has never been and does not form a part in the national economy. Therefore, from the scientific as well as the economic point of view, the questions remain: – whether the pace of changes in the processes corresponds to the current requirements; – how justified are the composition and spatial changes in high and medium technology processing businesses; – how this business option in the rural environment is influenced by the readiness of local people for innovative action.

Finding answers to these questions is possible only by developing cooperation between research institutions and scientists in creating synergies for the development of a sustainable and intelligent rural area.

ACKNOWLEDGEMENTS. The research is financially supported by National research programme EKOSOC-LV.

REFERENCES

Bioeconomic Strategy of Latvia. Informative report. (03.05.2017), 10 pp. Access: https://www.zm.gov.lv/public/files/CMS_Discuss_Doc/00/00/00/12/74/ZMZino_31072017_LIBRA.pdf (in Latvian).

Campligio, E. 2014. The structural shift to green services: A two-sector growth model with public capital and open-access resources. *Structural Change and Economic Dynamics* Vol. **30**, pp. 148–161.

Castells, M. 2000. *The Rise of the network Society*. 2nd ed. Blackwell Publishing, Oxford, UK, 594 pp.

Chen, S., Jeffersen, G.H., Zhang, J. 2011. Structural change, productivity growth and industrial transformation in China. *China Economic Review* **22**, 133–150.
Chotovinský, O. & Altmann, V. 2017. Performance analysis of biodegradable municipal solid waste collection in the Czech Republic. *Agronomy Research* **15**(4), 1559–1570.
CORK 2.0. Declaration 2016. A Better Life in Rural Areas. Access: https://ec.europa.eu/agriculture/events/rural-development-2016_en
COTER. 2017. Territorial Impact Assessment. Smart specialisation. Brussels, 3.03.2017. Access: http://cor.europa.eu/en/events/Documents/COTER/TIA/smart-specialisation.pdf
European Commission. 2017. Review of the 2012 European Bioeconomy StrategyLuxembourg: Publications Office of the European Union.
EUROSTAT. 2008. NACE Rev. 2 .Statistical classification of economic activites in the European Community. Luxembourg: Office for Official Publications of the European Communities http://ec.europa.eu/eurostat/documents/3859598/5902521/KS-RA-07-015-EN.PDF
Hartwig, J. 2010. Testing the growth effects of structural change, KOF Working Papers No. **264**, Zurich.
Lankauskiene, T. & Tvaronaviciene, M. 2013. Economic Sector Performance and Growth: Contemporary Approaches in the Context of Sustainable Development. *Intellectual Economics*, Vol. **7**, **3**(17), 355–374 doi:10.13165/IE-13-7-3-07
Lankauskiene, T. 2015. *Economic Structure and Economic Growth Evaluation. Doctoral Dissertetition*. Vilnius Gediminas Technological University, Vilnius 'Technica', pp.37–44.
Macionis, J. 2004. *Society: the Basics*. Pearson, 544 pp.
OECD 2005. *The Measurement of Scientific and Technological Activities Guidelines for Collecting and Interpreting Innovation Data: Oslo Manual, Third Edition*, 71 pp. Access: https://stats.oecd.org/glossary/detail.asp?ID=6871
Padilla-Perez, R. & Villareal, F.G. 2017. Structural change and productivity growth in Mexico, 1990–2014. *Structural Change and Economic Dynamics* **41**, 53–63.
Palan, N. 2010. Measurement of specialization. The choice of indices. *FIW Working Paper* Nr. 62.
Pilvere, I., Nipers, A. & Silamikele, I. 2016. *Output of Bioeconomy Strategy in Latvia*. 16–22 pp. Access: http://www.norden.lv/Uploads/2016/08/26/1472194599_.pdf
Ploeg, J.D. van der etc. 2000. Rural Development: From Practices snd Policies towards Theory. *Sociologia Ruralis* **40**, 391–408.
Rivza, B., Kruzmetra, M. & Zaluksne, V. 2016. Performance Trends for Smart Growth in the Rural Territories of Latvia. *Agronomy Research* **14**(5), 1684–1693.
Rivza, B., Kruzmetra, M. & Zaluksne, V. 2017. Through Economic Growth to the Viability of Rural Space. *Agronomy Research* **15**(5), 2079–2089.
Rivza, B., Kruzmetra, M. 2017. Through economic growth to the viability of rural space. *Entrepreneurship and Sustainability Issues* **5**(2), 283–296 Access: https://doi.org/http://doi.org/10.9770/jesi.2017.5.2(9)
Ronkkoi, E. & Aarrevaara, E. 2017. Towards Strengths-based Planning Strategies for Rural Localities in Finland. *European Countryside* **9**(3), 397–415. DOI: 10.1515/euco-2017-0024
Sipilova, V. 2015. *Structural Changes in Manufacturing and their Impact on Economic Growth*. Doctoral Thesis. Daugavpils University, 117 pp. (in Latvian).
Sztompka, P. 1993. *The Sociology of Social Changes*. Oxford UK, Cambridge US: Wiley-Blackwell. 368 pp.
Vu, K.M. 2017. Structural change and economic growth: Empirical evidence and policy insights from Asian economies. *Structural Change and Economic Dynamics* **41**, 64–77.
Woods, M. 2012. New directions in rural studies? *Journal of Rural Studies* **28**, 1–4.

Agronomy Research **16**(3), 872–883, 2018
https://doi.org/10.15159/AR.18.079

Effects of Monopotassium-phosphate, Nano-calcium fertilizer, Acetyl salicylic acid and Glycinebetaine application on growth and production of tomato (*Solanum lycopersicum*) crop under salt stress

T.K. Sajyan[1,*], N. Shaban[1], J. Rizkallah[2] and Y.N. Sassine[3]

[1]University of Forestry, 10 Kliment Ohridski blvd, BG1797 Sofia, Bulgaria
[2]Lebanese University, Faculty of Agricultural Engineering and Veterinary Medicine, Department of Food Technology, Dekwaneh, Beirut, Lebanon
[3]Lebanese University, Faculty of Agricultural Engineering and Veterinary Medicine, Department of Horticulture, Dekwaneh, Beirut, Lebanon
[*]Correspondance: Tony.sajyan@hotmail.com

Abstract. Salinity problem is increasingly affecting tomato production in Lebanon leading to economic losses. The study investigated the potential effects of nano-Calcium (LITHOVIT®), monopotassium-phosphate (MKP: 0-52-34) fertilizers, Acetyl salicylic acid (Aspirin) and the osmoregulator glycinebetaine (GB) on salt tolerance of potted determinate tomato (variety Sila) plants in open-field. Salt stress was induced by irrigation solutions of EC = 2, 4, 6, 8 and 10 mS cm^{-1} and MKP (2, 3 and 3.5 g L^{-1}), Aspirin (50, 75 and 100 mg L^{-1}), LITHOVIT® (0.5, 0.75 and 1 g L^{-1}) and GB (4.5, 6 and 7.5 g L^{-1}) were applied through foliar application or fertigation. Comparisons between treated and non-treated plants at each salinity level (control) showed that LITHOVIT® decreased the salinity-induced reductions in stem diameter, leaf area and chlorophyll content. Medium concentrations of LITHOVIT® and Aspirin improved stem diameter and all products except Glycinebetaine improved flower number compared to control. Root dry weight and Root Mass Fraction were mostly enhanced in MKP and Aspirin-treated plants. Best improvement in plant yield (76%) was obtained with low concentrations of MKP and LITHOVIT® at EC = 8 mS cm^{-1} due to improvement in fruit number rather than fruit weight. Consequently, LITHOVIT® and MKP showed superior effects under salt stress compared to Aspirin and Glycinebtaine.

Key words: osmoregulator, foliar fertilizers, salt-tolerance, fruit yield, fruit quality.

INTRODUCTION

Salinity is a major problem affecting plant growth and development (Aly et al., 2003). Tomato is a moderately sensitive crop to salinity (Maksimovic & Ilin, 2012) and severe salt stress could alter plant physiology causing reductions in growth, photosynthesis, respiration and metabolic accumulation (Ebrahim, 2005). This is mainly due to ion toxicity caused by sodium (Na^+) accumulation in soils and plants (Munns, 2002) which affects water potential and availability (Franco et al., 2011) and interferes with nutrient uptake from roots (Chavarria & dos Santos, 2012). In addition, plant production is reduced (Tantawy et al., 2013) by salinity-induced reductions in flowering capacity (Boamah et al., 2011), size and number of marketable fruits (del Amor et al., 2001). On the contrary, salinity has a stimulatory effect on fruit quality (Boamah et al., 2011). It increases sugars, acidity, pH (Cuartero & Fernàndez-Muñoz, 1999), total soluble solids (TSS) contents as well as titratable acidity (del Amor et al., 2001). One way to improve salt tolerance of plants is through the application of compatible solutes (Ben Ahmed et al., 2010; Saxena et al., 2013) such as the osmoregulator glycinebetaine (GB) (Sakamoto & Murata, 2002; Chen & Murata, 2011) which accumulates in the cytoplasmic compartments while ions are sequestered in the vacuole (Salisbury & Ross, 1992). GB maintains the osmotic balance (McCue & Hanson, 1992) and protects membrane functions from high concentrations of Na^+ and chloride (Cl^-) (Fariduddin et al., 2013). It has been reported to ameliorate net photosynthesis, increase stomatal conductance, decrease photorespiration and improve fruit set and yield on tomato (Mäkelä et al., 1999; Tantawy et al., 2009). On the other hand, potassium and phosphorus fertilization has been reported as a method to alleviate salinity effects on crops (Yurtseven et al., 2005; Tantawy et al., 2013; Afzal et al., 2015). In specific, on tomato monopotassium-phosphate (MKP) application could improve plant growth, fruit quality (Fan et al., 2011), chlorophyll content and dry matter accumulation (Chapagain & Wiesman, 2004). On the same crop, it was stated that Acetyl salicylic acid (Aspirin) that is an artificial analogue of salicylic acid (Senaratna et al., 2000) could have a potential role in counteracting salinity impacts through foliar application due to its ability to increase photosynthetic pigments, soluble compounds in fruits as well as leaf water content and membrane stability (Agamy et al., 2013). Moreover, nano-fertlizers are being increasingly used in agriculture (Froggett, 2009), however there were minor reports regarding their role under salt stress. Their importance resides in their ability to improve nutrient use efficiency causing higher crop productivity (Solanki et al., 2015). They could increase photosynthesis rate and dry matter production through foliar application (Hediat & Salama, 2012; Suriyaprabha et al., 2012; Tarafdar et al., 2012). Under salt-stress, Tantawy et al. (2014) found that nano-calcium (LITHOVIT) treatment improved tomato yield and fruit nutritional status.

In the last 20 years, salinity was amplified in arid and semi-arid areas of the Mediterranean region (Cirillo et al., 2016). In Lebanon, this problem is dominant in cultivated areas of southern coasts where seawater intrusion was caused by excessive groundwater pumping (El Moujabber et al., 2004; Korfali & Jurdy, 2010). In addition, soil EC of more than 52% of open field sites in the semiarid northern areas are in the range of slightly saline to saline (Darwish et al., 2002) which has been limiting the type and production rate of crops grown there (El Moujabber et al., 2005). Tomato is one of the most important agricultural crops in Lebanon and is widely cultivated in regions subjected to salinity (Darwish, 1995). Based on all previous statements, the experiment was carried out in order to evaluate if the application of nano-Ca, MKP, GB and Acetyl salicylic acid (Aspirin) could be adopted as a strategy to mitigate negative salinity impacts in local cultivation of tomato crop.

MATERIALS AND METHODS

Plant material and treatments

In late-May, tomato seedlings were transplanted at the stage of 2–3 true leaves into plastic pots containing washed sandy clay soil with a Cation Exchange Capacity of 1 meq per 100 g. Seedlings were left to grow in open-field conditions under natural lighting (25–20) ±2 °CC day/night temperature with air relative humidity of 60%. Soil salinity (ECe) was analyzed prior to transplantation in saturated paste extracts and it was of 0.17 mS cm^{-1}. Plants were subjected to five salinity levels (EC = 2, 4, 6, 8 and 10 mS cm^{-1}) and to the application of four various products with 3 different concentrations: LITHOVIT® (LITHO-Low: 0.5 g L^{-1}, LITHO-Med: 0.75 g L^{-1} and LITHO-High: 1 g L^{-1}), ASPIRIN (ASP-Low: 50 mg L^{-1}, ASP-Med: 75 mg L^{-1} and ASP-High: 100 mg L^{-1}), MKP (MKP-Low: 2 g L^{-1}, MKP-Med: 3 g L^{-1} and MKP-High: 3.5 g L^{-1}) and GB (GB-Low: 4.5 g L^{-1}, GB-Med: 6 g L^{-1} and GB-High: 7.5 g L^{-1}). LITHOVIT® is a natural mineral (based on limestone) containing a lot of CO_2 bonds and consisting of (Ca; Mg) $CaCO_3$ and other micronutrient (Bilal, 2010). LITHO and ASP were applied through foliar spray, MKP through fertigation while GB through both methods. GB, LITHO and MKP were dissolved in distilled water while ASP was mixed with ethanol at high temperature prior to dilution. Each product was applied 3 times during growth cycle (15, 29 and 43 DAT: Days after transplantation). Plants were irrigated with tap water (EC = 0.4 mS cm^{-1}) until 14 DAT and saline irrigation started at 19 DAT with an interval of 3 days between consecutive irrigations; NaCl solutions were prepared after dissolving in water tanks of 100 L the corresponding weight of salt needed to reach each level. A continuous monitoring of the EC of the saline solution was done using an EC meter. At each salinity level, enough drainage was allowed until obtaining an $EC_{water\ drainage} = EC_{irrigation\ solution}$. Adjustment of $EC_{water\ drainage}$ was done using the corresponding saline solution. This was done to guarantee that the $EC_{root\ zone}$ is stable at the set point and to ensure a steady state value of the EC during the entire growing period.

Measured indicators

Leaf number and stem diameter were evaluated at the date of destructive sampling (55 DAT). Plant height was measured twice; at 24 and 55 DAT. Number of trusses, flowers and fruits was counted on plants. Fruit set consisted of the ratio of fruit number on flower number and expressed in percentage. Fruit diameter was measured using a sliding caliper and weight of individual fruit (g) was recorded for determining plant yield (g per plant). Aboveground and underground parts of plants were separated and oven-dried at 100 °C until constant weight for measuring dry weights, consequently Root Mass Fraction (RMF) was calculated as follows: RMF (g/g) = root dry mass ⁄ total plant dry mass (Poorter et al., 2012). Chlorophyll content and cell electrolyte leakage were assessed as described by Levent Tuna et al. (2007) using the upper most expanded leaves (del Amor et al., 2001). On fruits, Total soluble solids (TSS) was measured using Euromex RF (360) refractometer and titratable acidity was assessed by titration with NaOH (Garner et al., 2005).

Statistical analysis

The experimental design consisted on a Complete Randomized Block Design (CRBD) with 2 factors: salinity (5 salinity levels) and product application (4 products x

3 concentrations) and 10 replicates. Data was subjected to analysis of variance which consisted on means ± SE compared by Fisher's least-significant differences test (*LSD*) using STATISTICA 10 program. Repeated Measures ANOVA was used to evaluate the evolution of plant growth with time.

RESULTS AND DISCUSSION

Results of Factorial ANOVA (Table 1) showed that the separated effects of EC and Treatment were significant on averages of all parameters ($P < 0.05$) with the exception of those of EC on plant height, number of flowers and number of fruits. The 2-way interactive effects of EC and Treatment were significant on averages of all parameters except fruit weight, yield, dry weight of roots and root mass fraction. The non-interactive of Time, the 2way and 3way interactive effects of Time, EC and Treatment were significant on all parameters.

Table 1. Effects of the experimental factors (EC, Treatment and Time) and their interactions on the different measurements averages

	EC	Treatment	EC* Treatment	TIME* EC	TIME* Treatment	TIME*EC* Treatment
Plant height (cm)	NS	**	**	**	**	**
Leaf number	**	**	**	**	**	**
Number of clusters	**	**	**	**	**	**
Number of fruits	NS	**	**	**	**	**
Stem diameter (cm)	**	**	*	-	-	-
Number of flowers	NS	**	**	-	-	-
Fruit set (%)	**	**	*	-	-	-
AWF (g)	**	**	NS	-	-	-
ADF (cm)	**	**	*	-	-	-
Yield/plant (g)	**	**	NS	-	-	-
RMF (g/g)	**	**	NS	-	-	-

AWF: Average weight of individual fruit, ADF: Average diameter of fruit, DWR: Dry weight of roots; RMF: Root Mass Fraction.

Plant growth

In general, average plant height in salt-stressed plants was mostly enhanced at late stages of growth (55 DAT) mainly by MKP-Low and MKP-Med at EC4 and by MKP-Med and MKP-High at EC8, while it was the most improved by LITHO-Med and LITHO-High at EC10 compared to control (Fig. 1).

An improvement in average leaf number was observed at EC4 following MKP-Low and ASP-Med application, and at EC8 and EC10 with MKP-High and MKP-Low respectively (Fig. 2).

Stem diameter was reduced with increasing salinity levels (by 0.20 cm between EC2 and EC10), however it was enhanced by ASP-Med at EC4, EC8 and EC10 (by 0.18 cm, 0.29 cm, and 0.34 cm respectively), MKP-Low at EC8 (by 0.38 cm) and LTHO-Med at EC6 (by 0.29 cm) compared to control (Fig. 3).

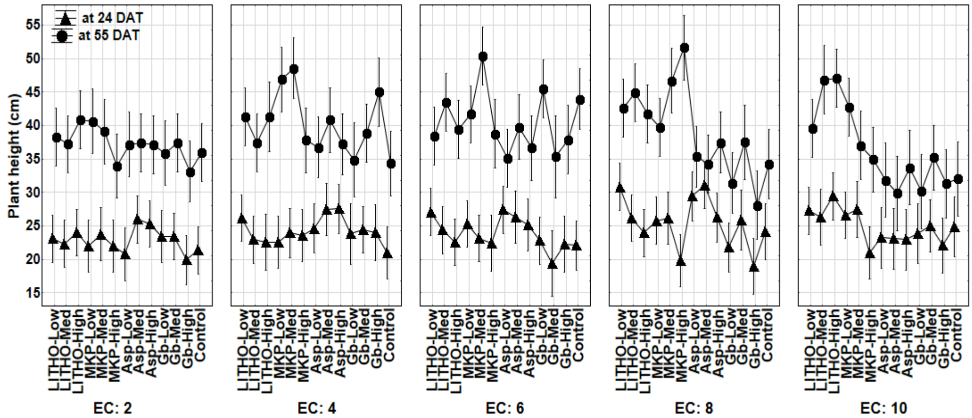

Figure 1. Averages (middle markers) and the 95% limits of confidence (±2 xSE) (vertical bars) of the plant height.

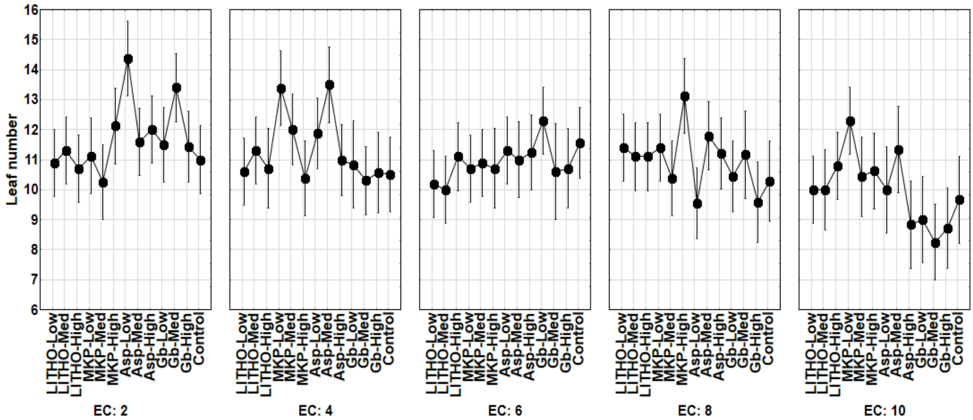

Figure 2. Averages (middle markers) and the 95% limits of confidence (±2 xSE) (vertical bars) of the leaf number.

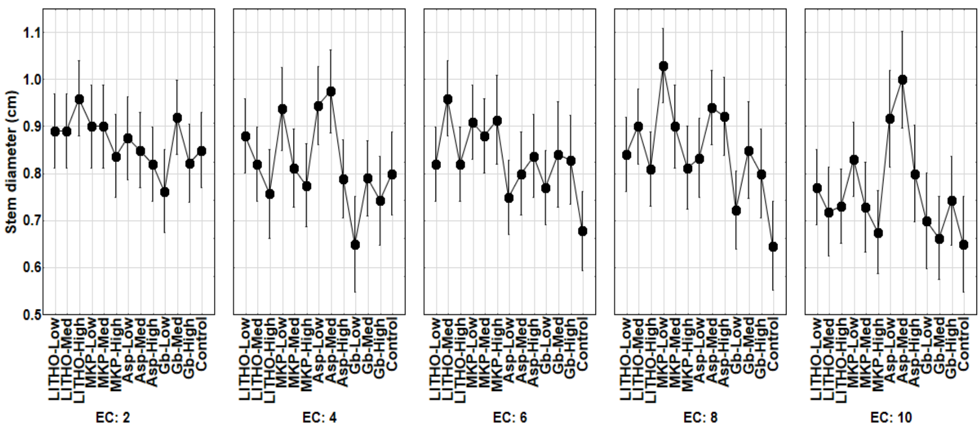

Figure 3. Averages (middle markers) and the 95% limits of confidence (±2 xSE) (vertical bars) of the stem diameter.

Flowering, production and fruit quality

Salinity-induced reductions in the majority of flowering and productive indicators were not statistically significant; however they were observed at high salinity levels (EC8 and EC10) in control plants. Application of LITHOVIT®, MKP and ASP with low, medium and high doses increased the average number of trusses at EC8 while at EC10 improvement in this parameter was significant following LITHO-Low, LITHO-Med, LITHO-High and MKP-Low applications compared to control. Also, at those salinity levels, all products except GB decreased the reductions in average flower number per plant, with various significance depending on the application dose (Figs 4, 5).

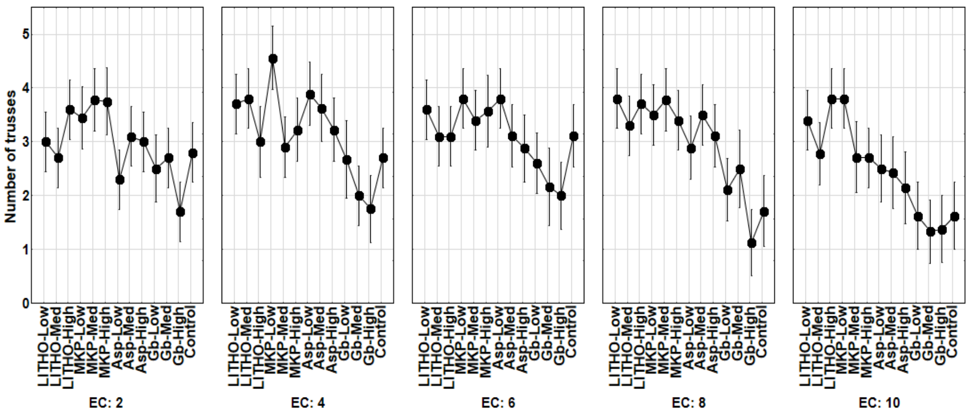

Figure 4. Averages (middle markers) and the 95% limits of confidence (±2 x SE) (vertical bars) of the number of trusses.

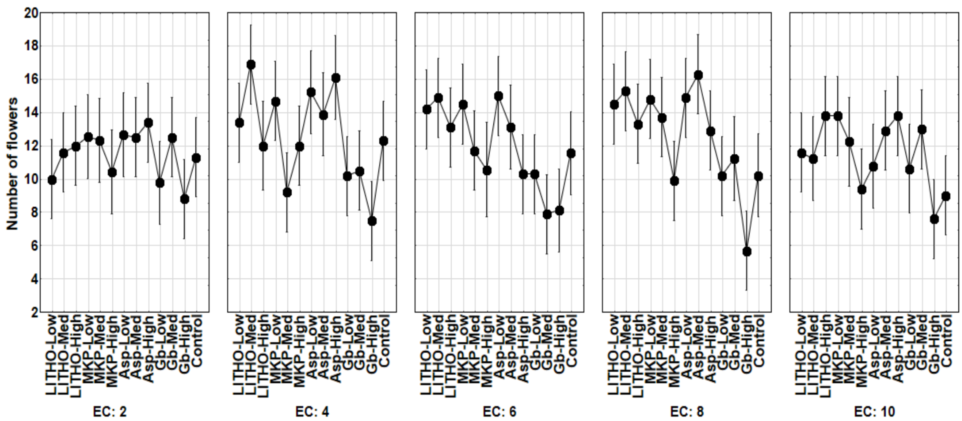

Figure 5. Averages (middle markers) and the 95% limits of confidence (±2 x SE) (vertical bars) of the number of flowers.

Fruit set was the highest in LITHO-treated plants compared to other treatments. When comparing with control, significant increase in fruit set was observed at EC2 and EC8 with LITHO-Low and at EC2 and EC10 with MKP-Med and MKP-Low respectively. Moreover, although none of the products have shown a significant effect on average values of individual weight and diameter of fruits, however MKP and LITHO enhanced average fruit number and average yield while ASP and GB did not. In specific, MKP-Low increased fruit number by 4 at EC4 and EC6 and by 6 at EC8 and EC10, while MKP-Med increased it by 4 at EC2 and EC6 compared to control. Also, at EC6 number of fruits was increased by 4 following LITHO application with various doses, and by 6 and 5 fruits with LITHO-Low and LITHO-Med respectively at EC8 (Fig. 6).

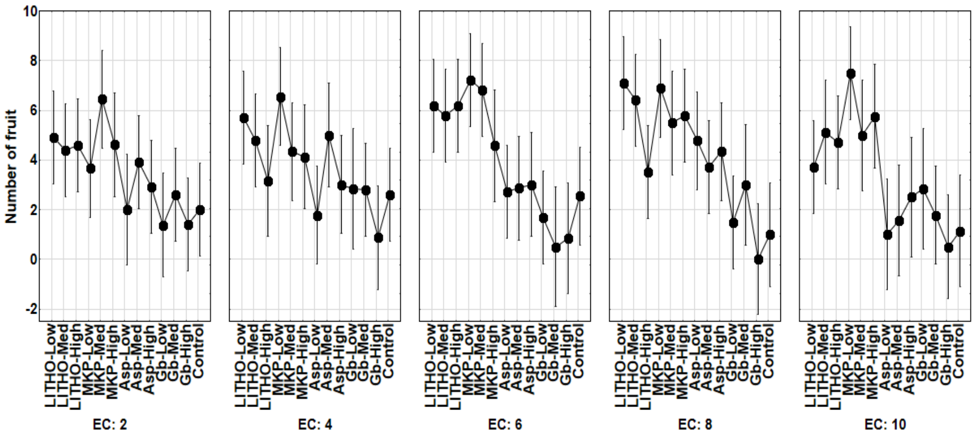

Figure 6. Averages (middle markers) and the 95% limits of confidence (±2 x SE) (vertical bars) of the number of fruits.

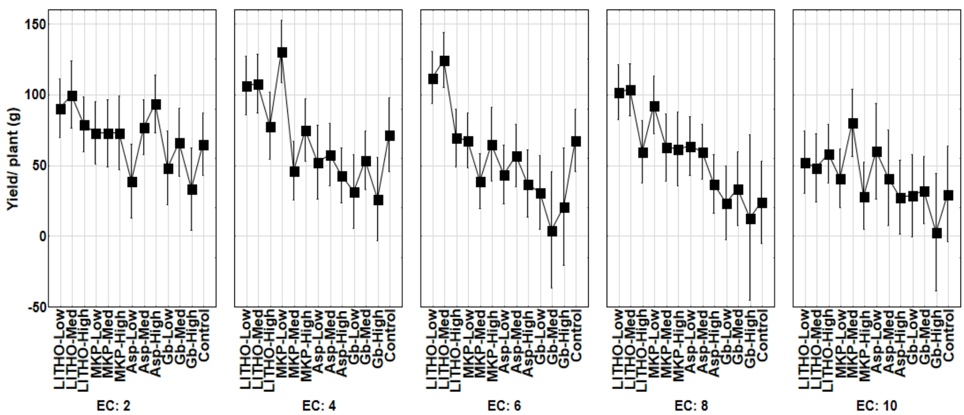

Figure 7. Averages (middle markers) and the 95% limits of confidence (±2 x SE) (vertical bars) of yield/ plant.

In addition, compared to control, improvements in yield by around 45% and 74% were observed at EC4 and EC8 respectively with MKP-Low and by 39% and 76% with LITHO-Low and by 46% and 76% with LITHO-Med at EC6 and EC8 respectively (Fig. 7). Fruit quality was improved with increasing salinity where TSS and titratable acidity contents were the highest in control fruits. Various investigated products did not affect fruit quality except for MKP positive effect on TSS content which was greatly improved mainly with MKP-Med under more severe salt stress (9.7% and 10.2% in treated plants compared to 8.2% and 8.95% in non-treated plants at EC8 and EC10 respectively) (figures not included).

Physiological indicators

Increasing salinity levels had negatively influenced dry weight of aboveground plant parts; however dry weights were in general higher with LITHO (Med) and MKP (Low, Med and High) treatments mainly at EC6, 8 and 10 mS cm^{-1}. On the other hand, dry weight of roots and consequently RMF were the highest in ASP-Low treated plants at EC2, 4 and 6 and in MKP-Low and LITHO-Med treated plants at EC8 and EC10 respectively (Fig. 8).

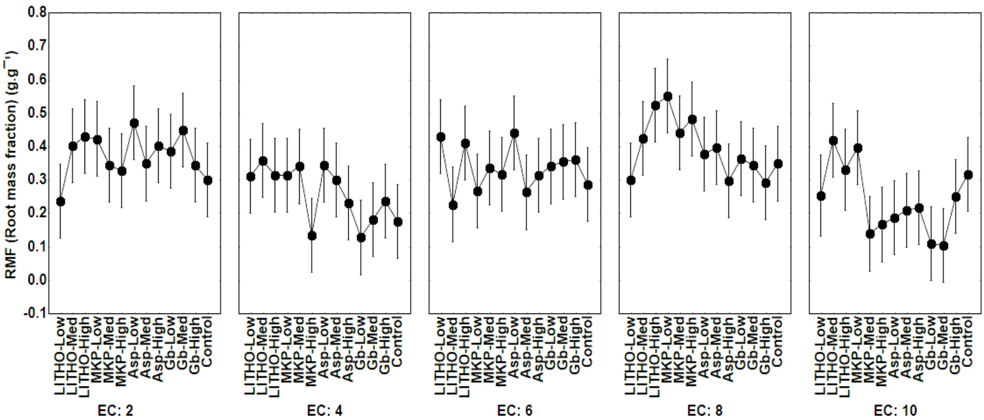

Figure 8. Averages (middle markers) and the 95% limits of confidence (±2 x SE) (vertical bars) of root mass fraction.

Furthermore, although increasing salinity between EC2 and EC10 decreased average leaf area by 142.4 cm^2, and did not affects total chlorophyll content. LITHOVIT® application induced amelioration in both parameters with all application doses. It also decreased the injury level in cells of plant leaves that was reflected by lower percentages of cell electrolyte leakage in LITHO-Low at EC2, 4, 6 and 8 mS cm^{-1} (70%, 78.9%, 78.9% and 84.2% compared to 73.3%, 80%, 82.4% and 87.5% in control plants).

Increasing salinity did not reduce plant height and leaf number which contradicted earlier findings (Oztekin & Tuzel, 2011; Parvin et al., 2015). On the contrary, a similar decline in stem diameter under salt stress was observed by Saberi et al. (2011) and could be attributed to the reduction in water potential leading to turgor in expanding tissues (Zhu, 2002). High salinity has negatively affected fruiting and physiological indicators causing yield reductions due to decline in fruit number confirming the results of del Amor et al. (2001). MKP application enhanced plant growth and yield confirming the results of Kaya et al. (2001) and this was due to the presence of K^+ playing a major role in osmotic adjustment, enzyme activation, cell turgor (Marschner, 1995) and lowering Na^+ uptake (Plaut et al. 2013). It improved the fertilization mechanism and ovary development causing fruit set (Satti et al., 1994). Lithovit® application has also shown a positive effect on plant height and stem diameter. This ameliorative effect was observed by Sabina (2013) on *Koelreuteria paniculata* when tested as fertilizer and on tomato yields by Tantawy et al. (2014). In fact, LITHOVIT acts as a long term CO_2 reservoir supplying plants with CO_2 (Kumar, 2011).

Moreover, since Calcium was applied in a micronization form as CaCO3 and CaO, plants could absorb enough Ca. In addition, Lithovit contains a lot of micronutrients such as Mg, Fe and Mn which contribute to the nutritional status of the plant (Bilal, 2010) and may reflect on its response to salinity compared to control. It is well known that salinity can disturb plant uptake of nutrients (Chavarria & dos Santos, 2012), hence providing these nutrients through foliar application would compensates for this disturbance. Mg is essential for chlorophyll formation and its foliar application may result in higher chlorophyll content hence better plant growth. In fact, LITHOVIT® has enhanced leaf area and chlorophyll content due to its stimulatory impact on photosynthetic rate caused by atmospheric CO_2 amelioration (del Amor, 2013).

Furthermore, the limited positive effect of Aspirin on leaf number and stem diameter could be related to enhanced root biomass, thus the higher water and nutrient absorption. The effect of this product was less studied on tomato salt-stressed plants. However, according to Sun et al. (1994) in stress conditions the positive activity of Acetyl salicylic acid is mainly to maintain the function of cellular membranes and to prevent lethal stress load. Finally, although some early studies have pointed out the efficiency of Glycinebetaine under salt-stress, however it had no evident effect in this experiment. Similar findings were reported by Heuer (2003) where GB was ineffective due to its inhibitory effect on ion accumulation in plant cells.

CONCLUSIONS

In conclusion, under the tested conditions, Aspirin effect was the most significant at rooting stage, while LITHOVIT® was the most beneficial at leaf formation, flowering and fruiting. MKP application improved plant performance at all stages of growth and production. Consequently, different combinations of treatments could be applied at different stages of plant growth under salt stress; mainly Aspirin (50 mg L^{-1}) and MKP (2 g L^{-1}) at early growth stages and MKP (2 to 3 g L^{-1}) and LITHOVIT® (0.75 g L^{-1}) at later growth stages. On the contrary, Glycinebetaine that had no effect under the current experimental conditions could be tested in upcoming studies with different application doses and timing.

ACKNOWLEDGEMENTS. Authors deeply thank the TRIBOdyn AG Company for providing the LITHOvit product and ensuring its shipping to Lebanon.

REFERENCES

Afzal, I., Hussain, B., Basra, S.M.A., Ullah, S.H, Shakeel, Q. & Kamran, M. 2015. Foliar application of potassium improves fruit quality and yield of tomato plants. *Acta Sci Pol Hortorum Cultus*. **14**(1), 3–13.

Agamy, R.A., Hafez, E.E. & Taha, T.H. 2013. Acquired Resistant Motivated by Salicylic Acid Applications on Salt Stressed Tomato (*Lycopersicon esculentum* Mill.). *American-Eurasian J Agric & Environ Sci.* **13**, 50–57.

Aly, M.M., El-Sabbagh, S.M., El-Shouny, W.A. & Ebrahim, M.K.H. 2003. Physiological response of *Zea mays* to NaCl stress with respectto *Azotobacter chroococcum* and *Streptomyces niveus*. *PakistanJ Biological Science* **6**(24), 2073–2080.

Ben Ahmed, C., Ben Rouina, B., Sensoy, S., Boukhriss, M. & Ben Abdullah, F. 2010. Exogenous proline effects on photosynthetic performance and antioxidant defense system of young olive tree. *Journal of Agricultural and Food Chemistry* **58**, 4216–4222.

Bilal., B.A. 2010. Lithovit®: An innovative fertilizer. The 3rd e- Conference on Agricultural Biosciences (IeCAB 2010), 1st- 15th June 2010. http://www.slideserve.com/madison/lithovitan-innovative-fertilizer.

Boamah, P.O., Sam-Amoah, L.K. & Onumah, J. 2011. Effect of salinity level of irrigation water on the yield of tomato. *ARPN Journal of Agricultural and Biological Science* **6**(8), 49–53.

Chapagain, B.P. & Wiesman, Z. 2004. Effect of Nutri-Vant-PeaK foliar spray on plant development, yield, and fruit quality in greenhouse tomatoes. *Scientia Horticulturae* **102**, 177–188.

Chavarria, G. & dos Santos, HP. 2012. Plant water relations: Absorption, transport and control mechanisms. *InTechOpen*. **5**, 105–132.

Chen, T.H. & Murata, N. 2011. Glycinebetaine protects plants against abiotic stress: mechanisms and biotechnological applications. *Plant Cell Environ* **34**, 1–20.

Cirillo, C., Rouphael, Y., Caputo, R., Raimondi, G., Sifola, M.I. & De Pascale, S. 2016. Effects of high salinity and the exogenous of an osmolyte on growth, photosynthesis and mineral composition in two ornamental shrubs. *J. Hortic. Sci. Biotechnol*. **91**, 14–22.

Cuartero, J. & Fernández-Muñoz, R. 1999. Tomato and salinity. *Sci Hort*. **78**, 83–125.

Darwish, T. 1995. Implementation and perspectives of fertigation in crop production in Lebanon. In: *Short Advanced Course on Fertigation. FAO/RNE,* CIHEAM/IAM-B, Lebanese University, pp. 207–220.

Darwish, T., Atallah, T., El-Khatib, M. & Hajhasan, S. 2002. Impact of irrigation and fertilization on NO3 leaching and soil-ground water contamination in Lebanon. In: *Transactions 17th World Congress of Soil Science*. Bangkok, Thailand, pp. 1–11.

del Amor, F.M., Martinez, V. & Cerda, A. 2001. Salt Tolerance of Tomato Plants as Affected by Stage of Plant Development. *HortScience*. **36**(7), 1260–1263.

del Amor, F.M. 2013. Variation in the leaf 13 °C is correlated with salinity tolerance under elevated CO2 concentration. *Journal of Plant Physiology* **170**, 283–290.

Ebrahim, M.K.H. 2005. Amelioration of sucrose-metabolism and yield changes, in storage roots of $NaCl^-$ stressed sugarbeet, by ascorbic acid. *Agrochimica* **3**(4), 93–103.

El Moujabber, M., Atallah, T., Darwish, T. & Bou Samra, B. 2004. Monitoring of groundwater salination by seawater intrusion on the lebanese coast. *Lebanese Science Journal* **5**, 21–36.

El Moujabber, M., Darwich, T., Shaban, A., Atallah, T., Abi Saab, M. & Janho, R. 2005. Regional water balance as a tool to monitor groundwater contamination by seawater intrusion on the Lebanese Coast. In: *International Conference on Water, land and Food Security in Arid and Semi- Arid Regions*. MAIB, pp. 1–13.

Fan, M., Bie, Z.L., Krumbein, A. & Schwarz, D. 2011. Salinity stress in tomatoes can be alleviated by potassium depending on rootstock and K concentration employed. *Scientia Hort*. **130**, 615–623.

Fariduddin, Q., Varshney, P., Yusuf, M., Ali, A. & Ahmad, A. 2013. Dissecting the role of glycine betaine in plants under abiotic stress. *Plant Stress.* **7**, 8–18.

Franco, J.A., Bañón, S., Vicente, M.J., Miralles, J. & Martínez-Sánchez, J.J. 2011. Root development in horticultural plants grown under abiotic stress conditions. *A review J Hortic Sci Biotechnol*. **86**, 543–556.

Froggett, S. 2009. Nanotechnology and agricultural trade. *OECD Conference on the Potential Environmental Benefits of Nanotechnology*: Fostering Safe Innovation-Led Growth.

Garner, D., Cristo, C.H. & Wiley, P. 2005. Measurement of pH and Titratable Acidity. In: Quality Evaluation Methodology. USA: Kearney Agricultural Center, 1 pp.

Hediat, M. & Salama, H. 2012. Effects of silver nanoparticles in some crop plants, Common bean (Phaseolus vulgaris L.) and corn (*Zea mays* L.). *International Research Journal of Biotechnology* **3**(10), 190–197.

Heuer, B. 2003. Influence of exogenous application of proline and glycinebetaine on growth of salt-stressed tomato plants. *Plant Sci.* **165**, 693–699.

Kaya, C., Kirnak, H. & Higgs, D. 2001. Enhancement of growth and normal growth parameters by foliar application of potassium and phosphorus on tomato cultivars grown at high (NaCl) salinity. *J Plant Nutr*. **24**, 357–367.

Korfali, S.I. & Jurdi, M. 2010. Deterioration of coastal water aquifers: causes and impact. *European waters* **29**, 3–10.

Kumar, P. 2011. Nanotechnology in agriculture. *Financing Agriculture* **34**, 8–10.

Levent Tuna, A., Cengiz, K., Mura, D., İbrahim, Y., Betül, B. & Hakan, A. 2007. Comparative effects of various salicylic acid derivatives on key growth parameters and some enzyme activities in salinity stressed maize (*zea mays* L.). *Plants. Pak. J. Bot*. **39**(3), 787–798.

Mäkelä, P., Kontturi, M., Pehu, E. & Somersalo, S. 1999. Photosynthetic response of drought- and salt-stressed tomato and turnip rape plants to foliar-applied glycinebetaine. *Physiologia Plantarum*. **105**, 45–50.

Maksimovic, I. & Ilin, Ž. 2012. Effects of Salinity on Vegetable Growth and Nutrients Uptake. In: Lee T.S. (ed.): *Irrigation Systems and Practices in Challenging Environments,* ISBN: 978-953-51- 0420-9, InTech, pp. 170–190.
Available from: http://www.intechopen.com/books/irrigation-systems-and-practices-inchallenging-environments/effects-of-salinity-on-vegetable-growth-and-nutrients-uptake.

Marschner, H. 1995. *Mineral Nutrition of Higher Plants*. 2nd edn. Academic Press, London, 889 pp.

McCue, K.F. & Hanson, A.D. 1992. Salt-inducible betaine aldehyde dehydrogenase from sugar beet: cDNA cloning and expression. *Plant Mol Biol.* **18**, 1–11.

Munns, R. 2002. Comparative physiology of salt and water stress. *Plant Cell Environ*. **25**, 239–250.

Oztekin, G.B. & Tuzel, Y. 2011. Comparative salinity responses among tomato genotypes and rootstocks. *Pak. J. Bot*. **43**(6), 2665–2672.

Parvin, K., Ahamed, K.U., Islam, M.M. & Haque, M.N. 2015. Response of Tomato Plant Under Salt Stress: Role of Exogenous Calcium. *Journal of Plant Sciences* **10**, 222–233.

Plaut, Z., Edelstein, M. & Ben-Hur, M. 2013. Overcoming Salinity Barriers to Crop Production Using Traditional Methods. *Critical Reviews in Plant Sciences* **32**(4), 250–291.

Poorter, H., Niklas, K.J., Reich, P.B., Oleksyn, J., Poot, P. & Mommer, L. 2012. Biomass allocation to leaves, stems and roots: meta-analyses of interspecific variation and environmental control. Tansley review. *New Phytol.* **193**, 30–50.

Saberi, A.R., Aishah, H.S., Halim, R.A. & Zaharah, A.R. 2011. Morphological responses of forage sorghums to salinity and irrigation frequency. *Afr. J. Biotechnol*. **10**, 9647–9656.

Sabina, P.D. 2013. Research concerning the use of some seed and material preparation methods in the production of biological material in generative *Koelreuteria paniculata* LAXM. *Journal of Horticulture, Forestry and Biotechnology* **17** (2), 185–188.

Sakamoto, A. & Murata, N. 2002. The role of glycine betaine in the protection of plants from stress: clues from transgenic plants. *Plant Cell and Environment* **25**(2), 163–171.

Salisbury, F.B. & Ross, C.W. 1992. *Plant Physiology*. 4th edn. Wadsworth Publishing, Belmont, 674 pp.

Satti, S.M.E., Lopez, M. & Al-Said, F.A. 1994. Salinity induced changes in vegetative and reproductive growth in tomato. *Communications in Soil Science and Plant Analysis* **5**(6), 501–510.

Saxena, S.C., Kaur, H., Verma, P., Petla, B.P., Andugula, V.R. & Majee, M. 2013. Osmoprotectants: potential for crop improvement under adverse conditions. In: Tuteja N. & Singh S. G. (eds.): *Plant Acclimation to Environmental Stress.* Springer. New York, NY, pp. 197–232.

Senaratna, T., Touchell, D., Bumm, E. & Dixon, K. 2000. Acetylsalicylic (Aspirin) and salicylic acid induce multiple stress tolerance in bean and tomato plants. *Plant Growth Regul*. **30**, 157–61.

Solanki, P., Bhargava, A., Chhipa, H., Jain, N. & Panwar, G. 2015. Nano-fertilizers and Their Smart Delivery System. In: M. Rai et al. (eds.): *Nanotechnologies in Food and Agriculture*. Springer, Cham, pp. 81–101.

Sun, W.Q., Irving, T.C. & Leopold, A.C. 1994. The role of sugar, vitrification and membrane phase transition in seed desiccation tolerance. *Physiol. Plant* **90**, 621–628.

Suriyaprabha, R., Karunakaran, G., Yuvakkumar, R., Rajendran, V. & Kannan, N. 2012. Silica nanoparticles for increased silica availability in maize (*Zea mays* L) seeds under hydroponic conditions. *Curr Nanosci*. **8**, 902–908.

Tantawy, A.S., Abdel-Mawgoud, A.M.R., El-Nemr, M.A. & Chamoun, Y.G. 2009. Alleviation of salinity effects on tomato plants by application of amino acids and growth regulators. *Eur J Sci Res*. **30**. 484–494.

Tantawy, A.S., Salama, Y.A.M., Abdel-Mawgoud, A.M.R. & Zaki, M.F. 2013. Interaction of Fe and salinity on growth and production of tomato plants. *World Applied Sciences Journal* **27**(5), 597–609.

Tantawy, A.S., Salama, Y.A.M., Abdel-Mawgoud, M.R. & Ghoname, A.A. 2014. Comparison of Chelated Calcium with Nano Calcium on Alleviation of Salinity Negative Effects on Tomato Plants. *Middle East Journal of Agriculture Research* **3**(4), 912–916.

Tarafdar, J.C., Agrawal, A., Raliya, R., Kumar, P., Burman, U. & Kaul, R.K. 2012. ZnO nanoparticles induced synthesis of polysaccharides and phosphatases by Aspergillus fungi. *Advanced Sci, Eng. and Medicine* **4**, 1–5.

Yurtseven, E., Kesmez, G.D. & Unlukara, A. 2005. The effect of water salinity and potassium level on yield, fruit quality and water consumption of a native central Anatolian tomato species (*Lycopersicon esculentum*). *Agric Water Manage* **78**, 128–135.

Zhu, J.K. 2002. Salt and drought stress signal transduction in plants. *Ann. J. Plant Biol*. **14**, 267–273.

Agronomy Research **16**(3), 884–891, 2018
https://doi.org/10.15159/AR.18.132

Effect of Automatic Feeding Station use on fattening performance in lambs and intake activity periods

L. Šenfelde* and D. Kairiša

Latvia University of Life Sciences and Technologies, Faculty of Agriculture, Institute of Agrobiotechnology, Liela street 2, LV-3001 Jelgava, Latvia
*Correspondence: shenfeldel@gmail.com

Abstract. Implementation of precise farming technology is very important for productivity increasing of livestock. One of the highest components of the production costs is feeding expenses. An automatic concentrate feeding stations (AFS) can ensure economic feed distribution and intake registration for animals individually. The aim of this research was to study the possibility and benefits of using AFS in fattening of lambs. Results show that during all the research average number of daily visits to AFS per lamb were 13 ± 0.2 visits, average daily live weight gain per lamb was 254 ± 15.7 g. For 1 kg lamb live weight gain 5.35 kg concentrate was used. More intesively acitivity periods of lambs was noted during following hours of day time: 02:00–02:59, 08:00–09:59 and 19:00–20:59. Significant ($P \leq 0.05$) moderate positive correlation (r = 0.470) was found between average daily number of visits to the AFS per lamb and total amount of concentrate consumed during the research per lamb. Significant ($P \leq 0.05$) strong negative correlation (r = -0.806) was found between average daily number of visits to the AFS per lamb and average amount of concentrate consumed during one visit.

Key words: sheep, feed intake, live weight gain, feeding station.

INTRODUCTION

Behaviour of animals is relevant to the welfare requirements and has influence on the productivity traits (Konig von Borstel et al., 2011; Dodd et al., 2012; Jogman et al., 2017). Although the animals would stay in the pasture most of the time (Shepley et al., 2017), but it is not always possible to provide under the production circumstances. Therefore the total periods of daily activity (eating, walking, sleeping, drinking) and intake speed have been analysed in various research studies (Silva et al., 2015; Simeonov et al., 2015; Rahman et al., 2017) as well as behaviour of the animals by daily hours (Tobler et al., 1991; Refinetti et al., 2016), to improve as much as possible the feeling of comfort of animals also in the barn.

Ruminants, allowed in the pasture, consume first major part of the daily food intake already in the morning, which means by 09:00, and the maximal daily food intake has been consumed till 20:00 (Thompson et al., 1985). During the two major feeding times the animals consume daily the 60%–80% from the total daily food quantity, thus the total quantity of daily intake closely correlates with the quantity of food taken in the major feeding times (Jarrige et al., 1995). Intake speed under limited food distribution to animals is higher than in cases, when animals have unlimited access to food. Should there be unlimited access to food, the animals themselves determinate intervals and eating times, wherein the food intake occurs considerably more slowly (Zorrilla et al., 2005). Moreover, the pH level in rumen depends significantly ($P < 0.001$) on the feeding time. Animals, having continuous access to the food, can remain constant pH level during the whole 24 hours (Felix et al., 2017).

The aim of this research was to study the possibility and benefits of using automatic concentrate feeding stations (AFS) in fattening of lambs. The following tasks were set: 1) to analyze frequency of visits to automatic feeding station daily and during the lamb activity; 2) to analyze the amount of concentrate intake during the one visit in the automatic feeding station in fattening periods; 3) to analyze the lamb live weight changes and daily live weight gain during fattening.

MATERIALS AND METHODS

The study about lamb fattening effect and behaviour using AFS was carried out on the farm 'Mežoki' located in Latvia (57.016996, 21.632202). The study was carried out in production conditions. In total the research was carried out from 16 July 2017 to 10 September 2017.

Ten male 50% Romanov × 50% Dorper (RD) and twelve (seven female and five male) unknown crossbreed (XX) lambs were used. Lambs were born in the period from 3 March 2017 to 15 May 2017. The characterizations of both groups of lambs are enclosed below (Table 1).

Table 1. Characterizations of the groups of lambs before research start-up depending on breed

Characterizations	RD (n = 10)	XX (n = 12)
	$\bar{x} \pm S_{\bar{x}}$	
Age, days	77 ± 2.2^{a}	89 ± 5.7^{a}
Live weight before the research, kg	21.1 ± 0.86^{a}	24.1 ± 0.92^{b}
Place of borth	Germany, imported in farm, Mežoki'on 15 July 2017	Latvia, farm, Mežoki'
Keeping conditions before weaning	on pasture	indoor
Concentrate consumtion before the research	had not received	received unlimited in free access

[ab] – traits with different subscriptions are significantly different ($P \leq 0.05$).

The study was started after lamb weaning, adapting period was not ensured. During the research lambs were kept apart in a separate pen and provided continuous access to an automatic concentrate feeding station. The lambs were given free access to water as well. At the automatic feeding station lambs were offered concentrate of the following content: 46% of cereals (barley (*Hordeum vulgare L.*), maize (*Zea mays*), wheat (*Triticum*), wheat (*Triticum*) bran), 36% plant-based protein sources (feed beans (*Vicia faba*), sunflower (*Helianthus annuus*) coarse meal, rapeseed (*Brassica napus*) meal) and 18% the remaining ingredients (oats (*Avena sativa*), lime flour, molasses – liquid, NaCl). Concentrate content: 84% of dry matter (DM), protein 20.4% in DM, crude fibre 8.2% in DM, metabolizable energy (ME) 10.48 MJ kg^{-1} of DM, neutral detergent fibre (NDF)

24% in DM, acid detergent fibre (ADF) 11% in DM, P 0.59% in DM, Ca 1.66% in DM. Under the study the daily concentrate feed rations for one animal were determined steadily increasing from 1,510 g (17 July 2017) to 1,780 g (10 September 2017).

Live weight monitoring of lambs was organized with a New Zealand company's Tru-Test automatic weigh scales. Weighing accuracy is ± 0.1 kg for animals with live weight up to 50 kg and ± 0.2 kg for animals with live weight 50–100 kg. Live weight control dates: 16 July 2017, 30 July 2017, 13 August 2017, 27 August 2017, 10 September 2017.

Concentrate distribution was organized using BioControl Norway JSC compound concentrate feeding station for feeding of individual sheep, identically as for the research made in 2015 (Šenfelde & Kairiša, 2016; Šenfelde & Kairiša, 2017). The external measurements of the feeding station are 2 × 8 × 1 m, its mode of operation – continuous. Form of the concentrate feed – pellets. One standard dose dispensed in the feeding station – 25 g, entrance gates closes after the dispensing the dose and remains closed for 30 seconds or longer if the next dose dispenses within 30 seconds, maximum limit intake at one visit to the feeding station – 300 g. Using the concentrate feeding station the following data were recorded: electronic ID number of the animal visiting the feeding station, date and time of the visit to the feeding station for each lamb, the amount of concentrate dispensed per visit, the amount of concentrate dispensed per day for each lamb after each visit, total concentrate amount for each lamb per day. The data from the concentrate feeding station were collected from 17 July 2017 to 10 September 2017, except 9 August 2017 when there was a failure in power supply. The obtained data were analyzed in the periods between live weight controls: from 17 July 2017 to 30 July 2017 (1st period), from 31 July 2017 to 13 August 2017 (2nd period), from 14 August 2017 to 27 August 2017 (3rd period) and from 28 August 2017 to 10 September 2017 (4th period).

Data were analyzed within the framework of breed, regarding the total number of visits during the whole period of research, comparing results of lambs, visiting the AFS a less number of times (RD1 (n = 5) and XX1 (n = 6)) with results of those lambs visiting the AFS more often during the whole period of research (RD2 (n = 5) and XX2 (n = 6)).

The data were analyzed with mathematical processing methods, using software 'SPSS Statistics'. The number of visits, quantity of compound concentrate fed during one visit, live weight mean daily gain of lambs, standard error and the concentrate quantity necessary for 1 kg live weight gain were calculated. The amount of concentrate necessary for live weight gain of 1 kg was calculated dividing the total amount of concentrate (kg), which was fed, by the live weight gain (kg). The parameters obtained were compared between breeds, study periods and groups RD1-RD2, XX1-XX2 determining significance of their differences and designating with the upper-case alphabetical character; A, B, $P \leq 0.05$ (between breeds) and lower-case alphabetical character; a, b, c $P \leq 0.05$ (in other cases).

RESULTS AND DISCUSSION

Dividing the total number of AFS visits by hours of the day several periods may be observed, during which the lambs visited the AFS more often (Figs 1, 2). Considering the total number of visits depending on hour of the day (Fig. 1) one can note that the AFS were visited by lambs more intensively in following hours of the day: 02:00–02:59, 08:00–09:59 and 19:00–20:59. These periods of activity of lambs do not match with the results stated in other research studies. Tobler et al. (1991) have shown that the active periods of sheep kept indoors occurs within time period from approximately 06:00 till 19:00, but according to article of Refinetti et al. (2016) the activity periods of sheep occur from approximately 08:00 till 20:00. In the same time the results of research of Nugroho et al. (2015) reveal increase of the eating activity at 06:00–06:29, 12:00–12:29, 18:00–18:29 and 00:00–00:29. Factors that could affect the results reported is the various feeding systems, sheep breed and age, air temperature, air humidity, lighting in barn or other.

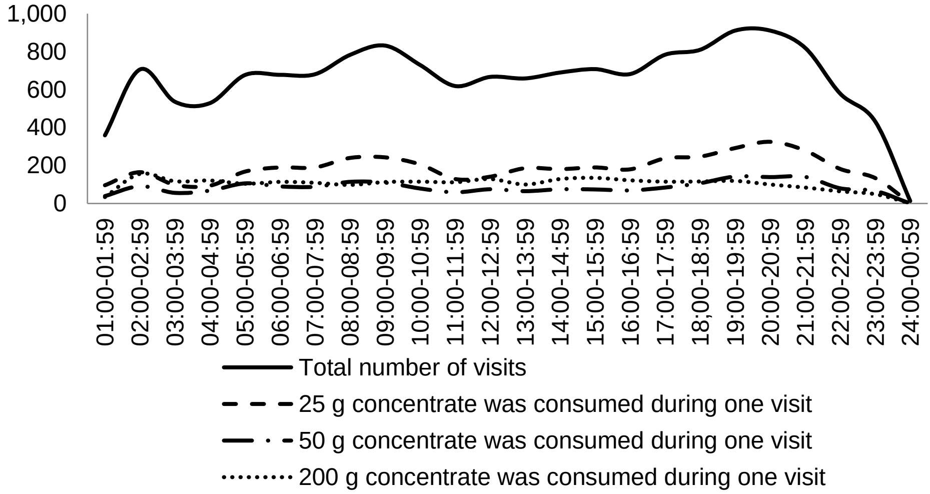

Figure 1. Number of visits to the AFS depending on concentrate consumed during one visit.

Analysing the number of AFS visits depending on the quantity of concentrate consumed per one visit, it may be concluded, that often (in 28% cases from the total number of visits) the lambs consumed 25 g of concentrate per one AFS visit. The most intensive eating periods during the day, when 25 g of the concentrate were consumed by lambs per one AFS visit conform to the intensity periods observed in the general curve of visits (02:00–02:59, 08:00–09:59 and 19:00–20:59). Amount of 50 g of concentrate were consumed by lambs per one AFS visit in 13% cases, but 200 g of concentrate – in 16% cases from the total number of AFS visits. Considering the number of visits depending on the quantity of concentrate consumed per one AFS visit (Fig. 1) it may be noted that the eating intensity within the above mentioned periods of the day is not typical for all other quantities of concentrate (except 25 g). It could be explained with the fact that should there be a queue formed in front of the AFS, the lambs consume 25 g per one AFS visit, because immediately after opening of the gate (30 s after dispensing out of the first portion) there comes the next lamb to the AFS and the previous one must leave the AFS. Should there be no queue at the AFS, the lamb can manage to require dispensing out of the next portion and consume higher dose per one visit (max 300 g).

Proportion of the rest quantity of concentrate consumed by lambs per one AFS visit from the total number of visits was as follows: 75 g – 9%, 175 g – 9%, 150 g – 7%, 225 g – 7%, 100 g – 6%, 125 g – 4.8%, 250 g, 275 g and 300 g was generally fixed in 0.2% of all cases.

Analyzing the number of AFS visits by research periods, numerically the largest number of AFS visits (4655 AFS visits) was achieved by lambs in the third research period (from 14 August 2017 to 27 August 2017), and the lowest number of AFS visits (2869 AFS visits) in the fourth research period (from 28 August 2017 to 10 September 2017). The eating activity increases in the same hours of the day, which were observed under the total number of AFS visits (at 02:00–02:59, 08:00–09:59 and 19:00–20:59, Fig. 2).

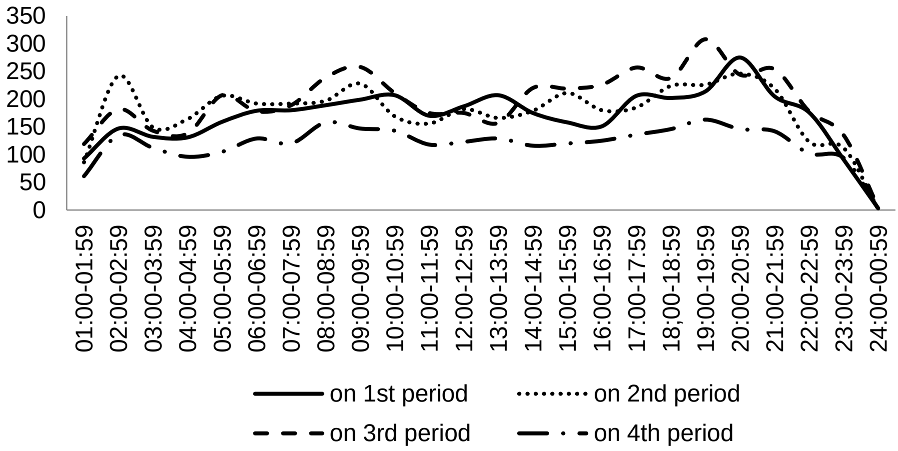

Figure 2. Number of visits to the AFS depending on research periods.

Among the breeds (Table 2) significantly different ($P \leq 0.05$) results was observed in the average number of daily AFS visits per lamb (RD 13 ± 0.2 visits, XX 14 ± 0.2 visits, $P = 0.000609$) and in the average quantity of concentrate consumed per one AFS visit (RD 108 ± 0.9 g, XX 105 ± 0.8 g, $P = 0.026812$). The average increase of daily live weight gain per lamb among breeds does not differ significantly ($P > 0.05$). The average daily live weight gain of RD lambs per day was less (246 ± 26.3 g) than average daily live weight gain of XX lambs (261 ± 18.8 g). In this research the average daily live weight gain of RD lambs was less than it could have been stated in the published results of other research studies (275 g – 388 g per day per lamb) of purebred Dorper sheep and their crossbreeds (Deng et al., 2012; Gallo et al., 2014; Gavojdian et al., 2015). The necessary quantity of concentrate for 1 kg live weight gain of RD lambs was higher (5.39 kg) than of XX lambs (5.32 kg).

Significantly different results for both breeds ($P \leq 0.05$) were obtained in the fourth research period, in comparison with other research periods: the average daily number of AFS visits was significantly less (RD 10 ± 0.2 visits, XX 10 ± 0.2 visits), the average quantity of concentrate consumed per one AFS visit was significantly higher (RD 140 ± 2.0 g, XX 146 ± 1.8 g), the average daily live weight gain was significantly smaller (RD 89 ± 27.8 g, XX 113 ± 22.8 g) and the necessary quantity of concentrate for 1 kg live weight gain was the highest (RD 14.83 kg, XX 12.83 kg). In beginning of fourth research period the age of lambs were 125 ± 3.5 days (RD 119 ± 2.2 days, XX 131 ± 5.7 days). Daily live weight gain reduction and concentrate consumption gain in fourth period can be explained with peak productivity of lambs at the end of third research period (Šenfelde & Kairiša, 2017a).

Table 2. Daily number of visits to the AFS per lamb, concentrate consumed during one visit (g), daily live weight gain (g) per lamb and concentrate necessary for 1 kg live weight gain (kg)

Breed	Research period	Daily number of visits per lamb	Concentrate consumed during one visit, g	Daily live weight gain per lamb, g	Concentrate necessary for 1 kg live weight gain, kg
		$\bar{x} \pm S_{\bar{x}}$			
RD	1	11 ± 0.5^{a}	103 ± 1.8^{a}	395 ± 44.5^{a}	2.95
	2	15 ± 0.4^{b}	97 ± 1.6^{b}	204 ± 44.9^{b}	6.56
	3	15 ± 0.4^{b}	100 ± 1.6^{ab}	297 ± 39.5^{ab}	5.00
	4	10 ± 0.2^{a}	140 ± 2.0^{c}	89 ± 27.8^{c}	14.83
	Total	13 ± 0.2^{A}	108 ± 0.9^{A}	246 ± 26.3^{A}	5.39
XX	1	15 ± 0.4^{a}	96 ± 1.4^{a}	367 ± 30.0^{a}	3.82
	2	15 ± 0.5^{ab}	95 ± 1.4^{a}	238 ± 25.8^{b}	7.28
	3	16 ± 0.4^{b}	99 ± 1.4^{a}	328 ± 22.2^{a}	4.30
	4	10 ± 0.2^{c}	146 ± 1.8^{b}	113 ± 22.8^{c}	12.83
	Total	14 ± 0.2^{B}	105 ± 0.8^{B}	261 ± 18.8^{A}	5.32
RD, XX	Total	13 ± 0.2	106 ± 0.6	254 ± 15.7	5.35

^{abc} – traits with different subscriptions are significantly different ($P \leq 0.05$) between research periods; ^{AB} – traits with different subscriptions are significantly different ($P \leq 0.05$) between breeds; RD – 50% Romanov × 50% Dorper lambs; XX – unknown crossbreed lambs.

Analysing data depending on the number of AFS visits (Table 3), it may be noticed, that the average quantity of concentrate consumed by lambs, who visited the AFS less times (RD1 and XX1 group) was significantly ($P \leq 0.05$) higher (RD1 112 ± 1.3 g, XX1 108 ± 1.1 g), in comparison with lambs visiting the AFS more often (RD2 104 ± 1.2 g, XX2 103 ± 1.1 g). The average daily live weight gain among groups within the framework of one breed does not differ significantly ($P > 0.05$).

Table 3. Concentrate consumption during one visit (g) and live weight gain (g) depending on number of visits to the AFS

Group	Concentrate consumed during one visit, g	Daily live weight gain per lamb, g	Concentrate necessary for 1 kg live weight gain, kg
	$\bar{x} \pm S_{\bar{x}}$		
RD1	112 ± 1.3^{a}	256 ± 42.9^{a}	4.99
RD2	104 ± 1.2^{b}	236 ± 31.6^{a}	5.83
XX1	108 ± 1.1^{a}	245 ± 24.7^{a}	5.41
XX2	103 ± 1.1^{b}	277 ± 28.4^{a}	5.25

^{ab} – traits with different subscriptions are significantly different ($P \leq 0.05$) between groups within breed; RD1 and XX1 – groups of lambs, visiting the AFS a less number of times, RD2 and XX2 – groups of lambs, visiting the AFS more often during the research.

The correlation was calculated for average daily number of visits to the AFS per lamb and average amount of concentrate consumed during one visit to the AFS (Fig. 3, a). The results showed the strong negative correlation ($r = -0.806$) between mentioned factors, also the correlation was significant ($P \leq 0.05$).

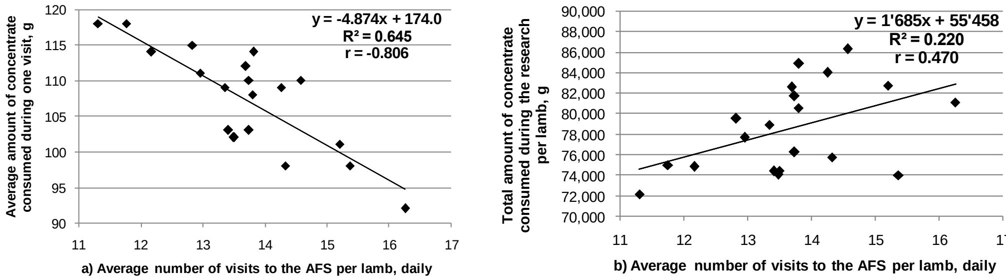

Figure 3. Correlation between average daily number of visits to the AFS and: a) average amount of concentrate consumed during one visit, g; b) total amount of concentrate consumed during the research, g.

Significant ($P \leq 0.05$) moderate positive correlation ($r = 0.470$) results showed between average daily number of visits to the AFS per lamb and total amount of concentrate consumed during the research per lamb (Fig. 3, b). Regarding both graphs (Fig. 3, a, b) one can note that lambs during all the research totally consumed more concentrate in case if they visited AFS more often and during one visit to the AFS consumed less concentrate.

CONCLUSIONS

By using AFS it is possible to ensure continuous access (24 hour per day) to the concentrate for lambs during fattening with reduced human participation and costs. The average daily number of visits to the AFS per lamb achieved 13 ± 0.2. Generally, in the research following periods of the day may be noted, when the eating activity of lambs was increased: at 02:00–02:59, 08:00–09:59 and 19:00–20:59.

During one visit the lambs most often consumed 25 g, 50 g and 200 g of concentrate, which was fixed respectively in 28%, 13% un 16% of the cases from the total number of visits. If the lambs visited AFS more often, they consumed less concentrate during one visit to the AFS, but it did not affect the live weight gain.

The average daily live weight gain per lamb was 254 ± 15.7 g in the whole research and the necessary quantity of concentrate for 1 kg live weight gain was 5.35 kg. Continuous access to the AFS for food consumption reduces the level of stress of the lambs and ensures better food conversion after intake.

REFERENCES

Deng, K. D., Diao, Q. Y., Jiang, C. G., Tu, Y., Zhang, N. F., Liu, J., Ma, T., Zhao, Y. G. & Xu, G. S. 2012. Energy requirements for maintenance and growth of Dorper crossbred ram lambs. *Livestock Science* **150**, 102–110.

Dodd, C. L., Pitchford, W. S., Hocking Edwards, J. E. & Hazel, S. J. 2012. Measures of behavioural reactivity and their relationships with production traits in sheep: A review. *Applied Animal Behaviour Science* **140**, 1–15.

Félix, A., Repetto, J. L., Hernández, N., Pérez-Ruchel, A. & Cajarville, C. 2017. Restricting the time of access to fresh forage reduces intake and energy balance but does not affect the digestive utilization of nutrients in beef heifers. *Animal Feed Science and Technology* **226**, 103–112.

Gavojdian, D., Cziszter, L. T., Budai, C. & Kusza, S. 2015. Effects of behavioral reactivity on production and reproduction traits in Dorper sheep breed. *Journal of Veterinary Behavior* **10**, 365–368.

Gallo, S. B., Merlin, F. A, Macedo, C. M. & Silveira, R. D. O. 2014. Whole grain diet for Feedlot Lambs. *Small Ruminant Research* **120**, 185–188.

Jarrige, R., Dulphy, J.P., Faverdin, P., Baumont, R. & Demarquilly, C. 1995. Activites d'ingestion et de rumination. In: Nutrition des Ruminants Domestiques, INRA Editions, Paris, Ed. by Jarrige, R., Ruckebusch, Y., Demarquilly, C., Farce, M.H., Journet, M., pp. 123–181.

Jongman, E. C., Rice, M., Campbell, A. J. D., Butler, K. L. & Hemsworth, P. H. 2017. The effect of trough space and floor space on feeding and welfare of lambs in an intensive finishing system. *Applied Animal Behaviour Science* **186**, 16–21.

König von Borstel, U., Moors, E., Schichowski, C. & Gauly, M. 2011. Breed differences in maternal behaviour in relation to lamb (*Ovis orientalis aries*) productivity. *Livestock Science* **137**, 42–48.

Nugroho, T. A., Dilaga, W. S. & Purnomoadi, A. 2015. Eating behaviour of sheep fed at day and/or night period. *Journal of the Indonesian Tropical Animal Agriculture* **40**(3), 176–182.

Rahman, M. A., Chuanqi, X., Huawei, S. & Binghai, C. 2017. Effects of hay grass level and its physical form (full length vs. chopped) on standing time, drinking time, and social behavior of calves. *Journal of Veterinary Behavior* **21**, 7–12.

Refinetti, R., Wassmer, T., Basu, P., Cherukalady, R., Pandey, V. K., Singaravel, M., Giannetto, C. & Piccione, G. 2016. Variability of behavioral chronotypes of 16 mammalian species under controlled conditions. *Physiology & Behavior* **161**, 53–59.

Shepley, E., Bergeron, R. & Vasseur, E. 2017. Daytime summer access to pasture vs. free-stall barn in dairy cows with year-long outdoor experience: A case study. *Applied Animal Behaviour Science* **192**, 10–14.

Šenfelde, L. & Kairiša, D. 2016. Use of automatic fodder feeding station for feeding of young sheep. In: *Proceedings of the Scientific and Practical Conference 'Harmonius Agriculture'*, Jelgava, Latvia, pp. 189–192 (in Latvian).

Šenfelde, L. & Kairiša, D. 2017. Concentrate distribution to sheep using automatic feeding station. In: *23rd Annual International Scientific Conference 'Research for Rural Development 2017'*, Jelgava, Latvia, Vol. **2**, pp. 81–88.

Šenfelde, L. & Kairiša, D. 2017a. Automatic concentrate distribution for fattening of Romanov × Dorper lambs. In Proceedings of the 8th international scientific conference "Rural Development 2017: Bioeconomy Challenges", Kaunas, Lithuania, pp. 143–147.

Silva, T. P. D., Marques, C. A. T, Torreão, J. N. C, Bezerra, L. R., Araújo, M. J., Gottardi, F. P., Edvan, R. L. & Oliveira, R. L. 2015. Ingestive behaviour of grazing ewes given two levels of concentrate. *South African Journal of Animal Science* **45**(2), 180–187.

Simeonov, M., Nedelkov, K. & Bozakova, N. 2015. Feeding behavior of early weaned lambs deprived of roughage. *Emirates Journal of Food and Agriculture* **27**(12), 919–926.

Thomson, B.C., Cruickschank, G.J., Poppi, D.P. & Sykes, A.R. 1985. Diurnal patterns of rumen fill in grazing sheep. *Proceeding of New Zealand Society of Animal Production* **45**, 117–120.

Tobler, I., Jaggi, K., Arendt, J. & Ravault, J. P. 1991. Long-term 24-hour rest-activity pattern of sheep in stalls and in the field. *Experimentia* **47**, 744–749.

Zorrilla, E.P., Inoue, K., Fekete, E.M., Tabarin, A., Valdez, G.R. & Koob, G.F. 2005. Measuring meals: structure of prandial food and water intake of rats. *American Journal of Physiology, Regulatory Integrative and Comparative Physiology* **288**, R1450–R1467.

Agronomy Research **16**(3), 892–899, 2018
https://doi.org/10.15159/AR.18.133

Evaluation of different lighting sources on the growth and chemical composition of lettuce

D. Sergejeva[1], I. Alsina[1], M. Duma[2], L. Dubova[1], I. Augspole[2], I. Erdberga[1] and K. Berzina[3]

[1]Latvia University of Life Sciences and Technologies, Faculty of Agriculture, Institute of Plant and Soil Science, Liela street 2, LV-3001 Jelgava, Latvia
[2]Latvia University of Life Sciences and Technologies, Faculty of Food Technology, Department of Chemistry, Liela street 2, LV-3001 Jelgava, Latvia
[3]Riga Technical University, Faculty of Power and Electrical Engineering, Kalku street 1, LV-1050 Riga, Latvia
Correspondence: ina.alsina@llu.lv

Abstract. Experiment were carried out in Latvia University of Agriculture in plant growth room. Lettuce *Lactuca sativa* L. var *foliosum* cv. 'Dubacek' and *L .sativa* L. cv. 'Michalina' were grown under 4 types of lights (luminescence lamps, commercial light emitting diodes (LED) lamps (V-TAC premium series – for plant growing) and two different Lumigrow LED strips - dominant wavelength- blue or red with 14 h photoperiod and total photosynthetic active radiation (PAR) 100 μmol m^{-2} s^{-1} in all variants. Plant weight, length, amount of leaves were measured. Content of chlorophylls, carotenoids, phenols, flavonoids in lettuce was determined three times per vegetation period. In experiments were found that higher lettuce yield was under commercial LED (V-TAC premium series), but these plants contain less soluble sugars, pigments and phenols. Better plant quality was obtained with luminescence lamps. These lettuces have higher sugar, phenols and flavonoids content. Lettuce growth under blue dominate LED (LEDb) was delayed, but these plants contain higher chlorophylls content. The differences in plant growth, response to light and biochemical content between cultivars were detected.

Key words: LED lamps, *Lactuca sativa*, pigments, phenols, flavonoids.

INTRODUCTION

Light is one of most important factor in plant life what can affect their growth and development in a complicated manner. Plant response to the light is made by interaction of many different responses (Hogewoning et al., 2010).

In controlled environments growers use electric lamps such as fluorescent, high-pressure sodium and metal halide (Wheeler, 2008). The light emitting diodes (LED) becomes popular among growers due to spectral output matched to plant photoreceptors (Dougher & Bugbee, 2001). LEDs turn on instantly and do not need warmup time. They are easily integrated into digital control system (Morrow, 2008). Small lighting elements gives more uniform distribution of lighting than use of few larger such as incandescent and fluorescent lamps, that allows to get maximum production without wasting energy

(Yano & Fujiwara, 2012). LEDs are environmentally friendlier than other currently used lamps in horticulture (Dougher & Bugbee, 2001; Morrow, 2008).

Traditional light sources create light with an ionized gas, superheated element or arc discharge. LEDs create light through a semiconductor process. Material which are used to form the semiconductor junction determined by the wavelength of the emitted light. LEDs can give the light with wavelengths from 250 nm (ultraviolet) to 1,000 nm (infrared) and even more (Bourget, 2008).

If plants were grown in greenhouses light effect on the plants are complex and caused by mixed with natural and supplemental light.There for results from greenhouses and growing room by using same lightening source can give different results.

The spectral composition of LEDs light is extensively studied, but due to no systematic research approach, the results sometimes are contradictory (Viršile et al., 2017).

Red and blue light are the major energy source for the photosynthetic CO_2 assimilation in plants. Therefore influence of the red and blue light on plant physiologic processes gives easily noticeable changes (Lin et al., 2013). Red light is necessary for normal plant growth and photosynthesis. Red light with different wavelengths can effect plants uneven. Lettuce biomass yield increased if LED wavelength was increased from 660 to 690 nm. Red light gives positive impact on antioxidant system (Olle & Viršilė, 2013).

Blue light (440–476 nm) stimulated biomass accumulation in lettuce (Johkan et al., 2010), promote lettuce growth after transplanting,increased concentration of carotenoids and anthocyanins, enhanced antioxidant status (Olle & Viršilė, 2013).

Combination of blue and red light reduced nitrate content and significantly increased soluble sugar content (Viršile et al., 2017).

Understanding of wavelengths effects on the plant will allow researchers to develop specific lighting systems for the current plant species with changeable light spectrum and intensity during plant development (Massa et al., 2015).

The aim of the study is to evaluate lettuce growth, yield and its chemical composition to improve plant nutrition quality with the use of different lighting sources.

MATERIALS AND METHODS

Lettuce *Lactuca sativa* L. var *foliosum* cv. 'Dubacek' and *L.sativa* L. cv. 'Michalina' were used in experiments. 10 plants per pot were grown in 3 L vegetation pots filled with commercial peat substratum (Kekkila – peat fraction > 25 mm, EC – 25 mS m^{-1}, pH_{H2O} 5.6, N – 80 mg L^{-1}, P – 30 mg L^{-1} K – 200 mg L^{-1}).

Experiments were arranged in growing room without natural lighting.. Plants were grown under 4 different lighting sources- luminescence lamp (OSRAM, Cool-white, 36 W), commercial LED (V-TAC premium series – for plant growing, 18 W, 1,530 Lm) and two different Lumigrow LED strips – dominant wavelength- blue (LEDb) or red (LEDr). In all variants plants were grown in 14 h photoperiod with total PAR 100 µmol m^{-2} s^{-1}. Light spectrum of used illumination sources were shown in Fig. 1. Relative spectral distribution 440 nm : 660 nm are: luminescence lamp (LL) 79 : 21, commercial LED (LEDc) 50 : 50, LEDb 77 : 23, LEDr 15 : 85. Temperature in plant growth room during day and night time were 22 ± 2 °C.

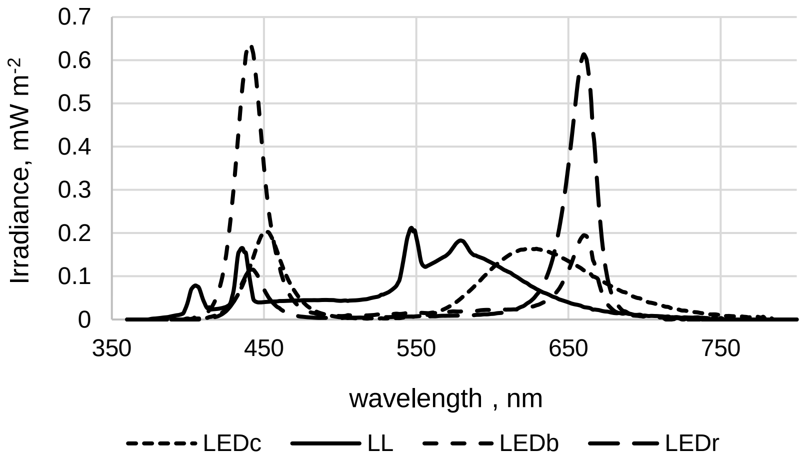

Figure 1. Spectrum of used lighting sources (determined with Gigahertz-Optic MSC15).

All plant analyses were made three times during the plant vegetation with two week interval. Plant weight, dry weight, dry matter content (dried at 60 °C for 24 h), number of leaves, and plant biochemical parameters was detected.

Phytochemical extraction and determination

All the chemicals used were with the analytical grade. For absorbance measurements UV spectrometer UV-1800 Shimadzu Corporation, Japan was used.

Chlorophylls and carotenoids content was analysed spectrophotometrically in ethanol extract according to the method described by Duma et al. (2014) and results were expressed as mg g^{-1} fresh matter (FM).

Total phenolics in lettuce leaves was extracted with methanol- distilled water- hydrochloric acid solution (79 : 20 : 1 v/v/v). Total phenolics content was determined with Folin- Ciocalteu reagent. Absorption was measured at 765 nm and results was expressed as mg g^{-1} gallic acid equivalent (GAE) (Duma et al., 2017).

Flavonoids were extracted with ethanol. Total flavonoid content was determined by method described by Duma et al. (2016). Absorption was measured at 506 nm and results were expressed mg rutin equivalent (RE) 100 g^{-1} FM.

The total soluble solids content (°Brix) from lettuce leaf juice was determined with Refractometer DR301-95 made by company A.KRÜSS Optronic.

Biochemical analyses were performed in three replicates. Two-way analyses of variance (ANOVA) was used. Fisher LSD post-hoc test were made to determine significance of differences. For mathematical data processing $p < 0.05$ was regarded as statistically significant. Data were expressed as means ± standard deviation.

RESULTS AND DISCUSSION

Plant growth significantly depends on used illumination source, plant cultivar and development stage. Tallest plants were obtained under LEDr illumination. Under that illumination atypical stem elongation for the rosette type plants was observed and decrease of leaf number by 10–17% for cv. 'Michalina' and 10–21% for cultivar

‘Dubacek’ was stated. Similar results are reported also by Lin et al. (2013) and Chen et al. (2014). Till the 4th week of plant growth there are no significant differences in plant weight grown under LEDr and other lighting sources, but at the end of experiment this variant and LEDb were the worst. The decrease of plant biomass by 7–49% for cv. ‘Dubacek’ and 3–49% for ‘Michalina’ was observed in comparison with other lighting sources (Fig. 2). It is contrary to Son & Oh (2013) results. They reported the highest lettuce weight under monochromatic red light. The next best result was observed in variant illuminated with light in relative proportion 13% of blue light and 87% of red light (Son & Oh, 2013). Similar positive effect of red light was reported by Bian et al. (2016), Viršilė et al. (2017). That is completely opposite to ours LEDr, were plant weight was one of the lowest (Fig. 2).

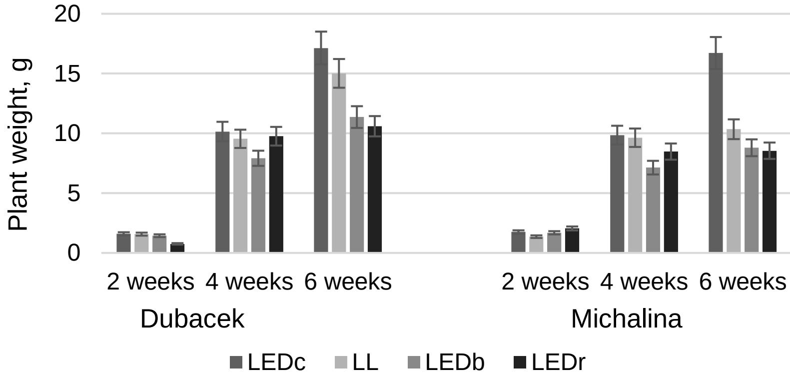

Figure 2. The lettuce weight during vegetation period.

Under LEDc, LL light sources plant growth was harmonious. The largest and vigorous plant was obtained under LEDc. At the 6th week of cultivation lettuce of cv.‘Dubacek’ weighted 14.1%, but cv.’Michalina’ 61.6% more in comparison with plants grown under luminescent lamps. Retarded growth was observed under dominant LEDb. (Figs 1 and 3.) It corresponds to the results of other authors (Li & Kubota, 2009, Stutte et al., 2009, Lin et al., 2013, Chen et al., 2014).

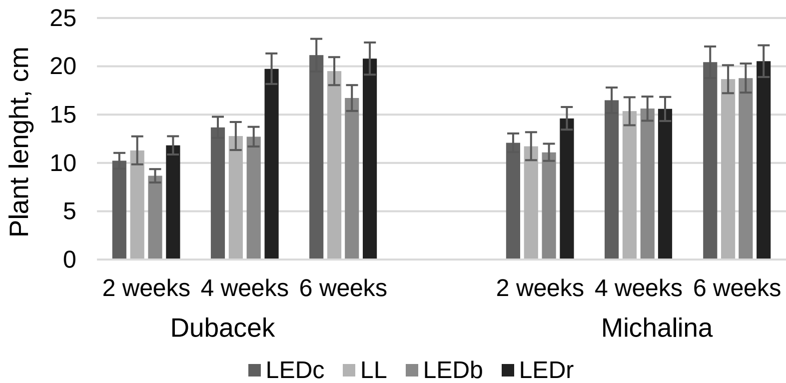

Figure 3. The lettuce length during vegetation period.

The impact of illumination source on the dry matter content significantly depended on cultivar and sampling time. (Fig. 4) For cv. ‘Dubacek’ significant differences as result of light source was observed only at the 4th week of vegetation, but cv. ‘Michalina’ after 4 and 6 weeks of cultivation. The highest content of the dry matter was in variant with commercial LED. Knowing that the dry matter content in plants increases with the plant age, it can be hypothesized that commercial LED stimulates plant aging.

Results corresponds to Son & Oh (2013) data where also the highest dry matter content was observed in variants with blue and red light proportion close to 50 : 50 calculated from.

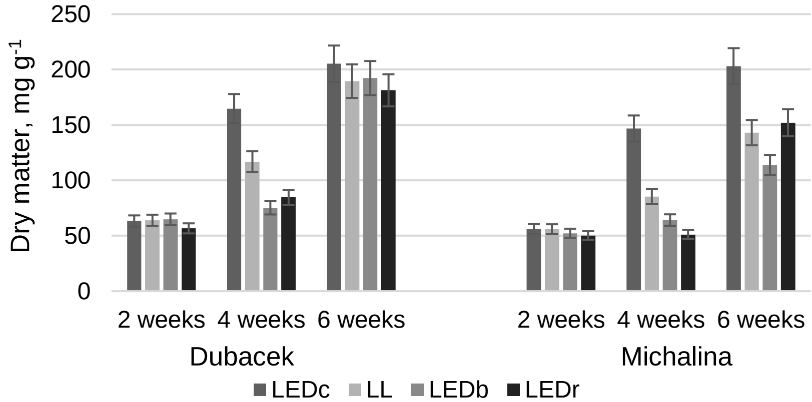

Figure 4. Dry matter content in the lettuce plants during vegetation period.

The content of soluble solids (°Brix) depended on cultivar. Slightly higher content was observed in cv. ‘Dubacek’. Significantly higher soluble solids content was detected in lettuce grown under LL, the less one- under LEDr (Fig. 5). The decrease of soluble sugar content by adding red light is reported also by Lin et al. (2013). Soluble sugars are main product of photosynthesis and effects lettuce nutrition quality as well as together with other compounds- plant taste. Higher soluble sugar content by luminescence lamp use in comparison with LED is reported also by Chen et al. (2014).

Plant pigments have specific wavelength absorption patterns and LED lamps are manufactured taking into account these spectrums. In average higher chlorophyll content was in the lettuce grown under LEDb. After 2 weeks of cultivation the highest content of total chlorophyll (0.827 mg g^{-1}) and carotenoids (0.190 mg g^{-1}) was detected in the leaves cv. ‘Dubacek’ under the LEDb. Higher chlorophylls content in cv. ‘Michalina’ leaves was detected at 4th week 0.685 mg g^{-1} under the same – LEDb light. Difference in pigments content as result of lighting increased with the plant aging (Table 1). The impact of light spectrum on the chlorophylls content is reported also by other researchers. Son & Oh (2013) detected higher chlorophylls value in red: blue light proportion 50:50. Increase of red wavelength proportion leads to decrease of chlorophyll content, but there is no significant positive effect of blue light reported (Son & Oh, 2013). Lin et al. didn’t find significant differences in chlorophylls and carotenoids content due to different light spectrum (Lin et al., 2013).

Table 1. The effect of light source on the biochemical content of lettuce plants

	Dubacek					Michalina				
	LEDc	LL	LEDb	LEDr	$LSD_{0.05}$	LEDc	LL	LEDb	LEDr	$LSD_{0.05}$
Chlorophylls'content, mg g^{-1}										
2 weeks	0.678	0.662	0.827	0.656	0.101	0.564	0.496	0.598	0.560	0.039
4 weeks	0.582	0.712	0.706	0.648	0.073	0.654	0.674	0.685	0.664	0.037
6 weeks	0.557	0.531	0.663	0.584	0.108	0.206	0.345	0.561	0.402	0.066
Carotenoides content, mg g^{-1}										
2 weeks	0.119	0.154	0.190	0.154	0.035	0.128	0.109	0.136	0.128	0.015
4 weeks	0.129	0.151	0.151	0.156	0.035	0.142	0.150	0.146	0.144	0.012
6 weeks	0.123	0.114	0.145	0.136	0.031	0.057	0.082	0.123	0.098	0.015
Phenols content, mg g^{-1}										
2 weeks	1.381	0.732	2.050	1.311	0.010	0.687	0.840	0.872	0.849	0.012
4 weeks	2.840	2.865	3.242	1.395	0.024	2.316	3.413	1.844	1.761	0.031
6 weeks	6.340	3.112	4.002	3.133	0.003	4.451	3.960	1.568	2.959	0.003
Flavonoids content, mg 100 g^{-1}										
2 weeks	4.918	5.136	6.211	5.648	0.199	3.980	4.130	5.220	4.390	0.139
4 weeks	6.462	7.021	6.801	6.109	0.494	5.740	5.300	5.450	4.800	0.250
6 weeks	6.743	5.967	8.396	6.601	0.350	6.430	6.280	4.310	5.310	0.384

Results showed that phenols and flavonoids content in lettuce leaves significantly increased with the plant age. Larger phenol and flavonoids content was detected in cv. 'Dubacek'. After 6 weeks of cultivation highest phenol content was in variant with LEDc – 6.340 mg g^{-1} FM for 'Dubacek' and 4.451 mg g^{-1}FM for 'Michalina'. The smallest amount of phenols at 4th week of vegetation was in variants with LEDr (Table 1, Fig. 5). Opposite results were obtained in experiments with lettuce made by Li & Kubota (2009) and Zukauskas et al. (2011) – phenol content under red light wavelengths increased. Taulavuori et al. (2017) reported that accumulation of phenols is higher in lettuce leaves grown in at high ratios of blue light.

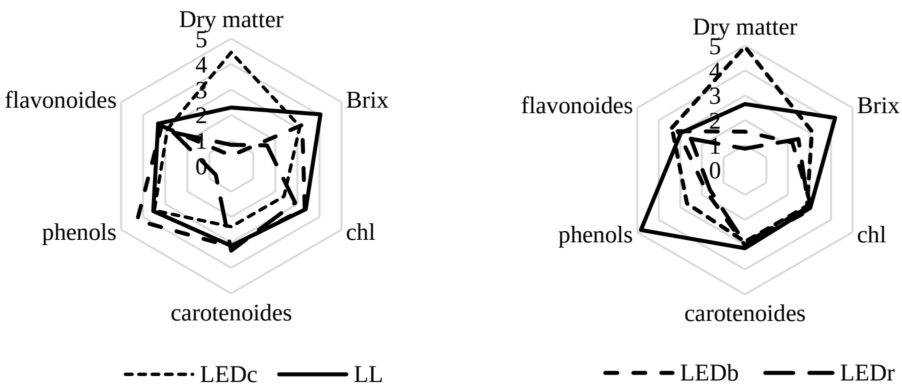

Figure 5. Relative dry matter, soluble solids, chlorophylls, carotenoids, total phenols and flavonoids content in the cv. 'Dubacek' (left) and cv. 'Michalina' (right) leaves at the 4th week of vegetation.

Lithuanian researchers reported that the significant increase of total phenols was found under both blue (455 nm, 470 nm) and 535 nm green LEDs lighting (Samuoliene et al., 2012).

Flavonoid content is one of the important factors influenced lettuce nutrition quality. Flavonoids content affect colour, flavour and fragrance of plants (Son & Oh, 2013). Our results showed the significant effect of cultivar, sampling time and light spectrum. In average cv. ‘Dubacek’ had 24% higher flavonoids content. Increase of flavonoid content during vegetation was observed (Table 1). Illumination spectrum effect depended on cultivar. In average increase of flavonoid content as result of LEDb treatment was observed for cv. ‘Dubacek’, but the same light for cv. ‘Michalina ’at the end of vegetation was the worst one. Contradictory results are reported also in other studies (Son & Oh, 2013, Viršilė et al., 2017, Taulavuori et al., 2017).

The obtained results show that the influence of light is complex and depends on lighting spectral conditions, plant variety and sampling time. The highest fresh and dry matter derived from plants grown under the comercial LEDs, the highest soluble dry matter content for both varieties was detected in plants grown under LL. Under the same illumination source also more physiologically active compounds were detected.

CONCLUSIONS

Higher lettuce yield was obtained under commercial LED (V-TAC premium series), but these plants contain less soluble sugars, pigments and phenols.

Better plant quality was obtained with luminescence lamps. These lettuces have higher sugar, phenols and flavonoids content.

Lettuce growth under LEDb was delayed, but these plants contain higher chlorophylls content.

The differences in plant growth, response to light and biochemical content between cultivars were detected.

ACKNOWLEDGEMENTS. Study was supported by European Regional Development Fund project ‘New control methods for energy and ecological efficiency increase of greenhouse plant lighting systems (uMOL)’, Grant Agreement Nr. 1.1.1.1/16/A/261

REFERENCES

Bian, Z.H., Cheng, R.F., Yang, Q.C. & Wang, J. 2016. Continuous light from red, blue, and green light-emitting diodes reduces nitrate content and enhances phytochemical concentrations and antioxidant capacity in lettuce. *J Amer Soc Hort Sci.* **141**, 186–195.

Bourget, C.M. 2008. An introduction to light-emitting diodes. *HortScience* **43**(7), 1944–1946.

Chen, X.L., Guo, W.Z., Xue, X.Z., Wang, L.C. & Qiao, X.J. 2014. Growth and quality responses of ‘Green Oak Leaf’ lettuce as affected by monochromic or mixed radiation provided by fluorescent lamp (FL) and light-emitting diode (LED). *Sci. Hortic.* **172**,168–175.

Dougher, T.A.O. & Bugbee, B. 2001. Differences in the Response of Wheat, Soybean and Lettuce to Reduced Blue Radiation. *Photochemistry and Photobiology* **73**(2), 199–207.

Duma, M., Alsina, I., Zeipina, S., Lepse, L. & Dubova, L. 2014. Leaf Vegetables As Source of Phytochemicals. *9th Baltic Conference on Food Science and Technology – Food for Consumer Well-Being: Foodbalt 2014*, 262–265.

Duma, M., Alsina, I. & Dubova, L. 2016. Changes of chemical composition of rhubarb during vegetation. *Acta Horticulturae* **1142**, 253–259.

Duma, M., Alsina, I., Dubova, L. & Erdberga, I. 2017. Quality of tomatoes during storage. *11th Baltic conference on food science and technology "Food science and technology in a changing world" : conference proceedings, Jelgava, April 27-28, 2017 / Latvia University of Agriculture. Faculty of Food Technology. - Jelgava:* LLU, 130–133.

Hogewoning, S.W., Trouwborst, G., Maljaars, H., Poorter, H., van Ieperen, W. & Harbinson, J. 2010. Blue light dose-responses of leaf photosynthesis, morphology, and chemical composition of Cucumis sativus grown under different combinations of red and blue light. *Journal of Experimental Botany* **61**(11), 3107–3117.

Johkan, M., Shoji, K., Goto, F., Hahida, S. & Yoshihara, T. 2010. Blue light-emitting diode light irradiation of seedlings improves seedling quality and growth after transplanting in red leaf lettuce. *HortScience* **45**, 1809–1814.

Li, Q. & Kubota, C. 2009. Effects of supplemental light quality on growth and phytochemicals of baby leaf lettuce. *Environmental and Experimental Botany* **67**(1), 59–64.

Lin, K.H., Huang, M.Y., Huang, W.D., Hsu, M.H., Yang, Z.W. & Yang, C.M. 2013. The effects of red, blue, and white light-emitting diodes on the growth, development, and edible quality of hydroponically grown lettuce (Lactuca sativa L. var. capitata). *Scientia Horticulturae* **150**, 86–91. https://doi.org/10.1016/j.scienta.2012.10.002

Massa, G., Graham, T., Haire, T., Flemming, C., Newsham, G. & Wheeler, R. 2015. Light-emitting diode light transmission through leaf tissue of seven different crops. *HortScience* **50**(3), 501–506.

Morrow, R.C. 2008. LED Lighting in Horticulture. *HortScience* **43**(7), 1947–1950.

Olle, M. & Viršilė, A. 2013. The effects of light-emitting diode lighting on greenhouse plant growth and quality. *Agricultural food and science* **22**, 223–234.

Samuolienė, G, Sirtautas, R, Brazaitytė, A, Duchovskis, P. 2012. LED lighting and seasonality effects antioxidant properties of baby leaf lettuce. *Food Chem* **134**(3),1494–1499.

Son, K.H. & Oh, M.M. 2013. Leaf Shape, Growth, and Antioxidant Phenolic Compounds of Two Lettuce Cultivars Grown under Various Combinations of Blue and Red Light-emitting Diodes *HortScience* **48**(8), 988–995.

Stutte, G.W., Edney, S. & Skerritt, T. 2009. Photoregulation of bioprotectant content of red leaf lettuce with light-emitting diodes. *HortScience* **44**(1), 79–82.

Taulavuori, E., Taulavuori, K., Holopainen, J.K., Julkunen-Tiitto, R., Acar, C. & Dincer, I. 2017. Targeted use of LEDs in improvement of production efficiency through phytochemical enrichment. *J Sci Food Agric*. **97**(15), 5059–5064.

Viršilė, A., Olle, M. & Duchovskis, P. 2017. LED Lighting in Horticulture. In: Dutta Gupta S. (eds) *Light Emitting Diodes for Agriculture*. Springer, Singapore, 113–147.

Zukauskas, A., Bliznikas, Z., Breivė, K., Novičkovas, A., Samuolienė, G., Urbonavičiūtė, A., Brazaitytė, A., Jankauskienė, J. & Duchovskis, P. 2011. Effect of supplementary pre-harvest LED lighting on the antioxidantproperties of lettuce cultivar. *Acta Horticulturae* **907**, 87–90.

Wheeler, R.M. 2008. A historical background of plant lighting: An introduction to the workshop. *HortScience* **43**(7), 1942–1943

Yano, A. & Fujiwara, K. 2012. Plant lighting system with five wavelength-band light-emitting diodes providing photon flux density and mixing ratio control. Plant Methods **8**(46), 1–12.

Agronomy Research **16**(3), 900–909, 2018
https://doi.org/10.15159/AR.18.084

Molecular genetics analysis of milk protein gene polymorphism of dairy cows and breeding bulls in Latvia

D. Smiltina* and Z. Grislis

Latvia University of Life Sciences and Technologies, Faculty of Agriculture, Institute of Agrobiotechnology, Liela street 2, LV-3001 Jelgava, Latvia
*Correspondence: dace.smiltina@llu.lv

Abstract. Milk protein is the most valuable component of milk from a dietary point of view. More than 95% of ruminants' milk proteins are coded by six structural genes: two whey proteins (α – lactalbumin and β – lactoglobulin) and four caseins (α_{S1} – and α_{S2} – caseins, β – casein, κ – casein). The object of the research was the genetic polymorphisms of milk protein genes in populations of cows and breeding bulls of milk producing breeds in Latvia. The aim was to promote cow breeding in Latvia by developing and testing molecular genetics analyses for future quantity and quality analysis of the dairy cows' population in Latvia, based on the research of genes encoding milk protein polymorphism. In methodology the molecular markers were chosen which would be suitable for characterization of polymorphism of five milk protein genes in the population of dairy cows reared in Latvia. As a genetic method chosen the Restriction Fragment Length Polymorphism (RFLP) method and most analysed alleles of milk proteins. Using data of 719 DNA samples of dairy cows, the analysis of Latvian cows' population was carried out through six SNP of five milk protein genes: C*SN1S1* c.–175A > G, *CSN2* – c.4451A > C, *CSN3* c.11625C > T and c.11661A > C, *LAA* c.15A > G and *LGB* c.3106T > C. The results of PCR-RFLP analysis showed, as it was expected, that all genotypes were found in the populations.

Key words: milk proteins, dairy cattle, polymorphisms, Latvian population.

INTRODUCTION

At the end of 2014 in Latvia agricultural holdings were breeding 422.0 thousand cattle (Central Statistical bureau of Latvia, 2015). But at the end of 2016, agricultural holdings were breeding 412.3 thousand cattle, the drop was due to the reduction in the number of dairy cows of 5.2% (Central Statistical bureau of Latvia, 2017).

The production of dairy cows or milk yield from the total milk, produced in the European Union, in year 2014 and 2015 was more than 96% (Eurostat, 2015; 2016). It is used not only in pure form (around 27% from all dairy products), but also in different dairy products. The amount of milk produced in Latvia (incl. goat milk) in 2014 comprised 971.8 thousand tons. The average milk yield from a dairy cow reached 5812 kg, (Central Statistical bureau of Latvia, 2015).

The primary genetic relationship with milk quality and quantity is sought in relation to milk proteins, which largely, till 95% depending from breed, (Artym, Zimecki, 2013; Tsabouri et al., 2014) consists of four caseins and two main whey proteins.

Caseins are the water insoluble fraction of milk proteins (Table 1): alfa$_{S1}$ – casein (gene *CSN1S1*), alfa$_{S2}$ – casein (*CSN1S2*), beta – casein (*CSN2*) and kappa – casein (*CSN3*), (Artym, Zimecki, 2013; Tsabouri et al., 2014). Cattle casein loci is located on chromosome 6, and closely interconnected in cluster (Caroli et al., 2009; Barłowska et al., 2012). The total casein locus varies from 250 kb to 370 kb for humans, but the gene sequence and genetic alignment are conservative (Vilotte et al., 2013).

The second groupe of milk proteins are whey or serum proteins – water soluble fraction. Two main whey proteins (Table 1) are α – lactalbumin (α – LA), which is encoded with *LAA (LALBA)*, and β – lactoglobulin (β – LG; progestagen-associated endometrial protein) or *LGB (PAEP)* gene (Artym, Zimecki, 2013; Tsabouri et al., 2014). α – LA gene is localized on chromosome 5, but *LGB* gene is located on chromosome 11 (11q28; Barłowska et al., 2012).

Table 1. Description of polymorphisms of five cow milk proteins

Gene		Polymorphisms of analyse			Protein alleles	
Abr.	Chr.	ID nr.	SNP^	Inr/Ex	Short	Full
CSN1S1	6q31	rs109817504	g.4646092A > G	5'UTR	B > C	A,**B**,D,F,G,H > **C**,E,I
CSN2	6q31	rs43703011	c.4451A > C	Ex 7	A1 > A2	**A1**,B,C,F,G > **A2**,A3,D,E,H1,H2,I,J
CSN3	6q31	rs43703015	c.11625C > T	Ex 4	A > B	**A**,A1,D,E,F2,G1,H,I > **B**,B2,C,J
		rs43703016	c.11661A > C	Ex 4		
LAA	5q21	rs209045823	c.15A > G	5'UTR	A > B	-
LGB	11q28	rs109625649	c.3106T > C	Ex 4	A > B	**A**,H > **B**,C,D,Dr,E,F,G,I,J,W

^ – Full name of polymorphisms taking in account position in gene (DNA) sequence.

In different studies in last 80 years have found out that all six major cows' milk proteins are variably not only in genome level (polymorphisms) but mainly after amino acid sequences of proteins. So far, various protein synthesis summaries (Hristov et al., 2014; Martin et al., 2013) have shown that for six proteins a total variation of alleles are 53: from 3 till 16 depending on gene/protein (Table 1), despite the fact that there are more polymorphisms in each gene. In the last five years, research on the dairy cow population in several of these genes has also been launched in Latvia (Petrovska et al., 2017a; 2017b; 2017c).

By 2008, more than 1200 breeds of dairy cows have been registered in the world (Utsunomiya et al., 2015), but in Latvia are registered 16 breeds in Agricultural Data Centre of Republic of Latvia. The number of dairy cows at 2014 were more than 125 thousands. More often farmed breed in Latvia is Holstein Black and White (HB; frequency around 33% in 2014, but in 2017 – around 47%), which is known in more than 128 countries (Utsunomiya et al., 2015). Dairy cows' milk yield per one cow of HB breed is greater than of Latvian local or historical breeds: Latvian Brown and Latvian Blue (Cielava et al., 2015; 2017), what's mean that in case of HB breed is a need more urgent to carry out a rebuilding of the bulk or additional costs of buying or growing new cows.

The aim of all research is to promote cow breeding in Latvia by developing and testing molecular genetics analyses for future quantity and quality analysis of the dairy cows' population in Latvia, based on the research of genes encoding milk protein polymorphism. But the task of this study is to make the primary characterization of selected polymorphisms of bovine milk protein genes in the population of dairy cows reared in Latvia.

MATERIALS AND METHODS

Research was elaborated in the period of April 2009 to June 2014.

Description of the study object

Research group of breeds of dairy cows raised in Latvia was formed from 719 cattle biological material, including blood of 625 cows and sperm samples of 94 breeding bulls from Breeding and artificial insemination stations (BAIS) of seven breeds (Latvian Brown (LB) and Latvian Blue (LZ), Holstein Black and White (HB), Holstein Red and White (HR), Sweden Red and White (SR), Danish Red (DR) and Angeln (AN)) of dairy cows raised in Latvia (Table 2).

Table 2. Description of cows' group and the number of animals with positive genotyping in each locus

Breed of dairy cow		Sample	Freq., %	Positive genotyping (number of cows)				
				CSN1S1	*CSN2*	*CSN3*	*LAA*	*LGB*
Latvian Brown	LB	367	51,04	352	365	299	292	342
Latvian Blue	LZ	179	24,90	154	178	65	142	138
Holstein Black and White	HB	79	10,99	79	79	52	79	79
Holstein Red and White	HR	15	2,09	15	15	14	15	15
Sweden Red and White	SR	4	0,56	4	4	3	4	4
Danish Red	DR	55	7,65	55	55	41	55	55
Angeln	AN	4	0,56	4	4	4	4	4
Breeds crossing	XX	16	2,23	12	16	9	12	12
Sum		719		675	716	487	603	649
Including breeding bulls of BAIS		94	13,07	86	94	74	94	86

Overall, biological material was obtained from 81 herds of dairy cows in different regions of Latvia. In research were used also samples of cows of Latvian Brown and Latvian Blue breeds from the Depository of Latvian animal genetic resources.

DNA extraction

DNA extraction was done from 625 cows' blood and 94 bulls' sperm samples. In work were used two kits of genomic DNA extraction: Genomic DNA Purification Kit #K512 (Fermentas, Vilnius, Lithuania) and PUREGENE® DNA Isolation Kit (QIAgene, USA). Methods of both kits were adjusted for work with different blood and sperm quantity than in protocol.

Cows' milk protein polymorphism analysis

Six SNPs of five cows' milk protein genes (Table 3) were analysed with one of the oldest DNA fingerprinting method (Restriction Fragment Length Polymorphism (RFLP)), where each restriction endonuclease targets different nucleotide sequences in a DNA strand and cuts at different sites. Respectively, in casein protein genes: C*SN1S1* c.–175A > G, which leading to the protein variation change B to C; *CSN2* – c.4451A > C

(Pro$_{67(82)}$His; A1 and A2 variations); for *CSN3* were selected two SNPs: c.11625C > T and c.11661A > C, which leading to Thr$_{136(157)}$Ile and Asp$_{148(169)}$Ala or A variation change to B variation. For whey proteins, respectively, for *LAA* was selected SNP located in no-translated region or c.15A > G, in which case it is considered that changes A variations of the B, but for *LGB* c.3106T > C, which leading to the amino acid change Val$_{118(134)}$Ala or protein variation change A to B.

Table 3. Description of PCR – RFLP for study of polymorphisms of milk protein genes at cows' population reared in Latvia

Gene	Polymorphism#	PCR		RFLP	
		sequence of primers	product, bp	**enzyme,** sequence	fragments, bp and protein variations
CSN1S1	c.–175A > G - B > C	F 5' – TGC ATG TTC TCA TAA TAA CC – 3' R 5' – GAA GAA GCA GCA AGC TGG – 3'	310	***MaeIII*** ↓GTNAC	214/96 – B 310 – C
CSN2	c.4451A > C Pro$_{67(82)}$His A1 > A2	F 5' – CCT TCT TTC CAG GAT GAA CTC CAG – 3' R 5' – GAG TAA GAG GAG GGA TGT TTT GTG GGA GGC TCT – 3'	121	***DdeI*** C↓TNAG	121 – A1 86/35 – A2
CSN3	c.11625T > C and c.11661A > C Thr$_{136(157)}$Ile and Asp$_{148(169)}$Ala A > B	F 5'– TAT CAT TTA TGG CCA TTG GAC CA – 3' R 5'– CTT CTT TGA TGT CTC CTT AGA GTT – 3'	228	***HinfI*** G↓ANTC ***HindIII*** A↓AGCTT	133/93 – A 135/95 – B
LAA (LALBA)	c.15A > G - A > B	F 5' – CTC TTC CTG GAT GTA AGG CTT– 3' R 5' – AGC CTG GGT GGC ATG GAA TA– 3'	166	***MnlI*** CCTCN$_7$↓	78/52/36 – A 114/52 – B
LGB (PAEP)	c.3106T > C Val$_{118(134)}$Ala A > B	F 5' – TGT GCT GGA CAC CGA CTA CAA AAA G – 3' R 5' – GCT CCC GGT ATA TGA CCA CCC TCT – 3'	247	***HaeIII*** GG↓CC	148/99 – A 74(x2)/99 – B

– Nucleotide replacement and, if so, the replacement amino acids in activated protein (inactive protein), and protein variations.

Data analysis

Numbers and frequencies of alleles and genotypes for entire population were estimated by direct counting, but for group of each breed were calculated by dividing samples.

Expected heterozygote indexes were estimated for both alleles at the locus or polymorphism. Population heterozygote was calculated as the ratio of the number of heterozygous individuals vs. the total number of subjects. Deviations from the Hardy – Weinberg equilibrium were tested by the *chi square (χ^2) test*.

Also for entire population was analysed association between non-parametrical indicators (number of alleles and genotypes for different sex or breeds of cows). For that calculation was used crosstab method with χ^2 *tes*t or *Pirson* χ^2 *test* at the confidence $p < 0.05$.

For all analyzes was used statistically programs: IBM SPSS Statistics version 22.0 and PAST (PAlaentological Statistics, ver. 1.63).

RESULTS AND DISCUSSION

DNA samples of 719 dairy cows raised in Latvia, including 94 breeding bulls, was analysed on polymorphisms of five milk proteins, by studding alleles and genotypes of each SNPs of each gene. Therefore we get a view about Latvian cows' population (Table 4).

Table 4. Distribution of polymorphisms of alleles and genotypes of the milk protein genes in population of dairy cows' in Latvia

Gene	Allele/	Frequency of allele/genotype									Statistic
	Genotype	All	LB	LZ	HB	HR	SR*	DR	AN*	XX	p_x
CSN1S1	B	0.96	0.97	0.95	0.97	0.97	1.00	0.97	0.88	0.92	0.42
	C	0.04	0.03	0.05	0.03	0.03	-	0.03	0.13	0.08	
	BB	0.93	0.93	0.90	0.94	0.93	1.00	0.95	0.75	0.83	0.76
	BC	0.07	0.07	0.10	0.06	0.07	-	0.05	0.25	0.17	
	CC	-	-	-	-	-	-	-	-	-	
CSN2	A1	0.67	0.69	0.76	0.43	0.60	0.38	0.63	0.50	0.53	1.25 x10^{-11}
	A2	0.33	0.31	0.24	0.57	0.40	0.63	0.37	0.50	0.47	
	A1A1	0.42	0.44	0.56	0.16	0.20	0.25	0.38	-	0.19	1.57 x10^{-9}
	A1A2	0.49	0.50	0.42	0.53	0.80	0.25	0.49	1.00	0.69	
	A2A2	0.09	0.06	0.03	0.30	-	0.50	0.13	-	0.13	
CSN3	A	0.92	0.93	0.72	1.00	1.00	1.00	1.00	1.00	1.00	2.32 x10^{-17}
	B	0.08	0.07	0.28	-	-	-	-	-	-	
	AA	0.86	0.88	0.54	1.00	1.00	1.00	1.00	1.00	1.00	2.66 x10^{-13}
	AB	0.11	0.10	0.35	-	-	-	-	-	-	
	BB	0.03	0.02	0.11	-	-	-	-	-	-	
LAA	A	0.06	0.03	0.08	0.18	0.10	0.13	0.02	-	-	8.04 x10^{-9}
	B	0.94	0.97	0.92	0.82	0.90	0.88	0.98	1.00	1.00	
	AA	-	-	-	0.01	-	-	-	-	-	2.70 x10^{-3}
	AB	0.12	0.06	0.15	0.34	0.20	0.25	0.04	-	-	
	BB	0.88	0.94	0.85	0.65	0.80	0.75	0.96	1.00	1.00	
LGB	A	0.22	0.17	0.20	0.42	0.33	0.38	0.25	0.50	0.04	7.16 x10^{-11}
	B	0.78	0.83	0.80	0.58	0.67	0.63	0.75	0.50	0.96	
	AA	0.03	0.01	0.01	0.14	0.13	0.25	0.05	0.25	-	3.25 x10^{-5}
	AB	0.37	0.33	0.37	0.57	0.40	0.25	0.40	0.50	0.08	
	BB	0.60	0.67	0.62	0.29	0.47	0.50	0.55	0.25	0.92	

* – sample only from bulls.

The analysis of polymorphism of milk protein genes

For **CSN1S1** gene the most frequently occurring allele is B (in all population 0.96) and genotype – BB (0.93) in Latvia (Table 4). There isn't difference of distribution of alleles or genotypes between dairy cow breeds.

Analysing frequencies of alleles depending from sex, we have recognized, that frequency of allele B of breeding bulls' is 0.07 lower than in cows (0.90 vs. 0.97; $p = 2.,07 \times 10^{-7}$). Looking at frequencies of genotypes, we can make conclusion, that samples with heterozygote are more common between breeding bulls than cows (20.93% for bulls and 5.43% for cows; $p = 4.99 \times 10^{-7}$ for all genotypes). So, it might imply, that breeding bulls are responsible about C allele in different stoking, because we didn't found among 675 samples any with homozygote genotype CC.

Investigating results of other researchers of different countries, we found out that result of research of Estonia (EE) is similar to ours. For Estonian native breed cows' (n = 118) α_{s1} – CN allele B is with frequency 0.92, but allele C – 0.08 (Lien et al., 1999). Also Lithuanian (LT) researchers have similar results: for dairy cows' population of LT (n = 427) allele B is with frequency 0.95 (Pečiulaitiene, 2005). In others countries of Europa, the results of similar studies are a little different. For example, for Bulgarian Grey breed (Neov et al., 2013) allele B is with frequency 0.43, but allele C – 0.57. As well as in this research, contrary to our, was found all three genotypes with frequencies: BB = 0.18, BC = 0.79, CC = 0.03. These results can be explained with this historical occurrence of breed (*Bos taurus brachiceros* x *Bos taurus primigenius*; Neov et al., 2013). In contrast, the Czech scientists' results for 440 Czech Fleckvieh breed cows' by alleles are closer to our results (B = 0.89, C = 0.11), but by genotypes – to Bulgarian' results with all three genotypes, respectively, BB = 0.80, BC = 0.18, CC = 0.16 (Kučerova et al., 2006).

In case of **CSN2** the common allele is A1 with frequency 0.67 and genotypes A1A1 (0.42), and A1A2 (0.49), despite the fact that in literature as preferable for cows' populations and as common allele more often is allele A2 (Cardak, 2005; Cieslinska et al., 2007; Pečiulaitiene et al., 2007). Looking at the population balance or deflection from Hardy – Weinberg at a given locus, there is statistically significant different ($p = 2.72 \times 10^{-3}$) between expected and obtained heterozygote frequencies. Similar results are for half of breeds (LB, LZ, HR and AN). For all investigated dairy breeds of Latvia the frequency of genotype A2A2 is very low. In addition, it appears that for HB breed, which has higher milk yield than other breeds, also observed higher frequency of A2A2 and equilibrium by Hardy – Weinberg equation.

Frequency of preferable allele A2 of CSN2 in Estonian native breed cows (Värv et al., 2009) is significantly higher (0.60) than in LB breed cows (0.31) or Latvian Blue (LZ) breed cows (0.24). We can conclude that in Estonian native breed frequency of benevolent allele A2 of CSN2 is two times higher than in Latvian native breeds.

In study included 94 breeding bulls are with small tendency to dominance of CSN2 allele A1 (0.54) over CSN2 allele A2 (0.46), but 622 dairy cows are with bigger tendency to CSN2 allele A1 dominance (0.69 vs. 0.31; between sex $p = 4.22 \times 10^{-5}$). Breeding bulls has higher frequency level of heterozygote and homozygote of CSN2 allele A2 genotypes ($p = 3.75 \times 10^{-3}$). So, there is a better background for CSN2 genotype A2A2 formation.

In Czech is the better situation for selection of CSN2 allele A2 than in Latvia. In their study was found that CSN2 alleles A1, A2, A3 and B are with frequencies 0.18, 0.80, 0.01 and 0.01, respectively (Kučerova et al., 2006).

In study of third casein protein gene **CSN3** we found, that in our population of dairy cows the common allele is A with frequency 0.92 and common homozygote genotype AA – 0.86. From literature is known that cows with genotype BB of CSN3 distinguished by better dairy technological features, the higher cheese outcome (Martin et al., 2002), but in our population this genotype and, respectively, CSN3 allele B are very rear (BB = 0.03 and B = 0.08). There is pronounced predominance of CSN3 allele A, as demonstrated by analyse of Hardy – Weinberg equation ($p = 1.19 \times 10^{-3}$). It should be noted that only in historical dairy cattle breeds of Latvia (LB and LZ) was found all three genotypes, but in other breeds – only genotype AA. The results differ from our colleges work (Petrovska et al., 2017 a, b, c), but the reason could be in fact, that in their collection have only genetic resources animals (bloodiness > 50%) and therefore groups of breeds are smaller.

Our data about very high occurrence of allele A of CSN3 in dairy cows of Latvian population comport with the research data in Lithuania and Estonia (Pečiulaitiene et al., 2007; Värv et al., 2009). Estonian researchers found higher frequency of CSN3 allele B in Estonian native breed cows (0.24) and in Estonian Red breed cows (0.37). Despite the low level of CSN3 allele B, Estonian scientists found that all parameters of milk coagulation were better to cows with genotype BB of CSN3 (Kübarsepp et al., 2005). In Lithuanian population of dairy cows' frequency of CSN3 allele A is 0.74 and of CSN3 allele B – 0.22 (Pečiulaitiene et al., 2007).

Second group is whey proteins, where for both **LAA** and **LGB** common allele is B (0.94 and 0.78, respectively) and common genotype is BB (0.88 and 0.60, respectively).

In *LAA* case analysed locus is in balance after Hardi – Weinberg equation across the population. In our all six breeds are observed predominance of LAA allele B (from 0.82 till 1.00). With the result can be recognized, that in result of genetic drift of LAA allele A is forced out of the population and the B allele frequency increases. Furthermore, LAA allele A is only in heterozygote genotypes, except in HB breed, where is one breeding bull with homozygote genotype after allele A. In this breed also frequency of LAA allele A is highest, which, compares to Latvian Brown breed, have six times higher (0.18 vs. 0.03). Looking to apportionment of rear LAA allele A in cows and breeding bulls, can be seen that for breeding bulls this allele is two times common than for cows (0.12 vs. 0.05; $p= 5.38 \times 10^{-4}$). Prevalence of LAA allele A resulting as double prevalence of frequency of heterozygote genotype (0.21 vs. 0.10; $p = 6.00 \times 10^{-4}$).

From data of different researches (Bell et al., 1981; Formaggioni et al., 1999) we can conclude that LAA variation B is typical or ancestral for *Bos taurus, Bos indicus, Bos (Poephagus) grunniens*, therefore LAA variation A isn't widespread in *Bos taurus*. Hypothetically, we can conclude that our data confirm the researchers' indicated the results about low frequency of variation A in different breeds and origins.

In our data, the highest frequency of LAA allele A is for dairy cows of HB breed (0.18) in Latvia. Comparing our results to the data of other researches, we conclude, that in other countries (Voelker et al., 1998; Bojarojc-Nosowicz et al., 2005) frequency of LAA allele A is higher (up to 0.77 or 76.60%) than in our studded breeds in Latvia.

In case of second largest whey protein or **LGB** in historical Latvian dairy cows' breeds frequency of LGB allele B is relative higher: in Latvian Brown 0.83, in Latvian Blue 0.80, but in Holstein Black and White (HB) only 0.58. Analysing variations of LGB genotypes of Latvian dairy cows' population, we found out that in tested HR, SR and AN breeds homozygote form of LGB rear allele A is markedly higher than in other breeds of Latvian population and average frequency of all population (0.03). Difference of distribution of LBG alleles and of genotypes between breeds is statistically significant ($p = 7.16 \times 10^{-11}$ and $p = 3.25 \times 10^{-5}$, respectively) in Latvia.

Comparing our results with other researches' publicised data (Pečiulaitiene, 2005; Kübarsepp et al., 2005; Zaton-Dobrowolska et al., 2006), we conclude that they show a slightly lower frequency of allele B, researching polymorphisms of whey milk protein LGB in different cows' breeds at national and/or special herds. Only one breed with higher frequency of allele B comparing to Latvian population is Lithuanian Red with frequency 0.92 (Pečiulaitiene, 2005).

CONCLUSIONS

The results of population analyse provide an opportunity to analyse B and C variations of CSN1S1, of A1 and A2 variations of CNS2 and of A and B variations of CSN3, LAA and LGB in association analyses with milk productivity indicators and with breeding bulls' estimated breeding values and yield index.

These loci can be used in future, after association analyses, as potential for gene, more precisely for marker assisted selection (MAS) in Latvian milk cattle breeding. Compared to the traditional breeding, MAS can be significantly more effective than traditional dairy cattle breeding. Judging by the data from scientific literature of different countries, it can be significant for increasing the productivity of animals, improving the quality and safety of milk products, by reducing the risks of milk and/or milk product related diseases and by promoting biological and food safety.

ACKNOWLEDGEMENTS. The results are part of D. Smiltina, Dr. agr., PhD Thesis. We thank Latvian Science Board for financial support to our investigations through grant Nr. 09.1461. The study financed by the ESF Project "Support for doctoral studies in LLU" No/2009/0180/1DP/1.1.2.1.2/09/IPIA/VIAA/0117 agreement No. 04.4-08/EF2.D1.13.

REFERENCES

Artym, J. & Zimecki, M. 2013. Milk-derived proteins and peptides in clinical trials. *Postepy Hig. Med. Dosw.* **67**, 800–816.

Barłowska, J., Wolanciuk, A., Litwińczuk, Z. & Król, J. 2012. Milk proteins' polymorphism in various species of animals associated with milk production utility. **In:** *Milk Protein*. Edited by W. L. Hurley, pp.235–264.

Bell, K., Hopper, K.E. & McKenzie, H.A. 1981. Bovine α - lactalbumin C and α_{S1} -, β -, κ - caseins of Bali (Banteng) cattle, Bos (Bibos) javanicus. *Aust. J. Biol. Sci.,* **34**, 149–159.

Bojarojc-Nosowicz, B., Kaczmarczyk, E., Bongar,c E. & Malolepszy, J. 2005. Natural BLY infection and polymorphismwithin the 5' flanking region of the a - lactalbumin gene in the black and white breed cattle. *Bull. Vet. Inst. Pulawy.* **49**, 439–442.

Cardak, A.D. 2005. Effects of genetic variants in milk protein on yield and composition of milk from Holstein-Friesian and Simmentaler cows. *S. Afr. J. Anim. Sci.* **35**(1), 41–47.

Caroli, A.M., Chessa, S. & Erhardt, G.J. 2009. Milk protein genetic variation in cattle: impact on animal breeding and human nutrition. *J. Dairy Sci.* **92**, 5335–5352.

Central Statistical bureau of Latvia. 2015. Agriculture of Latvia, Collection of statistical data. *Collection of Statistical Data*, Riga, pp.11–12.

Central Statistical bureau of Latvia. 2017. Agriculture of Latvia, Collection of statistical data. *Collection of Statistical Data*, Riga, pp.12–13.

Cielava, L., Petrovska, S., Jonkus, D. & Paura, L. 2015. The effect of different bloodiness level on Latvian brown cow productivity. *Proceedings of the 7 the international scientific conference rural development 2015*.

Cielava, L., Jonkus, D. & Paura, L. 2017. Lifetime milk productivity in farms with different housing and feeding system. *Agronomy Research* **15**(2), 369–375.

Cieslinska, A., Kaminski, S., Kostyra, E. & Sienkiewicz-Szlapka, E. 2007. Beta - casomorphin 7 in raw and hydrolysed milk derived from cows of alternative-casein genotypes. *Milchwissenschaft* **62**, 125–127.

Eurostat. 2015. Milk and milk product statistics. **In**: *Agriculture, forestry and fishery statistics - 2015*. Publications Office of the European Union, Luxembourg, pp.22–29.

Eurostat. 2016. Milk. **In**: *Agriculture, forestry and fishery statistics* - 2016. Publications Office of the European Union, Luxembourg, pp.113–122.

Formaggioni, P., Summer, A., Malacarne, M. & Mariani, P. 1999. Milk protein polymorphism: detection and diffusion of the genetic variants in B*os* genus. *AFMV Univ. Parma* **19**, 127–165.

Hristov, P.I., Teofanova, D.R., Neov, B.S., Zagorchev, L.I. & Radoslavov, G.A. 2014. Population Structure of Two Native Bulgarian Cattle Breeds with Regard to *CSN3* and *CSN1S1* Gene Polymorphism. *BJVM* **17**(1), 18–24.

Kübarsepp, I., Henno, M., Viinalass, H. & Sabre, D. 2005. Effect of k – Casein and β – Lactoglobulin Genotypes on the Milk Rennet Coagulation Properties. *Agronomy Research* **3**, 55–64.

Kučerova, J., Matejiček, A., Jandurova, O.M., Sorensen, P. E., Nemcova, E., Špitkova, M., Kott, T., Bouška, J. & Frelich, J. 2006. Milk protein genes *CSN1S1, CSN2, CSN3, LGB* and their relation to genetic values of milk production parameters in Czech Fleckvieh. *Czech J. Anim. Sci.* **51**(6), 241–247.

Lien, S., Kantanen, J., Olsaker, I., Holm, L.E., Eythorsdottir, E., Sandberg, K., Dalsgard, B. & Addalsteisson, S. 1999. Comparison of milk protein allele frequencies in Nordic cattle breeds. *Animal Genetics* **30**, 85–91.

Martin, P., Szymanowska, M., Zwierzchowski, L. & Leroux, Ch. 2002. The impact of genetic polymorphisms on the protein composition of ruminant milks. *Reprod. Nutr. Dev.* **42**, 433–459.

Martin, P., Bianchi, L., Cebo, C. & Miranda, G. 2013. Genetic polymorphism of milk proteins. **In***: Advanced Dairy Chemistry. 1A: Proteins: Basic Aspects*. 4th edition. New York: Fox, P.L. McSweeney ed., pp. 463–514.

Neov, B., Teofanova, D., Zagorchev, L., Radoslavov, G. & Hristov, P. 2013. Milk protein polymorphism in Bulgarian grey cattle population. *Bulg. J. Agric. Sci.* **19(**2), 194–196.

Pečiulaitiene, N., Miceikiene, I., Mišeikiene, R., Krasnopiorova, N. & Kriauziene, J. 2007. Genetic factors influencing milk production traits in Lithuanian dairy cattle breeds. *Žemes ūkio mokslai* **14**(1), 32–38.

Pečiulaitiene, N. 2005. Genetic Types of Milk Proteins Prevalence and their Relation with Production Traits in Lithuanian Dairy Cattle Breeds. Summary of doctoral thesis. *Biomedical sciences, zootechny* **13B**. Kaunas.

Petrovska, S., Jonkus, D. & Smiltiņa, D. 2017a. Influence of κ-casein genotype on milk productivity of Latvia local dairy breeds. *International Scholarly and Scientific Research & Innovation* **11**(3), 243–247.
Petrovska, S., Jonkus, D., Zagorska, J. & Ciprovica, I. 2017b. The influence of kappa-casein and beta-lactoglobulin genotypes on milk coagulation properties in Latvia dairy breed. *Agricultural sciences (Crop sciences, animal sciences)*, **2,** 74–80.
Petrovska, S., Jonkus, D., Zagorska, J. & Ciprovica, I. 2017c. Influence of κ-Casein Genotype on coagulation propertiesof milk collected from the local :atvian cow breeds. *Agronomy Research* **15**(S2), 1411–1419.
Tsabouri, S., Douros, K. & Priftis, K.N. 2014. Cow's milk allergenicity. *Endocr Metab Immune Disord Drug Targets*. **14**(1),16–26.
Utsunomiya, Y.T., Pérez O'Brien, A.M.P., Sonstegard, T.S., Sölkner, J. & Garcia, J.F. 2015. Genomic data as the "hitchhiker's guide" to cattle adaptation: Tracking the milestones of past selection in the bovine genome. *Front. Genet*. **5**, 1–13.
Värv, S., Belousova, A., Sild, E. & Viinalass, H. 2009. Genetic diversity in milk proteins among Estonian dairy cattle. *Veterinarija I Zootechnika* **48**(70), 93–98.
Vilotte, J. L., Chanat, E., Le Provost, F., Whitelaw, C.B.A., Kolb, A. & Shennan, D.B. 2013. Genetics and biosynthesis of milk proteins. **In:** *Advanced Dairy Chemistry – 1A: Proteins: Basic Aspects*. 4th edition. New York: Fox, P.L. McSweeney ed., pp. 431–461.
Voelker, Jr.G.R., Bleck, G.T. & Wheeler, M.B. 1999. Identification of variations in the α – lactalbumin gene in cattle and potential correlations to milk production traits. **In:** *Illini DairyNet Papers*. University of Illinois Extension (ASV).
Zaton-Dobrowolska, M., Čitek, J., Filistovicz, A., Rehout, V. & Szulc, T. 2006. An estimation of the genetic distance between Polish Red and other red cattle breeds on the basis of selected milk protein loci. *EJPAU* **9**(2, 10), 1–9.

Agronomy Research **16**(3), 910–916, 2018
https://doi.org/10.15159/AR.18.126

Sunlight potential for microalgae cultivation in the mid-latitude region – the Baltic states

A. Stunda-Zujeva*, M. Zuteris and K. Rugele

Riga Technical University, Faculty of Materials Science and Applied Chemistry, Institute of General Chemical Engineering, Pulka 3, LV-1007 Riga, Latvia
*Correspondence: agnese.stunda-zujeva@rtu.lv

Abstract. Products, e.g. food and feed from microalgae are a promising part of bioeconomy. One of the most investigated and highly demanded microalgae is *Spirulina*. Light is one of limiting factors for biomass cultivation by photosynthesis. Sunlight is cheap and climate friendly light source. The aim of this study was to evaluate available sunlight potential in the mid-latitude region - the Baltic states (Europe, 55–60 °N) for microalgae, e.g. *Spirulina* growth. The data of Climate atlas based on satellites of EUMETSAT and data from an observation station in Riga were analyzed. The latitude and climate (cloudiness) were main parameters affecting the total solar radiation received by Earth's surface. The sunlight potential in the Baltic states was higher than in most of Europe in similar latitude. Multi-year mean daylight intensity in the Baltic states was slightly less than in Southern France or Bulgaria, (26 klux and 30 klux, respectively, in summer) where *Spirulina* is commercially produced. Hourly solar radiation varied a lot in the Baltic states – from 880 W m^{-2} to 200 W m^{-2}, sunny and overcasted noon of summer day, respectively; average value (8 a.m.–4p.m.) was 450 W m^{-2}. Summer days are longer than 12 h, reaching 18 h in midsummer. The sunlight potential is suitable for microalgae, e.g. *Spirulina* cultivation in this period. From November till February days are shorter than 10 h and solar radiation is less than 300 W m^{-2} even in noon of sunny days.

Key words: Sunlight, solar radiation, microalgae, mid-latitude, Europe, the Baltic states.

INTRODUCTION

The bioeconomy is based on the innovative use of sustainable biological resources to cover the growing demand of food, energy and industrial sectors. In this context, algae represents emerging biological resource (Enzing et al., 2014). From ~ 50,000 microalgae species only 10 are commercially produced. Two most widely investigated and commercially produced species are tropical microalgae *Spirulina* and *Chlorella*. The estimated market value was about 600 million Euro in 2010. Main microalgae market applications are: human (74%) and animal nutrition (25%) and cosmetics (Egardt et al., 2013). Available light is one of the main limiting parameters for biomass cultivation by photosynthesis (Vonshak, 1997; Weyer et al., 2010). The Sun is the cheapest, the most energo-effective and climate friendly light source. However, the position of the Sun in the sky and amount of clouds varies a lot. Closer to the Equator (the low latitude) the Sun in the middle of a day is close to the zenith and it is rising and setting quite more rapidly compared to the higher latitude regions (closer to Earth's poles) where the Sun in the midday is in lower angle and days are longer. The aim of this study is to analyze sunlight potential in Baltic states (the mid-latitude, 55–60 °N) for microalgae *Spirulina*, growth. Another crucial factor for tropical algae is heat, the temperature as part of climate will be roughly overviewed but it will not be discussed deeply due to the limited space of the article.

Solar radiation through atmosphere

The Sun gives full spectra of the electromagnetic radiation. However due to atmosphere mostly visible, near infrared, and near ultraviolet part of spectra reaches Earth's surface (Chen & Julian, 2011). Solar radiation outside the atmosphere is 1,366 W m^{-2}. Under a clear sky reduction of solar radiance that reaches Earth's surface is about 22%. Due to Rayleigh scattering from molecules, especially water and carbon dioxide, and dust particles the short-wavelength radiation is reduced heavily. The reduction is proportional to the inverse power of the wavelength of the radiation. The solar radiation consists of direct and diffuse sunlight. If clouds are present direct sunlight intensity reduces and proportion of diffuse sunlight increases (Chen & Julian, 2011).

The theoretical maximum annual solar irradiance is a function of latitude, e.g. for latitude 0° it is approx. 364 W m^{-2}, for 30°–319 W m^{-2} and for 60°–206 W m^{-2} yearly average. At 60° latitude Earth's surface can receive only 57% of solar radiation that is received at 0° latitude (at the Equator) per year. However due to clouds and other absorptive atmospheric conditions the actual solar energy is reduced, for example, Kuala Lumpur, Malaysia (3° N) receives less energy than Màlaga, Spain (37 °N), 184 W m^{-2} and 197 W m^{-2} respectively (Weyer et al., 2010).

Photosynthesis and light

Light is only a part of the solar radiation spectra that reaches Earth's surface. Light is the part of the solar radiation spectra that is visible for human eye. For photosynthesis only a part of the visible spectra is used. The photosynthetically active radiation (PAR) is commonly defined as 400–700 nm. PAR is 45.8% of total solar energy (Weyer et al., 2010). Actual energy that is available for photosynthesis is determined by pigment types in plants. Photosynthesis is a set of chemical reactions that depends on photon amount, therefore for cultivation of plants photosynthetic photon flux density (PPFD) is used. PPFD is the number of photons (PAR) that fall on a square meter of target area per second (μmol of m^{-2} s^{-1}). The conversion coefficient from light intensity to PPFD (from lux to μmol m^{-2} s^{-1}) varies under different light sources, for sunlight the coefficient is 0.0185 and for cool white fluorescent lamps it is 0.0135 (Apogee Instruments, Inc., Environmental Growth Chambers, 2017). For example, full sunlight is 108 klux or 2,000 μmol m^{-2} s^{-1} on horizontal surface in Malaysia (Taisir et al., 2016) and China (Huang et al., 2017).

How much light do algae need?

Autotrophic microalgae growth in commercial pond is mostly light limited. Photosynthesis in most algal species is saturated at 1/3 the intensity of full solar radiation and in the most cases some photoinhibition is observed at 60–70% of full sunlight (Vonshak, 1987). However other studies have shown that optimal light intensity and optimal cell density are dependent variables. At higher light intensity higher cell density and higher mixing rate is necessary to prevent cells from photoinhibition due to overexposure to light. It is suggested to harvest some part of algae in afternoon for more efficient use of evening light and increase the overall productivity. In thin flat-plate bioreactors (optical path ~ 1 cm) the light intensity can be raised even up to several suns, because cell density is high and intensive mixing moves cells to dark zone of reactor before light causes damage of cells. Therefore, optimal light intensity for each algae strain should be determined experimentally for each growth environment (Richmond & Qiang, 2013). For example, the light saturation point of *Chlorella vulgaris* was 150 μmol m^{-2} s^{-1} in concentration range 0.2 till 1.4 g L^{-1}. The light saturation point of *C. vulgaris* was 30 μmol m^{-2} s^{-1} in concentration range 0.2 till 0.8 g L^{-1}. Photo-inhibition occurred with the high irradiance (200–300 μmol m^{-2} s^{-1}), specific growth rate was much slower for all 10 cultivation days, however it slightly increased after sixth day, probably due to increased concentration above 0.5 g L^{-1} that selfshaded cells (Jiang et al., 2016). The light intensity affects not only the productivity but also the composition of algae, for example, high light intensity (13–28 klux) during the cultivation of *Nostoc muscorum* stimulates the production of carotenoids, while the application of a low light intensity (1 klux) favors an increase in the production and accumulation of phycobiliproteins (Tarko et al., 2012).

The other important parameter of light is the length of photoperiod (light: dark cycle), for example, higher growth rate of *Nannochloropsis sp* was achieved at higher light intensity 350–370 μmol m^{-2} s^{-1} (on the back surface, depth of reactor 190 mm) and longer photo-period 18:6 h comparing to shorter one 12:12 h (Taisir et al., 2016).

MATERIALS AND METHODS

Seasonal changes and differences in various regions of Europe were compared using data on climate; multi-year (1982–2009) mean daylight intensity of seasons (Fig. 1) and global solar radiation and temperatures (Table 1) were taken from Climate atlas. Data in Table 1 was read from Latvia map of Climate atlas. The Climate atlas is based on Satellite Application Facility on Climate Monitoring datasets (CM SAF), new version of PVGIS (autumn 2010). The data used for PVGIS come mainly from geostationary satellites Meteosat, Metop, NOAA. Geostationary weather satellites take pictures of Earth at short intervals (every 15 or 30 minutes).

The solar radiation was analyzed as function of time of the day or year. Various days in the similar solar position was analyzed to find data on clear and cloudy days. The seasons of various years and spring comparing to summer or autumn were compared. Hourly mean solar radiation data of observation station 'Riga-University' is downloaded as a table (date/ hourly solar radiation for every hour) from public database of Latvian Environment, Geology and Meteorology Centre. Location of the station: latitude: 56.9506, longitude: 24.1161. The station is equipped with automatic device and corresponding software for data measurement and observation processing and transmission to the database.

RESULTS AND DISCUSSION

Seasonality

The total daylight intensity including direct, diffuse and reflected sunlight in summer and spring are shown in Fig. 1. In summer multi-year mean daylight intensity in Baltic states wa212qq6tdzddt43s about 65% of that in Mediterranean region, 22–28 klux and 26–40 klux respectively in summer, 16–20 klux and 18–28 klux in spring, 6 klux and 10–18 klux in autumn, 2 klux and 6–18 klux in winter. Due to local climate average light intensity can highly differ in relatively small area. Therefore, the daylight intensity in sunniest areas in the Baltic states were similar to cloudiest areas of Mediterranean region – approximately 27 klux in summer and 19 klux in spring.

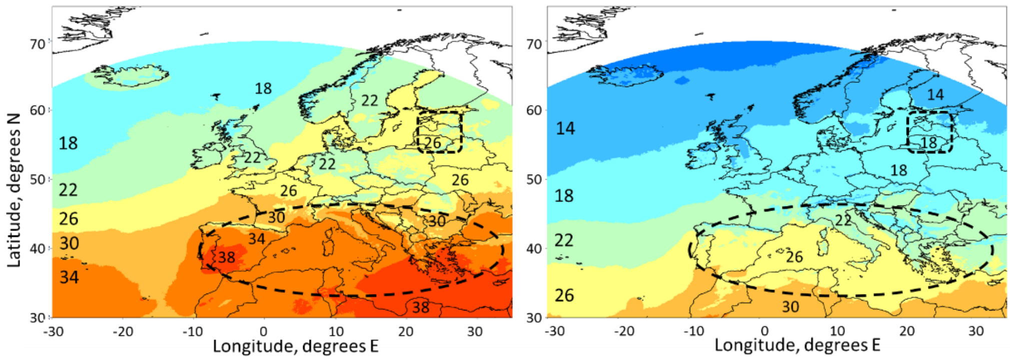

Figure 1. Multi-year mean daylight intensity (in klux) in summer (left) and spring (rigth) in Europe. The Baltic states are shown with square, Mediterranean region with oval shape.

The tropical algae *Spirulina* is successfully grown in commercial greenhouse ponds in Southern France (Spiruline La capitelle) at least for 4 months per year therefore 30 klux average daylight intensity is enough for Spirulina cultivation. In Bulgaria *Spirulina* and *Clorella* are cultivated in photobioreaktor inside greenhouse (bioLEED, 2018). There are also microalgal cultivation ponds of Bulgarian Academy of Sciences, running from March to October in Roupi thermal water region, SW Bulgaria (42 °N). There are 240 sunny days per year in Roupi region (Fournadzhieva et al., 2003). More to the north in the Netherlands (52 °N) is AlgaPARC, microalgae research pilot scale production center where various types of photobioreactors in open air and in greenhouse are running from May to September in open air and greenhouse (AlgaePARC 2014). Spirulina in commercial greenhouses (20,000 sqft) is cultivated also in Richmond, British Columbia, Canada (49 °N) (AlgaBloom Int'l, 2018). The sunlight was slightly less in the Baltic states than in the south of France or Bulgaria, ~26 and 30 klux respectively, but similar sunlight conditions were for the Netherlands and the Baltic States. There was lower cloudiness and higher mean sunlight intensity in the Baltic states than in the north of Germany, Denmark and Great Britain if the same latitude region (Europe, 55–60 °N) was compared (Fig. 3). Therefore the sunlight potential in the Baltic states was higher than in most of Europe in similar latitude.

The sunlight data for winter was not shown due to much lower precision caused by snow and low angle of the Sun above horizon. The main advantage of satellite-based methods is that they give a fairly uniform coverage of large areas comparing to ground stations. But drawbacks of using data from satellites are (1) that snow will look very much like clouds in the satellite images. There are methods to overcome this problem, but the uncertainty is higher in areas with snow (e.g. the Baltic states). (2) When the Sun is very low in the sky the calculation from satellite data becomes very difficult (Help of

PVGIS radiation database, 2017). Therefore, the data shown in Fig. 1. and Table 1 columns: 'Global solar radiation' and 'Light intensity' lowest precision is for February, March and October when snow covers large part of ground and/or the Sun is low.

Table 1. Multi-year mean meteorological data for Latvia

Month	Global solar radiation, W m^{-2}	Light intensity, klux	Length of day*, h	Sunny (clear sky), h day^{-1}	Average temp, °C	Average max. temp., °C
February	40…60	2...8	10	4…4.5	-7…-3	-4…0
March	80…100	8…12	12.3	6	-2…0	1…3
April	140…180	20...24	14.7	7…8	3…6	7…11
May	200…240	20...28	16.8	9…10	9…12	14…18
Jun	220…260	24...32	17.9	9…11	14…16	18…21
July	200…240	24...28	16.9	9…10	16…18	20…23
August	160…200	20...24	14.7	8…9	15…16	20…22
September	100…120	8...16	12.4	6	10…13	15…17
October	60…80	4...8	10	4…5	5…8	8…11

*21st date, from sunrise till sunset (http://www.suncalc.net/#/56.9496,24.1052,10).

Photoperiod ratio of light:dark at 18:6 h provided better results compared to 12:12 h (Habib et al., 2008; Taisir et al., 2016), thus the length of day that reach almost 18 h in the June and 6 months are longer than 12 h is an advantage.

Statistics of solar radiation was mostly gathered as average value of day, month or year. These data show that solar radiation potential or energy that can be converted in biomass is 2.2 times more in June and July than in March in the Baltic states. However, for algae growth it was also important to analyze diurnal cycle – the length of the day and change of sunlight intensity during the day.

Diurnal cycle

Solar radiation intensity variation during the day were characterized by the hourly mean radiation. The maximal hourly intensity reached approx. 880 W m^{-2} in the middle of the sunny day in June (see Fig. 2). Radiation level above 800 W m^{-2} lasted from 10 am till 1 pm in clear-sky days. Due to the lower angle of the Sun the sunlight intensity was lower in the middle of a day than in tropical countries (1,060 W m^{-2}) therefore cell growth will be less distracted by over exposure to light. Days can be strongly overcast when average hourly radiation in 8:00–16:00 did not exceeded 200 W m^{-2} (6 of 122 days in 2015, May 1st till August 30th) or 300 W m^{-2} (18 days in 2015) (see Fig. 3). Clouds increase the

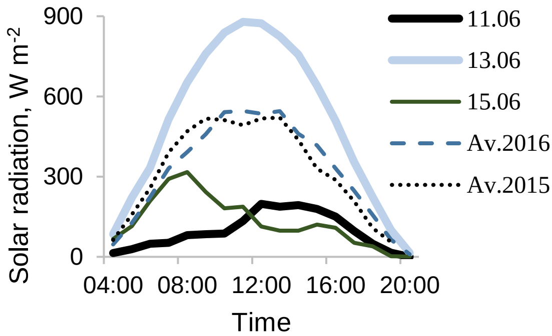

Figure 2. Change of total solar radiation (hourly average) during the day. Data on the sunniest (13.06.2016) and the cloudiest days (11.06.2016 and 15.06.2016) are shown and average values for period June 10 till June 31 in 2015 and 2016.

portion of diffused sunlight that is an advantage in illumination of photobioreactors, e.g. flat plate photobioreactors, because both sides receive similar radiation dose and there is less distinct direct light and shadow sides. Therefore medium cloudiness is an advantage.

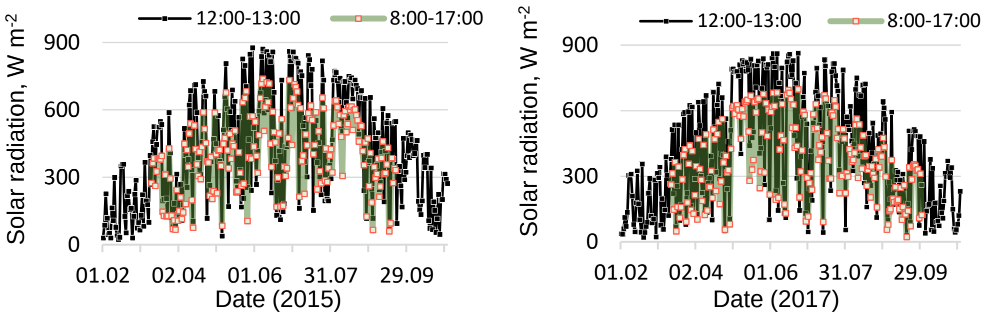

Figure 3. Fluctuation (due to clouds) of solar radiation intensity from February till October.

Maximum solar radiation intensity reached 880 W m^{-2} and was above 800 W m^{-2} from the beginning of May till the end of July, however radiation reached so high value no more than four hours per day and no more than 24 days per year (2015–2017). Average hourly radiation in 8:00–16:00 was approx. 450 W m^{-2} May 1st till August 30th in 2015–2017 that is approx. 42% of full sunlight. Therefore, in this period sunlight was enough for tropical microalgae, e.g. *Spirulina* cultivation. Main challenge for photobioreactor design and cultivation parameter setting will be strong fluctuations of light intensity.

In dark season – from November till February days are shorter than 10 h and solar radiation was less than 300 W m^{-2} even in noon of sunny days. Therefore, this period is too dark for commercial algae growth under sunlight.

CONCLUSIONS

The latitude was not the main parameter affecting total solar radiation received by Earth's surface as it could be expected by the Sun angle calculation. The other important factor that determines the amount of available sunlight was climate or cloudiness. The sunlight potential in the Baltic states was higher than in most of Europe in similar latitude.

The sunlight potential in mid-latitude region (e.g. the Baltic states) is suitable for cultivation of microalgae Spirulina at least four months of year. The advantages of higher latitude are long hours with moderate light intensity; six months with daytime longer than 12 h. The drawbacks are rapid changes of light intensity due to clouds; light intensity can reach the level of overexposure (light inhibition) of microalgae; at least 4 months per year it is too dark to cultivate microalgae under the sunlight.

ACKNOWLEDGEMENTS. This work has been supported by European Regional Development Fund within the project 'Influence of the magnetic field initiated stirring on biotechnological processes' No. 1.1.1.1/16/A/144.

REFERENCES

AlgaBloom Int’l https://www.algabloom.com/ Accessed 07.03.2018.

Apogee Instruments, Inc. *www.apogeeinstruments.co.uk* Accessed 17.12.2017.

AlgaePARC, 2014. *Winter Newsletter*, http://www.algaeparc.com/uploads/newsletterpdf_14-11-27_17-30-52.pdf.

Chen, C. Julian. 2011 Physics of Solar Energy, Wiley, ProQuest Ebook Central. Climate atlas (in Latvian) http://www2.meteo.lv/climate_atlas/curl.php Accessed 17.12.2017.

Climate atlas (in English) https://www.eumetsat.int/website/home/Images/ImageLibrary/DAT_2266050.html Accessed 17.12.2017.

bioLEED Ltd http://bioleed.com/ Accessed 07.03.2018.

Egardt, J., Lie, Ø., Aulie, J. & Myhre, P. 2013. Microalgae: A market analysis carried out as part of the Interreg KASK IVA project: Blue Biotechnology for Sustainable Innovations, *'Blue Bio'*, pp. 84

Enzing, C., Ploeg, M., Barbosa, M. & Sijtsma, L. 2014. *Microalgae-based products for the food and feed sector: an outlook for Europe*, pp. 82.

Fournadzhieva, S., Bojadgieva, K. & Pilarski, P. 2003. Bulgarian experience in aquaculture (microalgae) - cultivation , production and development. *Proceedings of the European Geothermal Conference*, pp. 8

Habib, M.A., Parvin, M., Huntington, T.C. & Hasan, M.R 2008. A Review on Culture, Production and Use of Spirulina As Food for Humans and Feeds for Domestic Animals and Fish. *FAO Fisheries and Aquaculture Circular* **1034**, pp.33.

Huang, Q. Jiang, F., Wang, L. & Yang, C. 2017. Design of Photobioreactors for Mass Cultivation of Photosynthetic Organisms. *Engineering* **3**(3), 318–329.

Jiang, L., Ji, Y., Hu, W., Pei, H., Nie, C., Ma, G. & Song, M 2016. Adjusting irradiance to enhance growth and lipid production of Chlorella vulgaris cultivated with monosodium glutamate wastewater. *Journal of Photochemistry and Photobiology B: Biology* **162**, 619–624.

Richmond, A. & Qiang, H., 2013. Part 2 Mass Cultivation and Processing of Microalgae. In *Handbook of Microalgal Culture : Applied Phycology and Biotechnology*, pp. 195.

Latvian Environment, Geology and Meteorology Centre (database in Latvian) https://www.meteo.lv/meteorologija-datu-meklesana/?nid=461 Accessed 01.12.2017-17.01.2018.

Spiruline La capitelle http://www.spirulinelacapitelle.com. Accessed 17.12.2017

Taisir, M., Teo, C.L., Idris, A., Yusuf, A.M. 2016. Cultivation of Nannochloropsis sp. using narrow beam angle light emitting diode in an internally illuminated photobioreactor. *Bioresources and Bioprocessing* **3**(1), 35.

Tarko, T., Duda-Chodak, A. & Kobus, M., 2012. Influence of growth medium composition on synthesis of bioactive compounds and antioxidant properties of selected strains of Arthrospira cyanobacteria. *Czech Journal of Food Science* **30**(3), 258–267.

Vonshak, A. 1997. Growth, Physiology and Biochemistry. In A. Vonshak, ed. *Spirulina platensis (Arthrospira)*. CRC Press, pp. 43–66.

Vonshak, A. 1987. Strain selection of Spirulina suitable for mass production. In *Hydrobiologia*. pp. 75–77.

Weyer, K.M., Bush, D.R., Darzins, A., Wilson, B.D. 2010. Theoretical maximum algal oil production. *Bioenergy Research* **3**(2), 204–213.

Agronomy Research **16**(3), 917–922, 2018
https://doi.org/10.15159/AR.18.138

Soil sampling automation using mobile robotic platform

E. Väljaots[1,*], H. Lehiste[2], M. Kiik[3] and T. Leemet[2]

[1]Tallinn University of Technology, School of Engineering: Department of Mechanical and Industrial Engineering, Ehitajate tee 5, EE19086 Tallinn, Estonia
[2]Estonian University of Life Sciences, Institute of Technology, Chair of Bioengineering Technologies, Fr.R.Kreutzwaldi 56, EE51014 Tartu, Estonia
[3]University of Tartu, Institute of Computer Science, J.Liivi 2, EE50409 Tartu, Estonia
[*]Correspondence: eero.valjaots@gmail.com

Abstract. Land based drone technology has considerable potential for usage in different areas of agriculture. Here a novel robotic soil sampling device is being introduced. Unmanned mobile technology implementation for soil sampling automation is significantly increasing the efficiency of the process. This automated and remotely controlled technology is enabling more frequent sample collection than traditional human operated manual methods. In this publication universal mobile robotic platform is adapted and modified to collect and store soil samples from fields and measure soil parameters simultaneously. The platform navigates and operates autonomously with dedicated software and remote server connection. Mechanical design of the soil sampling device and control software is introduced and discussed.

Key words: soil sampling, unmanned ground vehicle, autonomous navigation.

INTRODUCTION

Properly collecting soil samples is important step in any field soil fertility management program. Soil deterioration can be a considerable problem that builds up when fertility management is neglected in long term perspective. Trends toward reduced or zero tillage and technology for variable rate fertilization (VRF) have especially demanded that soil samples should be taken more comprehensively and intensively. Leading for more accurate fertilizer and soil amendment application. In general, soil sampling should reflect tillage, past fertilizer amendment placement, cropping patterns, soil type and texture including drainage and slopes (Oliver, 2010). Simultaneously compaction and moisture level should be measured.

Usefulness and accuracy of precision farming techniques are often dependent on soil sampling approach. Any error during extraction and analysistend to have cumulative effects and distort the soil maps and results. Soil samples are highly dependent of actual situation and conditions on the field which requires higher data acquisition frequency and precision. Conventional soil sampling procedure consists of driving through the fields with all-terrain-vehicle (ATV) and manually probing the soil and collecting the samples into the container (Fig. 1). As there is increasing demand to collect more soil samples, the traditional manual methods are cumbersome to carry out.

In precision agriculture, robotic research is mainly focused on mapping and sampling and is a research area with great potential impact (Bechar & Vigneault, 2017). Distribution of soil sampling points on test area has great effect on result quality. Grid sampling is usually preferred method for sample collection for soil fertility analysis (Ferguson & Hergert, 2000). As sampling pattern generation is a crucial task, automating the process has here clear benefits. To achieve better efficiency and quality, there is a great need for entire soil sampling process automation (Krishna, 2016).

Figure 1. Soil sampling in traditional way.

Several semi-automated commercial solutions are in use, meaning the sample taking is automated but the sampler is transported with ordinary vehicle (ATV or tractor) while human operator determines trajectory (Autoprobe, Falcon, Wintex, Magictec, Agriprobe etc.). They are claimed roughly to double probing speed in comparison with human operator and manual process. In some cases, soil sampling system is accompanied with penetrometer (Ghaffari et al., 2005). Being still monotonous and repetitive process for qualified personnel, it has suitable preconditions being conducted using autonomously navigating unmanned ground vehicle (UGV).

The scope of the current research is the development and implementation of an automated soil sampling system. Novelty is introduced here with proposed sampling system layout – mid-size autonomous UGV platform is to implement to carry soil sampling and storage apparatus. The hypothesis is set that automated fast acting collecting and storing mechanism is an efficient replacement for traditional manual method. Furthermore, accompanied with autonomous navigation technology and cloud-based data processing system, also conceivable replacement for current semi-automatic commercial solutions.

MATERIALS AND METHODS

Test platform

The articulated steering universal mobile robotic platform (Fig. 2) was developed in the Estonian University of Life Sciences for the purpose of practical testing of unmanned technologies and navigation for agricultural activities (Väljaots, 2017). While being somewhat similar to full-size unmanned tractor platforms (Oksanen, 2015), this UGV is classified as mid-size and weights 470 kg. It suits

Figure 2. Articulated steering UGV platform prototype with soil sampling mechanism.

perfectly for automating repeated light tasks usually carried out by humans like automated measurements and sampling.

The articulated steering universal mobile robotic platform (Fig. 2) was developed in the Estonian University of Life Sciences for the purpose of practical testing of unmanned technologies and navigation for agricultural activities (Väljaots, 2017). While being somewhat similar to full-size unmanned tractor platforms (Oksanen, 2015), this UGV is classified as mid-size and weights 470 kg. It suits perfectly for automating repeated light tasks usually carried out by humans like automated measurements and sampling.

UGV layout is modular, consisting of identical modules that are connected with each other through steering linkage. In comparison, different attempts are made to create modular agricultural robotic vehicle (Grimstad, 2017). All wheel drive (AWD) with differential axes is achieved by routing hydraulics lines to every wheel and body module. For powering the hydraulic pump, Kohler 15 kW 2-cylinder internal combustion engine is used. As it works continuously approximately 3 h and minimal pause is required for filling the tank, is well suited for agricultural tasks. The power unit is situated in one module, while the second is free for soil sampling or other useful equipment.

Soil sampling system

The soil sampling and collecting system is integrated into separate body module (Fig. 3, left). For robotic sampling, often drilling is used, especially in harder or variable grounds (Zhang et al., 2017). However, for soft field soils, sample probing with 25 mm diameter and 300 mm length tubular probe (pink in Fig. 3) is simple and durable.

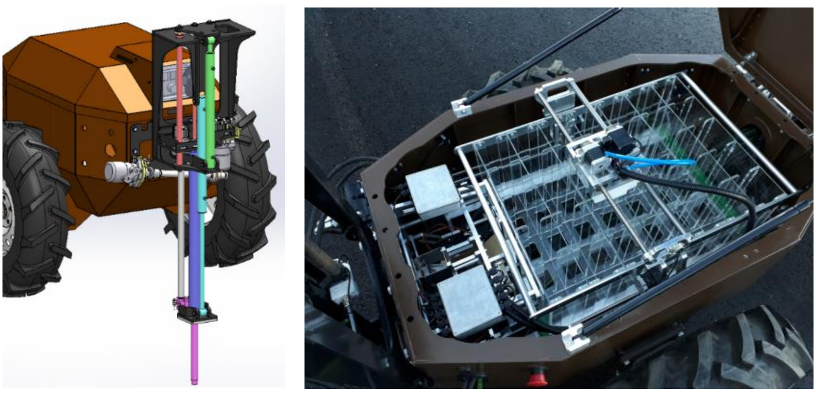

Figure 3. Soil sampling mechanism CAD-model (left) and sample storage system from the prototype.

As secondary actions use hydraulic cylinders, screw mechanism on probe maintains constant process speed and enables to integrate penetrometer drive with the probe. To measure the sampler mechanism position, the motor and screw mechanisms were fitted with rotary encoders and limit position detection with inductive sensors. As only fraction of soil amount in core is taken to container due to volume restriction, container end position is adjusted under the probe while the cleaner rod pushes collected core out of probe.

For automating sample handling and storage, other solutions use often robotic manipulator arm (Deusdado et al., 2016). The current solution uses simpler electric 3-axis coordinate system (Fig. 3, right) instead which is built into second body module. The separate multi-servo unit unpacks the standard carton container covers for sample feeding. The container block includes 140 slots for containers.

Software

The purpose of software development is to enable flexible functionality during autonomous soil sampling operation and solving the following tasks:

- creating the test plan, definition of test area and assigning sample points;
- optimal navigation trajectory generation between sample points;
- preventing the collision with obstacles in trajectory;
- probing for soil sample in test point, collecting the sample;

The input for creating the work tasks is GeoJSON data file with pre-agreed attribute marking. This file is used for creating area borders, restrictions and calculating the path segments for driving between sample points. The software is divided into two separate independent systems: firmware for driving the hardware and remote management system in server, including user interface (UI) for operator (Fig. 4). For achieving the maximum flexibility, the software uses service-oriented architecture. The remote management system software in server is based on NodeJS run-time environment and AngularJS framework. Using the separate library for communicating with operator, the server software manages robot tasks, work process, analyses telemetry and enables also manual control. Software system for the soil sampling device developed in this research is able to work with maps and spatial data.

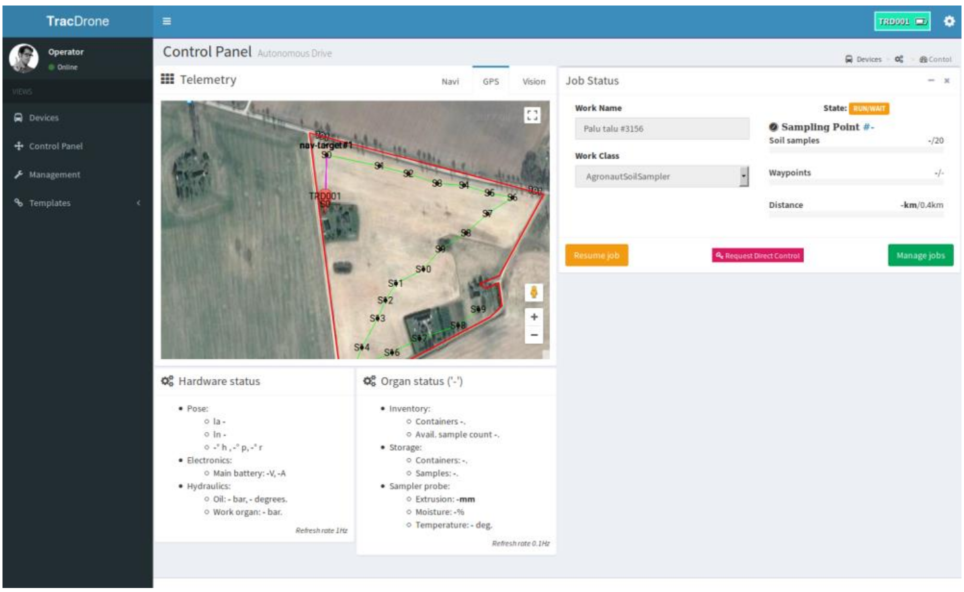

Figure 4. Soil sampling UI for work plan configuration view.

Test method

To observe the performance of the robotic platform equipped with soil sampling system and controlled by corresponding software, the was tested in real-conditions. The performance test was carried out in comparison with traditional method with human operator with ATV and manual probe. Operation speed as performance indicator is measured with sample count per time unit which depends on sample taking time and driving time between grid points. Sampling quality is determined how good representation of soil mean composition the collected samples are and is solved by control software during sampling path generation.

As initial testing was carried out in October after the field was harvested. For initial testing, flat field was chosen with good weather conditions. Sampling path is generated by operator in UI using iterative shortest path calculation algorithm. The resulting GeoJSON data file is transmitted to UGV for processing by its Nvidia control unit. One hour of sampling time was tested.

RESULTS AND DISCUSSION

In order to achieve best possible performance from sampling mechanism, the control unit is programmed to act in sequence presented on Fig. 5. Mean acting times were measured to calculate the summary sample taking times. While the robot platform navigation is still experimental, its control unit can navigate it between the sampling points approximately 2 times slower than operator with ATV. However, if human operator with ATV and manual probe can collect maximum 50 composite samples per hour, robot can collect 75 samples per hour due to faster process and beat traditional method while driving much slower.

Vehicle act.	Driving		Stopped		Driving			
Turret act.	Turn to sampl. pos							Turn to transp. pos
Cleaner act.		Cleaner up				Cleaner down		
Probe act.			Probe into soil	Probe up				Probe down
Support act.		Support down		Support up				
Container act.					Container forward		Container back	
Duration, s	4.80	1.30	1.80	4.30	1.10	1.30	1.10	4.80

Figure 5. Soil sampling mechanism tested action durations.

Further testing should include comparison with semi-automatic system fitted to car trailer, provided by Agricon company. In general, high speed systems that can used without stopping the vehicle, can take only short cores under 150 mm due to angular movement of probe during operation. As the current system probes 300 mm deep, it must be stopped, therefore having much slower collecting speed, yet can collect more measures from each spot.

CONCLUSIONS

A solution was proposed for automating the soil sampling process and mounted to mid-size mobile robot platform. Using cloud based control software, this hydraulic electro-mechanical device was tested for speed and efficiency. During testing, the current system was found out to be 50% faster of a traditional method. It does not require human intervention during the process, only the process planning, robot transportation and handling of collected samples is carried out by operator.

As the purpose of current project is sample collecting method and technical solution research, the system durability and efficiency can be improved further during the planned product development:

- As hydraulic actuators offer good speed and force capability, they should be kept on future development.
- Due to navigation system great impact on overall efficiency, process could also be improved much with validation of different path calculation algorithms.
- As the vehicle is stopped for probing, several soil parameters can be measured simultaneously with additional instruments: humidity, density, temperature etc.

ACKNOWLEDGEMENTS. This research was supported by funding of PRIA, project no. L160160TIPT 'Autonoomse mullaproovide kogumise seadme väljatöötamine'.

REFERENCES

Bechar, A. & Vigneault, C. 2017. Agricultural robots for field operations. Part 2: Operations and systems. *Biosystems Engineering* **153**, 110–128.

Deusdado, P., Pinto, E., Guedes, M., Marques, F., Rodrigues, P., Louren, A., Mendon, R., Silva, A., Santana, P., Corisco, J., Almeida, M., Portugal, L., Caldeira, R., Barata, J. & Flores, L. 2016. An Aerial-Ground Robotic Team for Systematic Soil and Biota Sampling in Estuarine Mudflats. In: *Robot 2015: Second Iberian Robotics Conference. Advances in Intelligent Systems and Computing*. Lisbon, vol. 418, pp. 15–26.

Ferguson, R.B. & Hergert, G.W. 2000. EC00-154: Soil Sampling for Precision Agriculture. In: *Precision Agriculture*. University of Nebraska-Lincoln, pp. 1–4.

Ghaffari, M., Cao, P. & Hall, E.L. 2005. Autonomous Techniques for Soil Sampling in Hazardous Fields. In: *International Conference on Human Impacts on Soil Quality Attributes in Arid and Semiarid Regions*, Isfahan, Iran, pp. 51–55.

Grimstad, L. & From, P.J. 2017. The Thorvald II Agricultural Robotic System. *Robotics 2017* **6(**24), 4588–4593.

Krishna, K.R. 2016. *Push Button Agriculture: Robotics, Drones, Satellite-Guided Soil and Crop Management*. Apple Academic Press, Oakville, 470 pp.

Oksanen, T. 2015. *Accuracy and performance experiences of four wheel steered autonomous agricultural tractor in sowing operation.* Field and Service Robotics, vol. **105** of Springer Tracts in Advanced Robotics, 425–438.

Oliver, M.A. 2010. *Geostatical Applications for Precision Agriculture*. Springer, London, 331 pp.

Väljaots, E. 2017. *Energy Efficiency Evaluation Method for Mobile Robot Platform Design*. Tallinn University of Technology, PhD thesis, 96 pp.

Zhang, T., Zhang, W., Wang, K., Gao, S., Hou, L., Ji, J. & Ding, X. 2017. Drilling, sampling, and sample-handling system for China's asteroid exploration mission. *Acta Astronautica* **137**, 192–204.

Agronomy Research **16**(3), 923–935, 2018
https://doi.org/10.15159/AR.18.102

The potential use of invasive plant species as solid biofuel by using binders

L. Zihare,* R. Soloha and D. Blumberga

Riga Technical University, Faculty of Electrical Engineering, Institute of Energy Systems and Environment, Āzenes iela 12/1, LV-1048 Riga, Latvia
*Correspondence to the author: lauma.zihare@rtu.lv

Abstract. The aim of the current research is to find sustainable pellet resources that are not made from forestry, agricultural materials, or food products. Evaluation has been carried out by experimentally determining the biofuel parameters of two invasive plant species. In comparison to the process of finding a new application, their use in the production of solid biofuel pellets would not require additional investment for the construction of a new pellet production plant. The article's hypothesis suggests that biofuel parameters for invasive plant species are sufficient for the production of solid biofuel and that their properties can be improved by binders that are available worldwide in the form of residues.
The experiment was carried out for two invasive plant species that are widespread in Latvia – *Heracleum sosnowskyi* Manden and *Solidago canadensis* L. The binders used include potato peel waste and spent coffee grounds. All of the tests have been carried out according to ISO standards on biofuel testing. Results show that *H sosnowskyi* is more suitable for solid biofuel than *S canadensis* as it has a higher calorific value and an ash content that is two times lower – 3wt%. Coffee grounds are a suitable binder because they increase calorific value.
The type and amount of binders partly confirms the hypothesis, since both binders reduced the amount of ash in pellets. Further research is needed to carry out pellet durability tests. It is also necessary to carry out an economic analysis in order to evaluate how beneficial it may be to use *H sosnowskyi* as a solid fuel in existing pellet production plants, thereby avoiding large initial investments and not encouraging the cultivation of invasive plant species.

Key words: *H sosnowskyi*, *S canadensis*, spent coffee grounds, potato peel waste, pellets.

INTRODUCTION

Currently one of the main challenges faced by the pellet industry is in the limitation of raw materials (Emadi et al., 2017). In the energy sector, one of the fastest growing markets is pellet production and consumption (Gravelsins et al., 2017). For the most part, pellets are prepared from wood as a raw material, but in order to be able to satisfy growing demand new materials have to be integrated into the production processes. Existing research offers non-woody materials such as herbaceous biomass, fruit biomass, and aquatic biomass (Konrád et al., 2017). In comparison with wood biomass, non-wood materials have a higher compound variation which creates a certain degree of challenge for the pellet production industry. Therefore, the quality of the raw material is important (Konrád et al., 2017).

Existing non-woody materials are agricultural biomass, wheat straw, rapeseed straw, maize straw, and others (I Niedziiolka et al., 2015). Research for substitute solid biofuel availability and energy sources concludes that herbaceous biomass has the potential for energy production (such as common reed and *H sosnowskyi*) (Beloborodko et al., 2013); therefore the focus in this study is on herbaceous biomass, which is available, and which is widespread and unused in Latvia. Agricultural residues are abundant and are an inexpensive source of renewable energy (Lu et al., 2014). Agricultural residues, such as straw, do not contain an adequate amount of natural binding components – lignin, protein, starch, or water soluble carbohydrates. One solution is to de-bond lignocellulosic matrix structures that free the lignin. However, that involves pre-treatment (including the use of chemicals, additives, a microwave, a steam explosion, or other methods). Another solution is to add a binder, in that way improving pellet durability and strength (Lu et al., 2014). Various types of natural binders are used for the improvement of pellet durability, such as rapeseed flour, coffee meal, bark, lignin powder, pine cones (Ahn et al., 2014), potato flour, potato peel residue, lignosulphonate (Kuokkanen, 2013), and others (Tarasov et al., 2013). The most important aspects are to find a binder that is of a low cost, does not require additional treatment, and is environmentally friendly.

Raw material selection is necessary when it comes to finding a sustainable solid biomass fuel, one which is not used in the production of any higher added value product. The aim of this study is to find good quality non-woody raw materials for solid biofuel. This has been managed by creating a methodology with sustainability criteria regarding solid biofuel raw materials and natural binders, as well as carrying out experimental analyses on selected biomass and binders.

MATERIALS AND METHODS

Methodology is focused on the selection of raw materials that can be used as a solid biofuel but which are not used in the forestry, agriculture, aquaculture, or food industries. Sustainability criteria are determined to select appropriate materials and binders, as well as to find low costs and, preferably, residue and/or waste bioresources. At first, samples were prepared with and without binders. Binders were used in the same proportion for each sample. The determination of main solid biofuel parameters (ash and moisture content, and calorific value) allowed for an evaluation of the quality of raw materials, the binder, and the mixed pellet. Materials with higher calorific values, and a lower ash and moisture content, were selected for further testing. In further sample preparation, different binder proportions are used (10w-%, 30w-%, and 50w-%). The parameters being tested are the same as previously. If the calorific value increases, the ash content remains the same or decreases, and the moisture content is lower than 10w-%, then the solid biofuel and binder can be classified as being justified. If the changes are significant and without clear tendency, more samples need to be tested in different proportions in order to discover the optimum proportion and results.

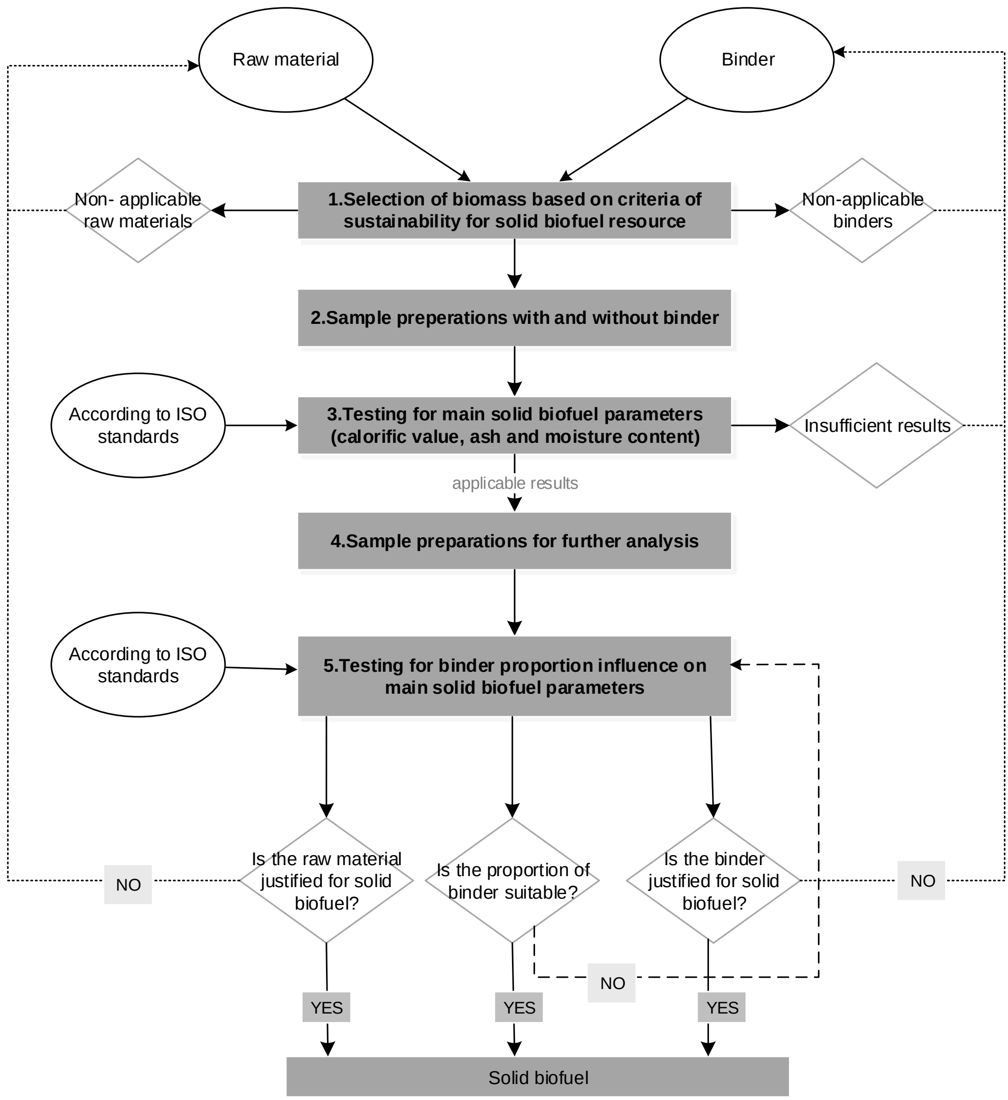

Figure 1. The validation of the resource-methodology algorithm.

Fig. 1 shows the methodology algorithm for resource validation as solid biofuel. The steps and criteria selected restrict the selection of biomass and biofuel. The methodology case study is conducted on invasive species.

1. The selection of biomass based on sustainability criteria for solid biofuel resources

After selecting raw materials and binders in accordance with the sustainability criteria, two raw materials and two binders have been selected for sample preparation and further analysis.

The sustainability criteria for the raw materials and binder selection for solid biofuel are as follows:

- non-woody resources;
- non-agricultural resources;
- resources that are not used in aquaculture;
- no fertiliser or additional water needed;
- a resource that is not used in the food industry;
- a bioresource (not fossil fuel);
- residue or waste that remains unused elsewhere;
- an available or local resource (which corresponds to geographical location and climate zone)
- a low cost resource;
- a resource that is not used in the production of a high added value product in the specific location (country);
- a positive impact on the environment and climate.

Invasive species that have invaded agricultural land and meadows meet the eligibility for sustainability criteria given above. Two of the most invasive plant species in Latvia have been selected for the case study: *Solidago canadensis L* and *Heracleum sosnowskyi* Manden. First of all, both have invaded agricultural land and meadows and are a waste product with no added value in Latvia. Secondly, these invasive species can grow on low nutrition land with no fertilisers or additional water. Thirdly, they are not used in the food industry and are available at a low cost. Mowing and utilising these plants to produce a valuable product would help to control their spread, as well as improving biodiversity. Two possible binders have been selected: potato peel waste and spent coffee grounds. The selected binders also correspond to the critera of sustainability.

2. Sample preparation

Raw materials have been collected in Riga. *H sosnowskyi* samples were collected at the end of October (2017) and *S canadensis* samples were collected at the end of August (2017). Plant materials were initially pre-dried in the laboratory at ambient conditions and afterwards dried completely in a dryer for eighteen hours at 105 °C. Afterwards, the samples were ground down in a mill (Vibrotehnik PM120) into particles smaller than 1mm in diameter. To ensure that particle size was less than 1mm, the mill contained a sieve with an aperture size of 1 mm.

The binders were air-dried for a week. The size of spent coffee grounds was already < 1 mm. This has been double-checked using the Retsch AS 400 sieve, with a sieve aperture size of 1mm. Potato peel waste was also ground down in the mill.

The first eight samples were prepared as follows: pure *S canadensis* (Sc), pure *H sosnowskyi* (Hs), pure coffee grounds (CG), pure potato peel waste (PPW), and S with 6wt% CG, S with 6wt% PPW, H with 6wt% CG, and finally H with 6wt% PPW.

All of the samples were prepared in accordance with the ISO (International Organisation for Standardisation) ISO 14780 standard.

3. Testing main biofuel parameters

The main biofuel characteristics were tested according to ISO standards for biofuel testing: ash content, moisture content, and calorific value.

3.1. Ash content

Ash content analysis has been carried out according to the ISO 18122 standard. The ash content has been calculated by taking into account the initial mass of the test portion and the mass of the ash that remained after the sample had been combusted. To prevent any absorption of moisture from the atmosphere, dishes containing the ash were kept in a desiccator.

The ash content was calculated according to Eq. (1):

$$A_d = \frac{(m_3 - m_1)}{(m_2 - m_1)} \times 100 \times \frac{100}{100 - M_{ad}} \tag{1}$$

where m_1 – mass of empty dish, g; m_2 – mass of dish plus the test portion, g; m_3 – mass of dish plus ash, g; M_{ad} – moisture content of the test portion used for a determination of ash content, w-%.

3.2. Moisture content

The sample was kept in air-tight plastic bags (according to EN 14778). The moisture content of the general analysis sample has been determined according to ISO 18134-3 (LVS EN ISO 18134-3:2016 Solid biofuels – Determining moisture content – oven dry method – Part3: moisture in a general analysis sample (ISO 18134-3:2015), 2016). The sample was dried in a drying oven at 105 °C.

It was assumed that the sample does not lose moisture during the preparation of the test portion. The mass of the test portion was in the range of 0.8–1.1 g.

Following sample preparation, a clean and empty weighing dish with its lid was dried at (105° ± 2) °C and then cooled to room temperature in a desiccator. The test portion was then placed in the dried dishes and dried for a period of one hour without its lid at (105° ± 2) °C, after which each dish with a sample and lid was weighed. In total each test portion was dried three times (three periods of one hour) to ensure that the sample dried completely.

$$M_{ad} = \frac{(m_2 - m_3)}{(m_2 - m_1)} \times 100 \tag{2}$$

where m_1 – mass of the empty dish plus lid, g; m_2 – mass of the dish, lid and test portion before drying, g; m_3 – mass of the dish, lid and test portion after drying, g.

3.3. Calorific value

A calorific value analysis was carried out according to the ISO 18125 standard. The experiment was handled in isoperibolic conditions, and the reference temperature was 30ºC (*LVS EN ISO 18125:2017 Solid biofuels – a determination of calorific value (ISO 18125:2017)*, 2017).

Due to the low density of solid dry biofuels, it is necessary to form a pellet in order to test the calorific value. The biofuel sample was pressed in a manual pellet press (IKA C21) to produce a compact and dense test piece weighing 1.0g ± 0.2 g.

The calculation for the gross calorific value of the dry mass (at a constant volume) is as follows:

$$Q_a^d = H_0 - \frac{Q_{N,S+}\, Q_S}{m} \tag{3}$$

Q_a^d – gross calorific value at a constant volume, J g^{-1}; m – mass of sample, g; $Q_{N,S}$ – heat correction, considering the formation of nitric acid, J; Q_S – heat correction, considering the formation of sulphuric acid, J; H_0 – gross calorific value of the analysed fuel, J g^{-1}.

The repeatability limit for non-wood solid biofuels is 140J/g (*LVS EN ISO 18125:2017 Solid biofuels – a determination of calorific value (ISO 18125:2017)*, 2017).

$$Q_S = 57 \cdot S^d \cdot m_s, \tag{4}$$

where S^d – sulphur content in the analysed sample (on a dry basis), %.

$$Q_{V,gr,d} = Q_{V,gr} \cdot \frac{100}{100 - M_{ad}}, \tag{5}$$

$Q_{V,gr,d}$ – gross calorific value of dry mass at a constant volume, J g^{-1}; M_{ad} – moisture content of the general analysis sample, wt%.

$$Q_{p,net,d} = Q_{V,gr,d} - 212.2 \cdot H^d - 0.8 \cdot (O^d + N^d), \tag{6}$$

where $Q_{p,net,d}$ – net calorific value of the dry mass at a constant pressure, J g^{-1}; H^d – hydrogen content in the analysed sample (on a dry basis), wt%; O^d – oxygen content in the analysed sample (on a dry basis), wt%; N^d – nitrogen content in the analysed sample (on a dry basis), wt%.

$$q_{p,net,ar} = q_{p,net,d} \cdot (1 + 0.01 \cdot M_{ar}) - 24.42 \cdot M_{ar}, \tag{7}$$

where $q_{p,net,ar}$ – net calorific value for the sample as received at constant pressure, J g^{-1}; M_{ar} – total moisture content, wt%.

4. Sample preparations for further analysis

After selecting samples for further analysis, new samples were formed using the best material (a higher calorific value shown for one of the species and increasing calorific value for the binder), which contained 10wt%, 30wt%, or 50wt% of binder accordingly.

5. Testing for binder influence. Validation

Validation for whether the resource and binder is justified as a solid biofuel is based on the results or calorific value, ash content, and moisture content. For resources the justification is based on calorific value – that closest to wood's calorific value, lower ash content, and lower moisture content. Binder justification is either based on increasing calorific value or it can remain the same if it does not change other parameters, ie. if the binder that is added serves to decrease the calorific value then it is not justified. A binder is also justified in terms of decreasing ash content. If adding a binder to the main resource means that it increases the ash content, then a binder is not justified and a different binder will have to be selected. By adding the binder, the moisture level will increase, but it is important to determine the optimum amount of binder added, so that the moisture level is also optimised.

RESULTS AND DISCUSSION

The results of tests involving moisture content (wt%), ash content (wt%), and calorific value (MJ kg^{-1}) have been determined during analysis. In order to be able to get reliable results for the calorific value, there is the necessity of determining and calculating the chemical composition of each sample. All of the results are corrected with chemical composition values for carbon (C), hydrogen (H), nitrogen (N), and sulphur (S).

The chemical composition (*C, H, N, S)* of the pure materials – coffee grounds (CG) (Somnuk et al., 2017), potato peel waste (PPW) (Krus & Lucas, 2014), and *S canadensis* (Sc) (Ciesielczuk et al., 2016) were taken from the available literature, *H sosnowskyi* (Hs) from experimental analysis by chromatograph, and mixed samples were calculated according to the proportions being mixed – see Table 1. Samples that were tested after selecting a suitable material and binder were: *H sosnowskyi* and spent coffee grounds accordingly. The proportions are as follows: Hs 90wt%:CG 10wt%, Hs 70wt%:CG 30wt% and Hs 50wt%:CG 50wt% and were calculated accordingly. According to EN plus pellet quality requirements for wood pellet quality classes, the N and S amount is very important for solid biofuel quality. The highest acceptable N amount is 1.0wt% and for S it is 0.05wt% (European Biomass Association (AEBIOM), 2015). If the aim is to compete with or to achieve qualities which are similar to wood, then no more than 30wt% of CG binder can be added.

Table 1. Chemical composition of the samples

	CG	PPW	Sc	Hs	Sc, PPW 6wt%	Sc, CG 6wt%	Hs, PPW 6wt%	Hs, CG 6wt%	Hs, CG 10wt%	Hs, CG 30wt%	Hs, CG 50wt%
C	52.95	43.90	44.80	46.52	44.75	45.29	46.36	46.91	47.16	48.45	49.74
H	6.76	7.20	6.46	5.79	6.50	6.48	5.87	5.84	5.88	6.08	6.27
N	2.10	0.80	0.37	0.59	0.40	0.47	0.60	0.68	0.74	1.04	1.35
S	0.12	0.10	0.20	0.00	0.19	0.19	0.01	0.01	0.01	0.04	0.06

Key: Sc, PPW 6wt% – *S canadensis* (94wt%) mixed with 6wt% potato peel waste; Sc, CG 6wt% – *S canadensis* (94wt%) mixed with 6wt% coffee grounds; Hs, PPW 6wt% – *H sosnowskyi* (94wt%) mixed with 6wt% potato peel waste; Hs, CG 6wt% – *H sosnowskyi* (94wt%) mixed with 6wt% coffee grounds.

According to the third step of the methodology algorithm, the first sample results are obtained for two species and two binders; further selection is carried out for species with a higher calorific value, and a lower ash and moisture content. The binder is further selected by positive changes in tested samples.

In Fig. 2 changes in biofuel parameters are shown for a pure materials sample (base sample – no binder added). The *H sosnowskyi* and PPW (Hs, PPW 6wt%) sample shows an increase in moisture content, and a small decrease in ash content and calorific values. *S canadensis* with both binders (PPW and CG) show a decrease in all parameters. Only *H sosnowskyi* with a CG binder shows an increase in calorific value and no important changes in moisture and ash content. Therefore, *H sosnowskyi* and CG were selected for further testing using different proportions of the binder. There are no similarities between either of the binders or their effect on biomass parameters; for example, the PPW binder decreases moisture for one biomass, but increases it for the other. Therefore further experiments with other types of biomass are preferable.

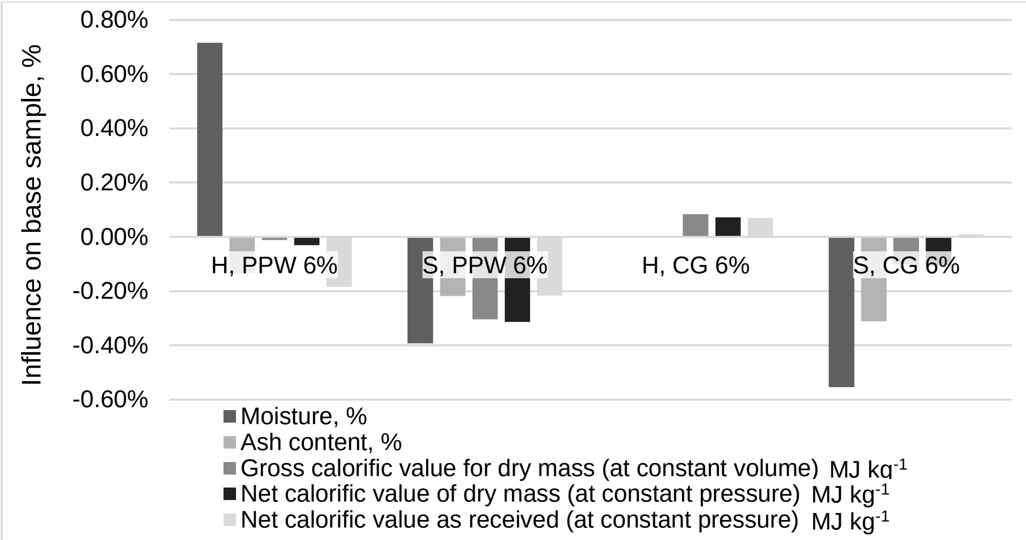

Figure 2. Biofuel parameter changes by binder type.

For the final results for all samples, see Table 2, which shows that the highest calorific value is for the pure coffee ground sample, whilst the lowest is for the potato peel waste. Potato peel waste has the highest moisture content. Thanks to these results, potato peel waste is proven not to be a very suitable binder. *Solidago canadensis* has a high moisture and ash content and, although the calorific value is good for non-woody material, *Heracleum* showed better results in all parameters and is therefore selected for further experiments.

Table 2. The results for solid biofuel parameters in all samples

Sample	Moisture (%)	Ash content (%)	Gross calorific value* (MJ kg^{-1})	Net calorific value ** (MJ kg^{-1})	Net calorific value *** (MJ kg^{-1})
Sc, 0%	7.3%	6.8%	18.24	16.84	15.43
Hs, 0%	3.1%	3.4%	19.45	18.19	17.56
Hs, PPW 6%	3.8%	3.3%	19.44	18.16	17.37
Sc, PPW 6%	6.9%	6.6%	17.94	16.52	15.22
Hs, CG 6%	3.1%	3.4%	19.53	18.26	17.63
Sc, CG 6%	6.7%	6.5%	18.14	16.73	15.44
Hs 90%, CG 10%	3.7%	3.4%	19.64	18.36	17.59
Hs 70%, CG 30%	4.8%	3.1%	20.42	19.10	18.07
Hs50%, CG 50%	6.1%	2.9%	21.09	19.73	18.39
CG 100%	9.2%	2.3%	22.73	21.27	19.08
PPW100%	15.9%	5.8%	17.90	16.33	13.36

* for dry mass at a constant volume; ** for dry mass at a constant pressure; *** for a sample as received at constant pressure.

Fig. 3 illustrates how the added amount of CG binder (10wt%, 30wt%, 50wt%) influences biofuel parameters. In comparison to a pure Hs sample, *H sosnowskyi* with CG increases calorific value (the gross calorific and net calorific value of dry mass; the net calorific value as received), lowers ash content, and increases moisture content. When analysing all parameters the optimal moisture content, ash content, and calorific value for *H sosnowskyi* shows no more than 30wt% CG binder.

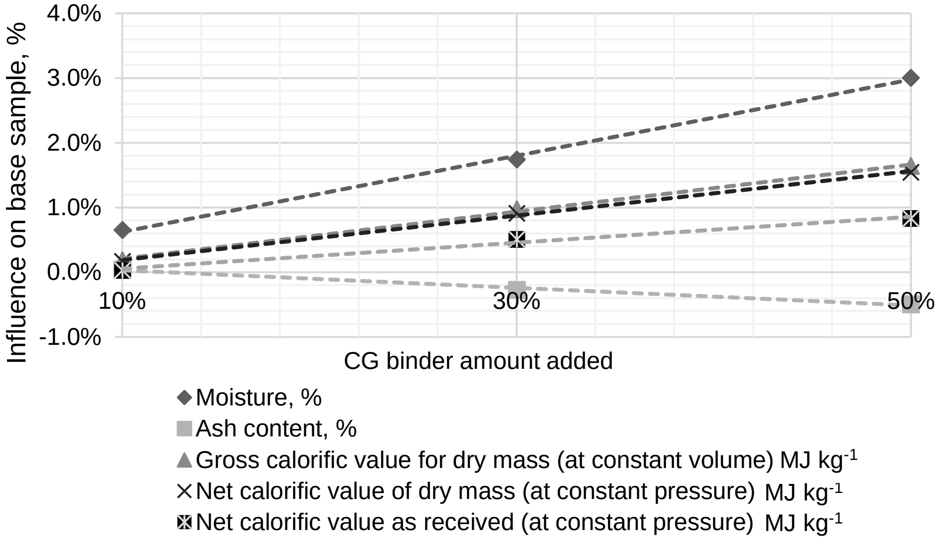

Figure 3. Biofuel parameter changes by different proportion of CG binder.

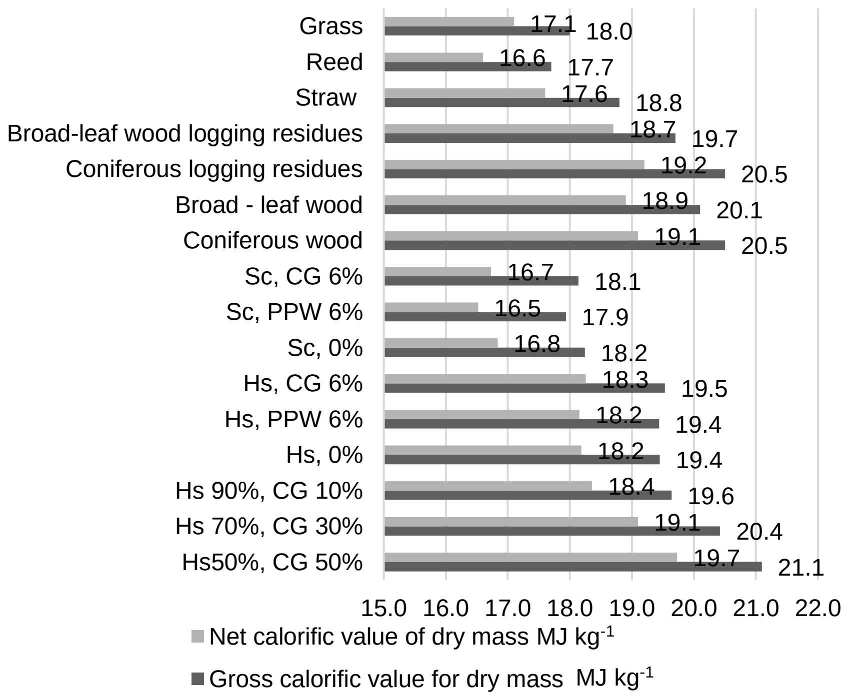

Figure 4. A comparison of calorific values between existing solid biomass fuels and tested samples.

In order to determine the quality of the tested sample, a comparison with other existing solid biomass fuels was carried out. Typical values have been taken from the ISO 17225-1:2014 standard. The main values taken for the comparison are grass (in general), virgin reed canary grass (summer harvest), virgin straw materials from wheat, rye, and barley, virgin wood logging residues for coniferous and for broad-leaf wood, and virgin wood materials for broad-leaf wood and coniferous wood.

The results for all *Solidago* samples – see Fig. 4 – corresponds to reed and grass calorific values with and without binders; however *Heracleum* is competitive with broad-leaf logging residues. Moreover, mixed samples are even comparable to the results for coniferous logging residues, broad-leaf wood, and coniferous wood. The best results are for the *Heracleum* sample with 50wt% coffee grounds. To determine the optimal proportion, ash content should also be taken into account.

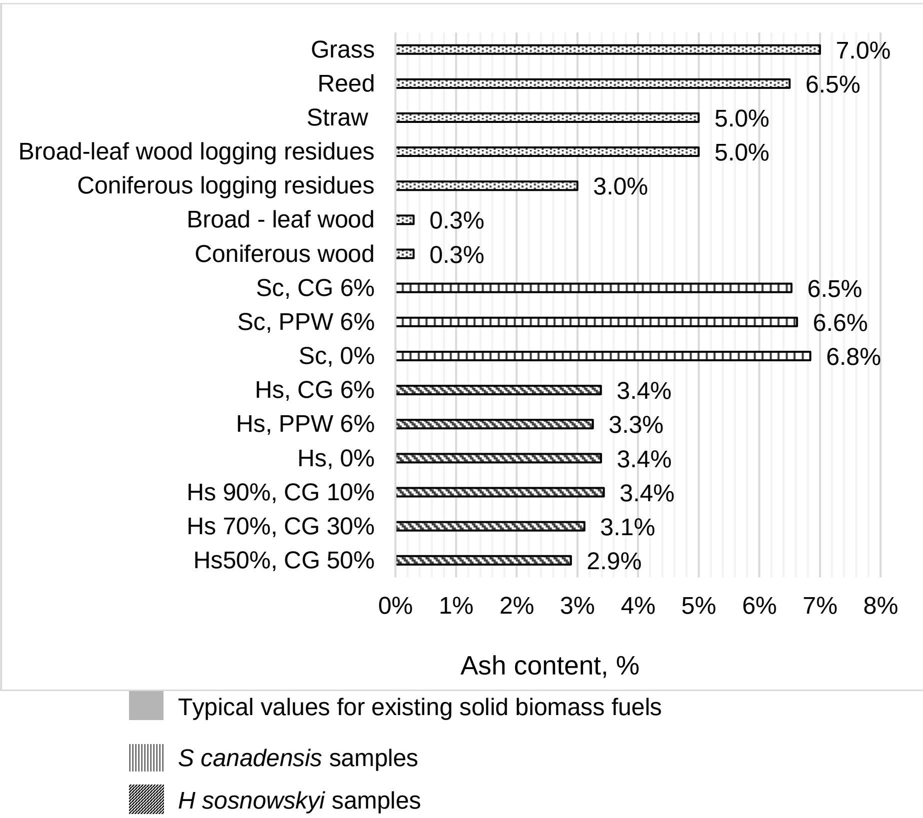

Figure 5. A comparison of ash content between existing solid biomass fuels and tested samples.

Fig. 5 shows the ash content values for existing solid biomass fuels and the tested samples. Typical values for existing solid biomass fuels are taken from the ISO 17225-1:2014 standard. The lowest ash content is for virgin wood material (broad-leaf and coniferous). Non-woody materials cannot compete with virgin wood materials. However, the average ash content for logging residues is between 3wt%-5wt%, which is similar to the ash content for *Heracleum*. The ash content of *Solidago* mixed samples are similar to those for virgin reed canary grass, but the results for pure *Solidago* are similar to those for grass (in general).

CONCLUSIONS

The article's hypothesis has been partly verified. Invasive plant species, in terms of sustainability criteria for biomass selection, can be a suitable resource for the production of solid biofuel pellets, one which is easily replaced if the selected biomass is no longer available. But not all species show the best results. Not all binders can improve the quality of pellets in terms of biofuel parameters, but the coffee grounds as a binder have shown good results with *H sosnowskyi*, and there is a necessity to continue research with this binder and other raw materials where the ash content is high and the calorific value should be improved.

The methodology that has been created allows the appropriate raw materials and binders to be validated for solid biofuel production, a production which is low on cost and underused. The methodology helps to determine the quality of the resource and the properties of the added binder, so that the most effective species with the most effective binder can be selected, where they are also low on cost and widely available. As well as determining the optimum amount of binder that can be added, the parameters do not change or there is an increase in the calorific value and a decrease in the ash content.

The methodology can be improved by adding more biofuel-characteristic parameters into the selection and is effective in comparison with other solid biofuels.

The optimum coffee ground binder percentage is no more than 30% as the moisture content increases significantly. The increasing moisture content in higher proportions with coffee grounds could be reduced by means of oven drying.

Overall, the experimental analysis turned out better for *H sosnowskyi* pellets with a coffee ground binder. The calorific value and ash content can be competitive against wood. Therefore, it is possible to use this bioresource as an effective energy source. From those conclusions it can be seen that the use of *H sosnowskyi* with a coffee ground binder has been fully validated, and it is advisable to use this in industrial pellet production plants. However, from the energy balance and economics point of view, it is preferable to conduct further analysis. Further investigation for durability and bulk density for industrial pellets is clearly needed.

ACKNOWLEDGEMENTS. This work has been supported by the National Research programme: 'Energy efficient and low-carbon solutions for a secure, sustainable, and climate-variability-reducing energy supply (LATENERGI)'.
Thanks are due to environmental science student, Ieva Laganovska, for her participation in the experimental part of the research.

REFERENCES

Ahn, B.J., Chang, H. sun, Lee, S.M., Choi, D.H., Cho, S.T., Han, G. seong, Yang, I. 2014. Effect of binders on the durability of wood pellets fabricated from Larix kaemferi C. and Liriodendron tulipifera L. sawdust. *Renew. Energy* **62**, 18–23. doi:10.1016/j.renene.2013.06.038

Beloborodko, A., Klavina, K., Romagnoli, F., Kenga, K., Rosa, M. & Blumberga, D., 2013. Study on availability of herbaceous resources for production of solid biomass fuels in Latvia. *Agron. Res.* **11**(2), 283–294

Ciesielczuk, T., Poluszyńska, J., Rosik-Dulewska, C., Sporek, M. & Lenkiewicz, M., 2016. Uses of weeds as an economical alternative to processed wood biomass and fossil fuels. *Ecol. Eng*. **95**, 485–491. doi:10.1016/j.ecoleng.2016.06.100

Emadi, B., Iroba, K.L. & Tabil, L.G. 2017. Effect of polymer plastic binder on mechanical, storage and combustion characteristics of torrefied and pelletized herbaceous biomass. *Appl. Energy* **198**, 312–319. doi:10.1016/j.apenergy.2016.12.027

European Biomass Association (AEBIOM). 2015. EN plus For Wood Pellets EN plus Handbook Part 3 : Pellet Quality Requirements 1–16. doi:10.1017/CBO9781107415324.004

Gravelsins, A., Muizniece, I., Blumberga, A. & Blumberga, D. 2017. Economic sustainability of pellet production in Latvia. *Energy Procedia* **142**, 531–537. doi:10.1016/j.egypro.2017.12.083

Konrád, K., Viharos, Z.J. & Németh, G. 2017. Evaluation, ranking and positioning of measurement methods for pellet production. Measurement. doi:10.1016/j.measurement.2017.12.036

Krus Carlos Galvão Lucas, 2014. Biogas Production from Potato Peel Waste. Dissertation, Faculdade de Ciências e Tecnologia, Universidade Nova de Lisboa, 1–106.

Kuokkanen, M. 2013. Development of an eco- and material-efficient pellet production chain—a chemical study. *Acta Univ.Oul.* **A 607**, 1–104.

Lu, D., Tabil, L.G., Wang, D., Wang, G. & Emami, S. 2014. Experimental trials to make wheat straw pellets with wood residue and binders. *Biomass and Bioenergy* **69**, 287–296. doi:10.1016/j.biombioe.2014.07.029

LVS EN ISO 18122:2016 Solid biofuels – Determination of ash content (ISO 18122:2015), 2016.

LVS EN ISO 18125:2017 Solid biofuels – Determination of calorific value (ISO 18125:2017), 2017.

LVS EN ISO 18134-3:2016 Solid biofuels – Determination of moisture content – Oven dry method – Part3: Moisture in general analysis sample (ISO 18134-3:2015), 2016.

Niedziiolka, I., Szpryngiel, M. Kachel-Jakubowska, M., Kraszkiewicz, A., Zawislak, K., Sobczak, P. & Nadulski, R. 2015. Assessment of the energetic and mechanical properties of pellets produced from agricultural biomass. *Renew. Energy* **76**, 312–317. doi:10.1016/j.renene.2014.11.040

Somnuk, K., Eawlex, P. & Prateepchaikul, G., 2017. Optimization of coffee oil extraction from spent coffee grounds using four solvents and prototype-scale extraction using circulation process. *Agric. Nat. Resour.* **51**, 181–189. doi:10.1016/j.anres.2017.01.003

Tarasov, D., Shahi, C. & Leitch, M. 2013. Effect of Additives on Wood Pellet Physical and Thermal Characteristics: A Review. *ISRN For*. **2013**, Article ID 876939, 6 pp. doi:10.1155/2013/876939

INSTRUCTIONS TO AUTHORS

Papers must be in English (British spelling). English will be revised by a proofreader, but authors are strongly urged to have their manuscripts reviewed linguistically prior to submission. Contributions should be sent electronically. Papers are considered by referees before acceptance. The manuscript should follow the instructions below.

Structure: Title, Authors (initials & surname; an asterisk indicates the corresponding author), Authors' affiliation with postal address (each on a separate line) and e-mail of the corresponding author, Abstract (up to 250 words), Key words (not repeating words in the title), Introduction, Materials and methods, Results and discussion, Conclusions, Acknowledgements (optional), References.

Layout, page size and font

- Use preferably the latest version of **Microsoft Word**, doc., docx. format.
- Set page size to **B5 Envelope or ISO B5 (17.6 x 25 cm)**, all margins at 2 cm.
- Use single line spacing and justify the text. Do not use page numbering. Use indent 0.8 cm (do not use tab or spaces instead).
- Use font Times New Roman, point size for the title of article **14 (Bold)**, author's names 12, core text 11; Abstract, Key words, Acknowledgements, References, tables and figure captions 10.
- Use *italics* for Latin biological names, mathematical variables and statistical terms.
- Use single ('…') instead of double quotation marks ("…").

Tables

- All tables must be referred to in the text (Table 1; Tables 1, 3; Tables 2–3).
- Use font Times New Roman, regular, 10 pt. Insert tables by Word's 'Insert' menu.
- Do not use vertical lines as dividers; only horizontal lines (1/2 pt) are allowed. Primary column and row headings should start with an initial capital.

Figures

- All figures must be referred to in the text (Fig. 1; Fig. 1 A; Figs 1, 3; Figs 1–3). Use only black and white or greyscale for figures. Avoid 3D charts, background shading, gridlines and excessive symbols. Use font **Arial** within the figures. Make sure that thickness of the lines is greater than 0.3 pt.
- Do not put caption in the frame of the figure.
- The preferred graphic format is EPS; for half-tones please use TIFF. MS Office files are also acceptable. Please include these files in your submission.
- Check and double-check spelling in figures and graphs. Proof-readers may not be able to change mistakes in a different program.

References

- **Within the text**

In case of two authors, use '&', if more than two authors, provide first author 'et al.':

Smith & Jones (1996); (Smith & Jones, 1996);
Brown et al. (1997); (Brown et al., 1997)

When referring to more than one publication, arrange them by following keys: 1. year of publication (ascending), 2. alphabetical order for the same year of publication:

(Smith & Jones, 1996; Brown et al., 1997; Adams, 1998; Smith, 1998)

- **For whole books**

Name(s) and initials of the author(s). Year of publication. *Title of the book* (*in italics*). Publisher, place of publication, number of pages.

Shiyatov, S.G. 1986. *Dendrochronology of the upper timberline in the Urals*. Nauka, Moscow, 350 pp. (in Russian).

- **For articles in a journal**

Name(s) and initials of the author(s). Year of publication. Title of the article. *Abbreviated journal title* (*in italic*) volume (in bold), page numbers.

Titles of papers published in languages other than English, German, French, Italian, Spanish, and Portuguese should be replaced by an English translation, with an explanatory note at the end, e.g., (in Russian, English abstr.).

Karube, I. & Tamiyra, M.Y. 1987. Biosensors for environmental control. *Pure Appl. Chem.* **59**, 545–554.

Frey, R. 1958. Zur Kenntnis der Diptera brachycera p.p. der Kapverdischen Inseln. *Commentat.Biol.* **18**(4), 1–61.

Danielyan, S.G. & Nabaldiyan, K.M. 1971. The causal agents of meloids in bees. *Veterinariya* **8**, 64–65 (in Russian).

- **For articles in collections:**

Name(s) and initials of the author(s). Year of publication. Title of the article. Name(s) and initials of the editor(s) (preceded by In:) *Title of the collection (in italics)*, publisher, place of publication, page numbers.

Yurtsev, B.A., Tolmachev, A.I. & Rebristaya, O.V. 1978. The floristic delimitation and subdivisions of the Arctic. In: Yurtsev, B. A. (ed.) *The Arctic Floristic Region*. Nauka, Leningrad, pp. 9–104 (in Russian).

- **For conference proceedings:**

Name(s) and initials of the author(s). Year of publication. Name(s) and initials of the editor(s) (preceded by In:) *Proceedings name (in italics)*, publisher, place of publishing, page numbers.

Ritchie, M.E. & Olff, H. 1999. Herbivore diversity and plant dynamics: compensatory and additive effects. In: Olff, H., Brown, V.K. & Drent R.H. (eds) *Herbivores between plants and predators. Proc. Int. Conf. The 38th Symposium of the British Ecological Society*, Blackwell Science, Oxford, UK, pp. 175–204.

Please note

- Use '.' (not ',') for decimal point: 0.6 ± 0.2; Use ',' for thousands – 1,230.4;
- Use '–' (not '-') and without space: pp. 27–36, 1998–2000, 4–6 min, 3–5 kg
- With spaces: 5 h, 5 kg, 5 m, 5°C, C : D = 0.6 ± 0.2; p < 0.001
- Without space: 55°, 5% (not 55 °, 5 %)
- Use 'kg ha^{-1}' (not 'kg/ha');
- Use degree sign ' ° ' : 5 °C (not 5 ^{O} C).